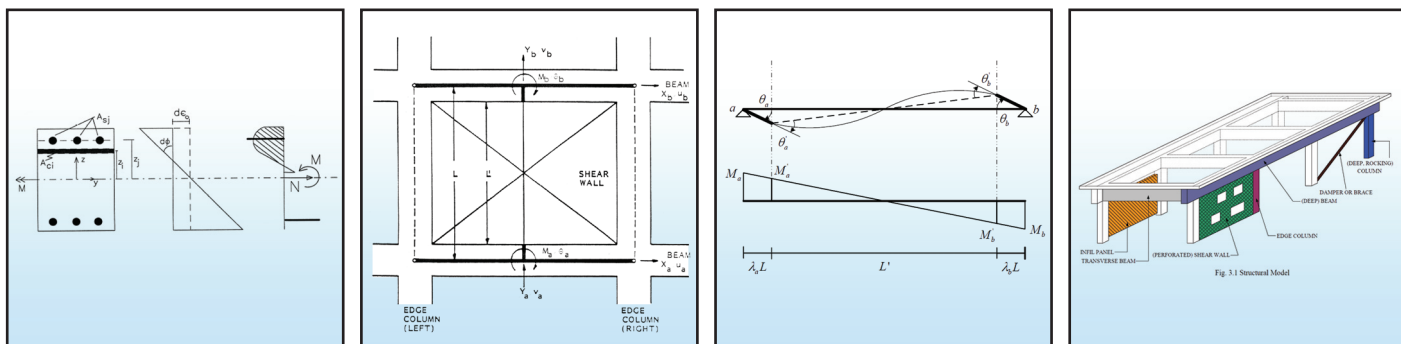


IDARC2D Version 7.0: A Program for the Inelastic Damage Analysis of Structures

by
A.M. Reinhorn, H. Roh, M. Sivaselvan, S.K. Kunnath, R.E. Valles, A. Madan, C. Li, R. Lobo and Y.J. Park



Technical Report MCEER-09-0006

July 28, 2009

DISCLAIMER

Considerable effort and time has been put in the development and testing of the computer program IDARC. Whenever possible, analytical results have been validated with experimental data. All modules and routines in the program have been carefully tested with examples. Nevertheless, the authors do not take any responsibility due to inadequate analysis results derived from flaws in the modeling techniques or in the program. The user is responsible to verify the results from the analysis. The program incorporates current knowledge in the field of nonlinear structural dynamic analysis. The user should be knowledgeable in this area to understand the assumptions in the program, adequately use it, and to verify and correctly interpret the results. The following DISCLAIMER OF WARRANTY applies to the user of the computer program IDARC and its associated subroutines.

DISCLAIMER OF WARRANTY

The program IDARC, the associated subroutines, and the data files, are provided "AS-IS" without warranty of any kind. The authors and the sponsoring institutions make no warranties, express or implied, that the program is free of error or is consistent with any particular standard of merchantability, or that the program will meet your requirements for any particular application. The program should not be relied on for solving a problem whose incorrect solution could result in injury to a person or loss of property. If you do use the program in such a manner, it is at your own risk. The authors and the sponsoring institutions disclaim all liability for direct or consequential damages resulting from your use of the program.

The ownership of the program remains with the developers. The program should not be resold or redistributed in whole or in part for direct profit. Neither the whole program nor routines of the program shall be incorporated into the source code or the executable binary code of other programs without prior written permission from the authors. Programs containing IDARC routines must acknowledge acceptance of the above DISCLAIMER OF WARRANTY and of the fact that no business relationship is created between the program's users and the authors of IDARC or the sponsoring institutions. The name of the authors and the name of sponsoring institutions should not be used to promote products derived from this program without specific prior written permission from the authors.

NOTICE

This report was prepared by the University at Buffalo, State University of New York as a result of research sponsored by MCEER through a grant from the Earthquake Engineering Research Centers Program of the National Science Foundation under NSF award number EEC-9701471 and other sponsors. Neither MCEER, associates of MCEER, its sponsors, the University at Buffalo, State University of New York, nor any person acting on their behalf:

- a. makes any warranty, express or implied, with respect to the use of any information, apparatus, method, or process disclosed in this report or that such use may not infringe upon privately owned rights; or
- b. assumes any liabilities of whatsoever kind with respect to the use of, or the damage resulting from the use of, any information, apparatus, method, or process disclosed in this report.

Any opinions, findings, and conclusions or recommendations expressed in this publication are those of the author(s) and do not necessarily reflect the views of MCEER, the National Science Foundation, or other sponsors.



IDARC2D Version 7.0: A Program for the Inelastic Damage Analysis of Structures

by

A.M. Reinhorn,¹ H. Roh,² M. Sivaselvan,³ S.K. Kunnath,⁴ R.E. Valles,⁵
A. Madan,⁶ C. Li,⁷ R. Lobo⁷ and Y.J. Park⁸

Publication Date: July 28, 2009
Submittal Date: March 20, 2009

Technical Report MCEER-09-0006

Previous Edition: Technical Report NCEER-96-0010

Task Number 10.2.6

NSF Master Contract Number EEC 9701471

- 1 Clifford C. Furnas Professor, Department of Civil, Structural and Environmental Engineering, University at Buffalo, State University of New York
- 2 Research Scientist, Department of Civil, Structural and Environmental Engineering, University at Buffalo, State University of New York
- 3 Assistant Professor, Department of Civil, Environmental and Architectural Engineering, University of Colorado, Boulder
- 4 Professor, Department of Civil and Environmental Engineering, University of California at Davis
- 5 Director General, DITEC Company, Mexico
- 6 Associate Professor, Department of Civil and Environmental Engineering, Indian Institute of Technology Delhi
- 7 Senior Structural Engineer, California Office of Statewide Health Planning and Development, Sacramento
- 8 Deceased

MCEER
University at Buffalo, State University of New York
Red Jacket Quadrangle, Buffalo, NY 14261
Phone: (716) 645-3391; Fax (716) 645-3399
E-mail: mceer@buffalo.edu; WWW Site: <http://mceer.buffalo.edu>

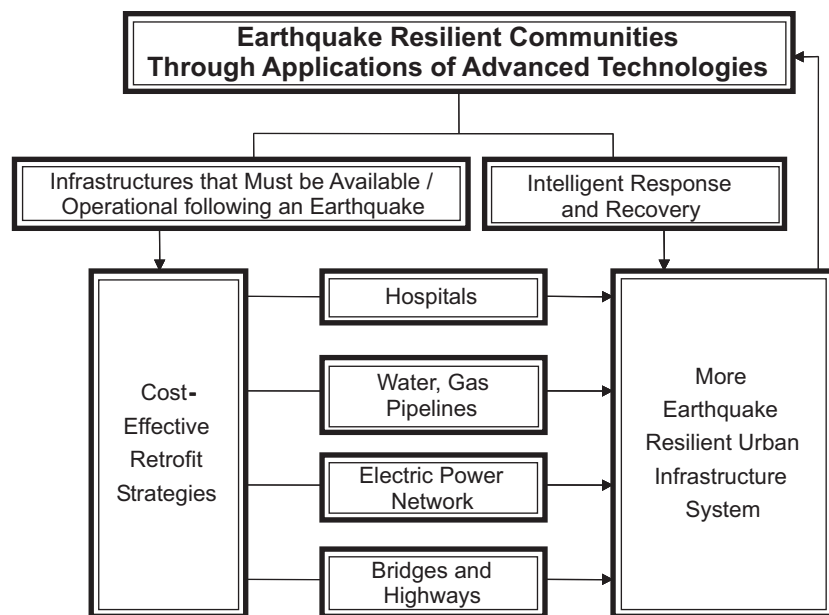
Preface

The Multidisciplinary Center for Earthquake Engineering Research (MCEER) is a national center of excellence in advanced technology applications that is dedicated to the reduction of earthquake losses nationwide. Headquartered at the University at Buffalo, State University of New York, the Center was originally established by the National Science Foundation in 1986, as the National Center for Earthquake Engineering Research (NCEER).

Comprising a consortium of researchers from numerous disciplines and institutions throughout the United States, the Center's mission is to reduce earthquake losses through research and the application of advanced technologies that improve engineering, pre-earthquake planning and post-earthquake recovery strategies. Toward this end, the Center coordinates a nationwide program of multidisciplinary team research, education and outreach activities.

MCEER's research is conducted under the sponsorship of two major federal agencies: the National Science Foundation (NSF) and the Federal Highway Administration (FHWA), and the State of New York. Significant support is derived from the Federal Emergency Management Agency (FEMA), other state governments, academic institutions, foreign governments and private industry.

MCEER's NSF-sponsored research objectives are twofold: to increase resilience by developing seismic evaluation and rehabilitation strategies for the post-disaster facilities and systems (hospitals, electrical and water lifelines, and bridges and highways) that society expects to be operational following an earthquake; and to further enhance resilience by developing improved emergency management capabilities to ensure an effective response and recovery following the earthquake (see the figure below).



A cross-program activity focuses on the establishment of an effective experimental and analytical network to facilitate the exchange of information between researchers located in various institutions across the country. These are complemented by, and integrated with, other MCEER activities in education, outreach, technology transfer, and industry partnerships.

This report summarizes the enhanced modeling and analysis capabilities of the IDARC program series for analysis, design and support of experimental studies. The analytical models described include frame structures with rigid or semi-rigid connections made of beams, columns, shear walls, connecting beams, edge elements, infill masonry panels, inelastic discrete springs (connectors), and damping braces (viscoelastic, viscous, friction and hysteretic). Hysteretic models with improved degradation parameters can trace sections to complete collapse. The nonlinear characteristics of the analytical models are based on a flexibility formulation and an improved distributed plasticity with yield penetration model. Properties of members are calculated by fiber models or by formulations based on mechanics. The analysis techniques include improved nonlinear static analysis (with monotonic and cyclic loadings), nonlinear dynamic analysis with multi-component ground motions and gravity loads, and quasi-static analysis of the type required by laboratory experiments. The analyses include enhanced evaluation of inelastic response through damage analysis of members and the global structure, using methods based on energy, stiffness and ductility including monitored damage progression. Finally, new case studies are included as examples of use of inelastic analyses.

ABSTRACT

This report summarizes the modeling of inelastic structures and enhancements to the program series IDARC developed for analysis, design and support of experimental studies. This report presents a synthesis of all the material presented in previous reports NCEER-87-0008, NCEER-92-0022, and NCEER-96-0010 (and in other related reports). The report presents also the new developments regarding modeling of inelastic elements and structures with supplemental damping devices, infill panels, etc.

The analytical models described herein include, frame structures with rigid or semi-rigid connections made of beams, columns, shear walls, connecting beams, edge elements, infill masonry panels, inelastic discrete springs (connectors), and damping braces (viscoelastic, fluid viscous, friction, hysteretic). The formulations are based on macromodels in which most structural members are represented by a single-comprehensive element with nonlinear characteristics.

The nonlinear characteristics of the basic macromodels are based on a flexibility formulation and a distributed plasticity with yield penetration. Properties of members are calculated by fiber models or by formulations based on mechanics. The solutions are obtained using step-by-step integration of equations of motion using Newmark beta method. One-step correction and iterative computations are performed to satisfy equilibrium. The nonlinear dampers are treated as time dependent Maxwell models, Kelvin Models or hysteretic models. Their solution is obtained by simultaneously solving their individual equations using a semi-implicit Runge-Kutta solution.

This report presents several analyses types which can be performed by the computer program, i.e., monotonic inelastic static analysis (push-over), time-history analysis with multi-components of ground motion and gravity loads, and quasi-static analyses of the type required by laboratory experiments. The analyses include evaluation of inelastic response through damage analysis of members and the global structure. Several damage indices formulations are presented (Park et al., Reinhorn & Valles, Cackmak et al.) based on energy, stiffness and ductility including monitored damage progression.

The previous report emphasized the improvements to this analytical platform which include: (i) improved plasticity and yield penetration model; (ii) new masonry

infill panels; (iii) new braces with damping; (iv) new hysteretic model and solution; (v) new global damping formulation; (vi) new “push-over” analyses including adaptable technique; (vii) new damage indicators, (viii) improved information on damage progression through snapshots; (ix) improved efficiency through reprogramming of stiffness formulations; (x) new case studies presented as examples of use of inelastic analyses.

The current report summarizes along with previous improvements, the new improvements from previous version 4.0 to latest version 7.0 of this analytical platform, which include: (i) added uniform flexibility formulation; (ii) added concentrated plasticity model; (iii) improved vertex oriented hysteretic model; (iv) developed smooth hysteretic model; (v) developed nonlinear elastic-cyclic model; (vi) developed deep beam and deep column elements; (vii) added new rocking column model; (viii) added shear failure state in output files; (ix) added story velocity in story output files; (x) new two case studies, as examples of the use of deep beam & column elements and rocking (constrained double hinged) columns characterized with the nonlinear elastic-cyclic behavior for used weakened structures.

For the sake of completion this report includes all background from previous reports as well as the latest improvements.

The computer program has a user’s manual which is presented in Appendix A and is distributed to members of the IDARC Users Group:

<http://civil.eng.buffalo.edu/idarc/>

http://civil.eng.buffalo.edu/users_ntwk_idarc (computational platform)

Additional information is posted in the Internet site (see Introduction).

ACKNOWLEDGMENTS

Financial support was provided for the development of IDARC indirectly through projects regarding modeling and evaluation of structural systems by the Multidiciplinary (former National) Center for Earthquake Engineering Research. MCEER was supported by the National Science Foundation, and by the State of New York. The support is gratefully acknowledged. Some enhancements to the current release were also sponsored and/or developed with cooperation from:

Dames and Moore, Inc., Los Angeles, CA, - Dr. M. Mehrain
John A. Martin and Associates (JAMA), Los Angeles, CA, Dr. F. Naeim
Larsa, inc., New York, NY-Dr. A. Karakaplan
National Institute of Standards and Technology (NIST), Gaithersbury, MD-Dr. J. Gross.
Sumitomo Construction, Co., Tokyo, Japan, - Dr. Myiazaki
Taylor Devices, Inc., N. Tonawanda, NY - Mr. D. Taylor
Tekton, Inc., Tempe, Arizona, - Mr. P. Attaway

Their cooperation is greatly appreciated.

The authors wish to thank the members of IDARC Users Group for their comments, that initiated some revisions. The members of the Users Group are further encouraged to provide feedback for the improvement of the program,
[see http://civil.eng.buffalo.edu/users_ntwk_idarc (computational platform)].

TABLE OF CONTENTS

SECTION	TITLE	PAGE
1	INTRODUCTION	1
2	THEORY AND BACKGROUND	5
2.1	Nonlinear Structural Analysis Software	5
2.2	IDARC Computer Program Series.....	5
2.3	Program Enhancements	13
3	FORMULATIONS OF STRUCTURAL ELEMENT MODELS.....	15
3.1	Introduction.....	15
3.2	Stiffness Formulation for Common Structural Elements.....	16
3.3	Fiber Model for Common Structural Elements	21
3.3.1	Moment-Curvature Envelope Computation.....	23
3.3.2	Ultimate Deformation Capacity.....	27
3.4	Spread Plasticity Model	29
3.4.1	Linear Variable Flexibility Distribution	32
3.4.2	Uniform Flexibility Distribution	34
3.5	Concentrated Plasticity Model.....	35
3.6	Yield Penetration Model	36
3.7	Element Moment Releases.....	40
4	ELEMENT MODELS LIBRARY	43
4.1	Column Elements.....	43
4.2	Beam Elements	46
4.3	Deep Beam and Column Elements	50
4.4	Rocking Column Elements	53
4.5	Shear Wall Elements.....	57
4.6	Edge Column Elements.....	59
4.7	Transverse Beam Elements.....	61
4.8	Rotational Inelastic Spring Elements.....	62
4.9	Visco-Elastic Damper Elements	63
4.10	Friction Damper Elements	67
4.11	Hysteretic Damper Elements	69
4.12	Infill Panel Elements.....	72
4.12.1	Masonry Infill Panels.....	72
5	HYSTERETIC RULES	79
5.1	Introduction.....	79
5.2	Polygonal Hysteretic Model (PHM)	80
5.2.1	Types of PHM.....	80
5.2.1.1	Trilinear model.....	80
5.2.1.2	Bilinear model.....	81
5.2.1.3	Vertex-Oriented model	81

TABLE OF CONTENTS (CONT'D)

SECTION	TITLE	PAGE
5.2.2	Backbone curves and types of Cyclic Behavior	81
5.2.3	“Points” and “Branches”	85
5.2.4	Operation of the Model – Force Vs. Displacement Control (Moment/Curvature Controlled)	86
5.2.5	Degradation.....	87
5.2.5.1	Stiffness Degradation.....	87
5.2.5.2	Strength Degradation	88
5.2.5.3	Pinching or Slip.....	89
5.2.5.4	Algorithm and Implementation.....	90
5.2.6	Nonlinear Elastic-Cyclic Model (NECM)	90
5.2.6.1	Backbone Curves and Types of Cyclic Behavior	90
5.2.6.2	NECM with “Negative Stiffness” Behavior	92
5.2.6.3	NECM without “Negative Stiffness” Behavior	95
5.2.6.4	“Points” and “Branches”	95
5.2.6.5	Operation of the Model – Force Vs. Displacement Control (Moment/Curvature Controlled)	95
5.2.6.6	Algorithm and Implementation.....	96
5.2.7	Examples.....	96
5.3	Smooth Hysteretic Model (SHM, Sivaselvan and Reinhorn model).....	96
5.3.1	Plain Hysteretic Behavior without Degradation	97
5.3.2	Spring 1: Post-yield Spring.....	97
5.3.3	Spring 2: Hysteretic Spring.....	97
5.3.4	Degradation.....	100
5.3.4.1	Stiffness Degradation.....	100
5.3.4.2	Strength Degradation	101
5.3.4.3	Pinching or Slip.....	101
5.3.4.4	Gap Closing Behavior.....	103
5.3.4.5	Solution of the SHM	104
5.3.5	Examples.....	105
5.4	Visco-Elastic Models	106
5.4.1	Kelvin Model	107
5.4.2	Maxwell Model	111
5.5	Complex Self Centering Model	114
5.6	Special Spring Base Isolator Model.....	124
6	ANALYSIS MODULES	127
6.1	Introduction.....	127
6.2	Incremental Nonlinear Static Monotonic Analysis.....	128
6.3	Incremental Nonlinear Static-Adaptive (Pushover) Analysis	129
6.3.1	Formulation.....	129
6.3.2	Vertical Lateral Force Distribution.....	130
6.4	Nonlinear Quasi-static Analysis	133

TABLE OF CONTENTS (CONT'D)

SECTION	TITLE	PAGE
6.5	Eigenvalue Analysis.....	134
6.6	Nonlinear Dynamic Analysis.....	135
6.6.1	Formulation.....	135
6.6.2	Damping Considerations.....	139
6.7	Analyses including P-Delta Effects	141
6.7.1	P-delta through Geometric Matrix	142
6.7.2	P-delta through Auxiliary Gravity Columns.....	144
7	DAMAGE ANALYSIS	145
7.1	Introduction.....	145
7.2	Modified Park & Ang Damage Model.....	146
7.3	Fatigue Based Damage Model.....	148
7.4	Global Damage Model.....	150
8	ADDITIONAL FEATURES IN THE PROGRAM.....	151
8.1	Structural Response Snapshots	151
8.2	Structural Collapse State.....	152
8.3	Element Stress Resultants Ratios.....	152
8.4	Special Ground Motions for Nonlinear Dynamic Analysis	152
9	PROGRAM VERIFICATIONS AND EXAMPLES: CASE STUDIES	155
9.1	Component Testing: Full Scale Bridge Pier Under Reversed Cyclic Loading....	155
9.2	Subassemblage Testing: 1:2 Scale Three-Story Frame	159
9.3	Seismic Simulation: Ten-Story Model Structure	167
9.4	Seismic Response: 1:3 Scale model Lightly Reinforced Concrete Structure.....	174
9.5	Damage Analysis: Cypress Viaduct Collapse During the 1989 Loma Prieta Earthquake.....	179
9.6	Pushover Analysis: Building in the Vicinity of the New Madrid Zone.....	185
9.7	Response Snapshots: Eight story building in Los Angeles.....	192
9.8	Steel Structure: Evaluation of Seismic Performance of a 11 Story Steel Moment Frame Building during the Northridge Earthquake.....	201
9.9	Passive Energy Dissipation Devices: 1:3 Scale Model Retrofitted Using Different Types of Dampers.	209
9.9.1	Viscous Dampers.	210
9.9.2	Friction Dampers.	210
9.9.3	Hysteretic Dampers.....	211
9.10	Masonry Infill Panels: Experimental Test of a Masonry Infilled Frame	221
9.11	Deep Beam & Column Elements: Performance of IDARC2D.....	225
9.12	Nonlinear Dynamic Analysis of Structures with Rocking Columns	233
9.13	Remarks and Conclusions.....	238

TABLE OF CONTENTS (CONT'D)

SECTION	TITLE	PAGE
10	CONCLUSIONS AND RECOMMENDATIONS	239
10.1	Conclusions.....	239
10.2	Further Development Recommendations	243
11	REFERENCES	245
	APPENDIX A USER'S GUIDE.....	255
	APPENDIX B SAMPLE INPUT.....	319
	APPENDIX C DEFAULT SETTINGS IN FILE IDDEFN.FOR.....	387
	APPENDIX D IMPLEMENTATION OF POLYGONAL HYSTERETIC MODEL	389
	APPENDIX E FORMULATION FOR MASONRY INFILL FRAMES.....	419

LIST OF FIGURES

FIGURE	TITLE	PAGE
3.1	Structural Model	17
3.2	Typical structural element with rigid zones.....	18
3.3	Section detail for fiber model analysis.....	22
3.4	Stress-strain curve for unconfined concrete.....	23
3.5	Stress-strain curve for unconfined steel.....	23
3.6	Fiber model analysis for a shear wall	24
3.7	Curvature distribution along an element.....	30
3.8	Spread plasticity model for linear flexibility distribution.....	31
3.9	Spread plasticity model for uniform flexibility distribution.....	31
3.10	Concentrated plasticity model.....	36
3.11	Yield penetration lengths for fully inelastic members: (a) linear flexibility distribution; (b) uniform flexibility distribution	40
3.12	Modeling of moment releases in structural elements	41
4.1	Typical column element with degrees of freedom.....	44
4.2	Typical beam element with degrees of freedom	47
4.3	Deformation parameters.....	49
4.4	Macroscopic model for deep beam & column elements.....	50
4.5	Moment-Curvature relationship and edge shapes of rocking columns.....	54
4.6	Typical shear wall element with degrees of freedom	58
4.7	Edge column elements	60
4.8	Transverse beam elements	61
4.9	Modeling of discrete inelastic springs	63
4.10	Viscoelastic damper installation detail (from Aiken, 1990)	65
4.11	Viscous walls and hysteresis loops (from Miyazaki, 1992)	66
4.12	Sumitomo friction damper and installation detail (from Aiken, 1990)	69
4.13	Masonry infill panel: a) Frame subassembly, b) Compression struts	74
4.14	Constitutive model for masonry.....	75
4.15	Strength envelope for masonry infill panel.....	75
4.16	Sivaselvan-Reinhorn model for smooth hysteretic response of infill panels.....	76
5.1	Trilinear hysteretic model	82
5.2	Bilinear hysteretic model	82
5.3	Backbone curves	83
5.4	Types of cyclic behavior	83
5.5	Points and branches of the Polygonal Hysteretic Model (PHM)	85
5.6	Illustration of branch transition.....	86
5.7	Modeling of stiffness degradation for positive excursion (for negative excursion the “+” sign changes accordingly).....	88
5.8	Schematic representation of strength degradation in the PHM	89
5.9	Modeling of slip	90

LIST OF FIGURES (CONT'D)

FIGURE	TITLE	PAGE
5.10	Points and Branches of Nonlinear Elastic-Cyclic Model (NECM) with “negative stiffness”	91
5.11	Points and Branches of Nonlinear Elastic-Cyclic Model (NECM) without “negative stiffness”	92
5.12	Stepwise strength reduction model in “negative stiffness” range.....	93
5.13	Examples of hysteretic behavior modeled by the PHM.....	98
5.14	Two-spring model for non-degrading hysteretic behavior	99
5.15	Three-spring model for hysteretic behavior with slip.....	102
5.16	Gap-closing spring in parallel.....	104
5.17	Examples of Hysteretic behavior modeled by the SHM.....	106
5.18	Kelvin model: a) Damper behavior b) Linear stiffness component c) linear damping component.....	107
5.19	Maxwell model for damping devices.....	111
5.20	Stiffness and damping versus frequency in Maxwell model	112
5.21	Complex self centering hysteretic model.....	116
5.22	Slip lock element: a) Influence on hysteretic response b) Slip-lock function	120
5.23	Influence of varying the slip-lock parameters	123
5.24	Typical behavior of spring base isolator	125
6.1	Unbalanced force correction	138
6.2	Computation of shear due to P-delta effects	142
6.3	Gravity columns in the structural model for P-delta effects consideration	144
8.1	Sample of collapsed state response	153
9.1	Configuration and loading of full-scale bridge pier.....	157
9.2	Comparison of observed vs. computed response	158
9.4	Progressive damage history during cyclic testing.....	159
9.4	Details of half-scale model frame	162
9.5	Comparison of observed vs. simulated force-deformation response	163
9.6	Correlation of dissipated energy and global damage	164
9.7	Study of collapse mechanism.....	165
9.8	Progressive story level damage.....	166
9.9	Configuration and reinforcement details for model structure	169
9.10	Achieved table motions for seismic testing	170
9.11	Computed versus observed peak acceleration response	171
9.12	Computed versus observed peak displacement response.....	171
9.13	Comparison with other programs.....	172
9.14	Comparison with other programs (Moderate intensity: Inelastic)	173
9.15	Comparison with other programs (Highly inelastic)	174
9.16	Details of gravity-load-designed frame building	176
9.17	Comparison with other programs – low intensity (0.05g)	177

LIST OF FIGURES (CONT'D)

FIGURE	TITLE	PAGE
9.18	Comparison with other programs – moderate intensity (0.22g)	178
9.19	Structural configuration and reinforcement details of type B1 bent.....	181
9.20	IDARC model used in damage analysis	182
9.21	Displacement response of type B1 bent.....	183
9.22	Damage history of pedestal region	184
9.23	Plan view of structure	187
9.24	NS frame elevations.....	188
9.25	EW frame elevations.....	189
9.26	Overall pushover capacity curves for different lateral load distributions.....	190
9.27	Story pushover capacity curves for different lateral load distributions (NS direction).....	191
9.28	Typical floor plan of structure	195
9.29	Perspective view of lateral load resisting elements	196
9.30	Response spectra used for evaluation	197
9.31	Pushover capacity curve with significant response stages (longitudinal direction).....	198
9.32	Lateral displacements, longitudinal direction, for various earthquake intensities	199
9.33	Frame elevation at grid line "M"	204
9.34	Typical moment connection at column flange.....	205
9.35	Material model used for the study	206
9.36	Nonlinear story shear versus story drift (NS direction)	207
9.37	Comparison of observed damage and computed damage indices (Grid line "M")	208
9.38	Location of dampers and measuring devices	212
9.39	Comparison of experimental and analytical displacements with viscous dampers	213
9.40	Comparison of experimental and analytical accelerations with viscous dampers	214
9.41	Pushover response of structure with viscous dampers for simplified evaluation.....	215
9.42	Comparison of experimental and analytical displacements with friction dampers (El Centro 0.3g).....	216
9.43	Comparison of experimental and analytical accelerations with friction dampers (El Centro 0.3g).....	217
9.44	Pushover response of structure with friction dampers for simplified evaluation.....	218
9.45	Analytical displacement response with hysteretic dampers (El Centro 0.3g)	219
9.46	Analytical acceleration response with hysteretic dampers (El Centro 0.3g)	220
9.47	Masonry infilled frame test specimen.....	222
9.48	Boundary conditions of infilled frame subassembly	223
9.49	Idealized structural model for analysis	223

LIST OF FIGURES (CONT'D)

FIGURE	TITLE	PAGE
9.50	Comparison of experimental and analytical force-deformation response (Specimen 1)	224
9.51	Frame model consisted of deep elements	227
9.52	Cases for performance of deep element.....	227
9.53	Moment-curvature and shear force-strain relationship of each cases.....	228
9.54	Simulated results of original and deep frames.....	229
9.55	Failure state and damage index.....	232
9.68	Quasi-static cyclic test of rocking columns	235
9.69	Model structure (Bracci et al., 1992) and alternative for weakening.....	236
9.70	Response histories of floor acceleration in conventional and weakened structures (White noise 0.3g)	236
9.71	Peak response of conventional and alternative structures: (a) story acceleration; (b) story shear; (c) floor displacement; and (d) story drift	237
A-1	Frame Discretization and Nodal Identification.....	256
A-2	Floor Heights and Nodal Weights.....	260
A-3	Stress Curve for Unconfined Concrete	262
A-4	Stress Curve for Reinforcing Bars	262
A-5 (a)	Qualitative View of Effects of Degrading Parameters on Hysteretic Behavior – Multilinear Model	266
A-5 (b)	Qualitative View of Effects of Degrading Parameters on Hysteretic Behavior – Smooth Model	267
A-6	Rectangular Columns Input Details	270
A-7	Circular column Input Details.....	271
A-8	Notation for User Input Trilinear Envelopes	275
A-9	P-M interaction diagram	275
A-10	Notation for User Input Trilinear Envelopes for rocking column	278
A-11	Input Details for Beam-Slab Sections.....	281
A-12	Typical Input Details for Shear Wall Sections	286
A-13	Shear Wall and Edge Column Details	287
A-14	Transverse Beam Input	292
A-15.	Element Connectivity for Sample Structure	300
A-16	Specification of Discrete Inelastic Springs	302
A-17	Specification of Moment Release	303
D.1	Overall flow of PHM module	389
D.2	Flowchart for Subroutine CONTROL1	390
D.3	Flowchart for Subroutine CONTROL2	391
D.4	Flowchart for Subroutine CONTROL3	392
D.5	Explanation for Rules which change Branches from 2 to 21 and 3 to 20.....	393

LIST OF TABLES

TABLE	TITLE	PAGE
4.1	Total stiffness of deep elements at various states	53
7.1	Interpretation of overall damage index (Park et al., 1986)	148
9.1	Element stress ratios for typical beams.....	200
9.2	Structural response, longitudinal direction, for various earthquake intensities ...	200
A-1.	Typical Range of Values for Hysteretic Parameters.....	265
C.1	Default Maximum Settings in File IDDEFN.FOR	387
D.1	Subroutines and their functions	394
D.2	Variables Governing PHM	395
D.3	Point Formulas	397
D.4	Map of Branch Connectivity.....	403
D.5	Starting and ending points of branches.....	406
D.6	Rules for Change of Branch.....	407
D.7	Variables governing nonlinear elastic-cyclic model (NECM).....	414
D.8	Definition of benchmark points in NECM (Fig. 5.10).....	415
D.9	Map of Branch Connectivity.....	416
D.10	Starting and ending points of branches.....	417
D.11	Rules of Branch Transition	417

SECTION 1

INTRODUCTION

Significant research has been carried out in an effort to understand the behavior of building structures subjected to earthquake motions. Due to the inherent complexities that buildings have, often, research has focused on understanding element behavior through component testing. The conclusions and models derived from these studies must later be integrated so that the response of the whole structure may be captured. The well known computer program DRAIN-2D (Kaanan and Powell, 1973) was introduced in 1973 with the state of the art knowledge at that time in an attempt to capture the structural response. The program has recently been updated and the new version is called DRAIN-2DX (Allahabadi and Powell, 1988).

A number of programs for the nonlinear dynamic analysis of building structures have been introduced since then. Among them, SARCF (Chung et al., 1988; Gomez et al., 1990), IDARC (Park et al., 1987; Kunnath et al., 1992) and ANSR (Oughourlian and Powell, 1982) became widely used by the research community. The computer program IDARC has been conceived, since its first release, as a platform for nonlinear structural analysis in which various aspects of concrete behavior could be modeled, tested and improved upon. Throughout the various releases of IDARC, program developments and enhancements have been based primarily on the need to link experimental research and analytical developments.

Structural design engineers have been aware of the inherent limitations that widely used elastic analysis have when trying to calculate the response of a building designed to respond inelastically. However, due to the computational effort required to perform a nonlinear analysis, the fact that building codes are mostly concerned with elastic analysis, the need for a more precise characterization of the input motion, etc., have forced structural engineers to continue using elastic analysis programs.

The introduction of new protective systems, such as base isolators and damper elements, require the use of nonlinear dynamic analysis programs for their design. To bridge this gap, commercial software for elastic analysis, such as ETABS (Habibullah, 1995) and SAP (Wilson, 1995), have incorporated nonlinear elements to model the behavior of such devices, allowing design engineers already familiar with those programs to easily incorporate the protective devices in the response of the structure. However, the structure itself is still modeled in the elastic range, therefore, not able to capture the inelastic response of structures. This drawback may not be significant for new buildings, however, retrofitted structures may considerably deviate from an elastic response.

The new release of IDARC incorporates the results from recent experimental testing on reinforced concrete components and structures, as well as structural steel structures, that have lead to enhancements in modeling using macromodels with new distributed plasticity models, new hysteretic models, and modifications to the combined model for shear-flexure capacity of members. IDARC is now enhanced to capture with greater accuracy the response of reinforced concrete and structural steel elements.

Furthermore, in parallel with an experimental program to study the response of buildings with damper elements for seismic protection, new mathematical models for such elements were incorporated and verified in the program. IDARC is now capable of accurately predicting the response of inelastic multistory buildings with viscoelastic, friction and hysteretic damper elements.

Moreover, combined with an experimental program, and a loss assessment program in a metropolitan area in the vicinity of the New Madrid zone, a model for infill panel elements was incorporated and tested. This model may be used to study the response of masonry buildings, commonly used as low to medium rise structures in metropolitan areas. IDARC is now capable of modeling buildings with masonry walls, or other type of infill panels.

In addition, the new method for seismic evaluation originally proposed in the ATC-

33 (1995) using the results from lateral pushover analysis, was already incorporated in previous versions of the program. However, in conjunction with an analytical program to estimate the inelastic response of structures, an extended and more realistic set of options to carry out the pushover analysis have been incorporated. Furthermore, the need to better characterize the structural performance of a building during a seismic event lead to an analytical investigation to develop a damage model from basic physical considerations. The new model, referred to as fatigue based damage model, developed by Reinhorn and Valles (1995) was also incorporated in the program, along with a global damage model, and the model by Park and Ang (1984) that was introduced in the first release of IDARC, and is now a benchmark damage quantification index. IDARC now offers a broader range of pushover and damage indices derived from strong physical considerations.

Finally, most of the program routines, internal variables and program structure have been checked and optimized to improve the performance, and considerably reduce execution time. In addition, the users manual was revised and restructured to facilitate the input data preparation. IDARC is now more efficient and user friendly.

This report summarizes the program modeling techniques used, and provides references for each of the broad topics considered. Appendix A has the user's manual for the program. Appendix B includes the sample input files described in Section 9. Appendix C summaries the maximum default numbers limited in the new version. The default numbers can be increased by User in the source file (iddefn.for). Appendix D addresses all variables used in the hysteretic rules.

SECTION 2

THEORY AND BACKGROUND

2.1 Nonlinear Structural Analysis Software

Building structures are often designed using results from elastic analyses, although inelastic behavior is expected during earthquakes. To estimate the actual response of structures when some of the elements behave inelastically, nonlinear structural analysis programs have been introduced. The well known computer program DRAIN-2D (Kaanan and Powell, 1973) was introduced in the early 1970's. The program included the state of the art knowledge at the time. Since then the program was not considerably modified in its structure, until DRAIN-2DX (Allahabadi and Powell, 1995) was introduced. Nevertheless, the new program has some limitations regarding the plasticity and flexibility rules.

Since then, a number of programs for nonlinear analysis of structures have been introduced. Among them SARCF (Chung et al., 1988; Gómez et al., 1990), IDARC (Park et al., 1987; Kunnath et al., 1992, Valles et al., 1996), ANSR (Oughourlian and Powell, 1982), DRAIN-3DX (Prakash et al., 1994), PERFORM3D (Computers and Structures, Inc., Ver. 4.0.3, 2007), OpenSees (Mazzoni et al., Ver. 2.0, 2008), and INDYAS (Elnashai et al., 2000) became widely used by the research community.

2.2 IDARC Computer Program Series

The computer program IDARC was conceived as a platform for nonlinear structural analysis in which various aspects of concrete behavior can be modeled, tested and improved upon. Program development and enhancements have been primarily to link experimental research and analytical developments.

The computer program IDARC was introduced in 1987 as a two-dimensional analysis program to study the non-linear response of multistory reinforced concrete buildings. The original program released included the following structural element types:

- a) Column Elements
- b) Beam Elements
- c) Shear Wall Elements
- d) Edge Column Elements
- e) Transverse Beam Elements

Column elements were modeled considering macromodels with inelastic flexural deformations, and elastic shear and axial deformations. Beam elements were modeled using a nonlinear flexural stiffness model with linear elastic shear deformations considered. Shear wall included inelastic shear and bending deformations, with an uncoupled elastic axial component. Edge column elements were introduced considering only inelastic axial deformations. Transverse beam elements, that have an effect on the rotational deformation of the shear walls or beams to which they are connected, in an attempt to consider 3D interactions, were modeled using elastic linear and rotational springs.

One of the significant features incorporated in the program, used to implement inelastic behavior in the macromodels, is the distributed flexibility model that replaced the commonly used hinge model developed for steel frames. The hinge model is not suitable for reinforced concrete elements and many other structural materials since the inelastic deformation is distributed along the member rather than being concentrated at critical sections (Park et al., 1987). To trace the hysteretic response of a section, a three parameter model was developed. Through the combination of three basic parameters and a trilinear polygonal skeleton, stiffness degradation, strength deterioration and pinching response can be modeled.

The original version of the program included the damage model developed by Park

and Ang (1984) to provide a measure of the accumulated damage sustained by the components of the structure, by each story level, and the entire building. This damage index included the ratio of the maximum to ultimate deformations, as well as the ratio of the maximum hysteretic energy dissipated to the maximum monotonic energy, therefore capturing both components of damage.

The original release of the program consisted of three parts (Park et al., 1987):

- a) System identification: static analysis to determine component properties, the ultimate failure mode of the building, and the initial stresses due to gravity loads before dynamic analysis.
- b) Dynamic response analysis: step by step inelastic dynamic analysis.
- c) Substructure analysis and damage analysis: analysis of selected substructures, and comprehensive damage evaluation.

Later versions of the program included:

- a) The addition of a fiber model routine to automatically calculate the envelope curve of column, beam, and shear wall elements.
- b) A quasi-static, or quasi-dynamic, analysis module for comparisons with experimental tests.
- c) Addition of P-Delta effects in the static and dynamic analysis.

The program version 4.0 provided a number of enhancements including:

- a) Viscoelastic, friction, and hysteretic damper macro elements.
- b) Macro model for infill panel elements.
- c) Spread plasticity and yield penetration
- d) New Hysteresis modules.
- e) New Damage indicators.
- f) New “Pushover” options.
- g) Response snapshots during analysis.
- h) Proportional damping options.

- i) Reprogrammed for improved efficiency.
- j) New case studies for program validation.

The major highlights of each improvement are briefly described below.

a) Viscoelastic, friction and hysteretic damper macro elements

Three main types of supplemental damper elements were included in the program. Damper elements are linked to the relative motion of two adjacent floors in the structure. Viscoelastic damper elements are modeled using either a Kelvin-Voight or a Maxwell model, depending on the characteristics of the dampers. Friction and hysteretic dampers are included using the Sivaselvan and Reinhorn's (similar to Bouc-Wen) smooth hysteretic model. All models are capable of capturing the response of the dampers during dynamic and quasi-static analyses.

An equivalent dynamic stiffness is used for the viscoelastic elements during quasistatic and pushover analysis, while the Sivaselvan and Reinhorn (1999) model was reformulated in terms of deformation increments to remove the time dependency in the original formulation. Furthermore, the instantaneous apparent dynamic stiffness of the damper elements is included in the global building stiffness matrix before the eigenvalue analysis takes place. Therefore, the eigenvalue analysis automatically incorporates the actual instantaneous contribution from the damper elements, which is often only accounted for using a user specified equivalent constant stiffness for these elements in other nonlinear analysis programs.

These new element types in the program allow the user to study the response of nonlinear structures with a wide variety of supplemental damping devices. Commercially available programs such as ETABS Version 6 (Habibullah, 1995) and SAP2000 (Computer and Structures, Inc., Ver. 12, 2008) are capable of capturing the response of some supplemental damping devices, but are incapable of capturing the nonlinear response of the building simultaneously. This shortcoming may be unimportant for the design of new structures that can be proportioned to remain elastic during the design

earthquake. However, when existing buildings are retrofitted using supplemental damping devices, often the new design will still allow some level of inelastic response in the structural elements in order to make the retrofit economically viable. Under such conditions, an analysis considering the inelastic response of in the structural elements must be performed to estimate the actual response of the retrofitted structure.

b) Macro model for infill panel elements

A new element was introduced in IDARC to capture the contribution of infill panels to the lateral load resistance of the structure. The hysteretic response of the infill element is captured using a smooth hysteretic model based on the Sivaselvan and Reinhorn model. The smooth hysteretic model includes stiffness decay, strength deterioration, and pinching response. An important improvement of the implemented model is that strength deterioration is related to a fatigue damage index of the panel element.

The infill panel element was implemented so that the modeling parameters could be easily changed to capture different types of hysteretic loops. Masonry infill walls can be modeled using the infill panel element. Provisions in the program were made so that if a masonry infill wall is used, the program will automatically calculate the hysteretic parameters based on geometric and material considerations. Other type of panel elements, structural or nonstructural, can be modeled using user defined parameters.

c) Spread plasticity and yield penetration

The spread plasticity model in the original release of the program was reformulated to enhance numerical precision and computation efficiency. The spread plasticity formulation includes the effect of shear distortions in the elements. The revised formulation can now handle flexural or shear failures with the possibility of numerical overflow eliminated. This effort is part of a larger project to model element collapse (loss) during analysis.

In addition to the reformulation of the spread plasticity model, yield penetration

rules were introduced to allow for varying plastic length zones. The formulation can capture the change in the plasticized length under single or double curvature conditions. The penetration length is updated at each step in the analysis as a function of the instantaneous moment diagram in the element, but the penetration length is never allowed to become smaller than the previous maximum.

d) New Hysteretic Models

The original IDARC program used the three parameter model to trace the hysteretic response of structural elements. The piece-wise linear three parameter model that included stiffness degradation, strength deterioration and slip was introduced to model the response of reinforced concrete structural elements. With a variation in the hysteretic parameters, and in the monotonic characteristic points, the user could simulate other hysteretic shapes, such as the one observed in steel structures, or other materials and systems.

A new set of routines were introduced to account for different hysteretic loops: steel and bilinear hysteresis. The polygonal model was redeveloped to identify branches and transitions in a clear fashion (Sivaselvan and Reinhorn, 1999). The structure of the program was modified to facilitate the addition of new hysteretic routines that can be developed in the future, or by other researchers. A new smooth hysteretic model with degradation of stiffness, strength and slip was developed (Sivaselvan and Reinhorn, 2000) and introduced in the program.

e) New Damage indicators

The original release of IDARC incorporated damage qualifications for the building, the building stories, and the structural elements based on the damage index proposed by Park et al. (1984). Since then, the Park and Ang damage model has become a benchmark damage qualification model. A new damage index has been developed (Reinhorn and Valles, 1995) based on basic principles and low cycle fatigue considerations.

The new damage quantification index, fatigue based damage index, was

incorporated in the newer releases of IDARC. The original Park and Ang damage model can be derived after simplifications of the fatigue based damage model. In addition, provisions in the program were made so that the user can request printing of the variation of the fundamental period of the structure as the analysis progresses.

The new fatigue based damage index, the Park and Ang damage model, and the history of the variation of the fundamental frequency of the structure provides the user with a more accurate description of the building performance for damage quantification. The extended damage index options provide three scope levels for quantification: building, story and element damage.

f) New “Pushover” options

“Pushover” (nonlinear inelastic) analyses are used to determine the force-deformation response characteristics of a structure. Using the results from this analysis, the actual nonlinear dynamic response of the structure can be estimated with suitable initial conditions and specific parameters of a problem (Valles et al., 1996). Furthermore, a new set of dynamic evaluation procedures (Reinhorn, 1997), as suggested also in the ATC-33 (1995), utilize the results obtained with pushover analyses.

A number of different options for the pushover analysis were added to the program: displacement control, user defined force control distribution, a generalized power distribution, and a modal adaptive lateral force distribution. These options allow a more realistic force distribution to be used in the pushover analysis. The generalized power distribution is also suggested in the ATC-33 (1995) to determine the load distribution as a function of the fundamental period of the structure. The modal adaptive force distribution (developed by Reinhorn, 1997) is able to capture the changes in the lateral load distribution as the building responds in the inelastic range.

g) Response snapshots during analysis

One of the new features of the program is that the user can request a series of response snapshots during the analysis. The response snapshots provide the user with

displacement profile, element stress ratios, collapse states, damage index states, and dynamic characteristics (eigenvalues and eigenvectors) of the building at an instant during the analysis.

The instant where response snapshots are taken can be specified in terms of a desired threshold in overall shear or drift levels. By default, the program can report snapshots at the end of the analysis, and when a column, beam or shear wall cracks, yields or fails. Response snapshots provide the user with the instantaneous building state, which is also required by the ATC-33 recommendations for seismic evaluation of existing buildings.

h) Proportional damping options

In the new version of IDARC, the damping matrix can be specified to be either Rayleigh or simply stiffness proportional, besides the mass proportional option available in the earlier versions of the program. Proportionality coefficients are calculated internally by the program using the first mode, or the first two modes in the case of Rayleigh damping.

i) Reprogrammed for improved efficiency

Most of the solution routines, including the eigenvalue routine, the shear calculation, the spread plasticity and yield penetration routines, and the matrix condensation routines were revised and reprogrammed to improve computational efficiency in the analysis. With these modifications, the program can readily be executed in a personal computer.

j) New case studies for program validation

Verification examples have been included to highlight the program capabilities and features, as well as to validate whenever possible, numerical models with experimental results. The case studies will also help new users of the program to get familiar with IDARC capabilities and input formats.

The program version 4.5 to version 5.5 enhanced through developing as following:

- a) Concentrated plasticity models.
- b) Uniform flexibility distribution.
- c) New Hysteretic modules for improved vertex oriented model.
- d) New Hysteretic modules for smooth hysteretic model.

2.3 Program Enhancements

For the latest release of the program, Versions 6.0 to 7.0, a number of additional enhancements are provided:

- a) New Deep Beam and Column Elements.
- b) New Rocking Column Model.
- c) New Nonlinear-Elastic-Cyclic Model.
- d) New “Case Studies” for program validation.
- e) User group and internet site support.

Several features such as multi-infill panels modeling, sign convention of brace systems, and nonlinear spring model from the previous version were corrected. The major highlights of each improvement are briefly described below.

a) New Deep Beam & Column Elements

The deep elements were developed by adding shear stiffness and hysteretic effect into the conventional beam and column elements. When the elements are reached to ultimate shear strength or strain, the elements are failed. The response snapshots of the shear failure state is shown in out-file during analysis. This development can be used to simulate a perforated shear wall with regular and irregular openings.

b) New Rocking Column Model

The rocking column is similar to a double-hinged column and does not develop a tensile resistance at the connection. However, the column provides a lateral resisting depending on an external axial load. The rocking column is used for weakening structures which reduce its story or global strength, to obtain better global behavior.

c) New Nonlinear-Elastic-Cyclic Model (NECM)

When structural element returns to the original position without loosing strength and stiffness capacities even after its plastic behavior, the Nonlinear-Elastic-Cyclic Model (NECM) is used to simulate the structural element behavior. This model can be used for beam, column, and shear wall elements also.

d) New case studies for program validation

Two case studies have been introduced: i) Verification example of “deep” elements and ii) Use of rocking columns for weakened structures. The case studies will help new users of the program to become familiar with IDARC capabilities and input formats.

e) Mail user group and internet site

Started in 1995, the user group for the program has been reorganized to allow for questions, suggestions or comments related to the program. The E-mail address is:

idarc@eng.buffalo.edu

A world-wide web site in the internet has been created where news, updates, comments and current developments are posted. The world-wide web address is:

<http://civil.eng.buffalo.edu/idarc/>

SECTION 3

FORMULATIONS OF STRUCTURAL ELEMENT MODELS

3.1 Introduction

The program was developed assuming that floor diaphragms behave as rigid horizontal links, therefore, only one horizontal degree of freedom is required per floor. This approach greatly reduces the total computational effort. Therefore, the building is modeled as a series of plane frames linked by a rigid horizontal diaphragm. Each frame is in the same vertical plane, and no torsional effects are considered. Since the floors are considered infinitely rigid, identical frames can be simply lumped together, and the stiffness contributions of each typical frame factored by the number of duplicate equal frames. Input is only required for each of the typical frames.

The computer program IDARC integrates different structural element models in the global stiffness matrix of the system, or treats them as loads in a pseudo-force formulation. Such arrangement allows for new element modules to be easily added to the global structure of the program.

Version 7.0 of IDARC includes the following types of structural elements:

- a) Column elements
- b) Beam elements
- c) Deep beam and column elements
- d) Rocking column elements
- e) Shear wall elements
- f) Edge column elements
- g) Transverse beam elements
- h) Rotational spring elements
- i) Visco-elastic damper elements

- j) Friction damper elements
- k) Hysteretic damper elements
- l) Infill panel elements
- m) Element moment releases

Figure 3.1 schematically shows a building with some of the element types available in IDARC Version 7.0. Each of the element types are discussed below.

3.2 Stiffness Formulation for Common Structural Elements

Most structural elements, i.e. columns, beams and shear walls, are modeled using the same basic macro formulation based on a flexibility method. Flexural, shear and axial deformations can be considered in the general structural macro element, although axial deformations are neglected in the beam elements. Figures 3.2 show a typical structural element with rigid zones. Flexural and shear components in the deformation are coupled in a “spread plasticity” formulation, as discussed in Section 3.4, and any of the following hysteretic models can be used for both the flexural and shear springs:

- a) Trilinear model.
- b) Bilinear model.
- c) Vertex oriented model.
- d) Nonlinear elastic-cyclic model
- e) Smooth hysteretic model.

Axial deformations are modeled using a linear elastic spring element uncoupled to the flexural and shear spring elements.

Rotations and moments at the face of the element are related by the basic element stiffness matrix, according to:

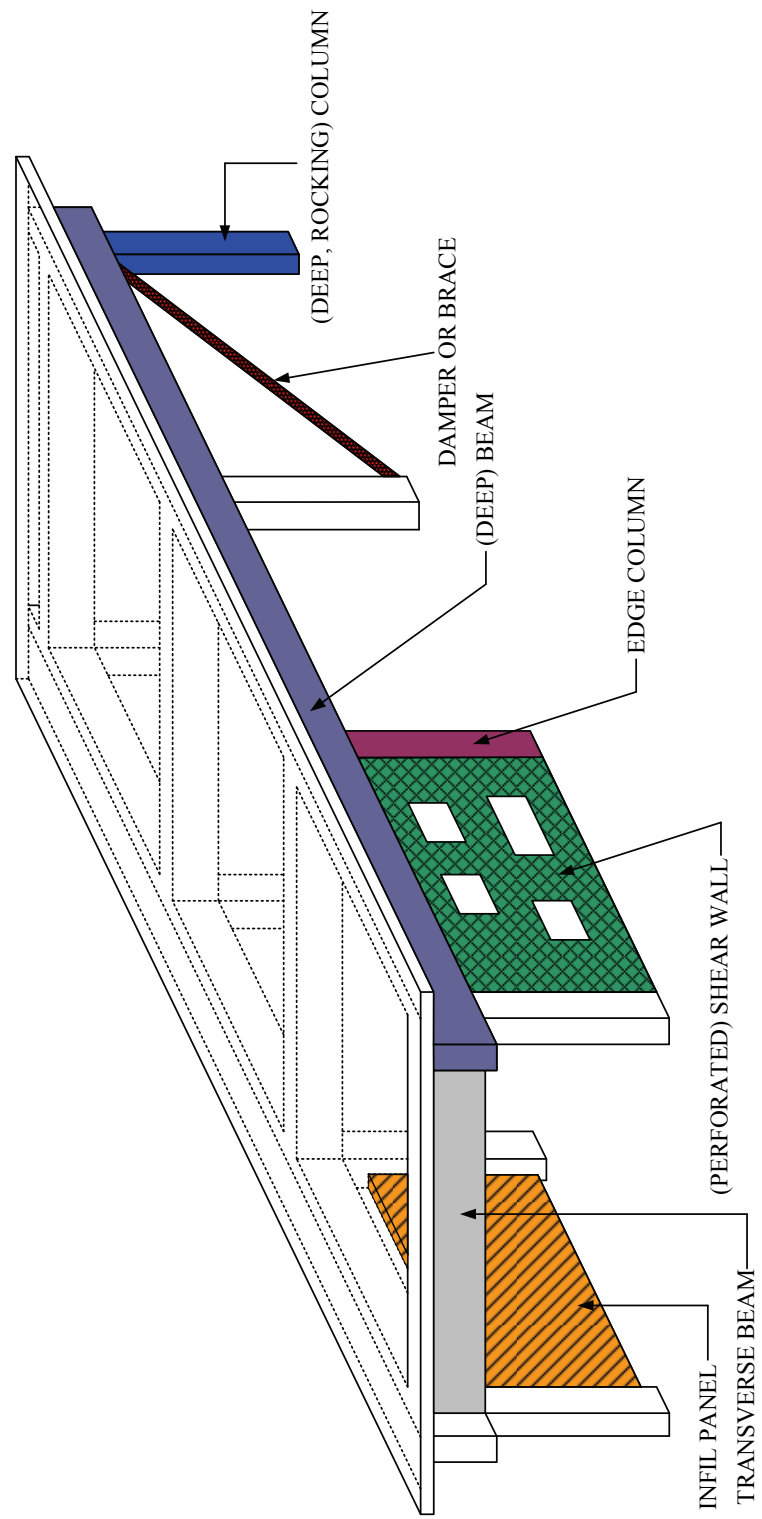


Fig. 3.1 Structural Model

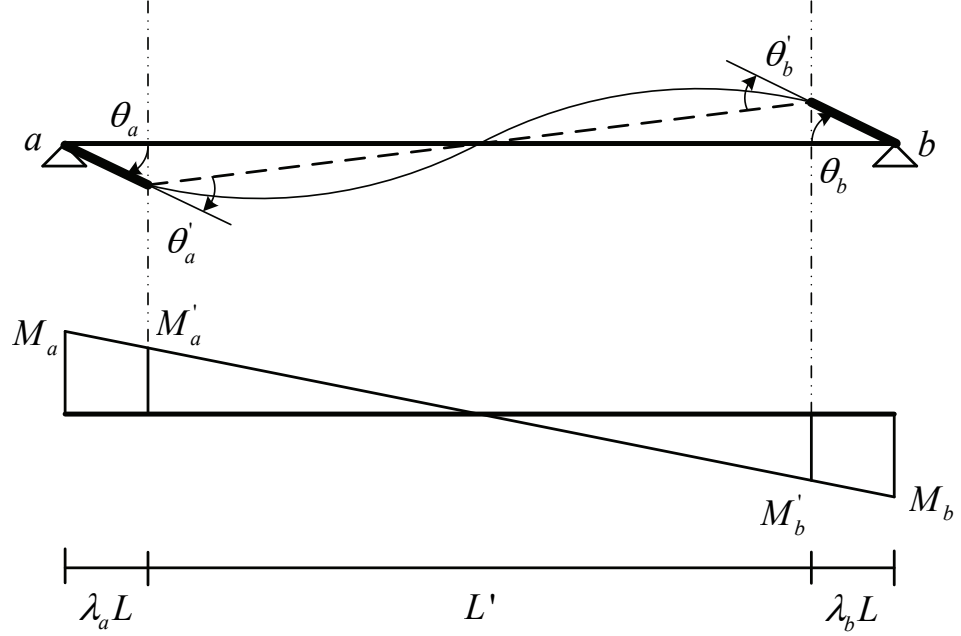


Fig. 3.2 Typical structural element with rigid zones

$$\begin{Bmatrix} M'_a \\ M'_b \end{Bmatrix} = [\mathbf{K}'] \begin{Bmatrix} \theta'_a \\ \theta'_b \end{Bmatrix} \quad (3.1)$$

where M'_a and M'_b are the moments at the face of the structural element; θ'_a and θ'_b are the rotations at the face of the element; and $[\mathbf{K}']$ is the basic stiffness matrix of the element based on a flexibility formulation including shear and flexural deformations, calculated using the spread or concentrated plasticity models described in Sections 3.4 and 3.5:

$$[\mathbf{K}'] = \begin{bmatrix} k_{aa} & k_{ab} \\ k_{ba} & k_{bb} \end{bmatrix} \quad (3.2)$$

where:

$$k_{aa} = \frac{12EI_0EI_aEI_b}{D_{et}L'} \left(f'_{bb}GA_zL'^2 + 12EI_0EI_aEI_b \right) \quad (a)$$

$$k_{ab} = k_{ba} = \frac{-12EI_0EI_aEI_b}{D_{et}L'} \left(f'_{ab}GA_zL'^2 + 12EI_0EI_aEI_b \right) \quad (b) \quad (3.3)$$

$$k_{bb} = \frac{12EI_0EI_aEI_b}{D_{et}L'} \left(f'_{aa}GA_zL'^2 + 12EI_0EI_aEI_b \right) \quad \text{---(c)}$$

with EI_0 being the elastic rotational stiffness; EI_a and EI_b the tangent rotational stiffness at the ends of the element; GA_z the shear stiffness; L' the length of the member; and the rest of the parameters declared from the flexibility method are described in Section 3.4.

Column and beam elements can include a rigid length zone to simulate the increased stiffness of the element at the joint, or in the connections with shear walls. The effect of the rigid length zone is negligible in typical shear wall elements. The user can specify the length of the rigid length zones depending on the dimensions of the connecting elements. From geometry, the relationship between rotations and moments at the face of the element, and these quantities at the nodes is expressed by the following transformation:

$$\begin{Bmatrix} M_a \\ M_b \end{Bmatrix} = [\tilde{\mathbf{L}}]^t \begin{Bmatrix} M'_a \\ M'_b \end{Bmatrix} \quad \text{---(a)} \quad (3.4)$$

$$\begin{Bmatrix} \theta'_a \\ \theta'_b \end{Bmatrix} = [\tilde{\mathbf{L}}]^t \begin{Bmatrix} \theta_a \\ \theta_b \end{Bmatrix} \quad \text{---(b)}$$

where:

$$[\tilde{\mathbf{L}}] = \frac{1}{1-\lambda_a - \lambda_b} \begin{bmatrix} 1-\lambda_b & \lambda_a \\ \lambda_b & 1-\lambda_a \end{bmatrix} \quad (3.5)$$

where λ_a and λ_b are the proportions of rigid zone in the element, as shown in Fig. 3.2. Combining the equations, the basic equation relating moments and rotations at the element nodes is:

$$\begin{Bmatrix} M_a \\ M_b \end{Bmatrix} = [\mathbf{K}_s] \begin{Bmatrix} \theta_a \\ \theta_b \end{Bmatrix} \quad (3.6)$$

where:

$$[\mathbf{K}_s] = [\mathbf{L}] [\mathbf{K}^t] [\mathbf{L}]^t \quad (3.7)$$

Considering force equilibrium of all the forces perpendicular to the axis of the element:

$$\begin{Bmatrix} X_a \\ M_a \\ X_b \\ M_b \end{Bmatrix} = [\mathbf{R}_e] \begin{Bmatrix} M_a \\ M_b \end{Bmatrix} \quad \text{---(a)} \quad (3.8)$$

$$\begin{Bmatrix} \theta_a \\ \theta_b \end{Bmatrix} = [\mathbf{R}_e]^t \begin{Bmatrix} u_a \\ u_b \\ \theta_a \\ \theta_b \end{Bmatrix} \quad \text{---(b)}$$

where X_a and X_b are the shear forces at ends “a” and “b”, respectively; and:

$$[\mathbf{R}_e] = \begin{Bmatrix} 1/L & 1/L \\ 1 & 0 \\ -1/L & -1/L \\ 0 & 1 \end{Bmatrix} \quad (3.9)$$

where L is the length of the member including rigid zone. Using Eqs. 3.8 and 3.9, Equation 3.6 can also be rewritten as:

$$\begin{Bmatrix} X_a \\ M_a \\ X_b \\ M_b \end{Bmatrix} = [\mathbf{K}_e] \begin{Bmatrix} u_a \\ \theta_a \\ u_b \\ \theta_b \end{Bmatrix} \quad (3.10)$$

where:

$$[\mathbf{K}_e] = [\mathbf{R}_e] [\mathbf{K}_s] [\mathbf{R}_e]^t \quad (3.11)$$

is the element stiffness matrix relating displacements and forces at the element joints, while $[\mathbf{K}_s]$ is the stiffness matrix relating rotations and moments at the element flexible ends, as given by Eq. 3.7.

Bending moments and axial forces are considered uncoupled in the formulation, hence, the force deformation relation for the resulting elastic axial stiffness is considered as follows:

$$\begin{Bmatrix} Y_a \\ Y_b \end{Bmatrix} = \frac{EA}{L'} \begin{bmatrix} 1 & -1 \\ -1 & 1 \end{bmatrix} \begin{Bmatrix} v_a \\ v_b \end{Bmatrix} \quad (3.12)$$

where Y_a and Y_b are the axial forces in the element at ends “a” and “b”, respectively; v_a and v_b are the vertical displacements at ends “a” and “b” of the structural element, respectively; and. EA/L' is the axial stiffness of the element.

The element basic stiffness matrix $[\mathbf{K}']$ is constantly varied throughout the analysis according to the formulation for the spread plasticity model presented in Section 3.4, and the hysteretic model selected. Depending on the hysteretic model considered, some characteristic values for the response of the element are required, namely moment-curvature or shear-shear distortion. For reinforced concrete elements, the user may select to specify the section dimensions and reinforcement, and use the fiber model to calculate the properties.

3.3 Fiber Model for Common Structural Elements

The moment curvature envelope describes the changes in the force capacity with deformation during a nonlinear analysis. Therefore, the moment-curvature envelopes for columns, beams and shear walls form an essential part of the analysis. The program IDARC now provides an option for users to input their own cross-section properties

directly, and the moment-curvature is computed internally based on a fiber model. Figure 3.3 shows a typical rectangular section subjected to a combination of axial load and moment. The procedure outlined below is applicable to all types of cross-sections: T-beams, shear walls, columns sections, etc. Some simplifying assumptions are made in the analysis and summarized here:

- a) Plane sections remain plain after bending
- b) Tensile strength of concrete is ignored beyond the tensile cracking capacity
- c) The effect of bond-slip between reinforcement and concrete is ignored
- d) The difference in properties between confined core and cover is ignored
- e) Stress strain properties for concrete and steel are shown in Figs. 3.4 and 3.5
- f) The axial force applied to the section is constant.

The procedure outlined below works with only a few iterations required to obtain convergence. The program IDARC uses this procedure to set up moment-curvature envelopes for columns (rectangular or circular), beams (rectangular or T-sections) and shear walls (with or without edge columns). Shear walls may be irregular and include “U” or “L” shaped core walls.

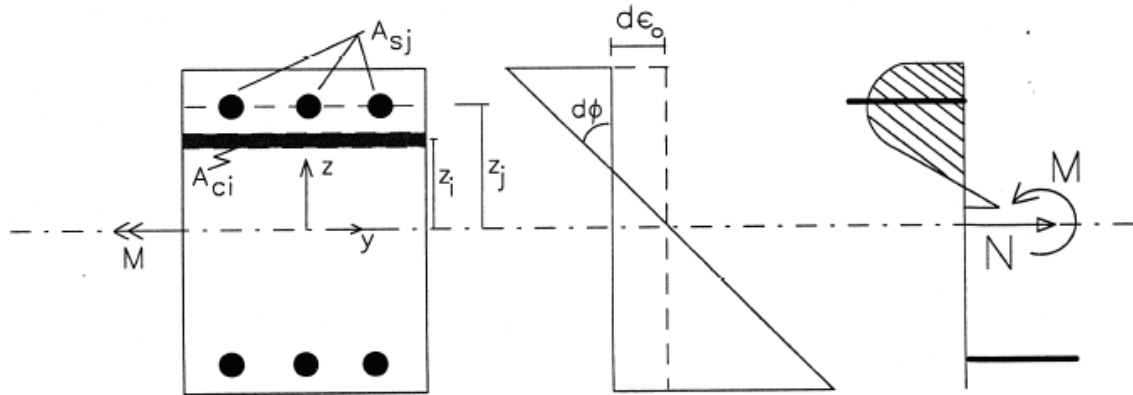


Fig. 3.3 Section detail for fiber model analysis

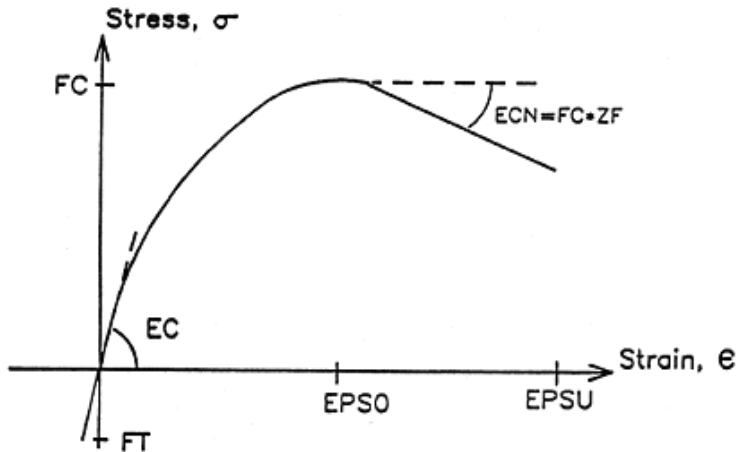


Fig. 3.4 Stress-strain curve for unconfined concrete

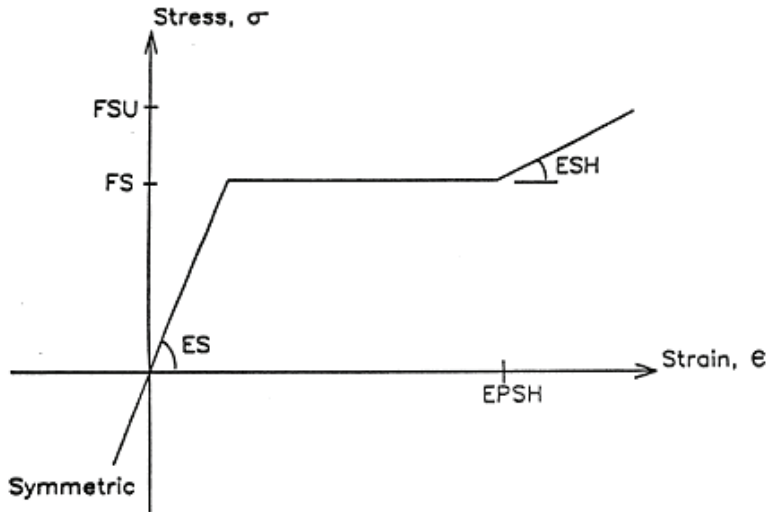


Fig. 3.5 Stress-strain curve for unconfined steel

3.3.1 Moment-Curvature Envelope Computation

The fiber element procedure used was outlined by Kunnath et al. (1992a), adapted from Mander (1984). The moment-curvature analysis is carried out on the cross-section by dividing the concrete area into a number of strips or fibers. The section is subjected to increments of curvature and the strain distribution is obtained from compatibility and equilibrium considerations. Steel areas and their respective locations are identified separately. The strain at any section is given by (see Fig. 3.3 and 3.6):

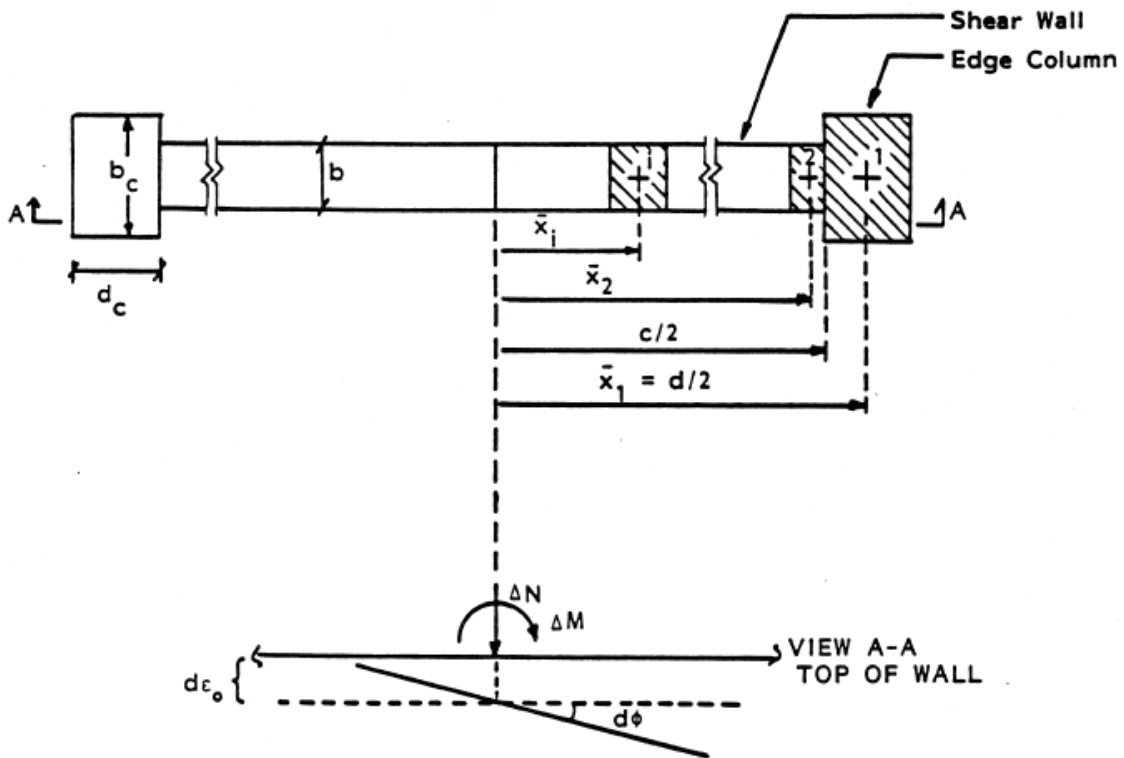


Fig. 3.6 Fiber model analysis for a shear wall

$$\varepsilon(z) = \varepsilon_0 + z\phi \quad (3.13)$$

where ε_0 is the centroidal strain, z is the distance from the reference axis, and ϕ is the curvature of the cross-section. The resulting axial load and moment in the cross section can be computed from:

$$N = \int E\varepsilon dA \quad (a) \quad (3.14)$$

$$M = \int Ez\varepsilon dA \quad (b)$$

where N is the axial force; M the flexural moment; E is the elastic modulus of the corresponding concrete or steel fiber; ε is the strain in the fiber; and z is the distance to the fiber from the reference axis. The axial load N should be equal to the applied load N_0 at all cases. This dictates a certain distribution of the axial strains $\varepsilon(z)$. Since the stress-strain relation is nonlinear and the axial strain increment $d\varepsilon$ cannot be

computed directly for a given value of the axial load and moment, it is necessary to develop an iterative procedure for the moment-curvature analysis. This is done through an iterative fiber analysis as follows.

Substituting Eq. 3.13 into Eq. 3.14 and replacing the integral by a finite summation over the discretized fibers, the following expression is obtained for any incremental step k of strain at neutral axis $\Delta\epsilon_0$ and curvature $\Delta\phi$

$$\begin{Bmatrix} \Delta N \\ \Delta M \end{Bmatrix}_k = \begin{bmatrix} k_A(\epsilon_{0,k}, \phi_k) & k_z(\epsilon_{0,k}, \phi_k) \\ k_z(\epsilon_{0,k}, \phi_k) & k_{zz}(\epsilon_{0,k}, \phi_k) \end{bmatrix}_k \begin{Bmatrix} \Delta\epsilon_0 \\ \Delta\phi \end{Bmatrix}_k \quad (3.15)$$

where:

$$k_A(\epsilon_{0,k}, \phi_k) = \sum_{i=1}^{NCC} E_{ci}(\epsilon_{0,k}, \phi_k) A_{ci} + \sum_{j=1}^{NSS} E_{sj}(\epsilon_{0,k}, \phi_k) A_{sj} \quad (a)$$

$$k_z(\epsilon_{0,k}, \phi_k) = \sum_{i=1}^{NCC} E_{ci}(\epsilon_{0,k}, \phi_k) A_{ci} z_i + \sum_{j=1}^{NSS} E_{sj}(\epsilon_{0,k}, \phi_k) A_{sj} z_j \quad (b) \quad (3.16)$$

$$k_{zz}(\epsilon_{0,k}, \phi_k) = \sum_{i=1}^{NCC} E_{ci}(\epsilon_{0,k}, \phi_k) A_{ci} z_i^2 + \sum_{j=1}^{NSS} E_{sj}(\epsilon_{0,k}, \phi_k) A_{sj} z_j^2 \quad (c)$$

where NCC and NSS are the number of concrete strips and steel areas considered in the section, respectively; E_{ci} and E_{si} are the concrete and steel section tangent moduli in the fibers “ i ” and “ j ”, respectively; and, A_{ci} and A_{si} are the areas of the concrete strip and steel, respectively.

With the above relations, the complete procedure for developing the moment-curvature envelope is as follows:

1) Apply a small incremental curvature $\Delta\phi_k$ to a previous known value $\Delta\phi_{k-1}$, i.e.

$$\phi_k = \phi_{k-1} + \Delta\phi_k$$

2) In the first step ($k = 0$), the entire axial load is applied. Since the computation assumes this axial load to be constant, the axial force increment ΔN_k^n must be zero for the remaining steps. Based on the previous stiffness matrix (in Eq. 3.15), compute the incremental centroidal strain as follows, where n is the iteration step number ($n \geq 1$):

$$\Delta \varepsilon_0^n = -k_{z,k}^{n-1} \Delta \phi_k / k_{A,k}^{n-1} \quad (3.17)$$

Note $k_{z,k}^0$ and $k_{A,k}^0$ are the stiffness characteristics at the previous step, $k-1$.

3) Update the new strains and curvatures:

$$\begin{Bmatrix} \varepsilon_0 \\ \phi \end{Bmatrix}_k^n = \begin{Bmatrix} \varepsilon_0 \\ \phi \end{Bmatrix}_k^{n-1} + \begin{Bmatrix} \Delta \varepsilon_0 \\ 0 \end{Bmatrix}_k^n \quad (3.18)$$

4) Recompute the terms of the stiffness matrix of Eq. 3.15 using the expressions in Eq. 3.16.

5) Find the unbalanced axial load from:

$$\Delta N_k^n = k_{A,k}^n \Delta \varepsilon_{0,k}^n + k_{z,k}^n \Delta \phi_k \quad (3.19)$$

6) If $|\Delta N_k^n| \geq \xi$ where ξ is a tolerance limit value, then continue the iteration procedure by returning to step (2). Otherwise calculate the moment increment:

$$\Delta M_k = k_{z,k}^n \Delta \varepsilon_{0,k}^n + k_{zz,k}^n \Delta \phi_k \quad (3.20)$$

and update the moment capacity, and continue to search for the moment-curvature relation by adding another increment $\Delta \phi_{k+1}$ to the process and continue to step (1).

In the fiber model analysis, the effect of hoop spacing on the moment-curvature of columns can also be considered. It is assumed that the capacity of the column remains unchanged after the concrete cover has spalled:

$$0.85 f'_c A_g = f'_{cc} A_{cc} \quad (3.21)$$

where f'_{cc} is the confined compressive strength; A_{cc} is the area of the core concrete; and A_g is the gross concrete area. An expression relating confined to unconfined strength of concrete is given by Park and Paulay (1975), and is based on the confining stress relation of Richart et al. (1928):

$$f'_{cc} = f_c + 2.05 \rho_s f_y \quad (3.22)$$

where ρ_s is the volumetric ratio of confinement steel to concrete cover:

$$\rho_s = \frac{A_h \pi d_c}{s A_{cc}} \quad (3.23)$$

and A_h is the cross-sectional area of the hoop steel; and s is the spacing of hoops. The modified compressive stress of concrete is obtained substituting Eq. 3.22 into Eq. 3.21:

$$f'_{cm} = \frac{(f_c + 2.05 \rho_s f_y) A_{cc}}{0.85 A_g} \quad (3.24)$$

3.3.2 Ultimate Deformation Capacity

The ultimate deformation capacity is expressed through the ultimate curvature of the section as determined from the fiber model analysis of the cross-section. The incremental curvature that is applied to the section is continued until one of the following

conditions is reached:

- a) The specified ultimate compressive strain in the concrete is reached ($\varepsilon \geq \varepsilon_{cu}$).
- b) The specified ultimate strength of one of the rebar is reached ($f_s \geq f_{su}$).

The attained curvature of the section when either of the two conditions is reached is recorded as the ultimate curvature. This parameter forms an important part of the damage analysis.

The only factor considered to influence the ultimate deformation capacity of the section is the degree of confinement. Since confinement does not significantly affect the maximum compressive stress, the present formulation only considers the effect of confinement on the downward slope of the concrete stress-strain curve (see Fig. 3.4). The factor ZF defines the shape of the descending branch. The expression developed by Kent and Park (1971) is used:

$$ZF = \frac{0.5}{\varepsilon_{50u} + \varepsilon_{50h} - \varepsilon_0} \quad (3.25)$$

where:

$$\varepsilon_{50u} = \frac{3 + \varepsilon_0 f_c'}{f_c' - 1000} \quad (a) \quad (3.26)$$

$$\varepsilon_{50h} = 0.75 \rho_s \sqrt{\frac{\bar{b}}{s_h}} \quad (b)$$

in which the concrete strength is prescribed in psi; ρ_s is the volumetric ratio of confinement steel to core concrete; \bar{b} is the width of the confined core; and s_h is the spacing of hoops. The effect of introducing this parameter is to define additional ductility to well-confined columns. Improved formulations for stress-strain behavior of confined concrete can be found in a publication by Paulay and Priestley (1992).

3.4 Spread Plasticity Model

The moment distribution along a member subjected to lateral loads is linear, as shown in Fig. 3.7. The presence of gravity loads will alter the distribution, and in cases of significant gravity load moments the structural elements should be subdivided to capture this variation. When the member experiences inelastic deformations, cracks tend to spread from the joint interface resulting in a curvature distribution as shown in Fig. 3.7. Sections along the element will also exhibit different flexibility characteristics, depending on the degree of inelasticity observed (see Fig. 3.8). The program IDARC includes a spread plasticity formulation based on the flexibility method in order to capture the variation of the section flexibility, and combine them to determine the element stiffness matrix.

The flexibility distribution in the structural elements is assumed to follow the two alternative distributions as shown in Fig. 3.8 and Fig. 3.9, where EI_A and EI_B are the current flexural stiffness of the sections at end “A” and “B”, respectively; EI_0 is the stiffness at the center of the element; GA_z is the shear stiffness of the element, assumed constant throughout the length; α_A and α_B are the yield penetration coefficients; and L' is the length of the element. The flexural stiffness EI_A and EI_B , and the shear stiffness GA_z , are determined from the hysteretic model. The stiffness EI_0 and the yield penetration coefficients α_A and α_B are determined as indicated in Section 3.6, depending on the moment distribution and the previous yield penetration history.

The flexibility matrix, including shear distortions, relating moments and rotations at the ends of the element is:

$$\begin{Bmatrix} \theta_A \\ \theta_B \end{Bmatrix} = \begin{bmatrix} f_{AA} & f_{AB} \\ f_{BA} & f_{BB} \end{bmatrix} \begin{Bmatrix} M_A \\ M_B \end{Bmatrix} \quad (3.27)$$

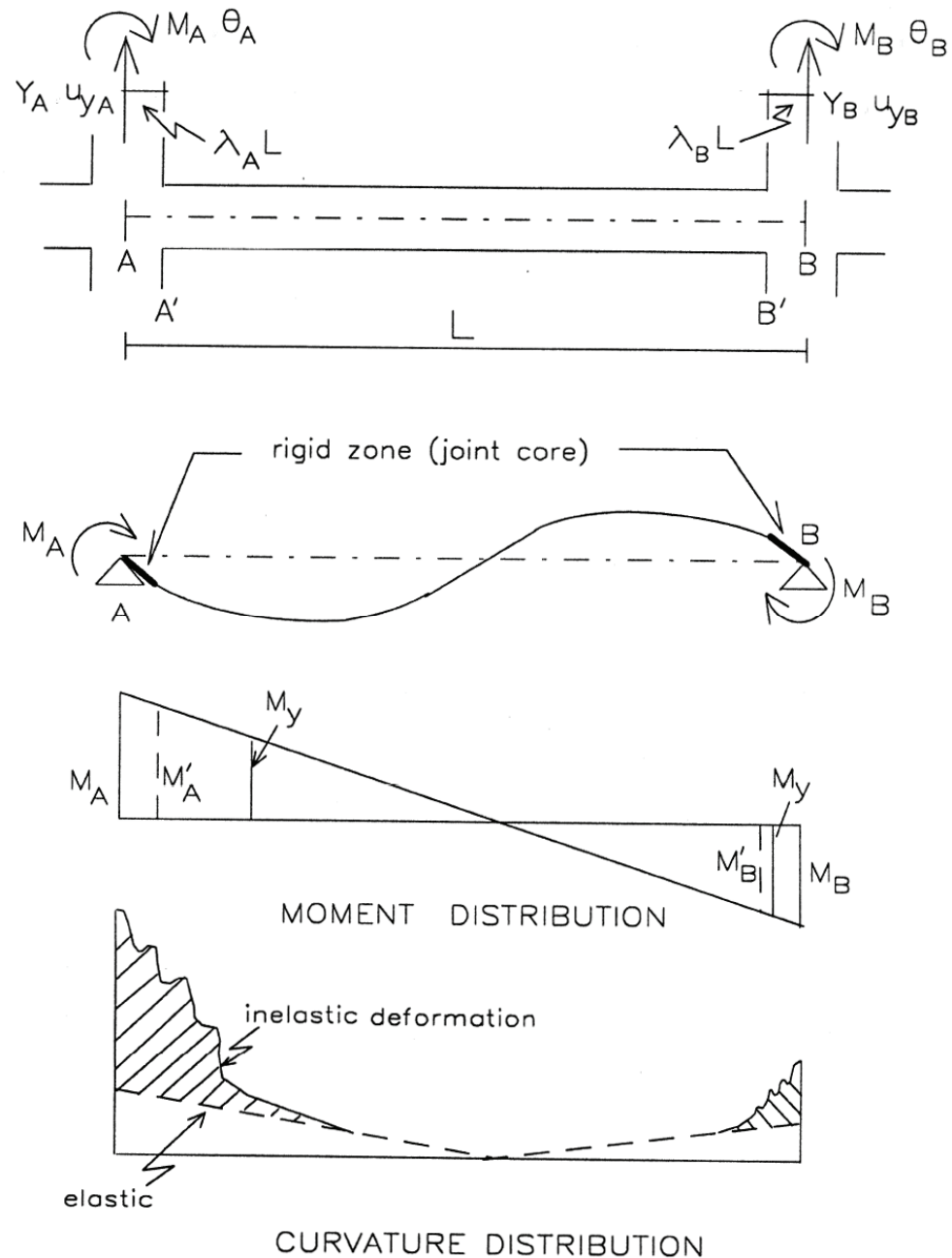


Fig. 3.7 Curvature distribution along an element

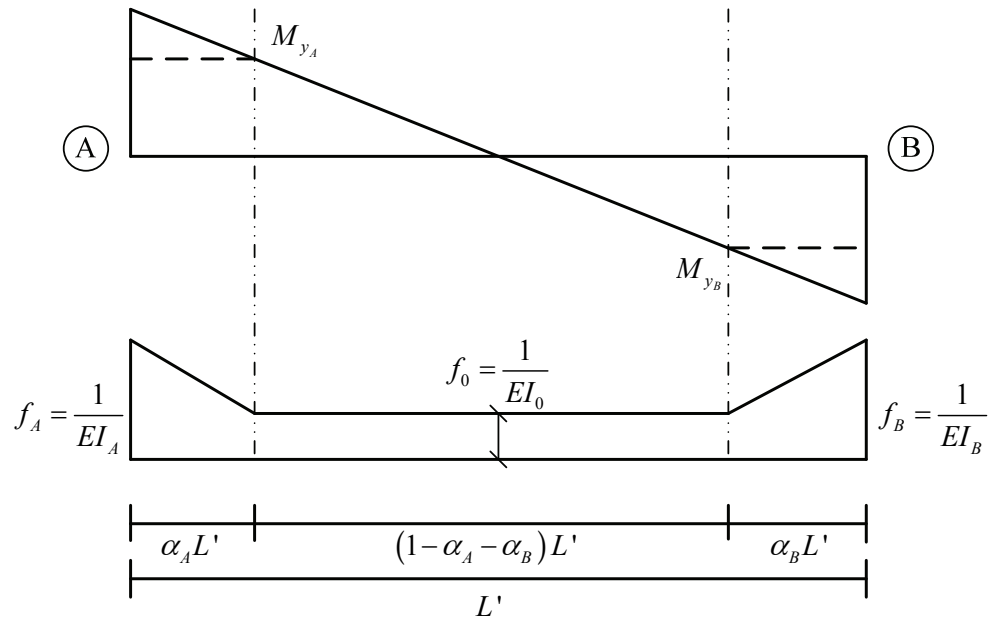


Fig. 3.8 Spread plasticity model for linear flexibility distribution

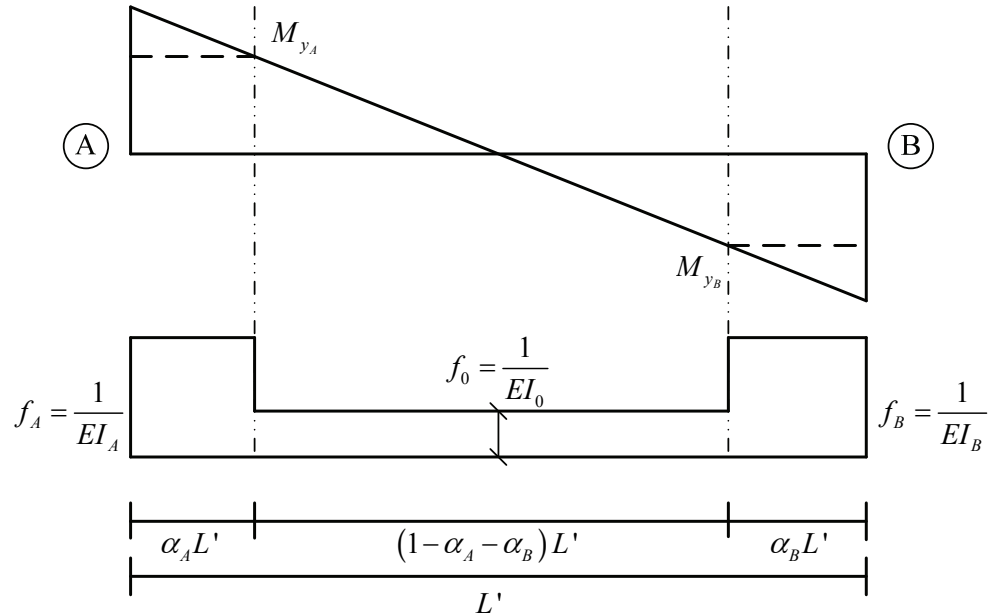


Fig. 3.9 Spread plasticity model for uniform flexibility distribution

where θ_A and θ_B are the rotations at the ends, M_A and M_B are the moments at the ends of the element. The flexibility coefficients are obtained from:

$$f_{ij} = \int_0^L \frac{m_i(x)m_j(x)}{EI(x)} dx + \int_0^L \frac{v_i(x)v_j(x)}{GA_Z} dx \quad (3.28)$$

where $m_i(x)$ and $m_j(x)$ are the moment distributions due to a virtual unit moment at end “ i ” or “ j ”, respectively; $v_i(x)$ and $v_j(x)$ are the corresponding shear distributions. Note that other influences such as temperature, torsion, and axial can be included using formulation provided suitable degree of freedoms are included.

Formulations of flexibility and stiffness coefficients for the two alternative distributions of spread plasticity are given in the following sections.

3.4.1 Linear Variable Flexibility Distribution

After some algebra using Eq. 3.28, the flexibility coefficients for the linear flexibility distribution can be written as (Lobo, 1994):

$$\begin{aligned} f_{AA} &= \frac{L'}{12} \left[\frac{4}{EI_0} + \left(\frac{1}{EI_A} - \frac{1}{EI_0} \right) (6\alpha_A - 4\alpha_A^2 + \alpha_A^3) + \left(\frac{1}{EI_B} - \frac{1}{EI_0} \right) \alpha_B^3 \right] + \frac{1}{GA_Z L'} \quad - (a) \\ f_{AB} &= \frac{L'}{12} \left[\frac{-2}{EI_0} - \left(\frac{1}{EI_A} - \frac{1}{EI_0} \right) (2\alpha_A^2 - \alpha_A^3) - \left(\frac{1}{EI_B} - \frac{1}{EI_0} \right) (2\alpha_B^2 - \alpha_B^3) \right] + \frac{1}{GA_Z L'} \quad - (b) \end{aligned} \quad (3.29)$$

$$f_{BA} = f_{AB} \quad ----- \quad (c)$$

$$f_{BB} = \frac{L'}{12} \left[\frac{4}{EI_0} + \left(\frac{1}{EI_B} - \frac{1}{EI_0} \right) (6\alpha_B - 4\alpha_B^2 + \alpha_B^3) + \left(\frac{1}{EI_A} - \frac{1}{EI_0} \right) \alpha_A^3 \right] + \frac{1}{GA_Z L'} \quad - (d)$$

In the current release of IDARC, the above formulation was rewritten, and close form solutions were derived for the element stiffness matrix to avoid numerical instabilities if

close to failure conditions are observed in flexure or shear.

The flexibility coefficients in the program for the linear distribution are:

$$\begin{aligned} f_{AA}' &= \frac{L'}{12EI_0EI_AEI_B} f_{AA}' + \frac{1}{GA_ZL'} \quad \text{----- (a)} \\ f_{AB}' = f_{BA}' &= \frac{L'}{12EI_0EI_AEI_B} f_{AB}' + \frac{1}{GA_ZL'} \quad \text{----- (b)} \\ f_{BB}' &= \frac{L'}{12EI_0EI_AEI_B} f_{BB}' + \frac{1}{GA_ZL'} \quad \text{----- (c)} \end{aligned} \quad (3.30)$$

where:

$$\begin{aligned} f_{AA}' &= 4EI_AEI_B + 4(EI_0 - EI_A)EI_B\alpha_A(3 - 3\alpha_A + \alpha_A^2) \\ &\quad + 4(EI_0 - EI_B)EI_A\alpha_B^3 \quad \text{----- (a)} \\ f_{AB}' &= -2EI_AEI_B - (EI_0 - EI_A)EI_B(2\alpha_A^2 - \alpha_A^3) \\ &\quad - (EI_0 - EI_B)EI_A(2\alpha_B^2 - \alpha_B^3) \quad \text{----- (b)} \\ f_{BB}' &= 4EI_AEI_B + (EI_0 - EI_A)EI_B\alpha_{AB}^3 \\ &\quad + (EI_0 - EI_B)EI_A(6\alpha_B - 4\alpha_B^2 + \alpha_B^3) \quad \text{----- (c)} \end{aligned} \quad (3.31)$$

Note that the total flexibility of the element is the sum of the flexural and shear contributions.

The element stiffness matrix, including shear deformations, relating moments and rotations at the element ends can be found by the following relation:

$$\begin{Bmatrix} M_A \\ M_B \end{Bmatrix} = \begin{bmatrix} k_{AA} & k_{AB} \\ k_{BA} & k_{BB} \end{bmatrix} \begin{Bmatrix} \theta_A \\ \theta_B \end{Bmatrix} = [\mathbf{K}'] \begin{Bmatrix} \theta_A \\ \theta_B \end{Bmatrix} \quad (3.32)$$

where the elements in the stiffness matrix are:

$$\begin{aligned} k_{AA} &= \frac{12EI_0EI_AEI_B}{D_{et}L'} (f_{BB}'GA_ZL'^2 + 12EI_0EI_AEI_B) \quad \text{----- (a)} \\ k_{AB} = k_{BA} &= \frac{-12EI_0EI_AEI_B}{D_{et}L'} (f_{AB}'GA_ZL'^2 + 12EI_0EI_AEI_B) \quad \text{----- (b)} \end{aligned} \quad (3.33)$$

$$k_{BB} = \frac{12EI_0EI_AEI_B}{D_{et}L'} (f'_{AA}GA_ZL'^2 + 12EI_0EI_AEI_B) \quad \text{---(c)}$$

$$D_{et} = GA_ZL'^2 (f'_{AA}f'_{BB} - f'^2_{AB}) + 12EI_0EI_AEI_B (f'_{AA} + f'_{BB} - 2f'_{AB}) \quad \text{---(d)}$$

In the present formulation shear or flexural failures of the element can be incorporated.

3.4.2 Uniform Flexibility Distribution

For uniform flexibility distribution as shown in Fig. 3.9, the flexibility coefficients and the elements in the stiffness matrix become:

$$f_{AA} = \frac{L'}{3} \left[\frac{1}{EI_0} + \left(\frac{1}{EI_A} - \frac{1}{EI_0} \right) \alpha_A (3 - 3\alpha_A - \alpha_A^2) + \left(\frac{1}{EI_B} - \frac{1}{EI_0} \right) \alpha_B^3 \right] \quad \text{---(a)}$$

$$f_{AB} = -\frac{L'}{6} \left[\frac{1}{EI_0} + \left(\frac{1}{EI_A} - \frac{1}{EI_0} \right) \alpha_A^2 (3 - 2\alpha_A) + \left(\frac{1}{EI_B} - \frac{1}{EI_0} \right) \alpha_A^2 (3 - 2\alpha_A) \right] \quad \text{---(b)} \quad (3.34)$$

$$f_{BA} = f_{AB} \quad \text{-----(c)}$$

$$f_{BB} = \frac{L}{3} \left[\frac{4}{EI_0} + \left(\frac{1}{EI_B} - \frac{1}{EI_0} \right) (3 - 3\alpha_B + \alpha_B^2) \alpha_B + \left(\frac{1}{EI_A} - \frac{1}{EI_0} \right) \alpha_A^3 \right] \quad \text{---(d)}$$

In the current release of IDARC, the formulation above was rewritten, and close form solutions were derived for the element stiffness matrix to avoid numerical instabilities if close to failure conditions are observed in flexure or shear.

The flexibility coefficients in the program for the uniform distribution are:

$$\begin{aligned} f'_{AA} &= 4EI_AEI_B + 4(EI_0 - EI_A)EI_B\alpha_A(3 - 3\alpha_A + \alpha_A^2) \\ &\quad + 4(EI_0 - EI_B)EI_A\alpha_B^3 \end{aligned} \quad \text{---(a)}$$

$$f'_{AB} = -2EI_A EI_B - 2(EI_0 - EI_A)EI_B \alpha_A^2 (3 - 2\alpha_A) \\ - 2(EI_0 - EI_B)EI_A \alpha_B^2 (3 - 2\alpha_B) \quad \text{----- (b)}$$

$$f'_{BB} = 4EI_A EI_B + 4(EI_0 - EI_A)EI_B \alpha_{AB}^3 \\ + 4(EI_0 - EI_B)EI_A \alpha_B (3 - 3\alpha_B + \alpha_B^2) \quad \text{----- (c)}$$

The elements in the stiffness matrix are again the same as for the linear flexibility distribution case.

3.5 Concentrated Plasticity Model

The concentrated plasticity model is called as “lumped plasticity model”. The first inelastic model known as the “two component model” was proposed by Clough and Johnston (1966). It consisted of a linear elastic member in parallel with an elastic perfectly plastic member. The elastic member accounted for the strain hardening characteristics of the reinforcing steel, while the elastic perfectly plastic member for the yielding of the reinforcement. The advantage of the two component model is that the end moments depend on the moments at both ends of the member. Giberson (1969) introduced the one componenet model which compresed of two nonlinear rotational springs at the ends of a perfectly elastic member. The advantage of this model is that the member-end deformation depends solely on the moment acting at the end, so that any moment-rotation hysteresis model can be assigned to the spring. Al-Haddad and Wight (1986) modified this model for varying plastic hinge locations at the member ends. This model accounted for rigid end zones in conjunction with an elastic line element. The inelastic actions were concentrated at the two plastic hinge locations.

The current IDARC2D uses a modified model from the previous models, which is shown in Fig. 3.10. The modified model consists of two nonlinear rotational springs at the ends while the member is considered as an elastic element. Also the model contains rigid end zones for a joint. Therefore, the plasticity of the member is concentrated into the rotational springs which represent the nonlinear properties of the member.

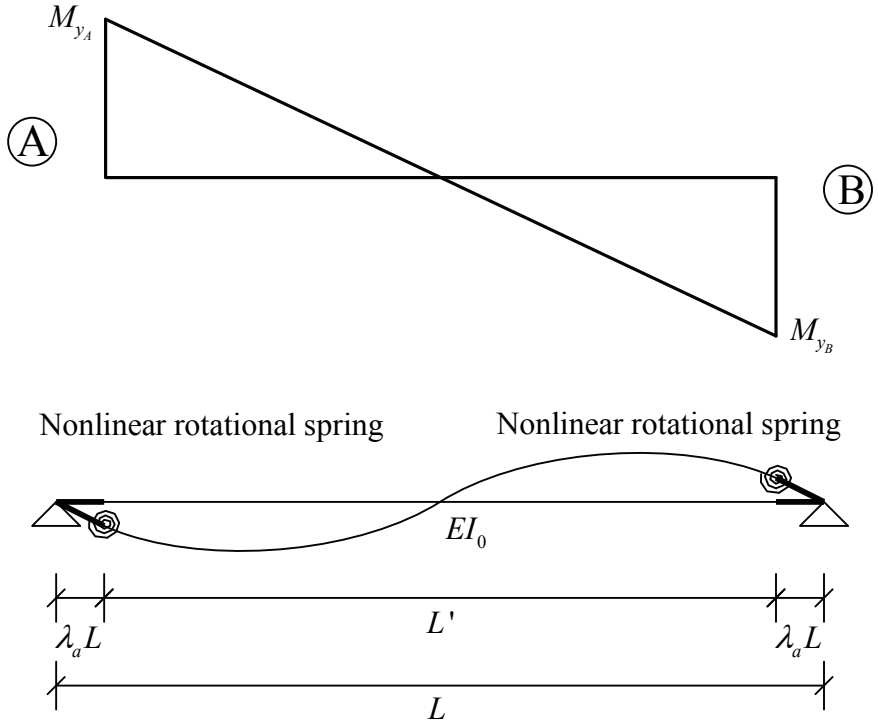


Fig. 3.10 Concentrated plasticity model

3.6 Yield Penetration Model

The yield penetration model establishes length of the nonlinear stress regions, which is combined with the spread plasticity formulation to capture the variation of the stiffness in structural elements. The spread and uniform plasticity formulations described in Sections 3.4 and 3.5 are dependent on the yield penetration parameters α_A and α_B , and of the flexural stiffness EI_0 at the center of the element. The rules for the variation of these parameters as the moment diagram changes in the element are described below.

The yield penetration parameters, α_A and α_B , specify the proportion of the element where the acting moment is greater than the section cracking moment, M_{Acr} or M_{Bcr} . These parameters are first calculated for the current moment distribution, and then checked with the previous maximum penetration lengths $\alpha_{A\max}$ and $\alpha_{B\max}$: the yield penetration parameters cannot be smaller than the previous maximum values regardless

of the current moment distribution. Two cases for the moment distribution are identified: single curvature and double curvature moment diagrams. A set of rules are specified for each of these cases.

a) Single Curvature Moment Diagram ($M'_A M'_B \geq 0$).

In the single curvature moment diagram, the moments at the end of the element have the same sign. Depending on the moment distribution four cases can be identified:

a.1) End moments smaller than the corresponding cracking moments

$$(|M'_A| \leq |M_{Acr}| \text{ and } |M'_B| \leq |M_{Bcr}|):$$

$$\alpha_A = 0 \text{ but } \alpha_A \geq \alpha_{A\max} \quad \text{---(a)}$$

$$\alpha_B = 0 \text{ but } \alpha_B \geq \alpha_{B\max} \quad \text{---(b)} \quad (3.36)$$

$$EI_0 = \frac{2EI_{A0}EI_{B0}}{EI_{A0} + EI_{B0}} \quad \text{---(c)}$$

a.2) Moment at end “A” greater than cracking moment

$$(|M'_A| > |M_{Acr}| \text{ and } |M'_B| \leq |M_{Bcr}|):$$

$$\alpha_A = \frac{M'_A - M_{Acr}}{M'_A - M'_B} \leq 1 \text{ but } \alpha_A \geq \alpha_{A\max} \quad \text{---(a)}$$

$$\alpha_B = 0 \text{ but } \alpha_B \geq \alpha_{B\max} \quad \text{---(b)} \quad (3.37)$$

$$EI_0 = \frac{2EI_{A0}EI_{B0}}{EI_{A0} + EI_{B0}} \quad \text{---(c)}$$

a.3) Moment at end “B” greater than cracking moment

$$(|M'_A| \leq |M_{Acr}| \text{ and } |M'_B| > |M_{Bcr}|):$$

$$\alpha_A = 0 \text{ but } \alpha_A \geq \alpha_{A\max} \quad \text{---(a)}$$

$$\alpha_B = \frac{M'_B - M_{Bcr}}{M'_B - M'_A} \leq 1 \text{ but } \alpha_B \geq \alpha_{B\max} \quad \text{---(b)} \quad (3.38)$$

$$EI_0 = \frac{2EI_{A0}EI_{B0}}{EI_{A0} + EI_{B0}} \quad \text{---(c)}$$

a.4) Moment at both ends greater than cracking moments

($|M'_A| > |M_{Acr}|$ and $|M'_B| > |M_{Bcr}|$):

$$\alpha_A = 0.5 \quad \text{---(a)}$$

$$\alpha_B = 0.5 \quad \text{---(b)}$$

$$EI_0 = \frac{2EI_AEI_B}{EI_A + EI_B} \quad \text{---(c)}$$

where M_{Acr} and M_{Bcr} are the cracking moments of the section corresponding to the sign of the applied moments; EI_{A0} and EI_{B0} are the elastic stiffness of the sections at the ends of the element.

b) Double Curvature Moment Diagram ($M'_A M'_B < 0$):

In the double curvature moment diagram, the moments at the end of the element have different signs. Depending on the moment distribution four cases can be identified:

b.1) End moments smaller than the corresponding cracking moments

($|M'_A| \leq |M_{Acr}|$ and $|M'_B| \leq |M_{Bcr}|$):

$$\alpha_A = 0 \text{ but } \alpha_A \geq \alpha_{A\max} \quad \text{---(a)}$$

$$\alpha_B = 0 \text{ but } \alpha_B \geq \alpha_{B\max} \quad \text{---(b)}$$

$$EI_0 = \frac{2EI_{A0}EI_{B0}}{EI_{A0} + EI_{B0}} \quad \text{---(c)}$$

b.2) Moment at end “A” greater than cracking moment

($|M'_A| > |M_{Acr}|$ and $|M'_B| \leq |M_{Bcr}|$):

$$\alpha_A = \frac{M'_A - M_{Acr}}{M'_A - M'_B} \leq 1 \text{ but } \alpha_A \geq \alpha_{A\max} \quad \text{---(a)}$$

$$\alpha_B = 0 \text{ but } \alpha_B \geq \alpha_{B\max} \quad \text{---(b)}$$

$$EI_0 = \frac{2EI_{A0}EI_{B0}}{EI_{A0} + EI_{B0}} \quad \text{---(c)}$$

b.3) Moment at end “B” greater than cracking moment

($|M'_A| \leq |M_{Acr}|$ and $|M'_B| > |M_{Bcr}|$):

$$\begin{aligned}\alpha_A &= 0 \text{ but } \alpha_A \geq \alpha_{A\max} && \text{---(a)} \\ \alpha_B &= \frac{M'_B - M'_{Bcr}}{M'_B - M'_A} \leq 1 \text{ but } \alpha_B \geq \alpha_{B\max} && \text{---(b)} \\ EI_0 &= \frac{2EI_{A0}EI_{B0}}{EI_{A0} + EI_{B0}} && \text{---(c)}\end{aligned}\quad (3.42)$$

b.4) Moment at both ends greater than cracking moments

$$\begin{aligned}(|M'_A| > |M_{Acr}| \text{ and } |M'_B| > |M_{Bcr}|): \\ \alpha_A &= \frac{M'_A - M_{Acr}}{M'_A - M'_B} \text{ but } \alpha_A \geq \alpha_{A\max} && \text{---(a)} \\ \alpha_B &= \frac{M'_B - M_{Bcr}}{M'_B - M'_A} \text{ but } \alpha_B \geq \alpha_{B\max} && \text{---(b)} \\ EI_0 &= \frac{2EI_AEI_B}{EI_A + EI_B} && \text{---(c)}\end{aligned}\quad (3.43)$$

where M_{Acr} and M_{Bcr} are the cracking moments of the section corresponding to the sign of the applied moments; EI_{A0} and EI_{B0} are the elastic stiffness of the sections at the ends of the element.

In the formulation described above, cracking moments are dependent on the sign of the applied moments. Special provisions are made in the program to adjust the flexibility distribution of members where yield penetration has taken place on the whole element, that is, when:

$$\alpha_A + \alpha_B > 1 \quad (3.44)$$

In such cases, the stiffness EI_0 is modified to capture the actual distribution considering a new set of yield penetration coefficients that will satisfy $\alpha_A + \alpha_B \leq 1$ (see Fig. 3.11).

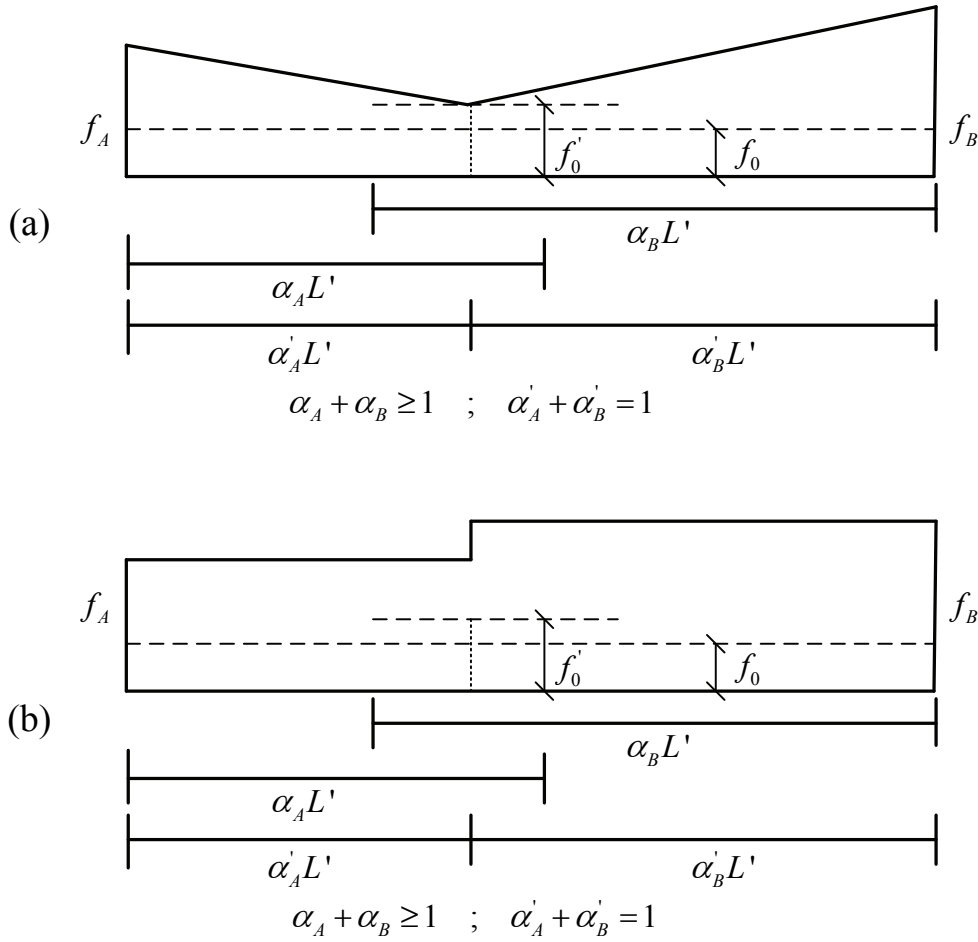


Fig. 3.11 Yield penetration lengths for fully inelastic members: (a) linear flexibility distribution; (b) uniform flexibility distribution

3.7 Element Moment Releases

A perfect hinge could have been modeled as an end spring with zero stiffness, however, the implications in the numerical analysis are leading often to singular matrices. Therefore, a perfect member hinge is modeled by setting the hinge moment to zero and condensing out the corresponding degree of freedom. If a hinge is assigned at the end “*b*” of an element, the relation between moments at the joint “*a*” and at the face of the element is given by (see Fig. 3.12):

$$M_a = \left(\frac{1}{1 - \lambda_a} \right) M'_a \quad (3.45)$$

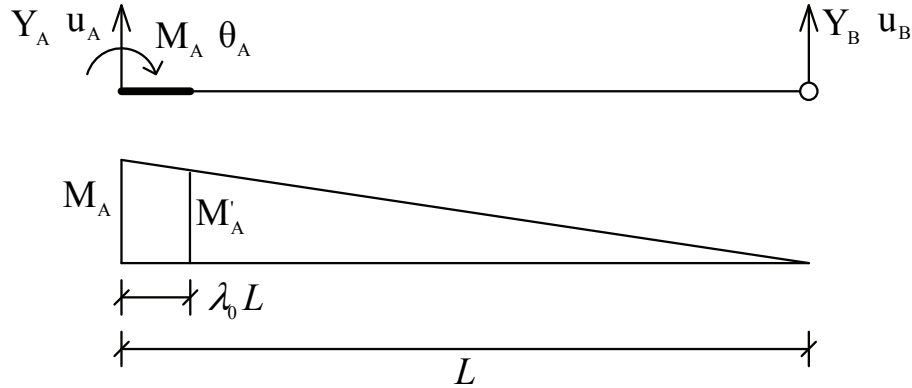


Fig. 3.12 Modeling of moment releases in structural elements

The element stiffness equation relating moments and rotations is:

$$\{M_a\} = k_s \{\theta_a\} \quad (3.46)$$

where k_s is a coefficient obtained by condensing the element stiffness matrix:

$$k_s = [\mathbf{K}_s]_{11} - \frac{([\mathbf{K}_s]_{12})^2}{[\mathbf{K}_s]_{22}} \quad (3.47)$$

where $[\mathbf{K}_s]_{ij}$ are the coefficients of the element stiffness matrix calculated considering the spread plasticity model.

The overall equilibrium equation for the entire element becomes:

$$\begin{Bmatrix} X_a \\ M_a \\ X_b \\ M_b \end{Bmatrix} = \left(\frac{1}{1-\lambda_a} \right)^2 k_s \{ \mathbf{R}_e \} \{ \mathbf{R}_e \}^t \begin{Bmatrix} u_a \\ \theta_a \\ u_b \\ \theta_b \end{Bmatrix} \quad (3.48)$$

where:

$$\{\mathbf{R}_e\} = \begin{Bmatrix} -1/L \\ 1 \\ 1/L \\ 0 \end{Bmatrix} \quad (3.49)$$

This element can be integrated into the global structural model as a standard element. In case of a single column structure the degree of freedom “*b*” is eliminated from the global stiffness matrix.

SECTION 4

ELEMENT MODELS LIBRARY

Based on model developed in Section 3, arbitrary models were developed for each of the elements indicated in Section 3.1. A detail presentation of models is shown below.

4.1 Column Elements

Column elements are modeled considering flexural and axial deformations. A typical column element with the corresponding degrees of freedom is shown in Fig. 4.1. Shear component does not contribute to the deformation since shear property is modeled as a rigid feature. The flexural component of the deformation is modeled using one of the following hysteretic models described in Section 5:

- a) Trilinear model
- b) Bilinear model
- c) Vertex oriented model
- d) Nonlinear elastic-cyclic model
- e) Smooth hysteretic model.

The axial deformation component is modeled using a linear-elastic spring. The column elements include a rigid length zone to simulate the increase in stiffness at the joint. The user can specify the length of the rigid zone depending on the dimensions of the connecting elements. The stiffness formulation for column elements is described in Section 3.2.

The element stiffness matrix $[K_s]$ is constantly varied throughout the analysis according to the formulation for the spread plasticity model presented in Section 3.4, and the hysteretic model selected. Depending on the hysteretic model considered some characteristic values for the response of the element are required, namely moment-

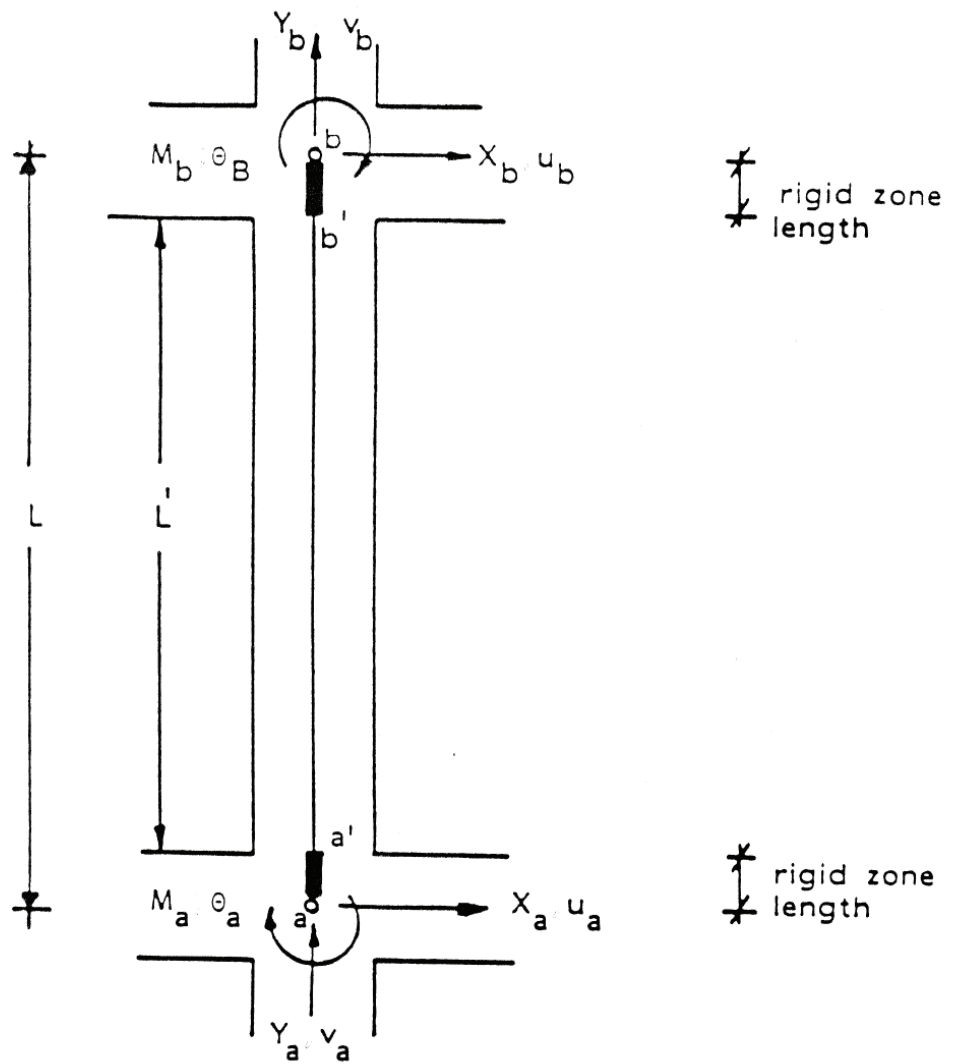


Fig. 4.1 Typical column element with degrees of freedom

curvature or shear-shear distortion. For reinforced concrete elements the user may select to specify the section dimensions and reinforcement, and use the fiber model to calculate the properties as described in Section 3.3, or provide user supplied values.

Simplified formulations can be used alternatively to determine the moment-curvature characteristics. For reinforced concrete columns, the following formulas may be used to estimate the characteristic values of the moment-curvature response of the element (Park et al., 1984):

a) Cracking moment:

$$M_{cr} = 11\sqrt{f'_c} Z_e + Nd / 6 \quad (4.1)$$

where f'_c is the concrete strength in ksi; Z_e is the section modulus in in^3 ; N is the axial load in kips; and d is the depth to rebar in inches.

b) Yield Curvature (Park and Paulay, 1974):

$$\varphi_y^* = \frac{\varepsilon_y}{(1-k)d} \quad (4.2)$$

where ε_y is the strain at yield stress of steel; and k is calculated according to:

$$k = \left\{ \left(\rho_t + \rho'_t \right)^2 \frac{1}{4\alpha_y^2} + \left(\rho_t + \beta_c \rho'_t \right) \frac{1}{\alpha_y} \right\}^{1/2} - \left(\rho_t + \rho'_t \right) \frac{1}{2\alpha_y}$$

$$\rho_t = \frac{A_t f_y}{b d f'_c}; \quad \rho'_t = \frac{A_c f_y}{b d f'_c}; \quad \alpha_y = \frac{\varepsilon_y}{\varepsilon_0}; \quad \beta_c = \frac{d_c}{d}$$

where A_t is the area of the tensile reinforcing bars; A_c is the area of the compressive reinforcing bars; ε_0 is the strain at maximum strength of the concrete; and d_c is the cover depth for compression bars. Note that this expression tends to underestimate the actual curvature since the inelasticity of concrete and the effect of axial loads is not taken into account. Based on the results on an iterative analysis (Aoyama, 1971) the following modification is introduced:

$$\varphi_y = \left[1.05 + (C_2 - 0.05) \frac{n_0}{0.03} \right] \varphi_y^* \quad (4.3)$$

where:

$$C_2 = 0.45 / (0.85 + \rho_t)$$

$$n_0 = N / (f_c' b d)$$

c) Yield Moment (Park et al., 1984):

$$M_y = 0.5 f_c' b d^2 \{ (1 + \beta_c - \eta) n_0 + (2 - \eta) \rho_t + (\eta - 2\beta_c) \alpha_c \rho_t \} \quad (4.4)$$

where:

$$\eta = \frac{0.75}{1 + \alpha_y} \left(\frac{\varepsilon_c}{\varepsilon_0} \right)^{0.7}$$

$$\alpha_c = (1 - \beta_c) \frac{\varepsilon_c}{\varepsilon_y} - \beta_c < 1.0$$

d) Ultimate Moment (Park et al., 1984):

$$M_u = (1.24 - 0.15 \rho_t - 0.5 n_0) M_y \quad (4.5)$$

e) Ultimate Curvature:

For ultimate curvature estimates, the relations suggested by Park and Paulay (1975) can be used.

More up to date relations of capacity of columns are presented by Mander et al. (1995), and could be used instead of those suggested.

4.2 Beam Elements

Beam elements are modeled as flexural elements without shear deformations coupled since shear property is modeled as a rigid feature. A typical beam element with the corresponding degrees of freedom is shown in Fig. 4.2. The flexural component of the deformation is modeled using one of the following hysteretic models described in Section 5:

- a) Trilinear model
- b) Bilinear model
- c) Vertex oriented model
- d) Nonlinear elastic-cyclic model
- e) Smooth hysteretic model.

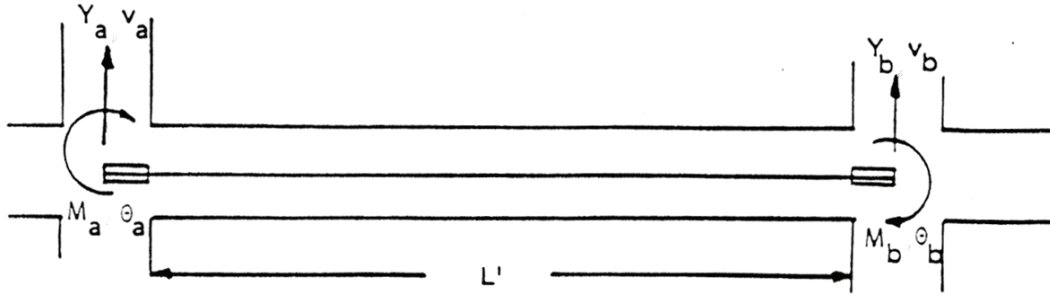


Fig. 4.2 Typical beam element with degrees of freedom

The beam elements include a rigid length zone to simulate the increase in stiffness at the joint. The user can specify the length of the rigid length depending on the dimensions of the connecting elements. The stiffness formulation for column elements is described in Section 3.2.

The element stiffness matrix $[K_s]$ is constantly varied throughout the analysis according to the formulation for the spread plasticity model presented in Section 3.4, and the hysteretic model selected. Depending on the hysteretic model considered, some characteristic values for the response of the element are required, namely moment-curvature or shear-shear distortion. For reinforced concrete elements, the user may select to specify the section dimensions and reinforcement, and use the fiber model to calculate the properties as described in Section 3.3, or provide user supplied values.

Simplified formulations can be used alternatively to determine the moment-curvature characteristics. For reinforced concrete beams, the following formulas may be used to estimate the characteristic values of the moment-curvature response:

a) Cracking Moments (Park et al., 1984):

$$M_{cr}^+ = 11.0 \sqrt{f_c'} \left(I_g / \bar{x} \right) \quad \text{---(a)} \quad (4.6)$$

$$M_{cr}^- = 11.0 \sqrt{f_c'} \left\{ I_g / (h - \bar{x}) \right\} \quad \text{---(b)}$$

where M_{cr}^+ and M_{cr}^- are the positive and negative cracking moments; I_g is the gross moment of inertia of the section; \bar{x} is the distance from the base to the centroid of the section; and h is the height of the section.

b) Yield Curvature (Park and Paulay, 1974):

$$\varphi_{yf}^+ = c \frac{\varepsilon_y}{(1-k)d} \quad \text{---(a)} \quad (4.7)$$

$$\varphi_{yf}^- = c \frac{\varepsilon_y}{(1-k')d'} \quad \text{---(b)}$$

where:

$$k = \left\{ \left(\rho_t + \rho_t' \right)^2 \frac{1}{4\alpha_y^2} + \left(\rho_t + \beta_c \rho_t' \right) \frac{1}{\alpha_y} \right\}^{1/2} - \left(\rho_t + \rho_t' \right) \frac{1}{2\alpha_y}$$

$$\rho_t = \frac{A_t f_y}{b d f_c'}; \quad \rho_t' = \frac{A_c f_y}{b d f_c'}; \quad \alpha_y = \frac{\varepsilon_y}{\varepsilon_0}; \quad \beta_c = \frac{d_c}{d}$$

and ε_y is the strain at yield stress of the steel; c is a factor to amplify the curvature due to inelasticity of the concrete; k' is the neutral axis parameter (similar to k); and the rest of the variables were defined in Section 3.2.

c) Yield Moment (Park et al., 1984):

$$M_y^+ = 0.5 f_c' b_{sl} d^2 \left[(2 - \eta) \rho_t + (\eta - 2\beta_c) \alpha_c \rho_t' \right] \quad \text{---(a)} \quad (4.8)$$

$$M_y^- = 0.5 f_c b (d')^2 \left[(2 - \eta) \rho_t + (\eta' - 2\beta_c) \alpha_c \rho_t' \right] \dots \text{(b)}$$

where:

$$\begin{aligned} \eta &= \frac{0.75}{1 + \alpha_y} \left(\frac{\varepsilon_c}{\varepsilon_0} \right)^{0.7}; \quad \eta' = \frac{0.75}{1 + \alpha_y} \left(\frac{\varepsilon_c'}{\varepsilon_0} \right)^{0.7} \\ \varepsilon_c &= \varphi_y d - \varepsilon_y; \quad \varepsilon_c' = \varphi_y' d' - \varepsilon_y' \\ \alpha_c &= (1 - \beta_c) \frac{\varepsilon_c}{\varepsilon_y} - \beta_c \leq 1.0; \quad \alpha_c' = (1 - \beta_c') \frac{\varepsilon_c'}{\varepsilon_y} - \beta_c' \leq 1.0 \end{aligned}$$

where M_y^+ and M_y^- are the positive and negative yield moments; ε_c and ε_c' are the maximum compression and tension strains in the concrete; and all additional parameters are defined in Fig. 4.3.

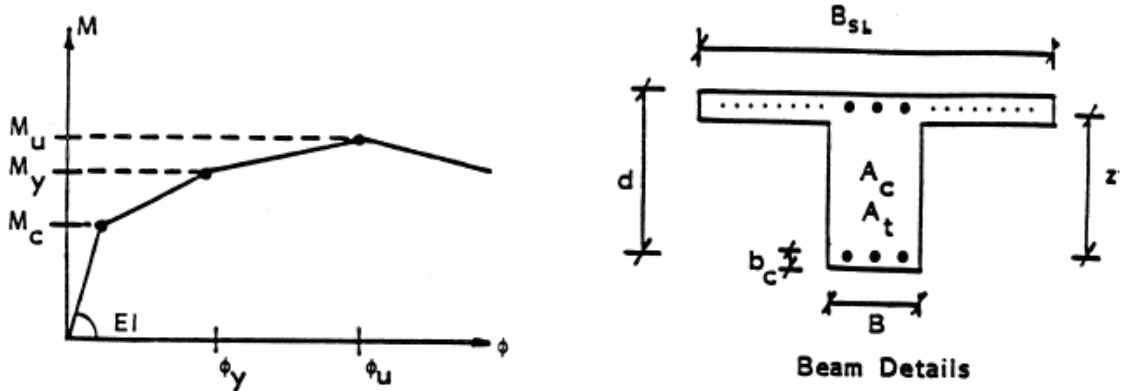


Fig. 4.3 Deformation parameters

d) Ultimate Moment (Park et al., 1984):

$$M_u^+ = (1.24 - 0.15 \rho_t) M_y^+ \dots \text{(a)} \quad (4.9)$$

$$M_u^- = (1.24 - 0.15 \rho_t') M_y^- \dots \text{(b)}$$

where M_u^+ and M_u^- are the positive and negative ultimate moments.

e) Ultimate Curvature:

For the ultimate curvature estimates, the relations suggested by Park and Paulay (1975) could be used as a rough approximation.

4.3 Deep Beam and Column Elements

Deep elements are modeled as flexural elements including shear deformations coupled as shown in Fig. 4.4. Flexural and shear components of the deformation are modeled using one of the following hysteretic models described in Section 5:

- a) Trilinear model
- b) Bilinear model
- c) Vertex oriented model
- d) Nonlinear elastic-cyclic model
- e) Smooth hysteretic model

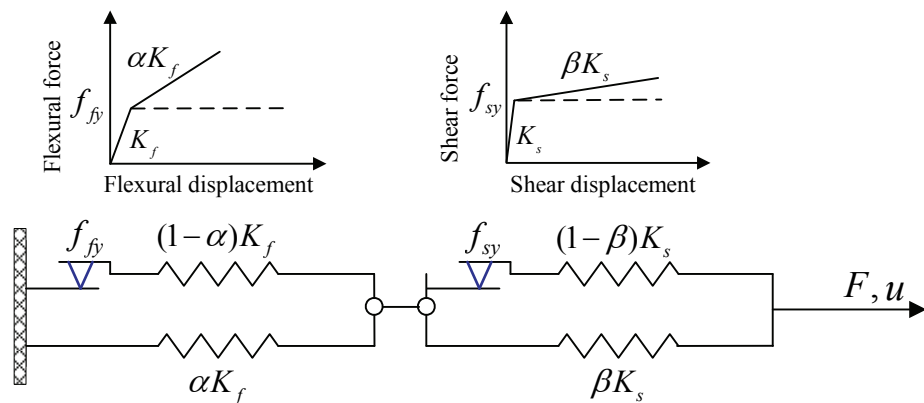


Fig. 4.4 Macroscopic model for deep beam & column elements

The axial deformation component is modeled using a linear-elastic spring. The deep elements are used to consider shear effects which play important role in the hysteretic behavior of the elements or structures. The deep elements include a rigid length zone to simulate the increase in stiffness at the joint. The user can specify the length of the rigid

zone depending on the dimensions of the connecting elements. The stiffness formulation for deep elements is described in Section 3.2.

The element stiffness matrix $[K_s]$ is constantly varied throughout the analysis according to the formulation for the spread plasticity model presented in Section 3.4, and the hysteretic model selected. Depending on the hysteretic model considered some characteristic values for the response of the element are required, namely moment-curvature and shear-shear distortion. For reinforced concrete elements the user may select to specify the section dimensions and reinforcement, and use the fiber model to calculate the properties as described in Section 3.3, or provide user supplied values.

Simplified formulations can be used alternatively to determine the moment-curvature characteristics. For reinforced concrete columns, the prescribed formulas in Section 3.4 may be used to estimate the characteristic values of the moment-curvature response of the element.

Deep elements consist of deep beam and deep column elements, and are characterized by horizontal springs and friction elements representing nonlinear shear and flexural behaviors as shown in Fig. 4.4. In the figure, K_f and K_s are the stiffnesses of shear and flexural components, respectively. The parameters α and β are the ratios of yield stiffness to initial stiffness for flexural and shear components, respectively. The parameters f_{fv} and f_{sy} are the friction forces at sliding which are the yielding forces of shear and flexural components, respectively. The stiffness of friction elements is infinite until yielding while the stiffness is zero after the yielding state. Therefore, in an elastic range, the initial stiffnesses of flexural ($(1-\alpha)K_f + \alpha K_f = K_f$) and shear ($(1-\beta)K_s + \beta K_s = K_s$) components operate. After yielding, the post yield stiffnesses of flexural (αK_f) and shear (βK_s) components contribute to the element behavior. In an elastic range, total stiffness of the element is close to the shear stiffness when the shear stiffness is relatively small comparing to its flexural stiffness.

$$K = \frac{K_s K_f}{K_s + K_f} = \frac{K_s}{\frac{K_s}{K_f} + 1} \cong K_s \quad (4.10)$$

When the shear stiffness is infinite (conventional elements); only flexural stiffness contributes to the element behavior.

$$K = \frac{K_s K_f}{K_s + K_f} = \frac{K_f}{\frac{K_f}{K_s} + 1} \cong K_f \quad (4.11)$$

Considering an inelastic behavior of the element the total stiffness and force relationship of deep beam and column elements is,

$$F = \left\{ \frac{[(1-\alpha)K_f \operatorname{sgn}(f_f) + \alpha K_f][(1-\beta)K_s \operatorname{sgn}(f_s) + \beta K_s]}{[(1-\alpha)K_f \operatorname{sgn}(f_f) + (1-\beta)K_s \operatorname{sgn}(f_s)] + [\alpha K_f + \beta K_s]} \right\} u \quad (4.12)$$

where:

$$\operatorname{sgn}(f_f) = \begin{cases} 1 & \text{for } f_f \leq f_{fy} \\ 0 & \text{for } f_f > f_{fy} \end{cases}$$

$$\operatorname{sgn}(f_s) = \begin{cases} 1 & \text{for } f_s \leq f_{sy} \\ 0 & \text{for } f_s > f_{sy} \end{cases}$$

Table 4.1 shows the total stiffness depending on the combinations of each state of the flexural and shear components. The deep elements can be used to analyze perforated shear walls. For more realistic results, the rotational model of panel zone where connects deep beam and deep column may be required if the zone is wide.

Table 4.1 Total stiffness of deep elements at various states

Flexural state	Flexural stiffness	Shear state	Shear stiffness	Total stiffness
$f_f < f_{fy}$	K_f	$f_s < f_{sy}$	K_s	$K = \frac{K_s K_f}{K_s + K_f}$
$f_f < f_{fy}$	K_f	$f_s \geq f_{sy}$	αK_s	$K = \frac{\alpha K_s K_f}{\alpha K_s + K_f}$
$f_f \geq f_{fy}$	βK_f	$f_s < f_{sy}$	K_s	$K = \frac{\beta K_s K_f}{K_s + \beta K_f}$
$f_f \geq f_{fy}$	βK_f	$f_s \geq f_{sy}$	αK_s	$K = \frac{\alpha \beta K_s K_f}{\alpha K_s + \beta K_f}$

4.4 Rocking Column Elements

The rocking columns (constrained double hinged column elements) are modeled considering flexural and axial deformations. The column elements are called “rocking column” elements as well. The rocking column element with the corresponding degrees of freedom is the same as the typical column element shown in Fig. 4.1. The contribution of shear component to the lateral deformation is very small, hence shear property is modeled as a constant feature. The flexural component of the deformation is modeled using the following hysteretic model described in Section 5:

- a) Nonlinear elastic-cyclic model

The axial deformation component is modeled using a linear-elastic spring. The column elements include a rigid length zone to simulate the increase in stiffness at the joint. The stiffness formulation for column elements is described in Section 3.2.

The element stiffness matrix $[K_s]$ is constantly varied throughout the analysis according to the formulation for the spread plasticity model presented in Section 3.4, and the hysteretic model selected.

Simplified formulations can be used alternatively to determine the moment-curvature characteristics shown in Fig. 4.5. The following formulas may be used to estimate the characteristic values of the moment-curvature response of the element:

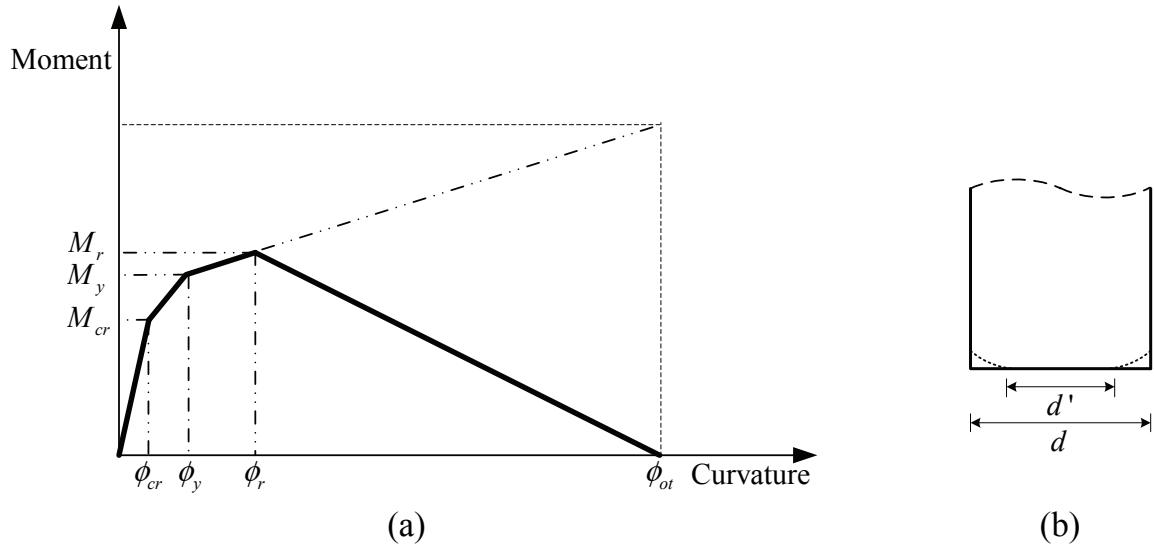


Fig. 4.5 Moment-Curvature relationship and edge shapes of rocking columns

a) Effective flexural rigidity:

$$EI_{eff} = \kappa_{eff} EI_0 \quad (4.13)$$

where EI_0 is the flexural rigidity at the ends, and κ_{eff} is an effective stiffness ratio of the rocking column. The ratio is ranged around 0.5 for reinforced concrete columns (Mander and Cheng, 1997; Priestley et al., 1996), but it is depended on the ratio of the axial load to the nominal strength.

b) Cracking moment:

$$M_{cr} = Nd / 6 \quad (4.14)$$

where N is the axial load; d is the depth of the column.

c) Yield Moment:

$$M_y = N \left(\frac{d}{2} - \frac{d_{c,y}}{3} \right) \quad (4.15)$$

where, $d_{c,y}$ is contact depth at yielding state and defined as $d_{c,y} = 2N/f_c' t$. The $d_{c,y} = 2N/f_c' t$. The parameter f_c' is the concrete strength and t is the column thickness.

d) Yield Curvature:

$$\phi_y = \frac{M_y}{K_{eff} E \left[A_{c,y} \left(\frac{d - d_{c,y}}{2} \right)^2 + I_{c,y} \right]} \quad (4.16)$$

where $A_{c,y}$ is the contact area at yielding state and the corresponding moment of inertia about the centroid of contact area are represented with $I_{c,y} = d_{c,y}^3 t / 12$.

e) Rocking Moment:

$$M_r = N \left(\frac{d - d_{c,r}}{2} \right) \quad (4.17)$$

where $d_{c,r}$ are contact depth at rocking point and defined as $d_{c,r} = d_{c,y} / 2$.

f) Rocking Curvature:

$$\phi_r = \frac{M_r}{K_{eff}E \left[A_{c,r} \left(\frac{d - d_{c,r}}{2} \right)^2 + I_{c,r} \right]} \quad (4.18)$$

where $A_{c,r}$ is the contact area at rocking point and the corresponding moment of inertia about the centroid of contact area are represented with $I_{c,r} = d_{c,r}^3 t / 12$.

h) Overturning Curvature:

When the rocking columns are reached at the overturning point, the moments at both ends are zero, which means that the end condition is symmetric. Considering the symmetric moment-curvature capacity, the curvature at the overturning point can be computed by using the relationship between moment-curvature and lateral force-displacement responses of a rocking column as follow.

$$\phi_{ot} = \phi_y + \frac{K_3 (\delta_{max} - \delta_y) L'}{EI_3} \frac{L'}{2} \quad (4.19)$$

where EI_3 is the tangential slope between “yielding” and “rocking” points in the moment-curvature envelope, and K_3 is the tangential lateral stiffness at the rocking point. The parameter δ_{max} is the maximum lateral displacement which can be estimated from the geometric configuration and depth of the column ends. If a damage at the edges of the column end during rocking behavior is small, the maximum displacement is close to the column depth ($\delta_{max} \approx d$). If the damage is not ignorable, the maximum displacement is evaluated with the consideration of the crushing or damage depth. For concrete rocking columns, the displacement is recommended as $d - 3d_{c,r}$ for a case of rectangular edges. When the column behaves cyclically and its edges are rounded or spherical as shown in Fig. 4.5, the moment-curvature relationship can be evaluated by

replacing d' instead of d and by replacing $\kappa_{eff} \left(2 - N'_0 / N_0\right)$ instead of κ_{eff} which is a effective stiffness ratio of the column having rectangular edge shapes, where N'_0 is the nominal strength of the column with spherical edge shapes and N_0 is the nominal strength of the column with rectangular edge shapes. The maximum displacement may close to the column depth because a minor damage will be developed at the edges.

More details are presented by Roh (2007) and Roh and Reinhorn (2008) except the definitions of base curvature, and could be used instead of those suggested.

4.5 Shear Wall Elements

Shear wall elements are modeled considering flexural, shear and axial deformations. A typical shear wall element with the corresponding degrees of freedom is shown in Fig. 4.6. Flexural and shear components of the deformation are modeled using one of the following hysteretic models described in Section 5:

- a) Trilinear model
- b) Bilinear model
- c) Vertex oriented model
- d) Nonlinear elastic-cyclic model
- e) Smooth hysteretic model

The axial deformation component is modeled using a linear-elastic spring. The user can specify the length of the rigid zone depending on the dimensions of the connecting elements. The stiffness formulation for shear wall elements is described in Section 3.2.

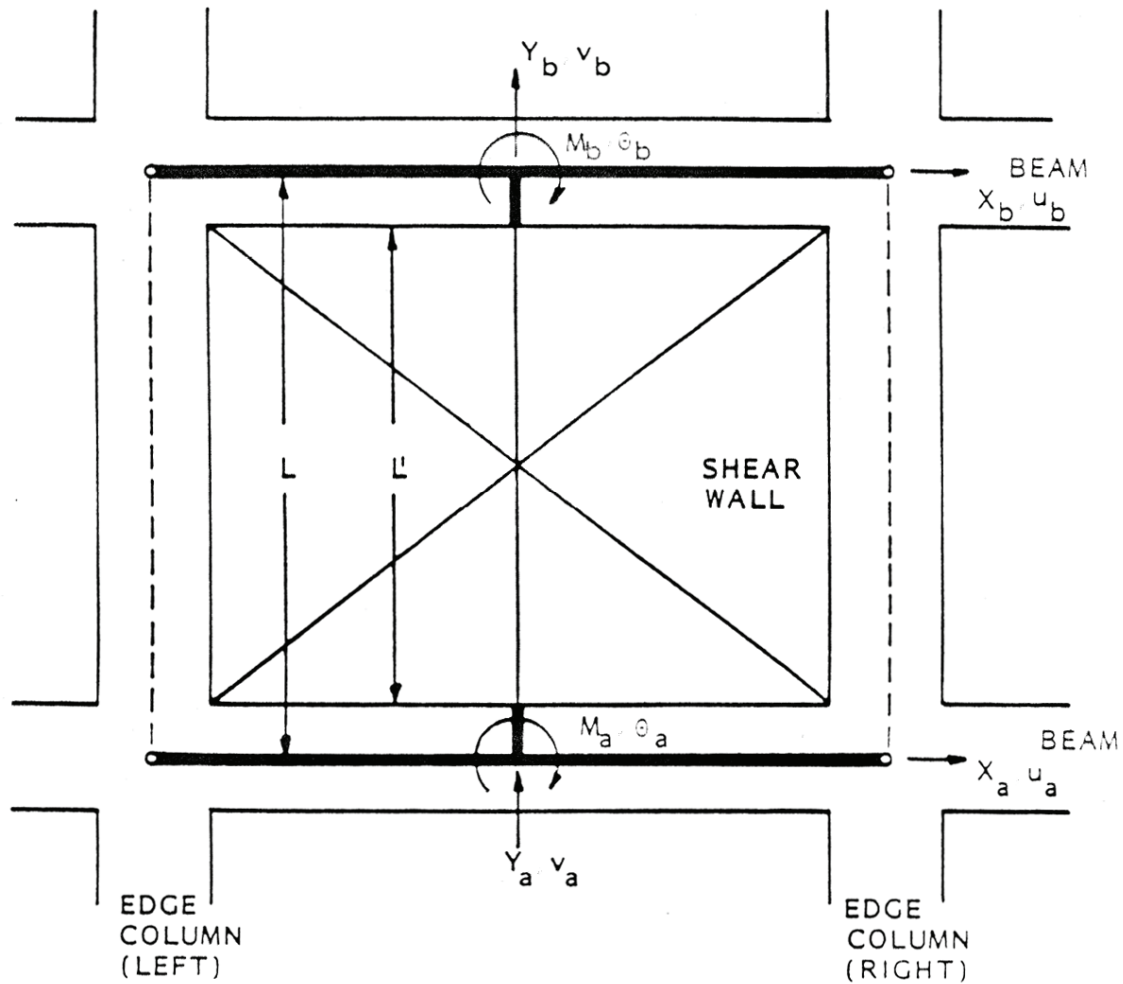


Fig. 4.6 Typical shear wall element with degrees of freedom

The element stiffness matrix $[K_s]$ is constantly varied throughout the analysis according to the formulation for the spread plasticity model presented in Section 3.4, and the hysteretic model selected. Depending on the hysteretic model considered some characteristic values for the response of the element are required, namely moment-curvature or shear-shear distortion. For reinforced concrete elements, the user may select to specify the section dimensions and reinforcement, and use the fiber model to calculate the shear wall flexural properties as described in Section 3.3, or provide user supplied values. Simplified formulations can be used alternatively to determine the moment-curvature characteristics.

The inelastic shear properties are evaluated based on a regression analysis of a large number of test data presented by Hirosawa (1975). The cracking and shear strengths, V_c and V_y are determined from the following empirical relations:

$$V_c = \frac{0.6(f'_c + 7.11)}{M/(VL_w) + 1.7} b_e L_w \quad \text{---(a)} \quad (4.20)$$

$$V_y = \left\{ \frac{0.08\rho_t^{0.23}(f'_c + 2.56)}{M/(VL_w) + 0.12} + 0.32\sqrt{f_y\rho_w} + 0.1f_a \right\} b_e L_w \quad \text{---(b)}$$

where $M/(VL_w)$ is the shear span ratio; ρ_t is the tension steel ratio in percent; ρ_w is the wall reinforcement ratio; f_a is the axial stress; b_e is the equivalent web thickness; and L_w is the distance between edge columns.

The shear deformation may be determined using the secant stiffness as follows:

$$k_y = \frac{0.5M}{VL_w} k_e \quad (4.21)$$

where k_e is the elastic shear stiffness (GA/L_w) . The above relations which resulted from the parametric analysis of test data (Hirosawa, 1975) was found to be the most suitable for defining the shear properties of walls. This formulation is incorporated in the program IDARC.

4.6 Edge Column Elements

Edge columns are the columns monolithically connected to the shear wall elements. Their behavior is primarily dependent on the deformation of the shear wall, and therefore are modeled as one dimensional axial springs. Fig. 4.7 shows a typical pair of edge

column elements with the corresponding degrees of freedom. These elements may also be used to model other transverse elements, such as secondary shear walls that can be lumped with the corresponding column element.

The stiffness matrix for the pair of elements is:

$$\begin{Bmatrix} Y_a \\ M_a \\ Y_b \\ M_b \end{Bmatrix} = \left(\frac{EA_l}{h} \begin{bmatrix} 1 & \lambda & -1 & -\lambda \\ \lambda & \lambda^2 & -\lambda & -\lambda^2 \\ -1 & -\lambda & 1 & \lambda \\ -\lambda & -\lambda^2 & \lambda & \lambda^2 \end{bmatrix} + \frac{EA_r}{h} \begin{bmatrix} 1 & -\lambda & -1 & \lambda \\ -\lambda & \lambda^2 & \lambda & -\lambda^2 \\ -1 & \lambda & 1 & -\lambda \\ \lambda & -\lambda^2 & -\lambda & \lambda^2 \end{bmatrix} \right) \begin{Bmatrix} v_a \\ \theta_a \\ v_b \\ \theta_b \end{Bmatrix} \quad (4.22)$$

where A_l and A_r are the cross-sectional areas for the left and right edge column elements; h is the length of the edge columns; and λ is half the distance between the edge columns. The stiffness matrix is added to the one determined for the shear wall elements.

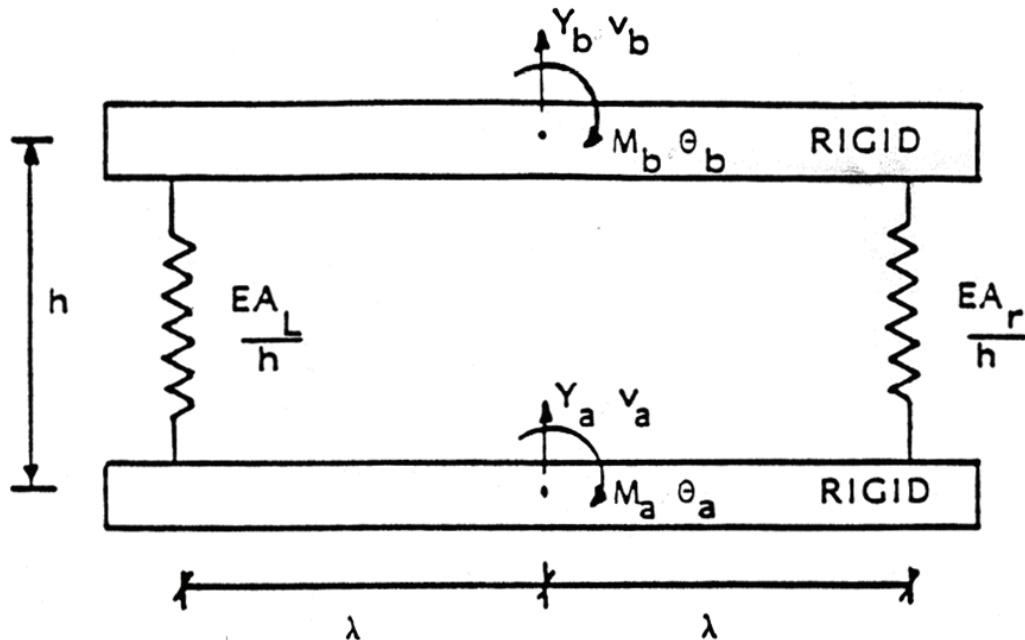


Fig. 4.7 Edge column elements

4.7 Transverse Beam Elements

Although the modeling of the structure is done using 2D (planar) frames, it is recognized that strong transverse beams may affect the frame behavior. Transverse beams are elements that connect nodes of different frames to take into account the contribution of beams perpendicular to the direction of analysis. The transverse beam elements are modeled by two springs, one to provide resistance to relative vertical motion, and the second, a rotational spring, to provide resistance to relative angular motions (see Fig. 4.8). Both springs are considered linear-elastic. The equation relating nodal forces and nodal displacements is:

$$\begin{Bmatrix} Y_a \\ M_a \\ Y_b \\ M_b \end{Bmatrix} = \left(k_v \begin{bmatrix} 1 & -L_v & -1 & 0 \\ -L_v & L_v^2 & L_v & 0 \\ -1 & L_v & 1 & 0 \\ 0 & 0 & 0 & 0 \end{bmatrix} + k_\theta \begin{bmatrix} 0 & 0 & 0 & 0 \\ 0 & 1 & 0 & -1 \\ 0 & 0 & 0 & 0 \\ 0 & -1 & 0 & 1 \end{bmatrix} \right) \begin{Bmatrix} v_a \\ \theta_a \\ v_b \\ \theta_b \end{Bmatrix} \quad (4.23)$$

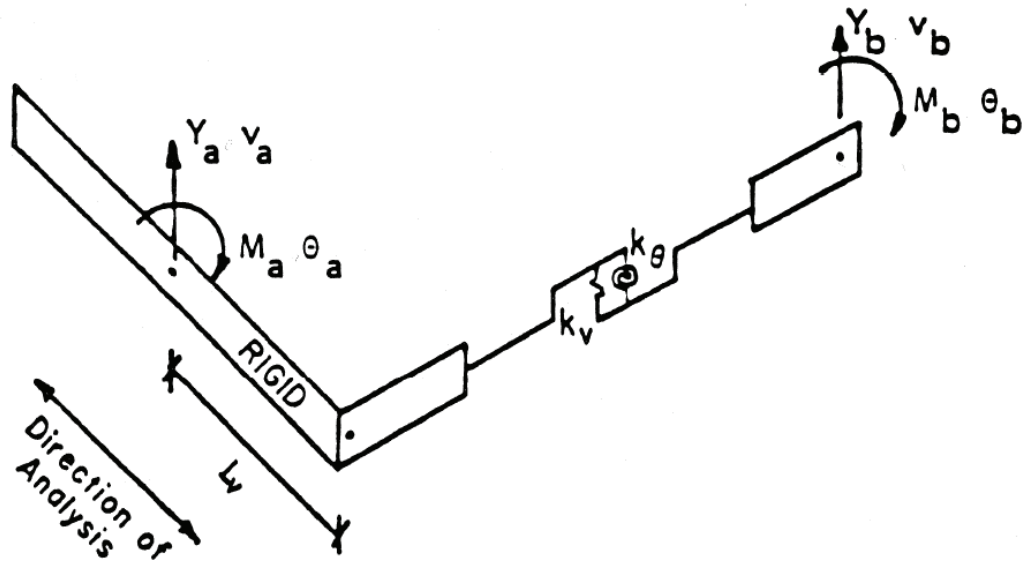


Fig. 4.8 Transverse beam elements

where k_v is the stiffness to vertical relative distortions; L_v is the offset to the center of a shear wall; and k_θ is the torsional stiffness of the transverse beam. When the transverse beam connects two columns the contribution of the shear stiffness may be neglected. These beams are assumed to remain elastic at all times, therefore, k_v and k_θ are constants.

4.8 Rotational Inelastic Spring Elements

Discrete inelastic spring elements may be identified and connected to beam or column element ends, to simulate a flexible or semi-rigid connection in the joint. Figure 4.9 shows four elements framing into a joint with three discrete inelastic springs. In general, more than one spring may be specified at the same location, however, the maximum number of springs that can be used in a particular joint must be one less than the number of elements framing into it. The moment deformation of the spring may be modeled using any of the following hysteretic models described in Section 5:

- a) Trilinear model
- b) Bilinear model
- c) Vertex oriented model
- d) Nonlinear elastic-cyclic model

The stiffness of the rotational spring element may be varied from a small quantity to simulate a hinge, to a large value to simulate a rigid connection. The spring stiffness is incorporated into the overall structural stiffness matrix as follows:

$$\begin{Bmatrix} M_{si} \\ M_f \end{Bmatrix} = k_{\theta i} \begin{bmatrix} 1 & -1 \\ -1 & 1 \end{bmatrix} \begin{Bmatrix} \theta_{si} \\ \theta_f \end{Bmatrix} \quad (4.24)$$

where M_{si} and M_f are the spring “ i ” and the fixed joint moment, respectively; θ_{si}

and θ_f are the corresponding rotations; and k_{θ_i} is the current tangent stiffness of the spring element. Spring rotations are expressed as a function of the fixed joint rotation.

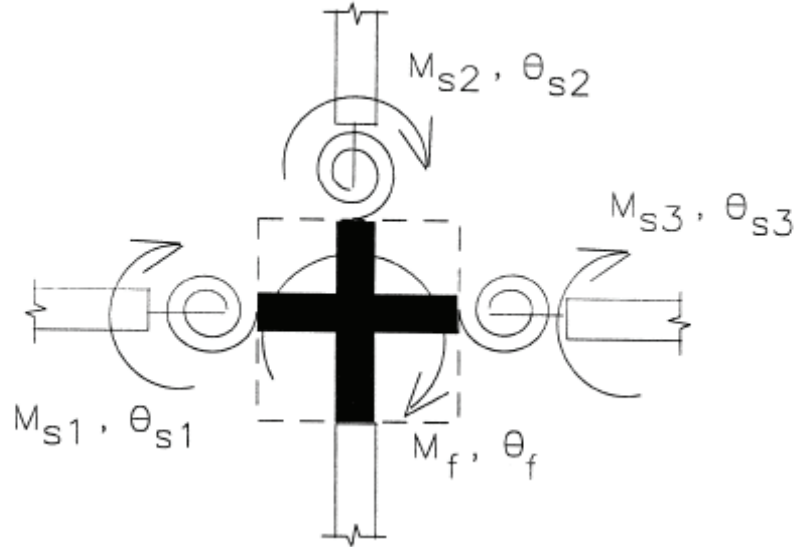


Fig. 4.9 Modeling of discrete inelastic springs

4.9 Visco-Elastic Damper Elements

An innovative approach to reduce earthquake hazard was introduced by adding protective devices to dissipate energy within the structure. Input energy during a seismic event is transformed into hysteretic, potential, damping and hysteretic energy. The performance of structures can be improved if the total energy input is reduced, or an important portion can be dissipated through supplemental damping devices (Reinhorn et al., 1995).

Supplemental damping devices can be broadly classified as viscous dampers, friction dampers, and hysteretic dampers. Viscous dampers exhibit an important velocity dependency. Several types of viscous dampers have been proposed:

- a) Viscoelastic elements
- b) Viscous walls
- c) Fluid viscous dampers

All of these devices can be modeled using a Kelvin Model, a Maxwell model, a Wierchert model, Fractional derivative models, or a convolution model (Reinhorn et al., 1995). The program IDARC includes routines for the Kelvin and Maxwell models. The Maxwell model is recommended when the damper exhibits a strong dependency on the loading frequency.

The above devices are modeled with an axial diagonal element. Forces at the ends of the elements are calculated according to:

$$\begin{Bmatrix} F_a \\ F_b \end{Bmatrix} = F_D \begin{Bmatrix} 1 \\ -1 \end{Bmatrix} \quad (4.25)$$

where F_D is the dynamic stiffness of the element, calculated considering a Kelvin or Maxwell model, as described in Sections 5.4.1 and 5.4.2. The forces in the damper elements are considered using a pseudo force approach, that is, the forces in the dampers are subtracted from the external load vector.

a) Viscoelastic dampers, made of bonded viscoelastic layers (acrylic polymers) have been developed by 3M Company Inc., and have been used in wind and seismic applications: World Trade Center in New York (110 stories), Columbia SeeFirst Building in Seattle (73 stories), the Number Two Union Square Building in Seattle (60 stories), and the General Service Administration Building in San Jose (13 stories). Fig. 4.10 shows a typical damper and an installation detail in a steel structure. See Lobo et al. (1993) for a summary.

b) Viscous Walls, consist of a steel plates moving in highly viscous fluid contained in a thin steel case (wall), as shown in Fig. 4.11. The viscous walls were developed by Sumitomo Construction Company Ltd., and the Building Research Institute in Japan. The devices were investigated by Sumitomo Construction Company (Arima, 1988), and

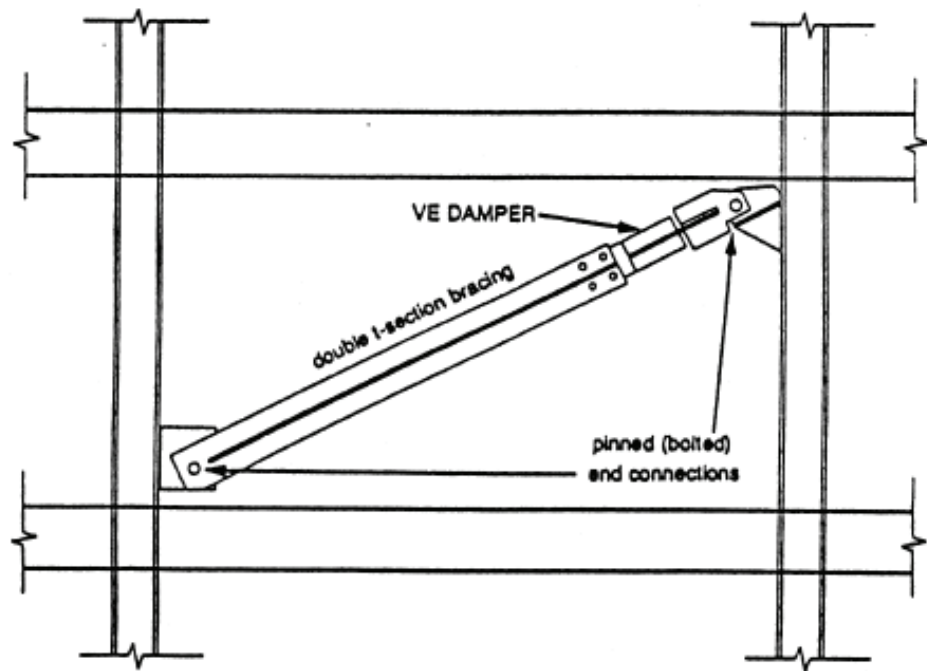
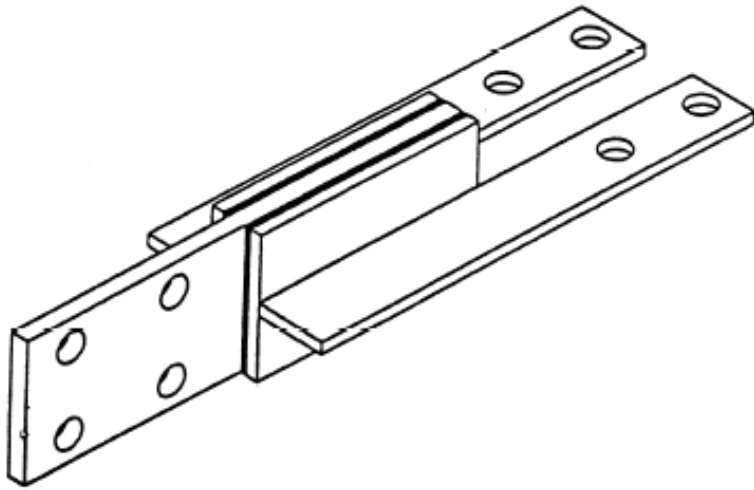


Fig. 4.10 Viscoelastic damper installation detail (from Aiken, 1990)

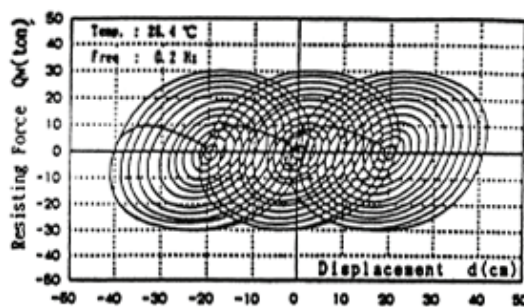
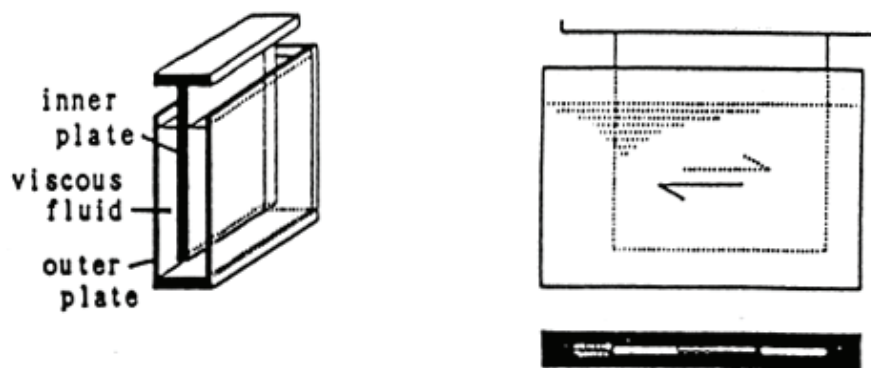


Fig. 4.11 Viscous walls and hysteresis loops (from Miyazaki, 1992)

installed in a 14 story building in Shizuoka city, 150 km west of Tokyo, Japan. Earthquake simulator tests of a 5 story reduced-scale building, a 4 story full-scale steel frame have been carried out (Arima, 1988). More recently, a 3 story 1:3 scale reinforced concrete building has been tested in the Earthquake simulator at the State University of New York at Buffalo (Reinhorn et al., 1994). The devices exhibit a nonlinear viscous behavior with stiffening characteristics at high frequencies (Reinhorn et al., 1995).

c) Fluid Viscous Dampers, have been extensively used in military applications for many years because of their efficiency and longevity. This kind of devices operates on the principle of fluid flow through orifices. The damper was used to reduce recoil forces.

Modern fluid dampers have only recently been used in large scale structural applications. The device is designed to be insensitive to significant temperature changes, and can be designed to exhibit linear or nonlinear viscous behavior (Reinhorn et al., 1995). The size of the device is very compact in comparison to force capacity and stroke. Experimental studies have been recently performed by Constantinou et al. (1993), and by Reinhorn et al. (1995).

4.10 Friction Damper Elements

Friction damper elements are one of the types of supplemental energy dissipation devices that have been introduced to enhance the seismic response of buildings. These types of devices dissipate input energy through frictional work. Several types of friction dampers, or friction like devices, have been proposed:

- a) Friction devices
- b) Lead extrusion devices
- c) Slotted bolted connections

Modeling of these devices is done using a complex self centering model (Reinhorn et al., 1995) without strength or stiffness degradation. Details of the hysteretic model used in IDARC are described in Section 5.5.

The friction devices are modeled with an axial diagonal element. Forces at the ends of the elements are calculated according to:

$$\begin{Bmatrix} F_a \\ F_d \end{Bmatrix} = F_D \begin{Bmatrix} 1 \\ -1 \end{Bmatrix} \quad (4.26)$$

where F_D is the dynamic stiffness of the element, calculated considering the hysteretic model described in Section 5.5. The forces in the damper elements are considered using a

pseudo force approach, that is, the forces in the dampers are subtracted from the external load vector.

- a) **Friction devices**, have been developed and manufactured for many years by Sumitomo Metal Ltd. (see Fig. 4.12). The behavior of the devices are nearly unaffected by amplitude, frequency, temperature, or the number of applied loading cycles (Reinhorn et al., 1995). The original application was in railway rolling stock bogie trucks, but since the mid 1980's the friction dampers were extended to the field of structural and seismic protection. Friction dampers were suggested as displacement control devices for bridge structures with sliding supports made of stainless steel-bronze surface (Constantinou et al., 1991). Recently, friction dampers manufactured by the Tekton company were tested in the seismic simulation laboratory of the State University of New York at Buffalo (Reinhorn et al., 1995). This type of friction dampers is manufactured with simple components to minimize the cost of manufacture. The friction force in the damper can be adjusted through appropriate torque of the bolts that control the pressure on the friction surfaces. A detailed evaluation of the dampers is presented by Li et al. (1995).
- b) **Lead extrusion devices (LED)**, lead extrusion was identified as an effective mechanism for energy dissipation in the 1970's (Robinson and Greenbank, 1976). The hysteretic behavior is similar to a friction device, and shows stable cycles unaffected by the number of loading cycles, environmental factors, or aging (Robinson and Cousins, 1987). Lead extrusion devices have been used in a 10-story base isolated building in Wellington, New Zealand (Charleston et al., 1987), and in seismically isolated bridges (Skinner et al., 1980). In Japan a 17-story and a 8-story building have lead extrusion devices connecting the precast concrete wall panels and the structural frame (Oiles Corp., 1991).
- c) **Slotted bolted connections**, are bolted connections designed to dissipate energy through friction steel plates and bolts (Grigorian and Popov, 1993). The development of slotted bolted connections is to attempt to use simple modifications to standard construction practice and materials widely available.

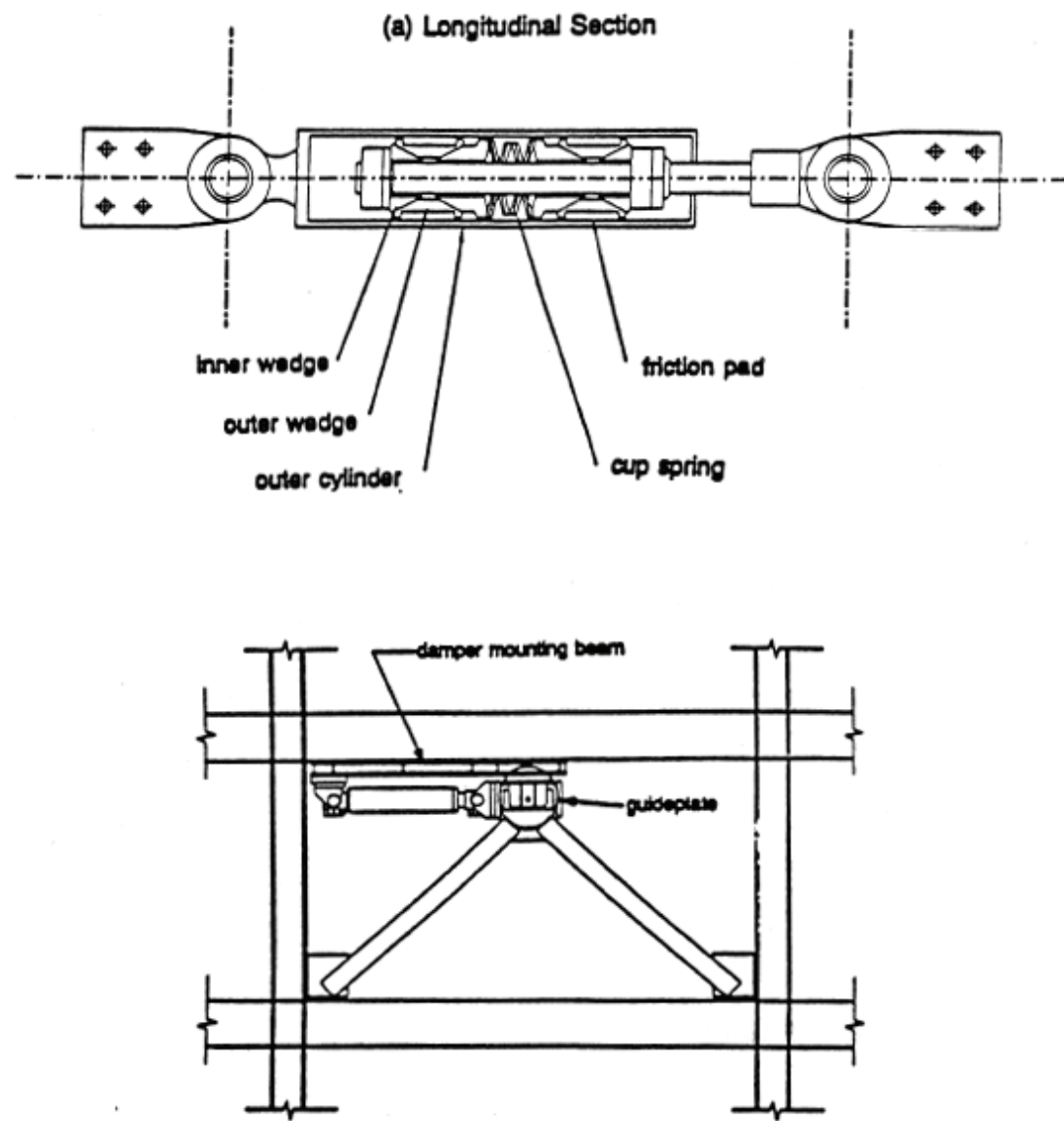


Fig. 4.12 Sumitomo friction damper and installation detail (from Aiken, 1990)

4.11 Hysteretic Damper Elements

Hysteretic damper devices are energy dissipation devices that reduce the dynamic response of structures subjected to earthquake loads. Hysteretic dampers dissipate energy through inelastic yielding of the device components. Several types of hysteretic dampers have been introduced:

- a) Yielding steel elements
- b) Shape memory alloys
- c) Eccentrically braced frames

Most of these devices can be modeled using a complex self centering model (Reinhorn et al., 1995) without strength or stiffness degradation. Details of the hysteretic model used in IDARC are described in Section 5.5.

The hysteretic dampers are modeled with an axial diagonal element. Forces at the ends of the elements are calculated according to:

$$\begin{Bmatrix} F_a \\ F_b \end{Bmatrix} = F_D \begin{Bmatrix} 1 \\ -1 \end{Bmatrix} \quad (4.27)$$

where F_D is the dynamic stiffness of the element, calculated considering the hysteretic model described in Section 5.5. The forces in the damper elements are considered using a pseudo force approach, that is, the forces in the dampers are subtracted from the external load vector.

a) Yielding steel elements, take advantage of the hysteretic behavior of mild steel when deformed in their post-elastic range. The devices exhibit stable behavior, long term reliability, and in general good resistance to environmental and temperature factors. Many of these devices use mild steel plates with triangular or hourglass shapes (Tyler, 1987; Stiemer et al., 1981) so that yielding occurs almost uniformly in the device. One such device, ADAS, uses X-shaped steel plates (Bergman and Goel, 1987; Whittaker et al., 1991). ADAS devices have been installed in a non-ductile reinforced concrete building in San Francisco (Fiero et al., 1993), and in two buildings in Mexico City.

Triangular plate energy dissipators were originally developed and used in base isolation applications (Boardman et al., 1983). The triangular plate concept was extended to building dampers in the form of triangular ADAS, or T-ADAS (Tsai and Hong, 1992). The T-ADAS device does not require rotational restraint at the top of the brace connection assemblage, and there is no potential for instability of the plate due to excessive axial load on the devices.

An energy dissipator for cross braced structures using mild steel round bars or flat plates was developed by Tyler (1985), and used in several industrial warehouses in New Zealand. Variations on the cross bracing device have been developed in Italy (Ciampi, 1991). A 29-story steel suspension building in Naples utilize tapered steel devices between the core and the suspended floors. A six-story government building in Wanganui, New Zealand, uses steel tube energy absorbing devices in precast concrete cross braced panels (Matthewson and Davey, 1979). The devices were designed to yield axially. Recent studies have been carried out to study different cladding connection concepts (Craig et al., 1992).

A number of mild steel energy dissipation devices have been introduced in Japan (Kajima Corp., 1991; Kobori et al., 1988). Honeycomb dampers, formed by X-plates loaded in the plane of the X, have been installed in a 15-story and a 29-story building in Tokyo. Kajima Corporation developed two types of omni-directional steel dampers: Bell dampers and Tsudumi dampers (Kobori et al., 1988). The Bell damper is a single tapered steel tube, and the Tsudumi damper is a double tapered tube intended to deform as an ADAS X-plate. Bell dampers have been used in the massive 1600 ft long artificial ski slope structure to allow for differential movement between four dissimilar parts of the structure under seismic loading. A joint damper between two buildings has also been developed (Sakurai et al., 1992), using a short lead tube loaded to deform in shear.

b) Shape memory alloys, are capable of yielding repeatedly without sustaining any permanent deformation because the material undergoes reversible phase transformations as it deforms rather than intergranular dislocations. Thus, the applied load induces crystal

phase transformations that are reversed when the loads are removed. The devices are therefore self-centering. Several tests with this type of dampers have been carried out: a 3-story steel model was tested with Nitinol (nickel-titanium) tension devices (Aiken et al., 1992), and a 5-story steel model was tested with a copper-zinc-aluminum device (Witting and Cozzarelli, 1992).

c) **Eccentrically braced frames** (EBF), have become a well recognized and widely used structural system for resisting lateral seismic forces. Hysteretic behavior is concentrated in specially designed regions, shear links, and other structural elements are designed to remain elastic under all but the most severe excitations. Extensive research has been devoted to EBF (Roeder et al., 1978; Popov et al., 1987; Whittaker et al., 1987) and the concept has gained recognition and acceptance by the structural engineering profession since the inclusion of design rules into seismic code practice.

4.12 Infill Panel Elements

Infill panel elements were included in the program IDARC using a complex self centering model that connects two stories in the building. Details of the hysteretic model used can be found in Section 5.5. The proposed analytical formulation assumes that the contribution of an infill panel can be modeled using compression struts (see Fig 4.13 for masonry infill element). This assumption is often used in the analysis of Masonry infill panels (Reinhorn et al., 1995d) and other types of infill panels. The formulation for the infill panel element is capable of modeling a variety of panel types by changing the values of the control parameters in the smooth hysteretic model. The masonry infill panels are described with greater detail below.

4.12.1 Masonry Infill Panels

The program is capable of determining the hysteretic parameters for masonry infilled frames. The stress-strain relationship for masonry in compression is commonly

idealized using a parabolic function (Reinhorn et al., 1995d) until the peak stress f_m' is reached, then it is assumed to drop linearly with increasing strains to a small fraction of the peak value, and then remains constant at this value of stress (see Fig. 4.14). The assumed constitutive model for the masonry struts is shown in Fig. 4.15. The struts are considered ineffective in tension, however, the combination of both struts provides resistance in both directions of loading. The lateral force-deformation relationship assumed for the system of compression struts is shown in Fig. 4.16. The analytical formulations for the envelope were developed based on the masonry constitutive model and a recent theoretical model for infilled masonry frames suggested by Saneinejad and Hobbs (1995). The formulations for masonry infilled frames are briefly summarized herein.

Considering the masonry infilled frame shown in Fig. 4.13, the maximum lateral force V_m and the corresponding displacement u_m are calculated as (Saneinejad and Hobbs, 1995):

$$V_m \leq A_d f_m' \cos \theta \quad \text{--- (a)} \quad (4.28)$$

$$\begin{aligned} &\leq \frac{v t l'}{(1 - 0.45 \tan \theta') \cos \theta} \\ &\leq \frac{0.83 (\text{MPa}) t l'}{\cos \theta} \\ u_m &= \frac{\dot{\varepsilon}_m L_d}{\cos \theta} \quad \text{--- (b)} \end{aligned}$$

in which t is the thickness or out-of-plane dimension of the masonry infill panel; f_m' is the masonry prism strength; $\dot{\varepsilon}_m'$ is the corresponding strain; v is the basic shear strength or cohesion of masonry; and A_d and L_d are the area and length of the equivalent diagonal struts obtained from (Saneinejad and Hobbs, 1995):

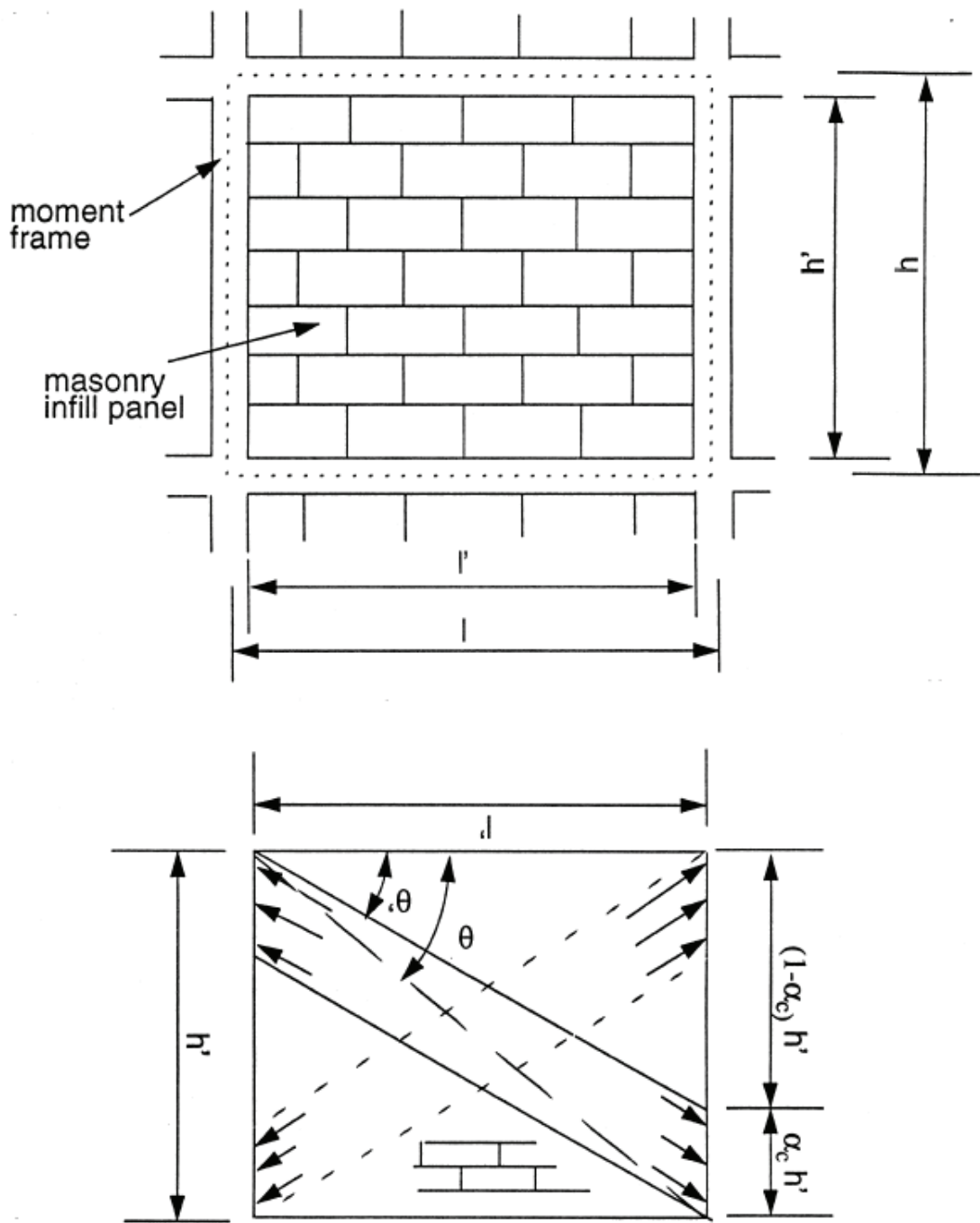


Fig. 4.13 Masonry infill panel: a) Frame subassembly, b) Compression struts

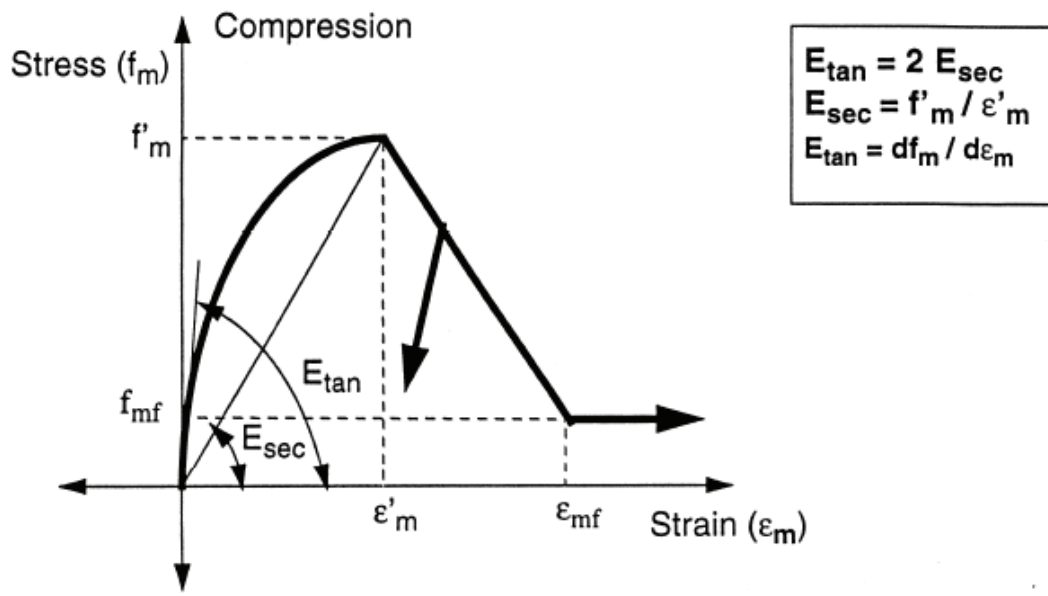


Fig. 4.14 Constitutive model for masonry

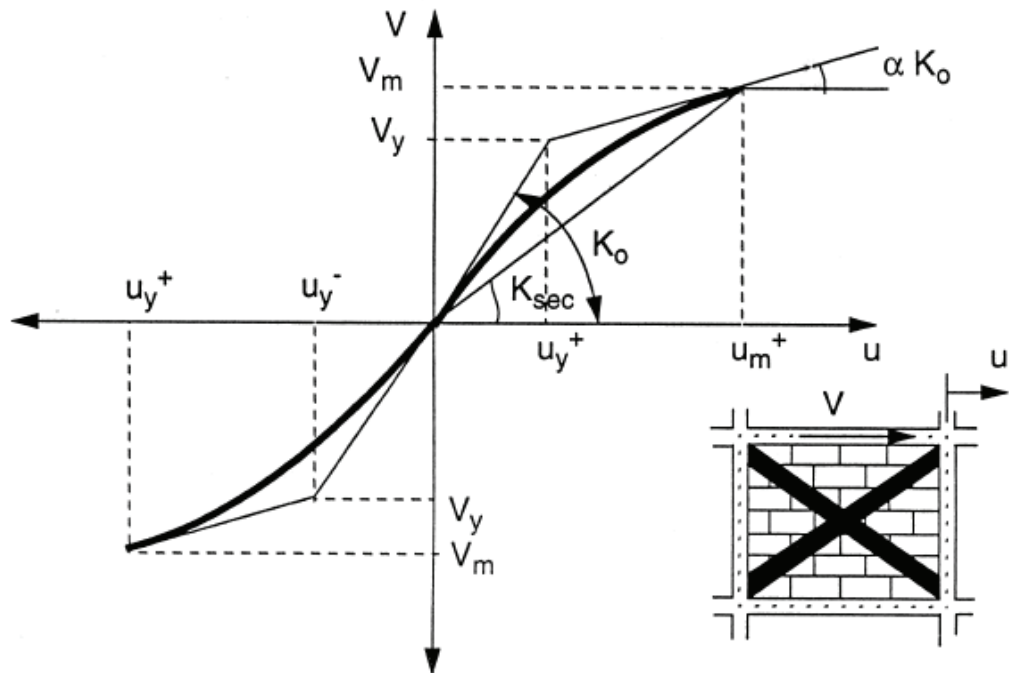


Fig. 4.15 Strength envelope for masonry infill panel

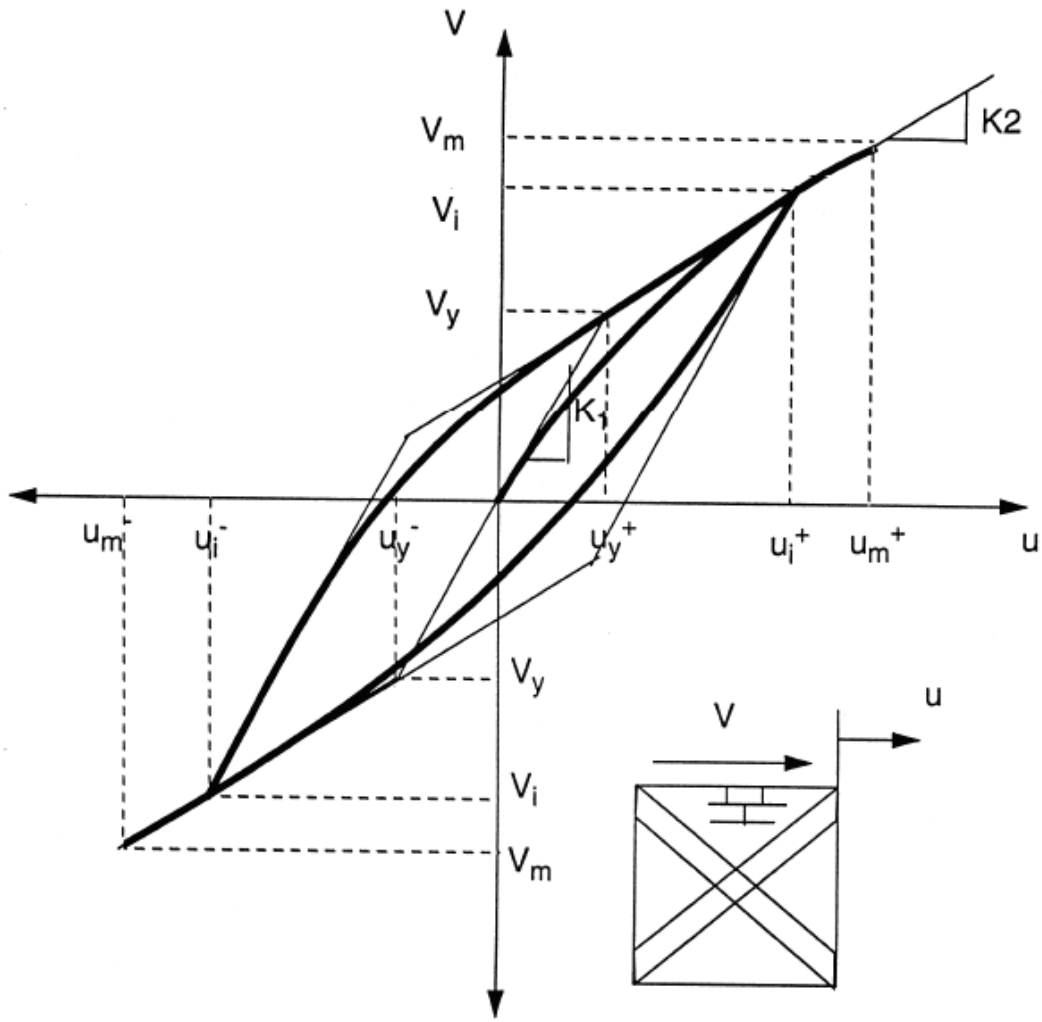


Fig. 4.16 Sivaselvan-Reinhorn model for smooth hysteretic response of infill panels

$$A_d = (1 - \alpha) \alpha_c t h' \frac{\sigma_c}{f_c} + \alpha_b t l' \frac{\tau_b}{f_c} \leq \frac{0.5 t h' (f_a / f_c)}{\cos \theta} \quad \text{---(a)} \quad (4.29)$$

$$L_d = \sqrt{(1 - \alpha)^2 h'^2 + l'^2} \quad \text{---(b)}$$

where the quantities α_c , α_b , σ_c , τ_b , f_a and f_c depend on the geometric and material properties of the frame and the infill panel. The relations used to calculate these quantities are presented in Appendix E.

The monotonic lateral force displacement curve is completely defined by the maximum force V_m , the corresponding displacement u_m , the initial stiffness K_0 and the ratio α of the post-yield to initial stiffness. The initial stiffness K_0 can be estimated using the following relation:

$$K_0 = \frac{V_m}{u_m} \quad (4.30)$$

The lateral yield force and displacement in the masonry infill can be calculated from (Reinhorn et al., 1995d):

$$V_y = \frac{V_m - \alpha K_0 u_m}{1 - \alpha} \quad (a) \quad (4.31)$$

$$u_y = \frac{V_m - \alpha K_0 u_m}{K_0 (1 - \alpha)} \quad (b)$$

A value of 0.1 is suggested for the post-yield stiffness ratio α . The monotonic force deformation model described was extended to account for hysteretic behavior due to loading reversals and strain softening.

A recommended set for the values of the controlling parameters for the hysteretic model described in Section 5.5 are listed in Appendix E. Other values, however, can be used to achieve different hysteretic response characteristics. More information on the solution of hysteretic model with slip is presented in Reinhorn et al. (1995d).

SECTION 5

HYSTERETIC RULES

5.1 Introduction

Modeling the hysteretic behavior of structural elements is one of the core aspects of a nonlinear structural analysis program. The release of IDARC includes two types of complex hysteretic models: the polygonal and smooth hysteretic models.

The Polygonal Hysteretic Model (PHM) refers to models based on piecewise linear behavior. Such models are most often motivated by actual behavioral stages of an element or structure, such as initial or elastic behavior, cracking, yielding, stiffness and strength degrading stages, crack and gap closures etc. One example in this category is the “three-parameter” model (1987). Sivaselvan and Reinhorn (1999) presented a detailed description of the more general framework for PHMs.

The Smooth Hysteretic Model (SHM), on the other hand, refers to models with continuous change of stiffness due to yielding, but sharp changes due to unloading and deteriorating behavior. The Bouc-Wen model (Bouc, 1967; Wen, 1976) and Ozdemir’s model (Ozdemir, 1976) are some examples of SHMs. Sivaselvan and Reinhorn (1999, 2000) developed a new versatile smooth hysteretic model based on internal variables, with stiffness and strength deterioration and with pinching characteristics, that unified many inelastic constitutive models.

The subsequent descriptions of both models incorporated in IDARC2D are based on the detailed report on hysteretic models by Sivaselvan and Reinhorn (1999, 2000).

5.2 Polygonal Hysteretic Model (PHM)

Polygonal Hysteretic Models (PHMs) are also referred to as *multi-linear* models. The PHM may be embodied in the bilinear model, double bilinear model, origin-oriented model, peak-oriented model, slip model, etc. The involved parameters can be assigned explicit physical meanings.

A general framework of *points* and *branches* is developed which can represent any of the aforementioned PHM as a special case, and includes various forms of degradation. This framework, along with the degradation rules, is discussed in the following paragraphs. The reformulation of the polygonal model was done such that the model is controlled by backbone curves specified by the material or structural properties. Furthermore, the cyclic behavior is represented by points and branches, which are functions of the backbone parameters and the current instantaneous forces and deformations. The behavior along a branch and the changes of branches follow a logic tree.

5.2.1 Types of PHM

The IDARC includes the following types of polygonal hysteretic response curves for different structural elements such as columns, beams, shear walls and rotational springs.

5.2.1.1 Trilinear model

The trilinear hysteretic model was first proposed by Park et al. (1987) as part of the original release of IDARC. The hysteretic model incorporates stiffness degradation, strength deterioration, non-symmetric response, slip-lock, and a trilinear monotonic envelope. The model traces the hysteretic behavior of an element as it changes from one linear stage to another, depending on the history of deformations. The model is therefore

piece-wise linear. Each linear stage is referred to as a branch. To capture the response of steel structures, this hysteretic model recommends no stiffness degradation, strength deterioration or slip, since it's intended to capture the loops of structural steel elements. Fig. 5.1 presents the branches of the hysteretic model and typical hysteretic curves.

5.2.1.2 Bilinear model

The commonly used bilinear hysteretic model was also included as an option for various structural elements. Fig. 5.2 presents the branches of the hysteretic model and typical hysteretic curves.

5.2.1.3 Vertex-Oriented model

The vertex-oriented hysteretic model is basically the same as the trilinear hysteretic model except the direction of the hysteretic loops to its previous peak response. For a complete description of the hysteretic model, see Sivaselvan and Reinhorn (1999).

5.2.2 Backbone curves and types of Cyclic Behavior

The PHM has been implemented with two types of backbone curves – bilinear and trilinear, which accommodate cracking models in addition to yielding (Fig. 5.3). With the trilinear backbone curve, the model could have two types of cyclic behavior – yield-oriented with slip and vertex-oriented (Fig. 5.4). In Figure 5.5, primed numbers denote points corresponding to bilinear behavior; double-primed numbers denote points of vertex-oriented behavior. The yield-oriented model with slip is the default and is denoted by unprimed points. The model is formulated in such a way that all of the above types of behavior have the same branch transition rules.

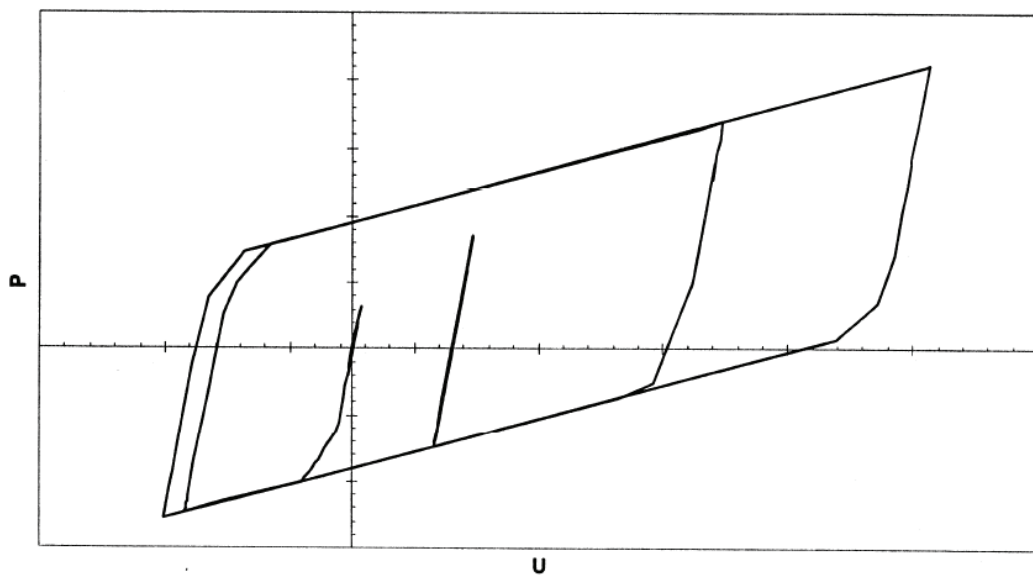
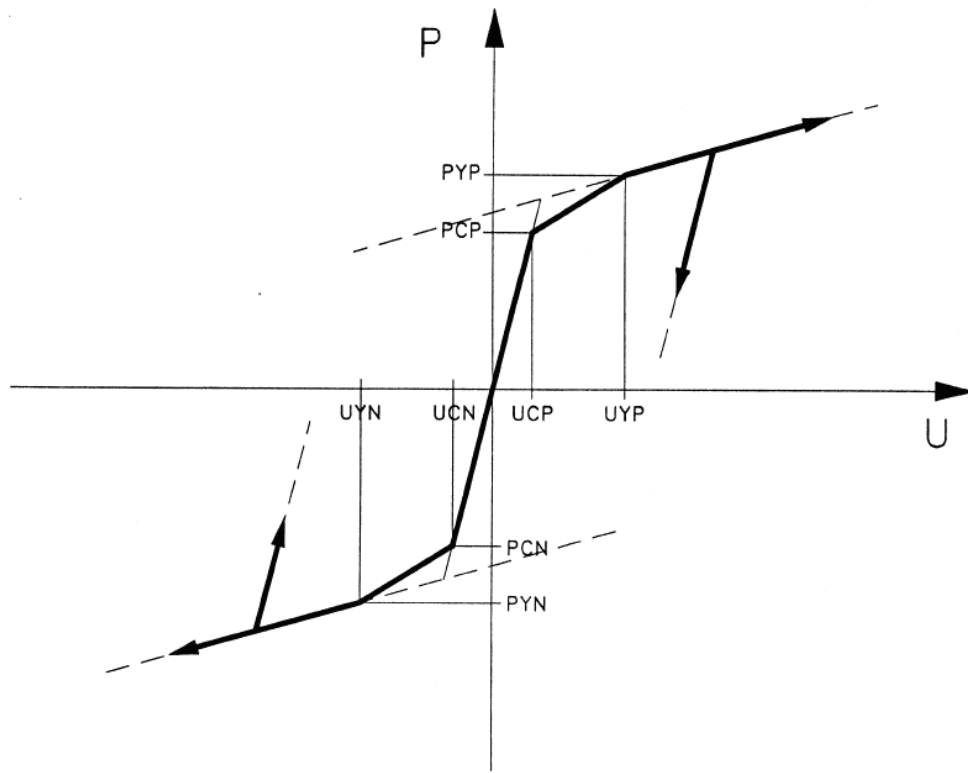


Fig. 5.1 Trilinear hysteretic model

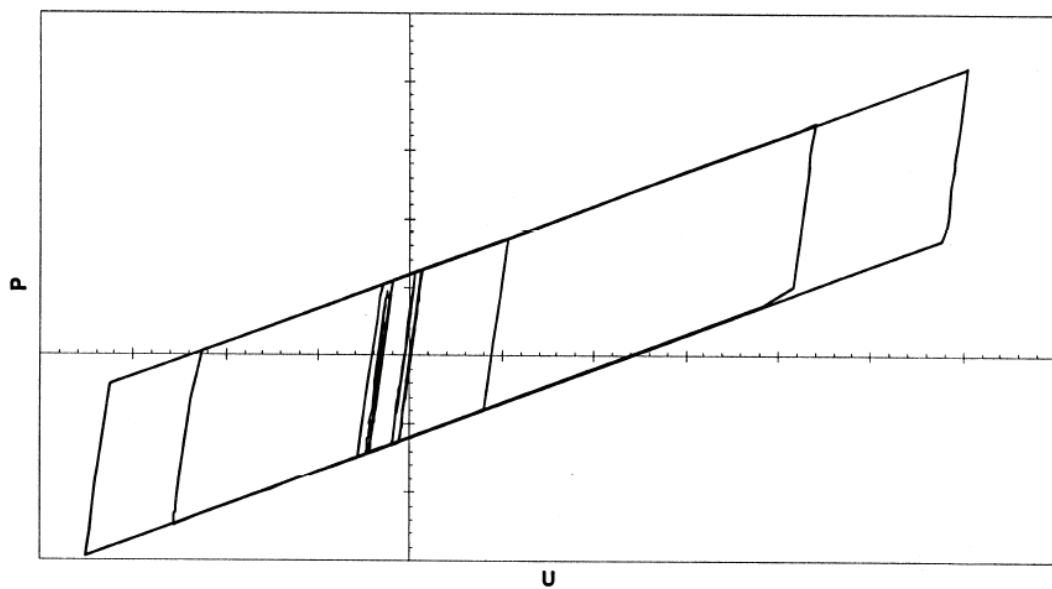
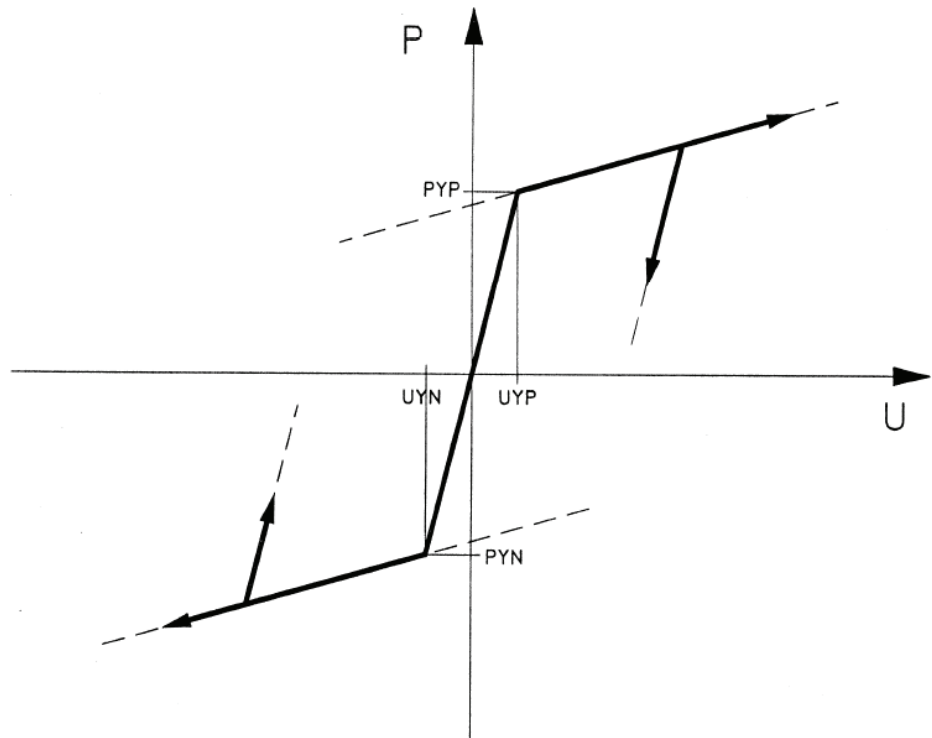


Fig. 5.2 Bilinear hysteretic model

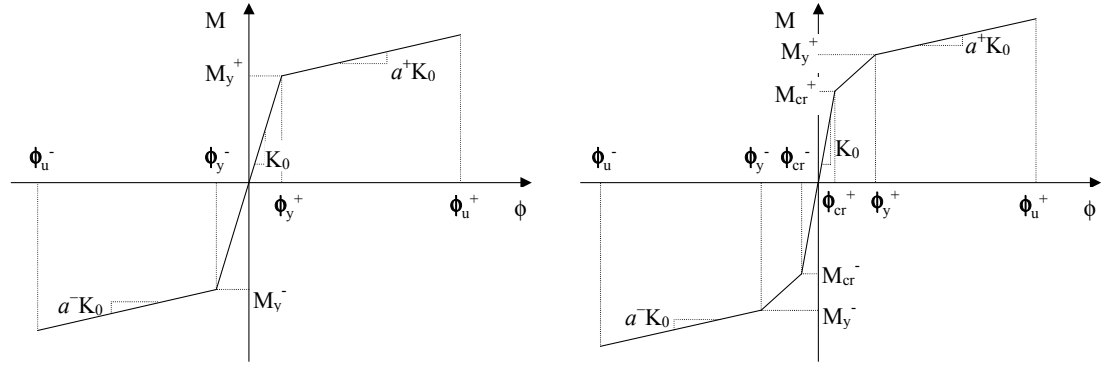


Fig. 5.3 Backbone curves

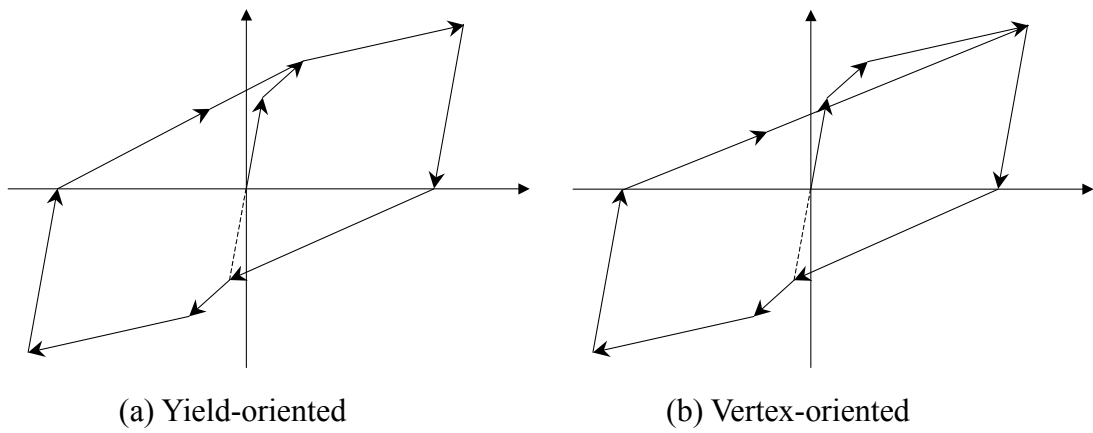


Fig. 5.4 Types of cyclic behavior

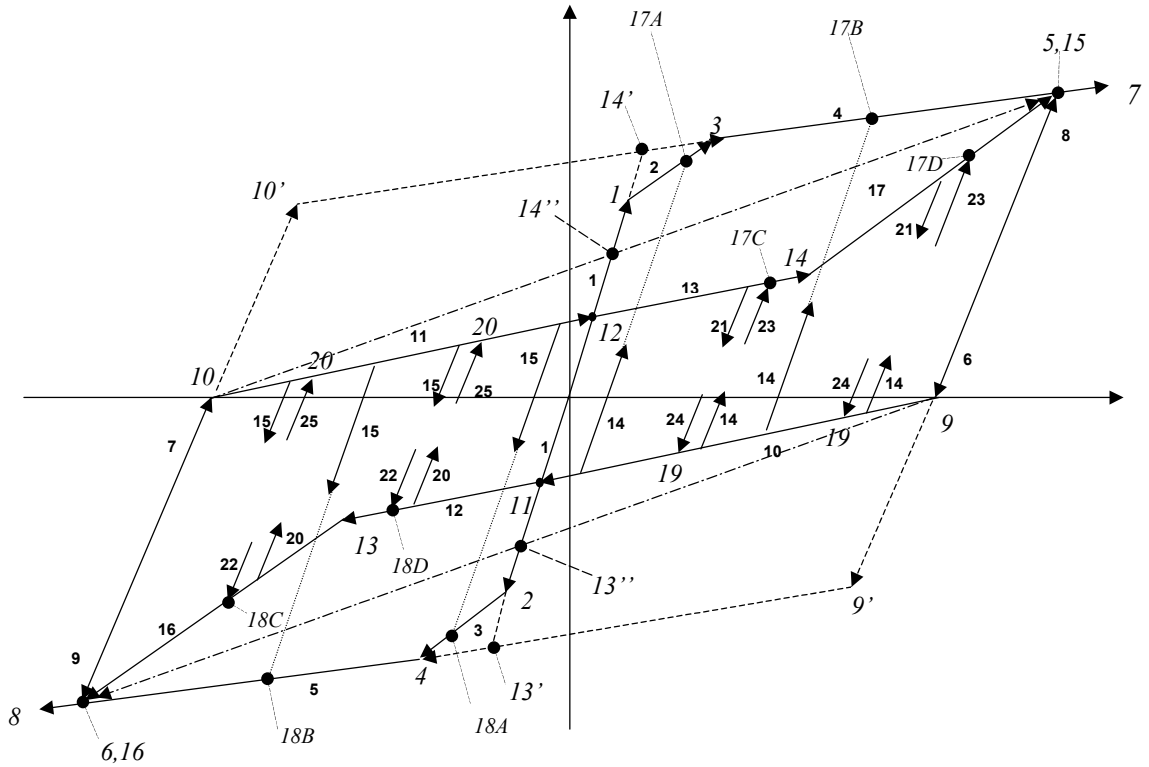


Fig. 5.5 Points and branches of the Polygonal Hysteretic Model (PHM)

5.2.3 “Points” and “Branches”

The state of the entity whose hysteresis is being modeled is completely defined by a set of *database variables*. These database variables are listed in Table D.2 (Appendix). A number of *control points* on the hysteresis loop are completely defined by these database variables and can be calculated given the values of these variables using functions as shown in Table D.3 (Appendix).

Lines between these points are called *branches* and represent the path along the hysteresis loop. Each branch leads to a set of other branches as shown in Table D.4 (Appendix). The end points of the branches are listed in Table D.5 (Appendix). The transitions between branches are governed by a set of rules (logic tree) as shown in Table D.6 (Appendix). The model of Reinhorn and Sivaselvan (1999) uses 21 control points

and 25 branches as shown in Fig. 5.5. Consider for example, unloading from branch 10, as shown in Fig. 5.6(a). In Appendix, the rules of Table D.4 and Table D.6 that govern this transition are depicted in Fig. 5.6(b)~(c).

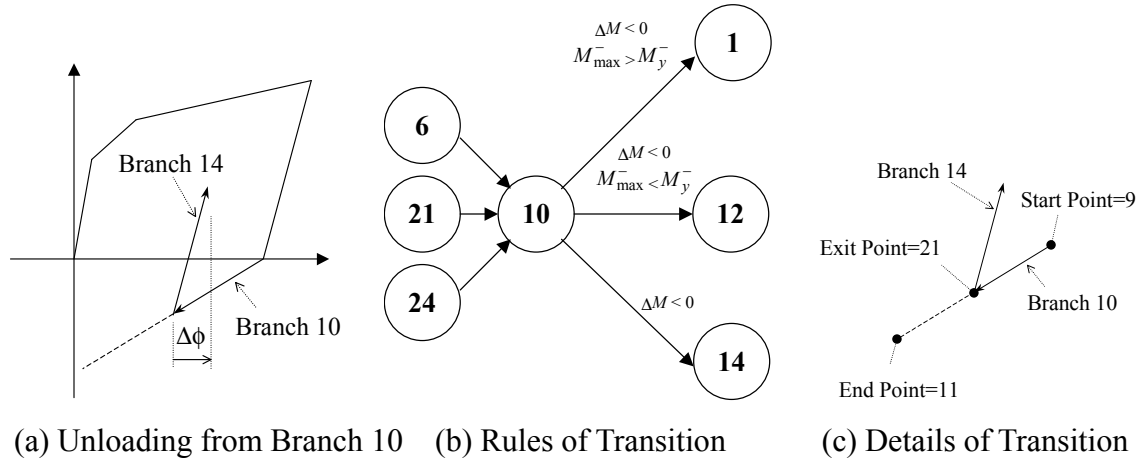


Fig. 5.6 Illustration of branch transition

5.2.4 Operation of the Model – Force Vs. Displacement Control (Moment/Curvature Controlled)

The PHM can be driven in three ways:

Force controlled – An incremental force is applied and the model responds by achieving that force increment and the corresponding displacement increment.

Quasi-Static force controlled – An incremental slowly varying force is given and the corresponding displacement increments are calculated using the stiffness of the current branch. This displacement is applied to the model, and it responds by achieving this displacement increment and returning the difference between the target force and the achieved force (capacity force). This method of driving the model is used while integrating the one-step correction method.

Displacement controlled – An incremental displacement is applied and the model responds by achieving that displacement increment and the corresponding force increment.

5.2.5 Degradation

The modeling of stiffness and strength degradation and pinching are discussed below. The hysteretic energy of PHMs is developed from a yielding moment. Therefore, the loading and unloading paths between cracking and yielding states should be the same.

5.2.5.1 Stiffness Degradation

Stiffness degradation occurs due to geometric effects. The elastic stiffness degrades with increasing ductility. It has been found that the phenomenon of stiffness degradation can be accurately modeled by the pivot rule (Park et al., 1987). According to this rule, the load-reversal branches are assumed to target a pivot point on the elastic branch at a distance of M_y on the opposite side, where α is the stiffness degradation parameter. This is shown in Fig. 5.7. It can be found that the stiffness degradation factor is given by

$$R_K^+ = \frac{M_{cur} + \alpha M_y}{K_0 \phi_{cur} + \alpha M_y} \quad (5.1)$$

where M_{cur} = current moment, ϕ_{cur} = current curvature, K_0 = initial elastic stiffness, α = stiffness degradation parameter, $M_y = M_y^+$ if (M_{cur}, ϕ_{cur}) is on the right side of the elastic branch and $M_y = M_y^-$ if (M_{cur}, ϕ_{cur}) is on the left side of the elastic branch. The current elastic stiffness is given by

$$K_{cur} = R_K K_0 \quad (5.2)$$

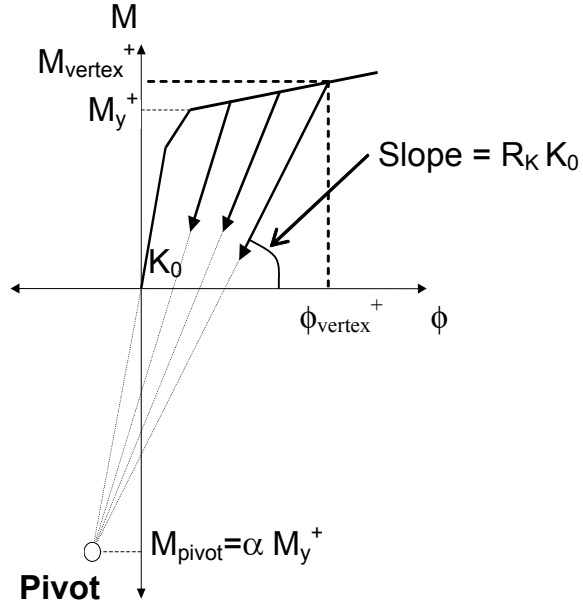


Fig. 5.7 Modeling of stiffness degradation for positive excursion (for negative excursion the “+” sign changes accordingly)

5.2.5.2 Strength Degradation

Strength degradation is modeled by reducing the capacity in the backbone curve as shown schematically in Fig. 5.8. The strength degradation rule is given by:

$$M_y^{+/-} = M_{y0}^{+/-} \left[1 - \left(\frac{\phi_{\max}^{+/-}}{\phi_u^{+/-}} \right)^{\frac{1}{\beta_1}} \right] \left[1 - \frac{\beta_2}{1 - \beta_2} \frac{H}{H_{ult}} \right] \quad (5.3)$$

where $M_y^{+/-}$ = positive or negative yield moment, $M_{y0}^{+/-}$ = initial positive or negative yield moment, $\phi_{\max}^{+/-}$ = maximum positive or negative curvature, $\phi_u^{+/-}$ = positive or negative ultimate curvature, H = hysteretic energy dissipated, H_{ult} = hysteretic energy dissipated when loaded monotonically to the ultimate curvature without any degradation, β_1 = ductility-based strength degradation parameter and β_2 = energy-based the strength degradation parameter.

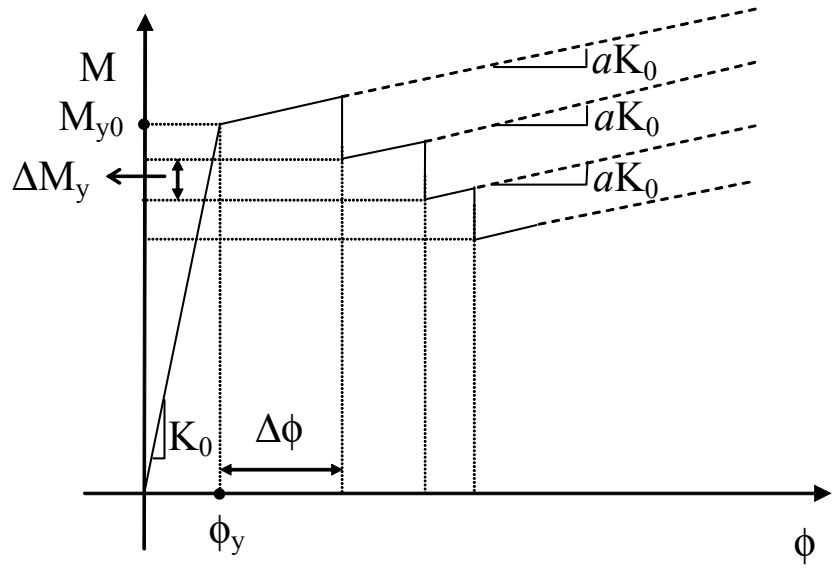


Fig. 5.8 Schematic representation of strength degradation in the PHM

The second term on the right-hand side of Eq. 5.3 represents strength degradation due to increased deformation, and the third term represents strength degradation due to hysteretic energy dissipated. The increment of the hysteretic energy is given by

$$\Delta H = \left[\frac{M + (M + \Delta M)}{2} \right] \left(\Delta\phi - \frac{\Delta M}{R_K K_0} \right) \quad (5.4)$$

5.2.5.3 Pinching or Slip

Slip or pinching occurs as a result of crack closure, bond slip, bolt slip, etc. Slip is modeled by defining the target point for the loading branch to be the crack closing point. The force level corresponding to this point is a fraction of the yield moment given by $F\gamma = \gamma F_y$ and the deformation level is obtained as a weighed average of the yield and ultimate deformations as shown in Fig. 5.9. The variable γ is the slip parameter.

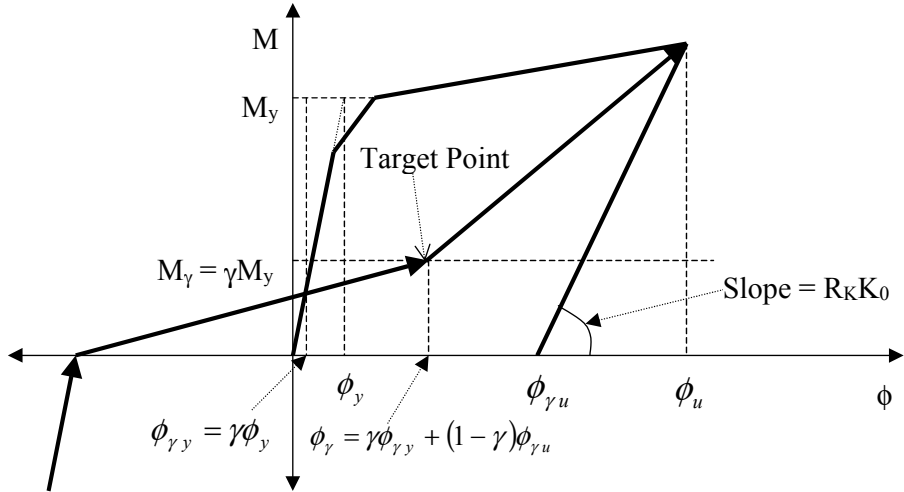


Fig. 5.9 Modeling of slip

5.2.5.4 Algorithm and Implementation

The PHM is implemented using a number of subroutines. These and their functions as well as the algorithms of these subroutines are listed in Figs. D.1~D.4 and Table D.1 (Appendix).

5.2.6 Nonlinear Elastic-Cyclic Model (NECM)

Nonlinear Elastic-Cyclic Model (NECM) assumes that the behavior of the element follows the same path for both loading and unloading without loss of energy. The nonlinear elastic model (NECM) is used to simulate the structural elements providing a nonlinear elastic behavior without noticeable hysteresis and thus very little equivalent hysteretic damping as compared to a conventional column. A detailed description of a general framework for the NECM is presented in Roh (2007).

5.2.6.1 Backbone Curves and Types of Cyclic Behavior

The nonlinear elastic-cyclic model is based on the backbone curve of for trilinear model. This model is governed by *branches* that occur during the response and *rules* that

d dictate the transitions between various branches. A general framework of *points* and *branches* is developed similar to Sivaselvan and Reinhorn (1999) and added to the existing framework so it can represent any of the aforementioned NECM. The behavior along a branch and the changes follow a logic tree. The nonlinear elastic-cyclic model is added to the polygonal hysteretic model (PHM) which was developed and implemented by Sivaselvan and Reinhorn (1999). With the trilinear backbone curve, the model could have two types of cyclic behavior – with “negative stiffness behavior” as shown in Fig. 5.10 and without “negative stiffness behavior” as shown in Fig. 5.11. In the figures, ϕ_{ns} is the curvature starting “negative stiffness behavior”, ϕ_u is the ultimate curvature at the total loss of strength, and M_u is the corresponding moment which is an imaginarily extended moment from yielding point. The “negative stiffness behavior” is as a matter of strength degradation due to stability reasons such as overturning motion or material recoverable losses.

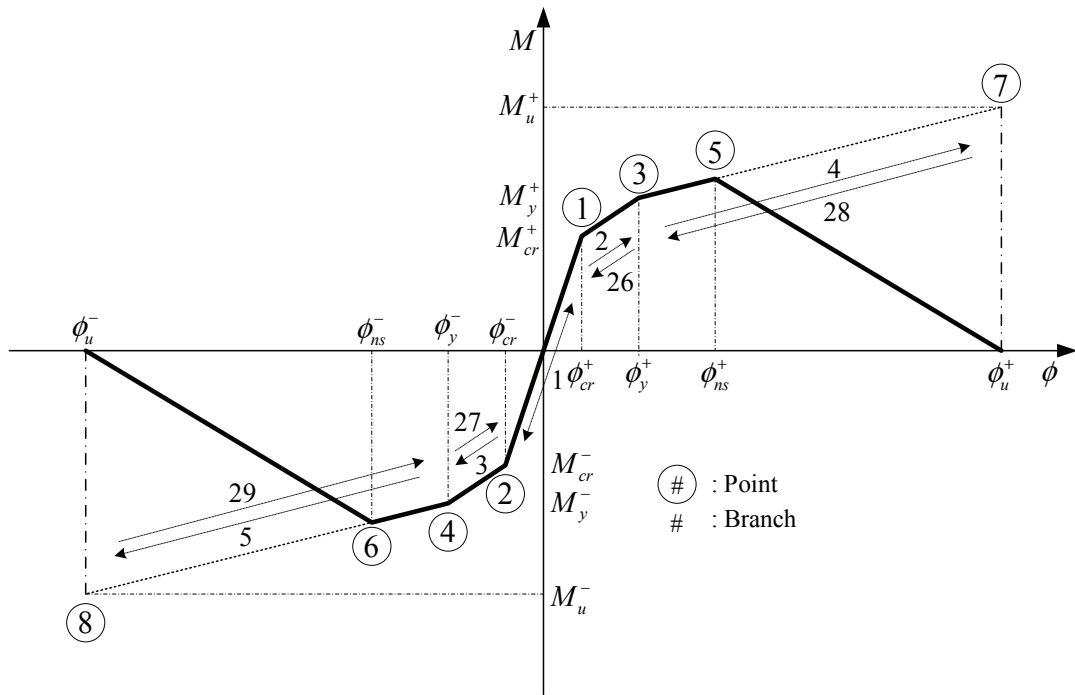


Fig. 5.10 Points and Branches of Nonlinear Elastic-Cyclic Model (NECM) with “negative stiffness”

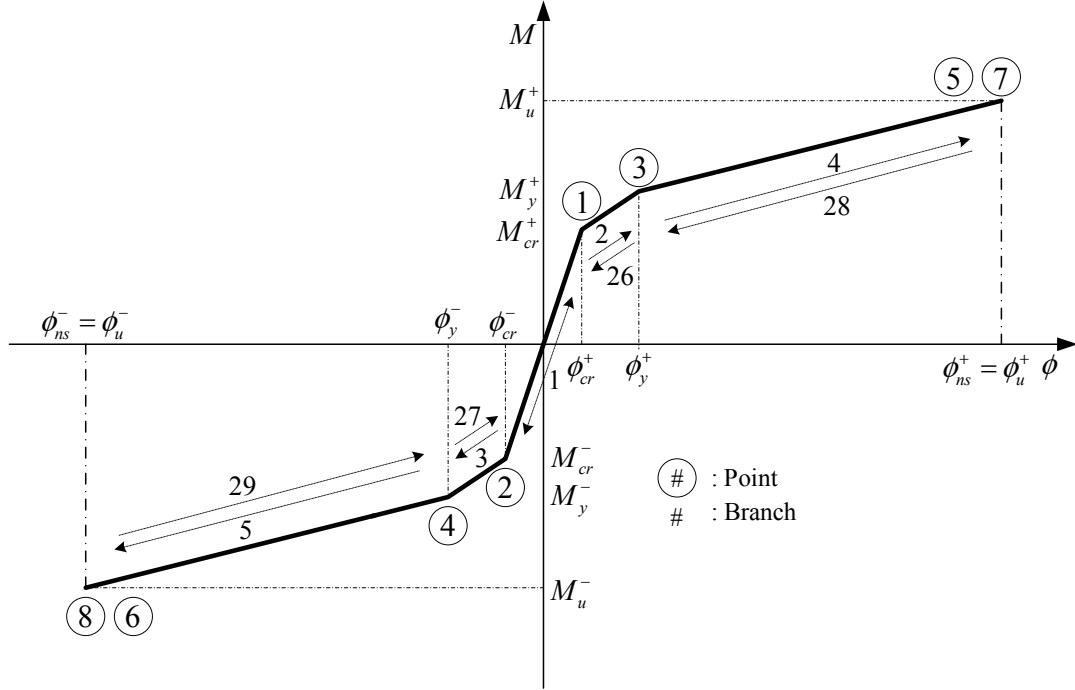


Fig. 5.11 Points and Branches of Nonlinear Elastic-Cyclic Model (NECM) without “negative stiffness”

5.2.6.2 NECM with “Negative Stiffness” Behavior

Figure 5.12 shows the tri-linear moment-curvature envelope curve and a schematic configuration for modeling of the “negative stiffness” range. The model called here the “stepwise strength reduction” provides a successive reduction of the apparent yielding moment, when the curvature exceeds the envelope limits. The result is a stepwise reduction of strength until reaching zero resistance associated with complete “collapse” or “overturning”. Assuming that M_u is the initial ultimate moment, $M_{u\Delta}$ is the reduced ultimate moment, M_y is the initial yield moment, and $M_{y\Delta}$ is the reduced yield moment. The reduced ultimate moment, $M_{u\Delta}$, is obtained by projecting the envelope at the ultimate curvature as follows:

$$M_{u\Delta} = M_{y\Delta} + (\phi_u - \phi_y) EI_3 \quad (5.5)$$

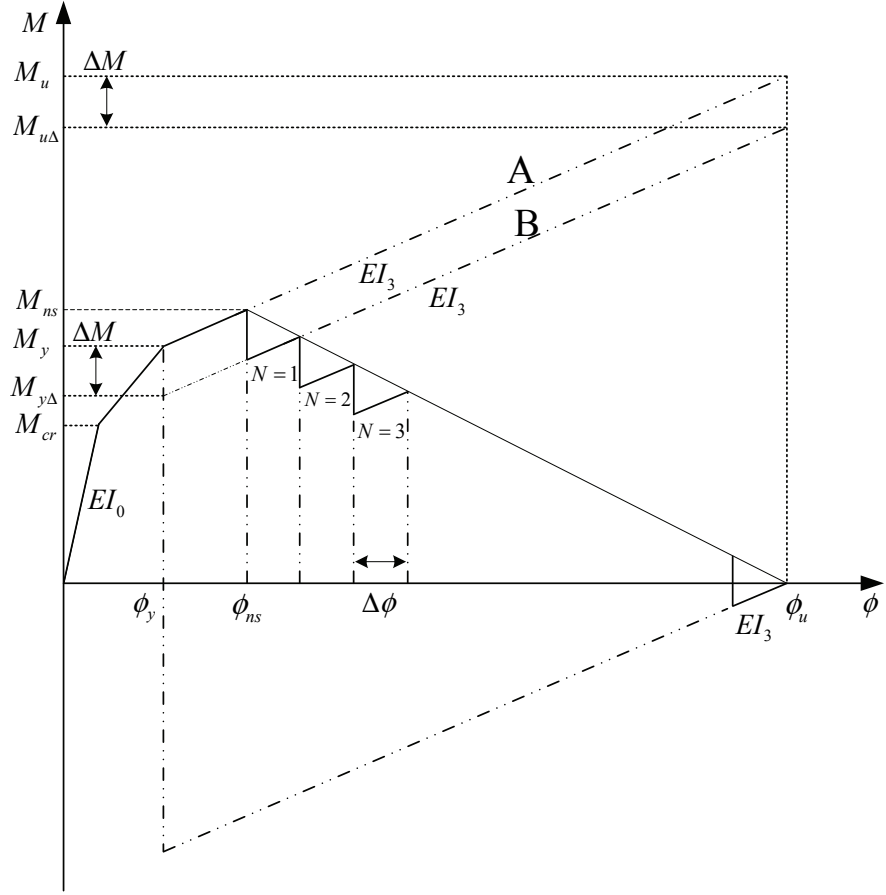


Fig. 5.12 Stepwise strength reduction model in “negative stiffness” range

The strength reduction is given by $M_{y\Delta} = M_y - \Delta M$. Herein, ΔM is the gradual moment reduction. When the yield moment is reduced, the ultimate moment is also reduced accordingly as shown in Eq. 5.5. The cracking moment M_{cr} does not change. In modeling of the “negative stiffness” stage, a curvature-control is adopted because this value increases consistently. When the curvature at the ends reaches the curvature starting the “negative stiffness” behavior, the yield moment is reduced by a certain quantity depending on $\Delta\phi$. The curvature increment after the onset of negative stiffness stage is

$$\Delta\phi = \frac{\phi_u - \phi_{ns}}{n} \quad (5.6)$$

where n is the total number of steps of “degradation” to be performed from the onset of

negative point to the ultimate point. Assume the incremental curvature step, $N = (\phi_{cur} - \phi_{ns} / \Delta\phi) + 1$, where N represents the step number (integer), $1 \leq N \leq n$. The moment reduction ΔM is calculated as

$$\Delta M = \frac{N\Delta\phi}{\phi_u - \phi_{ns}} M_{ns} + EI_3(N\Delta\phi) \quad (5.7)$$

where M_{ns} is the moment starting negative behavior, which is defined as $M_y + EI_3(\phi_{ns} - \phi_y)$. The same moment reduction is also applied to the ultimate state as shown in Fig. 5.12. Therefore, the envelope curve is changed from A to B. However, after the reduction of the end moments, the stiffness remains with the same positive value. This is important since it allows the use of the same solution algorithms in each step. The procedure using small incremental curvatures is continued until the curvature reaches the maximum ultimate and the moment resistance becomes zero.

The moment reduces with increased lateral displacement due to strength reduction. Also, the shear capacity at every story is also reduced. The reduction of story shear can be obtained using displacement-control or force-control. When displacement-control is used, the story shear reduction is not considered because the control of the curvature has a unique moment. However, for force-control, a shear force reduction procedure is required because of the reduced story shear at the level where the rocking columns have reacted the negative stiffness stage. The external force must be reduced as much as the reduced story shears to ensure that the total capacity is not exceeded and to capture the apparent negative stiffness. In current version of IDARC2D, the external forces, for concentrated, inverted triangular, uniform, and story height proportional lateral load distributions in nonlinear incremental static (pushover) analysis and quasi-static cyclic analysis, are decreased uniformly in all stories above the one in which a story shear reduction develops. For modal adaptive pushover analysis, the external force is proportionally decreased depending on the mode shapes considered. For dynamic

analyses, the solution is performed using one step “unbalanced force” correction (Park et al., 1987; Valles et al., 1996). A detailed description regarding to the unbalanced force correction is addressed in Roh (2007).

5.2.6.3 NECM without “Negative Stiffness” Behavior

From Fig. 5.10 which represents the cyclic behavior with “negative stiffness” behavior, the NECM without negative slope is achieved by extending the *points* 5 and 6 to the *points* 7 and 8 as shown in Fig. 5.11. The model is formulated in such a way that the above type of behavior has the same branch transition rules.

5.2.6.4 “Points” and “Branches”

The cyclic model is defined by a set of branches and rules (Sivaselavan and Reinhorn, 1999). It uses a database of variables listed in Table D.7 (Appendix). A number of control points on the loop are completely defined by these database variables. The control points are calculated using the functions shown in Table D.7 (Appendix). The points are defined by the circle numbers. The points 3 to 8 in Figs. 5.10~5.11 are variables. The variation rules of these points are described in Table D.8 (Appendix). Lines between these points are defined as branches and represent the cyclic loop path. Several new branches are added to the existing branches, and are defined as 26, 27, 28, and 29. Each branch leads to a set of other branches as shown in Table D.9 (Appendix). The end points of the branches are listed in Table D.10 (Appendix). The transitions between branches are governed by the set of rules as shown in Table D.11 (Appendix).

5.2.6.5 Operation of the Model – Force Vs. Displacement Control (Moment/Curvature Controlled)

The NECM can be implemented in two ways:

Force-control: An incremental force is applied. The model responds by achieving that force increment and the corresponding displacement increment are calculated. However, the applied force should be reduced when the structural elements are experiencing the strength reduction in the negative stiffness range. Force-control is used in Nonlinear Incremental Static (Pushover), Quasi-Static Cyclic, and Nonlinear Dynamic analyses.

Displacement-control: An incremental displacement is applied. The model responds by achieving that displacement increment and the corresponding force increment is calculated. Displacement-control is applied to Nonlinear Incremental Static (Pushover) and Quasi-Static Cyclic analyses.

5.2.6.6 Algorithm and Implementation

The Nonlinear Elastic-Cyclic Model (NECM) is implemented using a number of subroutines which are the same as the Polygonal Hysteretic Model (PHM) listed in Figs. D.1~D.4 and Table D.1 (Appendix).

5.2.7 Examples

Examples of various types of hysteretic behavior modeled by the PHM including the NECM are shown in Fig. 5.13.

5.3 Smooth Hysteretic Model (SHM, Sivaselvan and Reinhorn model)

The IDARC includes the smooth hysteretic response curves for different structural elements such as columns, beams, shear walls, and rotational springs. The smooth model discussed by Sivaselvan and Reinhorn (1999) is a comprehensive variation of the model originally proposed by Bouc (1967) and modified by several others (Wen, 1976; Baber and Noori, 1985; Casciati, 1991; Reinhorn et al., 1995c; Madan et al., 1997). The hysteretic energy of SHMs is developed from a yielding moment-curvature behavior.

Therefore, the loading and unloading paths between cracking and yielding states should be the same.

5.3.1 Plain Hysteretic Behavior without Degradation

Plain hysteretic behavior with post yielding hardening is modeled using two springs as shown in Fig. 5.14. When a moment is applied to the combination of springs, the two springs undergo the same deformation curvature. However, the springs share the applied moment in proportion to their instantaneous stiffness. The portion of the applied moment shared by the hysteretic spring is denoted by M^* .

5.3.2 Spring 1: Post-yield Spring

This is a linear elastic spring with the post-yielding stiffness of

$$K_{post-yield} = aK_0 \quad (5.8)$$

where K_0 = initial stiffness (elastic) and a = the ratio of post-yielding stiffness to the initial.

5.3.3 Spring 2: Hysteretic Spring

The hysteretic spring is a purely elasto-plastic spring with a smooth transition from the elastic to the inelastic range. All degradation phenomena occur in this spring and are described later in this section. The stiffness of this spring when it is non-degrading is given by

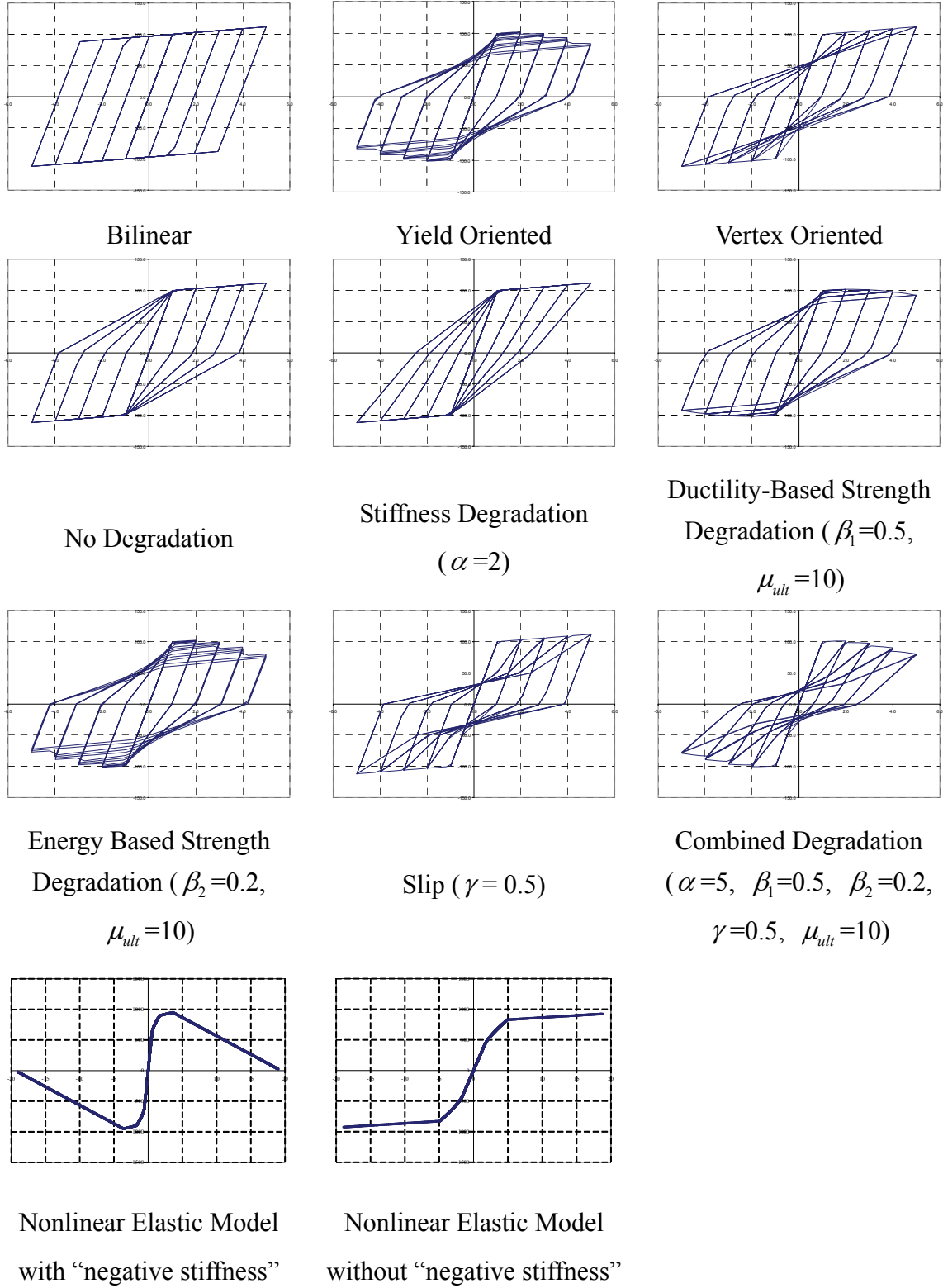


Fig. 5.13 Examples of hysteretic behavior modeled by the PHM

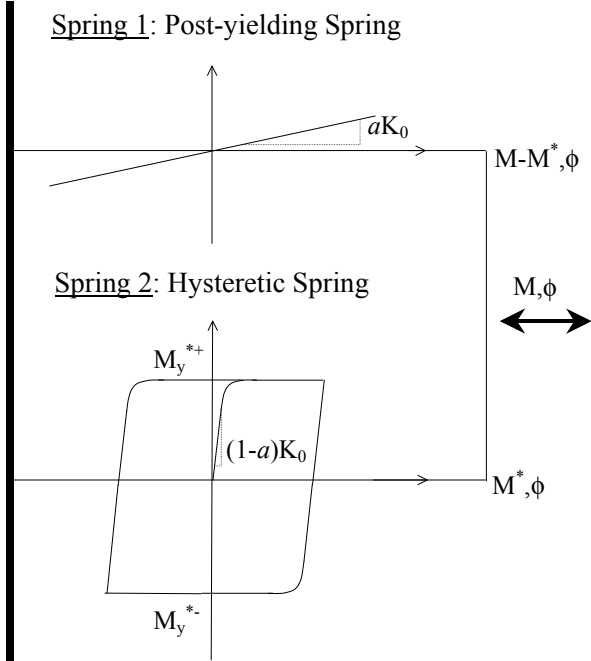


Fig. 5.14 Two-spring model for non-degrading hysteretic behavior

$$K_{hysteretic} = (1 - a)K_0 \left\{ 1 - \left| \frac{M^*}{M_y^*} \right|^N \left[\eta_1 \operatorname{sgn}(M^* \dot{\phi}) + \eta_2 \right] \right\} \quad (5.9)$$

where N is parameter controlling the smoothness of the transition from elastic to inelastic range, $\eta_1 = \eta$ is a parameter controlling the shape of the unloading curve, $\eta_2 = 1 - \eta$, $\phi_0 = \phi - \frac{M^*}{(1 - a)K_0}$, M^* is the portion of the applied moment shared by the hysteretic spring, $M_y^* = (1 - a)M_y$ is the yield moment of the hysteretic spring and $\operatorname{sgn}(x)$ is the signum function ($= +1$ for $x \geq 1$, $= -1$ for $x \leq -1$). $\eta_1 + \eta_2 = 1$ for the model to be compatible with plasticity.

Asymmetry can be modeled by defining

$$M_y^* = (1 - a) \left[\left(\frac{1 + \operatorname{sgn}(\dot{\phi})}{2} \right) M_y^+ + \left(\frac{1 - \operatorname{sgn}(\dot{\phi})}{2} \right) M_y^- \right] \quad (5.10)$$

where M_y^+ and M_y^- are the positive and negative yield moments respectively. The combined stiffness is given by,

$$K = K_{post-yield} + K_{hysteretic} \quad (5.11)$$

The SHM is represented by:

$$\dot{M} = K\dot{\phi} \quad (5.12)$$

5.3.4 Degradation

The stiffness and strength degradation rules for the SHM are the same as those for the PHM. They have been modified to fit the formulation of the SHM.

5.3.4.1 Stiffness Degradation

As mentioned earlier, stiffness degradation occurs only in the hysteretic spring. Thus the pivot rule is applied only to the hysteretic spring and the resulting hysteretic stiffness is given by

$$K_{hysteretic} = (R_K - a)K_0 \left\{ 1 - \left| \frac{M^*}{M_y^*} \right|^N [\eta_1 \operatorname{sgn}(M^* \dot{\phi}) + \eta_2] \right\} \quad (5.13)$$

where R_K = stiffness degradation factor given by Eq. 5.1.

5.3.4.2 Strength Degradation

The differential equations governing strength degradation in the SHM can be obtained by differentiating Eq. 5.3.

$$\frac{dM_y^{+/-}}{dt} = M_{y0}^{+/-} \left\{ \begin{aligned} & \left[1 - \frac{\beta_2}{1-\beta_2} \frac{H}{H_{ult}} \right] \left[-\frac{1}{\beta_1 (\phi_u^{+/-})^{\frac{1}{\beta_1}}} (\phi_{max}^{+/-})^{\frac{1-\beta_1}{\beta_1}} \right] \dot{\phi}_{max}^{+/-} \\ & + \left[1 - \left(\frac{\phi_{max}^{+1}}{\phi_u^{+/-}} \right)^{\frac{1}{\beta_1}} \right] \left[-\frac{\beta_2}{(1-\beta_2) H_{ult}} \right] \dot{H} \end{aligned} \right\} \quad \text{---(a)}$$

Writing Eq. 5.4 in the form of a differential equation, we have

$$\dot{H} = M \left(\dot{\phi} - \frac{\dot{M}}{R_K K_0} \right) = M \dot{\phi} \left[1 - \frac{(K_{post-yield} + R K_{hysteretic})}{R_K K_0} \right] \quad \text{---(b) (5.14)}$$

The evolution equations for the maximum positive and negative curvatures can be written as

$$\dot{\phi}_{max}^+ = \dot{\phi} U(\phi - \phi_{max}^+) U(\dot{\phi}) \quad \text{---(c)}$$

$$\dot{\phi}_{max}^- = \dot{\phi} U(\phi_{max}^- - \phi) (1 - U(\dot{\phi})) \quad \text{---(d)}$$

where $U(x)$ is the Heaviside step function ($=1$ for $x > 0$, $= 0$ for $x < 0$). The differential Eqs. 5.14(a)~(d) govern strength degradation in the SHM.

5.3.4.3 Pinching or Slip

To model this effect, an additional spring called the slip-lock spring (Baber and Noori, 1985; Reinhorn et al., 1995) is added in series to the hysteretic spring. The

resulting combination is shown in Fig. 5.15. The stiffness of the slip-lock spring can be written as

$$K_{Slip-Lock} = \left\{ \sqrt{\frac{2}{\pi}} \frac{s}{M_\sigma^*} \exp \left[-\frac{1}{2} \left(\frac{M^* - \bar{M}^*}{M_\sigma^*} \right)^2 \right] \right\}^{-1} \quad (5.15)$$

where s (slip length) = $R_s (\phi_{\max}^+ - \phi_{\max}^-)$; $M_\sigma^* = \sigma M_y^*$, a measure of the moment range over which slip occurs; $\bar{M}^* = \lambda M_y^*$, the mean moment level on either side about which slip occurs; R_s , σ and λ are parameters of the model and ϕ_{\max}^+ and ϕ_{\max}^- are the maximum curvatures reached on the positive and negative sides respectively during the response. It is chosen to be a Gaussian type distribution so that, $\int_{-\infty}^{\infty} \frac{1}{K_{slip-lock}} dM = s$, the slip length. Any other convenient distribution fulfilling this

condition could be chosen for the slip-lock stiffness.

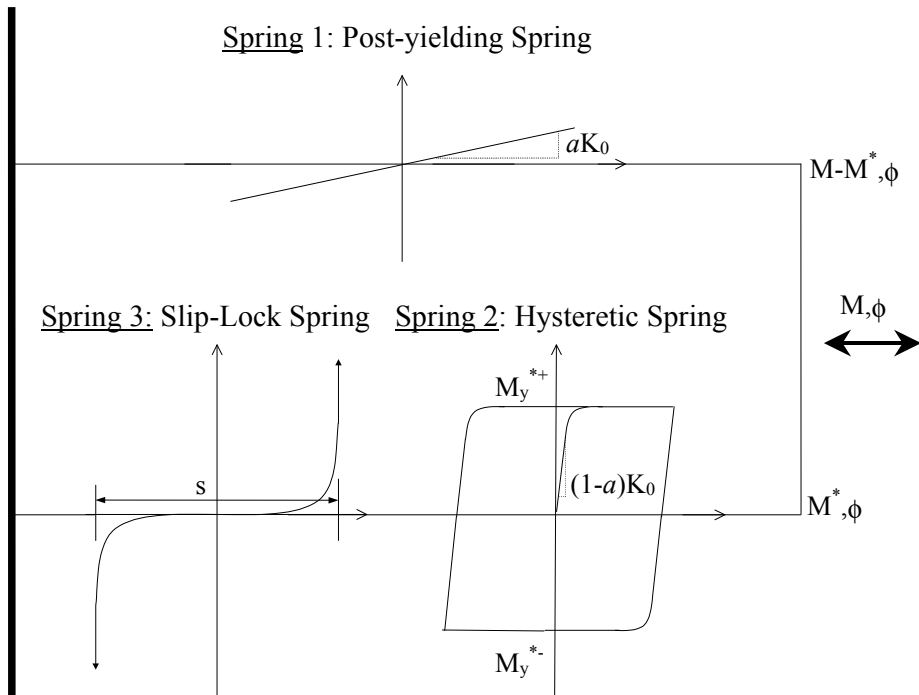


Fig. 5.15 Three-spring model for hysteretic behavior with slip

The stiffness of the combined system is given by

$$K = K_{post-yield} + \frac{K_{Hysteretic} K_{slip-lock}}{K_{slip-lock} + K_{Hysteretic}} \quad (5.16)$$

5.3.4.4 Gap Closing Behavior

Often, hysteretic elements exhibit stiffening under higher deformations. This happens for example in metallic dampers (Soong and Dargush, 1997) when axial behavior begins to predominate bending behavior and in bridge isolators (Reichman and Reinhorn, 1995; Priestley and Calvi, 1996) due to closing of the expansion gaps. Such behavior can be modeled by introducing an additional gap-closing spring in parallel as shown in Fig. 5.16.

The moment in this spring and the stiffness of this spring are given by

$$M^{**} = \kappa K_0 N_{gap} (|\phi| - \phi_{gap})^{N_{gap}-1} U(|\phi| - \phi_{gap}) \quad (a)$$

$$K_{gap-closing} = \kappa K_0 N_{gap} (|\phi| - \phi_{gap})^{N_{gap}-1} U(|\phi| - \phi_{gap}) \quad (b)$$

where M^{**} is the moment in the gap-closing spring, $K_{gap-closing}$ is the stiffness of the gap-closing spring, ϕ_{gap} is the gap-closing curvature, U is the Heaviside step function and κ and N_{gap} are parameters.

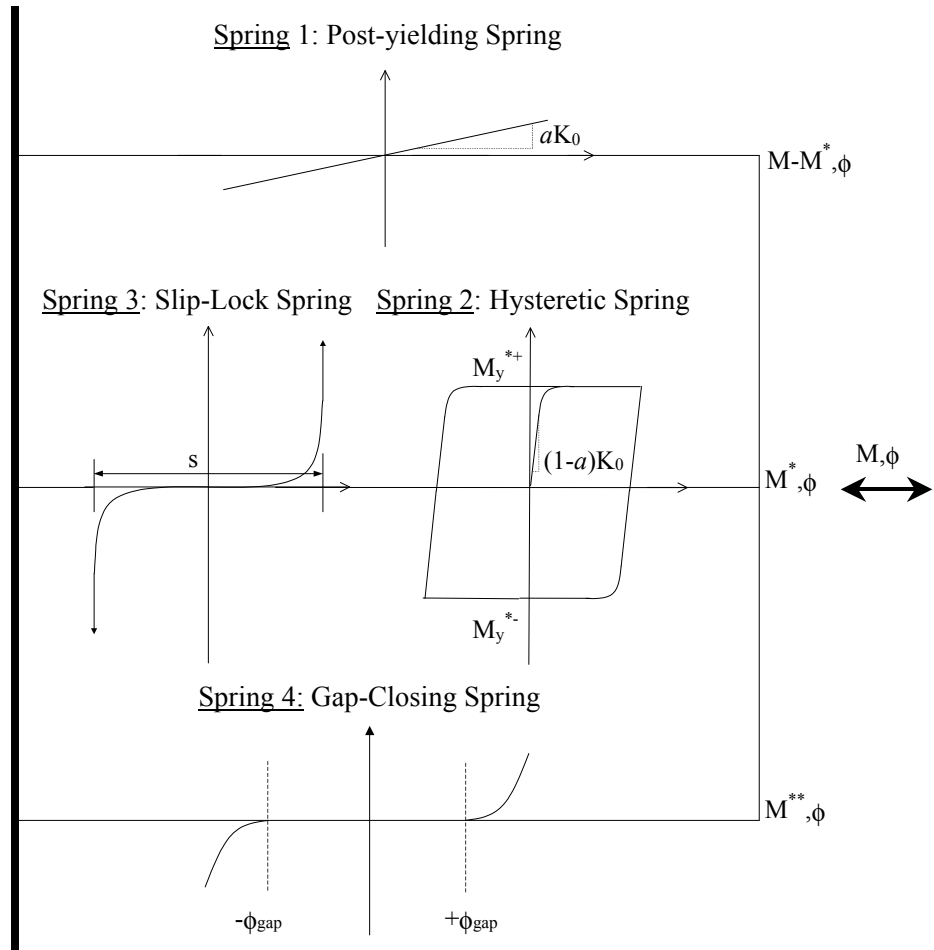


Fig. 5.16 Gap-closing spring in parallel

5.3.4.5 Solution of the SHM

There are two possible approaches to solving the equations governing the SHM –

(i) The conventional incremental approach and (ii) the State-Space Approach (SSA). Equations 5.12 and 5.14 can be used directly in the latter solution approach. However, only the former approach will be discussed here as implemented in the current version of IDARC2D. For this purpose, Eqs. 5.12 and 5.14 have to be written in time-independent manner. Also, since the post-yielding and gap-closing springs are algebraic, only the hysteretic and slip-lock springs are solved and the results added. This results in the following time-independent differential equations within a global time step:

$$\frac{dM^*}{d\phi} = \frac{K_{Hysteretic} K_{slip-lock}}{K_{slip-lock} + K_{Hysteretic}} \quad \text{---(a)}$$

$$\frac{dM_y^{*+}}{d\phi} = M_y^{*0+} \left\{ \begin{aligned} & \left[1 - \frac{\beta_2}{1-\beta_2} \frac{H}{H_{ult}} \right] \left[-\frac{1}{\beta_1 (\phi_u^+)^{\frac{1}{\beta_1}}} (\phi_{max}^+)^{\frac{1-\beta_1}{\beta_1}} \right] U(\phi - \phi_{max}^+) U(\Delta\phi) \\ & + \left[1 - \left(\frac{\phi_{max}^+}{\phi_u^+} \right)^{\frac{1}{\beta_1}} \right] \left[-\frac{\beta_2}{1-\beta_2} \frac{1}{H_{ult}} \right] M^* \left[1 - \frac{1}{(1-a)R_K K_0} \frac{K_{Hysteretic} K_{slip-lock}}{K_{slip-lock} + K_{Hysteretic}} \right] \end{aligned} \right\} \quad \text{---(b)}$$

$$\frac{dM_y^{*+}}{d\phi} = M_y^{*0-} \left\{ \begin{aligned} & \left[1 - \frac{\beta_2}{1-\beta_2} \frac{H}{H_{ult}} \right] \left[-\frac{1}{\beta_1 (\phi_u^-)^{\frac{1}{\beta_1}}} (\phi_{max}^-)^{\frac{1-\beta_1}{\beta_1}} \right] U(\phi_{max}^- - \phi) [1 - U(\Delta\phi)] \\ & + \left[1 - \left(\frac{\phi_{max}^-}{\phi_u^-} \right)^{\frac{1}{\beta_1}} \right] \left[-\frac{\beta_2}{1-\beta_2} \frac{1}{H_{ult}} \right] M^* \left[1 - \frac{1}{(1-a)R_K K_0} \frac{K_{Hysteretic} K_{slip-lock}}{K_{slip-lock} + K_{Hysteretic}} \right] \end{aligned} \right\} \quad \text{---(c)} \quad (5.18)$$

$$\frac{d\phi_{max}^+}{d\phi} = U(\phi - \phi_{max}^+) U(\Delta\phi) \quad \text{---(d)}$$

$$\frac{d\phi_{max}^-}{d\phi} = U(\phi_{max}^- - \phi) [1 - U(\Delta\phi)] \quad \text{---(e)}$$

$$\frac{dH}{d\phi} = M^* \left[1 - \frac{1}{(1-a)R_K K_0} \frac{K_{Hysteretic} K_{slip-lock}}{K_{slip-lock} + K_{Hysteretic}} \right] \quad \text{---(f)}$$

Equation 5.18 can be solved within each global integration step using any method such as the adaptive RK45 (Runge-Kutta 4/5 ODE solver with variable step size) or the Semi-implicit Rosenbrock methods (Nagarajaiah et al., 1989; Press et al., 1992).

5.3.5 Examples

Examples of various types of hysteretic behavior modeled by the SHM are shown in Fig. 5.17. For more comparisons between behavior predicted by the SHM and experimental results see.

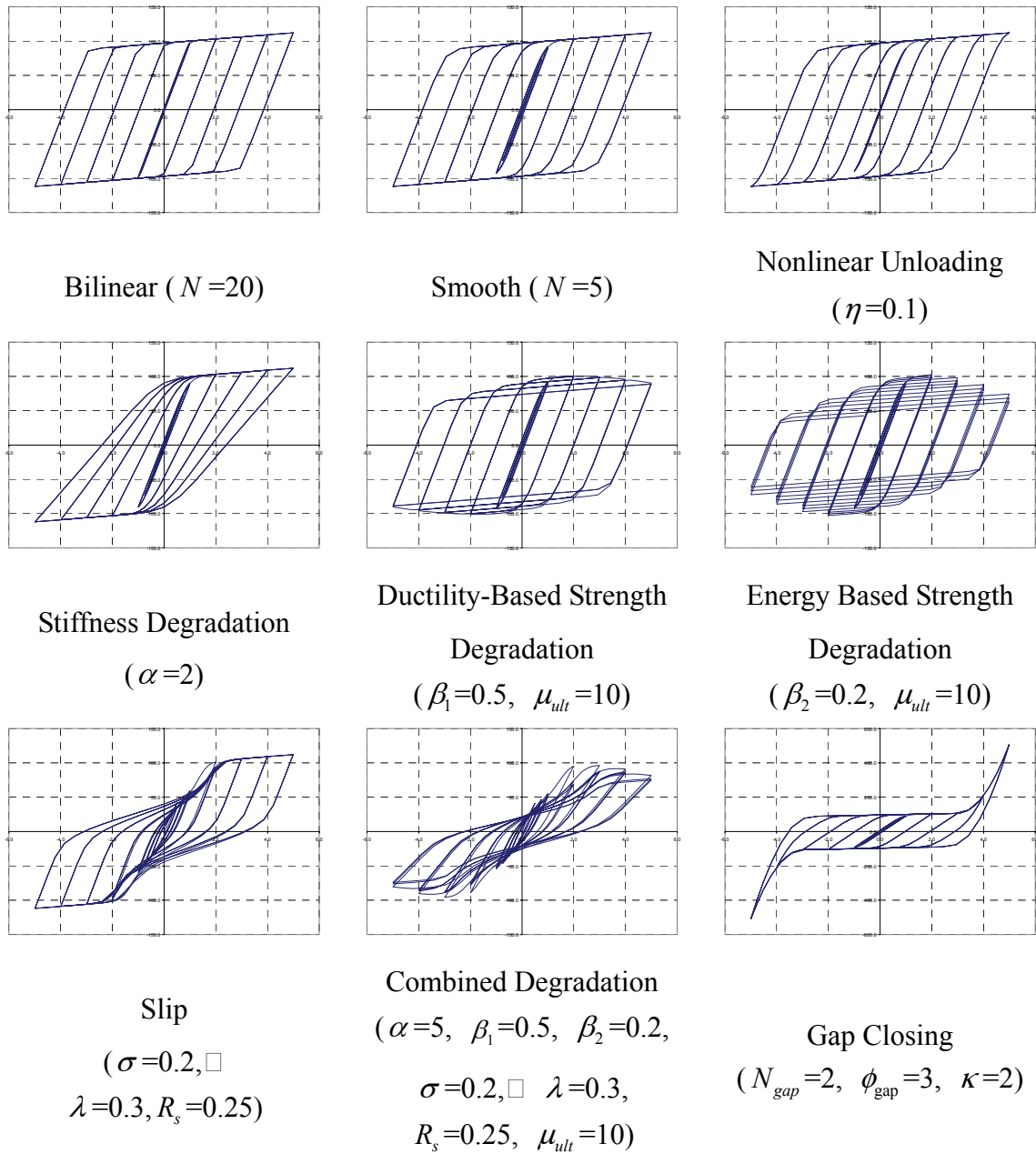


Fig. 5.17 Examples of Hysteretic behavior modeled by the SHM

5.4 Visco-Elastic Models

The behavior of Viscous Elastic (VE) dampers can be modeled using a Kelvin or a Maxwell models (Reinhorn et al., 1995a).

5.4.1 Kelvin Model

The Kelvin model includes the contribution of a stiffness element, and a linear viscous damper (see Fig. 5.18). The force displacement relation of a Kelvin element is:

$$F_d(t) = Ku(t) + Ci\dot{u}(t) \quad (5.19)$$

where $u(t)$ and $\dot{u}(t)$ are the relative displacement and velocity of the damper; K is the damper storage stiffness; and C is the damping coefficient.

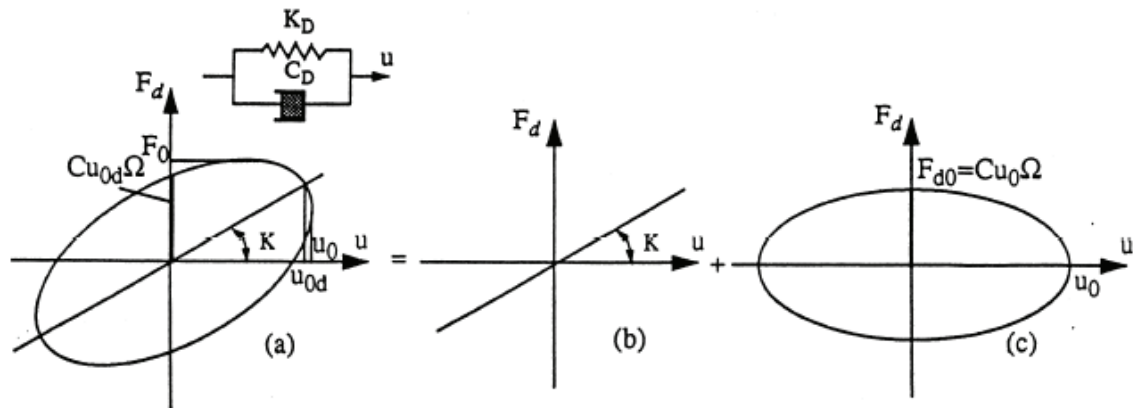


Fig. 5.18 Kelvin model: a) Damper behavior b) Linear stiffness component c) linear damping component

Considering the response of a damper element to a harmonic motion, the properties of the damper can be identified (Constantinou and Symans, 1992). Consider that the damper is subjected to a harmonic motion:

$$u(t) = u_0 \sin \Omega t \quad (5.20)$$

The force in the linear viscous element is:

$$F_v(t) = Cu_0\Omega \cos \Omega t \quad (5.21)$$

Eliminating time, force and displacements are related according to:

$$\left(\frac{F_v}{C\Omega u_0}\right)^2 + \left(\frac{u}{u_0}\right)^2 = 1 \quad (5.22)$$

that represents an ellipse with amplitude u_0 and $C\Omega u_0$ (see Fig. 5.18(c)). The energy dissipated by the viscous element is obtained by equating the area in the ellipse:

$$W_d = \pi C\Omega u_0^2 \quad (5.23)$$

The damping coefficient is therefore:

$$C = \frac{W_d}{\pi\Omega u_0^2} \quad (5.24)$$

Form the total element force, the following relation between force and displacements is obtained:

$$\left(\frac{F_d}{C\Omega u_0}\right)^2 + \left(\frac{u}{u_0}\right)^2 \left[1 + \left(\frac{K}{C\Omega}\right)^2 - 2 \left(\frac{K}{C\Omega}\right)^2 \left(\frac{F_0}{C\Omega u_0}\right)^2 \left(\frac{u_0}{u}\right)^2 \right] = 1 \quad (5.25)$$

The stiffness coefficient is therefore:

$$K = \frac{F_0}{u_0} \left[1 - \left(\frac{C\Omega u_0}{F_0}\right)^2 \right]^{1/2} \quad (5.26)$$

Most damping devices display frequency dependency properties, therefore, the stiffness and damping characteristics calculated in Eqs. 5.24 and 5.26 are dependent on the testing frequency Ω . Frequency dependency of the Kelvin model can be determined by Fourier transformation of Eq. 5.19:

$$F_d(\omega) = K(\omega)u(\omega) + i\omega C(\omega)u(\omega) \quad \text{---(a)} \quad (5.27)$$

or:

$$F_d(\omega) = [K_1(\omega) + iK_2(\omega)]u(\omega) = K^*(\omega)u(\omega) \quad \text{---(b)}$$

where the complex stiffness $K^*(\omega)$ has a real component, $K_1(\omega)$, known as the “storage” stiffness; and an imaginary component, $K_2(\omega)$ defined as the “loss” stiffness:

$$K_2(\omega) = \omega C(\omega) \quad (5.28)$$

In the current version of the computer program IDARC, the forces in the viscoelastic Kelvin elements are determined as:

$$F_{Di} = k_i u_i + c_i \dot{u}_i \quad (5.29)$$

in which k_i and c_i can be obtained for each device using Eqs. 5.24 and 5.26; and u_i and \dot{u}_i are the relative displacements and velocities in the damper “ i ” that can be obtained from the global displacement and velocity configurations of the structure. The force in dampers with identical properties can be modeled as:

$$\{F_D\} = [\Delta K]\{u\} + [\Delta C]\{\dot{u}\} \quad (5.30)$$

where $[\Delta K]$ and $[\Delta C]$ are the changes in the stiffness and damping matrices due to the addition of dampers. For damping braces with identical properties throughout the building, these matrices are:

$$[\Delta K] = k_i [\mathbf{B}] ; \quad [\Delta C] = c_i [\mathbf{B}] \quad (5.31)$$

where k_i and c_i are the properties of the base damper, and matrix $[\mathbf{B}]$ is a “location” matrix indicating the inclination of braces and the number of braces at each location. For the identical dampers case, this matrix is:

$$[\mathbf{B}] = \begin{bmatrix} N_j \cos^2 \theta_j & -N_j \cos^2 \theta_j & & \\ -N_j \cos^2 \theta_j & N_j \cos^2 \theta_j + -N_{j-1} \cos^2 \theta_{j-1} & -N_{j-1} \cos^2 \theta_{j-1} & \\ & & -N_3 \cos^2 \theta & \\ N_3 \cos^2 \theta_3 + N_2 \cos^2 \theta_2 & & & \\ -N_2 \cos^2 \theta_2 & -N_2 \cos^2 \theta_2 & & \\ & N_2 \cos^2 \theta_2 + N_1 \cos^2 \theta_1 & & \end{bmatrix} \quad (5.32)$$

where N_j is the number of dampers in brace level “ j ” with angle of incidence of θ_j .

Kelvin elements have a stiffening contribution also for monotonic or quasi-static loads. The dynamic stiffening contributes to a further reduction of displacements, and an increase in the base shear. For pushover and quasi-static analyses, the combined influence of the static and dynamic stiffening provided by the Kelvin element is accounted for using an equivalent dynamic stiffness defined as (Reinhorn et al., 1995d):

$$K_d = \sqrt{K_{1,eq}^2 + \omega^2 C_{1,eq}^2} \quad (5.33)$$

where $K_{1,eq}$ and $C_{1,eq}$ are determined using Eqs. 5.24 and 5.26 for a value of ω often taken as the fundamental circular frequency of the structure.

5.4.2 Maxwell Model

When a damper displays a strong dependency on frequency, the more refined model using a Maxwell model is recommended. This model was found suitable to represent fluid viscous dampers with accumulators (Constantinou and Symans, 1992). The Maxwell model consists of a damper and a spring in series (see Fig. 5.19). The force in the damper is defined by:

$$F_d(t) + \lambda \dot{F}_d(t) = C_D \dot{u}(t) \quad (5.34)$$

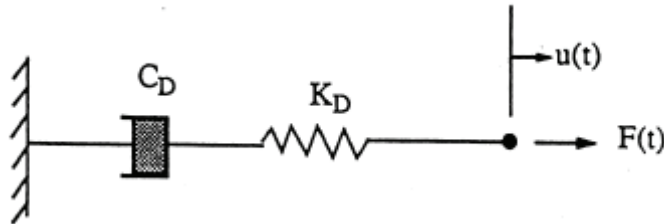


Fig. 5.19 Maxwell model for damping devices

in which λ is the relaxation time:

$$\lambda = \frac{C_D}{K_D} \quad (5.35)$$

where K_D is the stiffness at an “infinitely” large frequency; C_D is the damping constant at zero frequency. The Maxwell model can be expressed in the frequency domain as:

$$F_d(\omega) = [K_1(\omega) + iK_2(\omega)]u(\omega) \quad (5.36)$$

where the storage stiffness and the loss stiffness are:

$$K_1(\omega) = C_D \left(\frac{\lambda\omega^2}{1+(\lambda\omega)^2} \right) = K_D \left(\frac{(\lambda\omega)^2}{1+(\lambda\omega)^2} \right) \quad \text{--- (a)} \quad (5.37)$$

$$K_2(\omega) = \omega C(\omega) = \frac{\omega C_D}{1+(\lambda\omega)^2} \quad \text{--- (b)}$$

The dependence of the normalized damping and stiffness coefficients with frequency is shown in Fig. 5.20.

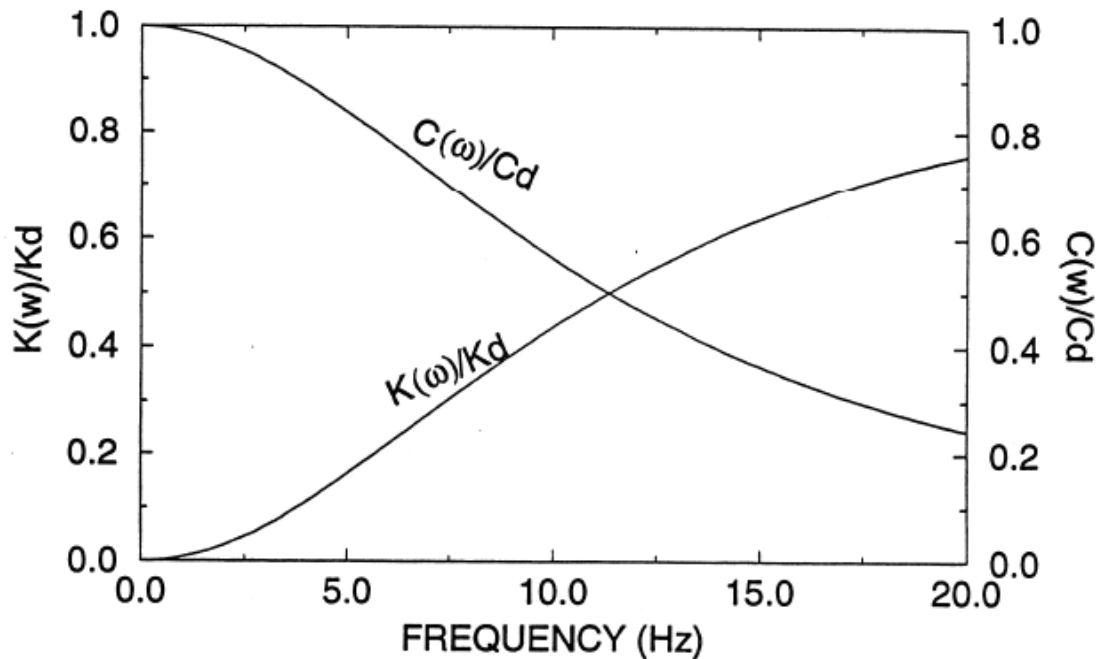


Fig. 5.20 Stiffness and damping versus frequency in Maxwell model

For convenience in the solution procedure, Eq. 5.34 can be expressed as:

$$\dot{F}(t) = f(F, u, \dot{u}, t) = -\frac{1}{\lambda} F(t) + \frac{C_D}{\lambda} \dot{u}(t) \quad (5.38)$$

that can be solved simultaneously with the other time dependent structural components. In the computer program IDARC, the forces in the viscoelastic Maxwell dampers are expressed as:

$$\dot{F}_{Di} = -\frac{1}{\lambda_i} F_i + \frac{C_{Di}}{\lambda_i} \dot{u}_i \quad (5.39)$$

The solution of which is found using the semi-implicit Runge-Kutta method (Rosenbrook, 1964):

$$(\Delta F_{Di})_k = f(F_k, u_k, \dot{u}_k) = R_1 k_k + R_2 l_k \quad (5.40)$$

where $(\Delta F_{Di})_k$ is the increment in force of damper “*i*” at time step “*k*”; k_k and l_k are determined from (Reinhorn et al., 1995a):

$$k_k = \left[1 - a_1 \Delta t \frac{\partial f(F_{k-1}, u_{k-1}, \dot{u}_{k-1})}{\partial F} \right]^{-1} f(F_{k-1}, u_{k-1}, \dot{u}_{k-1}) \Delta t \quad \text{---(a)} \quad (5.41)$$

$$l_k = \left[1 - a_2 \Delta t \frac{\partial f(F_{k-1} + c_1 k_k, u_{k-1}, \dot{u}_{k-1})}{\partial F} \right]^{-1} f(F_{k-1} + b_1 k_k, u_{k-1}, \dot{u}_{k-1}) \Delta t \quad \text{---(b)}$$

where the constant parameters R_1 , R_2 , a_1 , a_2 , b_1 and c_1 were selected to obtain a fourth order truncation error (Reinhorn et al., 1994): $R_1 = 0.75$, $R_2 = 0.25$, $a_1 = a_2 = 0.7886751$, $b_1 = -1.1547005$, and $c_1 = 0$.

Maxwell elements have a stiffening contribution in the dynamic response, and therefore will also have a contribution to the monotonic or quasi-static loads. The “dynamic stiffening” contributes to a further reduction of displacements, and an increase in the base shear. For nonlinear incremental static (pushover) and quasi-static analyses the combined influence of the static and dynamic stiffening provided by the Maxwell element is accounted for using an equivalent dynamic stiffness defined as (Reinhorn et al., 1995b):

$$K_d = \sqrt{K_{1,eq}^2 + \omega^2 C_{1,eq}^2} \quad (5.42)$$

where $K_{1,eq}$ and $C_{1,eq}$ are determined using Eq. 5.37 for a value of ω often taken as the fundamental circular frequency of the structure. At zero frequency the dynamic stiffness equals to the static while at large frequencies is governed by the “damping stiffness” ωC_{eq} .

5.5 Complex Self Centering Model

A hysteretic model is implemented in IDARC to model the response of friction dampers, hysteretic dampers, and infill panels. The hysteretic model which is also used for infill panels includes the effects of stiffness degradation, strength deterioration and pinching. Such effects are not included in the model used for dampers since no significant degradation, deterioration or pinching is observed in their response. The development of the present hysteretic model is based Sivaselvan and Reinhorn (1999), Madan et al. (1997), Kunnath and Reinhorn (1994), and Lobo (1994) models similar to on the Bouc-Wen model (Bouc, 1967; Wen, 1976; Baber and Noori, 1985). The hysteretic model with degradation and slip is described below.

The force displacement relationship for the smooth hysteretic model is (see Fig. 4.16):

$$V_i = V_y [\alpha \mu_i + (1 - \alpha) Z_i] \quad (5.43)$$

in which V_i and V_y are the instantaneous force and the yield force, respectively; μ is the normalized displacement calculated as:

$$\mu_i = \frac{u_i}{u_y} \quad (5.44)$$

where the subscript “ i ” is used to refer to the instantaneous values, while subscript “ y ” is used to denote yield values; α is the ratio of post-yielding to initial elastic stiffness ($\alpha = 0$ for friction dampers); and Z_i is the hysteretic component determined from the following equations:

$$\dot{Z}_i = \dot{\mu}_i [A - |Z_i|^n (\beta \operatorname{sgn}(\dot{\mu}_i Z_i) + \gamma)] \quad (5.45)$$

where:

$$\begin{aligned} \operatorname{sgn}(\dot{\mu}_i Z_i) &= 1 && \text{if } (\dot{\mu}_i Z_i) > 0 \\ \operatorname{sgn}(\dot{\mu}_i Z_i) &= -1 && \text{if } (\dot{\mu}_i Z_i) < 0 \end{aligned}$$

Eliminating the time differential dt , and noting that $\operatorname{sgn}(\dot{\mu}_i Z_i) = \operatorname{sgn}(d\mu_i Z_i)$, Eq. 5.45 can be rewritten for quasi-static or monotonic loading:

$$dZ_i = d\mu_i [A - |Z_i|^n (\beta \operatorname{sgn}(d\mu_i Z_i) + \gamma)] \quad (5.46)$$

In Eqs. 5.45 and 5.46 the parameters A , β and γ are constants that control

the shape of the generated hysteresis loops (β and γ identical to μ_1 and μ_2 in the Smooth Hysteretic Model (SHM). The parameter n controls the rate of transition from the elastic to the yield state (Lobo, 1994). A large value of n approximates a bilinear hysteretic curve, while a lower value will trace a smoother transition. Different hysteretic shapes with variations on the various parameters can be found in Fang (1991). To satisfy viscoplastic conditions the present development assumes that $A = \beta + \gamma = 1.0$.

An important characteristic in the hysteretic response of infill panels is the loss of stiffness due to deformation beyond yield (see Fig. 5.21). The stiffness deterioration due to plastic excursions of the infill panel is expressed as a function of the attained ductility (Lobo, 1994). The stiffness decay is incorporated directly in the hysteretic model by including the control parameter η . The differential equation for the hysteretic parameter Z (Eq. 5.46) may be modified to generate stiffness deterioration as follows:

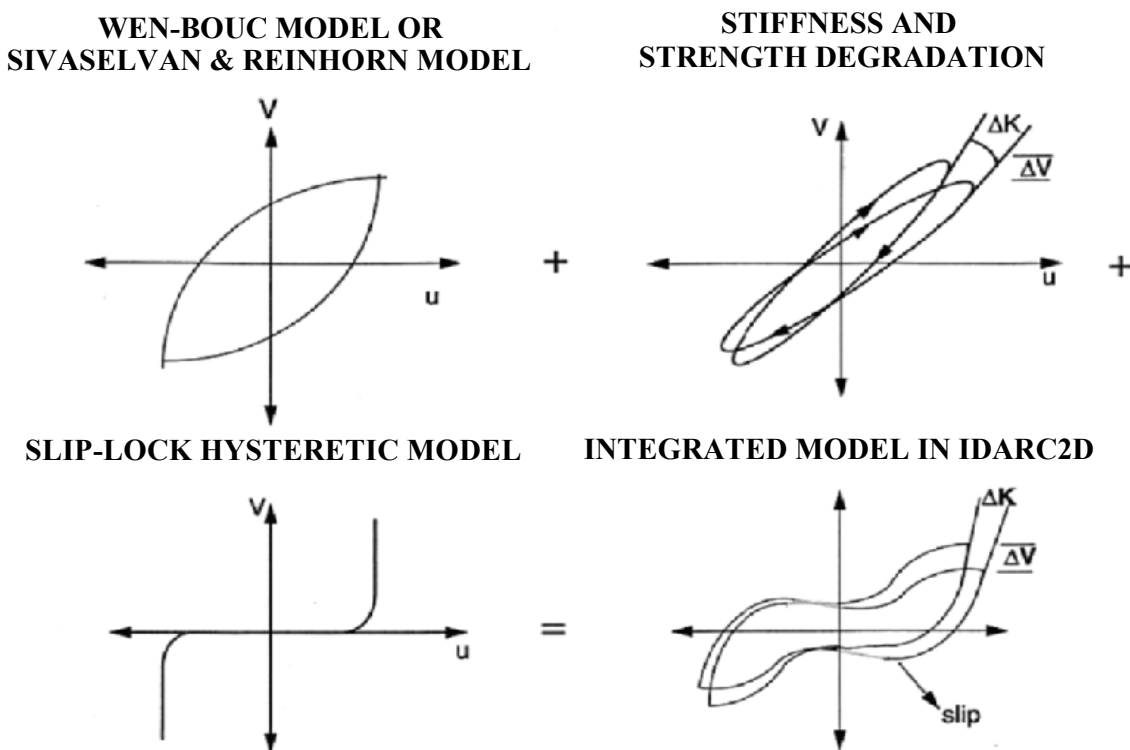


Fig. 5.21 Complex self centering hysteretic model

$$dZ_i = d\mu_i \frac{\left[A - |Z_i|^n (\beta \operatorname{sgn}(d\mu_i Z_i) + \gamma) \right]}{\eta_i} \quad (5.47)$$

The control parameter is defined as:

$$\eta = 1.0 + s_k \left(\frac{\mu_{\max}^p + \mu_i}{2} \right) \quad (5.48)$$

where s_k is a control parameter used to vary the rate of stiffness decay as a function of the current ductility μ_i , as well as the maximum attained ductility μ_{\max}^p before the start of the current unloading or reloading cycle (Reinhorn et al., 1995d). A value of $s_k = 0$ simulates a non-degrading system. A default value of $s_k = 0.1$ is suggested (Reinhorn et al., 1995d).

Degrading systems such as masonry infill panels also exhibit a loss of strength when subjected to cyclic loading in the inelastic range (see Fig. 5.21). The strength deterioration in the smooth hysteretic model was modeled reducing the yield force of the panel according to:

$$V_y^k = s_\beta V_y^0 \quad (5.49)$$

where V_y^k is the reduced yield force at the k -th cycle of loading; V_y is the initial non-degraded yield force.

The factor s_β determines the amount of deterioration from the original yield force. And depends on the cumulative damage in the infill panel during the response history. A

damage index (DI) was used to quantify the cumulative damage in the infill panel. The reduction factor s_β is related to the damage index according to:

$$s_\beta = 1 - DI \quad (5.50)$$

The damage index proposed in this development, known as fatigue based damage index, is a function of the attained ductility and dissipated cyclic energy (Reinhorn and Valles, 1995; see also Section 7.3):

$$DI = \frac{\mu_{\max}^p - 1}{\mu_c - 1} \frac{1}{\left(1 - \frac{s_{p1} \int dE_h}{4E_{hy}} \right)^{s_{p2}}} \quad (5.51)$$

in which μ_{\max}^p is the maximum attained ductility in the response history; μ_c is the ductility capacity of the infill panel; the parameters s_{p1} and s_{p2} control the rate of strength deterioration; $\int dE_h$ represents the cyclic energy dissipated before the start of the current reloading cycle; and E_{hy} is the monotonic energy capacity:

$$E_{hy} = V_y u_y (\mu_c - 1) \quad (5.52)$$

Thus, the damage index DI may also be expressed as (Reinhorn et al., 1995d):

$$DI = \frac{\mu_{\max}^p - 1}{\mu_c - 1} \frac{1}{\left(1 - 0.25 s_{p1} \int \left(\frac{V}{V_y} \right) \frac{d\mu}{(\mu_c - 2)} \right)^{s_{p2}}} \quad (5.53)$$

The damage index used in IDARC2D can reflect the cumulative effect of softening due to large inelastic excursions without load reversal as well as strength degradation due to repeated cyclic at moderate or small inelastic deformations.

Pinching of the hysteretic loops due to opening and closing of cracks is commonly observed in concrete and masonry structural systems subjected to cyclic loading. Baber and Noori (1985) proposed a general degradation model to incorporate pinching in the response of a single degree of freedom system. The infill masonry model implements the smooth degrading element developed by Bouc and modified by Baber and Wen (1981) in series with a time dependent slip-lock element (non-linear hardening spring). A rate dependent differential equation was proposed (Baber and Noori, 1995) relating the velocity contribution due to the slip-lock element with the hysteretic parameter Z , which was solved simultaneously with the equations of motion for the single-degree-of-freedom system to obtain the response of dynamically degrading pinching systems.

The concept of slip-lock element proposed by Baber and Noori (1985) has been adapted for this platform to formulate a more generalized hysteretic rule for degrading pinching elements. The hysteretic rule is rate-independent and defines the force deformation response of the pinching element for any arbitrary displacement history independent of the system differential equations. The present formulation incorporates a slip-lock element in series with the smooth degrading element to develop a hysteretic model for pinching response (see Fig. 5.22). The normalized displacement of the pinching smooth hysteretic element μ is the sum of the normalized displacement of the smooth degrading element μ_1 and the slip-lock element μ_2 . In incremental form, the relationship can be expressed as:

$$d\mu = d\mu_1 + d\mu_2 \quad (5.54)$$

in which $d\mu_1$ and $d\mu_2$ are the incremental normalized displacements of the smooth degrading element and the slip-lock elements, respectively.

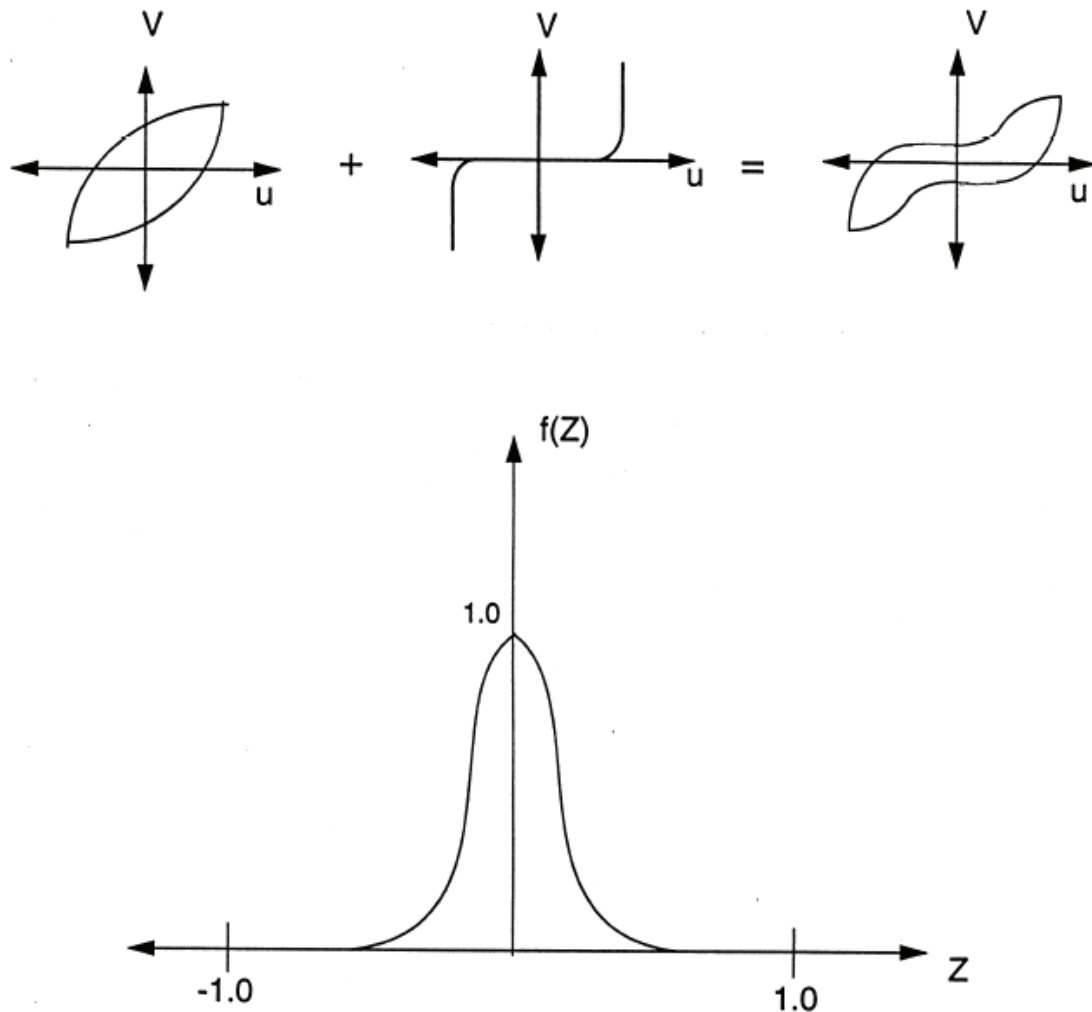


Fig. 5.22 Slip lock element: a) Influence on hysteretic response b) Slip-lock function

The smooth degrading element is based on the complex self centering model discussed earlier. Thus, the hysteretic parameter Z can be rewritten in terms of the displacement contribution μ_1 :

$$dZ = d\mu_1 \frac{[A - |Z|^n (\beta \operatorname{sgn}(d\mu_1 Z) + \gamma)]}{\eta} \quad (5.55)$$

The following relationship is proposed for the displacement component μ_2 in the slip-lock element:

$$d\mu_2 = af(Z) dZ \quad (5.56)$$

in which the function $f(Z)$ is taken as:

$$f(Z) = \exp\left(-\frac{Z}{Z_s}\right)^2$$

in which Z_s is the range of Z about $Z=0$, in which the slip occurs and thus controls the sharpness of the slip. The variation of $f(Z)$ is shown in Fig. 5.22(b). Upon substitution of Eqs. 5.54 and 5.56 into Eq. 5.55:

$$\frac{dZ}{d\mu} = \frac{A - |Z|^n (\beta \operatorname{sgn}(d\mu Z) + \gamma)}{\eta \left[1 + a \exp\left(-\frac{Z^2}{Z_s^2}\right) (A - |Z|^n (\beta \operatorname{sgn}(d\mu Z) - \gamma)) \right]} \quad (5.57)$$

In the present development, the slip length a is assumed to be a function of the attained ductility:

$$a = R_s (\mu^r - 1) \quad (5.58)$$

where R_s is a control parameter to vary slip length which may be linked to the size of crack openings or reinforcement slip (Lobo, 1994); and μ^r is the normalized displacement attained at the load reversal prior to the current loading or reloading cycle. The effect of varying the control parameters of the slip-lock element on the pinching of

hysteresis loops is shown in Fig. 5.23. The parameter Z_s , that controls the sharpness of the slip, is assumed to be independent of the response history. Slip occurs in the range of Z equal to Z_s , and is symmetric about $Z = 0$. In order to shift the effective slip region to be symmetric about an arbitrary $Z = \bar{Z}$, the value of Z used for slip may be offset by a value \bar{Z} :

$$\frac{dZ}{d\mu} = \frac{A - |Z|^n (\beta \operatorname{sgn}(d\mu Z) + \gamma)}{\eta \left[1 + a \exp \left(-\frac{(Z - \bar{Z})^2}{Z_s^2} \right) (A - |Z|^n (\beta \operatorname{sgn}(d\mu Z) - \gamma)) \right]} \quad (5.59)$$

Equations 5.48 and 5.58 with Eq. 5.59 furnish a modified Bouc-Wen model (complex self centering model) for hysteretic pinching elements subjected to dynamic or quasi-static loading. For dynamic analysis, Eq. 5.59 can be rewritten in a rate dependent form:

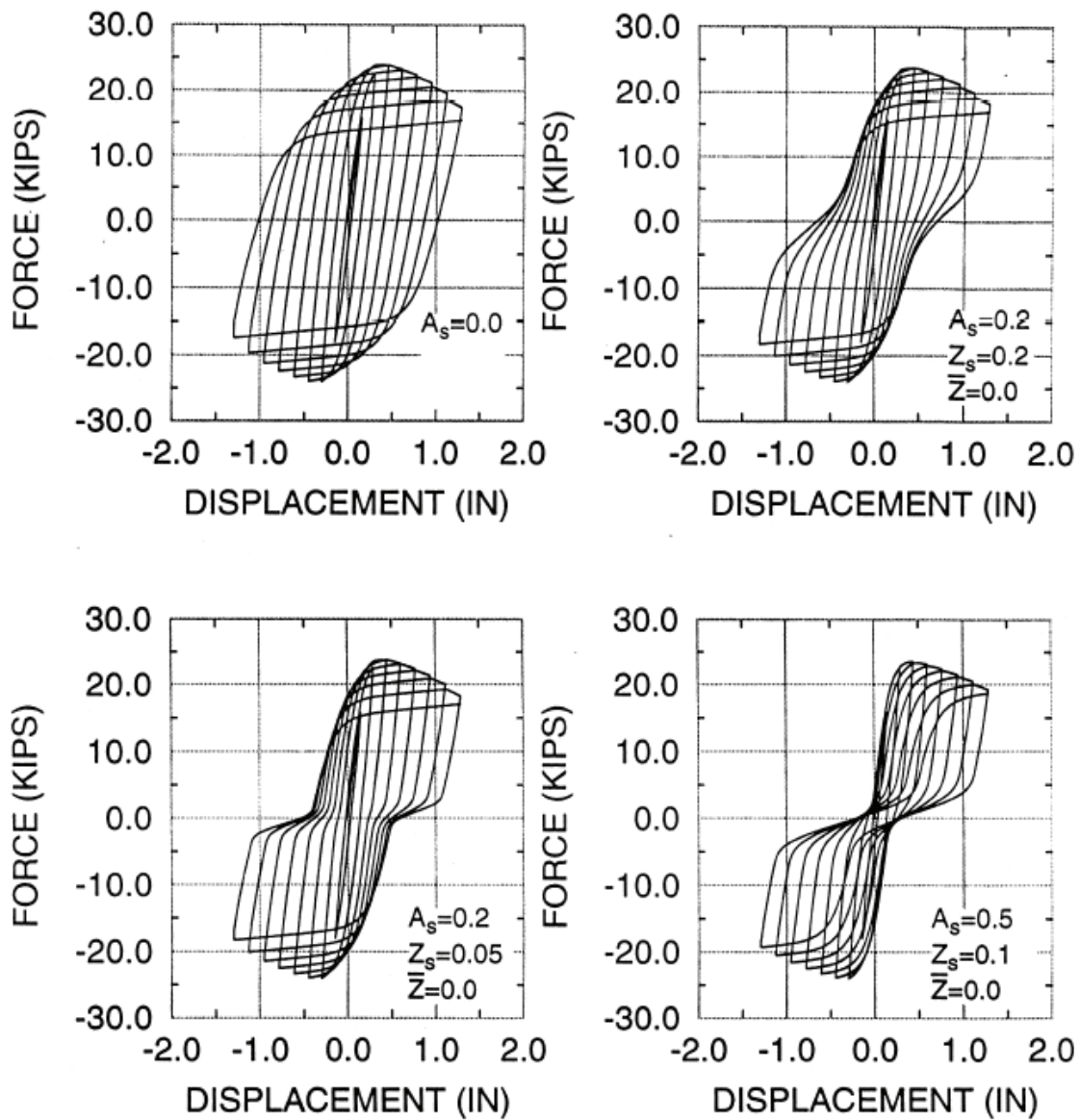
$$\dot{Z} = \dot{\mu} \frac{A - |Z|^n (\beta \operatorname{sgn}(\dot{\mu} Z) + \gamma)}{\eta \left[1 + a \exp \left(-\frac{(Z - \bar{Z})^2}{Z_s^2} \right) (A - |Z|^n (\beta \operatorname{sgn}(\dot{\mu} Z) - \gamma)) \right]} \quad (5.60)$$

The solution of the differential equation (Eq. 5.59 for quasi-static loading and Eq. 5.60 for dynamic loading) can be reduced to the following general form:

$$V'(u) = f(V, u) \quad \text{----- (a)} \quad (5.61)$$

in the quasi-static case, or:

$$\dot{V}(u) = f(V, u, \dot{u}) \quad \text{----- (b)}$$



Constant Parameters		
$A = 1.0$	$\alpha = 0.01$	$s_k = 0.1$
$\beta = 0.1$	$V_y = 25$ Kips	$s_{p1} = 0.8$
$\gamma = 0.9$	$K_0 = 125$ K/in	$s_{p2} = 1.0$
$n = 2$		$\mu_c = 25$

Fig. 5.23 Influence of varying the slip-lock parameters

in the dynamic case. Differential equations of this form can be incrementally integrated using the semi-implicit Runge-Kutta method (see Section 5.4.2). The increment ΔV is given by:

$$\Delta V_k = V_{k+1} - V_k = R_1 k_k + R_2 l_k \quad (5.62)$$

in which the subscript “ k ” denotes the k -th step. The quantities k_k and l_k are determined from:

$$k_k = \left[1 - a_1 \Delta x \frac{\partial f(V_k)}{\partial V} \right]^{-1} f(V_k) \Delta x \quad \text{---(a)} \quad (5.63)$$

$$l_k = \left[1 - a_2 \Delta x \frac{\partial f(V_k + c_1 k_k)}{\partial V} \right]^{-1} f(V_k + b_1 k_k) \Delta x \quad \text{---(b)}$$

To obtain a fourth order truncation error the coefficients are (Reinhorn et al., 1994): $R_1 = 0.75$, $R_2 = 0.25$, $a_1 = a_2 = 0.7886751$, $b_1 = -1.1547005$ and $c_1 = 0$.

5.6 Special Spring Base Isolator Model

The special hysteretic model is developed to simulate a spring base isolator as a protecting device. The model is basically incorporated with a hysteretic brace model implemented in this program. The device provides a “twisted hysteretic behavior” defined by a lower and upper bound curves as shown in Fig. 5.24. The stiffness variation of the upper bound of the isolator can be formulated with

$$k = k_0 \left[\alpha + (1-\alpha) \left(1 - \left| \frac{V_i}{V_y} \right|^n \right) \right] \dots \text{for } \left| \frac{V_i}{V_y} \right| \leq 1 \quad (5.64)$$

$$= \alpha k_0 \quad \dots \quad \text{for otherwise}$$

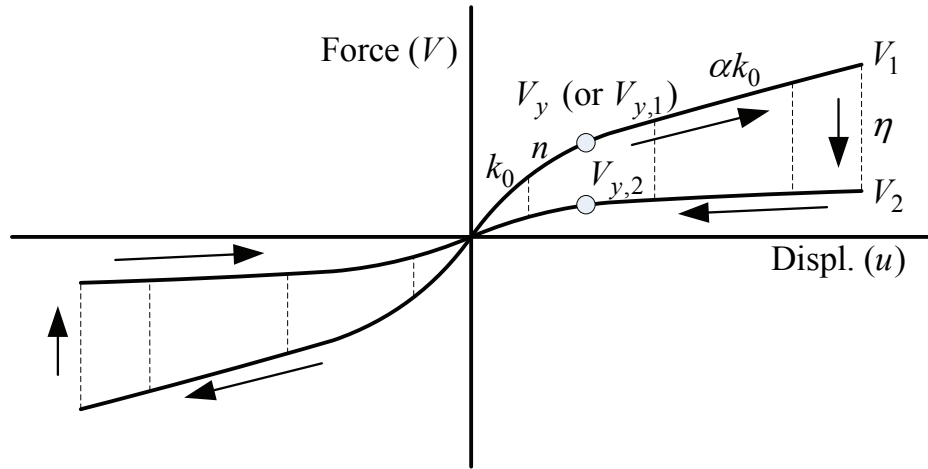


Fig. 5.24 Typical behavior of spring base isolator

where k_0 is an initial stiffness, α is a post-yield stiffness ratio, V_y is a yield force or a transitional force, and V_i is an instantaneous force. The stiffness variation of Eq. 5.64 is reformulated for both upper and lower bound curves with an unified equation as following:

$$k_i = k_0 \left[(1-\eta) + \eta \cdot \text{sgn}(V \cdot \dot{u})_{i-1} \right] \left[\alpha + (1-\alpha) \left(1 - \left| \frac{V_{i-1}}{V_y \left[(1-\eta) + \eta \cdot \text{sgn}(V \cdot \dot{u})_{i-1} \right]} \right|^n \right) \right] \quad (5.65)$$

where η is a strength decay or boundary control parameter which is defined by:

$$\eta = \frac{1}{2} \left(\frac{V_1 - V_2}{V_1} \right) \quad (5.66)$$

where V_1 and V_2 are reference forces of each bound as shown in Fig. 5.24. Alternatively, the reference forces can be replaced with V_{y1} and V_{y2} of each bound. When V_1 and V_2 are selected as reference forces, the stiffness and yield force of the

lower bound curve become automatically $k_0(1-2\eta)$ and $V_y(1-2\eta)$, respectively. In Eq. 5.65, \dot{u} is a velocity [or displacement increment (in time)]. The subscripts “ i ” and “ $i-1$ ” are the current and previous time steps, respectively. The absolute value ratio in the right parenthesis can be only ≤ 1.0 . If numerically the value is >1.0 , then the value must be limited to exactly 1.0.

The force at each instance in time is defined by:

$$V_i = V'_i \left[(1-\eta) + \eta \cdot \text{sgn}(V' \cdot \dot{u})_i \cdot \text{sgn}(V \cdot \dot{u})_{i-1} \right] \left[\frac{\text{sgn}(V' \cdot \dot{u})_i - \text{sgn}(V \cdot \dot{u})_{i-1}}{2} \right] / 2 \quad (5.67)$$

where the “prime” values of the instantaneous forces are obtained numerically from the solution of first order differential equation of forces as:

$$\begin{aligned} V'_i &= V'_{i-1} + k_i(u_i - u_{i-1}) && \text{for static analysis (first order computation)} \\ &= V'_{i-1} + k_i \cdot \dot{u}_i \cdot \Delta t && \text{for dynamic analysis (first order computation)} \end{aligned}$$

Higher order solutions can be obtained using semi-implicit Rosenbruck formulation (a higher order Runge-Kutta type solution, see Section 5.4.2)

SECTION 6

ANALYSIS MODULES

6.1 Introduction

The program evaluates the nonlinear response of the structure under the following four possible analysis options:

- a) Incremental Nonlinear Static Monotonic Analysis (Section 6.2)
- b) Incremental Nonlinear Static-Adaptive (Pushover) Analysis (Section 6.3)
- c) Nonlinear Quasi-static Analysis (Section 6.4)
- d) Eigenvalue Analysis (Section 6.5)
- e) Nonlinear Dynamic Analysis (Section 6.6)

The user may select any of the four options for the analysis, or a combination of a nonlinear static analysis with any of the three other analysis options.

For all four analysis options, the system to solve assumes the following form:

$$[\mathbf{K}_t]\{\Delta\mathbf{u}\} = \{\Delta\mathbf{F}\} \quad (6.1)$$

where $[\mathbf{K}_t]$ is the overall tangent stiffness matrix of the structure, $\{\Delta\mathbf{u}\}$ is the vector of unknown nodal displacement increments, and $\{\Delta\mathbf{F}\}$ is the vector of applied load increments. Since the stiffness matrix is banded and symmetric, the matrix is stored in a compact scheme with the diagonal elements in the first column and the remaining half width diagonal terms in the adjacent columns.

The element stiffness matrices are first calculated at the element level, and later assembled onto the global stiffness matrix. The stiffness matrix is then modified to account for P-Delta effects (see Section 6.7) if required by the user. The load vector in the structure is determined depending of the choice of analysis being performed. Element sub-matrices are stored to enable direct computation of the end moments and shears, and the hysteretic model checks for changes in the element stiffness. The global stiffness matrix is only upgraded, if an element stiffness is changed, otherwise remains constant. A single step force correction procedure is incorporated in all analysis options.

6.2 Incremental Nonlinear Static Monotonic Analysis

The incremental nonlinear static monotonic analysis is performed to detect the influence of static loads. The analysis is performed automatically before all analyses options for the evaluation of the initial stress states of members under dead and live loads that exist in the structure prior to the application of monotonic, cyclic, or earthquake loads. Static loads may be specified as distributed loads in the beams, or as concentrated forces or moments in the joints. When distributed loads are specified, the program internally calculates the fixed end forces (or/and moments).

Moments are assumed to have a linear distribution when the beam flexural matrix is generated, therefore, stress levels due to initial loads must be relatively small so that the assumed moment distribution pattern is not significantly violated. Otherwise, beam elements must be subdivided into sub-elements so that the moment distribution due to gravity loads is captured effectively.

The prescribed static loads are applied incrementally to capture stress redistribution due to inelastic response if such resources occurs. If the system is expected to remain elastic with the gravity loads applied, the entire load may be applied in a single step,

otherwise, care should be taken to sub-divide the static loads in a reasonable number of increments in order to trace the nonlinear response accurately. A simple technique to assure convergence in the static analysis is to increase the number of loading steps until consistent results are obtained. Note that this module is used also to perform nonlinear static (monotonic) analysis.

6.3 Incremental Nonlinear Static-Adaptive (Pushover) Analysis

6.3.1 Formulation

The nonlinear static or “pushover” analysis, or collapse mode analysis, is a simple and efficient technique to predict the capacity of the structure and its individual component members prior to a full dynamic and damage analyses. The nonlinear static (“pushover”) analysis can identify possible sequences of component yielding, the potential ductility capacity, and the total global lateral strength. The nonlinear static analysis option performs an incremental analysis of the structure subjected to a distribution of lateral forces. The system of equations solved in this module are:

$$[\mathbf{K}_t] \{\Delta\mathbf{u}\} = \{\Delta\mathbf{F}\} - \{\Delta\mathbf{P}_V\} - \{\Delta\mathbf{P}_{FR}\} - \{\Delta\mathbf{P}_{HY}\} - \{\Delta\mathbf{P}_{IW}\} + c_{corr} \{\Delta\mathbf{F}_{err}\} \quad (6.2)$$

where $[\mathbf{K}_t]$ is the tangent structural stiffness; $\{\Delta\mathbf{u}\}$ is the increment vector of lateral displacements; $\{\Delta\mathbf{F}\}$ is the increment vector of lateral forces; $\{\Delta\mathbf{P}_V\}$, $\{\Delta\mathbf{P}_{FR}\}$, $\{\Delta\mathbf{P}_{HY}\}$, and $\{\Delta\mathbf{P}_{IW}\}$ are the increment vectors of forces in viscous dampers, friction dampers, hysteretic dampers, and infill panels respectively; and $\{\Delta\mathbf{F}_{err}\}$ is the vector of the unbalanced forces in the structure; c_{corr} is a correction coefficient (usually taken as one).

The nonlinear static incremental analysis may be carried out using force control or displacement control. In the force control option, the structure is subjected to a distribution of incremental lateral forces while the incremental displacements are calculated. In the displacement control option, the structure is subjected to a displacement profile, and the lateral forces needed to generate that deformation are calculated. Typically, since the deformed profile is not known a priori, only an estimate of the lateral distribution of forces can be made, therefore, force control option is commonly used. For displacement control, the user must specify the target maximum deformation profile of the structure. This profile is internally divided by the number of steps specified by the user, and then incrementally applied to the structure.

6.3.2 Vertical Lateral Force Distribution

In the force control option, the user must specify the maximum force distribution, or select one of the force distributions available in the program:

- a) Uniform Distribution
- b) Inverted Triangular Distribution
- c) Generalized Power Distribution
- d) Modal Adaptive Distribution

Each of the distributions is briefly described below.

a) The uniform distribution considers a constant distribution of the lateral forces throughout the height of the building, regardless of the story weights. The force increment at each step for story “*i*” is given by:

$$\Delta F_i = \frac{\Delta V_b}{N} \quad (6.3)$$

where ΔV_b is the increment in the base shear of the structure, and N is the total number of stories in the building.

b) The inverse triangular distribution, often suggested in building codes, considers that the structure is subjected to a linear distribution of the acceleration throughout the building height. The force increment at each step for story “ i ” is calculated according to:

$$\Delta F_i = \frac{W_i h_i}{\sum_{l=1}^N W_l h_l} \Delta V_b \quad (6.4)$$

where W_i and h_i are the story weight and the story elevation, respectively, and ΔV_b is the increment of the building base shear.

c) The generalized power distribution was introduced to consider different variation of the story accelerations with the story elevation. This distribution was introduced to capture different modes of deformation, and the influence of higher modes in the response. The force increment at floor “ i ” is calculated according to:

$$\Delta F_i = \frac{W_i h_i^k}{\sum_{l=1}^N W_l h_l^k} \Delta V_b \quad (6.5)$$

where k is the parameter that controls the shape of the force distribution. The recommended value for k may be calculated as a function of the fundamental period of the structure (T):

$$k = 1.0 \quad \text{for } T \leq 0.5 \text{ sec}$$

$$k = 2.0 \quad \text{for } T \geq 2.5 \text{ sec}$$

$$k = 1 + \frac{T - 0.5}{2} \text{ for otherwise}$$

Nevertheless, any value for k may be used to consider different acceleration profiles. Note that $k = 0$ produces a constant variation of the acceleration, while $k = 1$ produces a linear variation (inverted triangle distribution), and $k = 2$ yields a parabolic distribution of story accelerations.

d) The modal adaptive distribution differs significantly from all the previous ones in that the story force increments are not constant. A constant distribution throughout the incremental analysis will force the structure to respond in a certain form. Often the distribution of forces is selected considering force distributions during an elastic response, however, it is clear that when the structure enters the inelastic range, the elastic distribution of forces may not be applicable anymore. If the incremental forces are not modified to account for the new stiffness distribution, the structure is forced to respond in a way that may considerably differ from what an earthquake may impose to the structure.

The modal adaptive distribution was developed (Reinhorn, 1996, 1997) to capture the changes in the distribution of lateral forces. Instead of a polynomial distribution, the “instantaneous” mode-shapes of the structure are considered. Since the inelastic response of the structure will change the stiffness matrix, the mode shapes will also be affected, and a distribution proportional to the mode shapes will capture this change. If the “instantaneous” fundamental mode is considered, the increment in the force distribution is calculated according to:

$$\Delta F_i = \frac{W_i \Phi_{i1}}{\sum_{l=1}^N W_l \Phi_{il}} \Delta V_b - F_i^{old} \quad (6.6)$$

where Φ_{il} is the value of the “instantaneous” first mode shape at story “ i ”, V_b is the

new base shear of the structure, and F_i^{old} is the force at floor “ i ” in the previous loading step.

The modal adaptive distribution may be extended to consider the contribution from more than one mode. In this case the “instantaneous” mode shapes are combined using the SRSS method and scaled according to their modal participation factor. The incremental force at story “ i ” is calculated according to:

$$\Delta F_i = \frac{W_i \left[\sum_{j=1}^{nm} (\Phi_{ij} \Gamma_j)^2 \right]^{1/2}}{\sum_{l=1}^N W_l \left[\sum_{j=1}^{nm} (\Phi_{lj} \Gamma_j)^2 \right]^{1/2}} \Delta V_b - F_i^{old} \quad (6.7)$$

where Φ_{ij} is the value of “instantaneous” mode shape “ j ” at story “ i ”, Γ_j is the modal participation factor for mode “ j ”, V_b is the new base shear of the structure, and F_i^{old} is the force at floor “ i ” in the previous loading step.

6.4 Nonlinear Quasi-static Analysis

A common testing procedure for components and sub-assemblages is to perform cyclic loading of the specimen against a reaction frame. The history of cyclic loads may be applied to the specimen in force or deformation control. The computer program IDARC is capable of performing both types of cyclic loading by specifying the force or displacement history at one or more story levels. In both cases the program internally interpolates between user-specified points for a more accurate analysis. The system of equations solved in the quasi-static routine are the same ones solved in the pushover routine (Eq. 6.2).

6.5 Eigenvalue Analysis

An eigenvalue analysis is carried out using the condensed stiffness matrix of the system:

$$([\mathbf{K}_d] - \omega_i^2 [\mathbf{M}_d]) \{\lambda_i\} = \{\mathbf{0}\} \quad (6.8)$$

where $[\mathbf{K}_d]$ is the condensed lateral stiffness matrix of the system relating lateral forces and lateral displacements; $[\mathbf{M}_d]$ is the diagonal lateral mass matrix of the structure; ω_i circular frequency of the structure for the mode “ i ”, and $\{\lambda_i\}$ is the corresponding eigenvector. The complete set of eigenvalues for the condensed degrees of freedoms is calculated, that is, the number of eigenvalues calculated equals the number of stories in the building.

The complete set of eigenvectors are stored by columns in the matrix $[\Phi]$. The modal equivalent masses in the structure are calculated according to:

$$[\mathbf{M}_{eq}] = [\Phi]^t [\mathbf{M}_d] [\Phi] \quad (6.9)$$

where $[\mathbf{M}_{eq}]$ is the matrix with the equivalent modal masses in the diagonal. The mass normalized eigenvectors are calculated according to:

$$[\Phi_N]_{i,j} = \frac{[\Phi]_{i,j}}{\sqrt{[\mathbf{M}_{eq}]_{i,i}}} \quad (6.10)$$

Such that $[\Phi_N]^t [\mathbf{M}_d] [\Phi_N] = [\mathbf{I}]$ and $[\Phi_N]^t [\mathbf{K}_d] [\Phi_N] = [\Omega^2]$, where $[\Omega^2]$ is the

diagonal matrix of eigenvalues. The modal participation is then calculated using the mass normalized eigenvectors:

$$\{\Gamma\} = [\Phi_N]^t [M_d] \{1\} \quad (6.11)$$

or for diagonal mass matrices:

$$\{\Gamma\}_i = \sum_{i=1}^N M_i [\Phi]_{i,j} \quad (6.12)$$

where $\{\Gamma\}_i$ is the modal participation factor for mode “ i ”, and $\{1\}$ is a vector of ones.

The program calculates the eigen properties before the dynamic analysis, at every step of the adaptive nonlinear static analysis and upon request by user.

Note: The program assembles the mass matrix using “nodal weights” which are the lumped masses in various nodes multiplied by g . The “nodal weights” expressed in force units, are used only for the calculation of mass matrix, and not considered in the gravity loads (nodal forces).

6.6 Nonlinear Dynamic Analysis

6.6.1 Formulation

The nonlinear dynamic analysis is carried out using a combination of the Newmark-Beta integration method, and the pseudo-force method. The solution is carried out in incremental form, according to:

$$[\mathbf{M}]\{\Delta\ddot{\mathbf{u}}\} + [\mathbf{C}]\{\Delta\dot{\mathbf{u}}\} + [\mathbf{K}_t]\{\Delta\mathbf{u}\} = -[\mathbf{M}]\left[\{\mathbf{L}_h\}\Delta\ddot{x}_{gh} + \{\mathbf{L}_v\}\Delta\ddot{x}_{gv}\right] - \{\Delta\mathbf{P}_V\} \\ - \{\Delta\mathbf{P}_{FR}\} - \{\Delta\mathbf{P}_{HY}\} - \{\Delta\mathbf{P}_{IW}\} + c_{corr}\{\Delta\mathbf{F}_{err}\} \quad (6.13)$$

where $[\mathbf{M}]$ is the lumped mass matrix of the structure; $[\mathbf{C}]$ is the equivalent viscous damping matrix of the structure; $[\mathbf{K}_t]$ is the tangent stiffness matrix; $\{\Delta\mathbf{u}\}$, $\{\Delta\dot{\mathbf{u}}\}$, and $\{\Delta\ddot{\mathbf{u}}\}$ are the incremental vectors of displacement, velocity and acceleration in the structure, respectively; $\{\mathbf{L}_h\}$ and $\{\mathbf{L}_v\}$ are the contribution vectors (of units) for the horizontal and vertical ground accelerations; $\Delta\ddot{x}_{gh}$ and $\Delta\ddot{x}_{gv}$ are the increment in the horizontal and vertical ground accelerations; $\{\Delta\mathbf{P}_V\}$, $\{\Delta\mathbf{P}_{FR}\}$, $\{\Delta\mathbf{P}_{HY}\}$, and $\{\Delta\mathbf{P}_{IW}\}$ are the restoring forces from viscous dampers, friction dampers, hysteretic dampers, and infill panels, respectively; c_{corr} is a correction coefficient (usually taken as one); and $\{\Delta\mathbf{F}_{err}\}$ is the vector with the unbalanced forces in the structure.

The solution of the incremental system is carried out using the Newmark-Beta algorithm (Newmark, 1959), that assumes a linear variation of the acceleration, therefore:

$$\{\dot{\mathbf{u}}\}_{t+\Delta t} = \{\dot{\mathbf{u}}\}_t + \Delta t \left[(1-\gamma)\{\ddot{\mathbf{u}}\}_t + \gamma\{\ddot{\mathbf{u}}\}_{t+\Delta t} \right] \quad (a)$$

$$\{\mathbf{u}\}_{t+\Delta t} = \{\mathbf{u}\}_t + \Delta t\{\dot{\mathbf{u}}\}_t + (\Delta t)^2 \left[(0.5 - \beta)\{\ddot{\mathbf{u}}\}_t + \beta\{\ddot{\mathbf{u}}\}_{t+\Delta t} \right] \quad (b)$$

where β and γ are parameters of the method. The program IDARC is by default set up to perform the unconditionally stable constant average acceleration for numerical integration, for which:

$$\beta = 1/4$$

$$\gamma = 1/2$$

but the parameters may be changed to perform a linear acceleration numerical integration, for which:

$$\beta = 1/6$$

$$\gamma = 1/2$$

Rearranging Eq. 6.14 yields the following expressions for the increment in velocity and acceleration:

$$\{\ddot{\mathbf{u}}\}_{t+\Delta t} = \left(1 - \frac{\gamma}{2\beta}\right) \Delta t \{\ddot{\mathbf{u}}\}_t - \frac{\gamma}{\beta} \{\dot{\mathbf{u}}\}_t + \frac{\gamma}{\beta \Delta t} \{\Delta \mathbf{u}\}_{t+\Delta t} \quad \text{---(a)}$$

$$\{\ddot{\mathbf{u}}\}_{t+\Delta t} = \frac{1}{\gamma \Delta t} \{\dot{\mathbf{u}}\}_{t+\Delta t} - \frac{1}{\gamma} \{\ddot{\mathbf{u}}\}_t \quad \text{---(b)}$$

When substituting in Eq. 6.13, the governing equation of motion can be rewritten as:

$$[\mathbf{K}_D] \{\Delta \mathbf{u}\}_{t+\Delta t} = \{\Delta \mathbf{F}_D\} \quad \text{---(6.16)}$$

where $[\mathbf{K}_D]$ and $\{\Delta \mathbf{F}_D\}$ are known as the equivalent dynamic stiffness and load vectors:

$$[\mathbf{K}_D] = \frac{1}{\beta(\Delta t)^2} [\mathbf{M}] + \frac{\gamma}{\beta \Delta t} [\mathbf{C}] + [\mathbf{K}_t] \quad \text{---(a)} \quad \text{---(6.17)}$$

$$\begin{aligned} [\Delta \mathbf{F}_D] &= -[\mathbf{M}] \left[\{\mathbf{L}_h\} \Delta \ddot{x}_{gh} + \{\mathbf{L}_v\} \Delta \ddot{x}_{gv} \right] - \{\Delta \mathbf{P}_V\} - \{\Delta \mathbf{P}_{FR}\} - \{\Delta \mathbf{P}_{HY}\} - \{\Delta \mathbf{P}_{IW}\} \\ &\quad + c_{corr} \{\Delta \mathbf{F}_{err}\} + \left(\frac{1}{2\beta} [\mathbf{M}] + \left(\frac{\gamma}{2\beta} - 1 \right) \Delta t [\mathbf{C}] \right) \{\ddot{\mathbf{u}}\}_t + \left(\frac{1}{\beta \Delta t} [\mathbf{M}] + \frac{\gamma}{\beta} [\mathbf{C}] \right) \{\dot{\mathbf{u}}\}_t \end{aligned} \quad \text{---(b)}$$

The increment in displacements is calculated when the system of linear algebraic equations in Eq. 6.16 is solved. Velocity and accelerations may be calculated by direct

substitution in Eqs. 6.15 (a) and (b), respectively.

The solution is performed incrementally assuming that the properties of the structure do not change during the time step of analysis. Since the stiffness of some elements is likely to change during the time step, the new configuration may not satisfy equilibrium. A compensation procedure is adopted to minimize the error by applying a one step unbalanced force correction.

At the end of step $t + \Delta t$ the difference between the restoring force calculated using the hysteretic model ($\{\mathbf{R}\}$), and the restoring force considering no change in stiffness during the step ($\{\mathbf{R}'\}$), yields the unbalanced force (see Fig. 6.1):

$$\{\Delta \mathbf{F}_{err}\} = \{\mathbf{R}\} - \{\mathbf{R}'\} \quad (6.18)$$

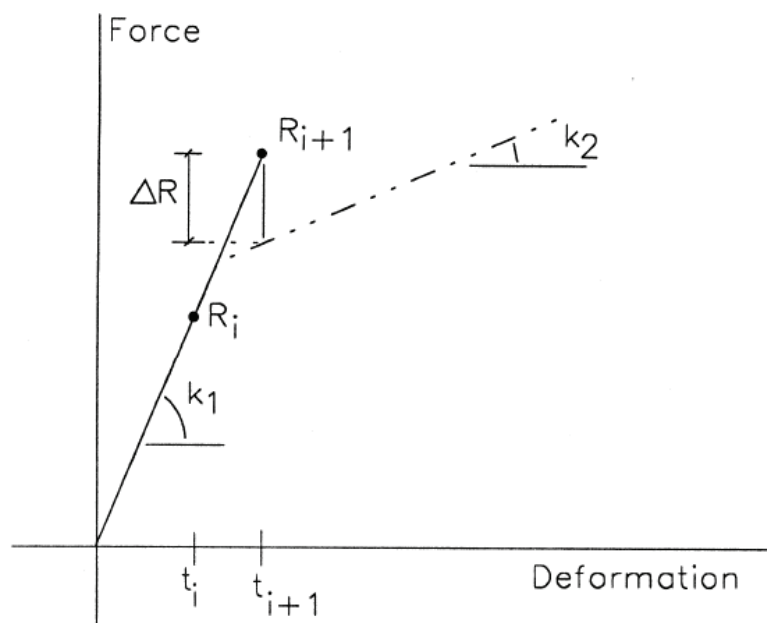


Fig. 6.1 Unbalanced force correction

This corrective force is then applied at the next time step of analysis. The unbalanced forces are computed when moments, shears and stiffness are being updated in the hysteretic model. Such a procedure was first adopted in DRAIN2D (Kannan and Powell, 1973) since the cost of performing iterations in the nonlinear analysis would become prohibitive, especially for large building systems. However, it must be pointed out that this technique is not physically accurate, since adding the unbalanced forces at the next time step has the effect of modifying the input loads. Such a procedure generally works well when small unbalanced forces occur. To minimize the magnitude of the unbalanced forces, a sufficiently small time increment must be selected for analysis. Numerical instabilities in the program are often due to an inadequate time step, that have lead to large unbalanced forces and problems in the hysteretic routines to trace the actual response of the elements. Warnings and directions are provided during analyses.

6.6.2 Damping Considerations

Damping in structures is handled in two ways: (i) describing the inherent damping by an equivalent viscous damping matrix and (ii) modeling the energy dissipation through hysteretic, viscous, and viscoelastic models in dedicated elements. When mixed damping should be considered it is strongly recommended to use minimal amounts of equivalent viscous damping.

The equivalent viscous damping matrix is calculated in the program using one of the following options:

- a) Mass proportional damping
- b) Stiffness proportional damping
- c) Rayleigh damping

All three options can be expressed as:

$$[\mathbf{C}] = \alpha_M [\mathbf{M}] + \alpha_K [\mathbf{K}] \quad (6.19)$$

where the coefficients α_M and α_K are calculated depending on the type of equivalent viscous damping matrix selected:

a) Mass proportional damping:

$$\alpha_M = 2\xi_i \omega_i \quad \text{---(a)} \quad (6.20)$$

$$\alpha_K = 0 \quad \text{---(b)}$$

where ξ_i and ω_i are the critical damping ratio and the circular frequency for mode “ i ”.

b) Stiffness proportional damping:

$$\alpha_M = 0 \quad \text{---(a)} \quad (6.21)$$

$$\alpha_K = \frac{2\xi_i}{\omega_i} \quad \text{---(b)}$$

c) Rayleigh damping:

Combining two distinct modes i and j .

$$\alpha_M = \frac{2\xi_i \omega_i \omega_j^2 - 2\xi_j \omega_j \omega_i^2}{\omega_j^2 - \omega_i^2} \quad \text{---(a)} \quad (6.22)$$

$$\alpha_K = \frac{2\xi_j \omega_j - 2\xi_i \omega_i}{\omega_j^2 - \omega_i^2} \quad \text{---(b)}$$

When the equivalent critical damping ratio is assumed same in both modes considered ($\xi_i = \xi_j = \xi$) the expressions simplify to:

$$\alpha_M = \frac{2\xi\omega_i\omega_j}{\omega_i + \omega_j} \quad \text{--- (a)} \quad (6.23)$$

$$\alpha_K = \frac{2\xi}{\omega_i + \omega_j} \quad \text{--- (b)}$$

In the program IDARC, the circular frequency ω corresponding to the first mode of vibration is used for the mass and stiffness proportional damping, while the circular frequencies corresponding to the first and second modes are used for the Rayleigh damping type. Under these conditions, mass proportional damping will yield a smaller damping ratio for the higher modes, while stiffness proportional and Rayleigh damping will yield a higher critical damping ratio for the higher modes.

6.7 Analyses including P-Delta Effects

The additional overturning moments generated by the relative inter-story drifts are generally referred to as P-delta effects. Such moments arise essentially due to gravity loads and are usually taken into consideration by evaluating axial forces in the vertical elements and computing a geometric stiffness matrix which is added to the element stiffness matrix.

There are two possibilities to consider P-delta effects: (a) For loads acting directly on the lateral resisting systems, the P-delta effects are included through a geometric stiffness matrix formulation (Section 6.7.1); (b) For gravity loads acting in “gravity columns” not modeled (considered) in the lateral load resisting system, the P-delta effects are included by modeling an auxiliary “gravity columns” (Section 6.7.2).

6.7.1 P-delta through Geometric Matrix

In the program IDARC, P-delta effects are represented by equivalent lateral forces, equal in magnitude to the overturning moments caused by eccentric gravity forces due to inter-story drift (Wilson and Habibullah, 1987). Consider a typical vertical element between two story levels shown in Fig. 6.2. Taking moments about the lower story level, the following equilibrium equation is obtained:

$$Ph_i - (M_i + M_{i-1}) - N_i(u_i - u_{i-1}) = 0.0 \quad (6.24)$$

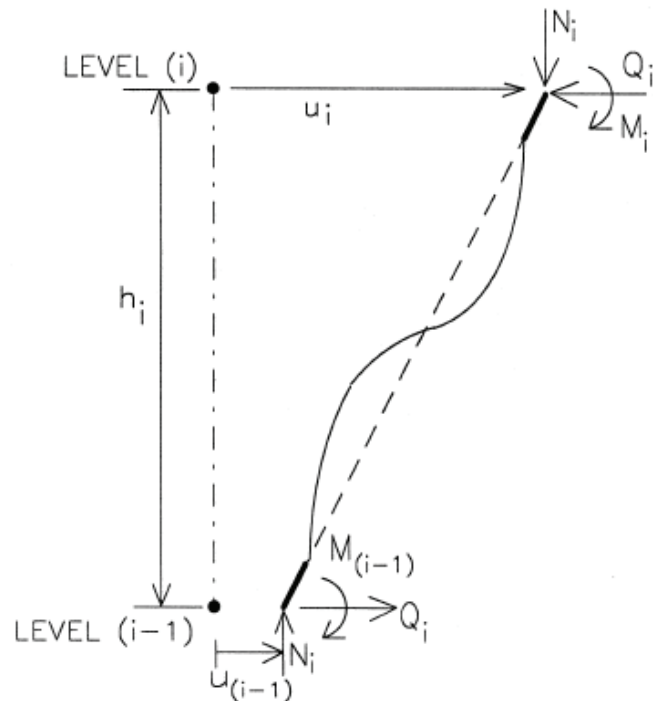


Fig. 6.2 Computation of shear due to P-delta effects

Considering equilibrium of the additional gravity load shears at story level “ i ”, the following expression is obtained:

$$P_i = \frac{N_i(u_i - u_{i-1})}{h_i} - \frac{N_{i+1}(u_{i+1} - u_i)}{h_{i+1}} \quad (6.25)$$

The above equations can be written in the following form for each component:

$$\{\mathbf{P}^*\} = [\mathbf{K}_G]\{\Delta\mathbf{u}\} \quad (6.26)$$

where $\{\Delta\mathbf{u}\}$ is the incremental vectors of story displacement. $[\mathbf{K}_G]$ is a tridiagonal matrix similar to the geometric stiffness matrix in the finite elements. This matrix is added to the overall stiffness prior to the start of a new analysis step.

$$[\mathbf{K}_G] = \begin{bmatrix} \frac{N_N}{h_N} & -\frac{N_N}{h_N} & 0 & . & . & . & . & . & 0 \\ -\frac{N_N}{h_N} & \frac{N_N}{h_N} + \frac{N_{N-1}}{h_{N-1}} & -\frac{N_{N-1}}{h_{N-1}} & 0 & . & . & . & . & . \\ 0 & -\frac{N_{N-1}}{h_{N-1}} & \frac{N_{N-1}}{h_{N-1}} + \frac{N_{N-2}}{h_{N-2}} & -\frac{N_{N-2}}{h_{N-2}} & 0 & . & . & . & . \\ . & . & . & . & . & . & . & . & . \\ . & 0 & -\frac{N_{i+1}}{h_{i+1}} & \frac{N_{i+1}}{h_{i+1}} + \frac{N_i}{h_i} & -\frac{N_i}{h_i} & 0 & . & . & . \\ . & . & 0 & -\frac{N_i}{h_i} & \frac{N_i}{h_i} + \frac{N_{i-1}}{h_{i-1}} & -\frac{N_{i-1}}{h_{i-1}} & 0 & . & . \\ . & . & . & . & . & . & . & . & . \\ . & . & . & 0 & -\frac{N_3}{h_3} & \frac{N_3}{h_3} + \frac{N_2}{h_2} & -\frac{N_2}{h_2} & 0 & . \\ . & . & . & . & 0 & -\frac{N_2}{h_2} & \frac{N_2}{h_2} + \frac{N_1}{h_1} & -\frac{N_1}{h_1} & . \\ 0 & . & . & . & . & 0 & -\frac{N_1}{h_1} & \frac{N_1}{h_1} & . \end{bmatrix} \quad (6.27)$$

where $N_i = \sum_{jj=i}^N N_{jj}$, and N_{jj} are the specific floor weights. The global stiffness matrix is defined as

$$[\mathbf{K}_t^*] = [\mathbf{K}_t] - [\mathbf{K}_G] \quad (6.28)$$

6.7.2 P-delta through Auxiliary Gravity Columns

The P-delta effects on the global structural system can be included by adding an auxiliary column to any frame in the structural models, connected through a “double hinged” link beam (or truss bar). The column must have its ends hinged such that the column has only “geometric stiffness” as described by the matrix in Eq. 6.26. The gravity loads (nodal axial force) at each level must be the sum of all gravity forces in the structure not attributed (supposed) by the lateral load resisting system, cumulative to that level. See Fig. 6.3 for additional information.

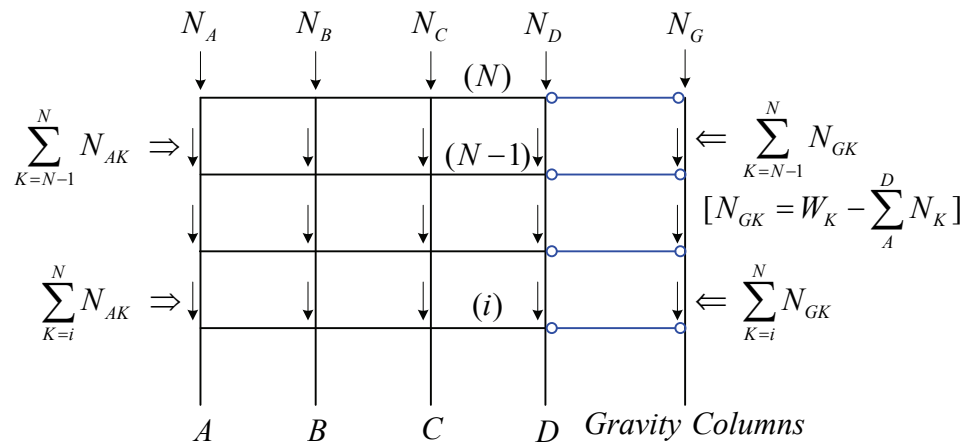


Fig. 6.3 Gravity columns in the structural model for P-delta effects consideration

SECTION 7

DAMAGE ANALYSIS

7.1 Introduction

Important research have been carried out to develop a damage indicators to qualify the response of structures. Reinhorn and Valles (1995) presents for a summary of various damage indices proposed. The current release of IDARC incorporates three models for damage indices: (i) a modified Park & Ang model (Park et al., 1984; Kunnath et al. 1992b), introduced in the previous releases of the program, (ii) a new fatigue based damage model introduced by Reinhorn and Valles (1995), based on Bracci (1990), and (iii) an overall damage qualification based on the variation of the fundamental period of the structure.

The Park & Ang and the fatigue based damage model can be used to calculate different damage indices: element, story (subassembly), and overall building damage. However, for the story and overall damage indices the ultimate inter-story deformation or top story displacement are required, as well as the corresponding story yield shear force or base shear yield force level. Such quantities can be readily determined from an incremental nonlinear lateral (pushover) analysis (see Section 6.3). To determine an estimate of the story and overall damage indices, weighting factors were introduced based on the energy absorption in the different structural elements or entire stories sub-structure. For a description of the methodology necessary to adequately determine story and overall damage indices see Valles et al. (1995).

7.2 Modified Park & Ang Damage Model

The Park & Ang damage model (Park et al., 1984) was incorporated in IDARC since the original release of the program (Park et al., 1987). Furthermore, the Park & Ang damage model is also an integral part of the three parameter hysteretic model since the rate of strength degradation is directly related to the parameter β described below (Park et al., 1987).

The original Park & Ang damage index for a structural element is defined as:

$$DI_{P\&A} = \frac{\delta_m}{\delta_u} + \frac{\beta}{\delta_u P_y} \int dE_h \quad (7.1)$$

where δ_m is the maximum experienced deformation; δ_u is the ultimate deformation of the element; P_y is the yield strength of the element; $\int dE_h$ is the cumulative hysteretic energy absorbed by the element during the response history; and β is a model constant parameter. A value of 0.1 for the parameter β has been suggested for nominal strength deterioration (Park et al., 1987). The Park & Ang damage model accounts for damage due to maximum inelastic excursions, as well as damage due to the history of deformations. Both components of damage are linearly combined.

Three damage indices are computed using this damage model:

1. Element damage index: column, beams or shear wall elements.
2. Story damage index: vertical and horizontal components and total story damage.
3. Overall building damage.

Equation 7.1 is the basis for the modified damage index developed for this program, although some considerations need to be taken into account as shown below.

$$DI_{P\&A} = \frac{\delta_m - \delta_y}{\delta_u - \delta_y} + \frac{\beta}{\delta_u P_y} E_h \quad (7.2)$$

where E_h is a total cumulative hysteretic energy: $\int dE_h$. Direct application of the damage model to a structural element, a story, or the overall building requires the determination of the corresponding overall element, story, or building ultimate deformations. Since the inelastic behavior is confined to plastic zones near the ends of some members, the relation between element, story or top story deformations, with the local plastic rotations is difficult to establish. For the element end section damage, the following modifications to the original model were introduced in IDARC version 3.0 (Kunnath et al., 1992b):

$$DI_{component} = \frac{\theta_m - \theta_r}{\theta_u - \theta_r} + \frac{\beta}{M_y \theta_u} E_h \quad (7.3)$$

where θ_m is the maximum rotation attained during the loading history; θ_u is the ultimate rotation capacity of the section; θ_r is the recoverable rotation when unloading; M_y is the yield moment; and E_h is the cumulative dissipated energy in the section. The overall element damage is defined as the biggest damage index of the end sections.

Two additional damage indices are defined as follows: (i) story and (ii) overall damage indices which are computed using weighting factors based on the hysteretic energy dissipated at component and story levels respectively:

(i) Story Damage

$$DI_{story} = \sum (\lambda_i)_{component} (DI_i)_{component} \quad (7.4)$$

$$\text{where } (\lambda_i)_{component} = \left(\frac{E_i}{\sum E_i} \right)_{component}$$

(ii) Overall Damage

$$DI_{overall} = \sum (\lambda_i)_{story} (DI_i)_{story} \quad (7.5)$$

$$\text{where } (\lambda_i)_{story} = \left(\frac{E_i}{\sum E_i} \right)_{story}$$

where λ_i are the energy weighting factors; and E_i are the cumulative energy absorbed by the component or story “ i ”.

The Park & Ang damage model has been calibrated using a database of observed structural damage of nine reinforced concrete buildings (Park et al., 1986). Table 7.1 presents the calibrated damage index with the degree of observed damage in the structure.

Table 7.1 Interpretation of overall damage index (Park et al., 1986)

LIMIT STATE DAMAGE INDEX	DEGREE OF DAMAGE	DAMAGE (SERVICE) STATE	USABILITY	APPEARANCE
(1)	(2)	(3)	(4)	(5)
	None	Undamaged		Undeformed / uncracked
0.00			Usable	
0.20-0.30	Slight	Serviceable		Moderate to severe cracking
0.50-0.60	Minor	Repairable	Temporarily	Spalling of concrete cover
	Moderate		Unusable	
	Severe	Unrepairable		Buckled bars, exposed core
> 1.0				
	Collapse	Collapse	Unusable	Loss of shear/axial capacity

7.3 Fatigue Based Damage Model

The fatigue based damage model was introduced by Reinhorn and Valles (1995). The damage model was developed based on basic structural response considerations, and a low-cycle fatigue rule. The damage index is:

$$DI = \frac{\delta_a - \delta_y}{\delta_u - \delta_y} \frac{1}{\left(1 - \frac{E_h}{4(\delta_u - \delta_y)F_y}\right)} \quad (7.6)$$

where δ_a is the maximum experienced deformation, rotation, or curvature; δ_y is the yield deformation capacity; δ_u is the ultimate deformation capacity; F_y is the yield force capacity; and E_h is the cumulative dissipated hysteretic energy.

The damage index proposed can be used to qualify the performance of structural elements, stories (subassemblies), or the overall response of the building. Yield and ultimate capacities for story and overall assemblies can be easily determined using the incremental nonlinear lateral (pushover) analysis option (See Section 6.3). However, since these capacities are not readily available during a time history analysis, weighting of element damage indices using dissipated energy considerations are used (see considerations described in the Park & Ang damage model). See Valles et al. (1995) for a detailed methodology on how story and overall building damages can be obtained combining the results from pushover and time history analysis.

Note that simplifying the fatigue based damage model for the case when the ratio $(\delta_a - \delta_y)/(\delta_u - \delta_y)$ is close to one, Eq. 7.6 simplifies (using Taylor expansion) to:

$$DI = \frac{\delta_a - \delta_y}{\delta_u - \delta_y} + \frac{E_h}{4(\delta_u - \delta_y)F_y} \quad (7.7)$$

That is the same as the modified Park & Ang damage formulation for $\beta = 0.25$. Therefore, the Park & Ang damage model is correlated to the fatigue based model for maximum deformations close to the ultimate capacity of the element. For more details on the fatigue based damage model see Reinhorn and Valles (1995). The fatigue based

damage model was introduced starting with version 4.0 and the indices of story and overall damage are computed using the same relationship of Eq. 7.4 and 7.5.

7.4 Global Damage Model

Another measure of damage of the structure is the variation in the fundamental period of vibration of the structure. This history is related to the overall stiffness degradation of the structure due to inelastic behavior. The history of the variation of the first mode of vibration is part of the “user defined snapshot options” in the program, as described in Section 8.1.

DiPasquale and Cakmak (1988) defined the softening of the structure as:

$$DI = 1 - \frac{(T_0)_{initial}}{(T_0)_{equivalent}} \quad (7.8)$$

Using the snapshot option to print the variation of the fundamental period, the softening of the structure can be estimated.

SECTION 8

ADDITIONAL FEATURES IN THE PROGRAM

This section presents several features added to the program to allow some post-processing of the analysis information. These features are *i*) Structural Response Snapshot, *ii*) Structural Collapse Snapshot, *iii*) Element Stress Resultants Ratios normalized to their capacity, and *iv*) Special Ground Motions.

8.1 Structural Response Snapshots

The program IDARC includes the option to determine the response of the structure at instants during the analysis. Several types of response snapshots can be specified:

- a) Displacement profile.
- b) Element stress ratios.
- c) Structural collapse state.
- d) Damage indices.
- e) Dynamic characteristics (eigenvalue analysis).

Response snapshots can be requested by the user during pushover, quasi-static or dynamic analysis.

Two types of response snapshots are specified in the program: default and user defined. Default snapshots will be reported, if requested by the user, for the first crack, yield or failure observed in any column, beam or shear wall in the structure during the analysis. Furthermore, all snapshot types are always reported at the end of the analysis. User defined snapshots can be specified for specific base shear or top displacement threshold levels. Using this feature the user can recover the response state of the structure

at any particular point during the analysis.

8.2 Structural Collapse State

During analysis the state of columns, beams and shear walls is observed. The program keeps track if a structural element has cracked, yielded or failed. The qualification is based on computing deformations to the specified envelope values. This information is automatically reported graphically, at the end of the analysis, but it can also be recovered at any step in the analysis using the response snapshot option. The structural collapse state is reported for each frame in the structure following a simple graphical convention to identify cracked or yielded elements (see Fig. 8.1), including shear state. Additional information on the state of the structure can be obtained from the damage analysis, presented in Section 7.

8.3 Element Stress Resultants Ratios

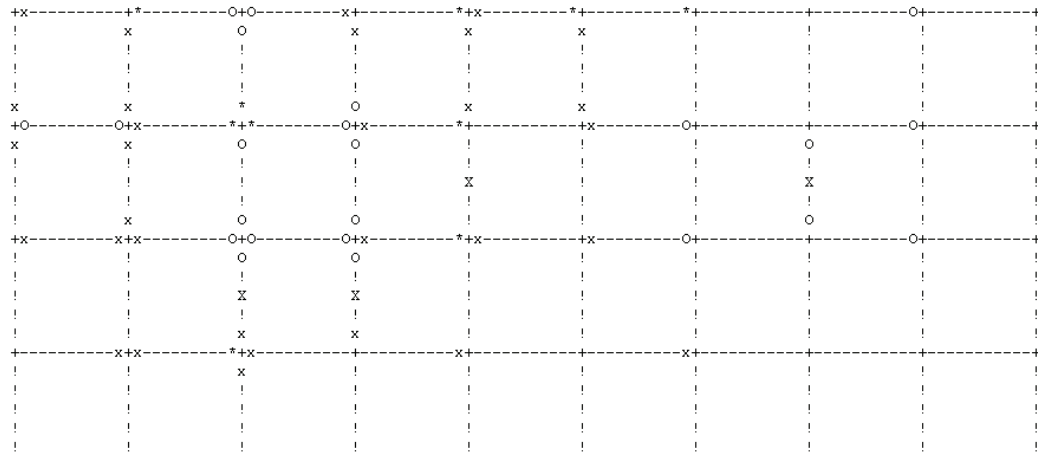
During analysis the stress ratios of the structural elements can be reported. This information can only be requested as a response snapshot. This option reports the ratios of demand to ultimate capacity in shear, axial and flexure for columns, beams and shear walls.

8.4 Special Ground Motions for Nonlinear Dynamic Analysis

For the nonlinear dynamic analysis, the user can consider the general ground motions, attaching the wave data file. However, in the new version, the user can define and generate a random white noise excitation, automatically. The white noise ground motion has a constant spectra density which will constantly interact with the structural response from elastic to plastic in frequency range. Thus, it may provides quite conservative results in plastic range.

***** CURRENT STATE OF FAILURE *****

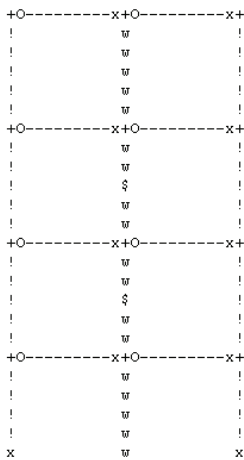
FAILURE MODE OF FRAME NO. 1



NOTATION:

- = BEAM	x = CRACKING(FOR CONCRETE)	
! = COLUMN	! = INITIAL YIELD(FOR STEEL)	
w = SHEAR WALL	o = PLASTIC HINGE DEVELOPED	
	*	= LOCAL FAULURE(EXCEED CRITERIA)
I = EDGE COLUMN	FOR EDGE COLS: C: COMPRESSION	
	T: TENSION	
	O: TENSILE YIELD	
	X = INITIAL SHEAR CRACK	
	\$ = SHEAR FAILURE	

FAILURE MODE OF FRAME NO. 2



NOTATION:

- = BEAM	x = CRACKING(FOR CONCRETE)	
! = COLUMN	! = INITIAL YIELD(FOR STEEL)	
w = SHEAR WALL	o = PLASTIC HINGE DEVELOPED	
	*	= LOCAL FAULURE(EXCEED CRITERIA)
I = EDGE COLUMN	FOR EDGE COLS: C: COMPRESSION	
	T: TENSION	
	O: TENSILE YIELD	
	X = INITIAL SHEAR CRACK	
	\$ = SHEAR FAILURE	

Fig. 8.1 Sample of collapsed state response

SECTION 9

PROGRAM VERIFICATIONS AND EXAMPLES: CASE STUDIES

9.1 Component Testing: Full Scale Bridge Pier Under Reversed Cyclic Loading

A series of full-scale and scale model circular columns were tested at the laboratories of the National Institute of Standards and Technology (Stone and Cheok, 1989; Cheok and Stone, 1990). These columns represent typical bridge piers deigned in accordance with Caltrans specifications. The piers were tested by applying both axial and lateral loads as shown in the experimental set-up in Fig. 9.1. The column analyzed in this sample investigation is a full-scale circular bridge pier measuring 30 feet with an aspect ratio of 6.0. The tests were performed using a displacement controlled quasi-static history as shown in Fig. 9.1. The column was made of 5.2 ksi concrete (measured compressive strength at 28 days) and had a modulus of elasticity of approximately 4110 ksi. Grade 60 steel with an actual yield stress of 68.9 ksi and elasticity modulus of 27438 ksi was used as longitudinal reinforcement. The steel exhibited good ductility in the material testing with a 2% strain and a strain hardening of 1454 ksi before actual rupture. The cross-section in Fig. 9.1 also shows the reinforcement details. The experiment was analyzed using data presented in the Input Data Sheet for Case Study #1 (see Appendix B).

The purpose of this analysis is to simulate the essential characteristics of the hysteretic behavior and compare it with the experimental recorded response. The modified three parameter hysteretic model was used with a stiffness degradation coefficient HC=9.0, strength degradation coefficient HBE=0.05; HBD=0.0 (very little deterioration in strength), and a pinching coefficient HS=1.0 (indicating no pinching). These parameters were estimated from the observed experimental loops, and could be used to represent well-detailed section. The response obtained from the analysis is compare with the test results in Fig. 9.2. The maximum loads attained in the analysis, 290

kips and 316 kips (positive and negative) compare well with those observed in the tests, 284 kips and 296 kips, respectively.

The damage evaluated using the analytical model is presented in Fig. 9.3. Part of the damage is due to permanent deformations while part is due to strength deterioration from hysteretic behavior. Note that the deformation damage stays constant during the phase in which the column was cycled repeatedly at a ductility of 4.0. The total damage reaches approximately 0.9, which is indicative of extremely large damage, usually beyond repair, as was the case for the tests presented here. It must also be pointed out that the specimen was able to sustain an additional one and half cycles before failure at a ductility of 0.8.

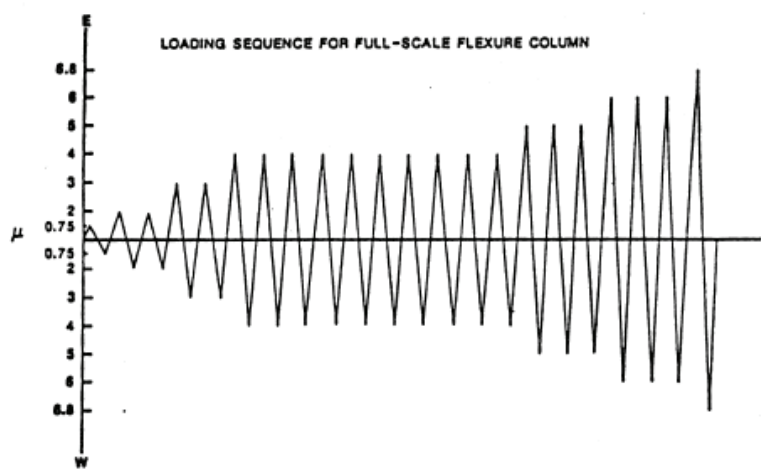
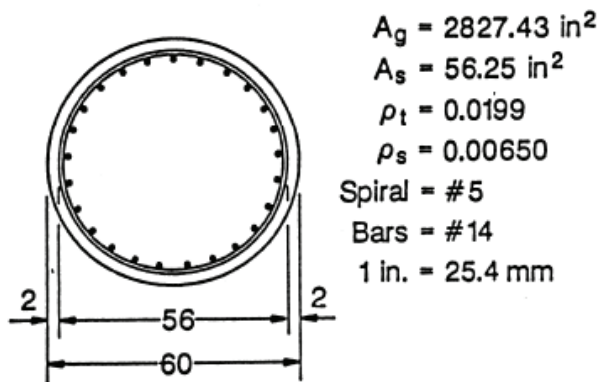
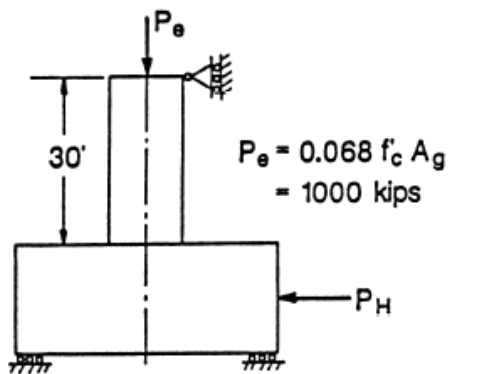


Fig. 9.1 Configuration and loading of full-scale bridge pier

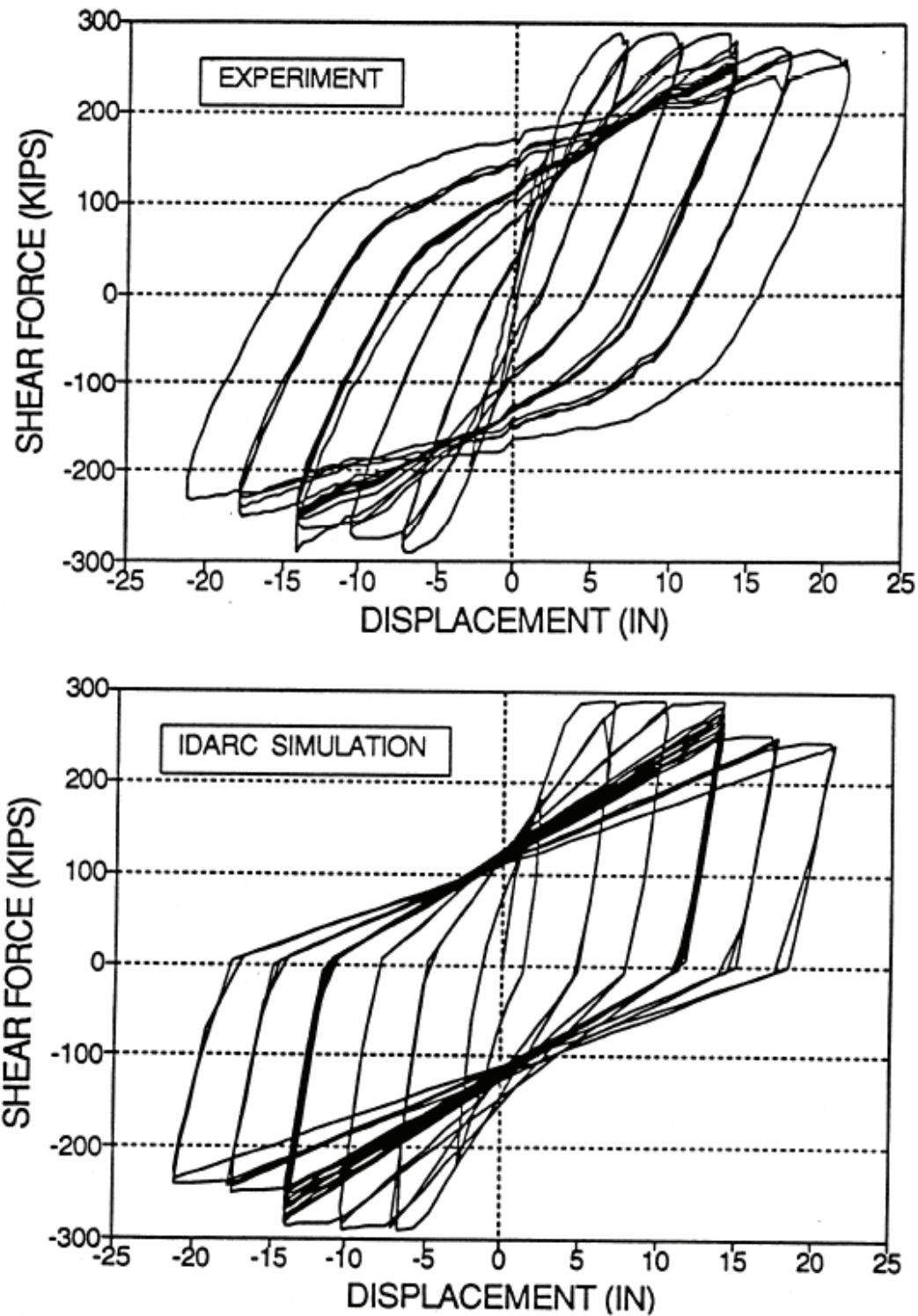


Fig. 9.2 Comparison of observed vs. computed response

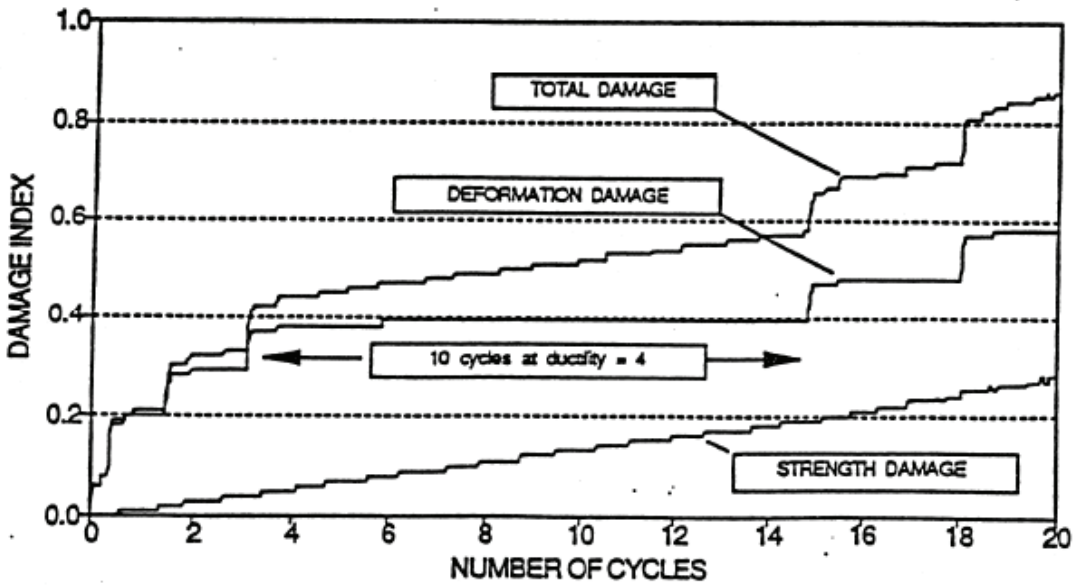


Fig. 9.3 Progressive damage history during cyclic testing

9.2. Subassemblage Testing: 1:2 Scale Three-Story Frame

A 1:2 scale model of a three-story frame, typical to construction practice of reinforced concrete structures in China, was tested in the laboratory by Yunfei et al. (1986). The structure was tested using a displacement controlled loading as shown in Fig.9.4. The geometry of the frame and the essential reinforcement used for the analysis is also shown in Fig. 9.4. The frame is made of 40.2 MPa concrete and is reinforced by Grade 40 steel (400MPa yield strength). Default parameters were used for the other material property information (see zero input in data Case Study #2, Appendix B). The first three cycles of loading produced cracking and first yielding. Subsequent loading of three cycles at the same ductility were applied until the frame collapsed.

The model was analyzed using the data specified in the data sheet for Case Study #2 in Appendix B. The hysteretic parameters were initially assigned based on well-detailed ductile sections obtained from the previous case study. These parameters were found to be adequate in reproducing the overall system response, however, a better

estimate was obtained by increasing the strength degrading parameter. The final parameters, HC=8 for stiffness degradation, HBE-0.1 for strength deterioration and HS=1.0 for bond slip (pinching), produced excellent agreement of force levels at the larger amplitude cycles as shown in Fig. 9.5.

The choice of hysteretic parameters is important, but not critical in establishing the overall system response. For example, values of HC between 4.0 and 9.0, and values between 0.05 and 0.10 would have produced almost comparable results. As will be pointed out later, a proper choice of hysteretic parameters becomes important for local failure cases due to effects of bar pull-out, pinching shear, etc., or when microconcrete is used for small-scale models (1:4 or greater). In this case study, no special connection behavior was modeled.

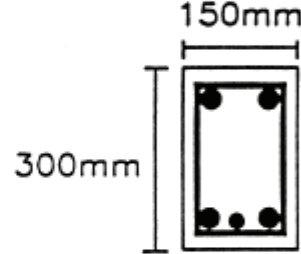
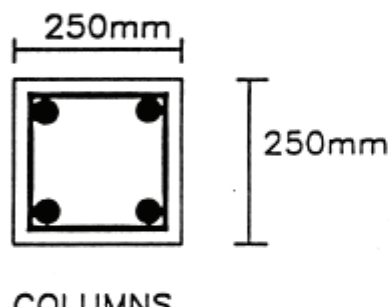
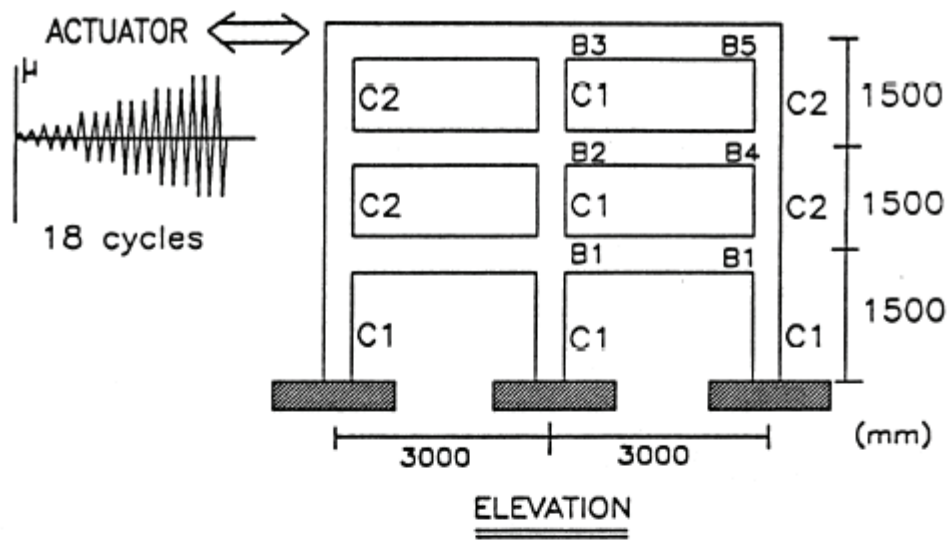
The present version of the program calculates the dissipated hysteretic energy of components that can be used as an identification target for the choice of hysteretic parameters. In the current analysis, the identification was directed towards the maximum force level which involves only the strength deterioration parameter. Hysteretic energy is also a known measure of structural damage. Fig. 9.6 presents a comparative representation of dissipated energy and total system damage. A maximum damage of about 0.6 was achieved in the analysis, indicating that the global damage index is less sensitive to local damage accumulated at individual sections. Therefore, it will be necessary to calibrate global indices before they can be used in damage assessment.

Another feature of the IDARC program is the push-over analysis under monotonically increasing lateral loads. This feature was used to determine the correspondence with the observed collapse mechanism. The frame developed a beam side sway collapse mechanism that was clearly documented in the experimental records through measured rebar yielding in the critical beam-column interface and column-base sections, and identified by visual observations. Fig. 9.7 shows the damaged frame with

observed plastic hinge locations and computed sequence of hinge formation using IDARC.

Finally, the progression of damage history is shown in Fig. 9.8 for each of the story levels. The upper two levels did not experience any column damage. Studies of this nature can be used to calibrate damage models using ductility demand and dissipated hysteretic energy as controlling criteria.

The two cases studies presented this far are based on displacement controlled loading, which is typical in laboratory testing of components and subassemblies. IDARC can also be used for force-controlled loading histories.



(dimensions in mm)

SECTION	NO OF BARS & BAR DIA	HOOPS
COLUMN C1	4 # 14	12mm@75 mm
COLUMN C2	4 # 12	8mm@75 mm
BEAM B1	TOP: 2 # 16 BOT: 2 # 16	6mm@75 mm
BEAM B2	TOP: 2 # 16 BOT: 2 # 16, 1 # 10	6mm@75 mm
BEAM B3	TOP: 2 # 12 BOT: 2 # 14	6mm@75 mm
BEAM B4	TOP: 2 # 18 BOT: 2 # 16	6mm@75 mm
BEAM B5	TOP: 2 # 14 BOT: 2 # 14	6mm@75 mm

Fig. 9.4 Details of half-scale model frame

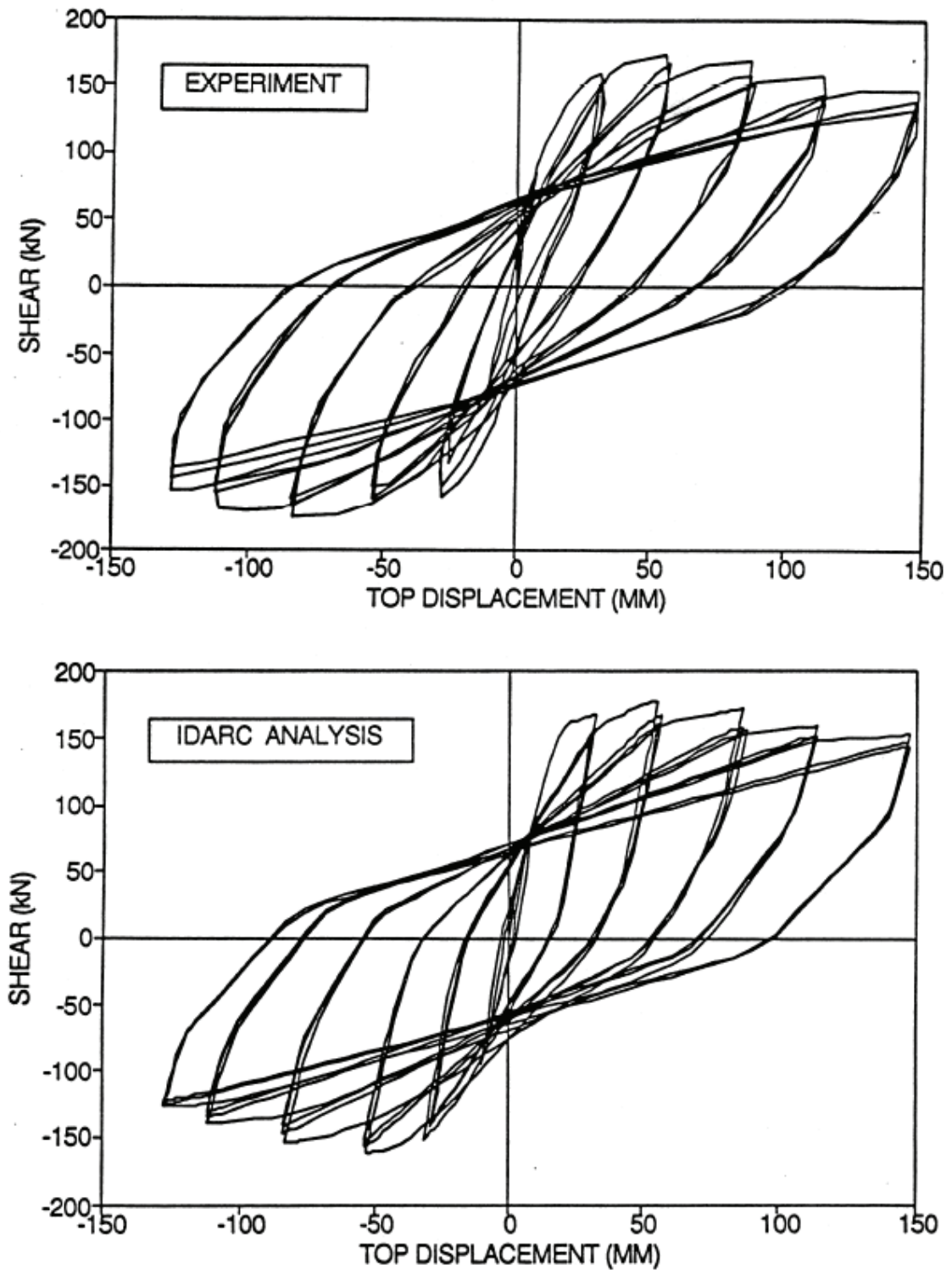


Fig. 9.5 Comparison of observed vs. simulated force-deformation response

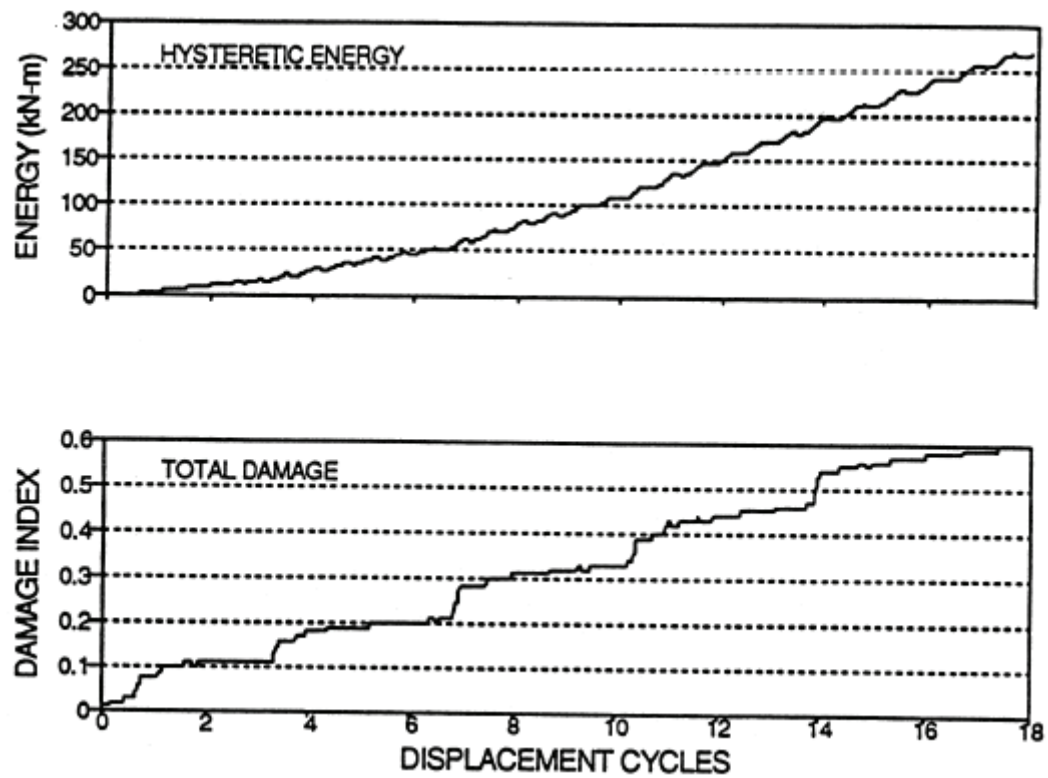
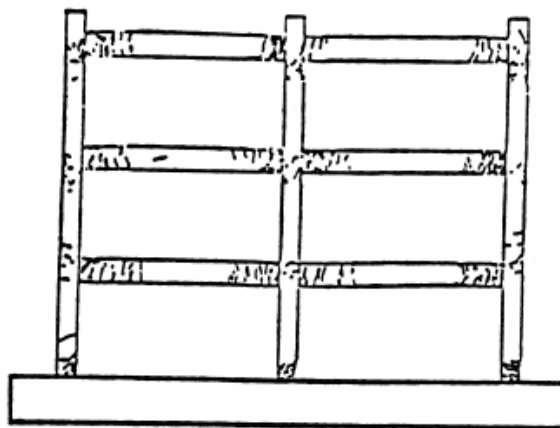
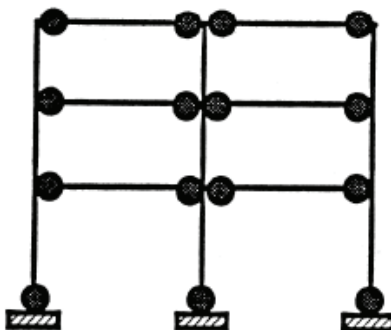


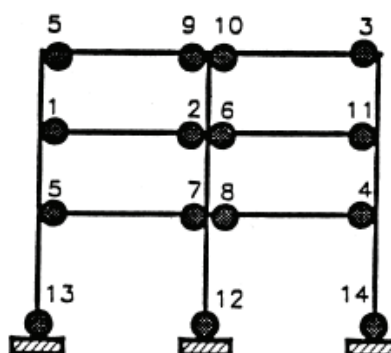
Fig. 9.6 Correlation of dissipated energy and global damage



(a) DAMAGED FRAME



(b) EXPERIMENT



NOTATION:

● PLASTIC HINGE

Numbers indicate sequence
of plastic hinge formation

(c) ANALYSIS

Fig. 9.7 Study of collapse mechanism

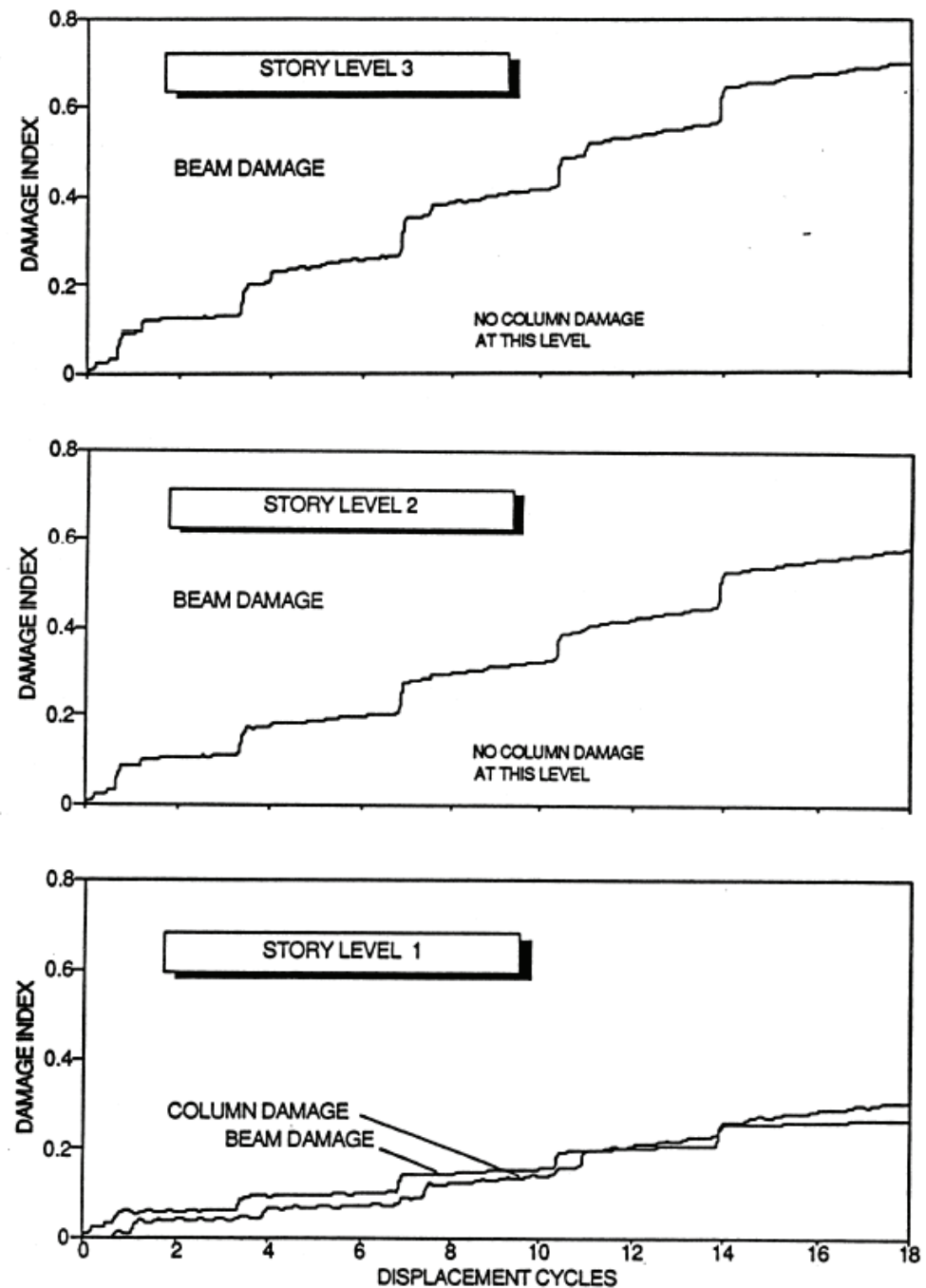


Fig. 9.8 Progressive story level damage

9.3 Seismic Simulation: Ten-Story Model Structure

This study is based on shaking table tests of a ten story, three-bay frame, scale model of a structure conducted at the University of Illinois, Urbana (Cecen, 1979). The model was subjected to similar earthquake ground motions at levels that produce strong inelastic behavior and damage. The geometrical configuration, element designation, dimensions and reinforcement details are shown in Fig. 9.9. The model is made of 4350 psi concrete and grade 60 steel with a measured yielding strength of 70 ksi and modulus of elasticity of 29000ksi. The initial concrete modulus was adjusted to provide a fundamental period consistent with observed response. This is an important consideration when initial conditions, such as cracking resulting from gravity loads or model construction, produce a system that is not consistent with gross moment of inertia computations.

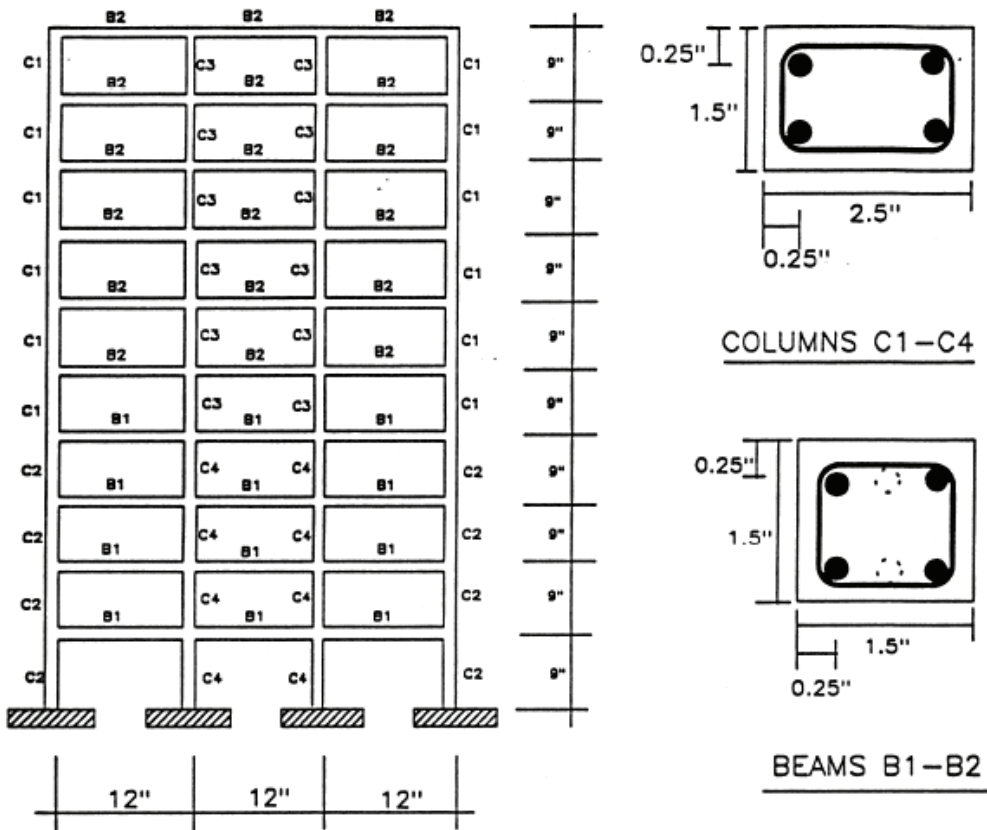
The model was subjected to scaled ground excitations with 2.5 time compression of the 1940 El Centro accelerogram. The peak base accelerations of the three successive seismic inputs were: 0.36g, 0.84g and 1.6g respectively, as shown in Fig. 9.10. The purpose of this case study is to compare the analytical response with the experimental results when severe nonlinearities resulting from progressive damage are observed. The second objective of the study is to compare the analytical performance with other analytical programs that perform similar tasks. The analysis was done using the information presented in the input data sheets for Case Study #3 (see Appendix B). The structure is modeled by mass similitude with a total floor weight of 1000 lbs per floor. The dynamic analysis is performed considering an integration time step of 0.001 sec. Hysteretic parameters used are listed in the input data sheet. There was no predetermined basis for the choice of hysteretic parameters. The program default values were used for both beams and columns, with the exception of the stiffness degrading parameter for columns where the program assigned default is 2.0. However, results of testing on relatively small scale components (1:4 or greater) indicate that the parameter HC is much

smaller, and a suggested value of $HC=0.5 - 1.0$ is recommended in such cases.

The comparison of the analytical and experimental results in terms of (i) peak accelerations is shown in Fig. 9.11; and (ii) peak displacements is shown in Fig. 9.12. The maximum displacement reported in Cecen (1979) is based on one-half the double amplitudes, while the IDARC values are absolute peak. The entire displacement histories compare more favorably as will be discussed next.

The analysis results are also compared with two other computer programs: (i) SARCF-III (Gomes et al., 1990) and (ii) DRAIN-2D (Kaanan and Powell, 1971). Since both SARCF and DRAIN use bilinear envelopes, only the initial stiffness and yield moments were provided as basic input. The default Takeda degrading model was used in DRAIN, while the damage-based hysteretic model was used in SARCF. The results are presented in Figs. 9.13 through 9.15. IDARC shows peak differences ranging between 3% to 10% of experimentally observed values. It can also be observed that an excellent agreement is obtained using IDARC for RUN H1-3 which has the largest inelastic response.

In all three programs, the three seismic inputs were provided successively as a continuous ground motion, so that the effects of each run were carried forth to the next without returning the system to undamaged conditions. Recording instruments, on the other hand, are typically reset to zero conditions between tests, thereby making it difficult to track permanent deformations, if any.



SECTION	LONG. REINF (each face)	TRANS. REINF.
BEAM B1	2#13	#16 gage@ 0.3"
BEAM B2	3#16	- " -
COLUMN C1	2#10	#16 gage@ 0.35"
COLUMN C2	2#7	- " -
COLUMN C3	2#13	- " -
COLUMN C4	2#8	- " -

Fig. 9.9 Configuration and reinforcement details for model structure

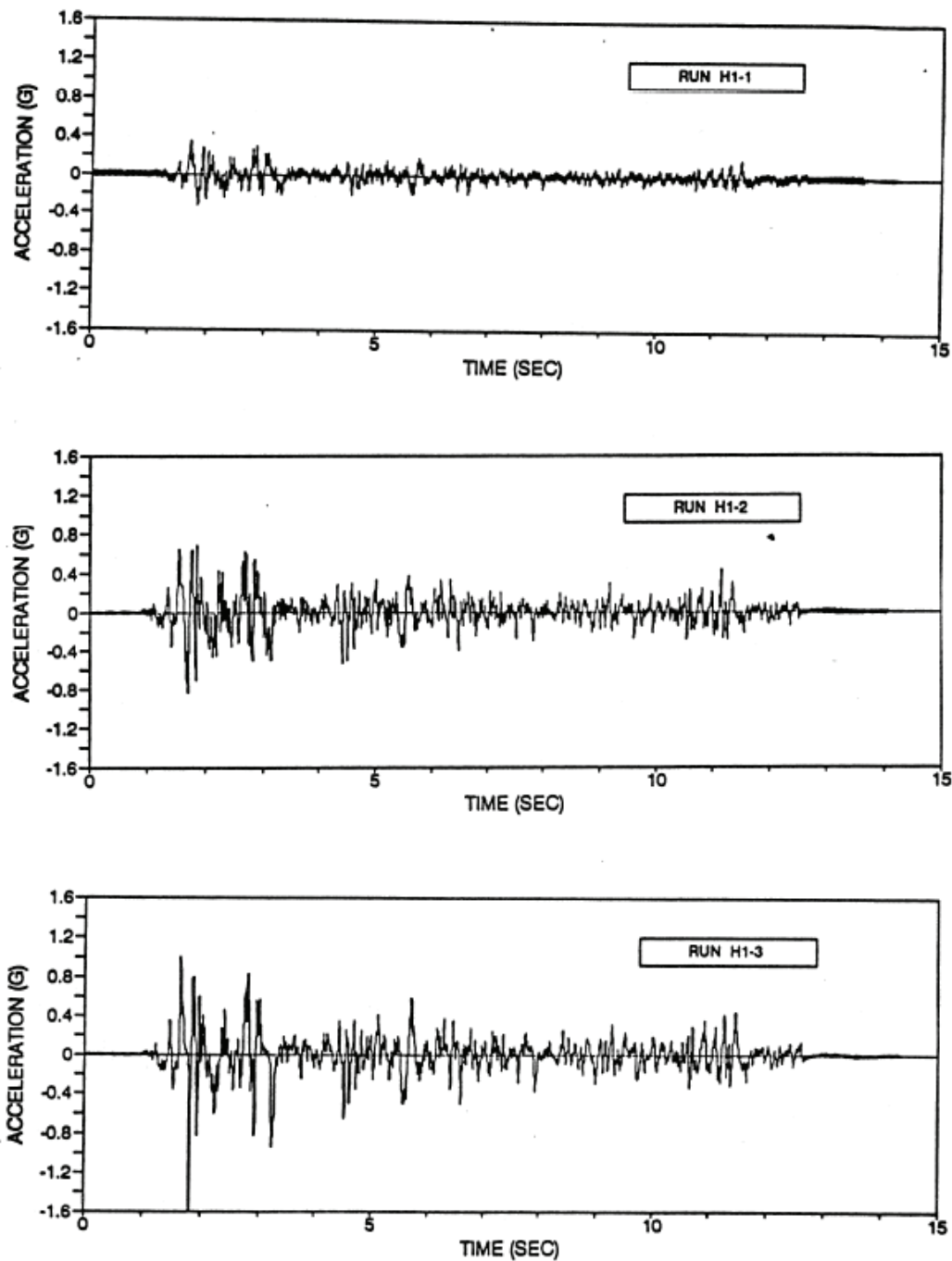


Fig. 9.10 Achieved table motions for seismic testing

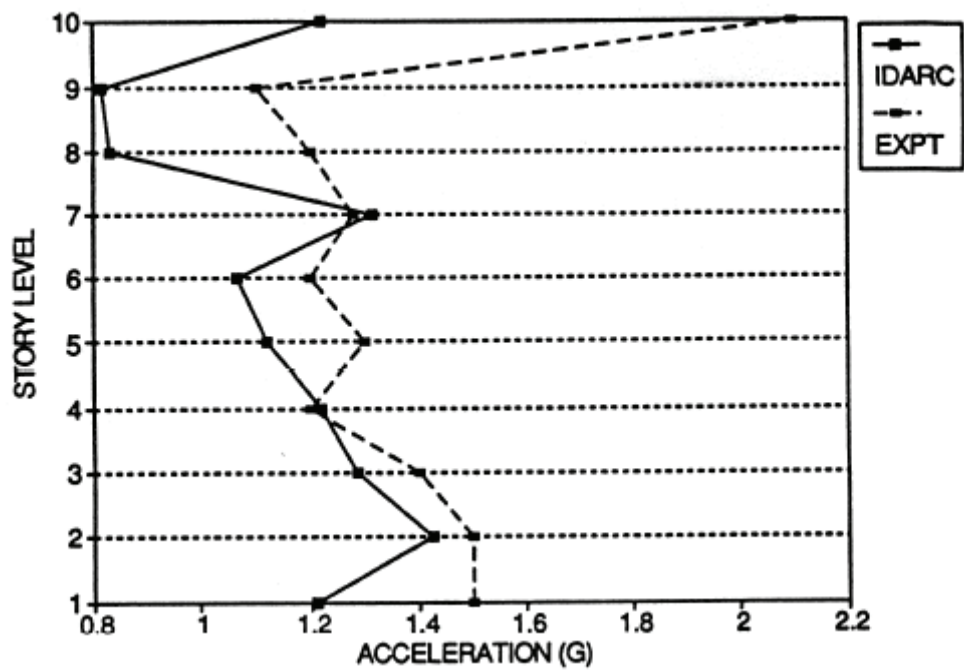


Fig. 9.11 Computed versus observed peak acceleration response

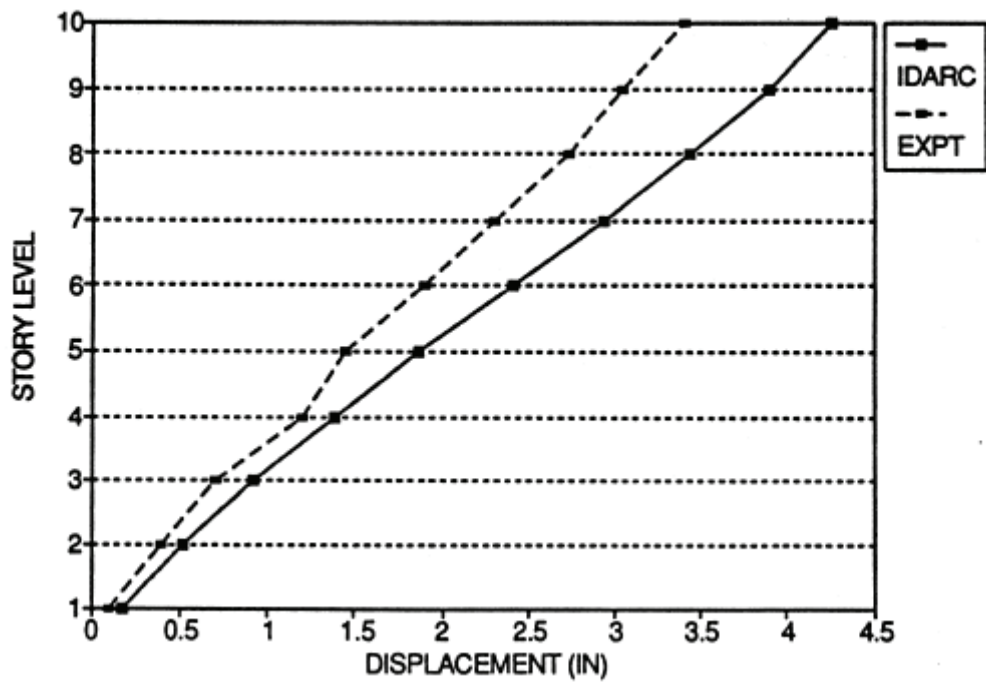


Fig. 9.12 Computed versus observed peak displacement response

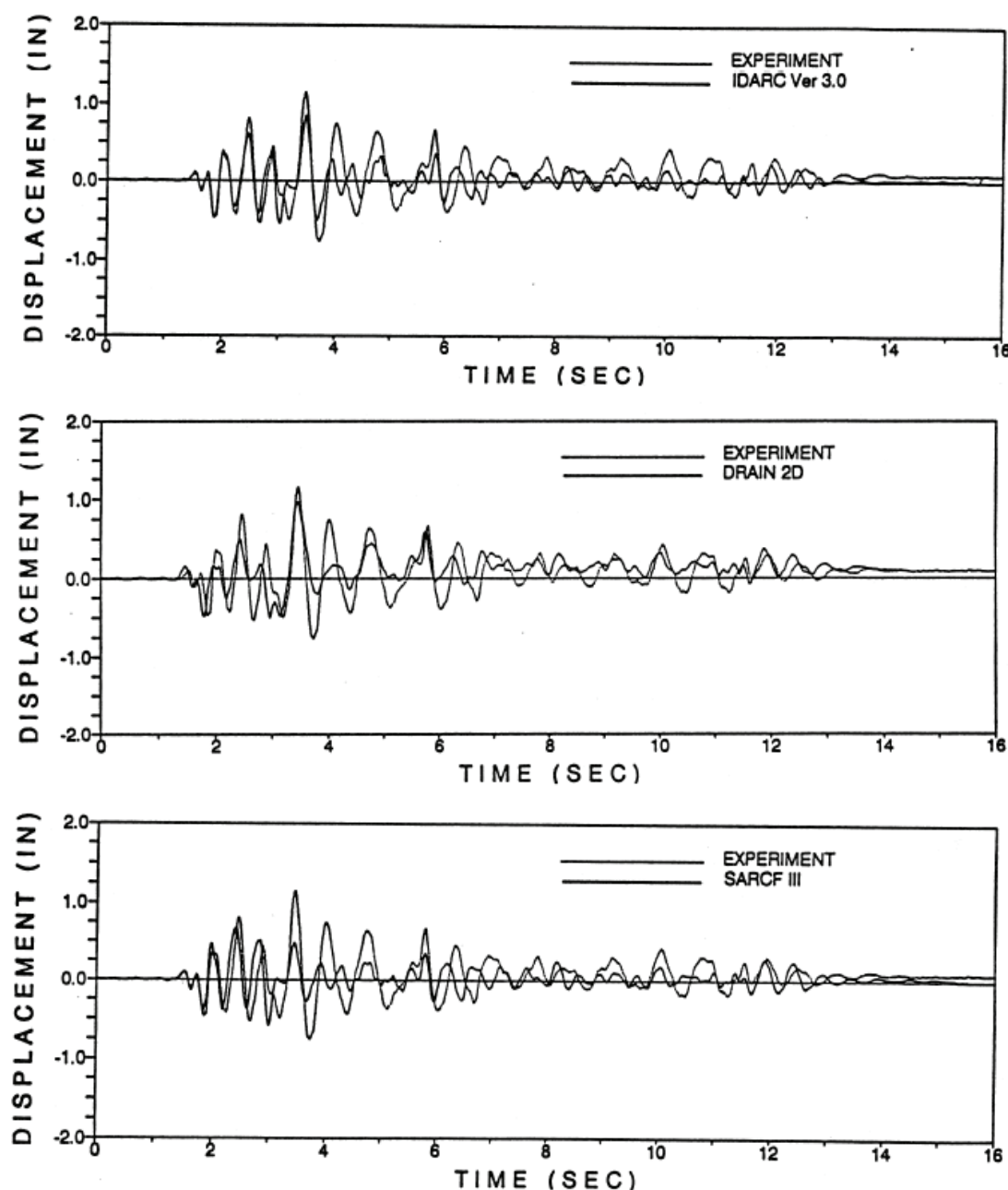


Fig. 9.13 Comparison with other programs

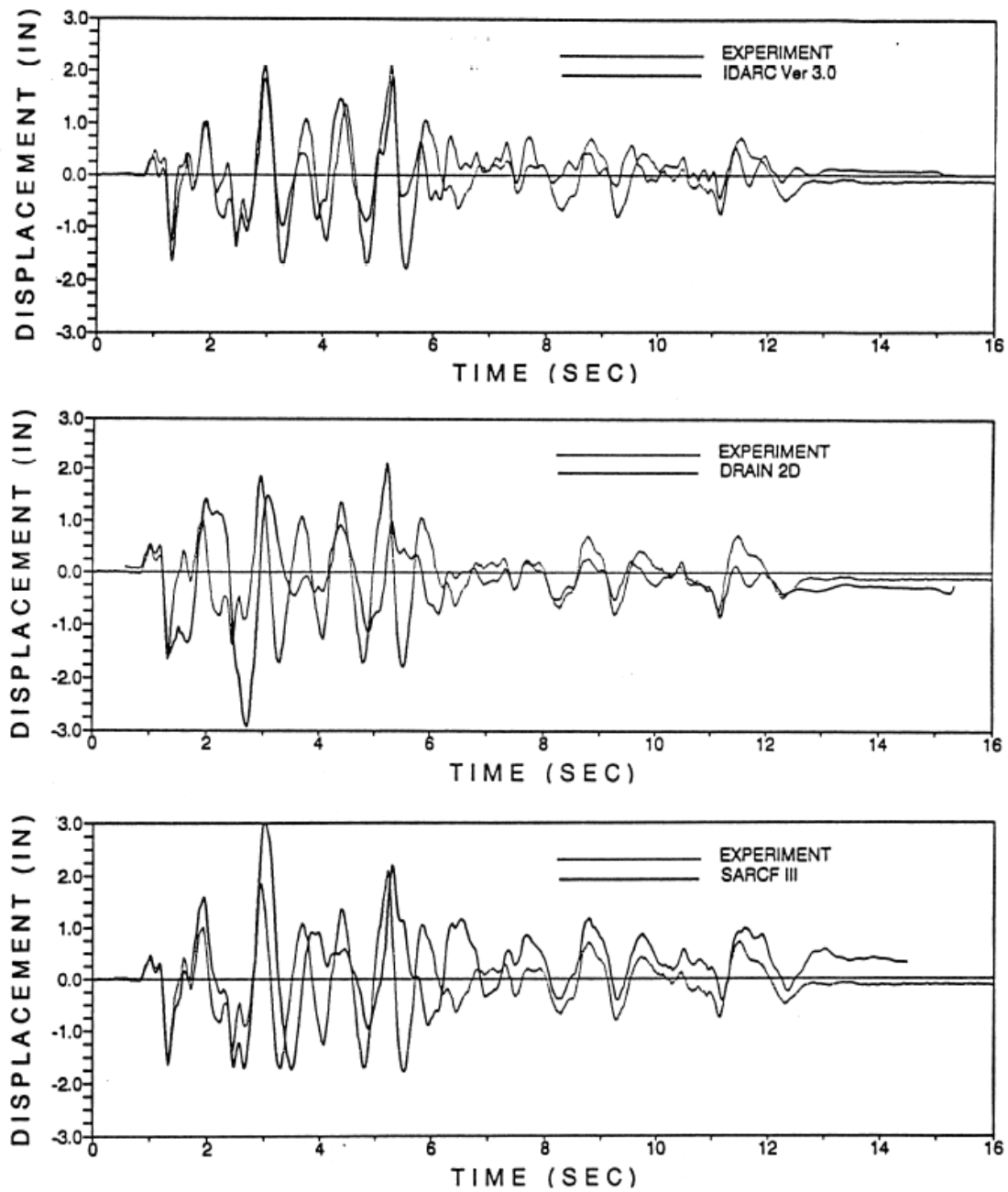


Fig. 9.14 Comparison with other programs (Moderate intensity: Inelastic)

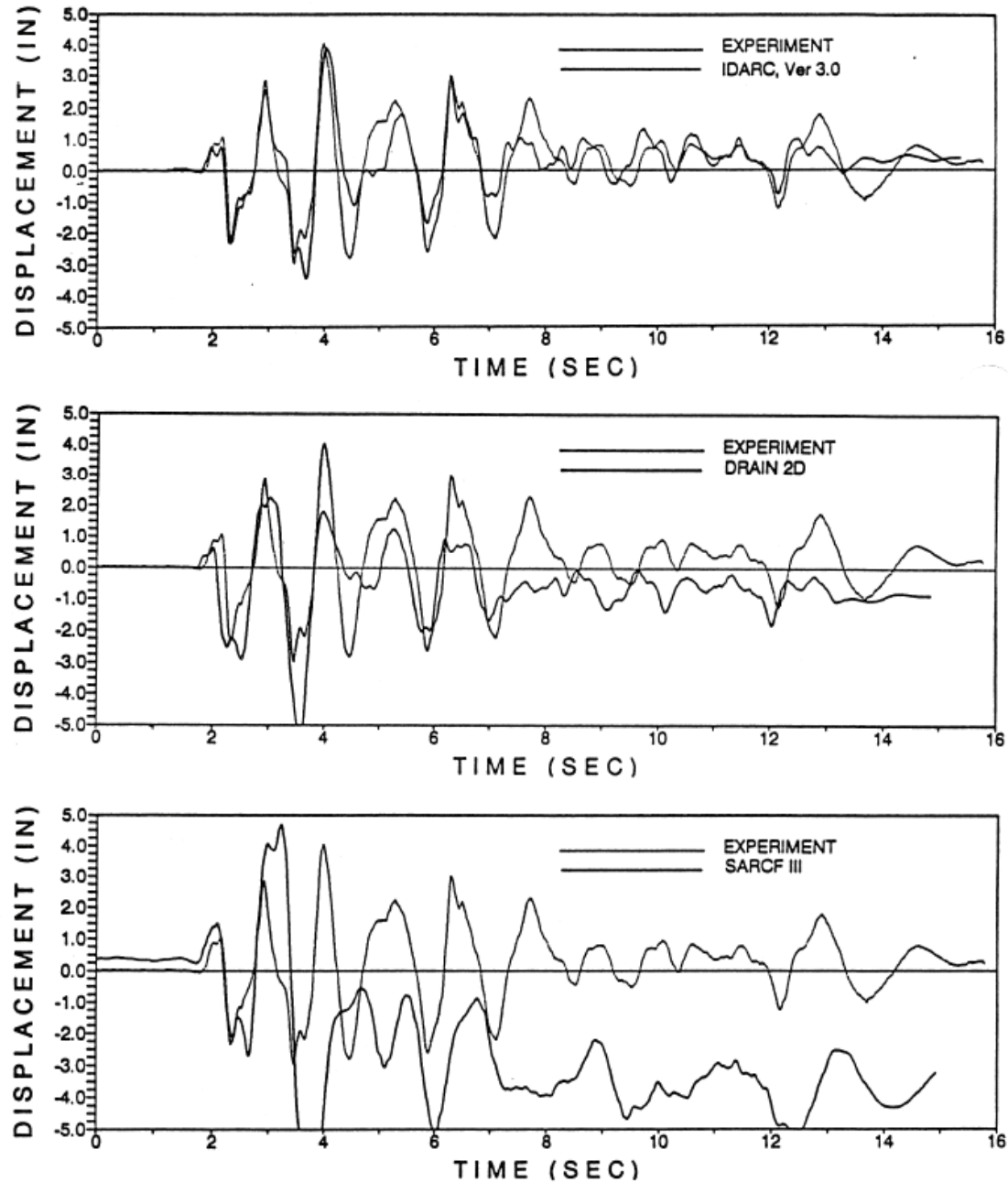


Fig. 9.15 Comparison with other programs (Highly inelastic)

9.4 Seismic Response: 1:3 Scale model Lightly Reinforced Concrete Structure

A comprehensive study of lightly reinforced frame structures was the subject of numerous investigations at the State University of New York at Buffalo (Bracci, 1992),

and at Cornell University (El-Altar, 1990). A 1:3 scaled model was constructed, tested, retrofitted and re-tested using simulated earthquake motion generated by the shaking table at SUNY/Buffalo. The model reflects a “slice” of a long structure with three-bay frames in the transverse direction. The “slice” has two parallel lightly reinforced frames as indicated by the model representation in the plan view in Fig. 9.16. Essential geometrical data and reinforcement details are also shown in the figure. Attained concrete strength were 4000 psi, 3000 psi and 3500 psi at the first, second and third story levels respectively, with an elastic modulus of 2700 ksi, 2300 ksi and 2530 ksi, respectively. The steel had an average yielding strength of 65 ksi after annealing with modulus of elasticity of approximately 29000 ksi. Additional details about the structure and the testing can be found in Bracci (1992).

The model was tested by a sequence of ground (table) motions reflecting a low level earthquake ($PGA=0.05g$), a moderate earthquake ($PGA=0.20g$) and a severe earthquake ($PGA=0.30g$). The ground motion was obtained by scaling the acceleration time history of Taft (1952) N21E component. Only two sets of results are presented here.

The main purpose of this study was to investigate the effectiveness of using identified component properties from separate sub-assemblage tests in predicting the dynamic response of the total structure. The data set used for in this example is presented in Appendix B. Only the second run at a measured peak acceleration of $0.22g$ is included, since the basic data is the same for both runs, with the exception of the initial stiffness and the input ground motion. As indicated, the data was derived entirely from the results of separate interior and exterior beam-column sub-assemblage tests which provided information on yield strength and hysteretic behavior. No attempt was made to fit the observed shaking table response.

The comparison of displacements for the top story during the mild and moderate earthquakes are shown in Fig. 9.17 and 9.18. IDARC predictions show good agreement

for both peak values and the total response history. The comparison includes predictions by DRAIN-2D and SARCF. More data on observed behavior in terms of deformations, stresses and damage mechanisms are reported in Bracci (1992).

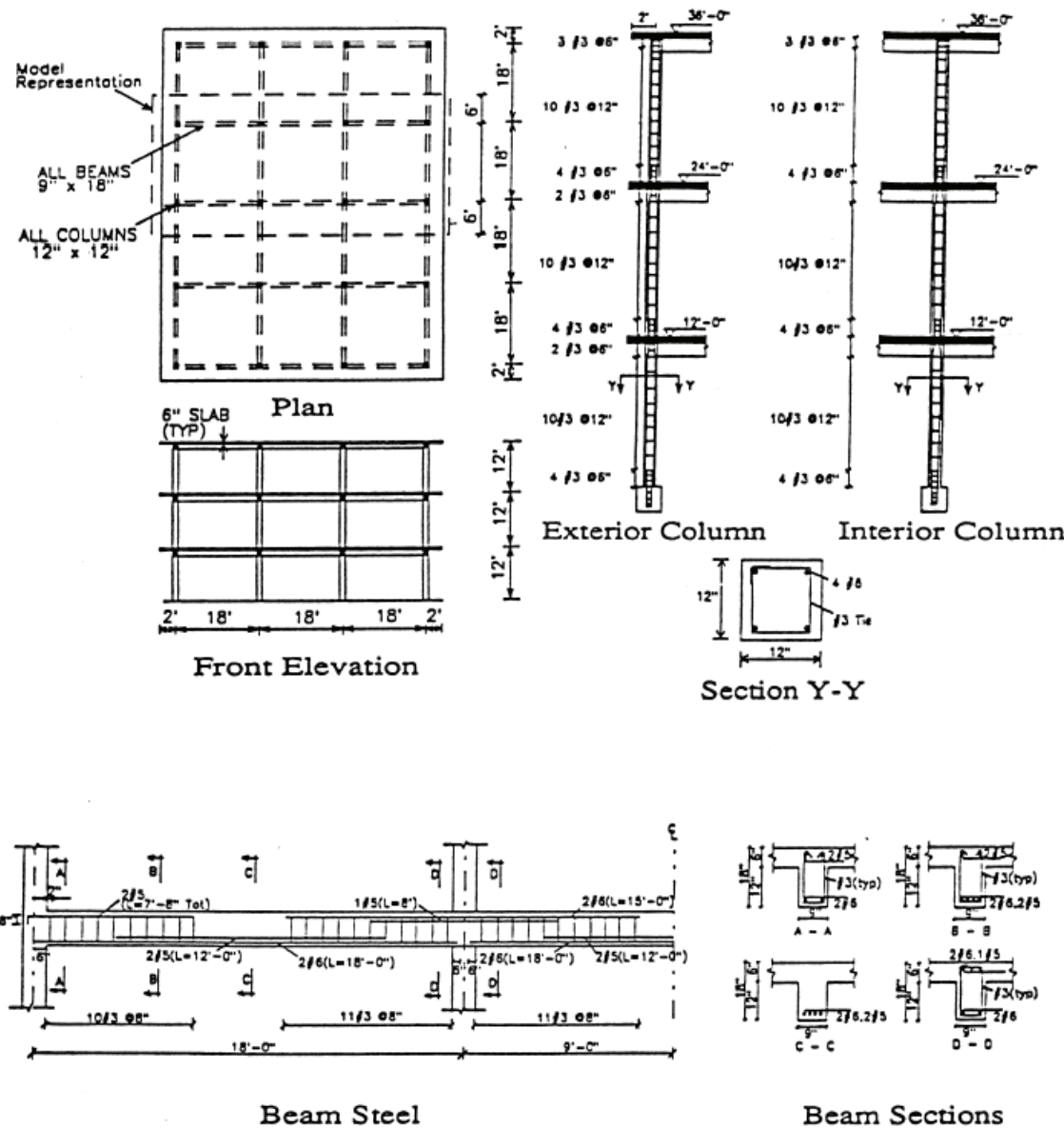


Fig. 9.16 Details of gravity-load-designed frame building

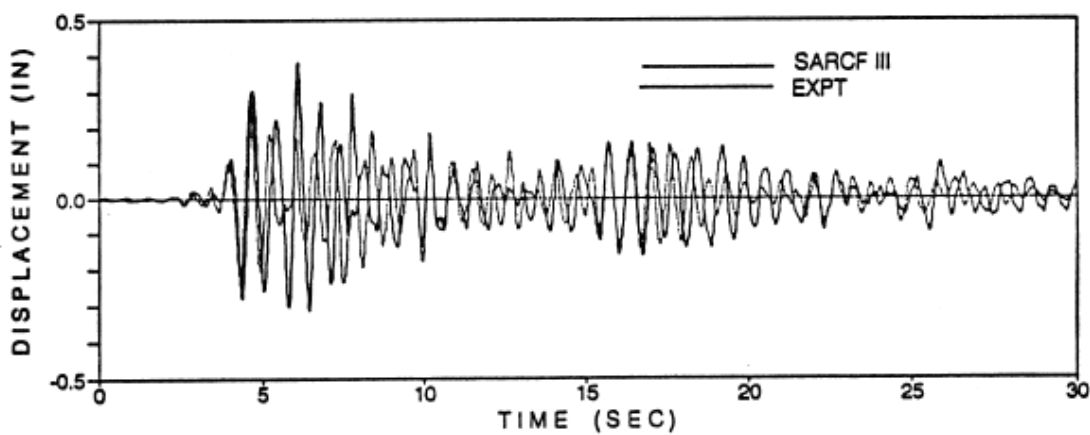
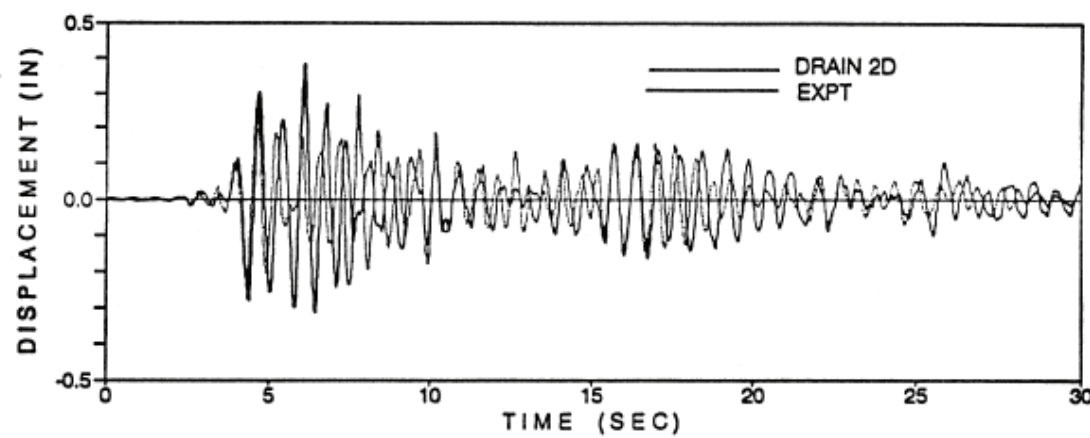
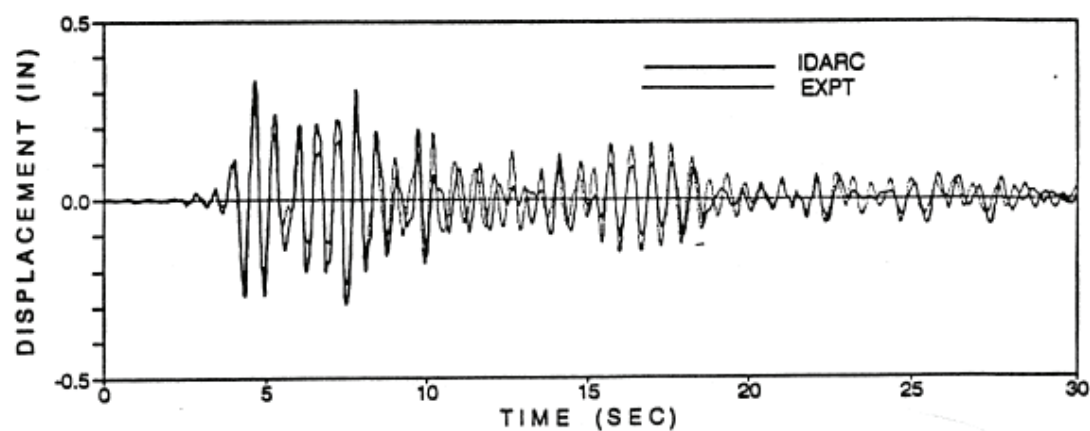


Fig. 9.17 Comparison with other programs – low intensity (0.05g)

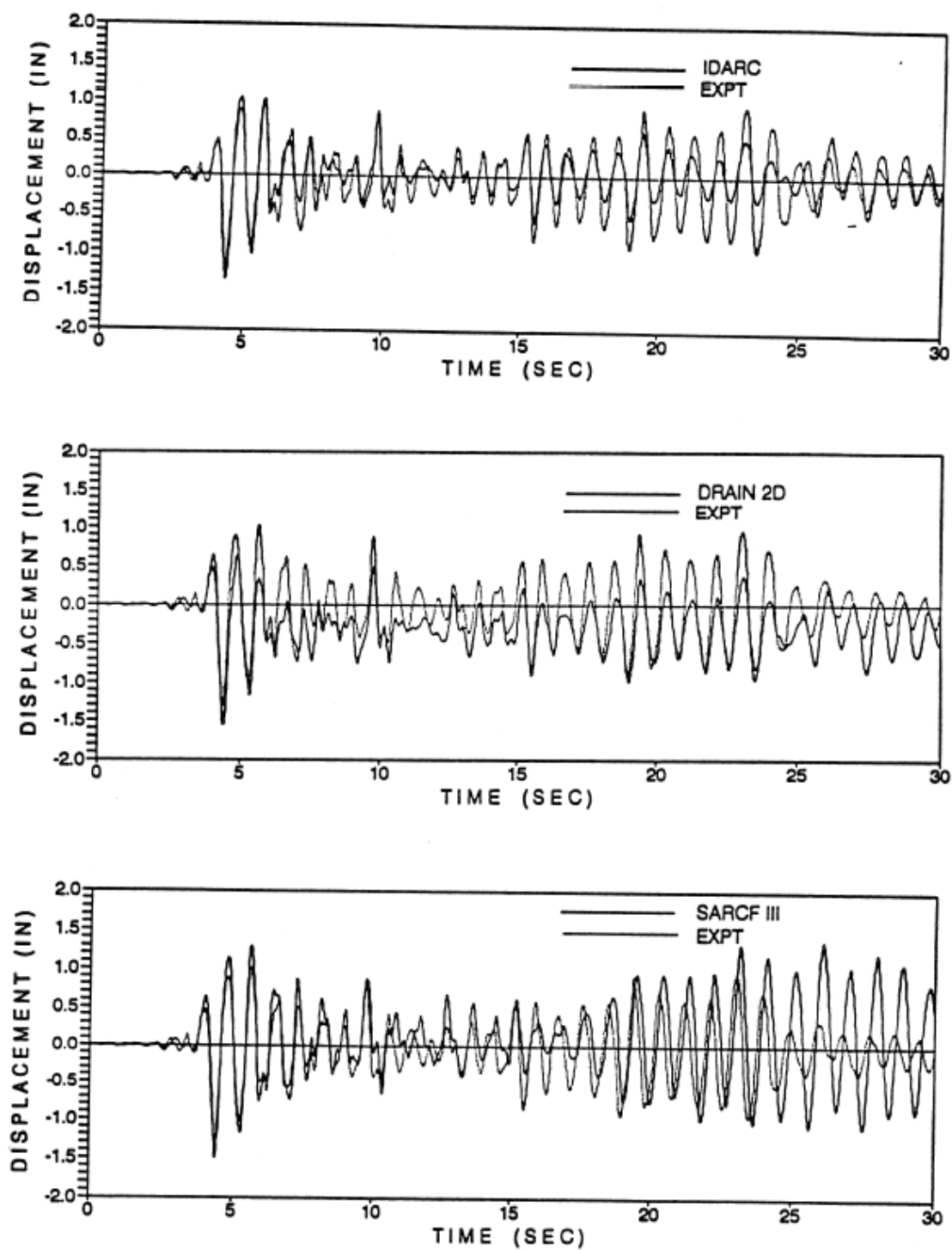


Fig. 9.18 Comparison with other programs – moderate intensity (0.22g)

9.5 Damage Analysis: Cypress Viaduct Collapse During the 1989 Loma Prieta Earthquake

The collapse of the Cypress Viaduct during Loma Prieta Earthquake in 1989 provided an excellent opportunity to verify IDARC in seismic damage evaluation of an existing structure. The Cypress structure consisted of a boxed girder roadway supported by a series of 83 reinforced concrete two-story bents. Eleven bent types were used in the construction of the viaduct. Fifty-three of the bents were designated as Type B1, which consist of two portal frames, one mounted on top of the other (Fig. 9.19). The upper frame is connected to the lower by shear keys (hinges). The dimensions of a typical B1 bent and its reinforcement details are shown in Fig. 9.19. Type B1 bents suffered the most damage and seemed to have failed in the same consistent manner throughout the freeway.

The structure was modeled using a combination of tapered column, shear-panel and beam elements. The pedestal region was modeled as a squat shear wall so that its impending shear failure could be monitored. The Outer Harbor Wharf horizontal strong-motion records were transformed to 94° , which is transverse to the alignment of the collapsed portion of the viaduct. The influence of gravity loads on the structure was simulated by imposing a ramp load in the form of a vertical excitation with magnitude of 1g. The actual ground motions were introduced after the resulting free vibrations had damped out. The data used for the analysis is presented in the data sheet for Case Study #5 in Appendix B.

The purpose of this analysis is to demonstrate the use of the program in the practical analysis of existing structures. The IDARC model of the bent is shown in Fig. 9.20. The imposed vertical and horizontal motions on the structure are shown along with the top level displacement response in Fig. 9.21. The analysis with IDARC revealed that the first element to fail was the left-side pedestal after approximately 12.5 seconds into

the earthquake, note that the plot shown in Fig. 9.22 includes an initial 4 seconds of gravity load input. A plot of the damage history of the pedestal is shown in Fig. 9.22, in which the horizontal input motion and the pedestal shear history are also shown for reference. Complete details of the analysis of the Cypress Viaduct using IDARC can be found in Gross and Kunnath (1992).

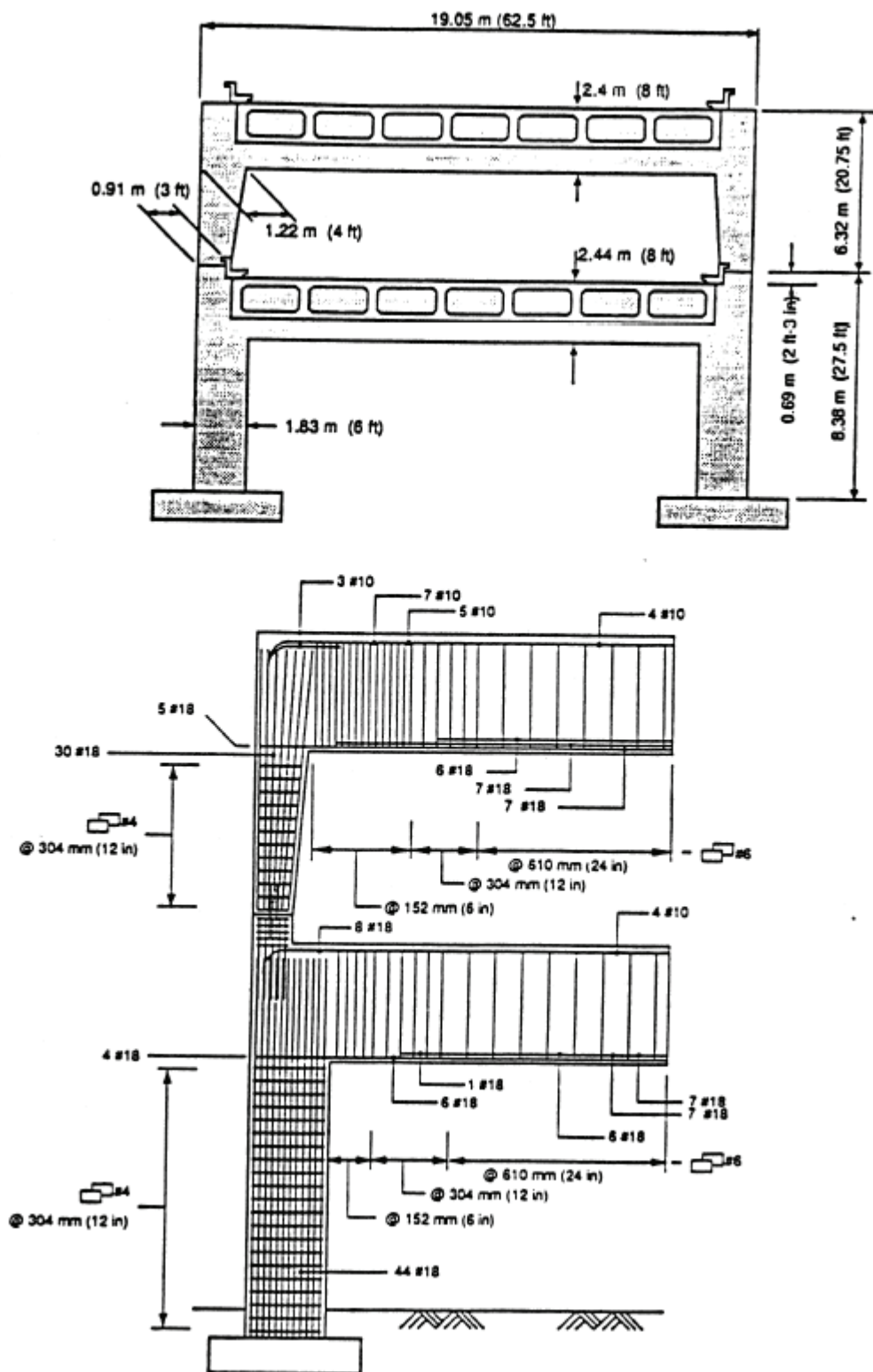


Fig. 9.19 Structural configuration and reinforcement details of type B1 bent

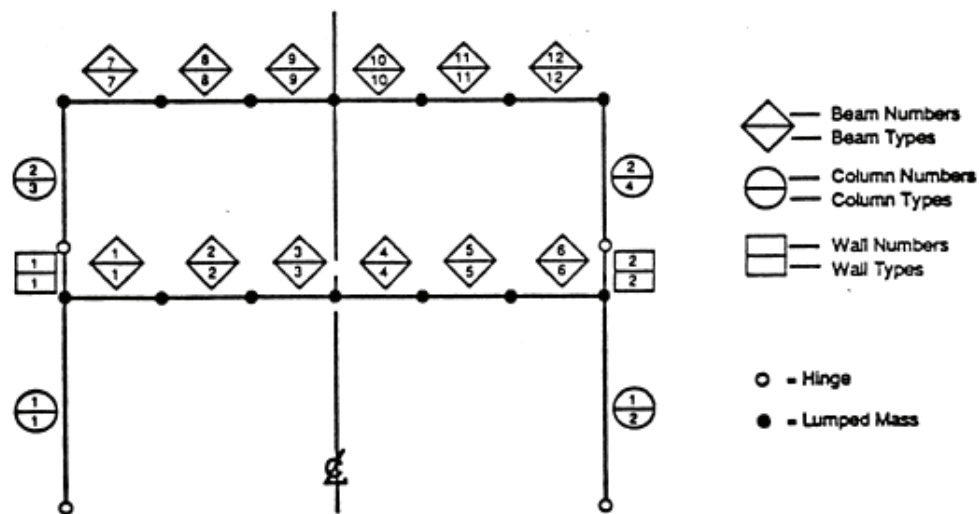
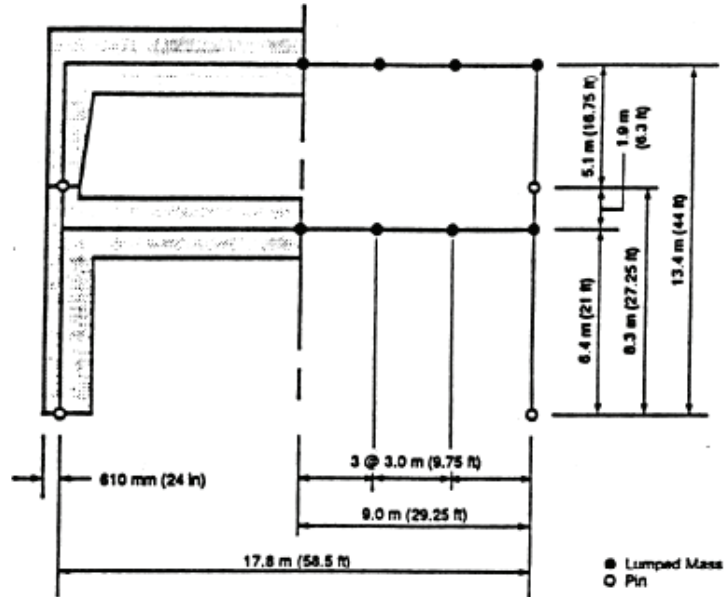


Fig. 9.20 IDARC model used in damage analysis

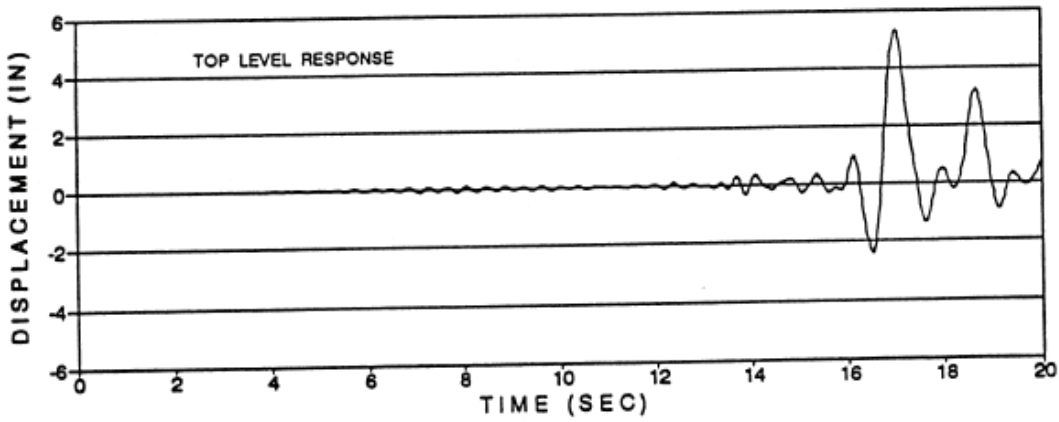
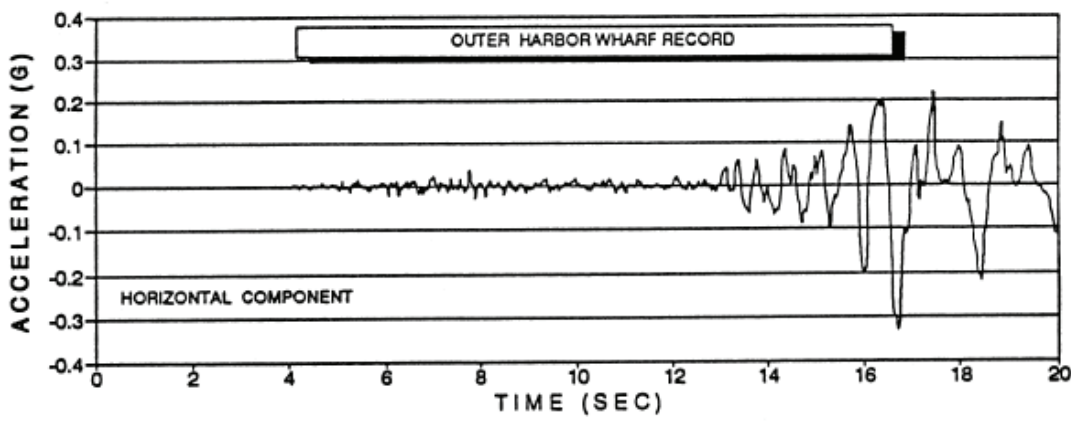
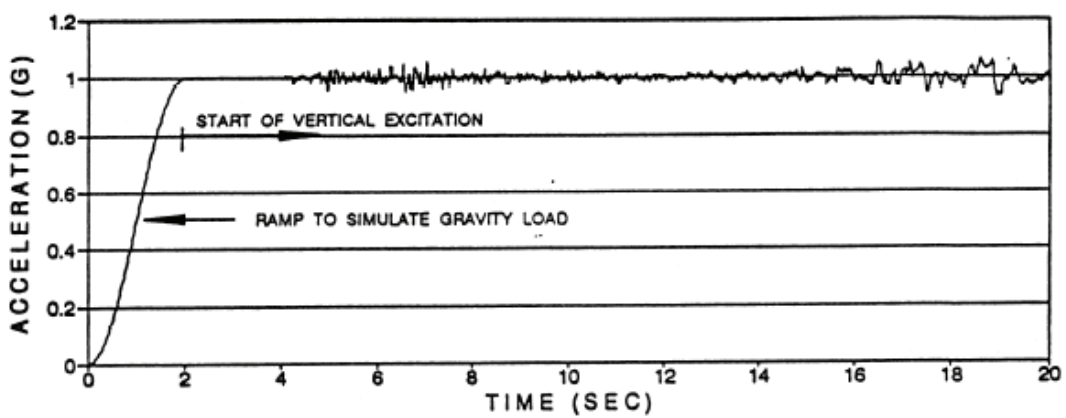


Fig. 9.21 Displacement response of type B1 bent

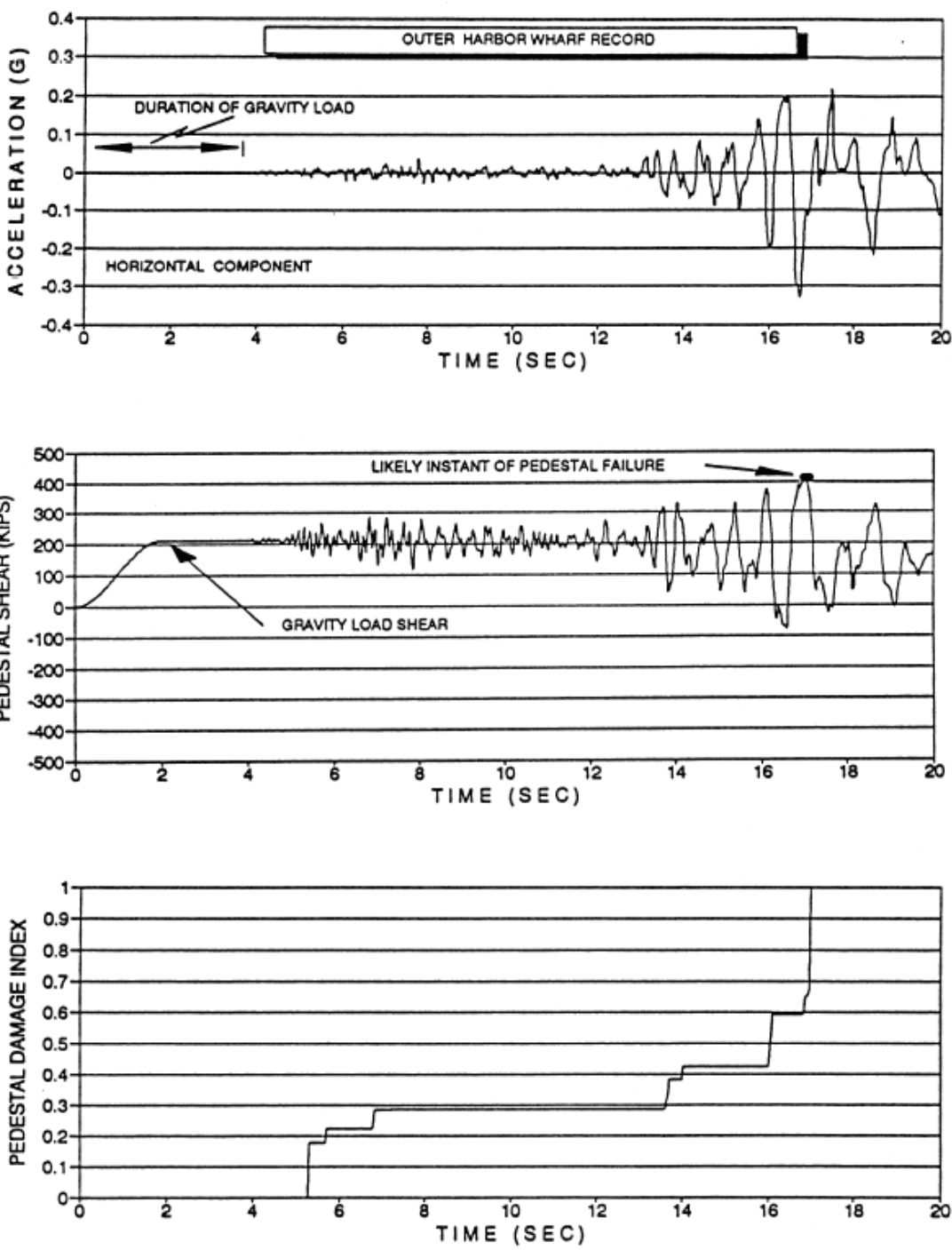


Fig. 9.22 Damage history of pedestal region

9.6 Pushover Analysis: Building in the Vicinity of the New Madrid Zone

This case study describes the different capabilities for pushover analysis available in the program. The pushover analysis was carried out to evaluate a four story reinforced concrete building, subjected to a set of static lateral loads representing the inertial forces that may be observed during an earthquake event. The typical floor framing plan of the building is shown in Fig. 9.23. The lateral load resisting system in both directions consists of shear walls and weak frames, as shown in Figs. 9.24 and 9.25.

The pushover consists of a static analysis of the structure under a set of incremental loads. The results describe the behavior of the structure in the elastic and inelastic ranges, and therefore are often used as a tool to identify the lateral load at which different elements crack, yield, or fail. Furthermore, it captures the sequence of gradual element failures as the structure collapses. A detailed description of the building is presented by Valles et al. (1995).

The pushover curves, often referred to as capacity curves, characterize the strength and displacement capacity of the building. However, the capacity curve is dependent on the force distribution along the height considered during the pushover analysis. Fig. 9.26 shows typical capacity curves for different lateral load distributions. The available options in the program for a pushover analysis are:

- 1) Force control: linear (inverted triangular)
- 2) Force control: uniform
- 3) Modal adaptive
- 4) Force control: user defined
- 5) Force control: generalized power distribution
- 6) Displacement control

In this study the global and the story response of the building were investigated and compared to the results from a non-linear dynamic analysis. The overall capacity curve is defined using the variation of the base shear versus the top story displacement (see Fig. 9.26). On the other hand, the capacity curve for a story was characterized using the variation of the inter-story drift versus the story shear (see Fig. 9.27). The figures include the results from the nonlinear time-history analysis with a black circle. Note that the generalized power distribution with power provides the best match between pushover and dynamic analysis. Further discussions on the results may be found in Valles et al. (1995).

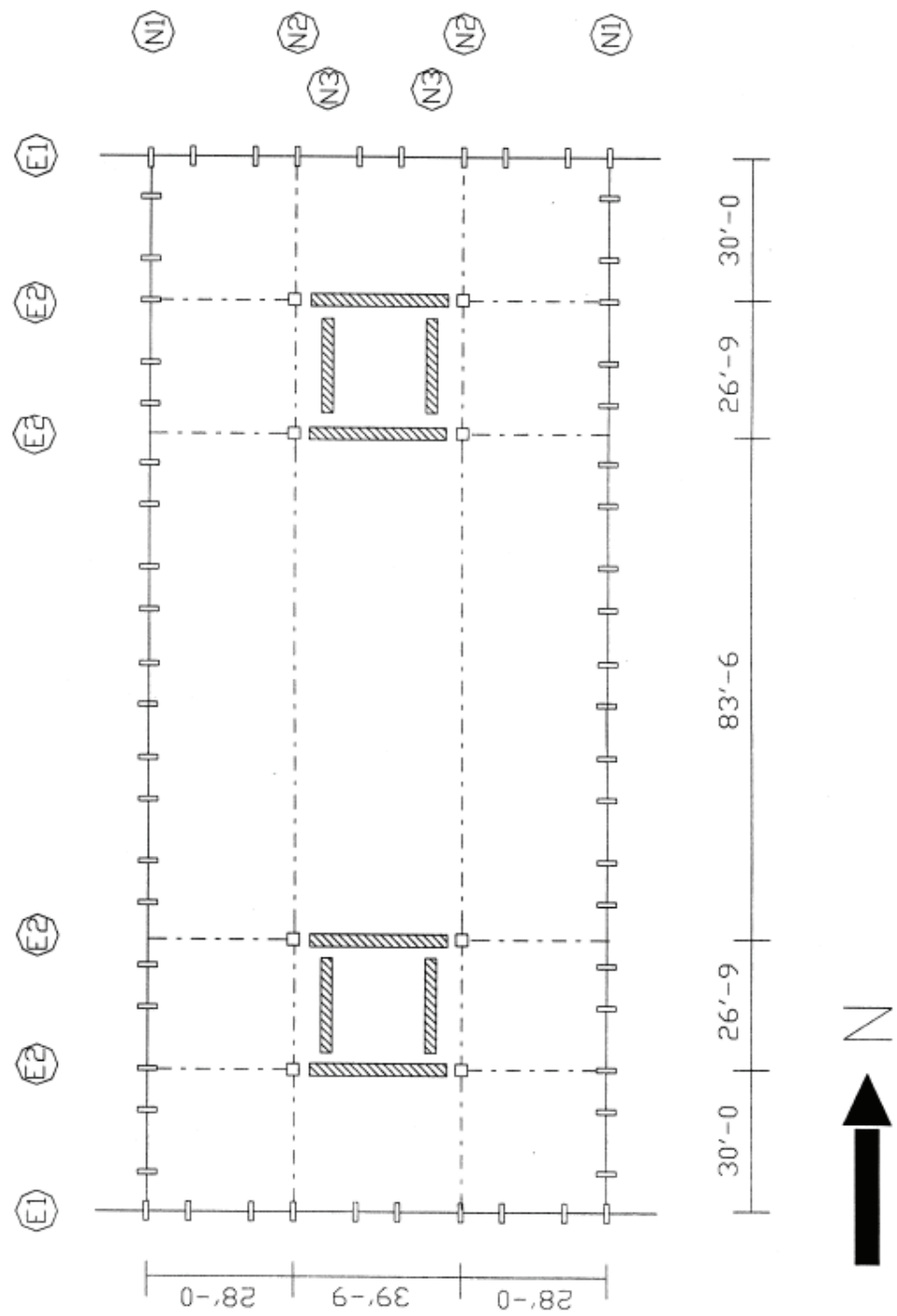


Fig. 9.23 Plan view of structure

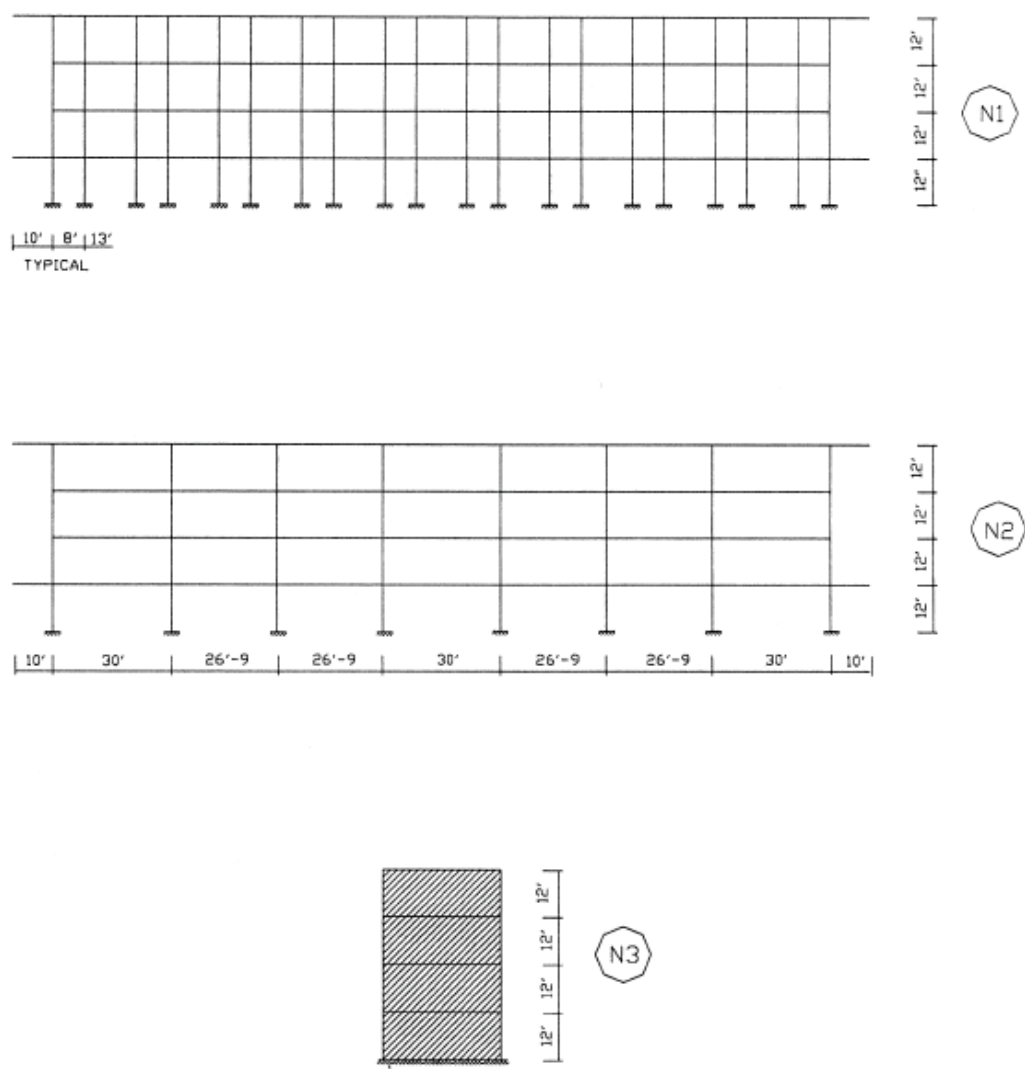


Fig. 9.24 NS frame elevations

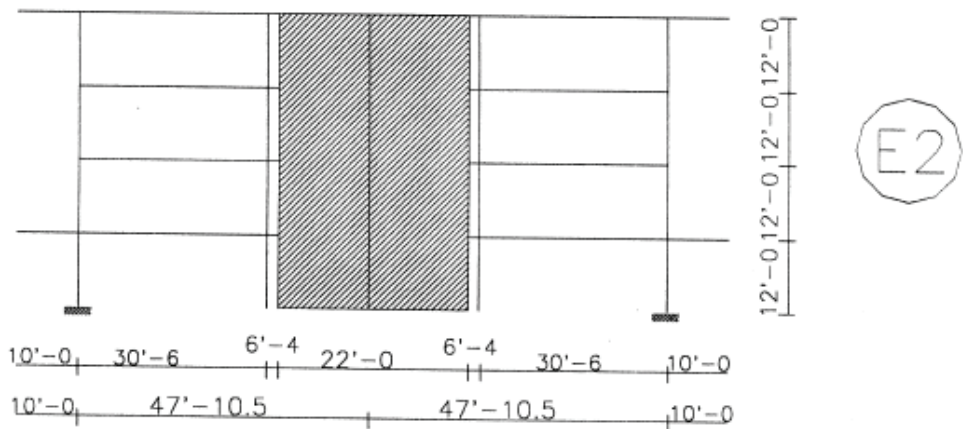
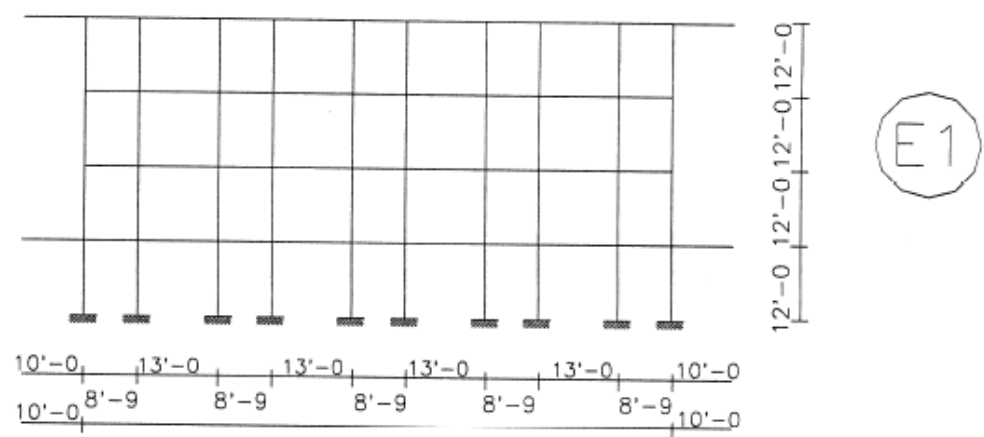


Fig. 9.25 EW frame elevations

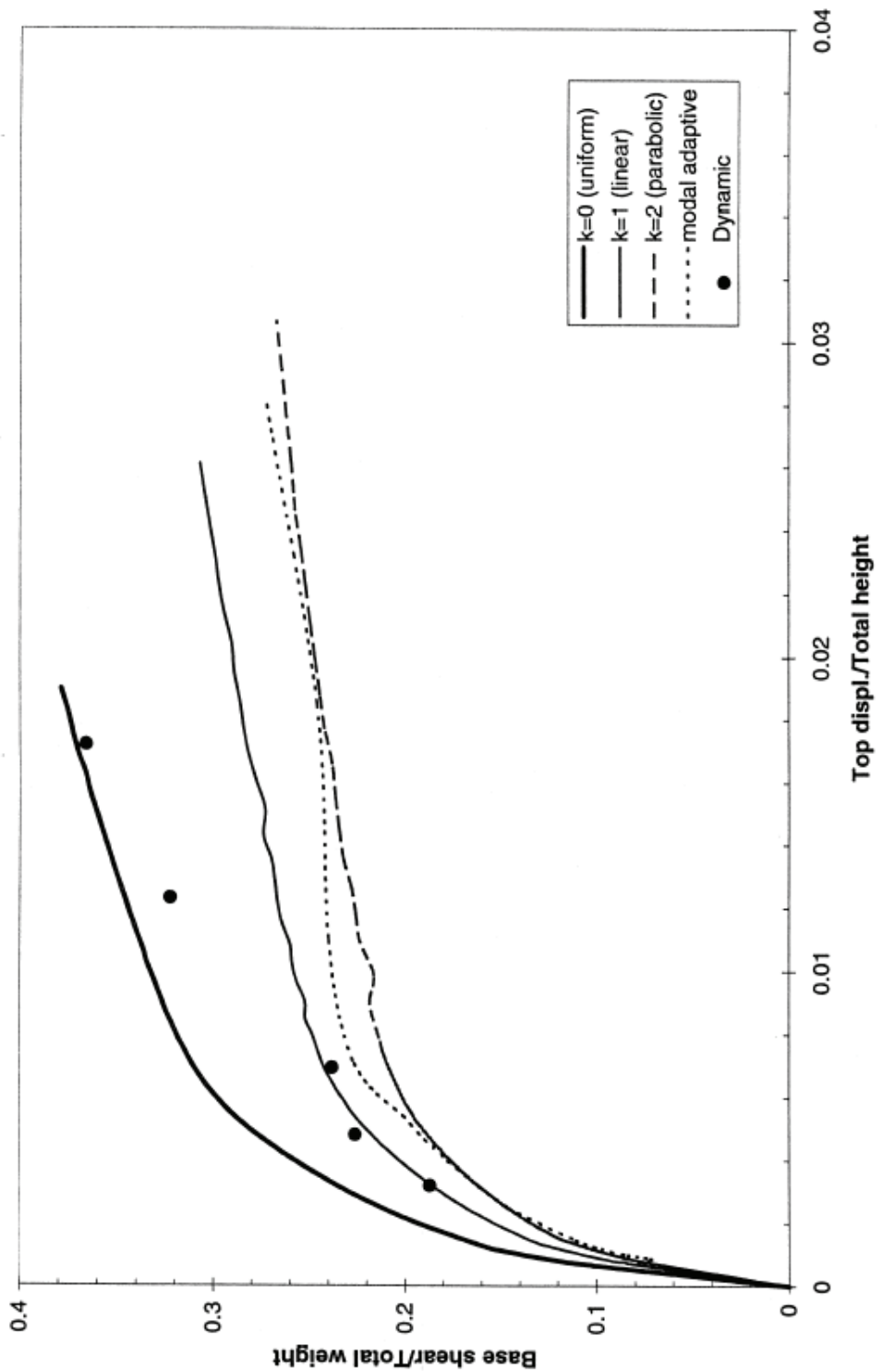


Fig. 9.26 Overall pushover capacity curves for different lateral load distributions

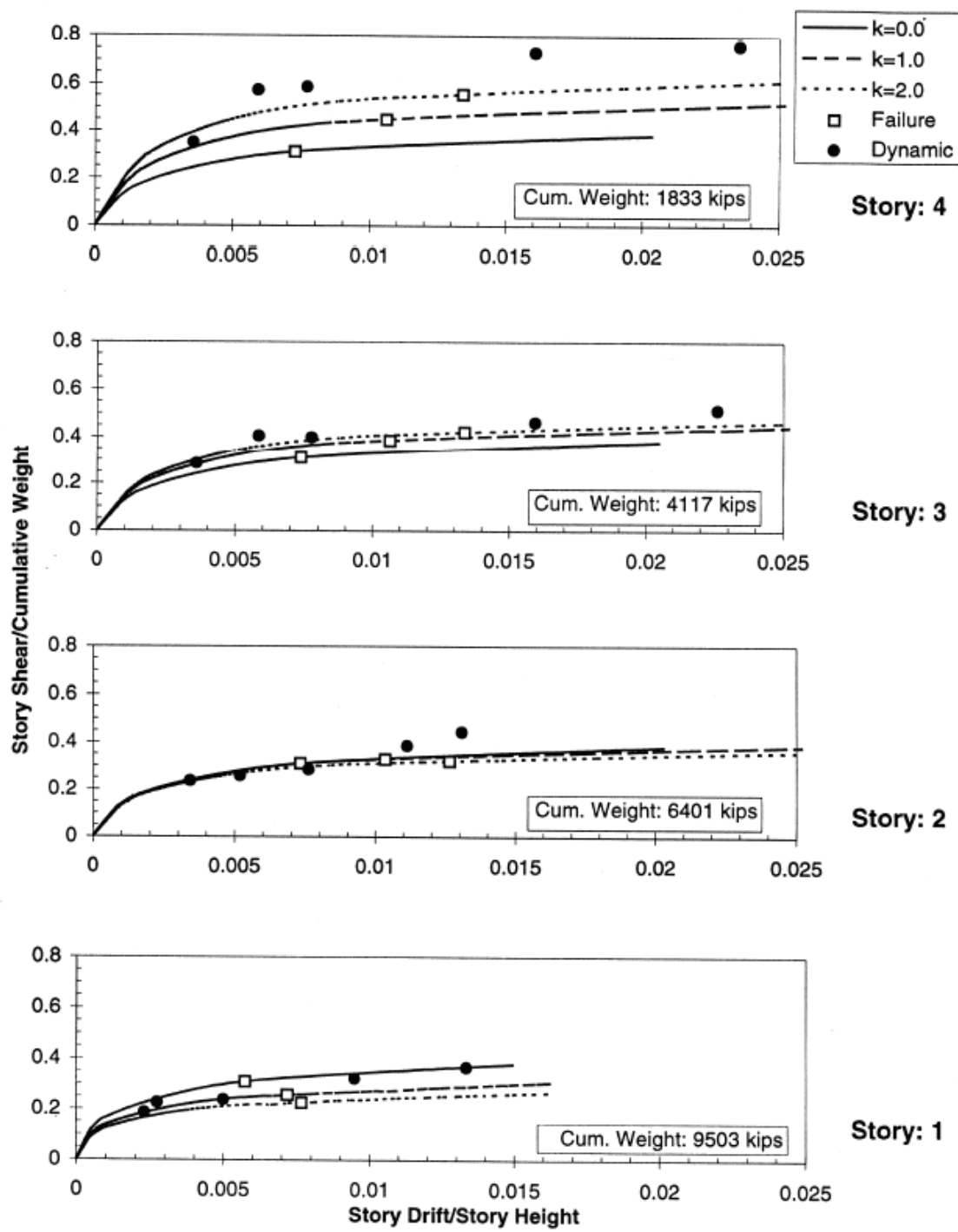


Fig. 9.27 Story pushover capacity curves for different lateral load distributions (NS direction)

9.7 Response Snapshots: Eight story building in Los Angeles

This case study presents the results of the application of the IDARC program in the evaluation of the seismic performance of a reinforced concrete building, using the ATC-33 (50% submittal) guidelines. During the evaluation process a number of response snapshots were required. The building was designed and constructed in 1961 according to the requirements of the 1959 Uniform Building Code. It consists of one subterranean basement level and seven above ground floors the typical floor framing plan of the building is shown in Fig. 9.28.

The lateral load resisting system in the longitudinal direction consist of non-ductile reinforced concrete moment-frames along column lines 2 and 3. Frames 1 and 4 were excluded in the analysis due to the architectural feature which seriously limits their participation. The lateral load resisting system in the transverse direction consist of 12" thick reinforced concrete exterior shear walls (along column lines A and W), and 8" thick reinforced concrete walls along column lines E, G, N, and V. These walls are assisted by several one-bay moment-frames spanning between lines 1-2 and 3-4. Hence, the lateral system in the transverse direction may be considered a dual system featuring shear wall-frame interaction, Figure 9.29.

The following models were considered in the analysis of the building, one three-dimensional linear elastic, and two 2-D non-linear models, one for each principal direction of the structure. Only the results corresponding to the inelastic analysis are shown, for more detailed information see Naeim and Reinhorn (1995). The nonlinear analysis was carried out using the pushover option along with user requested response snapshots to evaluate the seismic performance of the structure according to the recommendations of the ATC-33 (50% draft) guidelines (1995).

Three different response spectra were considered: a site specific smooth response

spectra representing the 1994 Northridge shaking at this site, as supplied by ATC (Somerville, 1995); and the ATC-33 5% damped design spectra corresponding to return periods of 500 years and 2500 years for soil type D and map area 7 which correspond to the ATC site classification for the building (Somerville, 1995). These spectra are shown in Fig. 9.30 where the initial and effective fundamental periods of the building in both directions are identified.

The longitudinal and transverse 2-D models of the structures were pushed using a lateral force distribution as specified in the ATC-33.02 (see generalized power distribution in Section 3.4.2). The exponents for the load distributions were calculated according to the ATC-33.02 recommendations: $k = 1.965$ in the longitudinal direction, and $k = 1.07$ in the transverse direction. In both directions the model was pushed beyond the specified target roof displacement according to the ATC-33 2500 year event.

Preliminary calculations conducted before the 1994 Northridge earthquake, indicated a significant potential for serious damage during a moderate to large earthquake. During the Northridge event, however, although extensive damage were observed in one or two neighboring buildings, no apparent signs of structural damage were observed. This observation is in accordance with the results of the pushover analyses, where no damage to very slight damage was predicted for the structure when subjected to this event.

Important information was obtained from the pushover analyses, including the variation of roof displacement versus base shear, and the response stages of the building. Figure 9.31 shows this variation for the longitudinal direction, with significant stages in the response identified. Using the response snapshots capability of the program, reports for the state of the building at different stages can be generated. User defined snapshots were requested for the three earthquake intensities considered. Figure 9.32 shows the lateral displacements, in the longitudinal direction, corresponding to the three earthquake intensities studied. Other response snapshots were requested, including element stress

ratios for beams (see Table 9.1). Based on the curvature demand/capacity ratios reported, beams are expected to undergo severe damage during the ATC 2500 year event. Relevant overall response snapshots are summarized in Table 9.2.

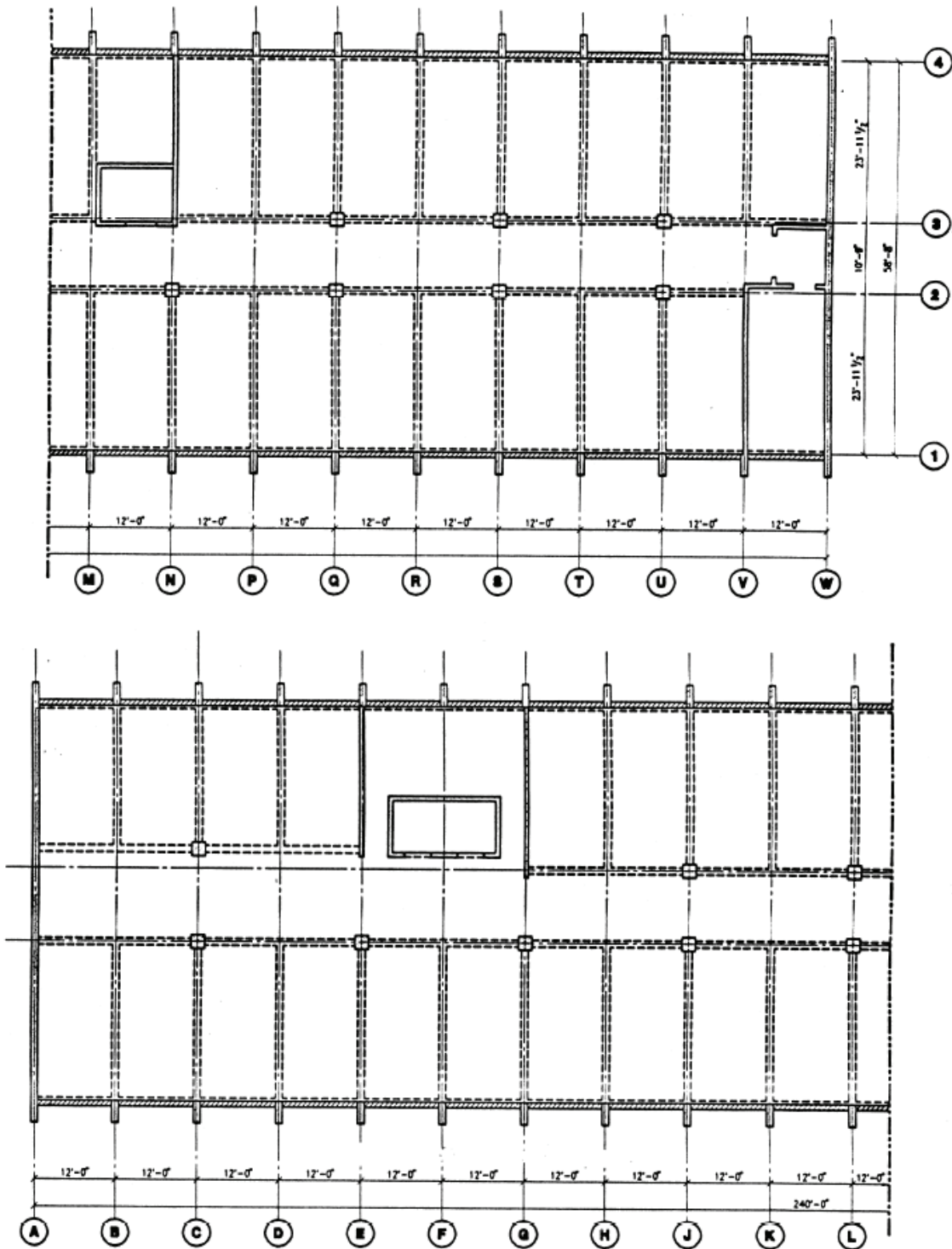


Fig. 9.28 Typical floor plan of structure

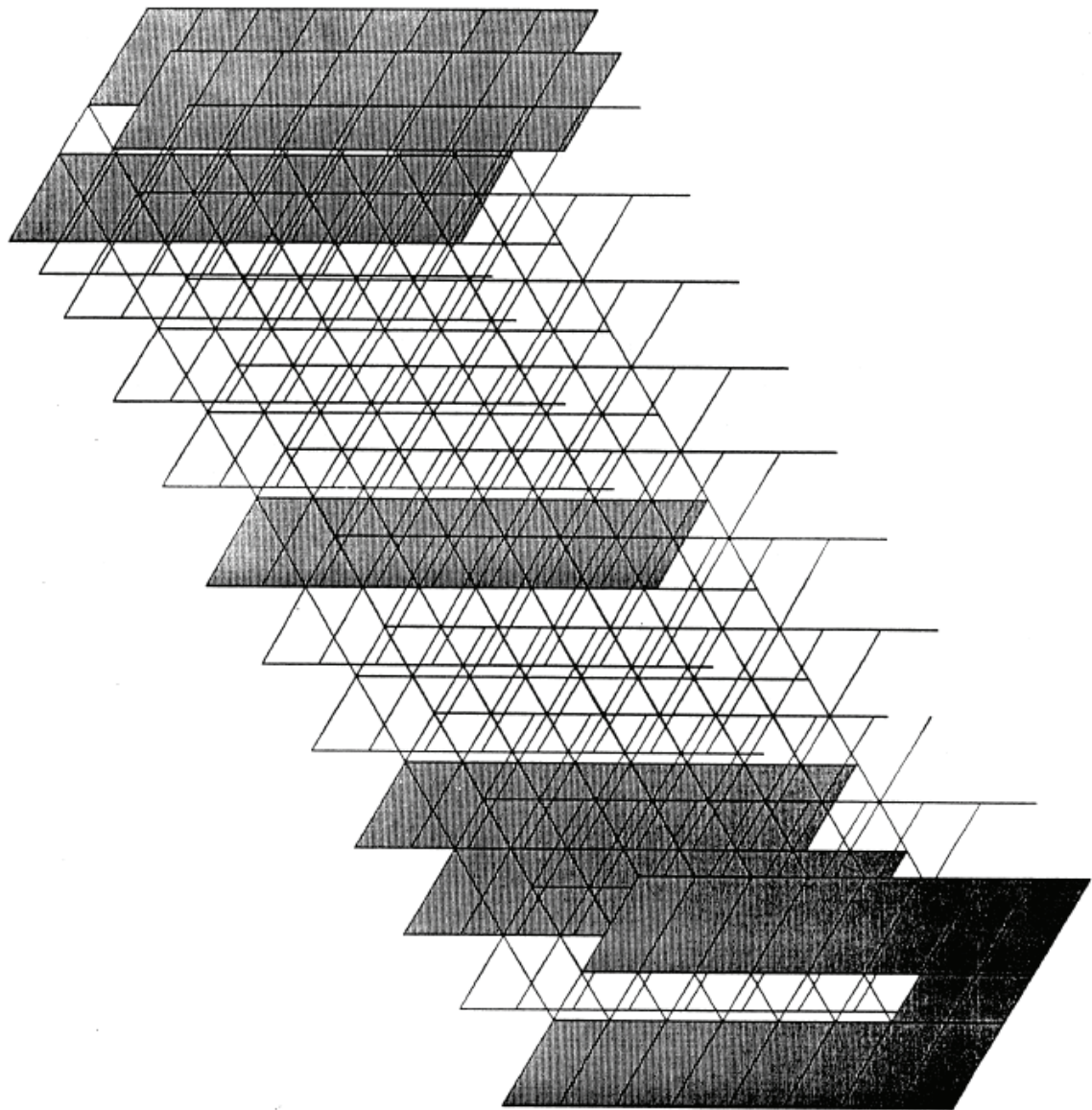


Fig. 9.29 Perspective view of lateral load resisting elements

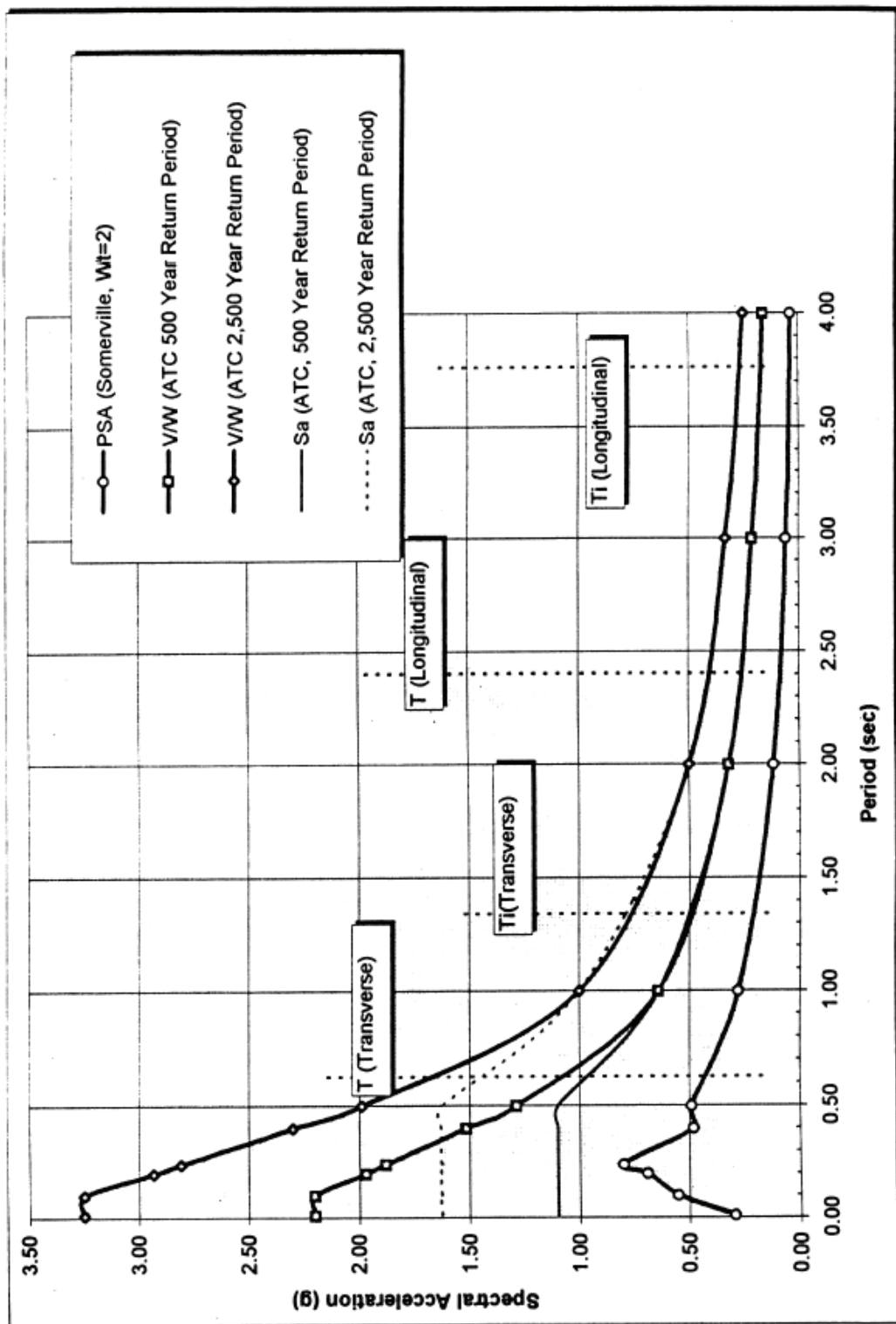


Fig. 9.30 Response spectra used for evaluation

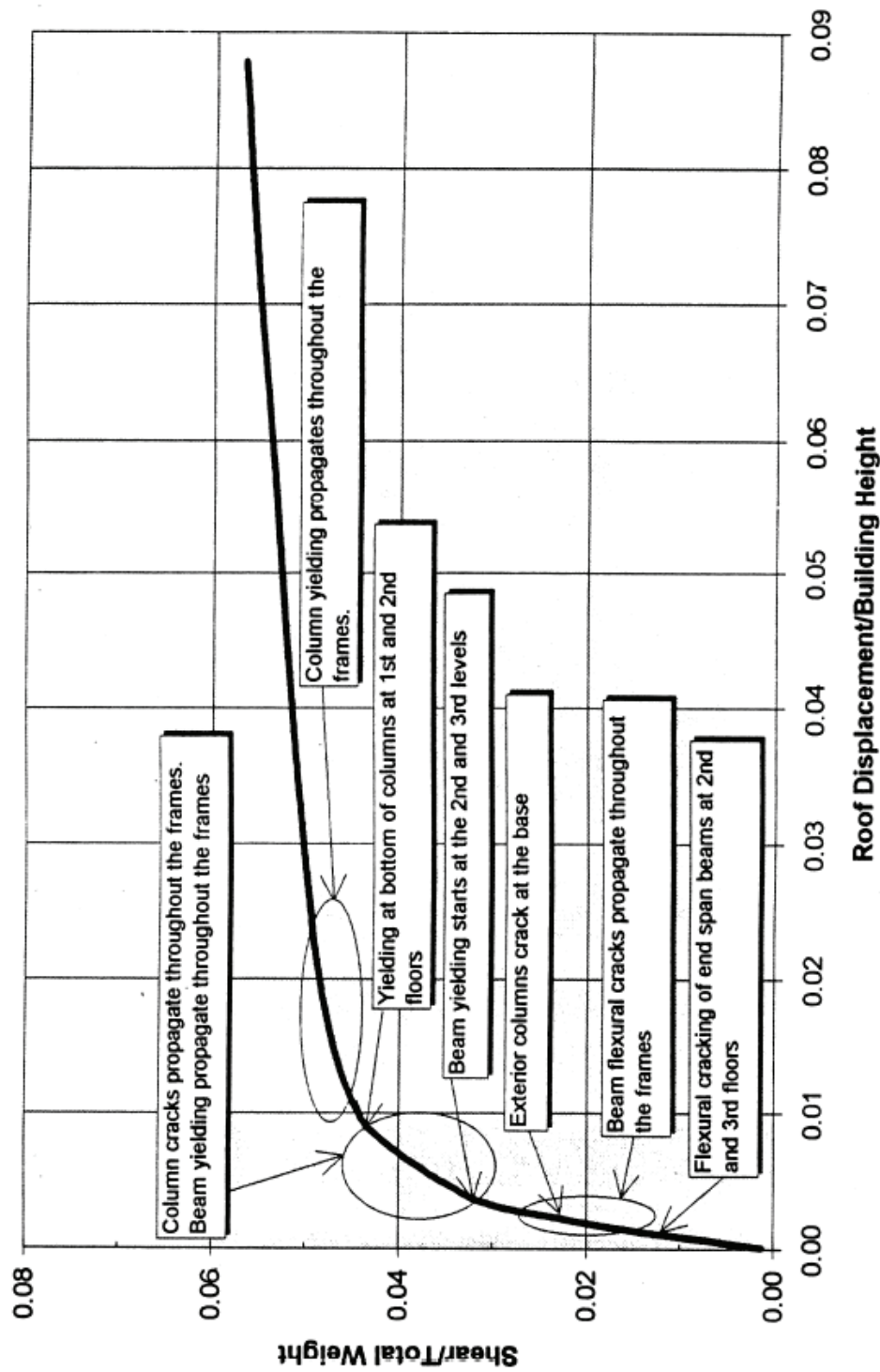


Fig. 9.31 Pushover capacity curve with significant response stages (longitudinal direction)

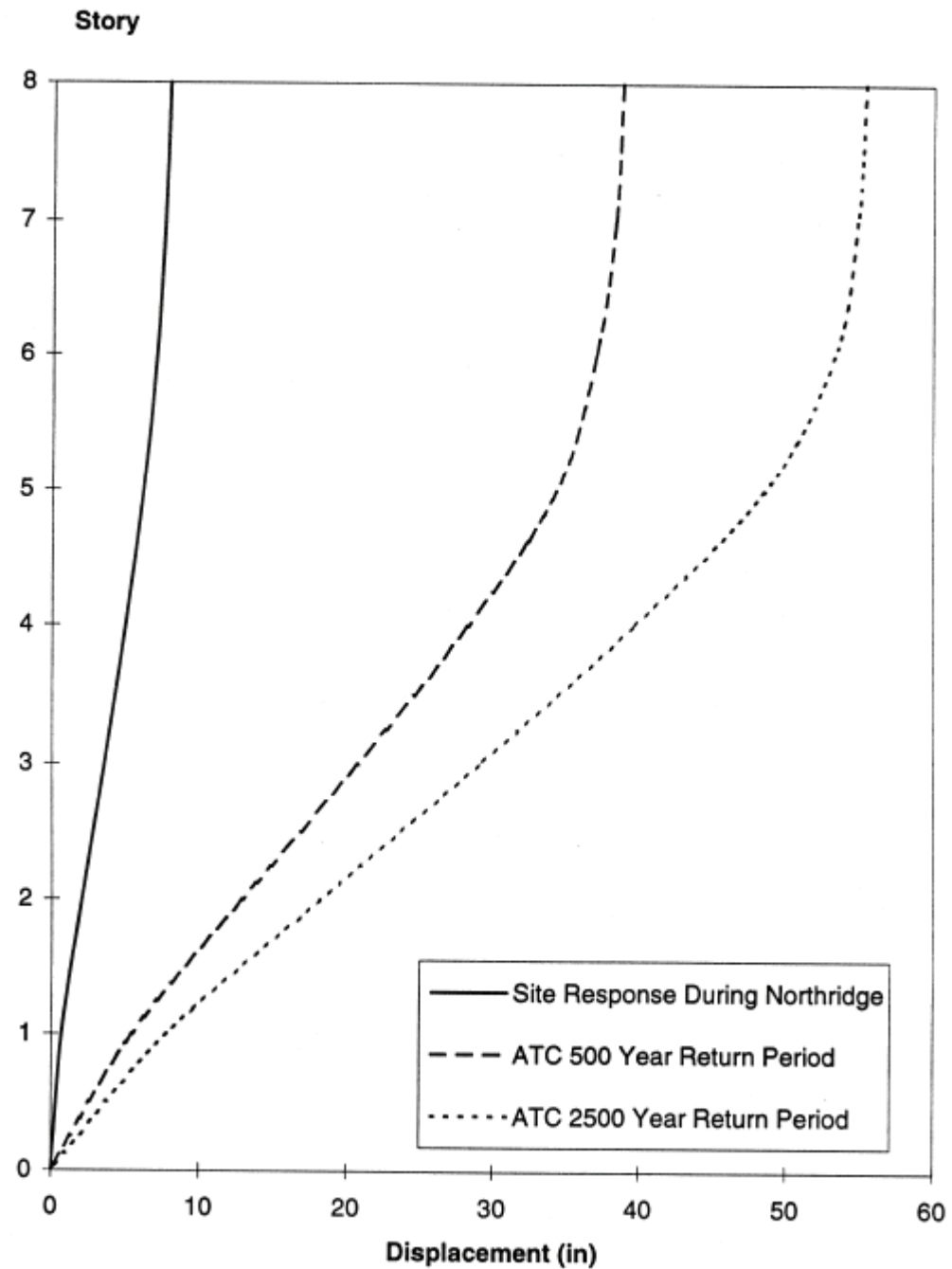


Fig. 9.32 Lateral displacements, longitudinal direction, for various earthquake intensities

Table 9.1 Element stress ratios for typical beams

	V/V _u	M/M _y	φ/φ _y
Northridge			
Story 8	0.1387	0.1935	0.0035
6	0.4394	0.7860	0.0277
4	0.5605	0.8760	0.2240
2	0.5809	0.8820	0.2611
1	0.5329	0.8625	0.1393
ATC 500			
Story 8	0.2370	0.3412	0.0062
6	0.5820	0.8837	0.2721
4	0.6122	0.9428	0.6416
2	0.6158	0.9482	0.6756
1	0.6110	0.9379	0.6111
ATC 2500			
Story 8	0.2433	0.3389	0.0062
6	0.5838	0.8868	0.2915
4	0.6287	0.9743	0.8390
2	0.6327	0.9810	0.8809
1	0.6264	0.9666	0.7911

Table 9.2 Structural response, longitudinal direction, for various earthquake intensities

	δ_{top} / H_{tot}	V_{base} / W_t	DI_{PARK}
Site Northridge	0.0062	0.0410	0.042
ATC 500	0.0256	0.0475	0.351
ATC 2500	0.0488	0.0502	0.502

9.8 Steel Structure: Evaluation of Seismic Performance of a 11 Story Steel Moment Frame Building during the Northridge Earthquake

This case study exemplifies one of the options incorporated in the present IDARC version, this is, the alternative for user to input their own moment-curvature properties directly. Thus, the program can be used to perform the analysis of buildings with frames made of different materials, besides reinforced concrete. This case presents some results of the inelastic analysis performed to an 11-story steel building subjected to earthquake loads.

This building, located in West Los Angeles, was damaged during the January 17, 1994, Northridge earthquake. An extensive field investigation of damage was performed prior to the start of the analytical study and then compared with the results of the extensive two and three dimensional, linear and non linear, static and dynamic analyses of the building in order to investigate and correlate observed damage with various elastic and inelastic damage predictors. As mentioned above, only some results corresponding to the inelastic analysis are shown. The reader can see the report by Naeim et al. (1995) for an ample description of the observations.

The building is made of composite concrete and steel metal deck slabs which are supported by A36 structural steel beams and columns. The exterior skin is made of precast concrete panels and glass plates. Structural steel columns are supported at the foundation by cast-in-place reinforced concrete friction piles. The seismic load resisting system consists of ordinary moment frames constructed of A36 structural steel, typical frames shown in Figure 9.33. Seismic loads are carried to the lateral resisting system by the composite concrete and steel deck slabs which act as horizontal diaphragms. Typical moment frame connections at the column flange and web are shown in Fig. 9.34.

The seismic loads considered were postulated ground motions for the site during

the 1994 Northridge earthquake. In addition, the following earthquake records were also considered:

1. The 1994 Northridge earthquake as recorded at the parking lot of the Sylmar County Hospital Building. This is considered to be one of the records with the highest damage potential for this event (Naeim, 1995).
2. The 1994 Northridge earthquake as recorded in Canoga Park (7769 Topanga Canyon Blvd.) which represents levels of shaking larger than the motion postulated for the site but less than that recorded at Sylmar.
3. The 1978 Iran earthquake records at Tabas to represent a larger event.
4. The 1940 El Centro earthquake as recorded at El Centro Irrigation district because it has been widely cited in previous studies and hence has certain value as a benchmark record.
5. A uniform risk design spectrum representing 10 % probability of exceedance in 50 years developed for the site of the Sylmar County Hospital (Somerville, 1995).

Two nonlinear 2-D computer models were constructed (one for the E-W and another for the N-S directions). In both mathematical models all frames in the direction under consideration were included and connected by the rigid floor diaphragm assumption, the columns were considered fixed at the foundation level, and 2% damping was assumed for the first mode and the mode nearest to 30 Hz.

Bilinear hysteretic behavior was assumed using a 5% strain-hardening ratio. The yield and ultimate curvatures correspond to the cross section's full elastic and full plastic strengths, respectively (Fig. 9.35). The ultimate deformation (curvature) for members was specified as the lowest of: (a) maximum strain at fracture ($\varepsilon_s = 15\%$) divided by the distance to neutral axis, or (b) using the maximum plastic moment and a post-yield hardening capacity of 0.05 (Fig. 9.35). The resulting ultimate curvature produces ultimate

rotations between 0.03 and 0.04 radians, depending on plastic penetration. Yielding curvature corresponds to a strain of 0.14%, and the curvature at the onset of strain-hardening corresponds to a strain of 1.5%. These assumptions are in basic agreement with the published A36 steel stress-strain relations.

To predict structural damage, damage indices were assigned at the element level (beams and columns), as well as story levels, and to the overall structure. The damage model developed by Park and Ang (1985) was utilized.

The following analyses were performed for models corresponding to N-S and E-W frames:

1. Static nonlinear pushover analysis with an inverted triangular lateral load distribution.
2. Nonlinear time history analysis with simultaneous applications of horizontal and vertical components of the synthetic ground motion representative of the Northridge earthquake at the site.
3. Nonlinear time history analysis with simultaneous application of horizontal and vertical components of the 1994 Northridge at the Sylmar County Hospital Parking Lot.

Typical plots of story shear versus story drift for the above analyses are presented in Fig. 9.36 for the N-S direction. In these figures, the maximum time history response to the synthetic motion at the site and that of the Sylmar time history are marked by a black circle and a square, respectively. The results of the pushover analyses and the time histories show a very good match at all stories. This is a strong indication that for this building, in spite of its complexity and vertical irregularities, the static pushover analysis may be used to obtain a good approximation to nonlinear dynamic analyses results with ground motions of widely differing severity.

The damage indices corresponding to inelastic dynamic and pushover analyses were computed. Typical damage indices corresponding to pushover analyses in one of the frames are shown in Fig. 9.37. This figure compares the damage observed in the field inspection and the numerical damage indices computed. Although there is no one-to-one correspondence between analysis results and observed damage, certain analytical indicators do provide strong indications of where damage might be present.

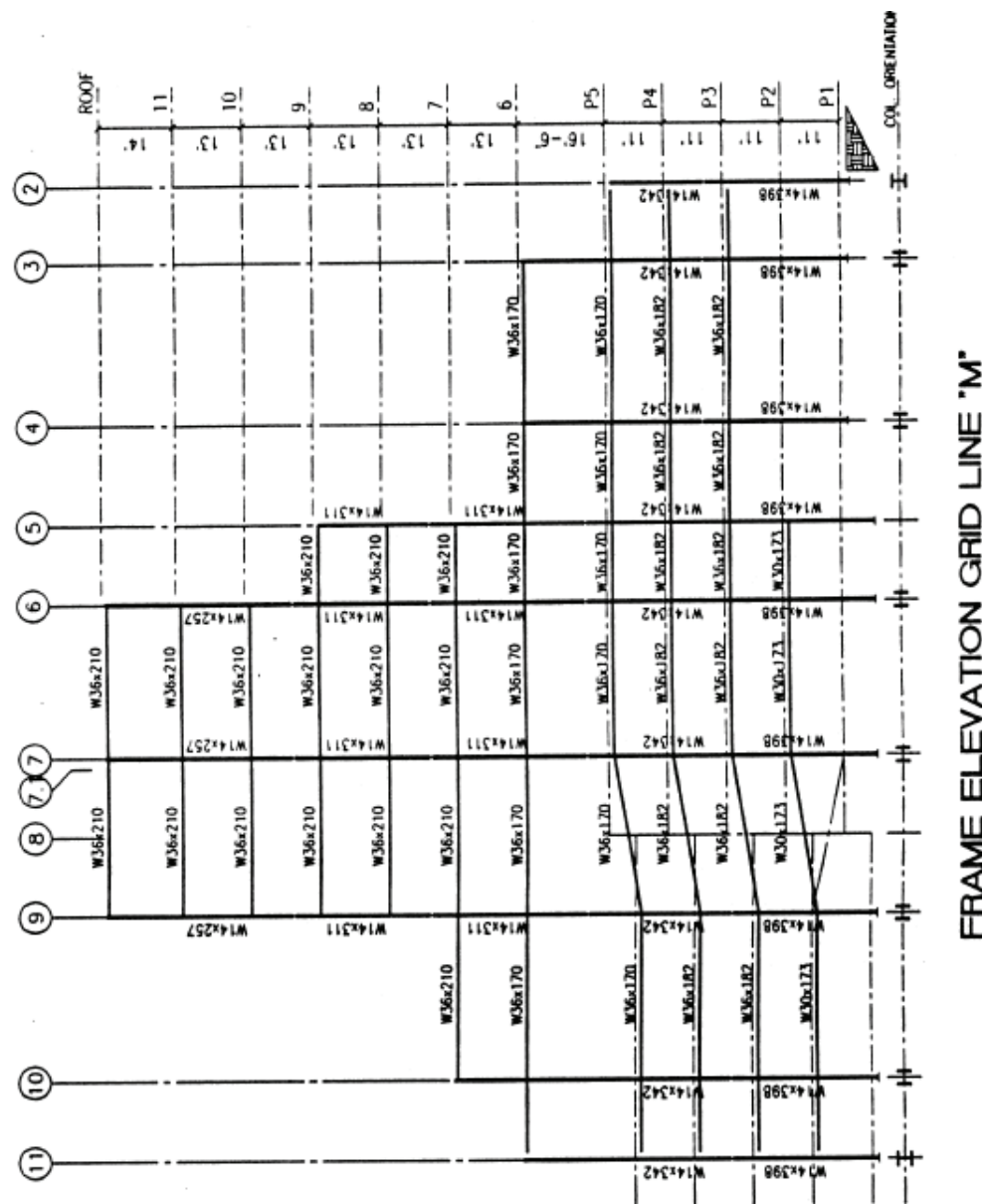


Fig. 9.33 Frame elevation at grid line "M"

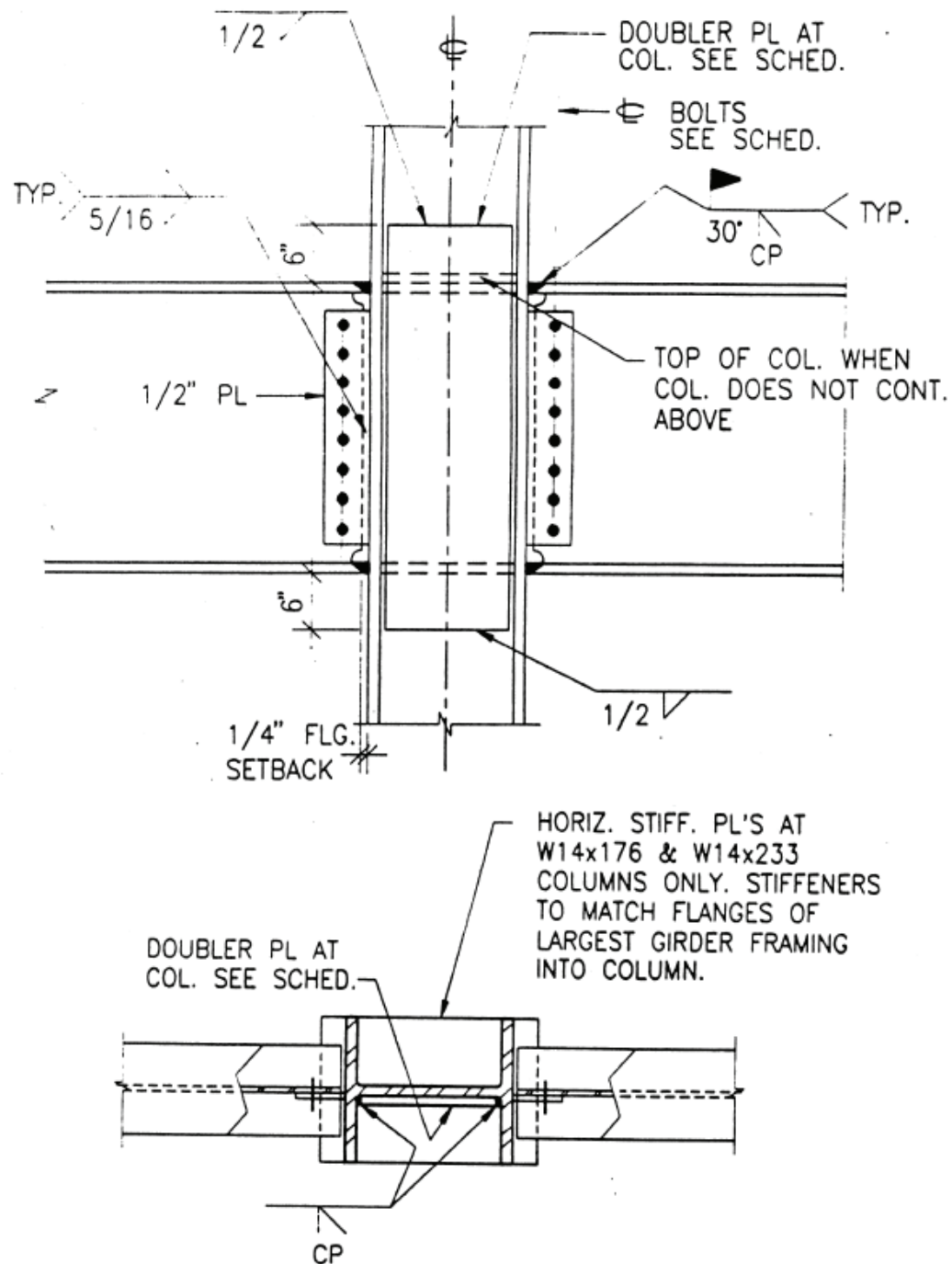


Fig. 9.34 Typical moment connection at column flange

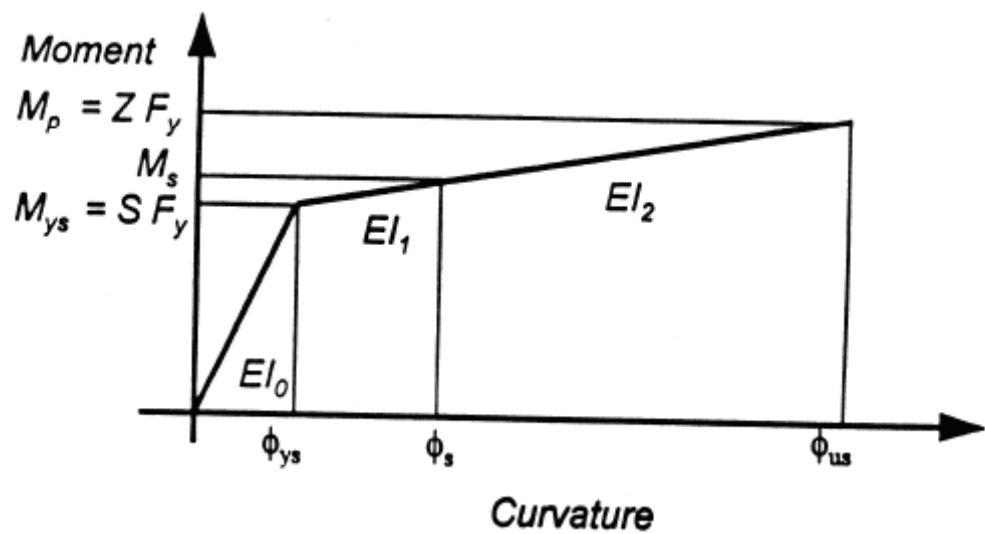


Fig. 9.35 Material model used for the study

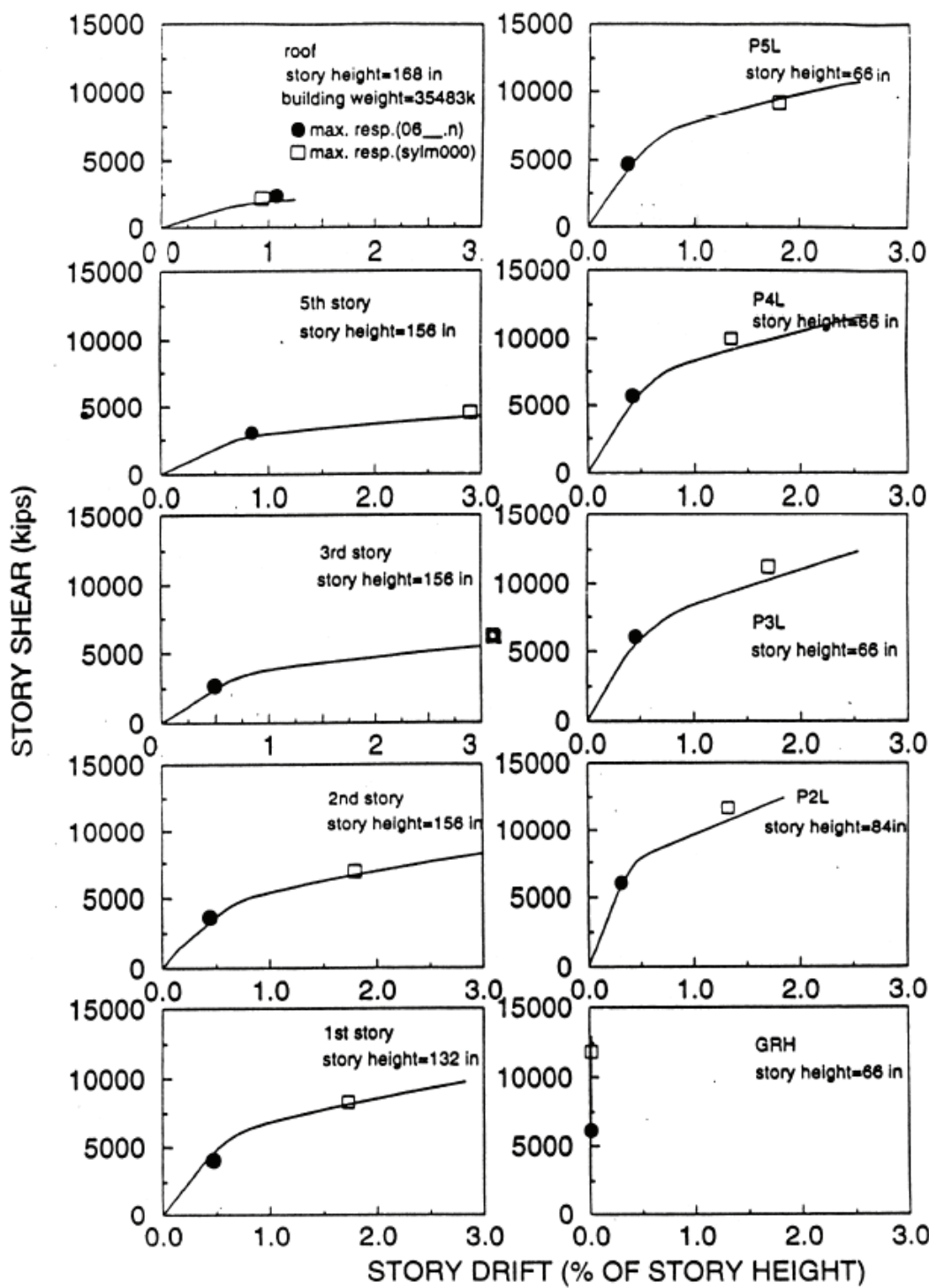


Fig. 9.36 Nonlinear story shear versus story drift (NS direction)

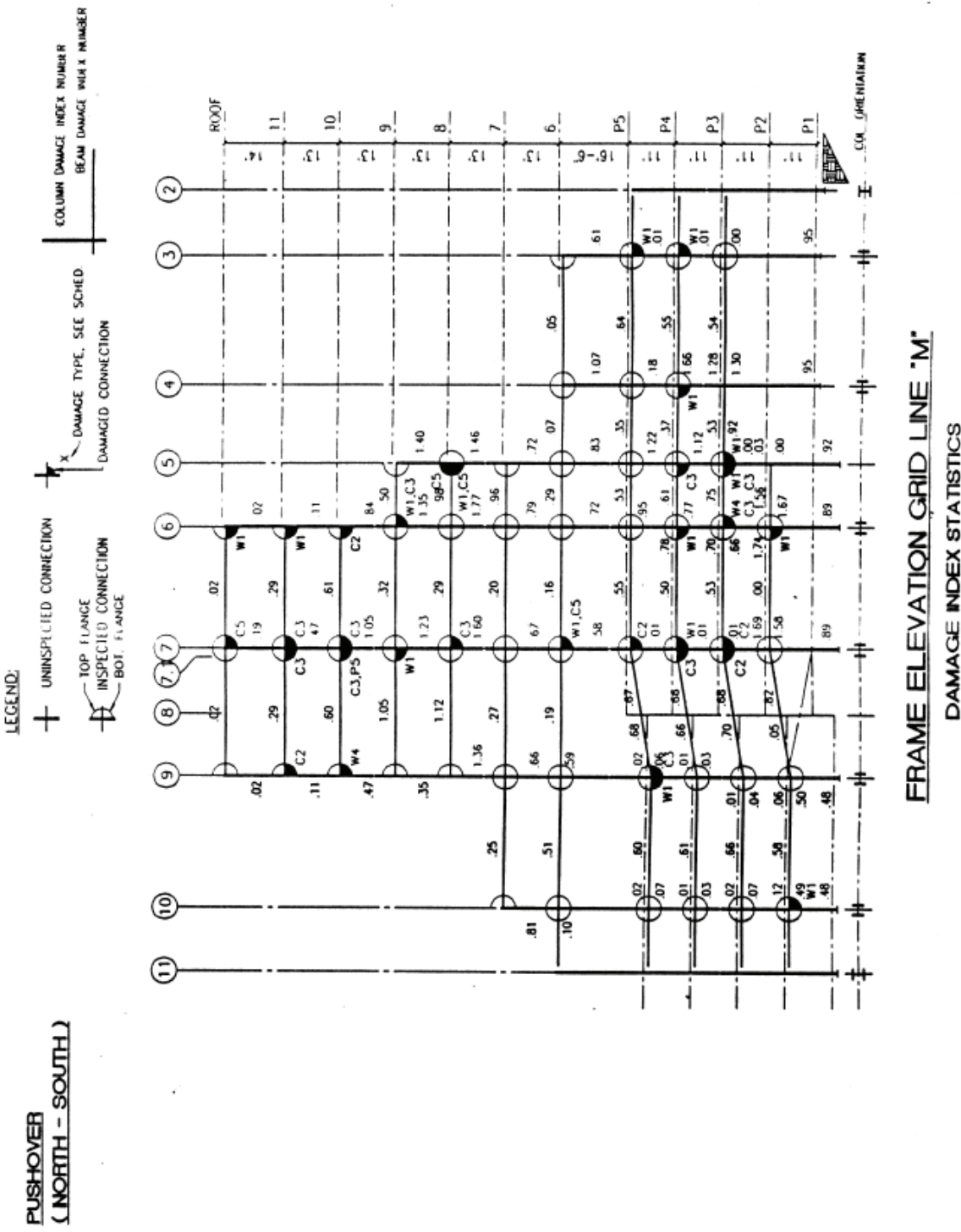


Fig. 9.37 Comparison of observed damage and computed damage indices (Grid line "M")

9.9 Passive Energy Dissipation Devices: 1:3 Scale Model Retrofitted Using Different Types of Dampers

The response of the 1:3 scale three story model structure described in Section 9.4 was investigated using different passive energy dissipation devices. This case study compares numerical predictions of the response with actual experimental measurements of the building with different types of dampers. The tested structure included conventional concrete jacketing in the interior columns and joint beam enhancements (Bracci et al., 1992) to retrofit the original damaged structure. The test program included the following types of dampers:

- a) Viscoelastic dampers by 3M company (Lobo et al., 1993; Shen et al., 1993).
- b) Fluid viscous dampers by Taylor Devices (Reinhorn et al., 1995a).
- c) Friction dampers by Sumitomo Construction Co. (Li and Reinhorn, 1995).
- d) Viscous walls by Sumitomo Construction Co. (Reinhorn et al., 1995b).
- e) Friction dampers by Tekton Co. (Li and Reinhorn, 1995).

The objectives for the retrofit test program was to reduce overall damage progression, provide data for analytical modeling of inelastic structures equipped with linear and nonlinear dampers, and to determine the force transfer in retrofitted structures and its local effects.

The new version of the computer program IDARC is capable of modeling viscous, friction and hysteretic dampers. Test results for the Taylor fluid viscous dampers and the Sumitomo friction dampers are summarized. The test program did not include any type of hysteretic dampers, but the numerical results for the structure with hysteretic dampers are included.

9.9.1 Viscous Dampers

The fluid viscous dampers by Taylor Devices were selected for this comparison. Results for the other types of viscous dampers tested can be found in the corresponding reference listed above. The viscous dampers installed in the brace (see Fig. 9.38), were selected from the catalog of Taylor Devices Inc. Model 3x4, rated to 10,000 lbs. (44.6 kN). The damper was connected to the brace using a load cell with a capacity of 30,000 lbs. The damper construction can prevent rotations between its two ends which is suitable to prevent buckling in the brace assembly.

Figures 9.39 and 9.40 present a comparison of story displacements and accelerations for El Centro 0.3g. Results show a good correlation between the experimental test results and the numerical prediction. Figure 9.41 shows the pushover response of the structure for a simplified evaluation, as presented by Reinhorn et al. (1995a).

9.9.2 Friction Dampers

For this comparison, the friction dampers by Sumitomo Construction Co. were selected. Results for the other type of friction damper tested can be found in the corresponding reference listed above. The damper was installed using the layout shown in Fig. 9.38, as described for the viscous damper example. Figures 9.42 and 9.43 present a comparison of story displacements and accelerations. Numerical results show good correlation with the experimental measurements. Figure 9.44 shows the pushover response of the structure that can be used in a simplified response evaluation as described in Reinhorn et al. (1995a).

9.9.3 Hysteretic Dampers

The test program on the three story scale model did not include retrofit using hysteretic damper elements. For completeness, the results considering a hysteretic damper are presented in Figs. 9.45 and 9.46.

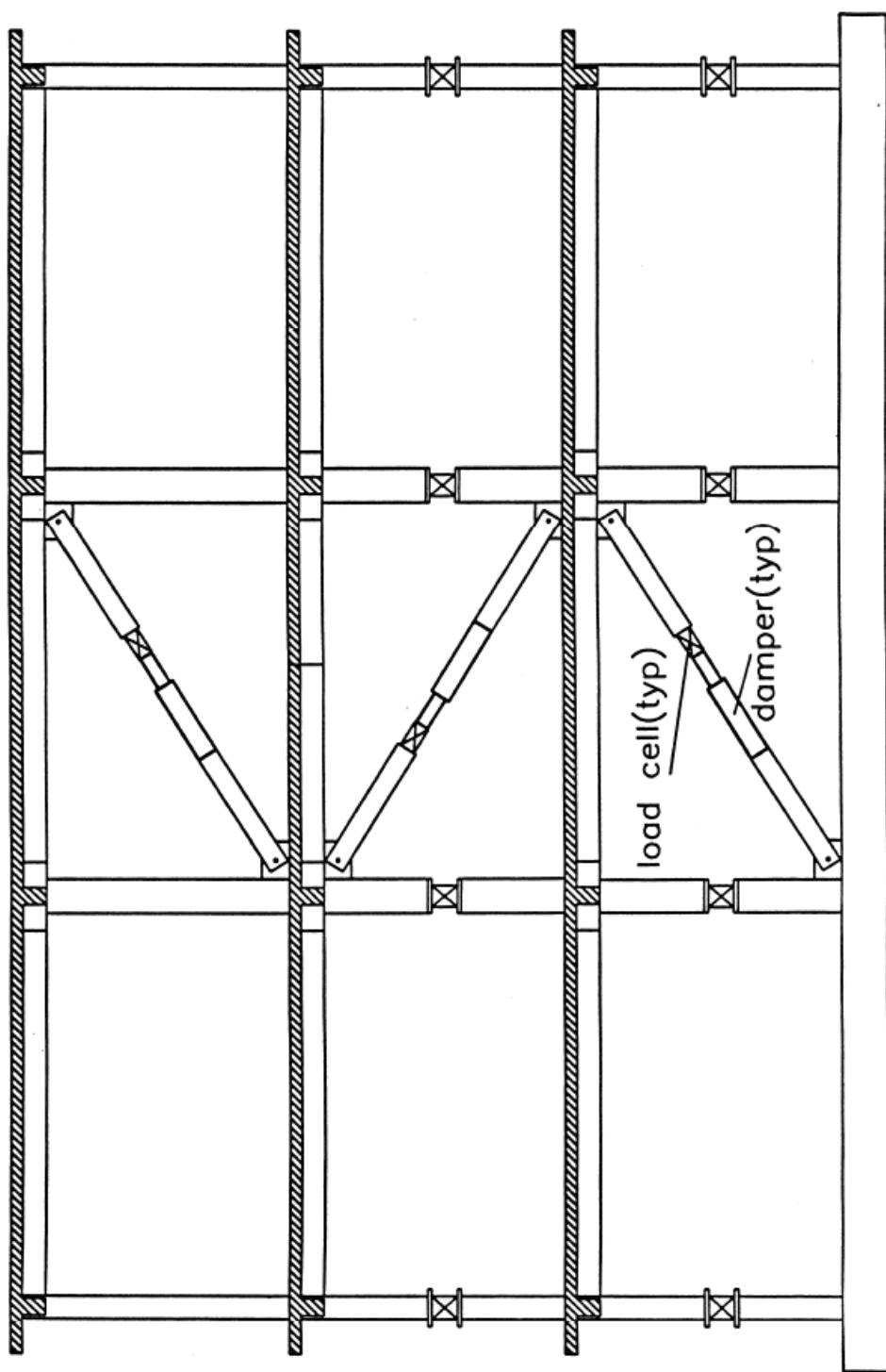


Fig. 9.38 Location of dampers and measuring devices

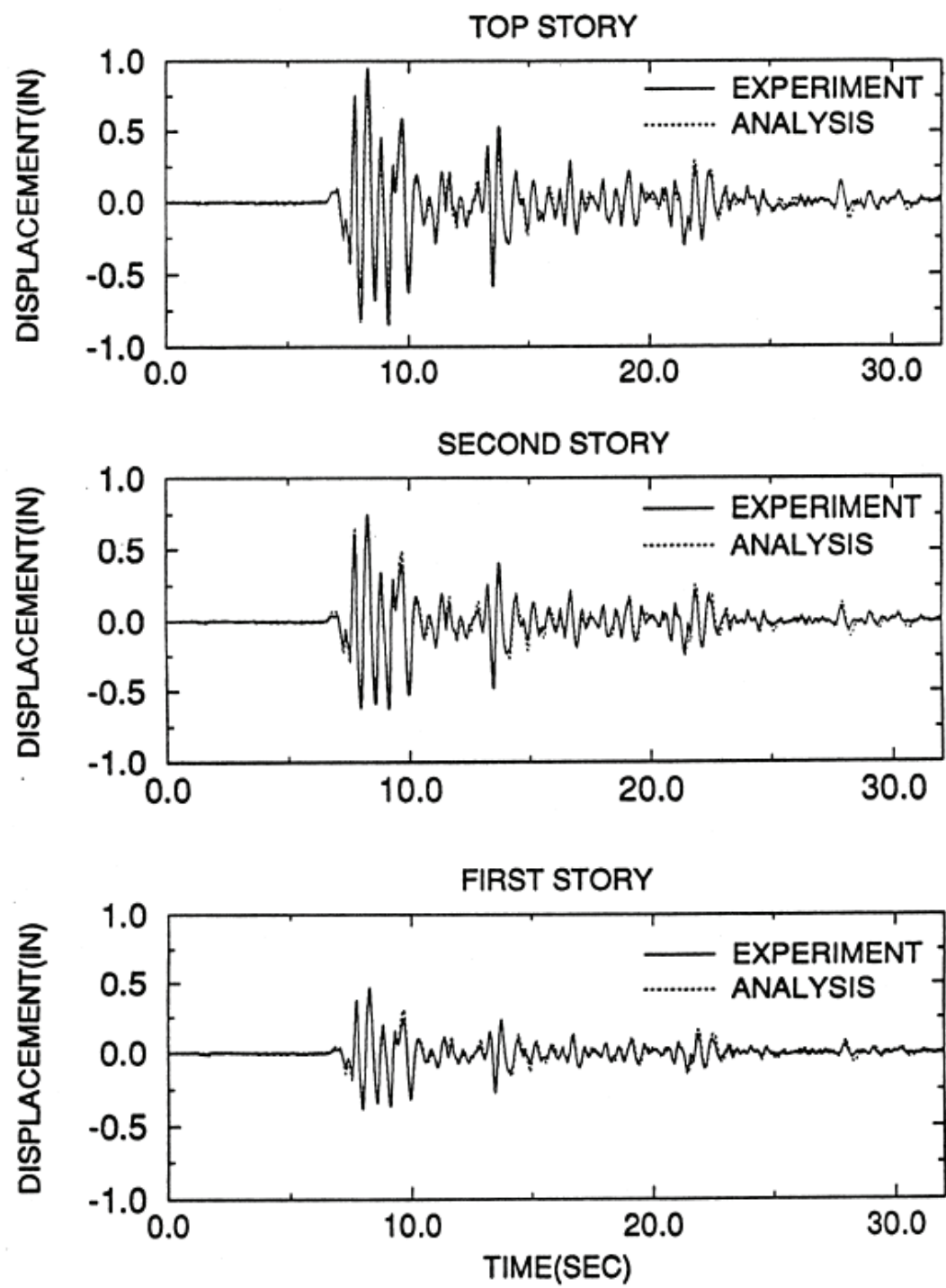


Fig. 9.39 Comparison of experimental and analytical displacements with viscous dampers

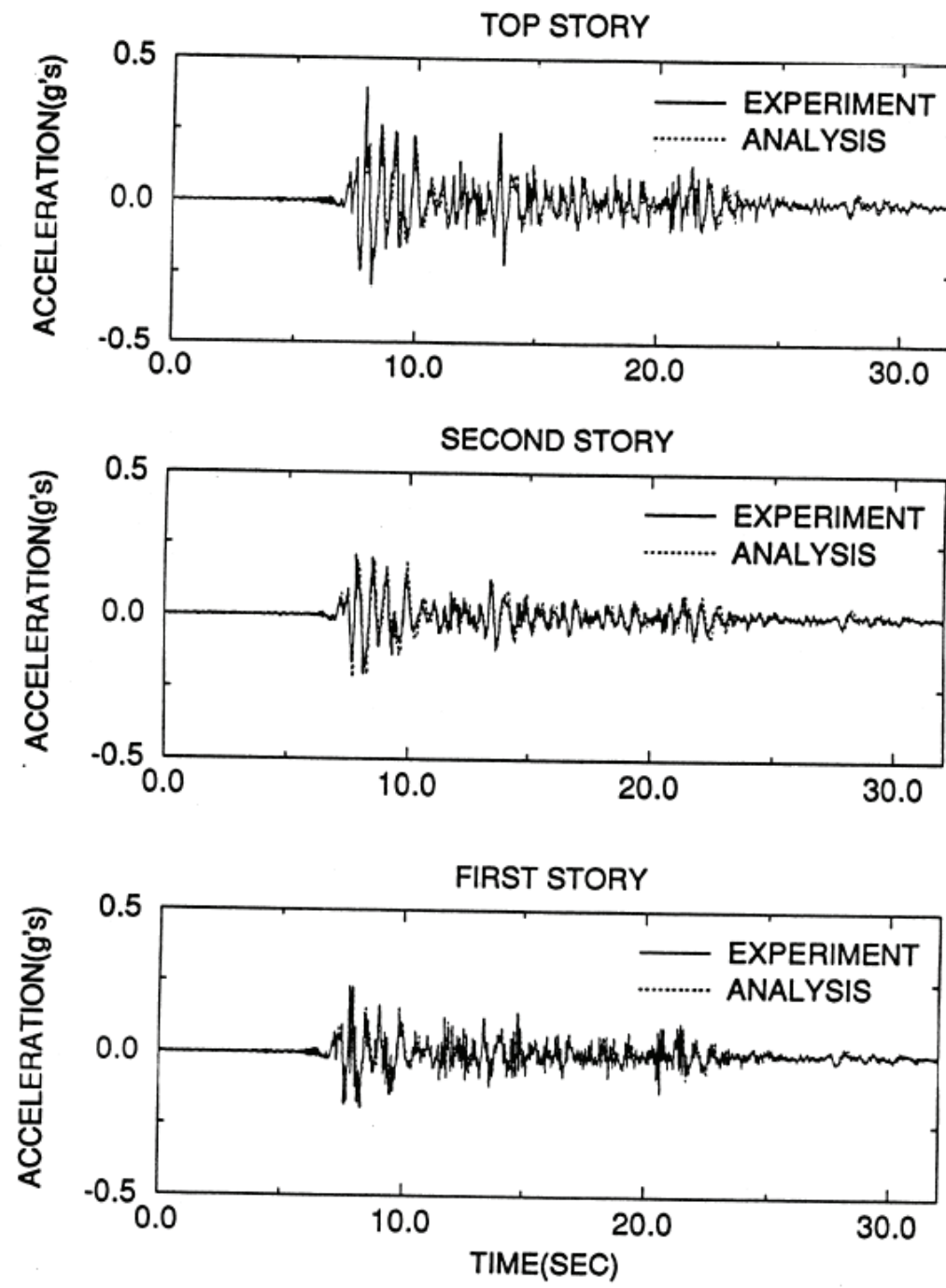


Fig. 9.40 Comparison of experimental and analytical accelerations with viscous dampers

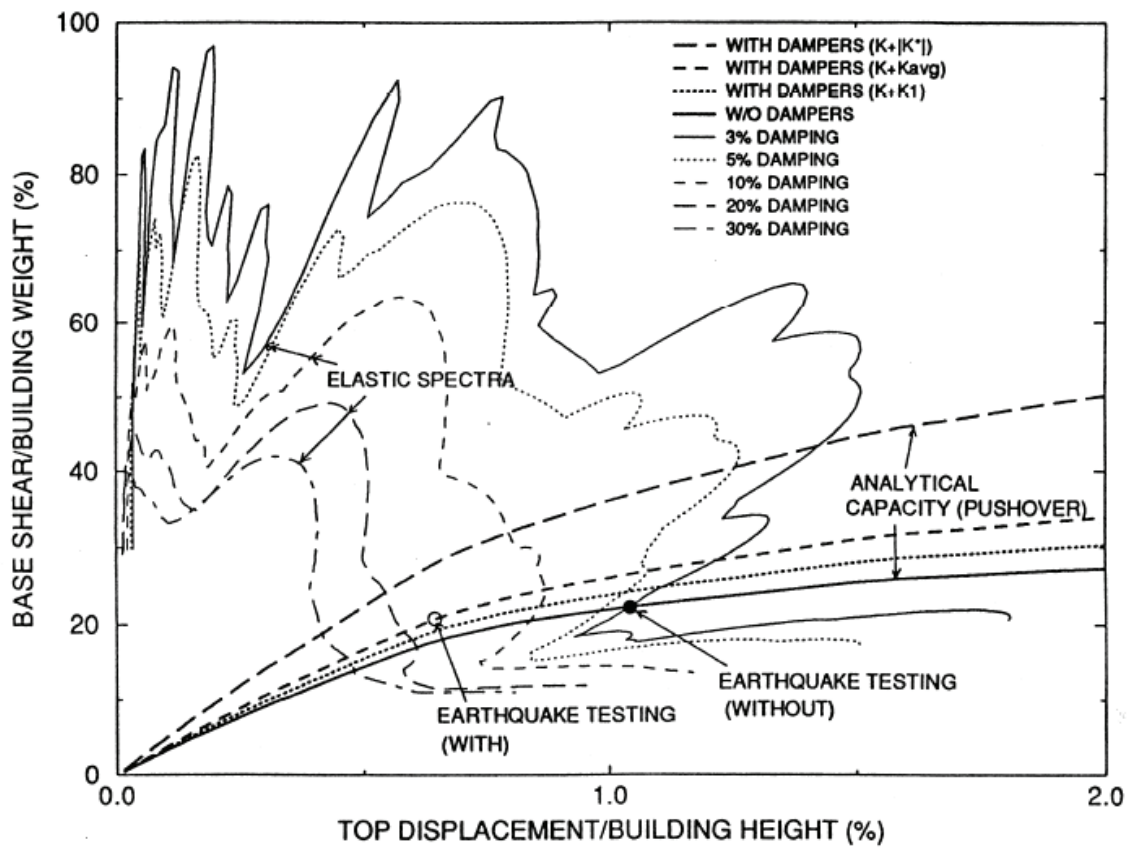


Fig. 9.41 Pushover response of structure with viscous dampers for simplified evaluation

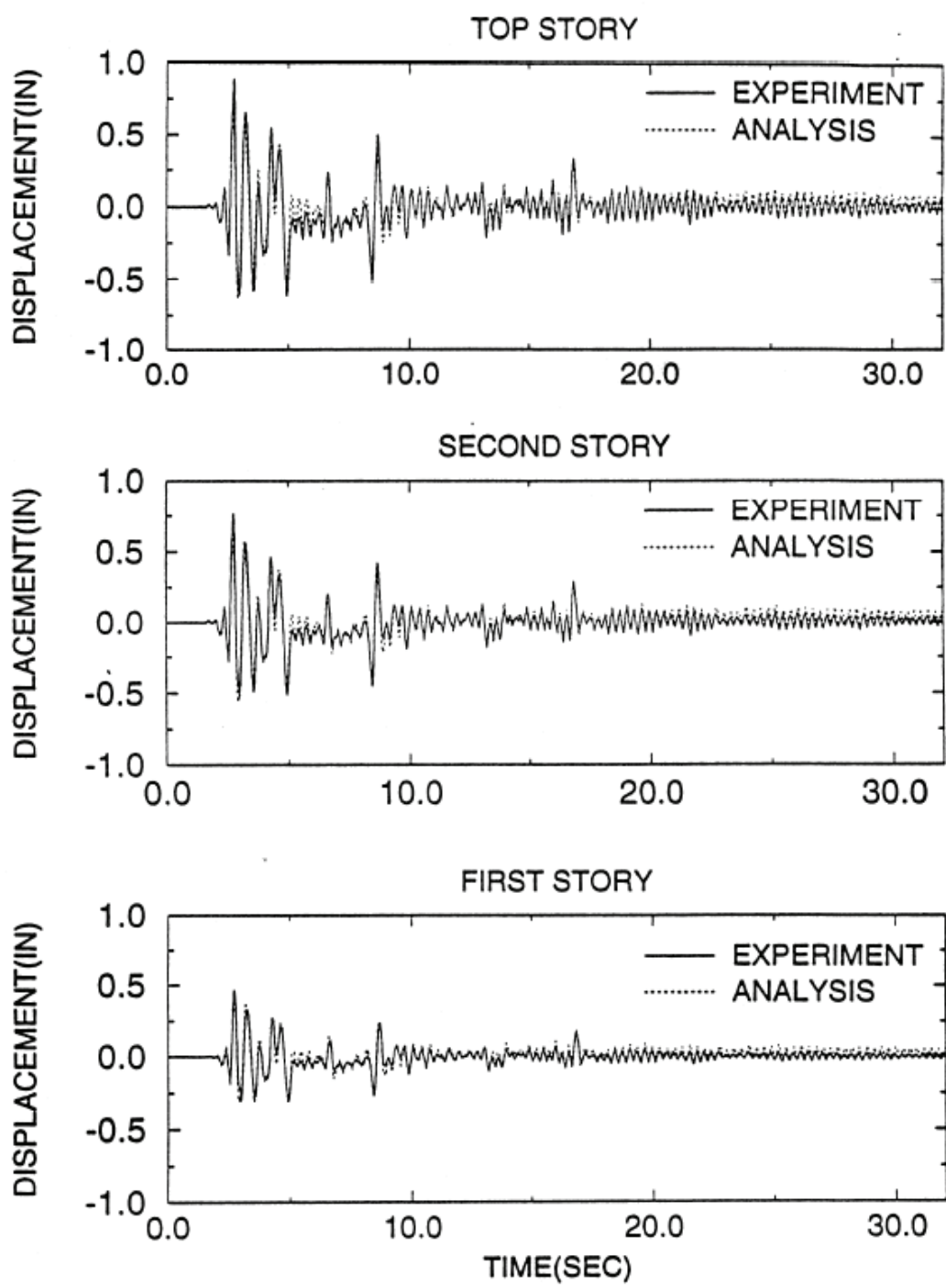


Fig. 9.42 Comparison of experimental and analytical displacements with friction dampers
(El Centro 0.3g)

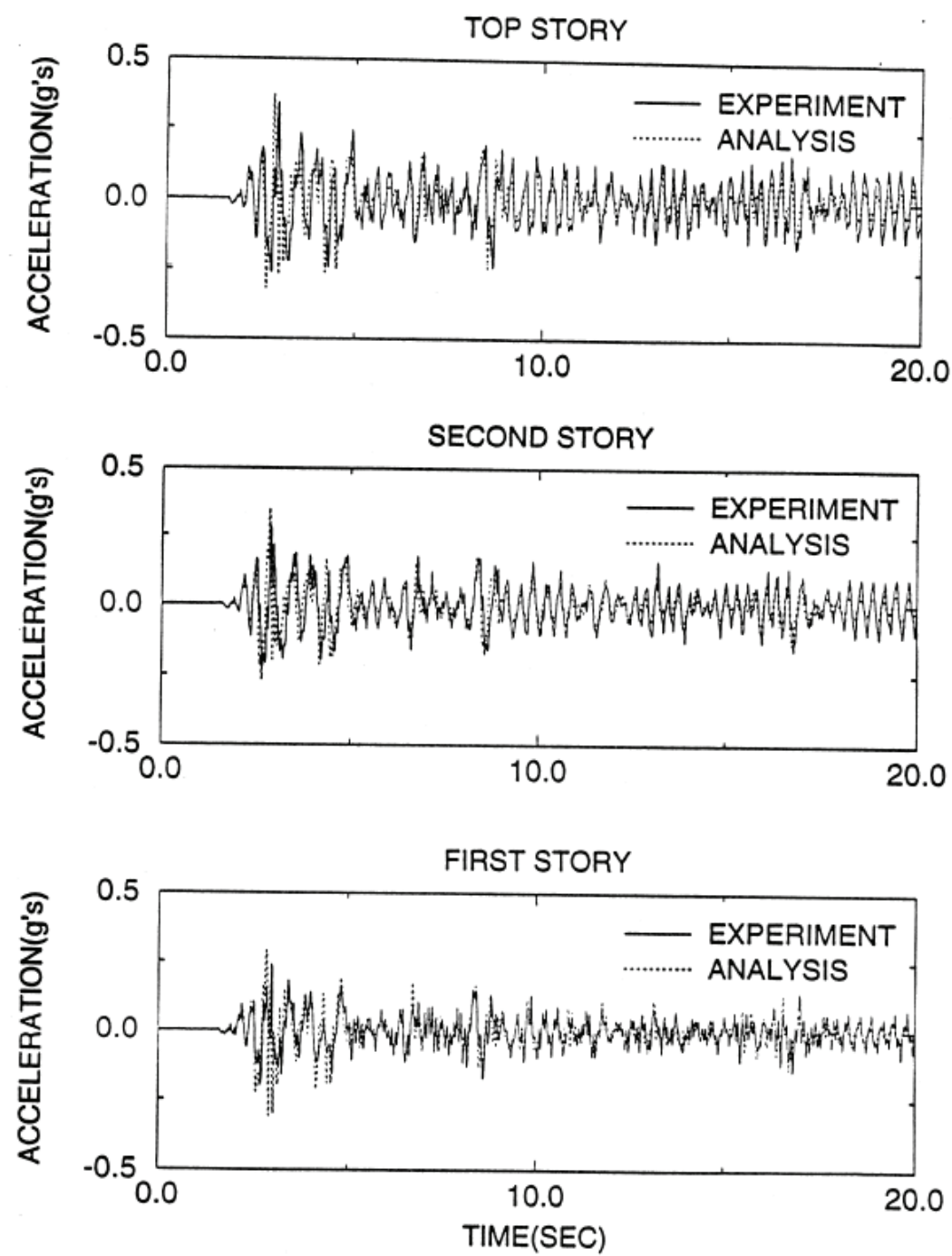


Fig. 9.43 Comparison of experimental and analytical accelerations with friction dampers
(El Centro 0.3g)

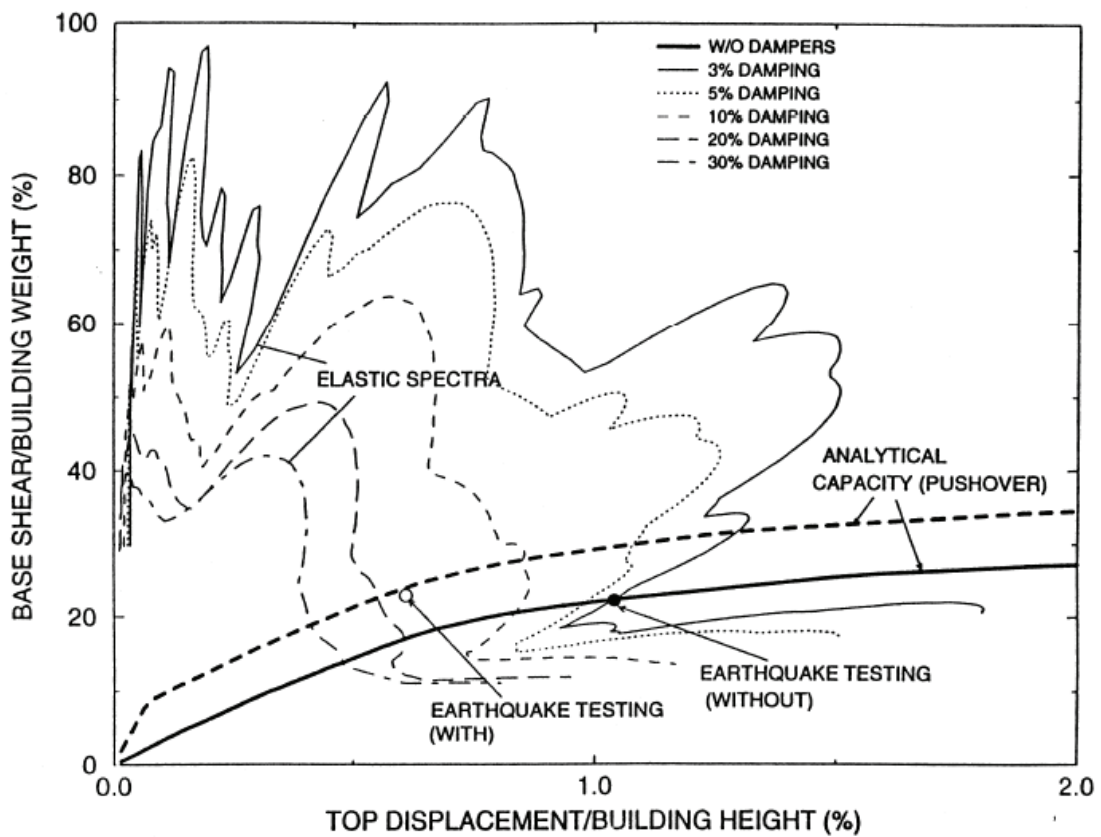


Fig. 9.44 Pushover response of structure with friction dampers for simplified evaluation

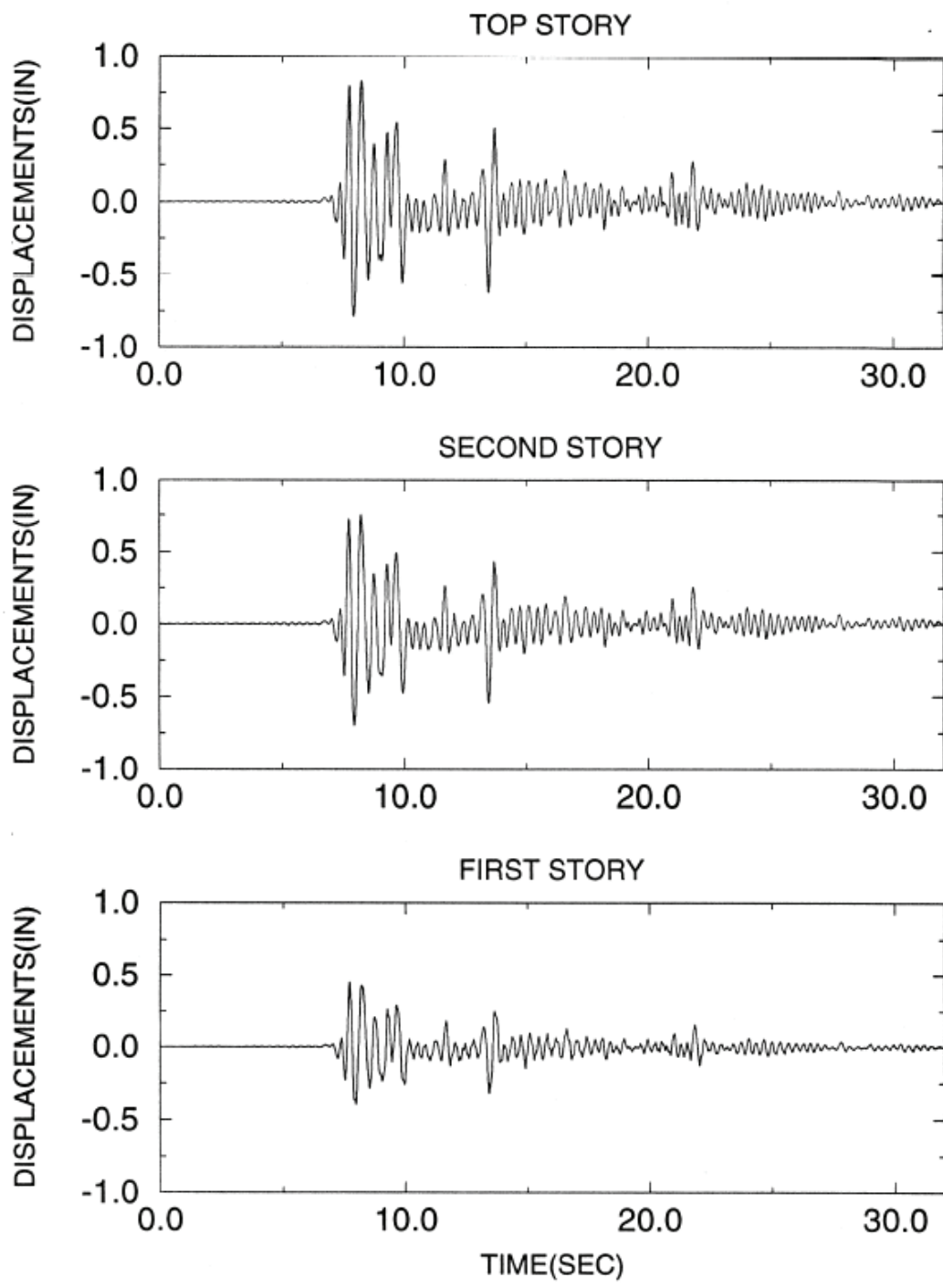


Fig. 9.45 Analytical displacement response with hysteretic dampers (El Centro 0.3g)

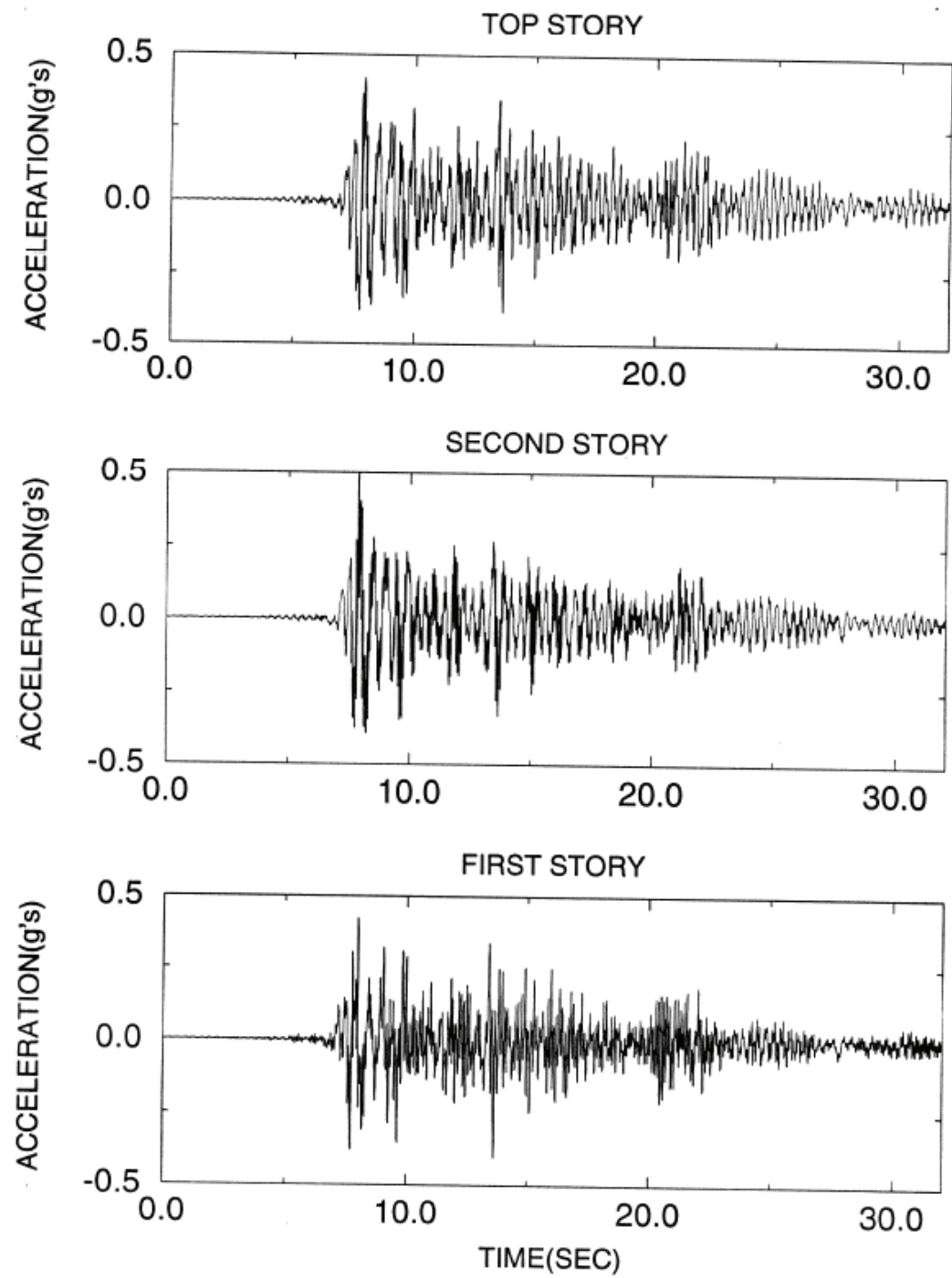


Fig. 9.46 Analytical acceleration response with hysteretic dampers (El Centro 0.3g)

9.10 Masonry Infill Panels: Experimental Test of a Masonry Infilled Frame

The computer program IDARC is capable of analyzing the response of buildings with infill panel elements. In this case study, the response of a masonry infill panel tested at the University of Buffalo (Mander and Nair, 1994) is investigated. The infill frame was part of a research program to obtain the hysteretic force deformation of masonry infilled frames. The subassemblies, constructed from bolted steel frames and infilled with clay brick masonry, were tested under in-plane quasi-static cyclic loading. The test specimens consisted of three story steel frames with the center story infilled with the brick masonry (see Fig. 9.47). Diagonal braces with stiffness similar to the infill were provided at the top and bottom stories.

Connections in the frame were designed to half the strength capacity of the connecting members to achieve concentrated yielding in the connections, preventing therefore damage to the principal members. The test setup was designed to simulate boundary conditions shown in Fig. 9.48, with plastic hinges at the beam ends and a compression strut in the infill. Such conditions exist in frames subjected to lateral loading with the infill being the critical element (Mander et al., 1994). Test specimens were subjected to a sinusoidal cyclic drift history with increasing amplitude.

The program IDARC Ver. 4.0 was used to simulate the observed experimental force deformation response of the masonry infill subassembly. The idealized structural model used for the analysis is shown in Fig. 9.49. The model parameters were determined using the formulas presented in Appendix D (see Reinhorn et al., 1995d, for more details). The same cyclic drift history used for the experimental test was used as input for the model. The comparison of the experimental and analytical force-deformation response for one of the subassemblies tested is presented in Fig. 9.50 (see Reinhorn et al., 1995d, for more comparisons). The figure shows the lateral force vs. interstory drift hysteresis loops obtained in the experiment and the simulation. The comparison indicates that the

theoretical model predicts the experimental results to a reasonable degree of accuracy. The proposed hysteretic rule is sufficiently versatile and adequate to generate the observed hysteretic loops.

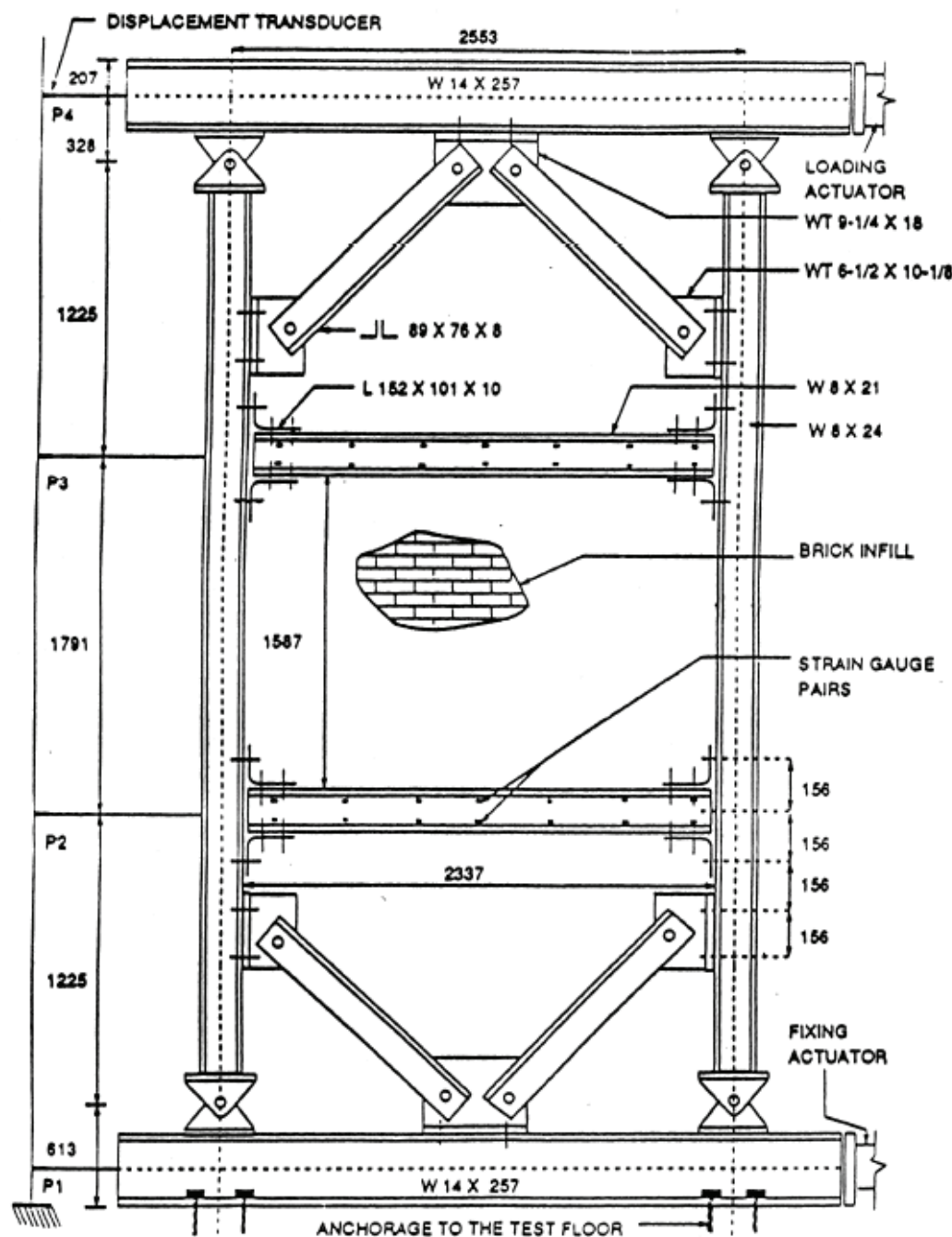


Fig. 9.47 Masonry infilled frame test specimen

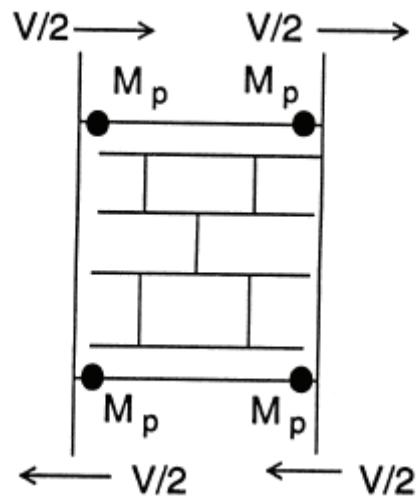


Fig. 9.48 Boundary conditions of infilled frame subassembly

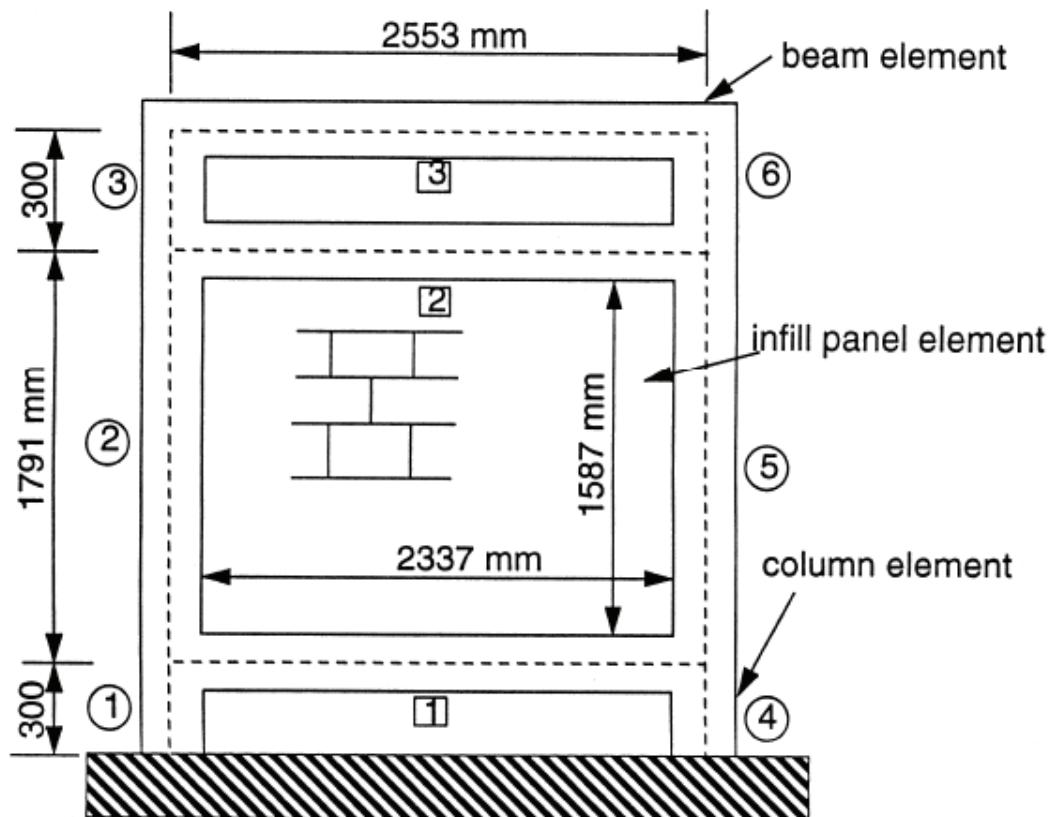


Fig. 9.49 Idealized structural model for analysis

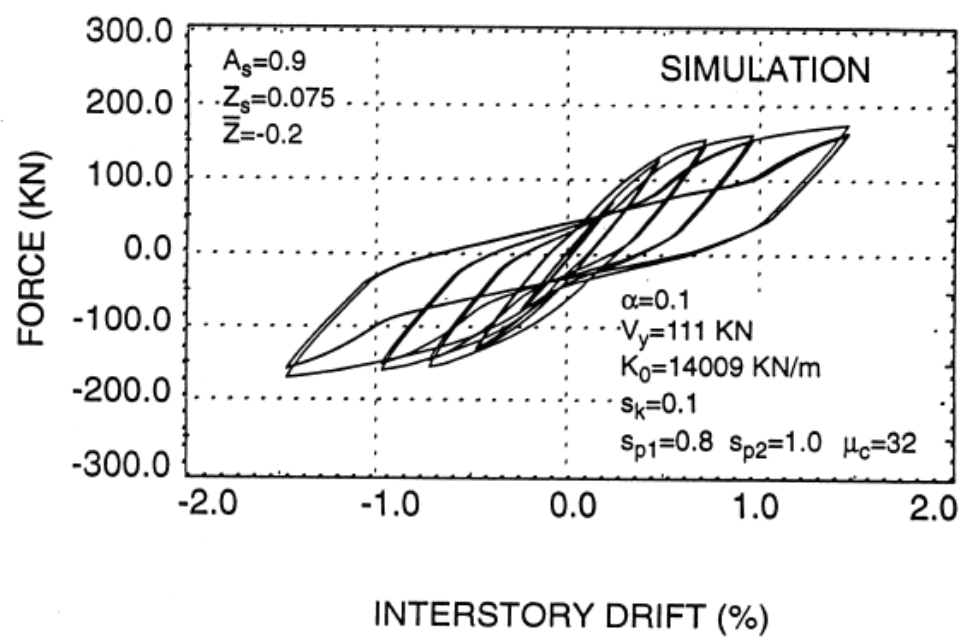
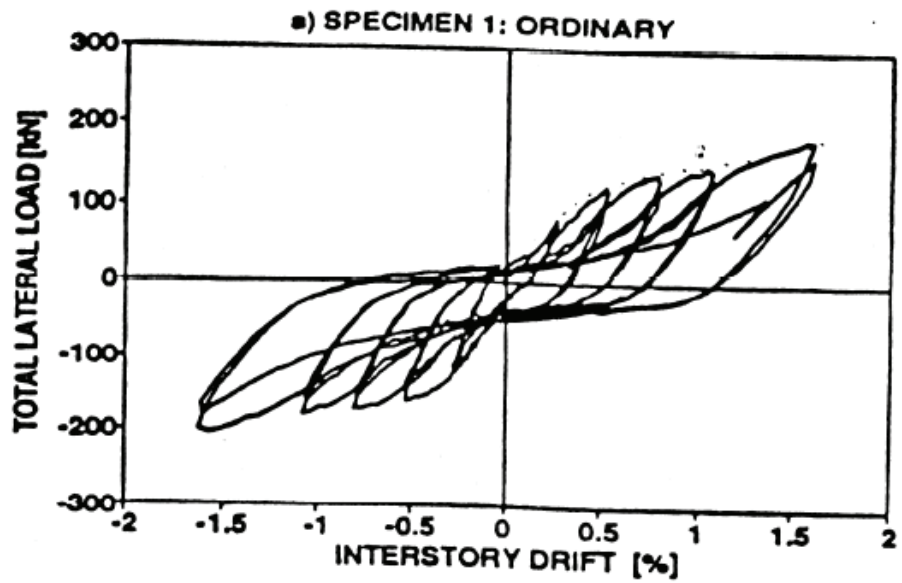


Fig. 9.50 Comparison of experimental and analytical force-deformation response
(Specimen 1)

9.11 Deep Beam & Column Elements: Performance of IDARC2D

This example is to present the IDARC2D performance for deep beam & column elements which consist of both nonlinear flexural and shear properties. One story and one bay frame is shown in Fig. 9.51. The frame structure is modeled with conventional elements (CEs), thus the frame is governed by flexural behavior only. The flexural properties of the two columns are designed as the same as the beam flexural properties.

In order to obtain Deep beam & column Elements (DEs), shear properties are added to the conventional elements. Herein, two cases are considered depending on the level of shear stiffness and shear strength as shown in Fig. 9.52. The case DE1 has the high shear stiffness and strength. In this case, the flexural failure is developed before the shear yielding. The case DE1 will be governed by flexural property only because of high shear stiffness. Eventually, the global and local behaviors of the DE1 will be the same as the behavior of the original frame. The case DE4 has the low shear stiffness and strength. In this case, the shear failure will be developed before its flexural yielding. Therefore, the case DE4 will be governed by the shear response in both elastic and plastic range.

The deep beam & column elements are based, therefore, on a series springs model of shear and flexure (see Fig. 3.10). The moment-curvature and shear force-strain envelopes used to both the beam and columns are shown in Fig. 9.53. The same shear properties and capacities are applied to the beam and column elements when these members are considered as a deep element. Quasi-static cyclic analyses are performed for the three types of the frame: a) frame designed with conventional elements, which is a type CE, b) frame designed with deep beam and conventional columns, which is a type DB, and c) frame designed with conventional beam and deep columns, which is a type DC. In the analysis, same loading history based on displacement control and same hysteretic control parameters are used.

Fig. 9.54 (a) is the results of the type CE. Figures 9.54(b)~(c) and (d)~(e) show also the results of the type DB and the type DC, respectively. Moment-curvature response and corresponding shear force-top displacement of each beam and column are sampled for the hysteretic behaviors.

The results of DB 1 (type DB + case DE1) and DC 1 (type DC + case DE1) are the same as the result of CE because the shear stiffness and the shear strength are relatively higher than their flexural properties. However, the cases DB 4 (type DB + case DE4) and DC 4 (type DC + case DE4) are more flexible than the case of CE due to the shear effect. The beam element in the DB 4 and the column element in the DC 4 are remained within elastic range in the flexural behavior. Furthermore, as expected, the maximum shear force of the beam and column in both cases, DB 4 and DC 4, are lower than the maximum shear force of the type CE.

Failure states and damage index of each case are shown in Fig. 9.55. The original frame is yielded in all elements. The same yielding states and same damage index are appeared in the cases of the DB 1 and the DC 1. However, when the beam is designed as low shear stiffness and low shear strength, the flexural yielding is developed at the bottom of the columns and shear yielding is appeared at the beam. Similarly to the case DB 4, only shear yielding is developed at the columns when the columns in the frame are designed as low shear stiffness and low shear strength.

From these results, this IDARC2D program performs well in the use of deep beam and column element, satisfying the concept of deep beam and deep column theories.

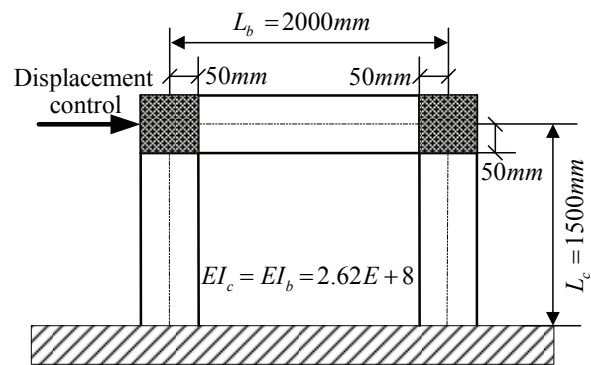


Fig. 9.51 Frame model consisted of deep elements

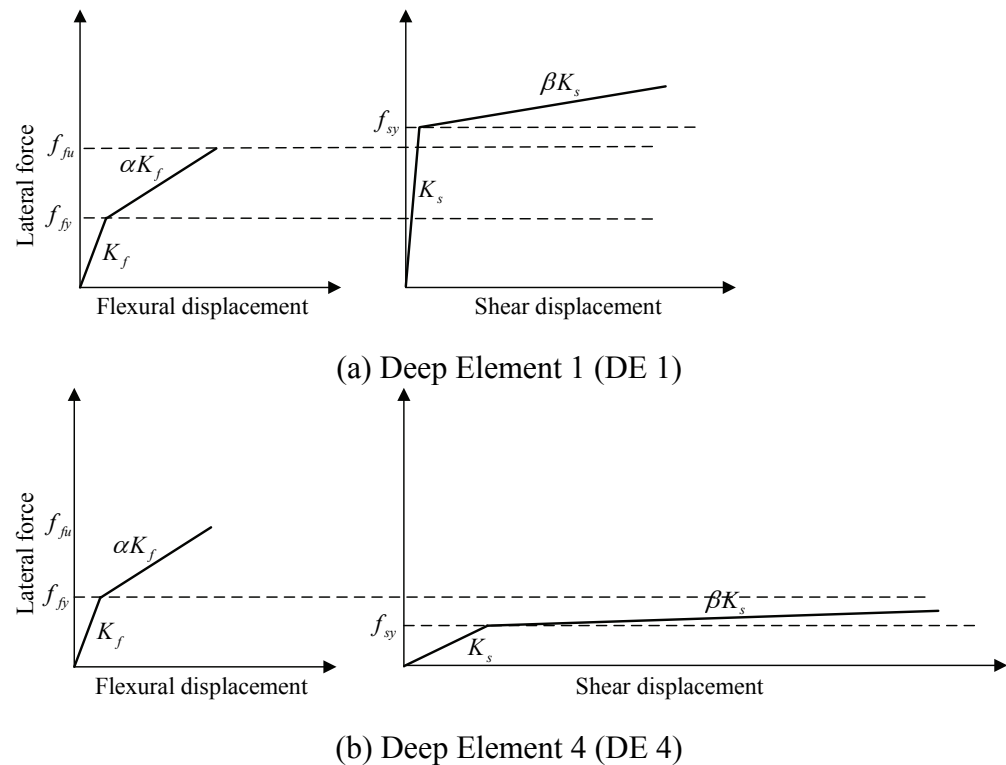
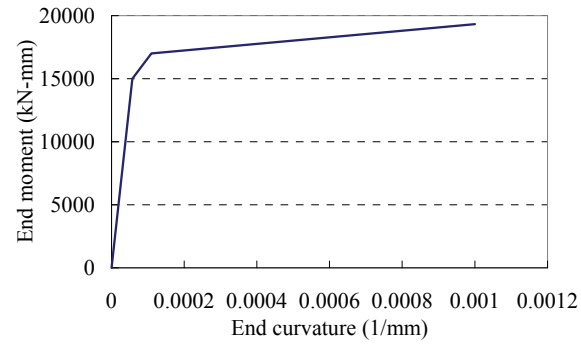


Fig. 9.52 Cases for performance of deep element



Conventional Element (CE)

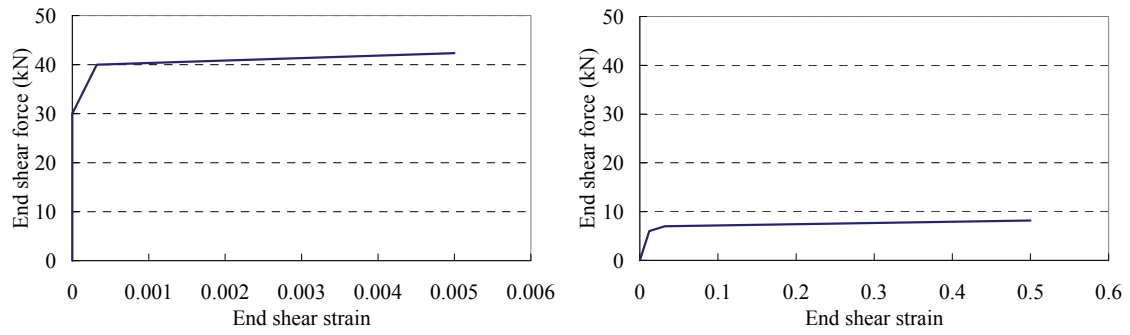


Fig. 9.53 Moment-curvature and shear force-strain relationship of each cases

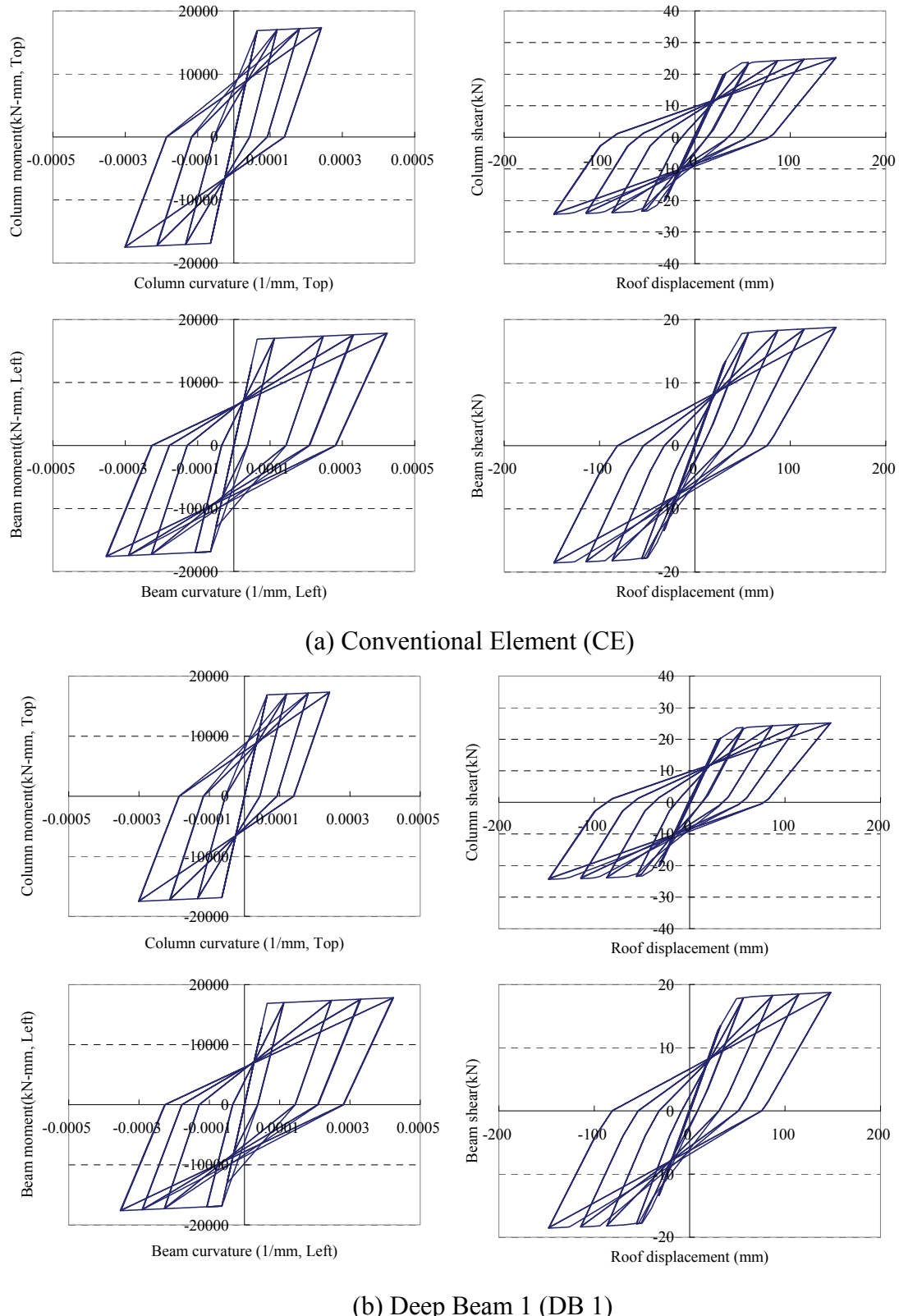
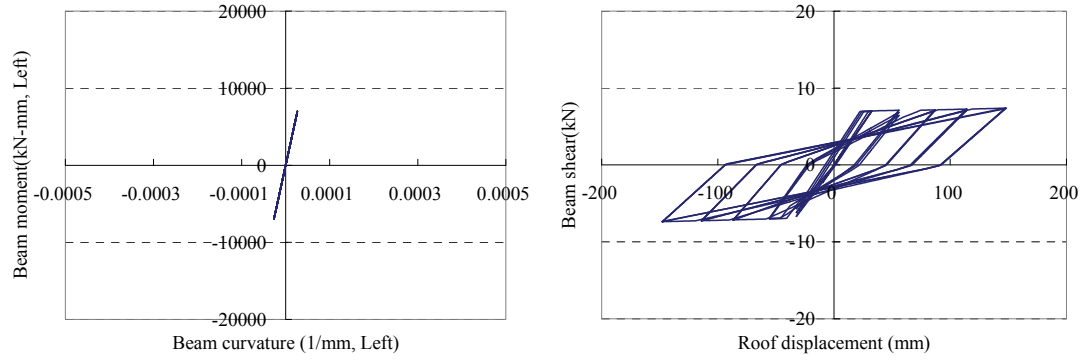
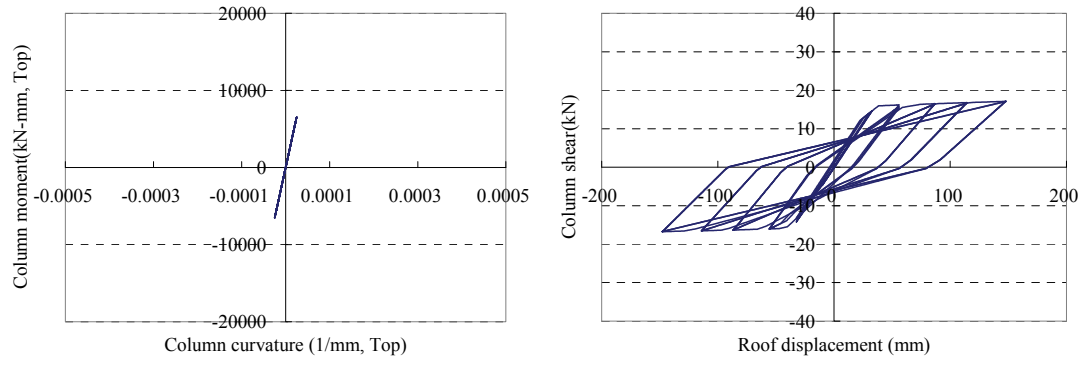
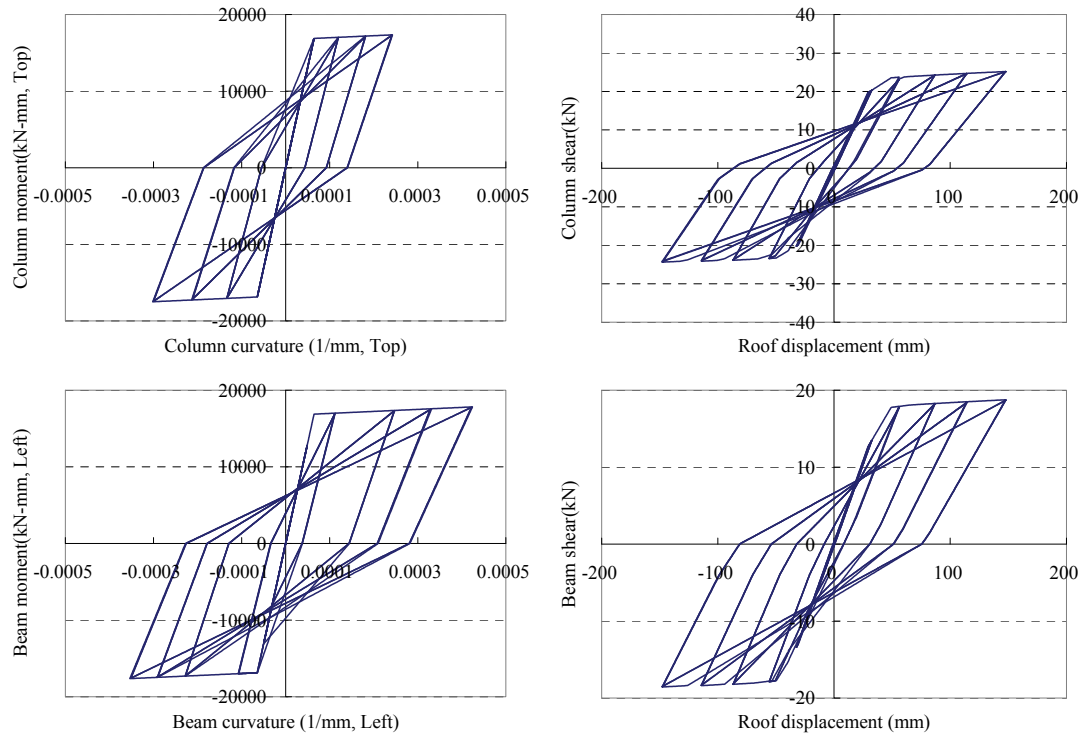


Fig. 9.54 Simulated results of original and deep frames

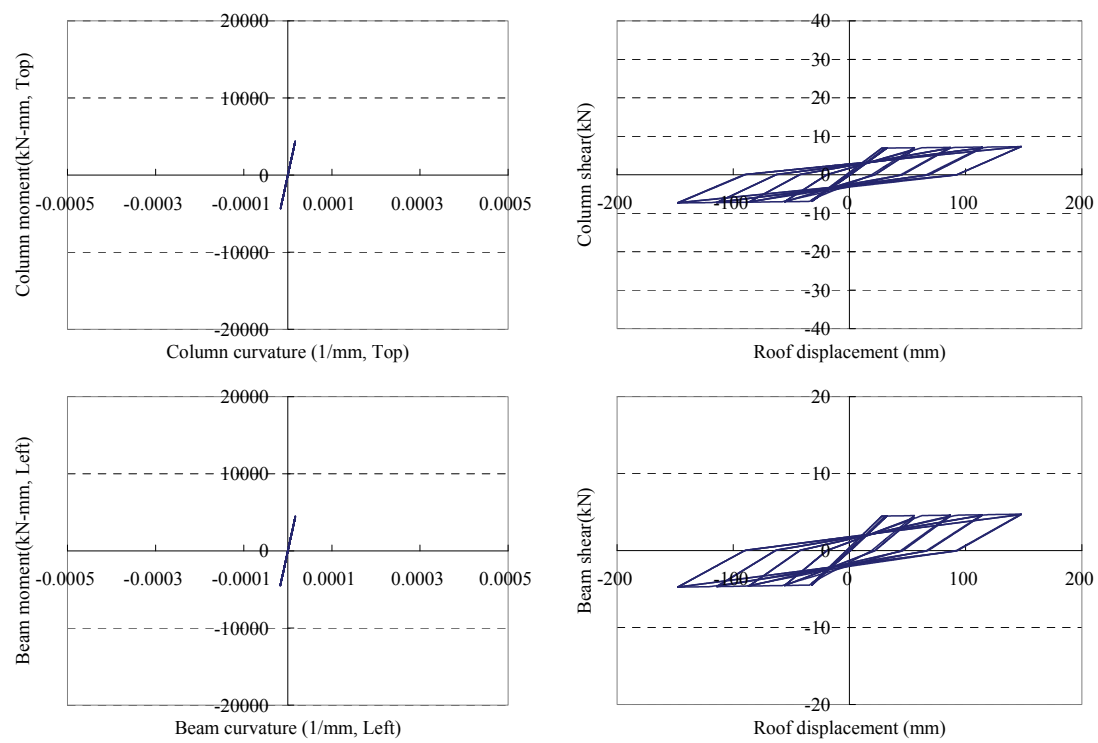


(c) Deep Beam 4 (DB 4)



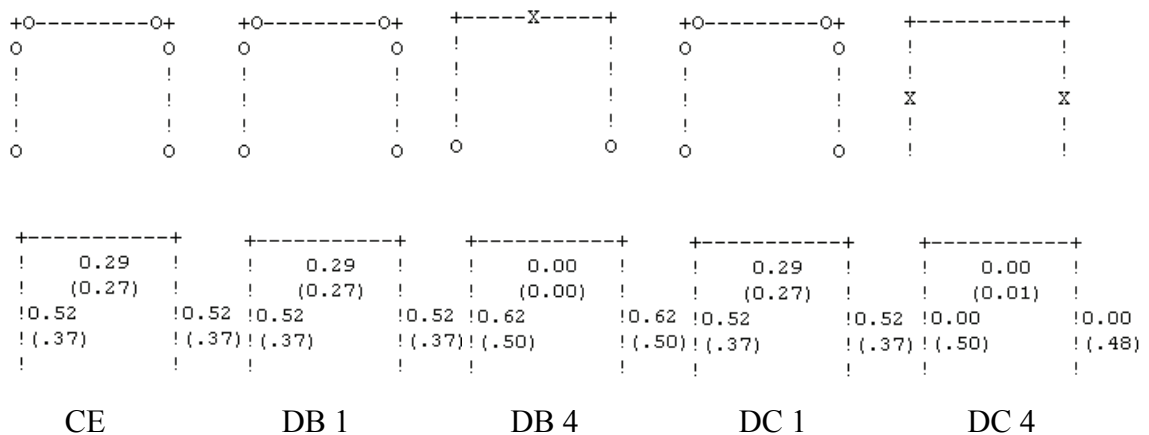
(d) Deep Column 1 (DC 1)

Fig. 9.54 Simulated results of original and deep frames (continued)



(e) Deep Column 4 (DC 4)

Fig. 9.54 Simulated results of original and deep frames (continued)



NOTATION:

- = BEAM x = CRACKING(FOR CONCRETE)
 ! = COLUMN INITIAL YIELD(FOR STEEL)
 W = SHEAR WALL O = PLASTIC HINGE DEVELOPED
 I = EDGE COLUMN * = LOCAL FAILURE(EXCEED CRITERIA)
 FOR EDGE COLS: C: COMPRESSION
 T: TENSION
 O: TENSILE YIELD
 X = INITIAL SHEAR CRACK OR YIELD
 \$ = SHEAR FAILURE

VALUES IN PARENTHESIS INDICATE ENERGY RATIOS

Fig. 9.55 Failure state and damage index

9.12 Nonlinear Dynamic Analysis of Structures with Rocking Columns

The purpose of most current seismic retrofit techniques is to improve performance by increasing the structural strength, stiffness, and energy dissipating capacity for better control. In such cases, although the displacements and the ductility demands decrease, there is an increase in the floor accelerations. The acceleration response of yielding structure is dependent on its structural strength. Therefore, in order to reduce accelerations to protect structural elements and acceleration-sensitive nonstructural components in inelastic structures, the overall strength of the structure should be decreased. In this study the use of “rocking columns”, a type of constrained double hinged column, is suggested to reduce the structural strength (passive controlled-weakened structure) for lessening the story accelerations.

The results of quasi-static cyclic test with rocking columns are shown in Fig. 9.68. From the results the rocking columns have non-negligible stiffness prior to rocking. Also, the rocking columns provide large lateral drift during three cycles. As shown in Fig. 9.68, after reaching the maximum lateral displacement in the first cycle, the rocking column returns to a steady envelope curve that remains constant in subsequent cycles without degradation, which can be modeled using a Nonlinear Elastic-Cyclic Model (NECM). Also, when the small external axial load was applied to the column, the envelope curves from first to last cycles were very close with providing almost a nonlinear elastic-cyclic behavior.

The rocking column can be used to achieve a weakening structure. The conventional model structure (Bracci et al., 1992) described in Section 9.4 is weakened for the alternative C(SA) by using rocking columns as shown in Fig. 9.69. This weakening strategy was applied to only frame B. The alternative C(SA) has all columns at all stories of frame B allowed to rock and was weakened proportionally to the original story strength, considering nodal weights as external vertical loads. The time history

responses of the conventional and weakened structures to 0.3PGA white noise ground motion are shown in Fig. 9.70.

Analysis results regarding to story peak acceleration, story shear force, floor displacement, and interstory drift obtained for the alternative are presented in Fig. 9.71. The alternative A in Fig. 9.71 presents the response of the conventional model structure. Throughout weakening the conventional structure, the peak acceleration and peak shear force decrease in all stories. In alternative C(SA) the peak accelerations, compared to the conventional structure, reduce by 33.78%, 31.81%, and 29.85% at first, second, and third stories, respectively. Peak floor displacements are increased proportionally with the level of weakening of the conventional structure. In peak story drift response shown in Fig. 9.71(d), all stories of the alternative C(SA) are deformed larger than the conventional structure.

The use of rocking columns as used in the alternatives instead of conventional lateral resisting columns is an appropriate technique to achieve weakening. However, weakening alone is not sufficient if the displacement response exceeds a desirable limit because the increased displacements and drifts are undesirable. The addition of damping, however, corrects this problem.

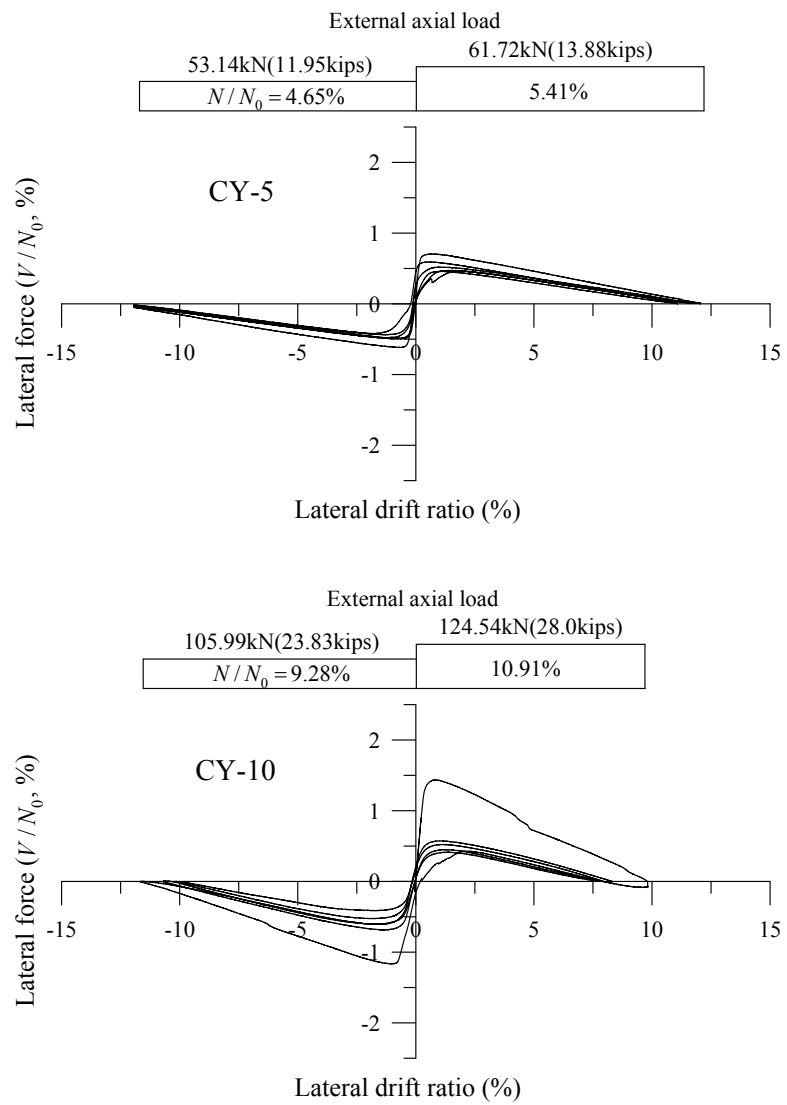


Fig. 9.68 Quasi-static cyclic test of rocking columns
(Roh, 2007; Roh and Reinhorn, 2008)

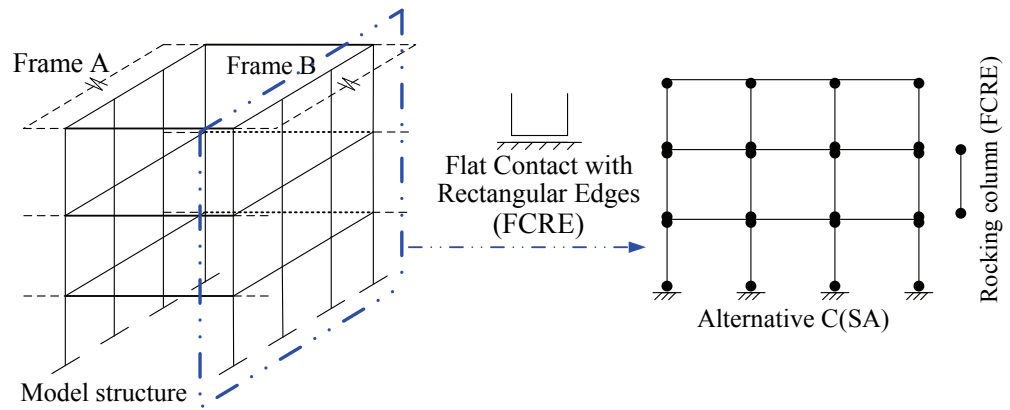


Fig. 9.69 Model structure (Bracci et al., 1992) and alternative for weakening

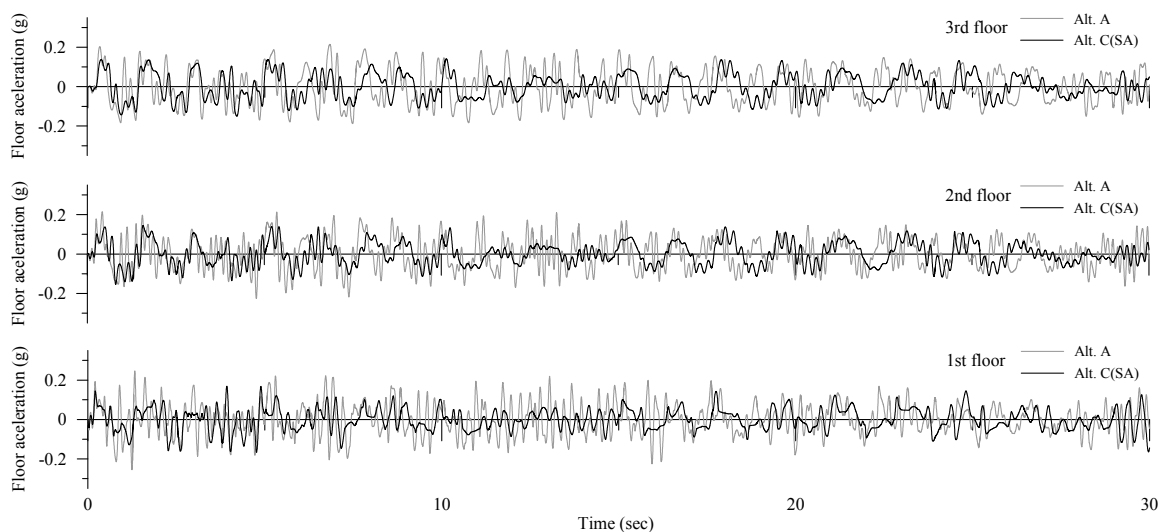


Fig. 9.70 Response histories of floor acceleration in conventional and weakened structures (White noise 0.3g)

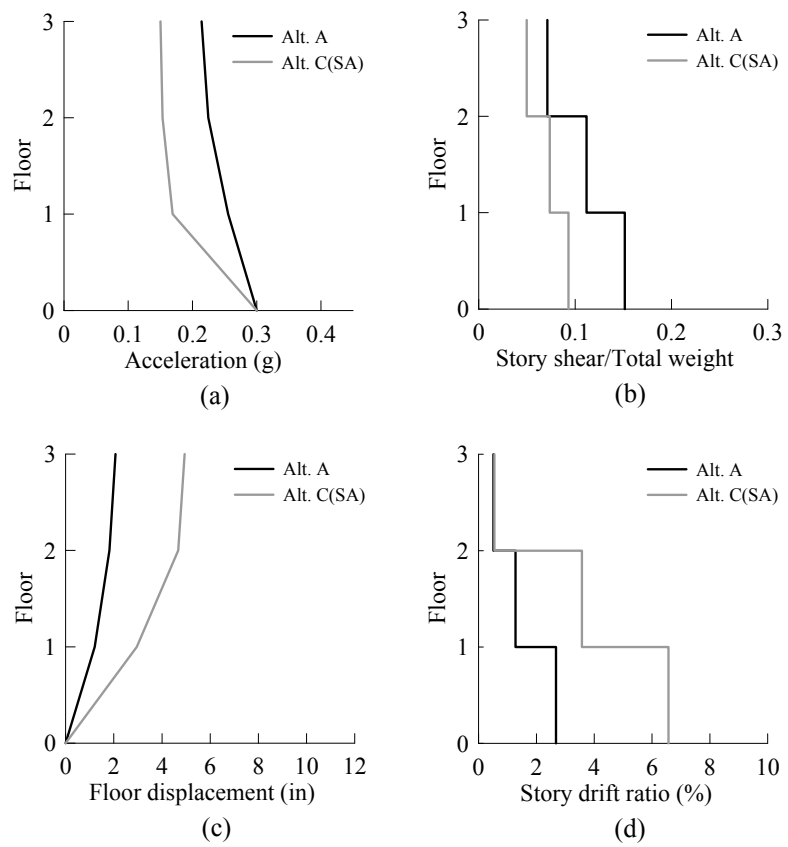


Fig. 9.71 Peak response of conventional and alternative structures: (a) story acceleration; (b) story shear; (c) floor displacement; and (d) story drift

9.13 Remarks and Conclusions

The case studies presented in this Section are only meant to show a representative sample of IDARC capabilities. The task of modeling different structures varies from case to case, depending upon the degree of complexity in structural configuration and member connections. While IDARC must still be regarded as a special-purpose program, it can be used with generality in analysis of structures ranging from buildings to bridges and partial subassemblies used in laboratory testing.

The input parameters to the program are obtained directly from engineering drawings or from separate computations of member properties. The only exceptions are the input of hysteretic parameters and the assigned viscous damping analysis. The case studies presented here cover a range of different structures from single components to scaled model frame buildings to full scale existing structures. They also include well-detailed ductile joints to gravity-load-designed non-ductile connections. The parameters used here can serve as a reference for the choice of appropriate parameters. It is recommended to use data from component test when available, either by actual testing or from the literature of past testing of similar configurations and details.

The choice of hysteretic parameters is critical only in the prediction of local failures at a beam-column interface. For systems with a large numbers of elements, the overall response is less sensitive to local behavior. Consequently, the prediction of global damage states is more reliable for single components, such as single bridge piers, and structures where the damage is more evenly distributed.

SECTION 10

CONCLUSIONS AND RECOMMENDATIONS

10.1 Conclusions

The present report summarizes the theory, developments, and capabilities of IDARC Ver.7.0 for the inelastic damage analysis of structures.

Significant changes and improvements of former version 4.0 are summarized below.

- a) Viscoelastic, friction and hysteretic damper elements. The three main types of supplemental damper elements were added to the new release of the program. Viscoelastic damper elements can be modeled using a Kelvin or a Maxwell model, depending on the specific characteristics of the damper used. Friction and hysteretic dampers are modeled using the Bouc-Wen smooth hysteretic model. All damper models are capable of capturing the response during dynamic, quasi-static and pushover analysis.
- b) Infill panel elements. Contribution of infill panel elements to the lateral load resistance of the structure was added. The hysteretic response is captured using a smooth hysteretic model that accounts for stiffness degradation, strength deterioration, and pinching of the hysteretic loops. A large variety of infill panel elements can be modeled with changes in the control parameters of the hysteretic model. Formulas to internally calculate the response parameters of masonry infill panels are available in the program.
- c) Spread plasticity and yield penetration. The spread plasticity model was

reformulated to include the effects of shear distortions with enhanced numerical precision. The new formulation can accommodate shear or flexural failure conditions. Yield penetration rules were introduced to track the variation of the plastic length zones.

- d) New damage indices. Three damage indices can now be calculated in the program: the Park & Ang damage model, the fatigue based damage index, and an overall measure of the lateral stiffness loss. The first two damage models can provide damage estimates for structural elements, stories (subassemblies), or the overall buildings response.
- e) Hysteresis modules. New set of routines were introduced to model different hysteretic responses, including a three branch steel model, and a bilinear model. The structure of the program was modified to facilitate the addition of new hysteretic routines that can be developed in the future, or by other researchers.
- f) New pushover options. A number of different options for the pushover analysis were added to the program: displacement control, user defined force control distribution, a generalized power distribution, and a modal adaptive lateral force distribution. These distributions allow for a more realistic force distribution to be used during pushover analysis.
- g) Response snapshots during analysis. The user can now request response snapshots during the analysis. Response snapshots provide the user with displacement profile, element stress ratios, collapse states, damage index states, and dynamic characteristics (eigenvalues and eigenvectors) of the building during the analysis.
- h) Proportional damping options. In the new version of IDARC the damping matrix

can be specified to be mass proportional, stiffness proportional, or Rayleigh proportional. Proportionality coefficients are calculated internally by the program using the first mode, or the first two modes in the case of Rayleigh damping.

- i) Reprogrammed for improved efficiency. Most of the solution routines, including the eigenvalue routine, the shear calculation, the spread plasticity and yield penetration routines, and the matrix condensation routines were revised and reprogrammed to improve computational efficiency in the analysis. The program can readily be executed in a personal computer.
- j) New case studies for program validation. Verification examples have been included to highlight the program capabilities and features, as well as to validate whenever possible numerical models with experimental results. The case studies will help the new user of the program to understand IDARC capabilities and input formats.

Significant changes and improvements were made in subsequent versions 4.5 to 5.5 and summarized below.

- a) Concentrated plasticity models.
- b) Uniform flexibility distribution based on spread plasticity model.
- c) New Hysteretic modules for vertex oriented model.
- d) New Hysteretic modules for smooth hysteretic model.

Significant changes and improvements were made in subsequent versions 6.0 to 7.0 and are summarized below.

- a) New deep beam and column elements. The deep elements were developed by

adding shear stiffness and hysteretic effect into the conventional beam and column elements. This development can be used to simulate a perforated shear wall.

- b) New rocking column model. Through cutting top and bottom faces of conventional column or fabricating pre-cast column, the rocking column can be achieved. The rocking column provides lateral resisting depending on the shapes of end faces and edges.
- c) New nonlinear elastic-cyclic model. When structural element returns to the original position without loosing strength and stiffness capacities even after its plastic behavior, the nonlinear elastic-cyclic model (NECM) is used to simulate the structural element behavior.
- d) White-noise ground motion

In the new version, the user can define and generate a random white noise excitation for both horizontal and vertical motions to determine extreme responses.

- e) New case studies for program validation. Four case studies have been introduced: i) verification example of deep elements and ii) use of rocking columns characterized with nonlinear elastic-cyclic behavior for weakened structure.
- f) A mail user group for the program is available for questions, suggestions or comments related to the program:

Email: reinhorn@buffalo.edu

Some minor errors from the previous versions were fixed such as the sign

convention of brace damper, the multi-infill panel model, and the vertical ground motion interaction, and the axial load consideration in P-delta effects.

A web site in the internet has been created where news, updates, comments and current developments will be posted:

<http://civil.eng.buffalo.edu/idarc/>

10.2 Further Development Recommendations

The following is a list of recommendations for further developments of the program:

- Generate automatically the shear envelope for deep beam and column elements.
- Include damage indices and final failure state in the snapshot control algorithms even though structures seem physically collapsed (without completing analysis).
- Include axial, shear, and moment interactions in the element capacity.
- Develop new flexibility formulation, if necessary, incorporating the yielding moment for the yield penetration length and the hysteretic rules.

SECTION 11

REFERENCES

- Al-Haddad, M. S. and Wight, J. K., (1986). "Feasibility and consequences of moving beam plastic hinging zones for earthquake design of R/C buildings" Report No. UMCE 86-1, Department of Civil Engineering, The University of Michigan, Ann Arbor
- Allahabadi, R. and Powell, G. H. (1988). "DRAIN-2DX User Guide". Report No. UCB/EERC-88/06. University of California, Berkeley.
- Applied Technology Council (1995), "Guidelines and Commentary for the Seismic Rehabilitation of Buildings," 3 Volumes, ATC-33.02, 50% Submittal, Second Draft, Federal Emergency Management Agency.
- Baber, T. T., and Noori, M. N. (1985), "Random Vibration of Degrading Pinching Systems," Journal of Engineering Mechanics, 111(8), 1010-1026.
- Baber T. T., and Wen, Y. K. (1981), "Random Vibration of Hysteretic Degrading Systems," Journal of Engineering Mechanics, 107(6), 1069-1089.
- Bracci, J. M. (1992), "Experimental and Analytical Study of Seismic Damage and Retrofit of Lightly Reinforced Concrete Structures in Low Seismicity Zones", Ph.D. Dissertation, Department of Civil Engineering, University at Buffalo, The State University of New York.
- Bouc, R. (1967), "Forced Vibration of Mechanical Systems with Hysteresis," Proceedings of the 4th Conference on Non-linear Oscillations, Prague.
- Bracci, J. M., Reinhorn, A. M., and Mander, J. B. (1992), "Evaluation of Seismic Retrofit

of Reinforced Concrete Frame Structures: Part III-Experimental Performance and Analytical Study of Retrofitted Structural Model Structure," Technical Report NCEER-92-0031, National Center for Earthquake Engineering Research, University at Buffalo, The State University of New York.

Casciati, F. (1989), "Stochastic Dynamics of Hysteretic Media," Structural Safety, Vol. 6, pp. 259-269.

Cecen, H. (1979), "Response of Ten Story Reinforced Concrete Model Frames to Simulated Earthquakes", Ph.D. Dissertation, Department of Civil Engineering, University of Illinois, Urbana.

Cheok, G. S. and Stone, W. C. (1990), "Behavior of 1/6 Scale Model Bridge Columns Subjected to Inelastic Cyclic Loading", ACI Structural Journal, 87(6), 630-638.

Chung, Y. S., Meyer, C. and Shinozuka, M. (1988), "SARCF User's Guide: Seismic Analysis of Reinforced Concrete Frames", Technical Report NCEER-88-0044, University at Buffalo, The State University of New York.

Clough, R. W. and Johnston, S. B., (1966), "Effect of stiffness degradation on earthquake ductility requirements" Proceedings, Japan Earthquake Engineering Symposium, Tokyo, Japan, Oct, 195-198.

Computers and Structures, Inc., (2007), PERFORM3D – Nonlinear Analysis and Performance Assessment for 3D Structures, Version 4.0.3.

Constantinou, M. C., and Symans, M. D. (1992), "Experimental and Analytical Investigation of Seismic Response of Structures with Supplemental Fluid Viscous Dampers," Technical Report NCEER-92-0032, National Center for Earthquake Engineering Research, University at Buffalo, The State University of New York.

DiPasquale, E., and Cakmak, A. S. (1988), "Identification of the Serviceability Limit State and Detection of Seismic Structural Damage," Technical Report NCEER-88-0022, National Center for Earthquake Engineering Research, Princeton University.

El-Attar, A. G. (1991), "A Study of the Seismic Behavior of Lightly Reinforced Concrete Structures", Ph.D. Dissertation, Department of Civil Engineering, Cornell University, Ithaca.

Elnashai A. S., Pinho R., Antoniou S., (2000), INDYAS - A program for inelastic dynamic analysis of structures, ESEE Report # 00-2, Imperial College, London, UK.

Giberson, M.F., (1996), "Two nonlinear beams with definitions of ductility," Journal of the Structural Division, Proceedings, ASCE, 95(2), 137-157.

Gomez, S. R., Chung, Y. S., and Meyer, C. (1990), "SARCF-II User's Guide: Seismic Analysis of Reinforced Concrete Frames," Technical Report NCEER-90-0027, University at Buffalo, The State University of New York.

Gross, J. L. and Kunnath, S. K. (1992), "Application of Inelastic Damage Analysis to Double Deck Highway Structures", Technical Report NISTIR-4857, U.S. Department of Commerce, National Institute of Standards and Technology, Gaithersburg, M. D.

Habibullah, A. (1995), "ETABS v6.0: Three Dimensional Analysis of Building Systems," User's Manual, Computers & Structures Inc.

Kabeyasawa, T., Shiohara, H., Otani, S., and Aoyama, H. (1983), "Analysis of the Full-Scale Seven-Story Reinforced Concrete Test Structure," Journal of the Faculty of Engineering, University of Tokyo, XXXVII(2), 432-478.

Kanaan, A. E. and Powell, G.H. (1973), "DRAIN-2D-A General Purpose Computer

Program for Dynamic Analysis of Inelastic Plane Structures", Reports No. UCB/EERC/73/06 and 73/22. University of California, Berkeley.

Kent, D. C., and Park, R. (1971), "Flexural Members with Confined Concrete", Journal of Structural Division, 97(7), 1969-1990.

Kunnath, S.K. and Reinhorn, A.M. (1994), "Efficient Modeling Scheme for Transient Analysis of Inelastic RC Structures," Microcomputers in Civil Engineering, International Journal of Computer-Aided Civil and Infrastructure Engineering, Vol. 10, 97-110.

Kunnath, S. K., Reinhorn, A. M., and Abel, J. F. (1992a), "A Computational Tool for Seismic Performance of Reinforced Concrete Buildings", Computers and Structures, Pergamon Press, 41(1), 157-173.

Kunnath, S. K., Reinhorn, A. M., and Lobo, R. F. (1992b), "IDARC Version 3.0: A Program for the Inelastic Damage Analysis of Reinforced Concrete Structures," Report No. NCEER-92-0022, National Center for Earthquake Engineering Research, University at Buffalo, The State University of New York.

Kunnath, S. K., Reinhorn, A. M., and Park, Y. J. (1990), "Analytical Modeling of Inelastic Seismic Response of R/C Structures", Journal of Structural Engineering, ASCE, 116(4), 996-1017.

Li, C., and Reinhorn, A. M. (1995), "Experimental and Analytical Investigation of Seismic Retrofit of Structures with Supplemental Damping: Part II-Friction Damping Devices," Report No. NCEER-95-0009, National Center for Earthquake Engineering Research, University at Buffalo, The State University of New York.

Lobo, R. F. (1994), "Inelastic Dynamic Analysis of Reinforced Concrete Structures in Three Dimensions," Ph.D. Dissertation, Department of Civil Engineering, University

at Buffalo, The State University of New York.

Lobo, R. F., Bracci, J. M., Shen, K. L., Reinhorn, A. M., and Soong, T.T. (1993), "Inelastic Response of Reinforced Concrete Structures with Viscoelastic Braces," Technical Report No. NCEER-93-0006, National Center for Earthquake Engineering Research, University at Buffalo, The State University of New York.

Madan, A., Reinhorn, A. M., Mander, J., and Valles, R., (1997), "Modeling of Masonry Infill Panels for Structural Analysis," Journal of Structural Engineering, 123(10), 1295-1302.

Mander, J. B. and Cheng, C-T. (1997). "Seismic resistance of bridge pier based on damage avoidance design." Tech. Rep. No. NCEER-97-0014, National Center for Earthquake Engineering Research, Dept. of Civil, Structural and Environmental Engineering, State University of New York, Buffalo, NY.

Mazzoni, S., McKenna, F., Scott, M. H., and Fenves, G. L., (2008), "Open System for Earthquake Engineering Simulation User Manual version 2.1.0," Pacific Earthquake Engineering Center, University at California, Berkeley, CA.

Mander, J. B., and Nair, B. (1994), "Seismic Resistance of Brick-Infilled Steel Frames with and without Retrofit," TMS Journal, 12(2), 24-37.

Mander, J. B. (1984), "Seismic Design of Bridge Piers", Ph.D. Dissertation, Department of Civil Engineering. University of Canterbury, New Zealand.

Naeim, F., DiJulio, R., Benuska, K., Reinhorn, A. M., and Li, C. (1995), "Evaluation of the Seismic Performance of an 11 Story Steel Moment Frame Building During the 1994 Northridge Earthquake," Report to SAC Joint Venture, SAC Task 3.1, Building No. 6, John A. Martin & Associates, Inc.

Naeim, F., and Reinhorn, A. M. (1995), "Seismic Performance Analysis of a 7 Story

Reinforced Concrete Building,” Report to the Applied Technology Council, Task 12, Subcontract No. 330.1-24-569, John A. Martin & Associates, Inc.

Nagarajaiah, S., Reinhorn, A. M. and Constantinou, M. C., (1989), “Nonlinear Dynamic Analysis of Tree-Dimensional Base Isolated Structures (3D-BASIS),” Technical Report NCEER-89-0019, University at Buffalo, The State University of New York, Buffalo, USA.

Otani, S. (1974), “SAKE: A Computer Program for Inelastic Response of RC Frames Subject to Earthquakes”, Civil Engineering Studies, Technical Report No. SRS 413, University of Illinois, Urbana.

Oughourlian, C. V. and Powell, G. H. (1982), “ANSR-III: General Purpose Computer Program for Nonlinear Structural Analysis,” Report No. UCB/EERC-82/21, Earthquake Engineering Research Center, University of California at Berkeley.

Park, R., and Paulay, T. (1975), “Reinforced Concrete Structures”, John Wiley.

Park, Y. J., Reinhorn, A. M., and Kunnath, S. K. (1986), “IDARC: Inelastic Damage Analysis of Reinforced Concrete Frame - Shear-Wall Structures”, Technical Report NCEER-87-0008, University at Buffalo, The State University of New York.

Park, Y. J., Ang, A. H-S., and Wen, Y.K. (1987), “Damage-Limiting Aseismic Design of Buildings,” Earthquake Spectra, 3(1), 1-26.

Park, Y. J., Ang, A. H.-S., and Wen, Y. K. (1984), “Seismic Damage Analysis and Damage-Limiting design of R/C Buildings”, Civil Engineering Studies, Technical Report No. SRS 516, University of Illinois, Urbana.

Paulay, T., and Priestley, M. J. N. (1992), “Seismic Design of Reinforced Concrete and Masonry Buildings”, John Wiley.

Prakash, V., Powell, G. H., and Filippou, F. C. (1992), "DRAIN-2DX: Base Program User Guide," Report No. UCB/SEMM-92/29, Department of Civil Engineering, University of California at Berkeley, December.

Prakash, V., Powell, G., H., Campbell, S. D., (1994), "DRAIN-3DX: Base Program Description and User Guide: Version 1.10," UCB/SEMM-1994/07, Dept. of Civil Engineering, University of California, Berkeley, CA.

Press, W. H., Teukolsky, S. A., Vetterling, W. T. and Flannery, B. P., (1992), "Numerical Recipes in Fortran, Cambridge University Press, New York.

Priestley, M. J. N., Seible, F., and Calvi, G. M. (1996). "Seismic design and retrofit of bridges." John Wiley & Sons, New York.

Reichman, Y. and Reinhorn, A. M., (1995), "Extending Seismic Life Span of Bridges," Structural Engineering Review – Progress in Bridge Engineering, Pergamon Press, 7(3), 207-218.

Reinhorn, A. M., (1996), "Introduction to Dynamic and Static Inelastic Analysis Techniques." Proceedings of Annual Meeting – Los Angels Tall Buildings Structural Design Council, May 10, 1996, (Keynote Speaker).

Reinhorn, A. M., (1997), "Inelastic Analysis Techniques in Evaluations," In: Fajfar P, Krawinkler H, editors. Seismic design methodologies for next generation of codes. Rotterdam: AA Balkema; 1997. p. 277–87.

Reinhorn, A. M., Li, C., and Constantinou, M. C. (1995a), "Experimental and Analytical Investigation of Seismic Retrofit of Structures with Supplemental Damping: Part I: Fluid Viscous Damping Devices," Report No. NCEER-95-0001, National Center for Earthquake Engineering Research, University at Buffalo, The State University of New York.

Reinhorn, A. M., and Li, C. (1995b), "Experimental and Analytical Investigation of Seismic Retrofit of Structures with Supplemental Damping: Part III-Viscous Damping Walls," Report No. NCEER-95-0013, National Center for Earthquake Engineering Research, University at Buffalo, The State University of New York.

Reinhorn, A. M., Madan, A., Valles, R. E., Reichman, Y., and Mander, J. B. (1995c), "Modeling of Masonry Infill Panels for Analysis of Frame Structures," Report No. NCEER-95-0018, National Center for Earthquake Engineering Research, University at Buffalo, The State University of New York.

Reinhorn, A. M., Nagarajaiah, S., Constantinou, M. C., Tsopelas, P., and Li, R. (1994), "3D-BASIS-TABS: Version 2.0: Computer Program for Nonlinear Dynamic Analysis of Three Dimensional Base Isolated Structures," Technical Report NCEER-94-0018, National Center for Earthquake Engineering Research, University at Buffalo, The State University of New York.

Richart, F. E., Brandtzaeg, A., and Brown, R. L. (1928), "A Study of the Failure of Concrete Under Combined Compressive Stresses", University of Illinois Engineering Experimental Station, Bulletin No. 185.

Roh, H. (2007), "Seismic Behavior of Structures using Rocking Columns and Viscous Dampers," Ph.D. Dissertation, Dept. of Civil, Structural and Environmental Engineering, University at Buffalo, The State University of New York.

Roh, H. and Reinhorn, A. M. (2008), "Dynamic Response of Weakened Structures Using Rocking Columns," Proceedings of 14th World Conference on Earthquake Engineering, October 12-17, 2008, Beijing, China.

Rosenbrock, H. H. (1964), "Some General Implicit Processes for the Numerical Solution of Differential Equations," Computer Journal, 18, 50-64.

Saneinejad, A. and Hobbs, B. (1995), "Inelastic Design of Infilled Frames," Journal of Structural Engineering, 121(4), 634-650.

Shen, K. L. (1994) "Viscoelastic Dampers: Theory, Experimental and Applications in Earthquake Engineering," Ph.D. Dissertation, Department of Civil Engineering, University at Buffalo, The State University of New York.

Sivaselvan, M. V. and Reinhorn, A. M. (1999). "Hysteretic models for cyclic behavior of deteriorating inelastic structures." Tech. Rep. No. NCEER-99-0018, National Center for Earthquake Engineering Research, Dept. of Civil, Structural and Environmental Engineering, University at Buffalo, The State University of New York, Buffalo, NY.

Sivaselvan M., and Reinhorn, A.M. (2000), "Hysteretic Models for Deteriorating Inelastic Structures", ASCE/Journal of Engineering Mechanics, 126(6), 633-640, with discussion by Wang and Foliente and closure in 127(11)

Somerville, P. (1995), "Site-Specific Northridge Response Spectra for ATC-33 Task 12, Subcontract No. 330.1-24-569.

Soong, T. T. and Dargush, G. F., (1997), Passive Energy Dissipation Systems in Structural Engineering, John Wiley & Sons, New York.

Stone, W. C., and Cheok, G. C. (1989), "Inelastic Behavior of Full-Scale Bridge Columns Subjected to Cyclic Loading", NIST Building Science Series 166, National Institute of Standards and Technology, Gaithersburg, M. D.

Valles, R. E., Reinhorn, A.M., and Kunzath, S.K., and Madan, A. (1996), "IDARC2D version 4.0: A computer program for the inelastic damage analysis of buildings," Technical Report NCEER-96-0010, National Center for Earthquake Engineering Research, University at Buffalo, The State University of New York.

Wen, Y. K., (1976), "Method of Random Vibration of Hysteretic Systems," Journal of Engineering Mechanics Division, ASCE, 102(2), 249-263.

Wight, J. K. (Editor) (1985), "Earthquake Effects on Reinforced Concrete Structures", U.S.-Japan Research, ACI Special Publication SP-84, American Concrete Institute, Detroit.

Wilson, E. L. (1995), "SADSAP: Static and Dynamic Structural Analysis Programs," Version 2.04, Structural Analysis Programs Inc., El Cerrito, CA.

Wilson, E. L., and Habibullah, A. (1987), "Static and Dynamic Analysis Multistory Buildings, Including P-Delta Effects", Earthquake Spectra, 3(2), 289-298.

Yunfei, H., Yufeng, C., Chang, S., and Bainian, H. (1986), "The Experimental Study of a Two-Bay Three Story Reinforced Concrete Frame Under Cyclic Loading", Proceedings of the 8th Symposium on Earthquake Engineering, Roorkee, India.

APPENDIX A

USER'S GUIDE

INPUT FORMAT

A free format is used to read all input data. Hence, conventional delimiters (commas, blanks) may be used to separate data items. Standard FORTRAN variable format is used to distinguish integers and floating point numbers. Input data must, therefore, conform to the specified variable type.

- Notes:*
1. Provision is made for a line of text between each set of data items. Refer to the sample data files accompanying this Manual.
 2. No blank lines are to be input.
 3. A zero input will result in program default values, where applicable.

SET A: GENERAL INFORMATION

- Title of Problem:

TITLE

Description: **TITLE:** Alpha-numeric title, up to 80 characters.

- Control Data (See Figure A-1):

USER_TEXT

NSO, NFR, NCON, NSTL, NMSR, NPDEL, IFLEX, IFLEXDIST, IPC

Description: **USER_TEXT:** Reference information, up to 80 characters of text.

NSO: Number of stories.

NFR: Number of typical (non-identical) frames

NCON: Number of different concrete material properties sets.

NSTL: Number of different steel reinforcement properties sets.

NMSR: Number of different masonry material properties sets.

NPDEL: 0 to ignore P-Delta effects, or
1 to include P-Delta effects.

IFLEX: 0 for Spread Plasticity

1 for Concentrated Plasticity

IFLEXDIST 0 for linear flexibility distribution

1 for uniform flexibility distribution

IPC: 0 for Unix operating system, or
1 for DOS/WINDOWS operating system.

Notes: For steel structures no information about material is required.

A structure must be decomposed into a series of parallel frames. Input is required only for non-identical frames, denoted here by the integer variable

NFR. The number of duplicates of each typical frame is specified later in this DATA SET. The entire group of frames can be defined in the IDARC L-I-J nodal locater system. This concept is shown graphically in Figure A-1.

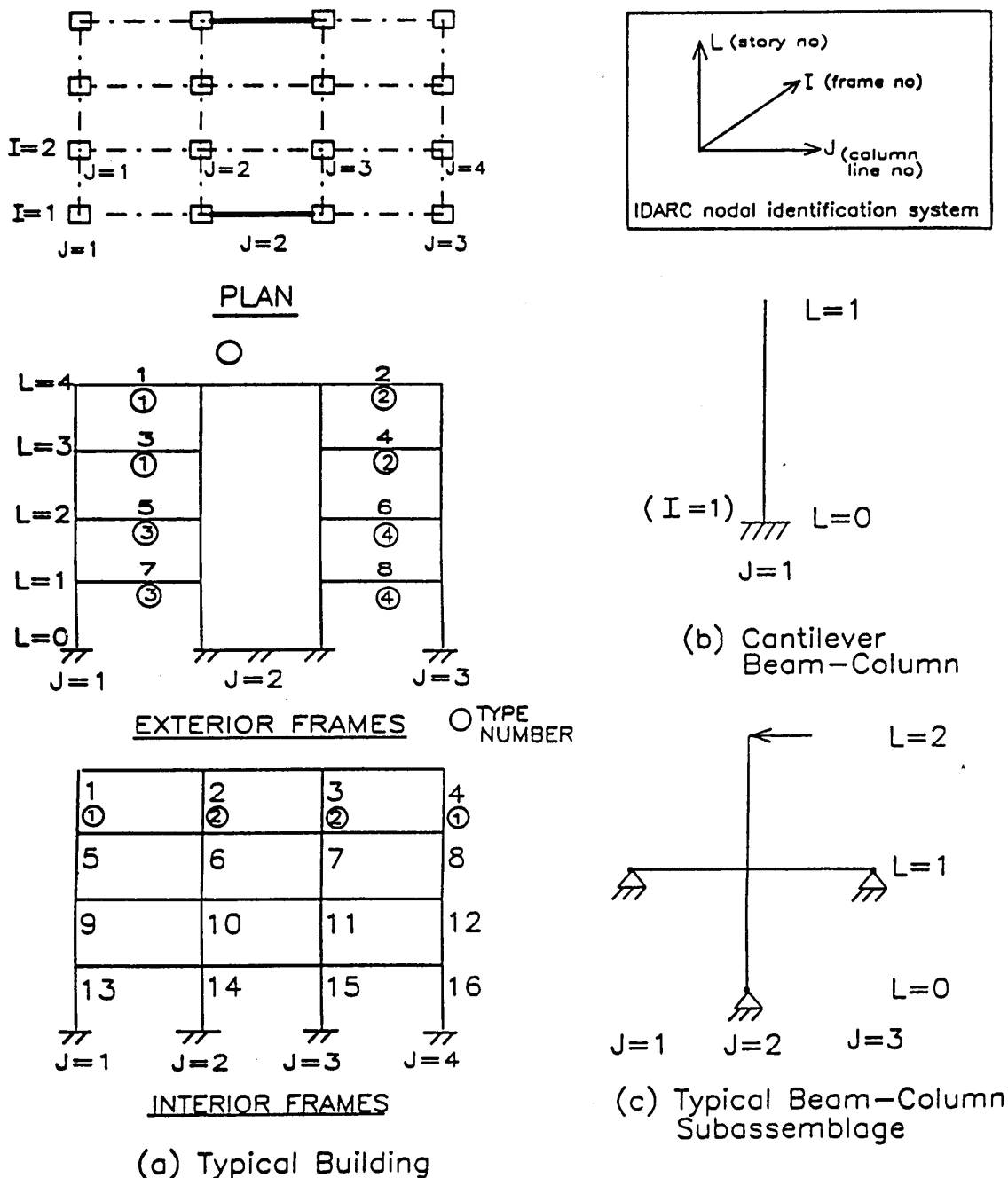


Fig. A-1 Frame Discretization and Nodal Identification

Three examples of different frame definitions are shown. In Figure A-1a, the four-story building made up of a total of four frames is assumed to have two pairs of identical frames, hence, only two of them need be input in IDARC (NFR=2). The cantilever beam/column shown in Figure A-1b is defined as a single-story structure with one column line. Likewise, the subassemblage shown in Figure 1c is defined as a 2-story structure with three column lines. The number of concrete and steel properties refer to the number of stress-strain envelopes to be input in Set B and Set C respectively.

SET A1: ELEMENT TYPES

- Control Data (See Figure A-1):

USER_TEXT

MCOL, MBEM, MWAL, MEDG, MTRN, MSPR, MBRV, MBRF, MBRH, MIW

Description: **USER_TEXT:** Reference information, up to 80 characters of text.

MCOL: No. of column types.

MBEM: No. of beam types.

MWAL: No. of shear wall types.

MEDG: No. of edge column types.

MTRN: No. of transverse beam types.

MSPR: No. of rotational spring types.

MBRV: No. of visco-elastic brace types.

MBRF: No. of friction brace types.

MBRH: No. of hysteretic brace types.

MIW: No. of infill panel types.

Notes: Elements are grouped into identical sets based on cross-section data and initial conditions such as axial loads. For example, in the exterior frame shown in Figure A-1a, there are 8 columns. Typically, the exterior columns at each level will be identical, hence, only 4 column types need to be defined. The interior frame, assuming identical interior and exterior columns in each floor, will require only 8 column types to define all 16 elements, i.e., 2 types per each level as shown in the Figure.

SET A2: ELEMENT DATA

- Control Data:

USER_TEXT

NCOL, NBEM, NWAL, NEDG, NTRN, NSPR, NMR, NBR, NIW

Description: **USER_TEXT:** Reference information, up to 80 characters of text.

NCOL: No. of columns.

NBEM: No. of beams.

NWAL: No. of shear walls.

NEDG: No. of edge columns.

NTRN:	No. of transverse beams.
NSPR:	No. of rotational springs.
NMR:	No. of moment releases.
NBR:	No. of braces (VE + friction + hysteretic).
NIW:	No. of infill panels.

Notes: NMR is used to specify moment releases (hinge locations) at member ends. Releasing a moment at a member end results in a hinge condition at that end thereby disallowing moments to develop at the section.

SET A3: SYSTEM OF UNITS

- Control Flag:

USER_TEXT
IU

Description: **USER_TEXT:** Reference information, up to 80 characters of text.

IU: System of units
1 for inch, kips
2 for mm, kN

DEFAULT SYSTEM OF UNITS: *inch, kip*

A zero input for IU will result in the use of *inch and kip units*.

SET A4: FLOOR ELEVATIONS

- Control Data (See Figure A-2):

USER_TEXT
HIGT(1), HIGT(2), ..., HIGT(NSO)

Description: **USER_TEXT:** Reference information, up to 80 characters of text.

HIGT(i): Elevation of story “i” from the base,
beginning with the first floor level.

SET A5: DESCRIPTION OF IDENTICAL FRAMES

- Control Data:

USER_TEXT

NDUP(1), NDUP(2), ..., NDUP(NFR)

Description: **USER_TEXT:** Reference information, up to 80 characters of text.

NDUP(i): List with the number of duplicate frames of typical (non-identical) frame “i”.

Notes: In the sample structure shown in Figure A-1, there are four frames. However, the two interior frames are identical as are the exterior frames. In this case, NFR=2, and NDUP(1) = NDUP(2) = 2. If there is no identical frame, NDUP=1.

SET A6: PLAN CONFIGURATION

- Control Data:

USER_TEXT

NVLN(1), NVLN(2), ..., NVLN(NFR)

Description: **USER_TEXT**: Reference information, up to 80 characters of text.

NVLN(i): Number of column lines (or J-locater points) in frame “i”.

Notes: *A set of NVLN points for each frame should define completely the column lines necessary to specify every vertical element in that frame. If a beam element is subdivided into two or more segments, then the number of column lines specified must include these internal beam nodes as well.*

SET A7: NODAL WEIGHTS

- Control Data (See Figure A-2):

USER_TEXT

LEVEL, IFR(1), WVT(1), WVT(2), ..., WVT(NVLN(1))

IFR(2), WVT(1), WVT(2), ..., WVT(NVLN(2))

.....repeat for NFR frames

....repeat for NSO levels (in ascending or descending order)

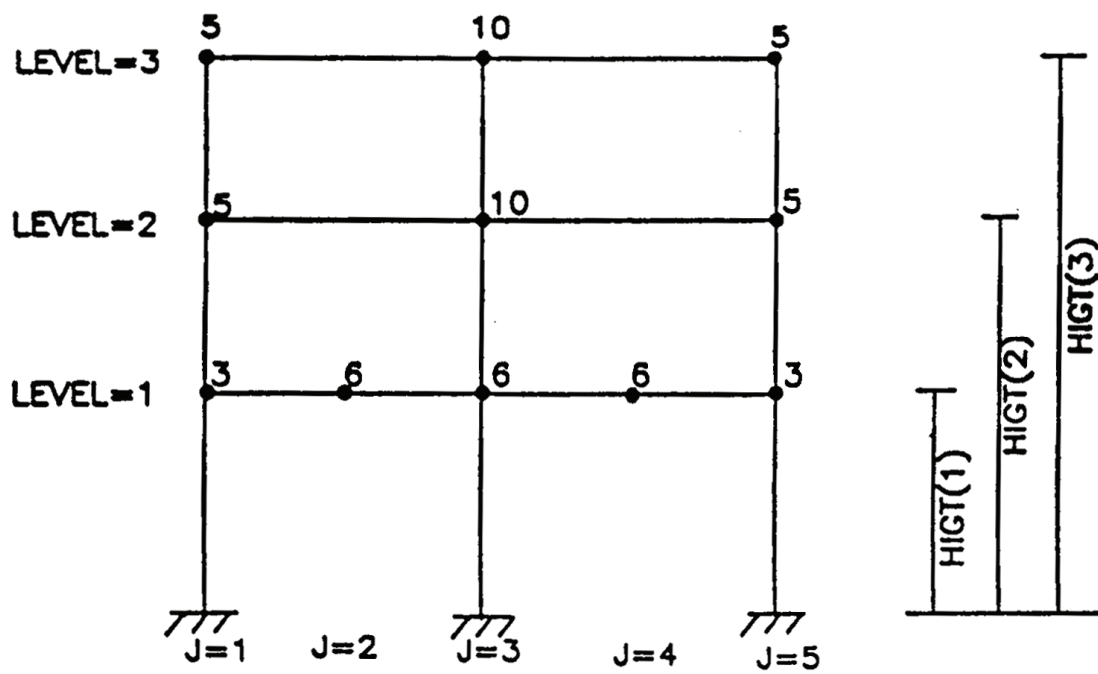
Description: **USER_TEXT**: Reference information, up to 80 characters of text.

LEVEL: Story level number.

IFR(J): Frame number.

WVT(K): Nodal weight.

Notes: 1. *Nodal weights in force units (kN) are used internally for the story mass computation, and they are not-cumulative quantities (from tributary area only). Nodal weights are not used to specify gravity or vertical loads.*
2. *Vertical loads need to be declared in SET M1, if necessary.*
3. *Nodal weights may be input in ascending or descending story level.*
4. *In ordinary analyses, reduced weight is used.*



FRAME #1
(numbers shown at nodes = nodal weights)

INPUT DATA:

1, 1, 3.0, 6.0, 6.0, 6.0, 3.0
2, 1, 5.0, 0.0, 10.0, 0.0, 5.0
3, 1, 5.0, 0.0, 10.0, 0.0, 5.0

Fig. A-2 Floor Heights and Nodal Weights

SET B: MATERIAL PROPERTIES SETS

- Envelope Generation Option:

USER_TEXT

IUSER

<i>Description:</i>	USER_TEXT: Reference information, up to 80 characters of text.
IUSER:	Code for specification of user properties: 0, produces IDARC generated envelopes for at least one element. 1, requires complete moment-curvature envelope data to be provided by user.

Note: If IUSER = 1 go directly to the SET C.

SET B1: CONCRETE PROPERTIES SETS (SEE FIGURE A-3)

(SKIP THIS INPUT IF IUSER=1 OR NCON=0)

- Reference text:

USER_TEXT

<i>Description:</i>	USER_TEXT: Reference information, up to 80 characters of text.
---------------------	---

- Characteristics of concrete stress-strain curve (one line for each of the NCON concrete types):

IM, FC, EC, EPS0, FT, EPSU, ZF

<i>Description:</i>	IM: Concrete property type (set) number.
	FC: Unconfined compressive strength.
	EC: Initial Young's Modulus of concrete.
	EPS0: Strain at max. strength of concrete (%).
	FT: Stress at tension cracking.
	EPSU: Ultimate strain in compression (%).
	ZF: Parameter defining slope of falling branch.

DEFAULT VALUES (if a zero was specified as data input):

$$EC = 57 * \sqrt{FC} * 1000 \text{ ksi} ; \quad EPS0 = 0.2\% ; \quad FT = 0.12 * FC ;$$

EPSU and ZF are derived from Eq. 3.25 and depends on section data.

SET B2: REINFORCEMENT PROPERTIES SETS (SEE FIGURE A-4)

(SKIP THIS INPUT IF IUSER=1 OR NSTL=0)

- Reference Text:

USER_TEXT

<i>Description:</i>	USER_TEXT: Reference information, up to 80 characters of text.
---------------------	---

- Characteristics of steel stress-strain curve (one line for each of the NSTL steel types):

IM, FS, FSU, ES, ESH, EPSH

<i>Description:</i>	IM:	Steel type (set) number.
	FS:	Yield strength.
	FSU:	Ultimate strength.
	ES:	Modulus of elasticity.
	ESH:	Modulus of strain hardening.
	EPSH:	Strain at start of hardening (%).

DEFAULT VALUES (if a zero was specified as data input):

$$FSU = 1.4 * FS ; \quad ES = 29,000 \text{ ksi} ; \quad ESH = (ES / 60) \text{ ksi} ; \quad EPSH = 3.0\%$$

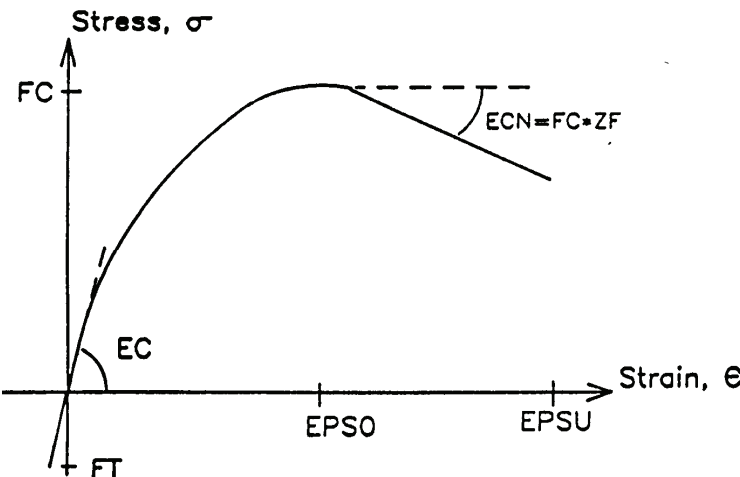


Fig. A-3 Stress Curve for Unconfined Concrete

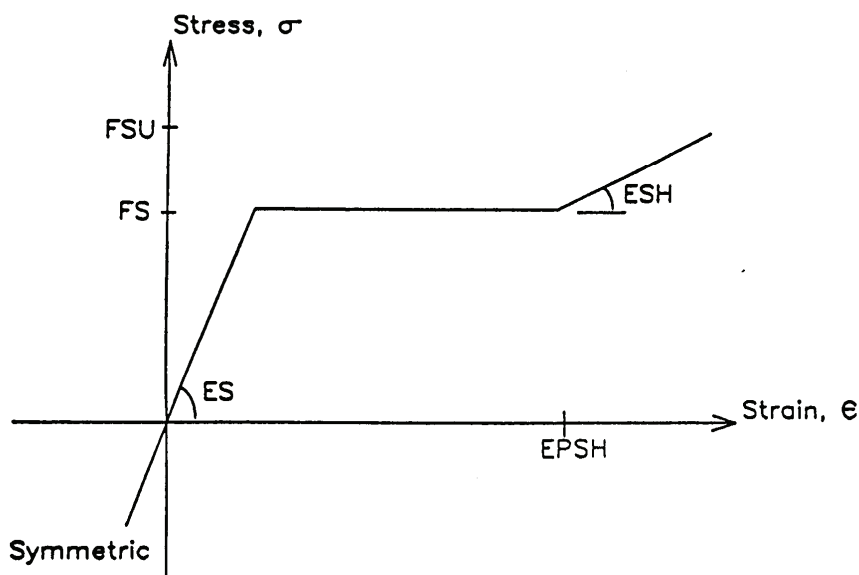


Fig. A-4 Stress Curve for Reinforcing Bars

SET B3: MASONRY INFILL PROPERTIES SETS

(SKIP THIS SECTION IF IUSER=1 OR NMSR=0)

- Reference text:

USER_TEXT

Description: **USER_TEXT:** Reference information, up to 80 characters of text.

- Characteristics of masonry (one line for each of the NMSR masonry types):

IM, FM, FMCR, EPSM, VM, SIGMM, CFM

Description: **IM:** Masonry type number.
FM: Prism strength of masonry.
FMCR: Cracking modulus of masonry
EPSM: Strain corresponding to prism strength (%).
VM: Basic shear strength of masonry bed joints.
SIGMM: Maximum allowable shear strength
CFM: Coefficient of friction of frame-infill interface.

DEFAULT VALUES (if a zero was specified as data input):

EPSM = 0.2% ; FMCR = 0.05*FM; VM = 0.04 ksi; SIGMM = 0.05*FM;
CFM=0.3

HSR:	Slip Length Parameter, R_s
HSS:	Slip Sharpness Parameter, σ (Default: 100 – No Slip)
HSM:	Parameter for Mean Moment Level of Slip, λ
NGAP:	Exponent of Gap Closing Spring, N_{gap}
PHIGAP:	Gap Closing Curvature Parameter, ϕ_{gap} (Default: 1000 – No Gap)
STIFFGAP:	Gap Closing Stiffness Coefficient, κ

Notes: Hysteretic behavior is specified at both ends of each member. Access to experimental results of the cyclic force-deformation characteristics of components typical to the structure being analyzed provides the best means of specifying the above degrading parameters. Table A-1 and Figure A-5 provide a number of qualitative insights into modeling of the hysteretic parameters. The loops shown in Figure A-5 are only meant to show the relative effects of changing the parameters. The general meaning of the parameters can be characterized as follows: An increase in HC retards the amount of stiffness degradation; an increase in HBD,HBE accelerates the strength deterioration; and an increase in HS reduces the amount of slip. (Also refer to Section 3.3 of this report)

Table A-1. Typical Range of Values for Hysteretic Parameters

Parameter	Meaning	Value	Effect
HC	Stiffness degrading parameter	4.0	Severe degrading
		10.0	Moderate degrading
		15.0	Mild degrading
		200.0	No degrading (Default)
HBD	Strength degrading parameter (ductility-based)	0.60	Severe degrading
		0.30	Moderate degrading
		0.15	Mild degrading
		0.01	No degrading (Default)
HBE	Strength degrading parameter (energy-controlled)	0.60	Severe deteriorating
		0.15	Moderate deteriorating
		0.08	Mild deteriorating
		0.01	No deteriorating (Default)
HS	Slip or Crack-closing parameter	0.05	Severe pinched loops
		0.25	Moderate pinching
		0.40	Mild pinching
		1.00	No pinching (Default)

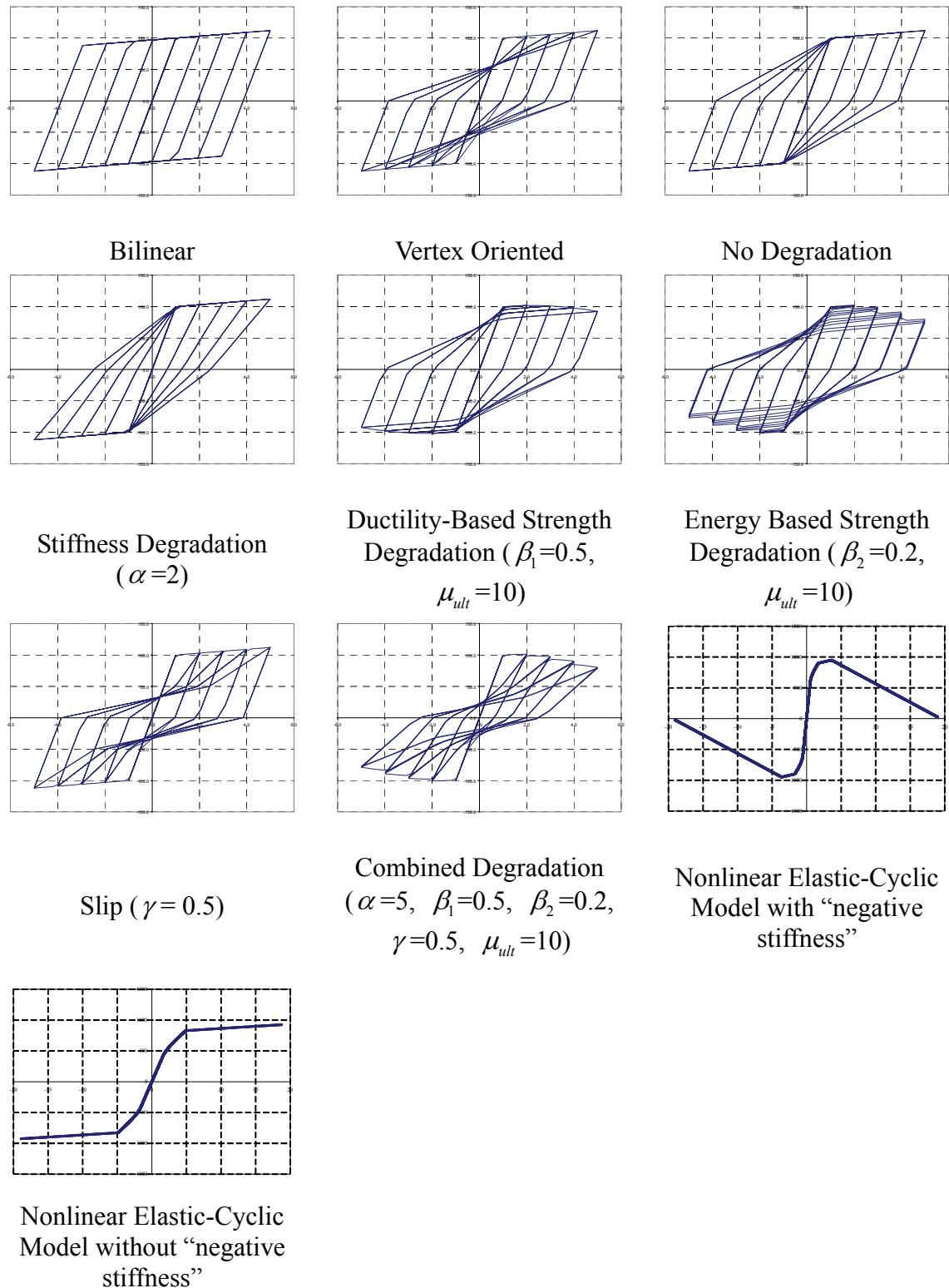


Fig. A-5 (a) Qualitative View of Effects of Degrading Parameters on Hysteretic Behavior

– Multilinear Model

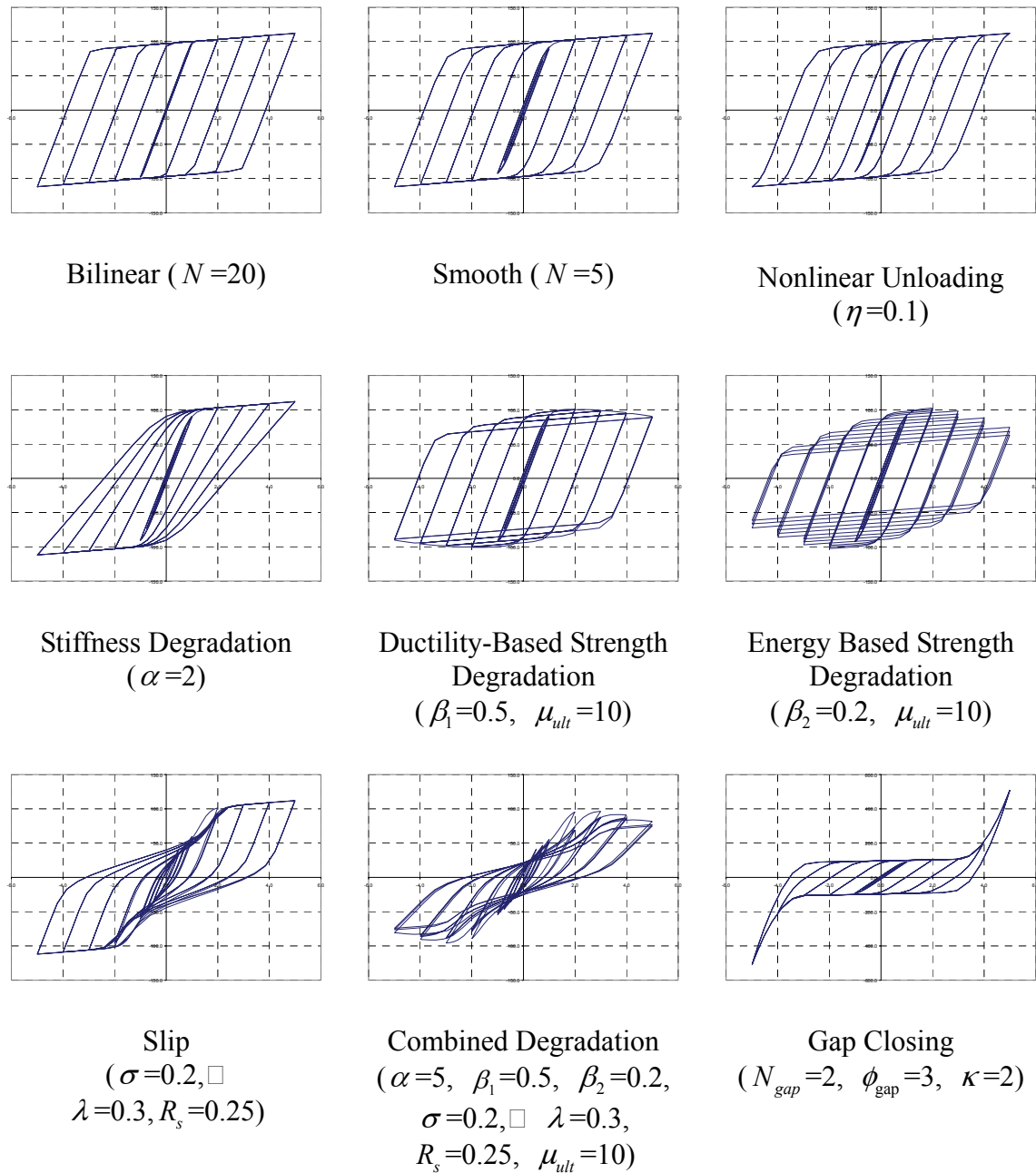


Fig. A-5 (b) Qualitative View of Effects of Degrading Parameters on Hysteretic Behavior
– Smooth Model

SET D: COLUMN PROPERTIES

(SKIP THIS INPUT IF THE STRUCTURE HAS NO COLUMNS)

- Control Data:

USER_TEXT

IUCOL

<i>Description:</i>	USER_TEXT: Reference information, up to 80 characters of text.
	IUCOL: Type of column input: 0;Section dimensions and reinf. to be specified, 1;Moment (Shear)-curvature (Strain) envelope to be specified

IF IUCOL = 1, GO TO SET D3

- Reference Text:

USER_TEXT

Description: **USER_TEXT:** Reference information, up to 80 characters of text.

- For each column type (MCOL), input the following:

ICTYPE

Data from **SET D1(a) (ICTYPE=1)**, **SET D1(b) (ICTYPE=2)**
or **SET D2 (ICTYPE=3)**

<i>Description:</i>	ICTYPE: Type of column: 1; rectangular regular 2; rectangular deep beam-column [User Input Properties(SET D3) is more preferable] 3; circular
---------------------	--

READ DATA FROM SET D1(a), D1(b) OR D2 (See below)

GO TO SET E WHEN FINISHED READING ALL COLUMN TYPES.

SET D1: ICTYPE=1; Rectangular Regular Column Data Set (SEE FIGURE A-6)

- General data:

KC, IMC, IMS, AN, AMLC, RAMC1, RAMC2

- Bottom section:

KHYSC, D, B, DC, AT, HBD, HBS, CEF

- Top section:

If KHYSC for bottom section is input with negative sign, section is symmetric, hence, do not input top section data, otherwise repeat as above, starting with KHYSC.

Description: **KC:** Column type set number.

IMC: Concrete type number.

IMS: Steel type number.

AN: Axial load.

AMLC: Center-to-center column height.

RAMC1: Rigid zone length at bottom.

RAMC2: Rigid zone length at top.

KHYSC:	Hysteretic rule number (may be negative)*.
D:	Depth of column.
B:	Width of column.
DC:	Distance from centroid of reinforcement to face of column.
AT:	Area of reinforcement on one face.
HBD:	Hoop bar diameter.
HBS:	Hoop bar spacing.
CEFF:	Effectiveness of column confinement.

*Notes: * An input value of KHYSC with negative sign for the bottom section will result in symmetric values being assigned to the top section.*

*** If the section has a not-symmetric reinforcement, the SET D3 has to be used.*

**** AN is used for evaluating the moment-capacity envelope only. Vertical loads need to be declared in SET M1, if necessary.*

EXAMPLE

1	1, 1, 1, 270.0, 3810.0, 762.0, 762.0
	-1, 1270.0, 254.0, 20.0, 645.16, 5.0, 150.0, 0.5

Return to input of ICTYPE for next column type. When done go to SET E.

SET D1(b): ICTYPE=2; Rectangular Deep Beam-Column Data Set

- Add shear hysteretic rule number in SET D1(a)

KHYSC

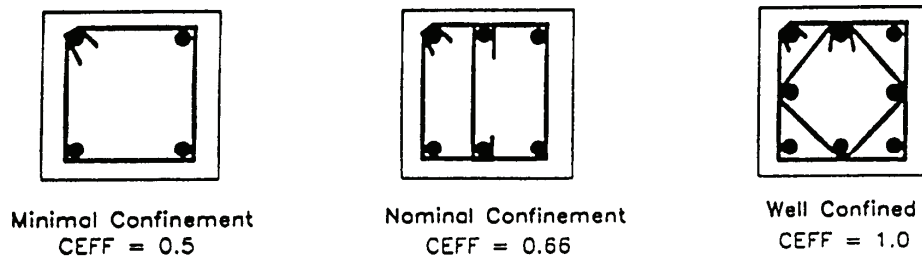
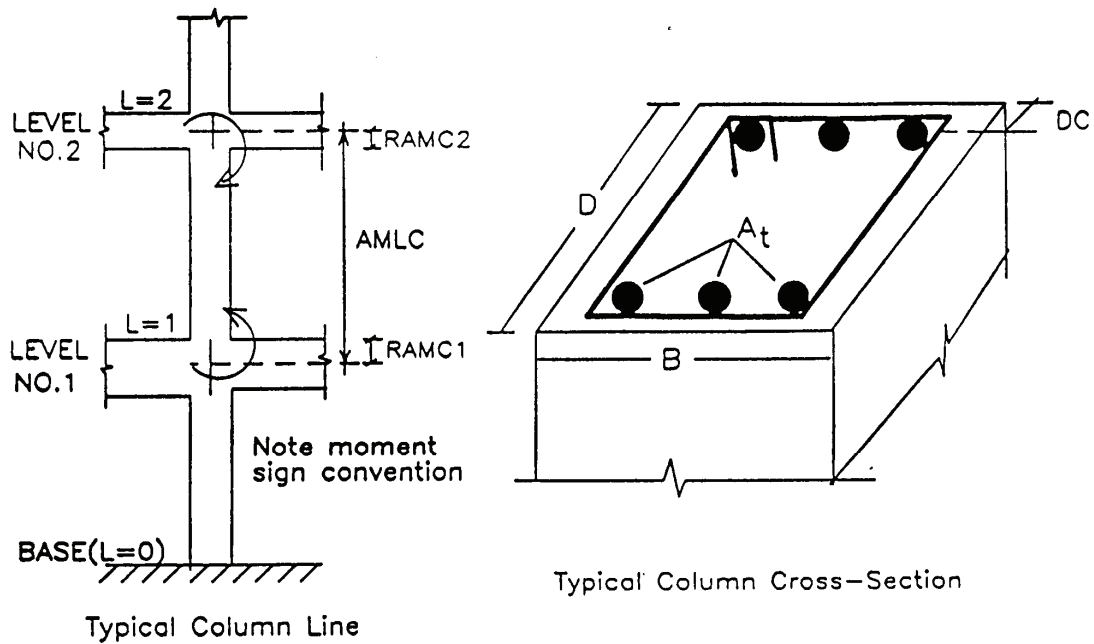
Description:

KHYSC: Hysteretic rule number (positive)

EXAMPLE

2	1, 1, 1, 270.0, 3810.0, 762.0, 762.0
	-1, 1270.0, 254.0, 20.0, 645.16, 5.0, 150.0, 0.5
	2

Return to input of ICTYPE for next column type. When done go to SET E.



Effectiveness of Confinement for Some Typical Hoop Arrangements

Fig. A-6 Rectangular Columns Input Details

SET D2: ICTYPE = 3; *Circular Column Input Data Set* (SEE FIGURE A-7)

- General Data:
KC, IMC, IMS, KHYSC, AMLC, RAMC1, RAMC2
- Column Section:
AN, DO, CVR, DST, NBAR, BDIA, HBD, HBS

<i>Description:</i>	
KC:	Column type set number.
IMC:	Concrete type number.
IMS:	Steel type number.
KHYSC:	Hysteretic Rule number.
AMLC:	Center-to-center column height.
RAMC1:	Rigid arm bottom.
RAMC2:	Rigid arm top.
AN:	Axial load on the column.
DO:	Outer diameter of column.
CVR:	Cover to center of hoop bar.
DST:	Distance between centers of long. bars.
NBAR:	Number of longitudinal bars.
BDIA:	Diameter of longitudinal bar.
HBD:	Diameter of hoop bar.
HBS:	Spacing of hoop bars.

EXAMPLE

3

1, 1, 1, 1, 360.0, 0.0, 0.0

1000.0, 60.0, 2.5, 54.5, 25, 1.69, 0.625, 3.5

Return to input of ICTYPE for next column type. When done go to SET E.

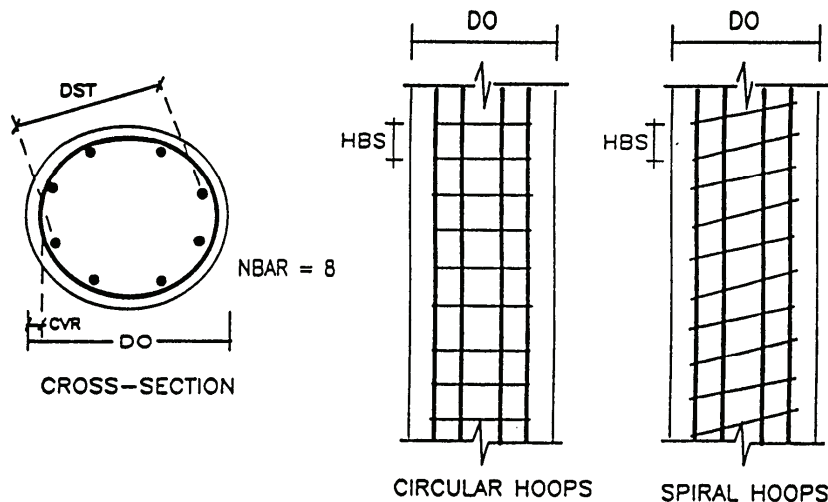


Fig. A-7 Circular column Input Details

SET D3: USER INPUT PROPERTIES (Rectangular or Circular)

- Reference Text:

USER TEXT

Description: **USER_TEXT**: Reference information, up to 80 characters of text.

- For each column type (MCOL), input the following:

ICTYPE

Data from SET D3(a)(ICTYPE=1), or SET D3(b)(ICTYPE=2)

READ DATA FROM SET D3(a), SET D3(b), OR SET D3(c) (See below)
GO TO SET E WHEN FINISHED READING ALL COLUMN TYPES.

SET D3(a): ICTYPE=1; Regular Column Input Data Set (SEE FIGURE A-8)

For each section type provide the following data:

- General Data:
KC, AN, ANY, ANB, AMLC, RAMC1, RAMC2
 - Bottom section:
**KHYSC, EI, EA, PCP, PYP, UYP, UUP, EI3P,
PCN, PYN, UYN, UUN, EI3N**
 - Top section:

If KHYSC for bottom section is input with negative sign, section is symmetric, hence, do not input top section data, otherwise repeat as above, starting with KHYSC.

Description:	
KC:	Column type number.
AN	Axial Force
ANY	Axial Yield Force
ANB	Axial Balance Force (Cut-off on PM diagram)
AMLC:	Column Length.
RAMC1:	Rigid Arm (Bottom).
RAMC2:	Rigid Arm (Top).
KHYSC:	Hysteretic rule number (may be negative)*.
EI:	Initial Flexural Rigidity (EI).
EA:	Axial Stiffness.
PCP:	Cracking Moment (positive). (When using bilinear model, use 99% of PYP)
PYP:	Yield Moment (positive).
UYP:	Yield Curvature (positive). (When using bilinear model, use 102% of PCP/EI ensuring post crack slope < post yield slope)
UUP:	Ultimate Curvature (positive).
EI3P:	Post Yield Flexural Stiffness (positive) as % of elastic.

PCN:	Cracking Moment (negative).
PYN:	Yield Moment (negative).
UYN:	Yield Curvature (negative).
UUN:	Ultimate Curvature (negative).
EI3N:	Post yield Flexural Stiffness (negative) as % of elastic.

*Notes: * AN is the axial force due to the static vertical loads.*

- ** An input value of KHYSC with negative sign for the bottom section will result in symmetric values being assigned to the top section.*
- *** All the negative quantities (PCN, PYN, UYN, UUN, EI3N) have to be put as positive ones.*

EXAMPLE

1

1, 270.0, 2000.0, 3500.0, 3810.0, 762.0, 762.0
 -1, .1981E+14, .8003E+04, .3112E+07, .5658E+07, .8516E-06, .2725E-03, 0.3683
 .3112E+07, .5658E+07, .8516E-06, .2725E-03, 0.3683

Repeat for each column type, starting with ICTYPE (DET D3). When done go to SET E

SET D3(b): ICTYPE=2; Deep Beam-Column Data Set (SEE FIGURE A-8)

- Add shear properties in **SET D3(a)**
- For shear properties

**KHYSC, GA, PCP, PYP, UYP, UUP, EI3P,
 PCN, PYN, UYN, UUN, EI3N**

<i>Description:</i>	KHYSC:	Hysteretic rule number. (positive)
	GA:	Shear Stiffness (Shear modulus*Shear Area).
	PCP:	Cracking Shear (positive). (When using bilinear model, use 99% of PYP)
	PYP:	Yield Shear (positive).
	UYP:	Yield Strain (positive). (When using bilinear model, use 102% of PCP/EI ensuring post crack slope < post yield slope)
	UUP:	Ultimate Strain (positive).
	EI3N:	Post yield Shear Stiffness (positive) as % of elastic.
	PCN:	Cracking Shear (negative).
	PYN:	Yield Shear (negative).
	UYN:	Yield Strain (negative).
	UUN:	Ultimate Strain (negative).

EI3N: Post yield Shear Stiffness (negative) as % of elastic.

Notes: All the negative quantities (PCN, PYN, UYN, UUN, EI3N) have to be put as positive ones.

EXAMPLE

2

1, 270.0, 2000.0, 3500.0, 3810.0, 762.0, 762.0
-1, .1981E+14, .8003E+04, .3112E+07, .5658E+07, .8516E-06, .2725E-03, 0.3683
.3112E+07, .5658E+07, .8516E-06, .2725E-03, 0.3683
2, 5.543E+06, 3000.0, 5000.0, 0.0058, 0.1, 0.5
3000.0, 5000.0, 0.0058, 0.1, 0.5

For considering a shear stiffness without shear hysteretic behavior (Constant shear stiffness), the shear cracking force (PCP) should be higher than the expected maximum shear force corresponding the flexural failure which is related to ultimate moments and element length

Repeat for each column type, starting with ICTYPE (SET D3). When done go to SET E.

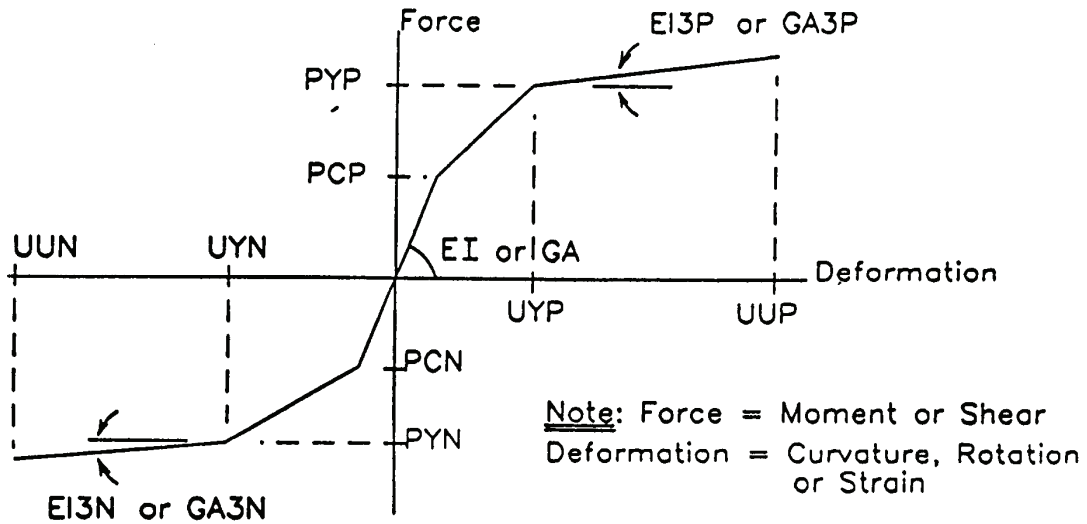


Fig. A-8 Notation for User Input Trilinear Envelopes

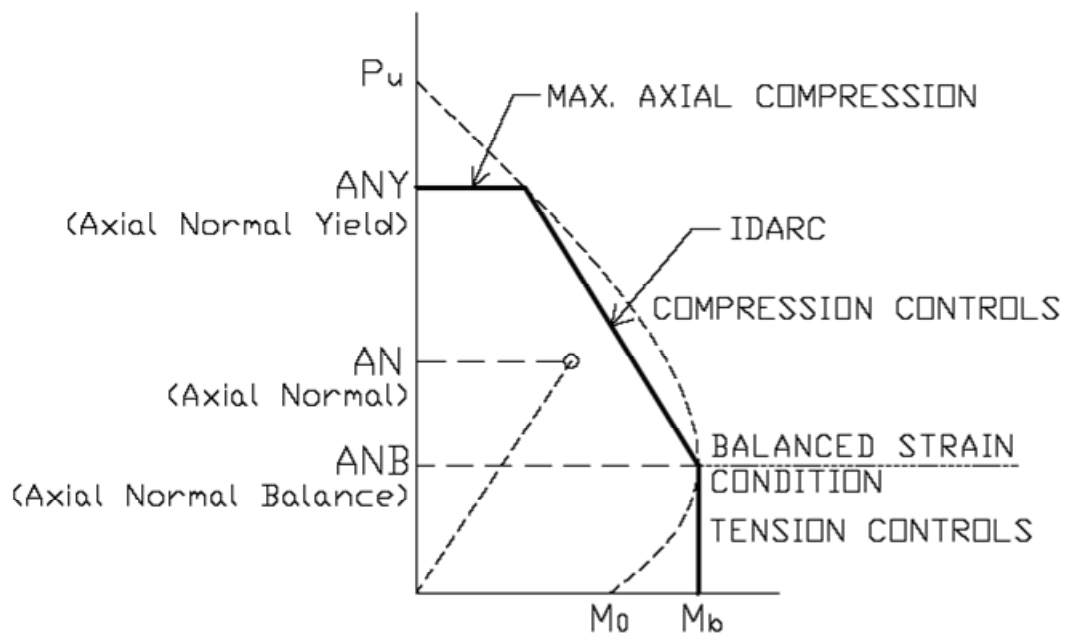


Fig. A-9 P-M interaction diagram

SET D3(c): ICTYPE=3; Rocking Column Input Data Set (SEE FIGURE A-10)

For each section type provide the following data:

- General Data:

KC, AN, ANY, ANB, AMLC, RAMC1, RAMC2, NEV

Description:	KC:	Column type number.
	AN	Axial Force
	ANY	Axial Yield Force
	ANB	Axial Balance Force (Cut-off on PM diagram)
	AMLC:	Column Length.
	RAMC1:	Rigid Arm (Bottom).
	RAMC2:	Rigid Arm (Top).
	NEV:	Type of input data for overturning point. 0; Maximum latral displacement capacity input corresponding to overturning point, 1; Overturning curvature input.

IF NEV = 1, GO TO SET D3(c-2)

SET D3(c-1): NEV=0; Latral Displacement Input correponding overturning point

- Bottom section:

**KHYSC, EI, EA, PCP, PYP, UYP, UNSP, ULP, EI3P,
PCN, PYN, UYN, UNSN, ULN, EI3N**

- Top section:

If KHYSC for bottom section is input with negative sign, section is symmetric, hence, do not input top section data, otherwise repeat as above, starting with KHYSC.

Description:	KHYSC:	Hysteretic rule number (may be negative)*.
	EI:	Initial Flexural Rigidity (EI).
	EA:	Axial Stiffness.
	PCP:	Cracking Moment (positive). (When using bilinear model, use 99% of PYP)
	PYP:	Yield Moment (positive).
	UYP:	Yield Curvature (positive). (When using bilinear model, use 102% of PCP/EI ensuring post crack slope < post yield slope)
	UNSP:	Rocking Curvature (positive).
	ULP:	Maximum Latral Displacement Capacity at overturning point (positive).
	EI3P:	Post Yield Flexural Stiffness (positive) as % of elastic.
	PCN:	Cracking Moment (negative).
	PYN:	Yield Moment (negative).
	UYN:	Yield Curvature (negative).
	UNSN:	Rocking Curvature (negative).
	ULN:	Maximum Latral Displacement Capacity at overturning point (negative).

EI3N: Post yield Flexural Stiffness (negative) as % of elastic.

SET D3(c-2): NEV=1; Overturning Curvature Input.

- Bottom section:

Replace ULP and ULN with UUP and UUN, respectively, from SET D3(c-1)

- Top section:

If KHYSC for bottom section is input with negative sign, section is symmetric, hence, do not input top section data, otherwise repeat as above, starting with KHYSC.

<i>Description:</i>	UUP:	Overshooting Curvature (positive).
	UUN:	Overshooting Curvature (negative).

Notes: * *AN is the axial force due to the static vertical loads.*

** *An input value of KHYSC with negative sign for the bottom section will result in symmetric values being assigned to the top section.*

*** *All the negative quantities (PCN, PYN, UYN, UNSN, ULN, UUN, EI3N) have to be put as positive ones.*

Repeat for each column type, starting with ICTYPE (SET D3). When done go to SET E.

EXAMPLE

3

1, 28.4, 200.0, 80.0, 1143.0, 76.2, 76.2, 0
-1, 129700000.0, 73400.0, 482.045, 1253.3, 0.000024, 0.000049, 60.96, 1.5
482.045, 1253.3, 0.000024, 0.000049, 60.96, 1.5

EXAMPLE

3

1, 300.0, 1500.0, 600.0, 4100.0, 100.0, 100.0, 1
-1, 2.0E+10, 1.0E+06, 800000.0, 1100000.0, 0.0002, 0.00025, 0.0019, 1.0
800000.0, 1100000.0, 0.0002, 0.00025, 0.0019, 1.0

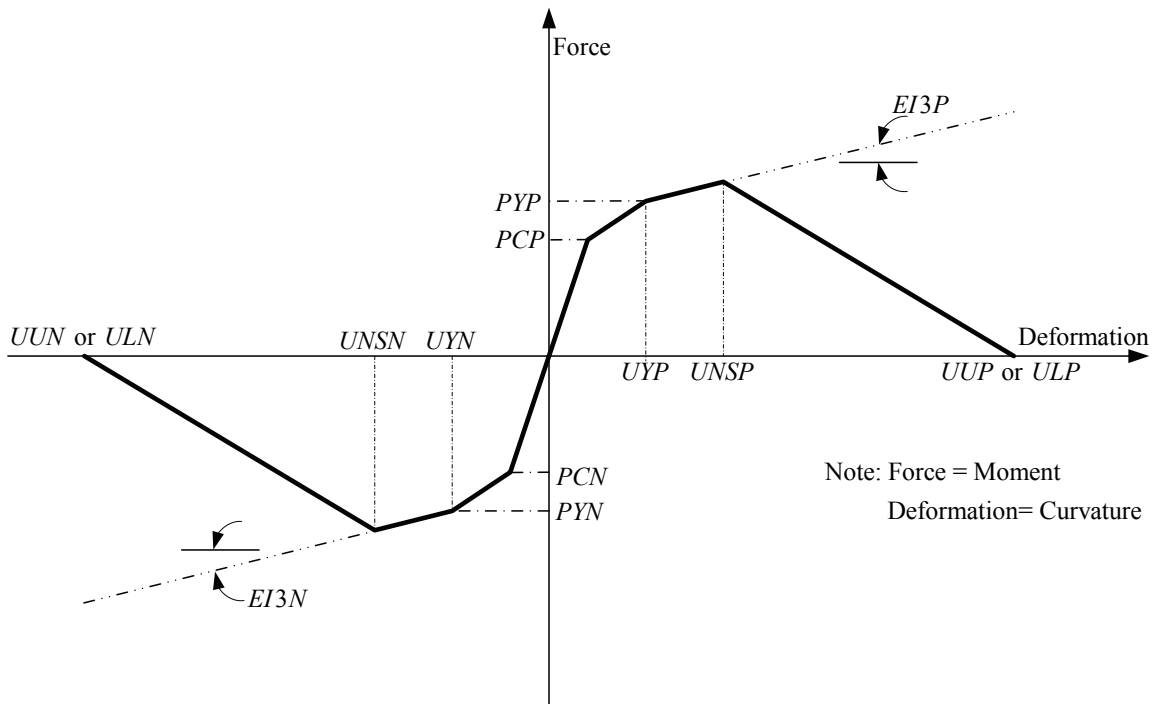


Fig. A-10 Notation for User Input Trilinear Envelopes for rocking column

SET E: BEAM PROPERTIES SETS

(SKIP THIS INPUT IF THE STRUCTURE HAS NO BEAMS)

- Control Data:

USER TEXT

IUBEM

Description: **USER_TEXT**: Reference information, up to 80 characters of text.

IUBEM: Type of beam input:
0; Section dimensions, and reinforcement details (internal computation of moment-curvature envelope),
1; User specified moment (Shear)-curvature (Strain) envelope.

IF IUBEM = 1, GO TO SET E2

- Reference Text:

USER TEXT

Description: **USER_TEXT**: Reference information, up to 80 characters of text.

- For each beam type (MBEM), input the following:

IBTYPE

Data from SET E1 (IBTYPE =1), or SET E2 (IBTYPE =2)

[User Input Properties(SET E2) is more preferable]

READ DATA FROM SET E1(a), OR SET E1(b)(See below)

GO TO SET F WHEN FINISHED READING ALL BEAM TYPES

SET E1(a): IBTYPE=1; *Regular Beam Data Set (SEE FIGURE A-11)*

- #### • Reference Text:

USER TEXT

Description: **USER_TEXT**: Reference information, up to 80 characters of text

For each section type provide the following data:

- General data

KB, IMC, JMS, AMLB, RAMB1, RAMB2

- ### • Left section:

KHYSB, D, B, BSL TSL, BC, AT1, AT2, HBD, HBS

- Right section:

If KHYSB for left section is input with negative sign, section is symmetric, hence, do not input right section data, otherwise input right section data starting with KHYSB as in the left section.

<i>Description:</i>	KB:	Beam type set number.
	IMC:	Concrete type number.
	IMS:	Steel type number.
	AMLB:	Member length.
	RAMB1:	Rigid zone length (left).
	RAMB2:	Rigid zone length (right).
	KHYSB:	Hysteretic rule number (may be negative)*.
	D:	Overall depth**.
	B:	Lower width**.
	BSL:	Effective slab width**.
	TSL:	Slab thickness**.
	BC:	Cover to centroid of steel.
	AT1:	Area of bottom bars.
	AT2:	Area of top bars.
	HBD:	Diameter of stirrup bars.
	HBS:	Spacing of stirrups.

Notes: * An input value of KHYSB with negative sign for the left section will result in symmetric values being assigned to the right section.

** For a rectangular beam or flat slab D is the overall depth, B=BSL&TSL=0

Repeat for each beam type starting with IBTYPE. When done, go to SET F

EXAMPLE

1

1, 1, 1, 2159.0, 1079.0, 0.0

-1, 1524.0, 254.0, 254.0, 0.0, 20.0, 774.192, 774.192, 5.0, 150.0

SET E1(b): IBTYPE =2; Deep Beam Data Set

- Add hysteretic rule number in **SET E1(a)**

KHYSB

Description: **KHYSB:** Hysteretic rule number (positive)

EXAMPLE

2

1, 1, 1, 2159.0, 1079.0, 0.0

-1, 1524.0, 254.0, 254.0, 0.0, 20.0, 774.192, 774.192, 5.0, 150.0

2

Repeat for each beam type starting with IBTYPE. When done, go to SET F

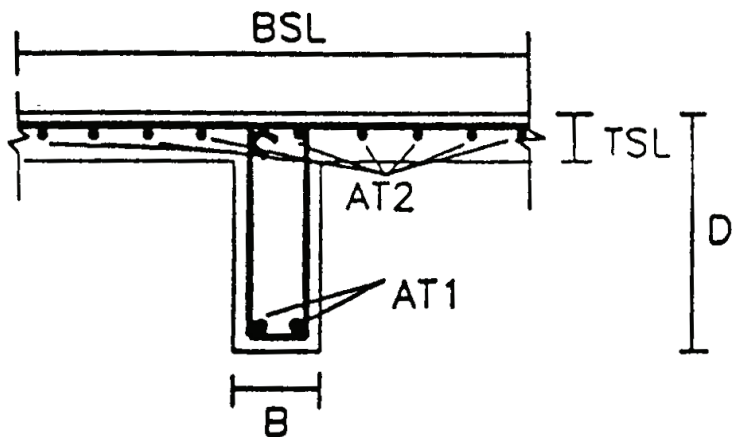
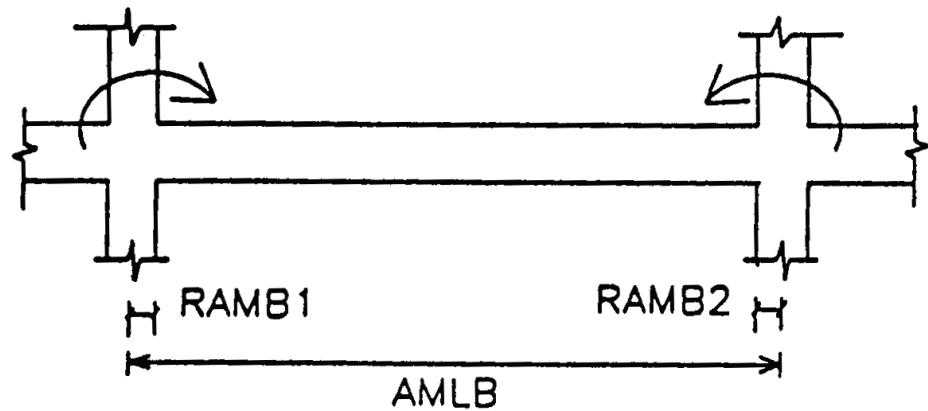


Fig. A-11 Input Details for Beam-Slab Sections

SET E2: USER INPUT PROPERTIES SETS

- Reference Text:

USER TEXT

Description: **USER_TEXT**: Reference information, up to 80 characters of text.

- For each beam type (MBEM), input the following:

IBTYPE

Data from **SET E2(a)** (**IBTYPE** =1), or **SET E2(b)** (**IBTYPE** =2),

READ DATA FROM SET E2(a), OR SET E2(b) (See below)

GO TO SET F WHEN FINISHED READING ALL BEAM TYPES.

SET E2(a): IBTYPE = 1; Beam Input Data Set (SEE FIGURE A-8)

For each section type provide the following data:

- General Data:

KB, AMLB, RAMB1, RAMB2

- Left section:

KHYSB, EI, PCP, PYP, UYP, UUP, EI3P, PCN, PYN, UYN, UUN, EI3N

- Right section

If KHYSB for left section is input with negative sign, section is symmetric, hence, do not input right section data, otherwise repeat as above, starting with KHYSB as in the left section.

Description:	
KB:	Beam type set number.
AMLB:	Beam Length.
RAMB1:	Rigid Arm (Left).
RAMB2:	Rigid Arm (Right).
KHYSB:	Hysteretic rule number (may be negative)*.
EI:	Initial Flexural Rigidity.
PCP:	Cracking Moment (positive). (When using bilinear model, use 99% of PYP)
PYP:	Yield Moment (positive).
UYP:	Yield Curvature (positive). (When using bilinear model, use 102% of PCP/EI ensuring post crack slope < post yield slope)
UUP:	Ultimate Curvature (positive).
EI3P:	Post Yield Flexural Stiffness (positive) as % of elastic..
PCN:	Cracking Moment (negative).
PYN:	Yield Moment (negative).
UYN:	Yield Curvature (negative).
UUN:	Ultimate Curvature (negative).

EI3N: Post yield Flexural Stiffness (negative) as % of elastic..

*Note: * An input value of KHYSB with negative sign for the left section will result in symmetric values being assigned to the right section.*

Repeat for each beam type, starting with IBTYPE(SET E2). When done go to SET F .

EXAMPLE

1

1, 3810.0, 762.0, 762.0
-1, .1981E+14, .3112E+07, .5658E+07, .8516E-06, .2725E-03, 0.3683
.3112E+07, .5658E+07, .8516E-06, .2725E-03, 0.3683

SET E2(b): ICTYPE=2; Deep Beam Data Set (SEE FIGURE A-8)

- Add shear properties in **SET E2(a)**
- For shear properties

**KHYSB, GA, PCP, PYP, UYP, UUP, EI3P,
PCN, PYN, UYN, UUN, EI3N**

<i>Description:</i>	KHYSB:	Hysteretic rule number. (positive)
	GA:	Shear Stiffness (Shear modulus*Shear Area).
	PCP:	Cracking Shear (positive). (When using bilinear model, use 99% of PYP)
	PYP:	Yield Shear (positive).
	UYP:	Yield Strain (positive). (When using bilinear model, use 102% of PCP/EI ensuring post crack slope < post yield slope)
	UUP:	Ultimate Strain (positive).
	EI3P:	Post Yield Shear Stiffness (positive) as % of elastic.
	PCN:	Cracking Shear (negative).
	PYN:	Yield Shear (negative).
	UYN:	Yield Strain (negative).
	UUN:	Ultimate Strain (negative).
	EI3N:	Post yield Shear Stiffness (negative) as % of elastic.

Notes: All the negative quantities (PCN, PYN, UYN, UUN, EI3N) have to be put as positive ones.

EXAMPLE

2

```
1, 3810.0, 762.0, 762.0
-1, .1981E+14, .3112E+07, .5658E+07, .8516E-06, .2725E-03, 0.3683
    .3112E+07, .5658E+07, .8516E-06, .2725E-03, 0.3683
2, 5.543E+06, 3000.0, 5000.0, 0.0058, 0.1, 0.5
    3000.0, 5000.0, 0.0058, 0.1, 0.5
```

For considering a shear stiffness without shear hysteretic behavior (Constant shear stiffness), the shear cracking force (PCP) should be higher than the expected maximum shear force corresponding the flexural failure which is related to ultimate moments and element length

Repeat for each beam type, starting with IBTYPE (SET E2). When done go to SET F.

SET F: SHEAR WALL PROPERTIES SETS (SEE FIGURES A-12 AND A-13)
(SKIP THIS INPUT IF THE STRUCTURE HAS NO SHEAR WALLS)

- Control Data:

USER_TEXT

IUWAL

<i>Description:</i>	USER_TEXT : Reference information, up to 80 characters of text.
IUWAL :	Type of wall input: 0; Section dimensions and reinforcement details (internal computation of moment-curvature and shear strain envelopes), 1; User specified moment-curvature and shear strain envelopes.

IF IUWAL = 1, GO TO SET F2

SET F1: WALLS SECTION DIMENSIONS SETS

- Reference Text:

USER_TEXT

<i>Description:</i>	USER_TEXT : Reference information, up to 80 characters of text.
---------------------	--

For each section type provide the following data:

- General Data:

KW, IMC, KHYSW(1), KHYSW(2), KHYSW(3), AN, AMLW, NSECT

- For each of the NSECT sections, input the following:

KS, IMS, DWAL, BWAL, PT, PW

<i>Description:</i>	KW : Shear wall type set number.
	IMC : Concrete type number.
	KHYSW(1) : Hysteretic Rule Number (bottom).
	KHYSW(2) : Hysteretic Rule Number (top).
	KHYSW(3) : Hysteretic Rule Number (shear).
	AN : Axial load.
	AMLW : Height of shear wall.
	NSECT : Number of Sections.
	KS : Section number.
	IMS : Steel type number.
	DWAL : Depth of section.
	BWAL : Width of section.
	PT : Vertical reinforcement ratio (%).
	PW : Horizontal reinf ratio (%).

Repeat for each wall type starting with General Data; When done go to SET G

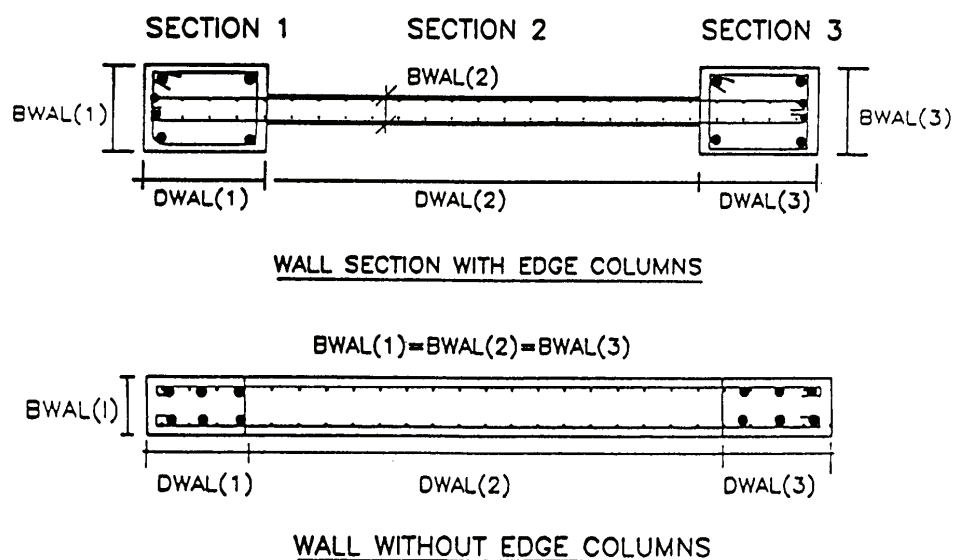


Fig. A-12 Typical Input Details for Shear Wall Sections

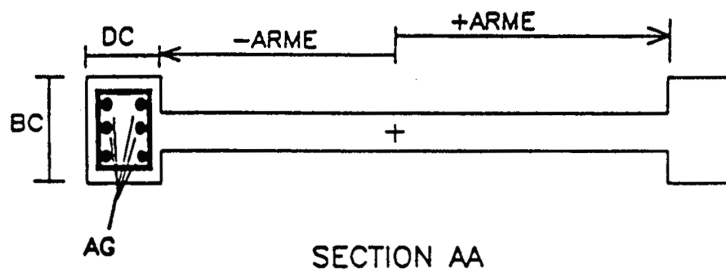
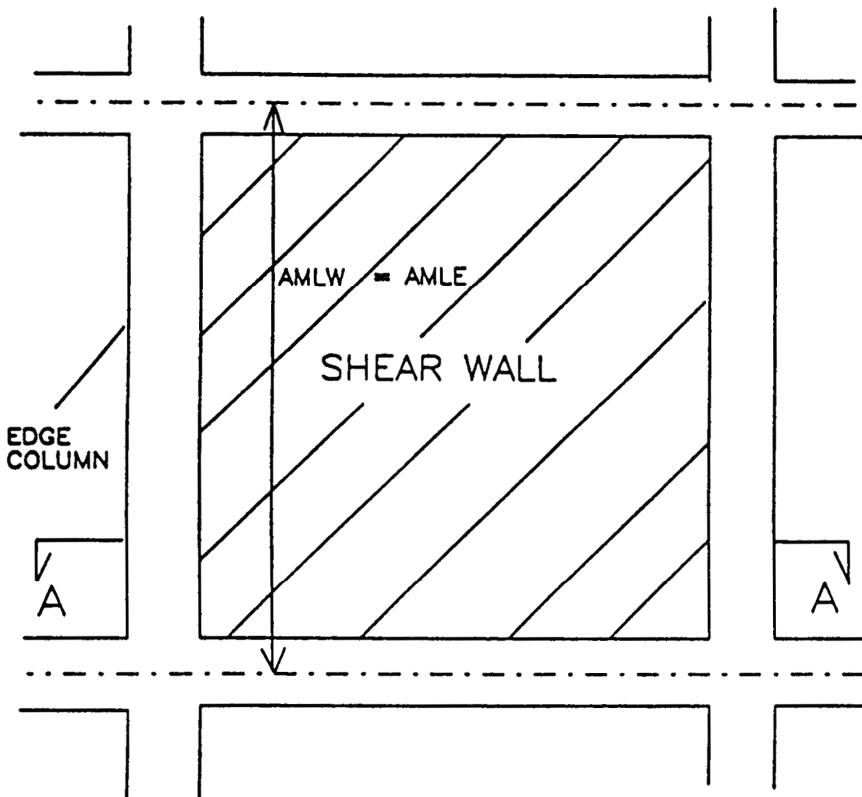


Fig. A-13 Shear Wall and Edge Column Details

SET F2: USER INPUT PROPERTIES SETS (SEE FIGURE A-8)

- Reference Text:

USER_TEXT

Description: **USER_TEXT:** Reference information, up to 80 characters of text.

For each section type provide the following data:

- General Data:

KW, AMLW, EAW

- Flexure BOT:

KHYSW, EI, PCP, PYP, UYP, UUP, EI3P, PCN, PYN, UYN, UUN, EI3N

- Flexure TOP:

If KHYSW for bottom section is input with negative sign, section is symmetric, hence, do not input top section data, otherwise repeat as above, starting with KHYSW.

- Shear:

KHYSW, GA, PCP, PYP, UYP, UUP, GA3P, PCN, PYN, UYN, UUN, GA3N

Description: **KW:** Wall type set number.

AMLW: Wall length.

EAW: Axial Stiffness (EA/L).

Data for Flexural Properties:

KHYSW: Hysteretic rule number (may be negative)*.

EI: Initial flexural stiffness (EI).

PCP: Cracking Moment (positive). (When using bilinear model, use 99% of PYP)

PYP: Yield Moment (positive).

UYP: Yield Curvature (positive). (When using bilinear model, use 102% of PCP/EI ensuring post crack slope < post yield slope)

UUP: Ultimate Curvature (positive).

EI3P: Post Yield Flexural Stiffness (positive) as % of elastic..

PCN: Cracking Moment (negative).

PYN: Yield Moment (negative).

UYN: Yield Curvature (negative).

UUN: Ultimate Curvature (negative).

EI3N: Post yield Flexural Stiffness (negative) as % of elastic..

Data for shear properties:

KHYSW: Hysteretic Rule Number.

GA: Initial Shear Stiffness (shear modulus*area).

PCP: Cracking Shear (positive). (When using bilinear model, use 99% of PYP)

PYP: Yield Shear (positive).

UYP:	Yield Shear strain (positive). (When using bilinear model, use 102% of PCP/EI ensuring post crack slope < post yield slope)
UUP:	Ultimate Shear strain (positive).
GA3P:	Post Yield Shear Stiffness (positive).
PCN:	Cracking Shear (negative).
PYN:	Yield Shear (negative).
UYN:	Yield Shear strain (negative).
UUN:	Ultimate Shear strain (negative).
GA3N:	Post Yield Shear Stiffness (negative).

*Note: * An input value of KHYSW with negative sign for the bottom section will result in symmetric values being assigned to the top section.*

Return to start of General Data (SET F2). Repeat for each wall type

SET G: EDGE COLUMN PROPERTIES SETS (SEE FIGURE A-13)

(SKIP THIS INPUT IF THE STRUCTURE HAS NO EDGE COLUMNS)

Do not duplicate edge column data if already input in SHEAR WALL data.

- Reference Text:

USER_TEXT

Description: **USER_TEXT**: Reference information, up to 80 characters of text.

- Edge Column Data (Provide one line for each MEDG edge column type):

KE, IMC, IMS, AN, DC, BC, AG, AMLE, ARME

Description: **KE**: Edge column type set number.
 IMC: Concrete type number.
 IMS: Steel type number.
 AN: Axial load.
 DC: Depth of edge column.
 BC: Width of edge column.
 AG: Gross area of main bars.
 AMLE: Member length.
 ARME: Arm length.

Repeat for each of MEDG elements starting with edge column type number.

SET H: TRANSVERSE BEAM PROPERTIES SETS (SEE FIGURE A-14)
(THIS INPUT NOT REQUIRED IF STRUCTURE HAS NO TRANSVERSE BEAMS
OR IS MADE OF IDENTICAL BEAMS ONLY)

- Reference Text:

USER_TEXT

Description: **USER_TEXT:** Reference information, up to 80 characters of text.

- Transverse Beam Data (Provide one line for each MTRN transverse beam type):

KT, AKV, ARV, ALV

Description: **KT:** Transverse beam type set number
AKV: Vertical Stiffness
ARV: Torsional Stiffness
ALV: Element length

Repeat for each of MTRN elements

Notes: 1. *Transverse elements are assumed to remain elastic. The degree of fixity at the ends will depend on the state of the joint and the state of the members that frame into the joint before and during the application of load. If the entire region is expected to stay elastic, then the vertical stiffness should be computed as : $AKV = 12EI / L^3$. In the extreme case that one of ends do not transmit stiffness due to yielding of adjoining members or deterioration of the joint, then $AKV = 3EI / L^3$. An intermediate value is a good average approximation.*
2. *If duplicate frames are present, extreme care should be taken in specifying transverse beam properties. The program multiplies the input values by the number of duplicate frames to which they are attached. For example, for the frames shown in Figure A-1, $NDUP(1) = NDUP(2) = 2$. The program will factor the input stiffness values by $(NDUP(1)+NDUP(2))=4.0$. Input stiffnesses should, therefore, be modified to account for this effect. If the modeling of transverse elements is not crucial to the analysis, the use of duplicate frames should be avoided.*

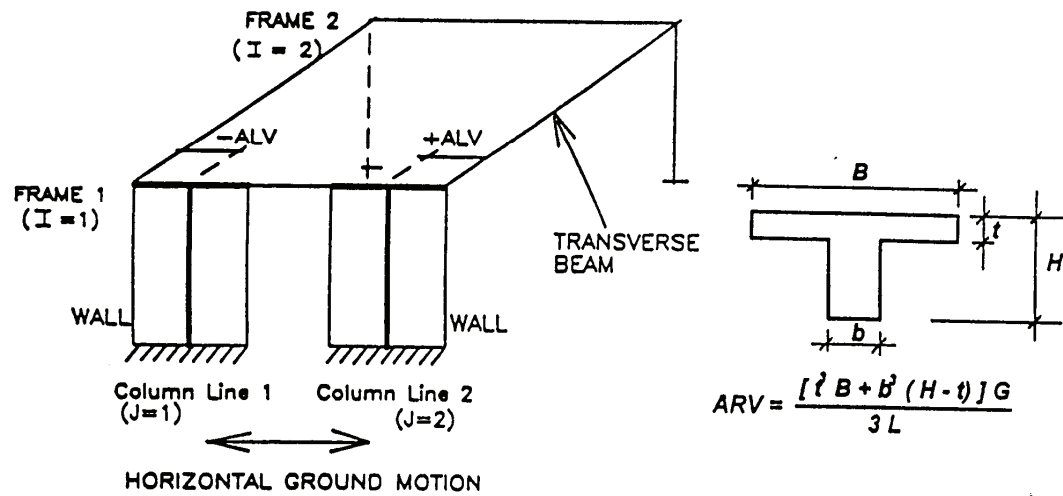


Fig. A-14 Transverse Beam Input

SET I: ROTATIONAL SPRINGS PROPERTIES SETS (SEE FIGURE A-8)
(THIS INPUT NOT REQUIRED IF ROTATIONAL SPRINGS ARE NOT SPECIFIED)

- Reference Text:

USER_TEXT

Description: **USER_TEXT**: Reference information, up to 80 characters of text.

- General Data (Provide one line of data for each MSPR spring type):

KS, KHYSR, EI, PCP, PYP, UYP, UUP, EI3P, PCN, PYN, UYN, UUN, EI3N

Description: **KS**: Rotational spring set number.
KHYSR: Hysteretic Rule Number.
EI: Initial Rotational Stiffness.
PCP: Cracking moment (positive). (When using bilinear model, use 99% of PYP)
PYP: Yield moment (positive).
UYP: Yield rotation (positive, radians). (When using bilinear model, use 102% of PCP/EI ensuring post crack slope < post yield slope)
UUP: Ultimate rotation (positive, radians).
EI3P: Post-yield stiffness ratio (positive) as % of elastic..
PCN: Cracking moment (negative).
PYN: Yield moment (negative).
UYN: Yield rotation (negative).
UUN: Ultimate rotation capacity (negative).
EI3N: Post yield stiffness ratio (negative) as % of elastic.

Repeat for each spring type

Notes: Spring properties, unlike other element types, are specified in terms of moment and rotation (in radians). The envelope follows the same nonsymmetric trilinear pattern as shown in Figure A-8.

SET J: BRACES PROPERTIES SETS

SET J1: VISCO-ELASTIC BRACE PROPERTIES SETS (SKIP THIS IF NO VISCO-ELASTIC BRACES ARE SPECIFIED)

- Control Information:

USER_TEXT

ITMODEL, ITDVCON

<i>Description:</i>	USER_TEXT: Reference information, up to 80 characters of text.
	ITMODEL: Model for viscous dampers: 0 for Maxwell model, 1 for Kelvin model.
	ITDVCON: Type of connection: 0 for diagonal braces, 1 for chevron braces.

SET J1-1: VISCO-ELASTIC BRACE PROPERTIES

- General Data (Provide one set of data for each MBRV visco-elastic brace type):

ITDV, CDV, KDV, ALPHADV

- Chevron Braces Data (Provide only if ITDVCON=1):

KDVCH, ANGDV

<i>Description:</i>	ITDV: Visco-elastic brace type set number.
	CDV: Damping constant C of this type of visco-elastic brace.
	KDV: Axial stiffness of this type of visco-elastic brace (EA/L).
	ALPHADV: Polynomial power α of velocity for non-linear dampers
	KDVCH: Axial stiffness of one leg of the Chevron bracing (EA/L).
	ANGDV: Angle of inclination of the brace with respect to a horizontal line.

Notes: *DEFAULT VALUES (if a zero was specified as data input):*
 ALPHADV=1.0 (i. e. linear damper)

Repeat set J1-1 for each visco-elastic brace type

SET J2: FRICTION DAMPER BRACE PROPERTIES SETS (SKIP THIS IF NO FRICTION DAMPER BRACES ARE SPECIFIED)

- Reference Text:

USER_TEXT

ITDFCON

<i>Description:</i>	USER_TEXT: Reference information, up to 80 characters of text.
	ITDFCON: Type of connection: 0 for diagonal braces, 1 for chevron braces.

SET J2-1: FRICTION DAMPER BRACE PROPERTIES

- General Data (Provide one line of data for each MBRF friction brace type):

ITDF, KDF, FYDF

- Chevron Brace Data (Provide only if ITDFCON=1):

KDFCH, ANGDF

<i>Description:</i>	ITDF: Friction (damper) brace type set number.
	KDF: Axial stiffness (EA/L).
	FYDF: Friction force of this type of friction dampers.
	KDFCH: Axial stiffness of one leg of the Chevron brace (EA/L).
	ANGDF: Angle of inclination of the brace with respect to a horizontal line.

Repeat set J2-1 for each friction damper brace type

SET J3: HYSTERETIC DAMPER BRACE PROPERTIES SETS

(SKIP THIS IF NO HYSTERETIC DAMPER BRACES ARE SPECIFIED)

- Reference Text:

USER_TEXT, ITDHCON

<i>Description:</i>	USER_TEXT: Reference information, up to 80 characters of text.
	ITDHCON: Type of connection: 0 for diagonal braces, 1 for chevron braces.

SET J3-1: HYSTERETIC DAMPER BRACE PROPERTIES

- General Data (Provide one line of data for each MBRH hysteretic brace type):

ITDH, 1, KDH, FYDH, RPSTDH

- Chevron Brace Data (Provide only if ITDHCON=1):

KDHCH, ANGDH

<i>Description:</i>	ITDH: Hysteretic damper brace type set number.
	KDH: Axial stiffness (EA/L).
	FYDH: Yield force of this type of hysteretic dampers.
	RPSTDH: Post yield stiffness ratio.
	KDHCH: Axial stiffness of one leg of the Chevron bracing (EA/L).
	ANGDH: Angle of inclination of the brace with respect to a horizontal line.

Repeat set J3-1 for each hysteretic damper type

SET K: INFILL PANEL PROPERTIES SETS

(SKIP THIS IF NO INFILL PANEL ELEMENTS ARE SPECIFIED)

- Reference Text

USER_TEXT

Description: **USER_TEXT:** Reference information, up to 80 characters of text.

SET K1: CONTROL DATA

- Control Information

USER_TEXT

IPT, ICTYPE

Description: **USER_TEXT:** Reference information, up to 80 characters of text.
IPT: Masonry infill panel type set
ICCTYPE: Type of infill panel input:
 0, Masonry panel dimensions to be specified
 for automatic generation of panel strength
 envelope parameters.
 1. User specified panel strength envelope
 parameters

SET K2-1: INPUT FOR GENERATION OF STRENGTH ENVELOPE

PARAMETERS

(SKIP TO K2-2 IF ICTYPE = 1)

- Infill panel dimensions (provide two lines of data for each IPT infill panel type set):

IMT,TMP,VLMP,VHMP

Description: **IMT:** Masonry property type number
TMP: Thickness of masonry infill panel
VLMP: Length of infill panel
VHMP: Height of infill panel

QMPC,QMPB, QMPJ

Description: **QMPC:** Plastic moment capacity of column
QMPB: Plastic moment capacity of beam
QMPJ: Plastic moment capacity of joint

SET K2-2: USER INPUT FOR STRENGTH ENVELOPE PARAMETERS

(SKIP THIS INPUT IF ICTYPE = 0)

- User specified infill panel strength envelope properties (provide one line of data for each IPT infill panel type set):

EAIW, VYIW

Description: **EAIW:** Initial elastic stiffness of the panel type
VYIW: Lateral yield force of the panel type

SET K3: INFILL PANEL HYSTERETIC PROPERTIES

- Hysteretic model parameters for infill panel (provide three lines of data for each IPT infill panel type set):

AIW, BTA, GMA, ETA, ALPHIW

IS, AS, ZS, ZBS

SK, SP1, SP2, MU

<i>Description:</i>		
AIW:	Parameter A in Wen's model.	
BTA:	Parameter beta in Wen's model.	
GMA:	Parameter gamma in Wen's model.	
ETA:	Parameter eta in Wen's model.	
ALPHIW:	Post yielding stiffness ratio.	
IS:	Flag to indicate no slip (=0), or slip (=1) in the hysteretic response.	
AS:	Control parameter for slip length.	
ZS:	Parameter that controls the sharpness of the slip.	
ZBS:	Offset value for slip response.	
SK:	Control parameter to vary the rate of stiffness decay.	
SP1:	Parameter to control the rate of strength deterioration.	
SP2:	Parameter to control the rate of strength deterioration.	
MU:	Ductility capacity of the infill panel.	

Notes: 1 *DEFAULT VALUES (if a zero was specified as data input):*

$AIW=1.0, BTA=0.1, GMA=0.9, ETA=2.0, ALPHIW=0.01$

$IS=1, AS=0.3, ZS=0.1, ZBS=0.0$

$SK=0.1, SP1=0.8, SP2=1.0, MU=5.0$

2 See Section 3.3 for details on the role of hysteretic model parameters,

Repeat Sets K1, K2 and K3 for each IPT infill panel type set.

Note: “*Infill*” model does not work in static analysis (including quasi-static, pushover), only work with the dynamic analysis. The capacity curve of structures with the *infill* model can be obtained by performing the dynamic analysis with incremental specific excitation levels (ex: 0.1g, 0.2g, 0.3g,), recording a maximum base shear versus a maximum overall displacement at each excitation level. Each pair of the maximum values at may not be recorded at the same time step.

SET L: ELEMENT CONNECTIVITIES

Notes: Element connectivity is established through the 3 positional locaters described in Figure A-1: a story level, a frame number and a column line. The L position locator (or story level) varies from 0 to the number of stories; the I position locator (or frame number) varies from 1 to the number of frames; and the J locator varies from 1 to the number of NVL positions (column lines) for each frame. NVLN can be different for each frame, being a 'local' information. The hypothetical structure shown below is used to demonstrate the input format. Only a representative data set is shown.

Element Type	Number	Type	IC	JC	LBC	LTC
COLUMNS	1	1	1	1	3	4
	2	2	1	2	3	4
	10	8	1	4	0	2
BEAMS	Number	Type	LB	IB	JLB	JRB
	1	1	4	1	1	2
	2	2	4	1	2	3
WALLS	Number	Type	IW	JW	LBW	LTW
	1	1	1	3	3	4
	2	2	1	3	2	3

SET L1: COLUMNS CONNECTIVITY (SEE FIGURE A-15)

(SKIP THIS INPUT IF THE STRUCTURE HAS NO COLUMNS)

- Reference Text:

USER_TEXT

Description: **USER_TEXT:** Reference information, up to 80 characters of text.

- Column Connectivities (Provide one line of data for each NCOL column):

M, ITC, IC, JC, LBC, LTC

Description: **M:** Column number.
ITC: Column type number.
IC: Frame number.
JC: Column Line number.
LBC: Story level at bottom of column.
LTC: Story level at top of column.

Notes: Input is required for each of the NCOL columns.

SET L2: BEAMS CONNECTIVITY (SEE FIGURE A-15)

(SKIP THIS INPUT IF STRUCTURE HAS NO BEAMS)

- Reference Text:

USER_TEXT

Description: **USER_TEXT:** Reference information, up to 80 characters of text.

- Beam Connectivities (Provide one line of data for each NBEM beam):

M, ITB, LB, IB, JLB, JRB

Description: **M:** Beam number.
ITB: Beam type number.
LB: Story level.
IB: Frame number.
JLB: Column Line number of left section.
JRB: Column Line number of right section.

Note: *Input is required for each of the NBEM beams.*

SET L3: SHEAR WALLS CONNECTIVITY (SEE FIGURE A-15)

(SKIP THIS INPUT IF STRUCTURE HAS NO SHEAR WALLS)

- Reference Text:

USER_TEXT

Description: **USER_TEXT:** Reference information, up to 80 characters of text.

- Wall Connectivities (Provide one line of data for each NWAL wall):

M, ITW, IW, JW, LBW, LTW

Description: **M:** Wall number.
ITW: Wall type number.
IW: Frame number.
JW: Column line number.
LBW: Story level at bottom.
LTW: Story level at top.

Note: *Input is required for each of the NWAL shear walls.*

SET L4: EDGE COLUMNS CONNECTIVITY

(SKIP THIS INPUT IF STRUCTURE HAS NO EDGE COLUMNS)

- Reference Text:

USER_TEXT

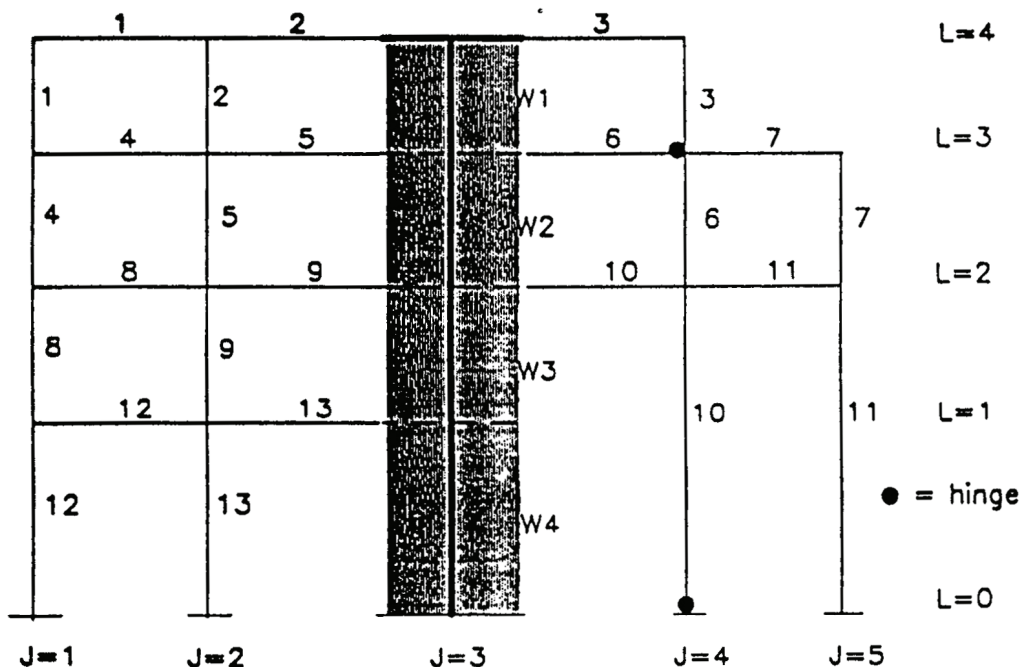
Description: **USER_TEXT:** Reference information, up to 80 characters of text.

Edge Column Connectivities (Provide one line of data for each NEDG edge column):

M, ITE, IE, JE, LBE, LTE

Description: **M:** Edge column number.
ITE: Edge column type number.
IE: Frame number.
JE: Column line number.

LBE: Story level at bottom of column.
LTE: Story level at top of column.



Element Type	Number	Type	IC	JC	LBC	LTC
COLUMNS	1	1	1	1	3	4
	2	2	1	2	3	4
	10	8	1	4	0	2
BEAMS	Number	Type	LB	IB	JLB	JRB
	1	1	4	1	1	2
	2	2	4	1	2	3
WALLS	Number	Type	IW	JW	LBW	LTW
	1	1	1	3	3	4
	2	2	1	3	2	3

Fig. A-15. Element Connectivity for Sample Structure

SET L5: TRANSVERSE BEAMS CONNECTIVITY

(SKIP THIS INPUT IF STRUCTURE HAS NO TRANSVERSE BEAMS)

- Reference Text:

USER TEXT

Description: **USER_TEXT**: Reference information, up to 80 characters of text.

- Transverse Beam Connectivities (Provide one line of data for each NTRN transverse beam):

M, ITT, LT, IWT, JWT, IFT, JFT

<i>Description:</i>	M:	Transverse beam number.
	ITT:	Transverse beam type number.
	LT:	Story level.
	IWT:	Frame number of origin of transverse beam*.
	JWT:	Column line of origin of transverse beam*.
	IFT:	Frame number of connecting wall or column.
	JFT:	Column line of connecting wall or column.

Note: *For beam-to-wall connections, IWT and JWT refer to the I,J locations of the wall.

SET L6: SPRINGS LOCATIONS (SEE FIGURE A-16)

(SKIP THIS INPUT IF ROTATIONAL SPRINGS ARE NOT SPECIFIED)

- Reference Text:

USER TEXT

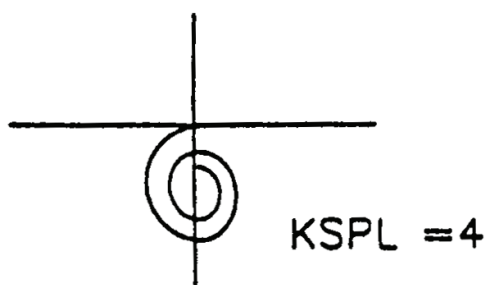
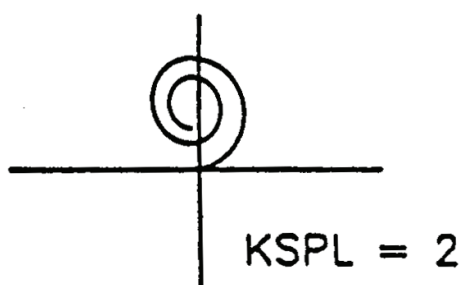
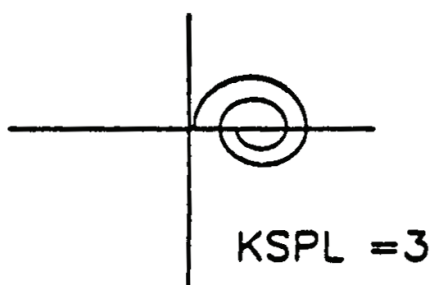
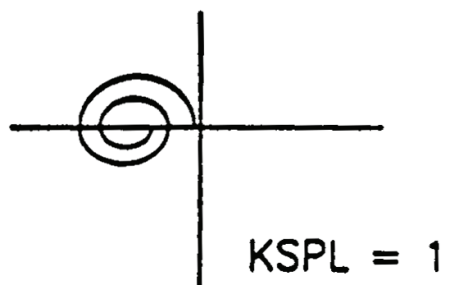
Description: **USER_TEXT**: Reference information, up to 80 characters of text.

- Spring Location (Provide one line of data for each NSPR springs):

M, ITRSP, ISP, JSP, LSP, KSPL

<i>Description:</i>	M:	Spring number.
	ITRSP:	Rotational Spring Type Number.
	ISP:	Frame number.
	JSP:	Column line number.
	LSP:	Story level.
	KSPL:	Relative spring location as follows: 1, for spring on beam, left of joint, or 2, for spring on column, top of joint, or 3, for spring on beam, right of joint, or 4, for spring on column, bottom of joint

Note: The number of springs at a joint is limited to one less than the total number of members framing into the joint.



SPRING LOCATION IDENTIFIERS

Fig. A-16 Specification of Discrete Inelastic Springs

SET L7: MOMENT RELEASES (SEE FIGURE A-17)
(SKIP THIS INPUT IF MOMENT RELEASES ARE NOT REQUIRED, NMR = 0)

- Reference Text:

USER_TEXT

Description: **USER_TEXT:** Reference information, up to 80 characters of text.

- Moment Release Locations (Provide one line of data for each NMR moment releases):

IDM, IHTY, INUM, IREG

Description: **IDM:** ID number.
 IHTY: Element type using following code:
 1 for COLUMN, or
 2 for BEAM, or
 3 for WALL.
 INUM: Column, Beam or Wall number.
 IREG: Location of hinge or moment release:
 1 for BOTTOM or LEFT,
 2 for TOP or RIGHT.

Sample Input (with reference to Fig A-13)

IDM	IHTY	INUM	IREG
1	1 (col)	10 (col #)	1 (bot)
2	2 (beam)	6 (beam#)	2 (right)

Fig. A-17 Specification of Moment Release

SET L8: BRACES CONNECTIVITIES
(SKIP THIS IF NO BRACES ARE SPECIFIED)

- Reference Text:

USER_TEXT

Description: **USER_TEXT:** Reference information, up to 80 characters of text.

- Brace Connectivities (Provide one line of data for each NBR braces):

M, IF, ITBR, ITD, LT, LB, JT, JB, AMLBR

<i>Description:</i>	M:	Brace number.
	IF:	Frame number.
	ITBR:	Brace type: 1, Visco-elastic brace, or 2, Friction damper brace, or 3, Hysteretic damper brace.
	ITD:	Property type number of specified brace.
	LT:	Story level at top side of the brace.
	LB:	Story level at bottom side of the brace.
	JT:	Column line number at top side of the brace.
	JB:	Column line number at bottom side of the brace.
	AMLBR:	Brace length (joint to joint).

SET L9: INFILL PANELS CONNECTIVITIES

(SKIP THIS IF NO INFILL PANELS ARE SPECIFIED)

- Reference Text:

USER_TEXT

<i>Description:</i>	USER_TEXT:	Reference information, up to 80 characters of text.
---------------------	-------------------	---

- Infill panels connectivities (Provide one line of data for each NIW panels):

M, IF, ITIW, LT, LB, JL, JR, JBMT

<i>Description:</i>	M:	Infill panel number.
	IF:	Frame number.
	ITIW:	Property type number of specified infill panel.
	LT:	Story level at top of infill panel.
	LB:	Story level at bottom of infill panel.
	JL:	Column line number at left side of the infill panel.
	JR:	Column line number at right side of the infill panel.
	JBMT:	Beam type number on top of infill panel

SET M: ANALYSIS OPTIONS

- General Data:

USER_TEXT

IOPT

<i>Description:</i>	USER_TEXT: Reference information, up to 80 characters of text.
IOPT:	Option for continuing analysis: 0 , STOP (Data check mode). 1 , for <u>Inelastic incremental static analysis</u> (with static loads.if specified) 2 , for <u>Monotonic "pushover" analysis</u> including static loads (if specified). 3 , for <u>Inelastic dynamic analysis</u> including static loads (if specified). 4 , for <u>Quasi-static cyclic analysis</u> including static loads (if specified).

Notes: It is generally advisable to use the "data check" mode for the first trial run of a new data set. The program performs only minimal checking of input data. Structural elevation plots generated by IDARC help identify errors in connectivity specification. Since IDARC prints all input data almost immediately after they are read, the task of detecting the source of input errors is generally expedited. It is also important to verify all printed output, especially section properties such as flexural stiffness and yield moment.

OPTION 1 permits an independent nonlinear static analysis. Static loads are input in data set M1. OPTIONS 2 - 4 may be combined with long-term static loads which is input in data set M1.

SET M1: LONG-TERM LOADING (STATIC LOADS)

- Control Information:

USER_TEXT

NLU, NLJ, NLM, NLC

<i>Description:</i>	USER_TEXT: Reference information, up to 80 characters of text.
NLU:	No. of uniformly loaded beams.
NLJ:	No. of laterally loaded joint.
NLM:	No. of specified nodal moments.
NLC:	No. of concentrated vertical loads.

Note: This input is required for all analysis options.

- Long Term Loading Analysis (Provide only when static loads are present):

JSTP, IOCRL

<i>Description:</i>	JSTP: No. of incremental steps in which to apply the static loads (default = 1 step).
---------------------	--

IOCRL: Steps between printing output (If IOCRL=0, only final results will be printed; if IOCRL=2, printout will result every 2 steps, and so on).

Notes: Dead and live loads that exist prior to the application of seismic or quasi-static cyclic loads can be input in this section. Such loads are typically specified through uniformly loaded beam members. An option is also available for lateral load analysis and the specification of nodal loads at joints. When used in conjunction with Options 2-4, the resulting forces are carried forward to the monotonic, dynamic and quasi-static analysis.

These loads are used for calculation of initial bending stresses, and do not affect the axial loads. The stresses are calculated through a global analysis of the structure (uniform loads on beams is automatically considered in columns).

- Uniformly Loaded Beam Data (Skip this input section if NLU=0):

USER_TEXT

Provide NLU lines of data as following:

IL, IBN, FU

Description: **USER_TEXT:** Reference information, up to 80 characters of text.
IL: Load number.
IBN: Beam number.
FU: Magnitude of load (Force/length).

- Laterally Loaded Joints (Skip this input section if NLJ=0):

USER_TEXT

Provide NLJ lines of data as following:

IL, LF, IF, FL

Description: **USER_TEXT:** Reference information, up to 80 characters of text.
IL: Load number (number of loaded beams).
LF: Story level number.
IF: Frame number.
FL: Magnitude of load.

- Nodal Moment Data (Skip this input section if NLM=0):

USER_TEXT

Provide NLM lines of data as following (See Figure A-9 for beam moment sign convention):

IL, IBM, FM1, FM2

Description: **USER_TEXT:** Reference information, up to 80 characters of text.
IL: Load number. (number of loaded nodes)
IBM: Beam number.
FM1: Nodal moment (left).
FM2: Nodal moment (right).

- Data on Concentrated Vertical Loads (Skip this input section if NLC=0):

USER_TEXT

Provide NLC lines of data as following:

IL, IFV, LV, JV, FV

<i>Description:</i>	USER_TEXT: Reference information, up to 80 characters of text.
IL:	Load number. (number of loaded columns)
IFV:	Frame number.
LV:	Story level number.
JV:	Column line number.
FV:	Magnitude of external nodal force.

IF IOPT = 2, CONTINUE TO SET M2.

IF IOPT = 3, CONTINUE TO SET M3.

IF IOPT = 4, CONTINUE TO SET M4.

SET M2: MONOTONIC PUSH-OVER ANALYSIS (FOR IOPT = 2 ONLY)

- General Data:

USER_TEXT

JOPT

<i>Description:</i>	USER_TEXT: Reference information, up to 80 characters of text.
JOPT:	Push over option: 1, force control 2, displacement control

For JOPT = 2 GO TO SET M2.2

SET M2.1: Force Controlled Input

(PROVIDE ONLY IF JOPT=1)

- Control Data:

USER_TEXT

ITYP

<i>Description:</i>	USER_TEXT: Reference information, up to 80 characters of text.
ITYP:	Option for lateral load distribution: 1 for linear (inverted triangle), or 2 for uniform, or 3 for modal adaptive pushover distribution, or 4 for user input, or 5 for distribution proportional to a power of the story elevation.

For ITYP = 4 GO TO Set M2.2

- Stop Criteria:

PMAX, MSTEPS, DRFLIM

<i>Description:</i>	PMAX:	Target ultimate base shear coefficient.
	MSTEPS:	Number of steps to reach PMAX.
	DRFLIM:	Upper limit for displacement of structure top-story (percentage of building height).

- Number of Modes for Modal Adaptive Option (Provide only if ITYP=3):

NMOD, POWER1, POWER2

<i>Description:</i>	NMOD:	Number of modes used during the modal adaptive pushover analysis.
	POWER1:	Power for Norm in Modal Adaptive Pushover Analysis. See Eq. A-1.
	POWER2:	<p>1 or 2: from story height for story force increments. Note: the numbers 1 and 2 are the power of story height</p> <p>3: from modal responses (more than one mode) for story force increments. Note: the number 3 is not a power, it's just a option.</p> <p>4: from fundamental mode only for story force increments. Note: the number 4 is not a power, it's just a option.</p>

$$Norm_{\text{POWER1}}(Value) = \text{POWER1} \sqrt{\sum_{n=1}^{\text{NMOD}} (Value_n)^{\text{POWER1}}} \quad (\text{A-1})$$

- Power for lateral distribution (Provide only if ITYP=5):

EXPK

<i>Description:</i>	EXPK:	Power for story elevation.
---------------------	--------------	----------------------------

Note: The lateral forces at story "i" are proportional to the story weight (W_i), and the story elevation (h_i) to the power EXPK, according to:

Error! Objects cannot be created from editing field codes.

The exponential distribution will take into account the effects of higher modes in the response. If EXPK<0 a default value is calculated as a function of the fundamental period (T):

Error! Objects cannot be created from editing field codes.

Continue to SET N

SET M2.2: Displacement Controlled Input (or User Defined Force Control)

(PROVIDE ONLY IF JOPT=2 OR JOPT=1 AND ITYP=4)

- Displacement Control Data (or User Defined Force Control Data):

USER_TEXT**NLDED**

NSTLD(1), NSTLD(2), ..., NSTLD(NLDED)

PX(1), PX(2), ..., PX(NLDED)**MSTEPS, DRFLIM**

<i>Description:</i>	USER_TEXT: Reference information, up to 80 characters of text.
NLDED:	number of loaded stories (levels).
NSTLD(i):	list of loaded stories.
PX(i):	list of maximum forces/displacements applied at loaded stories (levels).
MSTEPS:	number of steps to reach each ultimate story force/displacement.
DRFLIM:	upper limit for displacement of structure top story (percentage of building height).

Continue to SET N

SET M3: DYNAMIC ANALYSIS CONTROL PARAMETERS (FOR IOPT = 3 ONLY)

- Control Data:

USER_TEXT**GMAXH, GMAXV, DTCAL, TDUR, DAMP, ITDMP**

<i>Description:</i>	USER_TEXT: Reference information, up to 80 characters of text.
GMAXH:	Peak horizontal acceleration (g's).
GMAXV:	Peak vertical acceleration (g's).
DTCAL:	Time step for response analysis (secs).
TDUR:	Total duration of analysis (secs).
DAMP:	Damping coefficient (% of critical).
ITDMP:	Type of structural damping: 1 for Mass proportional (default), 2 for Stiffness proportional, or 3 for Rayleigh proportional damping.

Notes: 1. The input accelerogram is scaled uniformly to achieve the specified peak acceleration. DTCAL should not exceed the time interval of the input wave, DTINP. The nonlinear analysis of the structure is often very sensitive to the choice for DTCAL, a value of 0.005 is suggested for typical buildings, however, a smaller value may be necessary if drastic changes in the stiffness of the elements are expected, or if the structure consists of only a few elements. Larger values can be used for smoother transitions in the stiffness of the elements. Often an inadequate choice of this parameter will yield large unbalanced forces, that may cause numerical instabilities, and stop the execution of the program, or report extremely large values in the damage indices (DI>>3) of some or all elements.

2. The ratio (DTINP/DTCAL) must yield an integer number.

3. *TDUR may be less than the total duration of the earthquake. If TDUR is greater than the total time duration of the input wave, a free vibration analysis of the system will result for the remaining time.*

- Input Wave:

USER_TEXT

IGMOT, IWV, NDATA, DTINP

<i>Description:</i>	USER_TEXT: Reference information, up to 80 characters of text.
IGMOT:	0 for General types from wave input data files 1 Whitenose generation from program
IWV:	0 for Horizontal component of acceleration included, or 1 for Vertical component of acceleration included additionally.
NDATA:	Number of points in earthquake wave files.
DTINP:	Time interval of input wave.

IF IGMOT = 1, CONTINUE TO SET N.

- Wave Title:

NAMEW

<i>Description:</i>	NAMEW: Alpha-numeric title for input wave upto 80 characters.
---------------------	--

- Filename - Horizontal Component:

WHFILE

<i>Description:</i>	WHFILE: Name of file (with extension) from which to read horizontal component of earthquake record. Note: Filename should not exceed 12 characters.
	WINPH(I),I=1,NDATA Horizontal component of earthquake wave (NDATA points).

NOTE: This data is read from the file WHFILE specified in the previous data item.

- Filename - Vertical Component (Skip this input if IWV=0):

WVFILE

<i>Description:</i>	WVFILE: Name of file (with extension) from which to read vertical component of earthquake record. Note: Filename should not exceed 12 characters.
	WINPV(I),I=1,NDATA Vertical component of earthquake wave (NDATA points).

NOTE: This data is read from the file WVFILE specified in the previous data item.

Notes: Accelerogram data may be input in any system of units. The accelerogram is scaled uniformly to achieve the specified peak values of GMAXH and GMAXV. Since data is read in free format, as many lines as necessary to read the entire wave must be input. The data points of the input wave may, therefore, be entered sequentially until the last (or NDATA) point.

Continue to SET N

SET M4: QUASI-STATIC CYCLIC ANALYSIS (FOR IOPT=4 ONLY)

- Quasi-Static Data:

USER_TEXT

ICNTRL

NLDED

NSTLD(1), NSTLD(2), ..., NSTLD(NLDED)

NPTS

F(1,1), F(2,1), ..., F(NPTS,1)

F(1,2), F(2,2), ..., F(NPTS,2)

...

F(1,NLDED), F(2,NLDED), ..., F(NPTS,NLDED)

DTCAL

Description:

USER_TEXT: Reference information, up to 80 characters of text.

ICNTRL: Cyclic Analysis option:

0, Force controlled input, or

1, displacement controlled input.

NLDED: Number of story levels at which the force or displacement is applied.

NSTLD(j): List of story levels at which the force or displacement is applied.

NPTS: Number of points to be read in force or displacement history.

F(i,j): Quasi-Static force step “i”, at story NSTLD(j).

DTCAL: Analysis step (fraction of input steps).

The analysis is performed between (1/DTCAL) interpolated points on the input history.

SET N: OUTPUT CONTROL

SET N1: DEFORMATION, STRESS AND DAMAGE SNAPSHOTS

SET N1.1: Pushover Snapshot Control Data

(Provide only if Pushover analysis was selected in set M: IOPT=2)

- Control Data:

USER_TEXT

NPRNT

Description: **USER_TEXT:** Reference information, up to 80 characters of text.
 NPRNT: Additional number of snapshots of the structural response during pushover (≤ 10).

Notes: 1. Output in this set is written in file "DEFORMED.OUT". The story displacements, and the element stress ratios are provided at each snapshot.
2. By default the program will always identify the structural response at the first crack, first yield, or first collapse of a column, beam and wall.

- Ratios for which Additional Snapshots are Required (Provide only if NPRNT>0):

ITPRNT, UPRNT(1), UPRNT(2), ..., UPRNT(NPRNT)

Description: **ITPRNT:** Type of data provided to print snapshots:
 1 if Base shear/Total weight is specified, or
 2 if Top displacement/Total height is specified.
 UPRNT(i): List of base shear/total weight ratios (if ITPRNT=1), or top displacement/total building height (if ITPRNT=2), for which printing of additional snapshots is required.

Continue to set N1.3

SET N1.2: Dynamic and Quasistatic Analysis Snapshot Control Data

(Provide only if Dynamic or Quasistatic analysis was selected in set M: IOPT=3 or IOPT=4)

- Control Data:

USER_TEXT

NPRNT

Description: **USER_TEXT:** Reference information, up to 80 characters of text.
 NPRNT: Flag to indicate if additional snapshots during dynamic analysis are required:
 0 for no user defined additional snapshots,
 1 for user defined additional snapshots.

Notes: 1. Output in this set is written in file "DEFORMED.OUT". The story displacements, and the element stress ratios are provided at each snapshot.
2. By default the program will always identify the structural response at the first crack, first yield, or first collapse of a column, beam and wall.

- User Defined Snapshots (Provide only if NPRNT=1)

DTPRNT, DFPRNT, BSPRNT

Description:

DTPRNT:	Time increment for printing additional snapshots (Use DTPRNT≤0 to deactivate this option)
DFPRNT:	Threshold story drift ratio at which snapshots are desired (Use DFPRNT≤0 to deactivate this option)
BSPRNT:	Threshold base shear coefficient at which snapshots are desired (Use BSPRNT≤0 to deactivate this option)

Notes: 1. *Output in this set is written in file “DEFORMED.OUT”. The story displacements, and the element stress ratios are provided at each snapshot.*
 2. *By default the program will always identify the structural response at the first crack, first yield, or first collapse of a column, beam and wall.*

SET N1.3: General Snapshot Control Flags (Provide Always)

- Control Flags for Default Snapshots:

ICDPRNT(1), ICDPRNT(2), ICDPRNT(3), ICDPRNT(4), ICDPRNT(5)

Description:

ICDPRNT(1):	Flag to activate (=1), or deactivate (=0), printing of the <u>displacement profile</u> during default snapshots.
ICDPRNT(2):	Flag to activate (=1), or deactivate (=0), printing of the <u>element stress ratios</u> during default snapshots.
ICDPRNT(3):	Flag to activate (=1), or deactivate (=0), printing of the <u>element collapsed state</u> during default snapshots.
ICDPRNT(4):	Flag to activate (=1), or deactivate (=0), printing of the <u>structural damage indices</u> during default snapshots.
ICDPRNT(5):	Flag to activate (=1), or deactivate (=0), printing of the <u>structural dynamic characteristics</u> during default snapshots.

Notes: 1. *By default the program will identify the first crack, yield, and collapse of a column, beam and wall. At these stages during the pushover analysis, the user may indicate the program to report the displaced profile, the stress ratios, collapse state, damage indices, and periods.*

2. *Output for the default snapshots is written in the file “DEFORMED.OUT”.*

- Control Flags for User Defined Snapshots (Provide only if NPRNT>0):

ICPRNT(1), ICPRNT(2), ICPRNT(3), ICPRNT(4), ICPRNT(5)

Description:

ICPRNT(1):	Flag to activate (=1), or deactivate (=0), printing of the <u>displacement profile</u> during user defined snapshots.
-------------------	---

- ICPRNT(2):** Flag to activate (=1), or deactivate (=0), printing of the element stress ratios during user defined snapshots.
- ICPRNT(3):** Flag to activate (=1), or deactivate (=0), printing of the element collapsed state during user defined snapshots.
- ICPRNT(4):** Flag to activate (=1), or deactivate (=0), printing of the structural damage indices during user defined snapshots.
- ICPRNT(5):** Flag to activate (=1), or deactivate (=0), printing of the structural dynamic characteristics during user defined snapshots.

SET N2: STORY OUTPUT CONTROL

- Output Control Data:

USER_TEXT

NSOUT, DTOUT, ISO(1), ISO(2), ..., ISO(NSOUT)

FNAMES(1)

FNAMES(2)

...

FNAMES(NSOUT)

- Description:*
- USER_TEXT:** Reference information, up to 80 characters of text.
 - NSOUT:** No. of output histories.
 - DTOUT:** Output time/step interval¹.
 - ISO(i):** List of output story numbers.
 - FNAMES(i):** Filename to store time history output for story number ISO(i).

Notes: 1 If the pushover or quasi-static cyclic analysis option is used, DTOUT refers to the number of steps between output printing; for example, DTOUT=2 will print results every 2 steps.

SET N3: ELEMENT HYSTERESIS OUTPUT

- Control Data for Element Output:

USER_TEXT

KCOUT, KBOUT, KWOUT, KSOUT, KBROUT, KIWOUT

- Description:*
- USER_TEXT:** Reference information, up to 80 characters of text.
 - KCOUT:** Number of columns for which hysteresis output is required (≤ 10).
 - KBOUT:** Number of beams for which hysteresis output is required (≤ 10).
 - KWOUT:** Number of walls for which hysteresis output is required (≤ 10).

KSOUT:	Number of springs for which hysteresis output is required (≤ 10).
KBROUT:	Number of braces for which hysteresis output is required (≤ 10).
KIWOUT:	Number of infill panels for which hysteresis output is required (≤ 10).

SET N3.1: Column Output

- Column Output Specification (Skip this input if KCOUT=0):

USER_TEXT

ICLIST(1), ICLIST(2), ..., ICLIST(KCOUT)

Description: **USER_TEXT:** Reference information, up to 80 characters of text.

ICLIST(i): List of column numbers for which moment-curvature hysteresis is required.

SET N3.2: Beam Output

- Beam Output Specification (Skip this input if KBOUT=0):

USER_TEXT

IBLIST(1), IBLIST(2), ..., IBLIST(KBOUT)

Description: **USER_TEXT:** Reference information, up to 80 characters of text.

IBLIST(i): List of beam numbers for which moment-curvature hysteresis is required.

SET N3.3: Shear Wall Output

- Shear Wall Output Specification (Skip this input if KWOUT=0):

USER_TEXT

IWLIST(1), IWLIST(2), ..., IWLIST(KWOUT)

Description: **USER_TEXT:** Reference information, up to 80 characters of text.

IWLIST(i): List of shear wall numbers for which moment-curvature and shear-strain hysteresis is required.

SET N3.4: Spring Output

- Discrete Spring Output Specification (Skip this input if KSOUT=0):

USER_TEXT

ISLIST(1), ISLIST(2), ..., ISLIST(KSOUT)

Description: **USER_TEXT:** Reference information, up to 80 characters of text.

ISLIST(i): List of spring numbers for which moment-rotation hysteresis is required.

SET N3.5: Brace Output

- Brace Output Specifications (Skip this input if KBROUT=0):

USER_TEXT

IBRLIST(1), IBRLIST(2), ..., IBRLIST(KBROUT)

Description: **USER_TEXT**: Reference information, up to 80 characters of text.

IBRLIST(i): List of brace numbers for which force-displacement hysteresis is required.

SET N3.6: Infill Panel Output

- Infill Panel Output Specifications (Skip this input if KIWOUT=0):

USER_TEXT

IIWLIST(1), IIWLIST(2), ..., IIWLIST(KIWOUT)

Description: **USER_TEXT**: Reference information, up to 80 characters of text.

IIWLIST(i): List of infill panel numbers for which force-displacement hysteresis is required.

Notes: All the output generated in this section refers to moment-curvature hysteresis for beams, columns and shear-walls; in addition shear vs. shear strain history is generated for walls; whereas moment-rotation hysteresis is produced for the discrete spring elements. Output filenames are generated as follows:

IF $KCOUT = 2$, AND $ICLIST(1) = 3$ AND $ICLIST(2) = 12$, THEN THE FOLLOWING FILES WILL BE CREATED:

COL_003.PRN and COL_012.PRN

(where 3 and 12 refer to the element numbers for which output is requested)

END OF DATA INPUT

SPECIAL SPRING BASE ISOLATOR

The element can be used as diagonal brace, or as base isolator, if columns are infinitely flexible. To develop such element is required to follow the steps below. The development provided below is as an example for a “twisted hysteretic model” defined by a lower and upper bound curves.

SET J: BRACES PROPERTIES SETS

SET J3: HYSTERETIC DAMPER BRACE PROPERTIES SETS

(Provide ITDHCON=0 only)

SET J3-1: HYSTERETIC DAMPER BRACE PROPERTIES

- General Data (Provide one line of data for each MBRH hysteretic brace type):

ITDH, 2, KDH, FYDH, RPSTDH, POWER, ETA

Description: **ITDH:** Hysteretic damper brace type set number.

KDH: Axial stiffness (k_0).

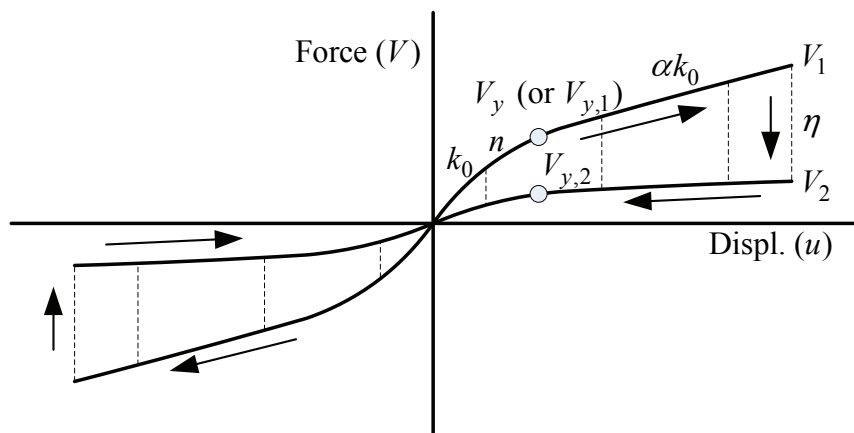
FYDH: Yield force of this type of hysteretic dampers (V_y).

RPSTDH: Post yield stiffness ratio (α).

POWER: Power of stiffness transition (n).

ETA: Ratio of forces in upper to lower bound curves (η).

Note: The program calculates the angle of inclination of the brace internally based on the length of columns and beams. For a base isolator provide “very small length” columns.



APPENDIX B

SAMPLE INPUT

CASE STUDY #1

*input filename: idarc.dat
data filename: case1.dat
output filename: idarc.out
results filename: case1.out*

file: idarc.dat

case1.dat
case1.out

file: case1.dat

CASE STUDY # 1 : Circular Column Test
CONTROL DATA
1, 1, 1, 1, 0, 1, 0, 0, 1
ELEMENT TYPES
1, 0, 0, 0, 0, 0, 0, 0, 0
ELEMENT DATA
1, 0, 0, 0, 0, 0, 0, 0
UNIT SYSTEM (KIPS/INCH)
1
FLOOR ELEVATIONS
360.0
DESCRIPTION OF IDENTICAL FRAMES
1
PLAN CONFIGURATION (SINGLE COLUMN LINE)
1
NODAL WEIGHTS
1, 1, 300.0
CODE FOR SPECIFICATION OF USER PROPERTIES
0
CONCRETE PROPERTIES
1, 5.2, 4110.0, 0.2, 0.624, 0.0, 0.0
REINFORCEMENT PROPERTIES
1, 68.9, 103.6, 27438.0, 0.0, 0.0
HYSTERETIC MODELING RULES
1
1, 1, 100.0, 0.01, 0.05, 1.0, 2
MOMENT CURVATURE ENVELOPE GENERATION
0
COLUMN DIMENSIONS
3
1,1,1,1, 360.0, 0.0, 0.0, 1000.0, 60.0, 2.5, 54.5, 25, 1.69, 0.625, 3.5
COLUMN CONNECTIVITY
1,1,1,1,0,1

ANALYSIS TYPE

4

STATIC ANALYSIS OPTION (Axial Force Only)

0,0,0,1

4,1

Nodal Loads

1, 1, 1, 1, 900.0

Quasistatic Analysis

1

1

1

301

0.0	2.5	0.0	-2.80	0.0	3.5	7.060	3.5	0.0	-3.5
-7.03	-3.5	0.0	3.50	7.08	3.5	0.0	-3.5	-7.02	-3.5
0.0	5.0	9.0	10.60	9.0	5.0	0.0	-5.0	-9.0	-10.55
-9.0	-5.0	0.0	5.0	9.0	10.6	9.0	5.0	0.0	-5.0
-9.0	-10.55	-9.0	-5.0	0.0	5.0	10.0	13.5	14.08	13.5
10.0	5.0	0.0	-5.0	-10.0	-13.5	-14.05	-13.5	-10.0	-5.0
0.0	5.0	10.0	13.5	14.07	13.5	10.0	5.0	0.0	-5.0
-10.0	-13.5	-14.05	-13.5	-10.0	-5.0				
0.0	5.0	10.0	13.5	14.08	13.5	10.0	5.0	0.0	-5.0
-10.0	-13.5	-14.08	-13.5	-10.0	-5.0				
0.0	5.0	10.0	13.5	14.08	13.5	10.0	5.0	0.0	-5.0
-10.0	-13.5	-14.07	-13.5	-10.0	-5.0				
0.0	5.0	10.0	13.5	14.10	13.5	10.0	5.0	0.0	-5.0
-10.0	-13.5	-14.07	-13.5	-10.0	-5.0				
0.0	5.0	10.0	13.5	14.10	13.5	10.0	5.0	0.0	-5.0
-10.0	-13.5	-14.07	-13.5	-10.0	-5.0				
0.0	5.0	10.0	13.5	14.12	13.5	10.0	5.0	0.0	-5.0
-10.0	-13.5	-14.07	-13.5	-10.0	-5.0				
0.0	5.0	10.0	13.5	14.12	13.5	10.0	5.0	0.0	-5.0
-10.0	-13.5	-14.07	-13.5	-10.0	-5.0				
0.0	5.0	10.0	13.5	14.12	13.5	10.0	5.0	0.0	-5.0
-10.0	-13.5	-14.07	-13.5	-10.0	-5.0				
0.0	5.0	10.0	13.5	14.12	13.5	10.0	5.0	0.0	-5.0
-10.0	-13.5	-14.07	-13.5	-10.0	-5.0				
0.0	5.0	10.0	13.5	14.10	13.5	10.0	5.0	0.0	-5.0
-10.0	-13.5	-14.07	-13.5	-10.0	-5.0				
0.0	5.0	10.0	13.5	14.12	13.5	10.0	5.0	0.0	-5.0
-10.0	-13.5	-14.07	-13.5	-10.0	-5.0				
0.0	5.0	10.0	13.5	14.12	13.5	10.0	5.0	0.0	-5.0
-10.0	-13.5	-14.07	-13.5	-10.0	-5.0				
0.0	5.0	10.0	13.5	14.10	13.5	10.0	5.0	0.0	-5.0
-10.0	-13.5	-14.07	-13.5	-10.0	-5.0				
0.0	5.0	10.0	13.5	14.12	13.5	10.0	5.0	0.0	-5.0
-10.0	-13.5	-14.07	-13.5	-10.0	-5.0				
0.0	5.0	10.0	16.0	17.66	15.5	10.0	5.0	0.0	-5.0
-10.0	-15.5	-17.66	-15.5	-10.0	-5.0				
0.0	5.0	10.0	16.0	17.66	15.5	10.0	5.0	0.0	-5.0
-10.0	-15.5	-17.66	-15.5	-10.0	-5.0				
0.0	5.0	10.0	16.0	17.66	15.5	10.0	5.0	0.0	-5.0
-10.0	-15.5	-17.66	-15.5	-10.0	-5.0				
0.0	6.0	12.0	20.0	21.30	20.0	12.0	6.0	0.0	-6.0
-12.0	-20.0	-21.19	-20.0	-12.0	-6.0				
0.0	6.0	12.0	20.0	21.32	20.0	12.0	6.0	0.0	-6.0
-12.0	-20.0	-21.27	-20.0	-12.0	-6.0	0.0			

0.005

SNAPSHOT OUTPUT

0,

0,0,0,0,0
OUTPUT CONTROL
1,6,1
CYC1.OUT
MISCELLANEOUS OUTPUT INFORMATION
1,0,0,0,0,0
COLUMN OUTPUT
1

CASE STUDY #2

*input filename: idarc.dat
data filename: case2.dat
output filename: idarc.out
results filename: case2.out*

file: idarc.dat

case2.dat
case2.out

file: case2.dat

CASE STUDY # 2: 1:2 SCALE THREE STORY FRAME
CONTROL DATA

3,1,1,1,0,0,0,0,1

ELEMENT TYPES

4,5,0,0,0,0,0,0,0

ELEMENT DATA

9,6,0,0,0,0,0,0,0

UNITS SYSTEM : KN - MM

2

FLOOR ELEVATIONS

1500.0, 3000.0, 4500.0

DESCRIPTION OF IDENTICAL FRAMES

1

PLAN CONFIGURATION: NO OF COLUMN LINES

3

NODAL WEIGHTS

1,1, 22.24, 22.24, 22.24

2,1, 22.24, 22.24, 22.24

3,1, 22.24, 22.24, 22.24

CODE FOR SPECIFICATION OF USER PROPERTIES

0

CONCRETE PROPERTIES

1, 0.0402, 0.0, 0.0, 0.0, 0.0, 0.0

REINFORCEMENT PROPERTIES

1, 0.4, 0.0, 0.0, 0.0, 0.0

HYSTERETIC MODELING RULES

2

1, 1, 200.0, 0.01, 0.01, 1.0, 2

2, 1, 200.0, 0.01, 0.01, 1.0, 2

MOMENT CURVATURE ENVELOPE GENERATION

0

COLUMN DIMENSIONS

1

1,1,1, 594.2, 1498.6, 149.86, 149.86,

1, 250.0, 250.0, 15.0, 100.2, 8.0, 55.0, 0.5

2, 250.0, 250.0, 15.0, 100.2, 8.0, 55.0, 0.5

1

2,1,1, 990.6, 1498.6, 149.86, 149.86,

1, 250.0, 250.0, 15.0, 307.7, 12.0, 75.0, 0.5

2, 250.0, 250.0, 15.0, 307.7, 12.0, 75.0, 0.5
 1
 3,1,1, 594.2, 1498.6, 0.0, 149.86,
 1, 250.0, 250.0, 15.0, 307.7, 12.0, 75.0, 0.5
 2, 250.0, 250.0, 15.0, 307.7, 12.0, 75.0, 0.5
 1
 4,1,1, 990.6, 1498.6, 0.0, 149.86,
 1, 250.0, 250.0, 15.0, 307.7, 12.0, 75.0, 0.5
 2, 250.0, 250.0, 15.0, 307.7, 12.0, 75.0, 0.5
 BEAM MOMENT CURVATURE ENVELOPE GENERATION
 0
 BEAM DIMENSIONS
 1
 1,1,1, 3000.0, 125.0, 125.0
 1, 300.0, 150.0, 150.0, 0.0, 0.0, 15.0, 401.9, 401.9, 6.0, 75.0
 1, 300.0, 150.0, 150.0, 0.0, 0.0, 15.0, 401.9, 401.9, 6.0, 75.0
 1
 2,1,1, 3000.0, 125.0, 125.0
 1, 300.0, 150.0, 150.0, 0.0, 0.0, 15.0, 480.6, 401.9, 6.0, 75.0
 1, 300.0, 150.0, 150.0, 0.0, 0.0, 15.0, 401.9, 509.0, 6.0, 75.0
 1
 3,1,1, 3000.0, 125.0, 125.0
 1, 300.0, 150.0, 150.0, 0.0, 0.0, 15.0, 401.9, 509.0, 6.0, 75.0
 1, 300.0, 150.0, 150.0, 0.0, 0.0, 15.0, 480.6, 401.9, 6.0, 75.0
 1
 4,1,1, 3000.0, 125.0, 125.0
 1, 300.0, 150.0, 150.0, 0.0, 0.0, 15.0, 307.7, 226.5, 6.0, 75.0
 1, 300.0, 150.0, 150.0, 0.0, 0.0, 15.0, 307.7, 307.7, 6.0, 75.0
 1
 5,1,1, 3000.0, 125.0, 125.0
 1, 300.0, 150.0, 150.0, 0.0, 0.0, 15.0, 307.7, 226.5, 6.0, 75.0
 1, 300.0, 150.0, 150.0, 0.0, 0.0, 15.0, 307.7, 307.7, 6.0, 75.0
 COLUMN CONNECTIVITY
 1,1,1,1,2,3
 2,2,1,2,2,3
 3,1,1,3,2,3
 4,1,1,1,1,2
 5,2,1,2,1,2
 6,1,1,3,1,2
 7,3,1,1,0,1
 8,4,1,2,0,1
 9,3,1,3,0,1
 BEAM CONNECTIVITY
 1,5,3,1,1,2
 2,4,3,1,2,3
 3,3,2,1,1,2
 4,2,2,1,2,3
 5,1,1,1,1,2
 6,1,1,1,2,3
 ANALYSIS TYPE
 4

STATIC ANALYSIS OPTION
 0,0,0,
 QUASI-STATIC CYCLIC ANALYSIS
 1
 1
 3
 249

0.0000	6.8580	0.0000	-6.8580	0.0000	10.1600
0.0000	-10.1600	0.0000	12.7000	25.4000	32.4104
25.4000	12.7000	0.0000	-12.7000	-25.4000	-32.0802
-25.4000	-12.7000	0.0000	12.7000	25.4000	31.9024
25.4000	12.7000	0.0000	-12.7000	-25.4000	-29.7180
-25.4000	-12.7000	0.0000	12.7000	25.4000	30.0482
25.4000	12.7000	0.0000	-12.7000	-25.4000	-28.7020
-25.4000	-12.7000	0.0000	20.3200	40.6400	50.8000
55.8800	50.8000	40.6400	20.3200	0.0000	-20.3200
-40.6400	-50.8000	-53.3400	-50.8000	-40.6400	-20.3200
0.0000	20.3200	40.6400	50.8000	57.4040	50.8000
40.6400	20.3200	0.0000	-20.3200	-40.6400	-50.8000
-54.3560	-50.8000	-40.6400	-20.3200	0.0000	20.3200
40.6400	50.8000	56.1340	50.8000	40.6400	20.3200
0.0000	-20.3200	-40.6400	-50.8000	-54.1020	-50.8000
-40.6400	-20.3200	0.0000	25.4000	50.8000	76.2000
86.8680	76.2000	50.8000	25.4000	0.0000	-25.4000
-50.8000	-76.2000	-83.3120	-76.2000	-50.8000	-25.4000
0.0000	25.4000	50.8000	76.2000	87.1220	76.2000
50.8000	25.4000	0.0000	-25.4000	-50.8000	-76.2000
-84.5820	-76.2000	-50.8000	-25.4000	0.0000	25.4000
50.8000	76.2000	88.6460	76.2000	50.8000	25.4000
0.0000	-25.4000	-50.8000	-76.2000	-84.5820	-76.2000
-50.8000	-25.4000	0.0000	38.1000	76.2000	106.6800
114.3000	106.6800	76.2000	38.1000	0.0000	-38.1000
-76.2000	-106.6800	-111.7600	-106.6800	-76.2000	-38.1000
0.0000	38.1000	76.2000	106.6800	114.3000	106.6800
76.2000	38.1000	0.0000	-38.1000	-76.2000	-106.6800
-112.2680	-106.6800	-76.2000	-38.1000	0.0000	38.1000
76.2000	106.6800	113.5380	106.6800	76.2000	38.1000
0.0000	-38.1000	-76.2000	-106.6800	-112.2680	-106.6800
-76.2000	-38.1000	0.0000	38.1000	76.2000	114.3000
139.7000	147.8280	139.7000	114.3000	76.2000	38.1000
0.0000	-38.1000	-76.2000	-114.3000	-121.9200	-127.7620
-121.9200	-114.3000	-76.2000	-38.1000	0.0000	38.1000
76.2000	114.3000	139.7000	147.0660	139.7000	114.3000
76.2000	38.1000	0.0000	-38.1000	-76.2000	-114.3000
-121.9200	-128.0160	-121.9200	-114.3000	-76.2000	-38.1000
0.0000	38.1000	76.2000	114.3000	139.7000	147.3200
139.7000	114.3000	76.2000	38.1000	0.0000	-38.1000
-76.2000	-114.3000	-121.9200	-127.0000	-121.9200	-114.3000
-76.2000	-38.1000	0.0000			

0.02
 SNAPSHOT OUTPUT CONTROL

0
0,0,0,0,0
STORY OUTPUT CONTROL
3,1,1,2,3
LEVEL1.OUT
LEVEL2.OUT
LEVEL3.OUT
ELEMENT HYSTERESIS OUTPUT INFORMATION
6,3,0,0,0,0
COLUMN OUTPUT
1 2 3 4 5 6
BEAM OUTPUT
1 2 3

CASE STUDY #3

input filename: idarc.dat
data filename: case3.dat
output filename: idarc.out
results filename: case3.out

file: idarc.dat

case3.dat
case3.out

file: case3.dat

CASE STUDY # 3 : TEN STORY MODEL STRUCTURE

CONTROL DATA

10,1,1,1,0,0,0,1,1

ELEMENT TYPES

20,2,0,0,0,0,0,0,0,0

ELEMENT DATA

40,30,0,0,0,0,0,0,0

UNITS SYSTEM

1

FLOOR ELEVATIONS

9.0,18.0,27.0,36.0,45.0,54.0,63.0,72.0,81.0,90.0

DESCRIPTION OF IDENTICAL FRAMES

2

PLAN CONFIGURATION

4

NODAL WEIGHTS

1, 1, 0.125, 0.125, 0.125, 0.125

2, 1, 0.125, 0.125, 0.125, 0.125

3, 1, 0.125, 0.125, 0.125, 0.125

4, 1, 0.125, 0.125, 0.125, 0.125

5, 1, 0.125, 0.125, 0.125, 0.125

6, 1, 0.125, 0.125, 0.125, 0.125

7, 1, 0.125, 0.125, 0.125, 0.125

8, 1, 0.125, 0.125, 0.125, 0.125

9, 1, 0.125, 0.125, 0.125, 0.125

10, 1, 0.125, 0.125, 0.125, 0.125

CODE FOR SPECIFICATION OF USER PROPERTIES

0

CONCRETE PROPERTIES

1, 4.35, 1000.0, 0.3, 0.435, 1.2, 100.0

REINFORCEMENT PROPERTIES

1, 70.0, 72.5, 29000.0, 40.0, 2.0

HYSTERETIC MODELING RULES

2

1, 1, 10.0, 0.01, 0.15, 1.0, 2

2, 1, 20.0, 0.01, 0.15, 1.0, 2

COLUMN MOMENT CURVATURE ENVELOPE GENERATION

0

COLUMN DIMENSIONS

1
 1,1,1,1.25,9.0,0.0,0.75,
 1, 2.0,1.5,0.25,0.049,0.0625,0.35,0.5
 1, 2.0,1.5,0.25,0.049,0.0625,0.35,0.5
 1
 2,1,1,1.12,9.0,0.75,0.75,
 1, 2.0,1.5,0.25,0.049,0.0625,0.35,0.5
 1, 2.0,1.5,0.25,0.049,0.0625,0.35,0.5
 1
 3,1,1,1.00,9.0,0.75,0.75,
 1, 2.0,1.5,0.25,0.049,0.0625,0.35,0.5
 1, 2.0,1.5,0.25,0.049,0.0625,0.35,0.5
 1
 4,1,1,0.88,9.0,0.75,0.75,
 1, 2.0,1.5,0.25,0.049,0.0625,0.35,0.5
 1, 2.0,1.5,0.25,0.049,0.0625,0.35,0.5
 1
 5,1,1,0.75,9.0,0.75,0.75,
 1, 2.0,1.5,0.25,0.049,0.0625,0.35,0.5
 1, 2.0,1.5,0.25,0.029,0.0625,0.35,0.5
 1
 6,1,1,0.63,9.0,0.75,0.75,
 1, 2.0,1.5,0.25,0.029,0.0625,0.35,0.5
 1, 2.0,1.5,0.25,0.029,0.0625,0.35,0.5
 1
 7,1,1,0.50,9.0,0.75,0.75,
 1, 2.0,1.5,0.25,0.029,0.0625,0.35,0.5
 1, 2.0,1.5,0.25,0.029,0.0625,0.35,0.5
 1
 8,1,1,0.38,9.0,0.75,0.75,
 1, 2.0,1.5,0.25,0.029,0.0625,0.35,0.5
 1, 2.0,1.5,0.25,0.029,0.0625,0.35,0.5
 1
 9,1,1,0.25,9.0,0.75,0.75,
 1, 2.0,1.5,0.25,0.029,0.0625,0.35,0.5
 1, 2.0,1.5,0.25,0.029,0.0625,0.35,0.5
 1
 10,1,1,0.13,9.0,0.75,0.75,
 1, 2.0,1.5,0.25,0.029,0.0625,0.35,0.5
 1, 2.0,1.5,0.25,0.029,0.0625,0.35,0.5
 1
 11,1,1,1.25,9.0,0.0,0.75,
 1, 2.0,1.5,0.25,0.041,0.0625,0.35,0.5
 1, 2.0,1.5,0.25,0.041,0.0625,0.35,0.5
 1
 12,1,1,1.13,9.0,0.75,0.75,
 1, 2.0,1.5,0.25,0.041,0.0625,0.35,0.5
 1, 2.0,1.5,0.25,0.041,0.0625,0.35,0.5
 1
 13,1,1,1.00,9.0,0.75,0.75,
 1, 2.0,1.5,0.25,0.041,0.0625,0.35,0.5

1, 2.0,1.5,0.25,0.041,0.0625,0.35,0.5
 1
 14,1,1,0.88,9.0,0.75,0.75,
 1, 2.0,1.5,0.25,0.041,0.0625,0.35,0.5
 1, 2.0,1.5,0.25,0.041,0.0625,0.35,0.5
 1
 15,1,1,0.75,9.0,0.75,0.75,
 1, 2.0,1.5,0.25,0.041,0.0625,0.35,0.5
 1, 2.0,1.5,0.25,0.013,0.0625,0.35,0.5
 1
 16,1,1,0.63,9.0,0.75,0.75,
 1, 2.0,1.5,0.25,0.013,0.0625,0.35,0.5
 1, 2.0,1.5,0.25,0.013,0.0625,0.35,0.5
 1
 17,1,1,0.50,9.0,0.75,0.75,
 1, 2.0,1.5,0.25,0.013,0.0625,0.35,0.5
 1, 2.0,1.5,0.25,0.013,0.0625,0.35,0.5
 1
 18,1,1,0.38,9.0,0.75,0.75,
 1, 2.0,1.5,0.25,0.013,0.0625,0.35,0.5
 1, 2.0,1.5,0.25,0.013,0.0625,0.35,0.5
 1
 19,1,1,0.25,9.0,0.75,0.75,
 1, 2.0,1.5,0.25,0.013,0.0625,0.35,0.5
 1, 2.0,1.5,0.25,0.013,0.0625,0.35,0.5
 1
 20,1,1,0.13,9.0,0.75,0.75,
 1, 2.0,1.5,0.25,0.013,0.0625,0.35,0.5
 1, 2.0,1.5,0.25,0.013,0.0625,0.35,0.5
 BEAM MOMENT CURVATURE ENVELOPE GENERATION
 0
 BEAM DIMENSIONS
 1
 1,1,1,12.0,0.75,0.75,
 2, 1.5,1.5,1.5,0.0,0.25,0.0092,0.0092,0.0625,0.3
 2, 1.5,1.5,1.5,0.0,0.25,0.0092,0.0092,0.0625,0.3
 1
 2,1,1,12.0,0.75,0.75,
 2, 1.5,1.5,1.5,0.0,0.25,0.013,0.013,0.0625,0.3
 2, 1.5,1.5,1.5,0.0,0.25,0.013,0.013,0.0625,0.3
 COLUMN CONNECTIVITY
 1 1 1 1 0 1
 2 2 1 1 1 2
 3 3 1 1 2 3
 4 4 1 1 3 4
 5 5 1 1 4 5
 6 6 1 1 5 6
 7 7 1 1 6 7
 8 8 1 1 7 8
 9 9 1 1 8 9
 10 10 1 1 9 10

11	11	1	2	0	1
12	12	1	2	1	2
13	13	1	2	2	3
14	14	1	2	3	4
15	15	1	2	4	5
16	16	1	2	5	6
17	17	1	2	6	7
18	18	1	2	7	8
19	19	1	2	8	9
20	20	1	2	9	10
21	11	1	3	0	1
22	12	1	3	1	2
23	13	1	3	2	3
24	14	1	3	3	4
25	15	1	3	4	5
26	16	1	3	5	6
27	17	1	3	6	7
28	18	1	3	7	8
29	19	1	3	8	9
30	20	1	3	9	10
31	1	1	4	0	1
32	2	1	4	1	2
33	3	1	4	2	3
34	4	1	4	3	4
35	5	1	4	4	5
36	6	1	4	5	6
37	7	1	4	6	7
38	8	1	4	7	8
39	9	1	4	8	9
40	10	1	4	9	10

BEAM CONNECTIVITY

1	2	1	1	1	2
2	2	2	1	1	2
3	2	3	1	1	2
4	2	4	1	1	2
5	1	5	1	1	2
6	1	6	1	1	2
7	1	7	1	1	2
8	1	8	1	1	2
9	1	9	1	1	2
10	1	10	1	1	2
11	2	1	1	2	3
12	2	2	1	2	3
13	2	3	1	2	3
14	2	4	1	2	3
15	1	5	1	2	3
16	1	6	1	2	3
17	1	7	1	2	3
18	1	8	1	2	3
19	1	9	1	2	3
20	1	10	1	2	3

```

21 2 1 1 3 4
22 2 2 1 3 4
23 2 3 1 3 4
24 2 4 1 3 4
25 1 5 1 3 4
26 1 6 1 3 4
27 1 7 1 3 4
28 1 8 1 3 4
29 1 9 1 3 4
30 1 10 1 3 4
ANALYSIS TYPE
3
STATIC ANALYSIS OPTION
0,0,0,0
DYNAMIC ANALYSIS CONTROL PARAMETERS
1.6163, 0.0, 0.01, 40.0, 2.0, 3
INPUT WAVE INFORMATION
0, 0, 1000,0.04
Recorded Table Motion
waveh.dat
SNAPSHOT CONTROL
0
0,0,0,0
OUTPUT CONTROL
5,0.02,1,2,3,4,5
LEVEL1.OUT
LEVEL2.OUT
LEVEL3.OUT
LEVEL4.OUT
LEVEL5.OUT
ELEMENT HYSTERESIS OUTPUT INFORMATION
1,1,0,0,0,0
COLUMN OUTPUT
1,37
BEAM OUTPUT
1,21

```

NOTES : The earthquake ground acceleration record is read separately from a file named ‘waveh.dat’ as specified in the input data

CASE STUDY #4

*input filename: idarc.dat
data filename: case4.dat
output filename: idarc.out
results filename: case4.out*

file: idarc.dat

case4.dat
case4.out

file: case4.dat

CASE4: Analysis of 1:3 Scale Three Story Model 0.05g

Control Data

3,1,0,0,0,0,0,1,1

Element types

6,1,0,0,0,0,0,0,0

Element data

12,9,0,0,0,0,0,0,0

Unit system

1

Floor elevations

45.0, 93.0, 141.0

Number of duplicate frames

2

No of column lines

4

Nodal weights

1, 1, 3.375, 3.375, 3.375, 3.375

2, 1, 3.375, 3.375, 3.375, 3.375

3, 1, 3.375, 3.375, 3.375, 3.375

Env generation option

1

Hysteretic Control

2

1, 1, 5.0, 0.01, 0.15, 1.0, 0

2, 1, 10.0, 0.01, 0.15, 1.0, 0

Column input option

1

Column data

1

1, 10, 20, 50, 48.0, 3.0, 3.0

1, 45400.0, 843.0, 10.0, 18.0, 0.00200, 0.006, 0.88

10.0, 18.0, 0.00200, 0.006, 0.88

1, 45400.0, 843.0, 10.0, 18.0, 0.00200, 0.006, 0.88

10.0, 18.0, 0.00200, 0.006, 0.88

1

2, 10, 20, 50, 48.0, 3.0, 3.0

1, 45400.0, 843.0, 10.0, 22.0, 0.00200, 0.006, 0.88

10.0, 22.0, 0.00200, 0.006, 0.88

1, 45400.0, 843.0, 10.0, 22.0, 0.00200, 0.006, 0.88

	10.0, 22.0, 0.00200, 0.006,	0.88
1		
3, 10, 20, 50, 48.0, 3.0, 3.0		
1, 45900.0, 900.0, 10.0, 22.0, 0.003, 0.006,	0.87	
10.0, 22.0, 0.003, 0.006,	0.87	
1, 45900.0, 900.0, 10.0, 22.0, 0.003, 0.006,	0.87	
10.0, 22.0, 0.003, 0.006,	0.87	
1		
4, 10, 20, 50, 48.0, 3.0, 3.0		
1, 45900.0, 900.0, 14.0, 29.0, 0.003, 0.006,	0.87	
14.0, 29.0, 0.003, 0.006,	0.87	
1, 45900.0, 900.0, 14.0, 29.0, 0.003, 0.006,	0.87	
14.0, 29.0, 0.003, 0.006,	0.87	
1		
5, 10, 20, 50, 45.0, 0.0, 3.0		
1, 45200.0, 960.0, 12.0, 28.0, 0.003, 0.008,	0.88	
12.0, 28.0, 0.003, 0.008,	0.88	
1, 45200.0, 960.0, 12.0, 28.0, 0.003, 0.008,	0.88	
12.0, 28.0, 0.003, 0.008,	0.88	
1		
6, 10, 20, 50, 45.0, 0.0, 3.0		
1, 45200.0, 960.0, 16.0, 38.0, 0.003, 0.008,	0.88	
16.0, 38.0, 0.003, 0.008,	0.88	
1, 45200.0, 960.0, 16.0, 38.0, 0.003, 0.008,	0.88	
16.0, 38.0, 0.003, 0.008,	0.88	

Beam input type

1

Beam data

1

1, 72.0, 2.0, 2.0

2, 140000.0, 15.0, 30.0, 0.001, 0.01,	1.71
30.0, 70.0, 0.001, 0.01,	1.71
2, 140000.0, 15.0, 30.0, 0.001, 0.01,	1.71
30.0, 70.0, 0.001, 0.01,	1.71

Column connectivity

1,1,1,2,3

2,2,1,2,2,3

3,2,1,3,2,3

4,1,1,4,2,3

5,3,1,1,1,2

6,4,1,2,1,2

7,4,1,3,1,2

8,3,1,4,1,2

9,5,1,1,0,1

10,6,1,2,0,1

11,6,1,3,0,1

12,5,1,4,0,1

Beam connectivity

1,1,3,1,1,2

2,1,3,1,2,3

3,1,3,1,3,4

4,1,2,1,1,2
5,1,2,1,2,3
6,1,2,1,3,4
7,1,1,1,1,2
8,1,1,1,2,3
9,1,1,1,3,4
Type of Analysis
3
Static loads
0,0,0,0
Dynamic Analysis Control Data
0.2, 0.0, 0.001, 30.0, 1.2, 3
Wave data
0, 0, 4100,0.01
TAFT - EARTHQUAKE
wave05.dat
SNAPSHOT CONTROL DATA
0
0,0,0,0,0
Output options
1, 0.01, 3
JELAS.PRN
Hys output
0,0,0,0,0,0

NOTES : The earthquake ground acceleration record is read separately from a file named 'wave05.dat' as specified in the input data

CASE STUDY #5

*input filename: idarc.dat
data filename: case5.dat
output filename: idarc.out
results filename: case5.out*

file: idarc.dat

case5.dat
case5.out

file: case5.dat

CASE 5: Seismic Damage Analysis of Cypress Viaduct

Control Data - 4 stories, 1 frame, 1 conc and 1 steel type

4, 1, 1, 1, 0, 0, 0, 0, 1

Element types: 2 cols, 12 beams, 2 walls

2, 12, 2, 0, 0, 0, 0, 0, 0

Element data: 4 columns, 12 beams, 2 walls

4, 12, 2, 0, 0, 4, 0, 0

System of units: k/in

1

Floor elevations

252.0 327.0 328.0 528.0

Duplicate frame info

1

No of column lines

7

Nodal weights (Note: Story 2 & 3 are dummy levels)

1 1 116.7 233.3 233.3 233.3 233.3 233.3 116.7

2 1 0.0 0.0 0.0 0.0 0.0 0.0 0.0

3 1 0.0 0.0 0.0 0.0 0.0 0.0 0.0

4 1 116.7 233.3 233.3 233.3 233.3 233.3 116.7

Option for M-phi input

1

Hysteresis Rules

4

1, 1, 18.0, 0.01, 0.15, 1.0, 0

2, 1, 18.0, 0.01, 0.15, 1.0, 0

3, 1, 18.0, 0.01, 0.15, 1.0, 0

4, 1, 15.0, 0.01, 0.3, 1.0, 0

Option for column input

1

COLUMN DATA

1

1 0.0 1.0e15 5.0e14 252.0 0.0 48.0

-1 8.38E+9 8.73e+4 50350 266300 5.12e-5 2.19e-4 1.63
50350 266300 5.12e-5 2.19e-4 1.63

1

2 0.0 1.0e15 5.0e14 201 0.0 48.0

1 1.02e+9 5.82e+4 12200 64350 1.04e-4 4.07e-4 1.81
12200 64350 1.04e-4 4.07e-4 1.81

1	2.32e+9	7.41e+4	19200	90300	7.24e-5	3.70e-4	1.38
			19200	90300	7.24e-5	3.70e-4	1.38

Option for beam input

1

BEAM DATA

1

1	117.0	48.0	0.0				
2	2.00E+10	45700	70500	2.29E-5	8.78E-4	0.31	
		47100	136800	2.51E-5	5.68E-4	0.58	
2	2.00E+10	45900	117800	2.48E-5	5.68E-4	0.51	
		40900	45600	2.27E-5	9.21E-4	0.21	

1

2	117.0	0.0	0.0				
2	2.00E+10	45900	117800	2.48E-5	5.68E-4	0.51	
		40900	45600	2.27E-5	9.21E-4	0.21	
2	2.00E+10	48500	208200	2.84E-5	3.07E-4	0.64	
		18500	20600	2.11E-5	8.23E-4	0.14	

1

3	117.0	0.0	0.0				
2	2.00E+10	48500	208200	2.84E-5	3.07E-4	0.64	
		18500	20600	2.11E-5	8.23E-4	0.14	
2	2.00E+10	49000	222300	2.87E-5	2.89E-4	0.65	
		18500	20600	2.10E-5	7.81E-4	0.15	

1

4	117.0	0.0	0.0				
2	2.00E+10	49000	222300	2.87E-5	2.89E-4	0.65	
		18500	20600	2.10E-5	7.81E-4	0.15	
2	2.00E+10	48500	208200	2.84E-5	3.07E-4	0.64	
		18500	20600	2.11E-5	8.23E-4	0.14	

1

5	117.0	0.0	0.0				
2	2.00E+10	48500	208200	2.84E-5	3.07E-4	0.64	
		18500	20600	2.11E-5	8.23E-4	0.14	
2	2.00E+10	45900	117800	2.48E-5	5.68E-4	0.51	
		40900	45600	2.27E-5	9.21E-4	0.21	

1

6	117.0	0.0	48.0				
2	2.00E+10	45900	117800	2.48E-5	5.68E-4	0.51	
		40900	45600	2.27E-5	9.21E-4	0.21	
2	2.00E+10	45700	70500	2.29E-5	8.78E-4	0.31	
		47100	136800	2.51E-5	5.68E-4	0.58	

1

7	117.0	24.0	0.0				
2	2.00E+10	44800	86800	2.39E-5	6.36E-4	0.38	
		44100	54500	2.31E-5	9.10E-4	0.25	
2	2.00E+10	49200	224300	2.98E-5	2.96E-4	0.64	
		25500	28600	2.24E-5	7.51E-4	0.18	

1

8	117.0	0.0	0.0				
2	2.00E+10	49200	224300	2.98E-5	2.96E-4	0.64	
		25500	28600	2.24E-5	7.51E-4	0.18	

2	2.00E+10	51200	301900	3.33E-5	2.16E-4	0.49
		21600	24000	2.14E-5	5.62E-4	0.29
1						
9	117.0	0.0	0.0			
2	2.00E+10	51200	301900	3.33E-5	2.16E-4	0.49
		21600	24000	2.14E-5	5.62E-4	0.29
2	2.00E+10	51200	301900	3.33E-5	2.16E-4	0.49
		21600	24000	2.14E-5	5.62E-4	0.29
1						
10	117.0	0.0	0.0			
2	2.00E+10	51200	301900	3.33E-5	2.16E-4	0.49
		21600	24000	2.14E-5	5.62E-4	0.29
2	2.00E+10	51200	301900	3.33E-5	2.16E-4	0.49
		21600	24000	2.14E-5	5.62E-4	0.29
1						
11	117.0	0.0	0.0			
2	2.00E+10	51200	301900	3.33E-5	2.16E-4	0.49
		21600	24000	2.14E-5	5.62E-4	0.29
2	2.00E+10	49200	224300	2.98E-5	2.96E-4	0.64
		25500	28600	2.24E-5	7.51E-4	0.18
1						
12	117.0	0.0	24.0			
2	2.00E+10	49200	224300	2.98E-5	2.96E-4	0.64
		25500	28600	2.24E-5	7.51E-4	0.18
2	2.00E+10	44800	86800	2.39E-5	6.36E-4	0.38
		44100	54500	2.31E-5	9.10E-4	0.25

Option for wall input

1

WALL DATA

1	75.0	2.83e+5				
-3	9.9e+15	9.9e+15	9.99e+15	2.0	10.0	0.10
		9.9e+15	9.99e+15	2.0	10.0	0.10
4	9.433e+5	400	520	9.380e-4	1.600e-3	1.59
		250	405	1.105e-3	5.333e-3	1.19
2	75	2.83e+5				
-3	9.9e+15	9.9e+15	9.99e+15	2.0	10.0	0.10
		9.9e+15	9.99e+15	2.0	10.0	0.10
4	9.433e+5	250	405	1.105e-3	5.333e-3	1.19
		400	520	9.380e-4	1.600e-3	1.59

Column connectivity

1, 1, 1, 1, 0, 1

2, 1, 1, 7, 0, 1

3, 2, 1, 1, 2, 4

4, 2, 1, 7, 3, 4

Beam connectivity

1, 1, 1, 1, 1, 2

2, 2, 1, 1, 2, 3

3, 3, 1, 1, 3, 4

4, 4, 1, 1, 4, 5

5, 5, 1, 1, 5, 6

6, 6, 1, 1, 6, 7

```

7,    7, 4, 1, 1, 2
8,    8, 4, 1, 2, 3
9,    9, 4, 1, 3, 4
10, 10, 4, 1, 4, 5
11, 11, 4, 1, 5, 6
12, 12, 4, 1, 6, 7
Shear wall connectivity
1,    1, 1, 1, 1, 2
2,    2, 1, 7, 1, 3
Moment releases
1, 1, 1, 1
2, 1, 2, 1
3, 1, 3, 1
4, 1, 4, 1
Phase II option (=0, STOP; =3, Seismic; =4, Quasistatic)
3
Long term loading: static loads
0 0 0 0
Control data for dynamic analysis
0.33, 1.065, 0.001, 20.0, 3.0, 3
Wave control data
0, 1, 2201, 0.02
GRAVITY LOAD PLUS OUTER HARBOUR WHARF RECORD
ohw_hori.dat
ohw_vert.dat
SNAPSHOT CONTROL DATA
0 1
0 0 0 0
Output control
2, 0.02, 1, 4
FIRST.PRN
SECOND.PRN
Hysteresis Output
0, 0, 2, 0, 0, 0
Wall numbers for output
1, 2

```

*NOTES : The earthquake ground acceleration record is read separately from files:
 ohw_hori.dat (horizontal component)
 ohw_vert.dat (vertical component)
 as specified in the input data*

CASE STUDY #6

*input filename: idarc.dat
data filename: case6_ew.dat
output filename: idarc.out
results filename: case6_ew.out*

file: idarc.dat

case6_ew.dat
case6_ew.out

file: case6_ew.dat

CASE 6: PATTERSON BUILDING EAST-WEST FRAMES HALF STRUCTURE (simplified)

CONTROL DATA

4, 2, 1, 1, 0, 1, 0, 1, 1

ELEMENT TYPES

12, 6, 4, 0, 0, 0, 0, 0, 0, 0

ELEMENT DATA

48, 44, 4, 0, 0, 0, 0, 0, 0

UNITS

1

FLOOR ELEVATIONS

144. 288. 432. 576.

IDENTICAL FRAMES

1, 2

COLUMN LINES

10, 3

NODAL WEIGHTS

1, 1, 87. 66. 66. 66. 66. 66. 66. 66. 87.
2, 349. 495. 349.

2, 1, 16. 39. 39. 39. 39. 39. 39. 39. 16.
2, 242. 484. 242.

3, 1, 16. 39. 39. 39. 39. 39. 39. 39. 16.
2, 242. 484. 242.

4, 1, 52. 39. 39. 39. 39. 39. 39. 39. 52.
2, 206. 293. 206.

ENVELOPE GENERATION

0

CONCRETE PROPERTIES

1, 3.0, 3122. 0.2, 0.36, 0.4, 0.

REINFORCEMENT PROPERTIES

1, 60. 0. 0. 0. 0.

HYSTERETIC RULES

1

1, 1, 12.0, 0.01, 0.1, 1.0, 0

COLUMN PROPERTIES

0

COLUMN DATA

1

1, 1, 1, 171. 144. 0. 8.
-1, 24. 30. 1.5 1.8 0.25 9. 0.5

1
 2, 1, 1, 183. 144. 0. 8.
 -1, 12. 30. 1.5 1.8 0.25 9. 0.5
 1
 3, 1, 1, 84. 144. 8. 8.
 -1, 24. 30. 1.5 1.8 0.25 9. 0.5
 1
 4, 1, 1, 117. 144. 8. 8.
 -1, 12. 30. 1.5 1.8 0.25 9. 0.5
 1
 5, 1, 1, 68. 144. 8. 8.
 -1, 24. 30. 1.5 1.8 0.25 9. 0.5
 1
 6, 1, 1, 78. 144. 8. 8.
 -1, 12. 30. 1.5 1.8 0.25 9. 0.5
 1
 7, 1, 1, 52. 144. 8. 8.
 -1, 24. 30. 1.5 1.8 0.25 9. 0.5
 1
 8, 1, 1, 39. 144. 8. 8.
 -1, 12. 30. 1.5 1.8 0.25 9. 0.5
 1
 9, 1, 1, 1039. 144. 0. 8.
 -1, 30. 36. 1.5 3.6 0.25 9. 0.5
 1
 10, 1, 1, 690. 144. 8. 8.
 -1, 30. 36. 1.5 3.6 0.25 9. 0.5
 1
 11, 1, 1, 448. 144. 8. 8.
 -1, 30. 36. 1.5 3.6 0.25 9. 0.5
 1
 12, 1, 1, 206. 144. 8. 8.
 -1, 30. 36. 1.5 3.6 0.25 9. 0.5

BEAM PROPERTIES

0
 BEAM DATA
 1
 1, 1, 1, 105. 6. 6.
 -1, 17. 60. 69. 3. 1.5 3.08 3.08 0.5 18.
 1
 2, 1, 1, 156. 6. 6.
 -1, 17. 60. 69. 3. 1.5 3.08 0. 0.5 18.
 1
 3, 1, 1, 105. 6. 6.
 -1, 17. 30. 39. 3. 1.5 1.76 1.76 0.375 18.
 1
 4, 1, 1, 156. 6. 6.
 -1, 17. 30. 39. 3. 1.5 2.2 0. 0.375 18.
 1
 5, 1, 1, 585. 18. 120.
 -1, 14. 24. 120 3. 1.5 2.48 1.6 0. 12.

1
 6, 1, 1, 585. 120. 18.
 -1, 14. 24. 120 3. 1.5 2.48 1.6 0. 12.
 SHEAR WALL PROPERTIES
 0
 SHEAR WALL DATA
 1, 1, 1, 1, 1, 1756. 144. 1
 1, 1, 264. 12. 0.09 0.14
 2, 1, 1, 1, 1, 1261. 144. 1
 1, 1, 264. 12. 0.09 0.14
 3, 1, 1, 1, 1, 777. 144. 1
 1, 1, 264. 12. 0.09 0.14
 4, 1, 1, 1, 1, 293. 144. 1
 1, 1, 264. 12. 0.09 0.14
 COLUMN CONNECTIONS
 1, 1, 1, 1, 0, 1
 2, 2, 1, 2, 0, 1
 3, 2, 1, 3, 0, 1
 4, 2, 1, 4, 0, 1
 5, 2, 1, 5, 0, 1
 6, 2, 1, 6, 0, 1
 7, 2, 1, 7, 0, 1
 8, 2, 1, 8, 0, 1
 9, 2, 1, 9, 0, 1
 10, 1, 1, 10, 0, 1
 11, 3, 1, 1, 1, 2
 12, 4, 1, 2, 1, 2
 13, 4, 1, 3, 1, 2
 14, 4, 1, 4, 1, 2
 15, 4, 1, 5, 1, 2
 16, 4, 1, 6, 1, 2
 17, 4, 1, 7, 1, 2
 18, 4, 1, 8, 1, 2
 19, 4, 1, 9, 1, 2
 20, 3, 1, 10, 1, 2
 21, 5, 1, 1, 2, 3
 22, 6, 1, 2, 2, 3
 23, 6, 1, 3, 2, 3
 24, 6, 1, 4, 2, 3
 25, 6, 1, 5, 2, 3
 26, 6, 1, 6, 2, 3
 27, 6, 1, 7, 2, 3
 28, 6, 1, 8, 2, 3
 29, 6, 1, 9, 2, 3
 30, 5, 1, 10, 2, 3
 31, 7, 1, 1, 3, 4
 32, 8, 1, 2, 3, 4
 33, 8, 1, 3, 3, 4
 34, 8, 1, 4, 3, 4
 35, 8, 1, 5, 3, 4
 36, 8, 1, 6, 3, 4

37, 8, 1, 7, 3, 4
38, 8, 1, 8, 3, 4
39, 8, 1, 9, 3, 4
40, 7, 1, 10, 3, 4
41, 9, 2, 1, 0, 1
42, 9, 2, 3, 0, 1
43, 10, 2, 1, 1, 2
44, 10, 2, 3, 1, 2
45, 11, 2, 1, 2, 3
46, 11, 2, 3, 2, 3
47, 12, 2, 1, 3, 4
48, 12, 2, 3, 3, 4

BEAM CONNECTIONS

1, 1, 1, 1, 1, 2
2, 2, 1, 1, 2, 3
3, 1, 1, 1, 3, 4
4, 2, 1, 1, 4, 5
5, 1, 1, 1, 5, 6
6, 2, 1, 1, 6, 7
7, 1, 1, 1, 7, 8
8, 2, 1, 1, 8, 9
9, 1, 1, 1, 9, 10
10, 3, 2, 1, 1, 2
11, 4, 2, 1, 2, 3
12, 3, 2, 1, 3, 4
13, 4, 2, 1, 4, 5
14, 3, 2, 1, 5, 6
15, 4, 2, 1, 6, 7
16, 3, 2, 1, 7, 8
17, 4, 2, 1, 8, 9
18, 3, 2, 1, 9, 10
19, 3, 3, 1, 1, 2
20, 4, 3, 1, 2, 3
21, 3, 3, 1, 3, 4
22, 4, 3, 1, 4, 5
23, 3, 3, 1, 5, 6
24, 4, 3, 1, 6, 7
25, 3, 3, 1, 7, 8
26, 4, 3, 1, 8, 9
27, 3, 3, 1, 9, 10
28, 3, 4, 1, 1, 2
29, 4, 4, 1, 2, 3
30, 4, 4, 1, 3, 4
31, 4, 4, 1, 4, 5
32, 4, 4, 1, 5, 6
33, 4, 4, 1, 6, 7
34, 4, 4, 1, 7, 8
35, 4, 4, 1, 8, 9
36, 3, 4, 1, 9, 10
37, 5, 1, 2, 1, 2
38, 6, 1, 2, 2, 3

39, 5, 2, 2, 1, 2
 40, 6, 2, 2, 2, 3
 41, 5, 3, 2, 1, 2
 42, 6, 3, 2, 2, 3
 43, 5, 4, 2, 1, 2
 44, 6, 4, 2, 2, 3
SHEAR WALL CONNECTIONS
 1, 1, 2, 2, 0, 1
 2, 2, 2, 2, 1, 2
 3, 3, 2, 2, 2, 3
 4, 4, 2, 2, 3, 4
ANALYSIS OPTION (PUSHOVER FORCE CONTROL)
 2
STATIC LOADS
 0 0 0 0
(FORCE CONTROL)
 1
DISTRIBUTION PROPORTIONAL WITH THE HIGTH
 3
 0.05 400 15.0
 1 3 3
RESPONSE SNAPSHOTS
 0
 0 0 0 0
STORY OUTPUT CONTROL
 4 1 4 3 2 1
 po_ew4m1.out
 po_ew3m1.out
 po_ew2m1.out
 po_ew1m1.out
ELEMENT HYSTERESIS OUTPUT
 0 0 0 0 0 0

ANALYSIS OPTIONS (Earthquake)
 3
STATIC LOADS
 0 0 0 0
DYNAMIC ANALYSIS
 0.52 0.0 0.0005 20.0 5.0 2
WAVE DATA
 0, 0, 1001, 0.02
DESIGN SIMULATED EARTHQUAKE
 design.qke
RESPONSE SNAPSHOTS
 0
 0 0 0 0
STORY OUTPUT CONTROL
 4, 0.005, 1, 2, 3, 4

```
dyn1_ew.out
dyn2_ew.out
dyn3_ew.out
dyn4_ew.out
ELEMENT HYSTERESIS OUTPUT
4 0 4 0 0 0
Column Output Specification
31 32 33 47
Shear Wall Output Specification
1 2 3 4
```

```
*****
ANALYSIS OPTION (PUSHOVER DISPLACEMENT CONTROL)
2
STATIC LOADS
0 0 0 0
MONOTONIC PUSHOVER ANALYSIS
2
(DISPLACEMENT) CONTROL
4
4 3 2 1
16 12 8 4
200 16
RESPONSE SNAPSHOTS
0
0 0 0 1 0
STORY OUTPUT CONTROL
4 1 4 3 2 1
dc_ew4V.out
dc_ew3V.out
dc_ew2V.out
dc_ew1V.out
ELEMENT HYSTERESIS OUTPUT
0 0 0 0 0 0
```

CASE STUDY #7

input filename: idarc.dat
data filename: case7.dat
output filename: idarc.out
results filename: case7.out

file: idarc.dat

case7.dat
case7.out

file: case7.dat

CASE 7: Physics Building in UCLA, Longitudinal model [kips-in]

CONTROL DATA

8 1 1 1 0 1 0,0,1

ELEMENT TYPES

10 4 0 0 0 0 0 0 0

ELEMENT DATA

88 80 0 0 0 0 0 0

UNIT SYSTEM

1

FLOOR ELEVATIONS

162 324 486 648 810 972 1134 1296

DESCRIPTION OF IDENTICAL FRAMES

2

PLAN CONFIGURATION

11

NODAL WEIGHTS

8 1 66.05 132.1 132.1 132.1 132.1 132.1 132.1 132.1 132.1 66.05

7 1 73.95 147.9 147.9 147.9 147.9 147.9 147.9 147.9 147.9 73.95

6 1 73.95 147.9 147.9 147.9 147.9 147.9 147.9 147.9 147.9 73.95

5 1 73.95 147.9 147.9 147.9 147.9 147.9 147.9 147.9 147.9 73.95

4 1 73.95 147.9 147.9 147.9 147.9 147.9 147.9 147.9 147.9 73.95

3 1 73.95 147.9 147.9 147.9 147.9 147.9 147.9 147.9 147.9 73.95

2 1 73.95 147.9 147.9 147.9 147.9 147.9 147.9 147.9 147.9 73.95

1 1 73.95 147.9 147.9 147.9 147.9 147.9 147.9 147.9 147.9 73.95

ENVELOPE GENERATION OPTION

0

CONCRETE PROPERTIES

1 3 0 0 0 0 0

REINFORCEMENT PROPERTIES

1 50 0 0 0 0

HYSTERETIC MODEL RULES

1

1, 1, 12.0, 0.01, 0.1, 0.4, 0

COLUMN PROPERTIES

0

RECTANGULAR COLUMNS

1

1 1 1 82.8 162 12 12
-1 12 144 2 1.6 0.625 18 0.5

1								
2	1	1	170.3	162	12	12		
-1	12	144	2	1.6	0.625	18	0.5	
1								
3	1	1	257.8	162	12	12		
-1	12	144	2	1.6	0.625	18	0.5	
1								
4	1	1	301.5	162	12	12		
-1	12	144	2	1.6	0.625	18	0.5	
1								
5	1	1	345.2	162	12	12		
-1	12	144	2	1.6	0.625	18	0.5	
1								
6	1	1	165.6	162	12	12		
-1	24	24	2	3.12	0.375	18	0.5	
1								
7	1	1	340.6	162	12	12		
-1	24	24	2	3.12	0.375	18	0.5	
1								
8	1	1	515.5	162	12	12		
-1	24	24	2	2.37	0.5	2.5		1
1								
9	1	1	603.3	162	12	12		
-1	24	24	2	2.37	0.5	2.5		1
1								
10	1	1	690.4	162	12	12		
-1	24	24	2	2.37	0.5	2.5		1

BEAM PROPERTIES

BEAM DATA												
1	1	1	1	288	12	12	0	2	3.12	3.54	0.375	12
1	-1	24	12	12	12	12	0	2	1.58	3.81	0.375	12
1	1	1	1	288	12	12	0	2	2.54	4.1	0.375	9
1	-1	24	12	12	12	12	0	2	2	4.1	0.375	9

COLUMN CONNECTIONS

1	1	1	1	7	8
2	1	1	1	6	7
3	2	1	1	5	6
4	2	1	1	4	5
5	3	1	1	3	4
6	3	1	1	2	3
7	4	1	1	1	2
8	5	1	1	0	1

9	6	1	2	7	8
10	6	1	2	6	7
11	7	1	2	5	6
12	7	1	2	4	5
13	8	1	2	3	4
14	8	1	2	2	3
15	9	1	2	1	2
16	10	1	2	0	1
17	6	1	3	7	8
18	6	1	3	6	7
19	7	1	3	5	6
20	7	1	3	4	5
21	8	1	3	3	4
22	8	1	3	2	3
23	9	1	3	1	2
24	10	1	3	0	1
25	6	1	4	7	8
26	6	1	4	6	7
27	7	1	4	5	6
28	7	1	4	4	5
29	8	1	4	3	4
30	8	1	4	2	3
31	9	1	4	1	2
32	10	1	4	0	1
33	6	1	5	7	8
34	6	1	5	6	7
35	7	1	5	5	6
36	7	1	5	4	5
37	8	1	5	3	4
38	8	1	5	2	3
39	9	1	5	1	2
40	10	1	5	0	1
41	6	1	6	7	8
42	6	1	6	6	7
43	7	1	6	5	6
44	7	1	6	4	5
45	8	1	6	3	4
46	8	1	6	2	3
47	9	1	6	1	2
48	10	1	6	0	1
49	6	1	7	7	8
50	6	1	7	6	7
51	7	1	7	5	6
52	7	1	7	4	5
53	8	1	7	3	4
54	8	1	7	2	3
55	9	1	7	1	2
56	10	1	7	0	1
57	6	1	8	7	8
58	6	1	8	6	7
59	7	1	8	5	6

60	7	1	8	4	5
61	8	1	8	3	4
62	8	1	8	2	3
63	9	1	8	1	2
64	10	1	8	0	1
65	6	1	9	7	8
66	6	1	9	6	7
67	7	1	9	5	6
68	7	1	9	4	5
69	8	1	9	3	4
70	8	1	9	2	3
71	9	1	9	1	2
72	10	1	9	0	1
73	6	1	10	7	8
74	6	1	10	6	7
75	7	1	10	5	6
76	7	1	10	4	5
77	8	1	10	3	4
78	8	1	10	2	3
79	9	1	10	1	2
80	10	1	10	0	1
81	1	1	11	7	8
82	1	1	11	6	7
83	2	1	11	5	6
84	2	1	11	4	5
85	3	1	11	3	4
86	3	1	11	2	3
87	4	1	11	1	2
88	5	1	11	0	1

BEAM CONNECTIVITY

1	1	8	1	1	2
2	2	8	1	2	3
3	2	8	1	3	4
4	2	8	1	4	5
5	2	8	1	5	6
6	2	8	1	6	7
7	2	8	1	7	8
8	2	8	1	8	9
9	2	8	1	9	10
10	1	8	1	10	11
11	3	7	1	1	2
12	4	7	1	2	3
13	4	7	1	3	4
14	4	7	1	4	5
15	4	7	1	5	6
16	4	7	1	6	7
17	4	7	1	7	8
18	4	7	1	8	9
19	4	7	1	9	10
20	3	7	1	10	11
21	3	6	1	1	2

22	4	6	1	2	3
23	4	6	1	3	4
24	4	6	1	4	5
25	4	6	1	5	6
26	4	6	1	6	7
27	4	6	1	7	8
28	4	6	1	8	9
29	4	6	1	9	10
30	3	6	1	10	11
31	3	5	1	1	2
32	4	5	1	2	3
33	4	5	1	3	4
34	4	5	1	4	5
35	4	5	1	5	6
36	4	5	1	6	7
37	4	5	1	7	8
38	4	5	1	8	9
39	4	5	1	9	10
40	3	5	1	10	11
41	3	4	1	1	2
42	4	4	1	2	3
43	4	4	1	3	4
44	4	4	1	4	5
45	4	4	1	5	6
46	4	4	1	6	7
47	4	4	1	7	8
48	4	4	1	8	9
49	4	4	1	9	10
50	3	4	1	10	11
51	3	3	1	1	2
52	4	3	1	2	3
53	4	3	1	3	4
54	4	3	1	4	5
55	4	3	1	5	6
56	4	3	1	6	7
57	4	3	1	7	8
58	4	3	1	8	9
59	4	3	1	9	10
60	3	3	1	10	11
61	3	2	1	1	2
62	4	2	1	2	3
63	4	2	1	3	4
64	4	2	1	4	5
65	4	2	1	5	6
66	4	2	1	6	7
67	4	2	1	7	8
68	4	2	1	8	9
69	4	2	1	9	10
70	3	2	1	10	11
71	3	1	1	1	2
72	4	1	1	2	3

73	4	1	1	3	4
74	4	1	1	4	5
75	4	1	1	5	6
76	4	1	1	6	7
77	4	1	1	7	8
78	4	1	1	8	9
79	4	1	1	9	10
80	3	1	1	10	11

ANALYSIS OPTION (PUSHOVER)
 2
 LONG-TERM LOADING
 0 0 0 0
 MONOTONIC PUSH-OVER ANALYSIS
 1
 FORCE CONTROL
 5
 0.2, 300, 10.0
 2
 SNAPSHOT OUTPUT CONTROL
 0
 0,0,0,0
 GLOBAL OUTPUT CONTROL
 8 1 8 7 6 5 4 3 2 1
 pushl8.out
 pushl7.out
 pushl6.out
 pushl5.out
 pushl4.out
 pushl3.out
 pushl2.out
 pushl1.out
 ELEMENT HYSTERSYS OUTPUT
 0 0 0 0 0 0
 END OF INPUT FILE

ANALYSIS OPTION (SYLM EARTHQUAKE)
 3
 LONG-TERM LOADING
 0 0 0 0
 DYNAMIC ANALYSIS
 0.084 0.054 0.001 25.0 0.05, 3
 INPUT WAVE
 0 1 3000 0.02
 SYLM EARTHQUAKE
 sylm000.wve
 sylmver.wve
 GLOBAL OUTPUT CONTROL

```
8 0.01 8 7 6 5 4 3 2 1
story8l.out
story7l.out
story6l.out
story5l.out
story4l.out
story3l.out
story2l.out
story1l.out
ELEMENT HYSTERESIS OUTPUT
2 0 0 0 0 0
COLUMN ELEMENTS
8 16
```

```
ANALYSIS OPTION (TABAS EARTHQUAKE)
3
LONG-TERM LOADING
0 0 0 0
DYNAMIC ANALYSIS
0.94 0.75 0.001 30.0 0.05, 3
INPUT WAVE
0 1 2490 0.02
TABAS EARTHQUAKE
taba344.wve
tabaver.wve
GLOBAL OUTPUT CONTROL
8 0.01 8 7 6 5 4 3 2 1
story8l.out
story7l.out
story6l.out
story5l.out
story4l.out
story3l.out
story2l.out
story1l.out
ELEMENT HYSTERESIS OUTPUT
0 0 0 0 0 0
```

CASE STUDY #8

*input filename: idarc.dat
data filename: case8.dat
output filename: idarc.out
results filename: case8.out*

file: idarc.dat

case8.dat

case8.out

file: case8.dat

Pushover analysis of frame #1, LINE 2,6,9 and 11, Olym. Ctr. CA.

control data

17, 4, 1, 1, 0, 0, 0, 1, 1

element types

32, 6, 0, 0, 0, 0, 0, 0, 0

element data

543, 289, 0, 0, 0, 0, 0, 0, 0

units

1

elevations

12,78,162,228,294,360,426,492,558,624,756,912,1068,1224,1380,1536,1704

description of identical frames

1, 1, 1, 1

plan configuration

9, 11, 11, 10

nodal weights

1, 1, 0, 0, 0, 0, 0, 0, 0, 0

2, 5, 5, 5, 5, 5, 5, 5, 5, 0

3, 0, 0, 0, 0, 0, 0, 0, 0, 0, 0

4, 0, 0, 0, 0, 0, 0, 0, 0, 0

2, 1, 0, 0, 0, 0, 0, 0, 0, 0

2, 10, 10, 10, 10, 10, 10, 10, 10, 10, 10, 10

3, 0, 10, 10, 10, 10, 10, 10, 10, 10, 10, 10, 10

4, 0, 0, 0, 0, 0, 0, 0, 0, 0

3, 1, 0, 0, 0, 0, 0, 0, 0, 0

2, 0, 0, 0, 0, 0, 0, 0, 0, 0

3, 92, 92, 92, 92, 92, 92, 92, 92, 92, 92

4, 0, 37, 37, 37, 37, 37, 37, 37, 37

4, 1, 73, 73, 73, 73, 73, 73, 73, 73, 73,

2, 129, 129, 129, 129, 129, 129, 129, 129, 129, 129

3, 0, 0, 0, 0, 0, 0, 0, 0, 0

4, 0, 0, 0, 0, 0, 0, 0, 0

5, 1, 0, 0, 0, 0, 0, 0, 0

2, 0, 0, 0, 0, 0, 0, 0, 0

3, 131, 131, 131, 131, 131, 131, 131, 131, 131, 131, 131

4, 0, 53, 53, 53, 53, 53, 53, 53, 53, 53

6, 1, 105, 105, 105, 105, 105, 105, 105, 105, 105

2, 179, 179, 179, 179, 179, 179, 179, 179, 179, 179

3, 0, 0, 0, 0, 0, 0, 0, 0, 0

4, 0, 0, 0, 0, 0, 0, 0, 0, 0
 7, 1, 0, 0, 0, 0, 0, 0, 0, 0
 2, 0, 0, 0, 0, 0, 0, 0, 0, 0
 3, 250, 250, 250, 250, 250, 250, 250, 250, 250, 250
 4, 0, 53, 53, 53, 53, 53, 53, 53, 53, 53
 8, 1, 100, 100, 100, 100, 100, 100, 100, 100, 100
 2, 175, 175, 175, 175, 175, 175, 175, 175, 175, 175
 3, 0, 0, 0, 0, 0, 0, 0, 0, 0
 4, 0, 0, 0, 0, 0, 0, 0, 0
 9, 1, 0, 0, 0, 0, 0, 0, 0, 0
 2, 0, 0, 0, 0, 0, 0, 0, 0, 0
 3, 250, 250, 250, 250, 250, 250, 250, 250, 250, 250
 4, 0, 53, 53, 53, 53, 53, 53, 53, 53
 10, 1, 100, 100, 100, 100, 100, 100, 100, 100, 100
 2, 175, 175, 175, 175, 175, 175, 175, 175, 175, 175
 3, 0, 0, 0, 0, 0, 0, 0, 0, 0
 4, 0, 0, 0, 0, 0, 0, 0, 0
 11, 1, 125, 125, 125, 125, 125, 125, 125, 0
 2, 219, 219, 219, 219, 219, 219, 219, 219, 219, 219
 3, 157, 157, 157, 157, 157, 157, 157, 157, 157, 157
 4, 0, 63, 63, 63, 63, 63, 63, 63, 63
 12, 1, 169, 169, 169, 169, 169, 169, 0, 0, 0
 2, 0, 169, 169, 169, 169, 169, 0, 0, 0, 0
 3, 0, 169, 169, 169, 169, 169, 169, 169, 169, 0
 4, 0, 0, 0, 0, 0, 0, 0, 0
 13, 1, 139, 139, 139, 139, 139, 139, 0, 0, 0
 2, 0, 139, 139, 139, 139, 139, 0, 0, 0, 0
 3, 0, 0, 0, 139, 139, 139, 139, 139, 139, 0
 4, 0, 0, 0, 0, 0, 0, 0, 0
 14, 1, 134, 134, 134, 134, 134, 134, 0, 0, 0
 2, 0, 134, 134, 134, 134, 134, 0, 0, 0, 0
 3, 0, 0, 0, 134, 134, 134, 134, 134, 134, 0
 4, 0, 0, 0, 0, 0, 0, 0, 0
 15, 1, 0, 138, 138, 138, 138, 0, 0, 0
 2, 0, 138, 138, 138, 138, 0, 0, 0, 0
 3, 0, 0, 0, 138, 138, 138, 138, 138, 0
 4, 0, 0, 0, 0, 0, 0, 0, 0
 16, 1, 0, 144, 144, 144, 144, 0, 0, 0, 0
 2, 0, 144, 144, 144, 144, 144, 0, 0, 0, 0
 3, 0, 0, 0, 144, 144, 144, 144, 144, 144, 0
 4, 0, 0, 0, 0, 0, 0, 0, 0
 17, 1, 0, 190, 190, 190, 190, 0, 0, 0, 0
 2, 0, 0, 190, 190, 190, 190, 0, 0, 0, 0
 3, 0, 0, 0, 190, 190, 190, 190, 190, 0
 4, 0, 0, 0, 0, 0, 0, 0, 0
 envelope generation
 1
 hys prop
 1
 1, 1, 2.0, 0.0, 0.0, 0.5 0
 column property option

1
 column data
 1
 1, 10, 50, 20, 156, 0, 0
 -1, 8.70E7, 1.99E6, 13511, 14198, .00025, 0.005, 6.89, 13511, 14198, .00025, 0.005,
 6.89
 1
 2, 10, 50, 20, 168, 0, 0
 -1, 9.80E7, 2.19E6, 14945, 15747, .00026, .0059, 5.52, 14945, 15747, .00026, .0059,
 5.52
 1
 3, 10, 50, 20, 156, 0, 0
 -1, 9.80E7, 2.19E6, 14945, 15747, .00026, .0059, 5.52, 14945, 15747, .00026, .0059,
 5.52
 1
 4, 10, 50, 20, 156, 0, 0
 -1, 1.11E8, 2.42E6, 16516, 17438, .00025, .0054, 6.44, 16516, 17438, .00025, .0054,
 6.44
 1
 5, 10, 50, 20, 132, 0, 0
 -1, 1.11E8, 2.42E6, 16516, 17438, .00025, .0054, 6.44, 16516, 17438, .00025, .0054,
 6.44
 1
 6, 10, 50, 20, 156, 0, 0
 -1, 1.26E8, 2.65E6, 18210, 19275, .00024, .0056, 6.03, 18210, 19275, .00024, .0056,
 6.03
 1
 7, 10, 50, 20, 132, 0, 0
 -1, 1.26E8, 2.65E6, 18210, 19275, .00024, .0056, 6.03, 18210, 19275, .00024, .0056,
 6.03
 1
 8, 10, 50, 20, 168, 0, 0
 -1, 5.25E7, 2.93E6, 7966, 9107, 0.00051, .016, 5.30, 7966, 9107, 0.00051, .016, 5.30
 1
 9, 10, 50, 20, 156, 0, 0
 -1, 5.25E7, 2.93E6, 7966, 9107, 0.00051, .016, 5.30, 7966, 9107, 0.00051, .016,
 5.30
 1
 10, 10, 50, 20, 156, 0, 0
 -1, 1.42E8, 2.93E6, 20114, 21345, .00025, .0057, 6.27, 20114, 21345, .00025, .0057,
 6.27
 1
 11, 10, 50, 20, 156, 0, 0
 -1, 1.58E8, 3.16E6, 21857, 23017, .00025, .0059, 6.46, 21857, 23017, .00025, .0059,
 6.46
 1
 12, 10, 50, 20, 132, 0, 0
 -1, 1.58E8, 3.16E6, 21857, 23017, .00025, .0059, 6.46, 21857, 23017, .00025, .0059,
 6.46
 1
 13, 10, 50, 20, 66, 0, 0

-1, 6.29E7, 3.39E6,	9418, 10789, .00051, .016,	3.08, 9418, 10789, .00051, .016,
3.08		
1		
14, 10, 50, 20, 84, 0, 0		
-1, 6.29E7, 3.39E6,	9418, 10789, .00051, .016,	3.08, 9418, 10789, .00051, .016,
3.08		
1		
15, 10, 50, 20, 66, 0, 0		
-1, 1.74E8, 3.39E6,	23619, 24923, .00025, .006,	6.44, 23619, 24923, .00025, .006,
6.44		
1		
16, 10, 50, 20, 66, 0, 0		
-1, 1.51E10, 7.25E7,	749952, 852151, .00016, .005,	5.16, 749952, 852151, .00016, .005,
5.16		
1		
17, 10, 50, 20, 66, 0, 0		
-1, 8.70E7, 1.99E6,	13511, 14198, .00025, 0.005,	6.89, 13511, 14198, .00025, 0.005,
6.89		
1		
18, 10, 50, 20, 66, 0, 0		
-1, 1.26E8, 2.65E6,	18210, 19275, .00024, .0056,	6.03, 18210, 19275, .00024, .0056,
6.03		
1		
19, 10, 50, 20, 84, 0, 0		
-1, 1.74E8, 3.39E6,	23619, 24923, .00025, .006,	6.44, 23619, 24923, .00025, .006,
6.44		
1		
20, 10, 50, 20, 42, 30, 0		
-1, 1.51E10, 7.25E7,	749952, 852151, .00016, .005,	5.16, 749952, 852151, .00016, .005,
5.16		
1		
21, 10, 50, 20, 168, 0, 0		
-1, 8.70E7, 1.99E6,	13511, 14198, .00025, 0.005,	6.89, 13511, 14198, .00025, 0.005,
6.89		
1		
22, 10, 50, 20, 132, 0, 0		
-1, 8.70E7, 1.99E6,	13511, 14198, .00025, 0.005,	6.89, 13511, 14198, .00025, 0.005,
6.89		
1		
23, 10, 50, 20, 66, 0, 0		
-1, 8.70E7, 1.99E6,	13511, 14198, .00025, 0.005,	6.89, 13511, 14198, .00025, 0.005,
6.89		
1		
24, 10, 50, 20, 168, 0, 0		
-1, 1.11E8, 2.42E6,	16516, 17438, .00025, .0054,	6.44, 16516, 17438, .00025, .0054,
6.44		
1		
25, 10, 50, 20, 66, 0, 0		
-1, 1.26E8, 2.65E6,	18210, 19275, .00024, .0056,	6.03, 18210, 19275, .00024, .0056,
6.03		
1		

26, 10, 50, 20, 132, 0, 0
 -1, 5.25E7, 2.93E6, 7966, 9107, 0.00051, .016, 5.30, 7966, 9107, 0.00051, .016,
 5.30
 1
 27, 10, 50, 20, 66, 0, 0
 -1, 5.25E7, 2.93E6, 7966, 9107, 0.00051, .016, 5.30, 7966, 9107, 0.00051, .016,
 5.30
 1
 28, 10, 50, 20, 66, 0, 0
 -1, 5.25E7, 2.93E6, 7966, 9107, 0.00051, .016, 5.30, 7966, 9107, 0.00051, .016,
 5.30
 1
 29, 10, 50, 20, 84, 0, 0
 -1, 1.42E8, 2.93E6, 20114, 21345, .00025, .0057, 6.27, 20114, 21345, .00025, .0057,
 6.27
 1
 30, 10, 50, 20, 66, 0, 0
 -1, 6.29E7, 3.39E6, 9418, 10789, .00051, .016, 3.08, 9418, 10789, .00051, .016,
 3.08
 1
 31, 10, 50, 20, 42, 20, 20
 -1, 1.51E10, 7.25E7, 749952,852151, .00016, .005, 5.16, 749952,852151, .00016, .005,
 5.16
 1
 32, 10, 50, 20, 66, 0, 0
 -1, 6.21E7, 1.50E6, 13511, 14198, .00025, 0.005, 9.65, 13511, 14198, .00025, 0.005,
 9.65
 beam property option
 1
 beam data
 1
 1, 344, 7, 7
 -1, 2.62E8, 18080., 18968., 0.00011, 0.0021, 7.25, 18080., 18968., 0.00011, 0.0021, 7.25
 1
 2, 344, 7, 7
 -1, 3.05E8, 21000., 21980., 0.0001, 0.002, 6.79, 21000., 21980., 0.0001, 0.002, 6.79
 1
 3, 344, 7, 7
 -1, 3.28E8, 22600., 23646., 0.0001, 0.002, 6.71, 22600., 23646., 0.0001, 0.002, 6.71
 1
 4, 344, 7, 7
 -1, 3.83E8, 26400., 27297., 0.0001, 0.002, 7.05, 26400., 27297., 0.0001, 0.002, 7.05
 1
 5, 344, 7, 7
 -1, 4.06E9, 280000, 318126, 0.00022, 0.0069, 5.34, 280000, 318126, 0.00022, 0.0069, 5.34
 1
 6, 344, 7, 7
 -1, 2.62E8, 18080., 18968., 0.00011, 0.0021, 7.25, 18080., 18968., 0.00011, 0.0021, 7.25
 column connectivities
 1, 2, 1, 2, 16, 17
 2, 8, 1, 3, 16, 17

3, 2, 1, 4, 16, 17
4, 2, 1, 5, 16, 17
5, 3, 1, 2, 15, 16
6, 9, 1, 3, 15, 16
7, 3, 1, 4, 15, 16
8, 3, 1, 5, 15, 16
9, 3, 1, 2, 14, 15
10, 9, 1, 3, 14, 15
11, 3, 1, 4, 14, 15
12, 3, 1, 5, 14, 15
13, 6, 1, 6, 14, 15
14, 1, 1, 13, 14
15, 6, 1, 2, 13, 14
16, 11, 1, 3, 13, 14
17, 6, 1, 4, 13, 14
18, 6, 1, 5, 13, 14
19, 6, 1, 6, 13, 14
20, 1, 1, 1, 12, 13
21, 6, 1, 2, 12, 13
22, 11, 1, 3, 12, 13
23, 6, 1, 4, 12, 13
24, 6, 1, 5, 12, 13
25, 6, 1, 6, 12, 13
26, 4, 1, 1, 11, 12
27, 6, 1, 2, 11, 12
28, 11, 1, 3, 11, 12
29, 6, 1, 4, 11, 12
30, 6, 1, 5, 11, 12
31, 6, 1, 6, 11, 12
32, 5, 1, 1, 10, 11
33, 7, 1, 2, 10, 11
34, 12, 1, 3, 10, 11
35, 7, 1, 4, 10, 11
36, 7, 1, 5, 10, 11
37, 7, 1, 6, 10, 11
38, 17, 1, 7, 10, 11
39, 17, 1, 8, 10, 11
40, 18, 1, 1, 9, 10
41, 10, 1, 2, 9, 10
42, 13, 1, 3, 9, 10
43, 10, 1, 4, 9, 10
44, 10, 1, 5, 9, 10
45, 10, 1, 6, 9, 10
46, 17, 1, 7, 9, 10
47, 17, 1, 8, 9, 10
48, 17, 1, 9, 9, 10
49, 18, 1, 1, 8, 9
50, 10, 1, 2, 8, 9
51, 13, 1, 3, 8, 9
52, 10, 1, 4, 8, 9
53, 10, 1, 5, 8, 9

54,10,1, 6, 8, 9
55,17,1, 7, 8, 9
56,17,1, 8, 8, 9
57,17,1, 9, 8, 9
58,18,1, 1, 7, 8
59,10,1, 2, 7, 8
60,13,1, 3, 7, 8
61,10,1, 4, 7, 8
62,10,1, 5, 7, 8
63,10,1, 6, 7, 8
64,17,1, 7, 7, 8
65,17,1, 8, 7, 8
66,17,1, 9, 7, 8
67,18,1, 1, 6, 7
68,10,1, 2, 6, 7
69,13,1, 3, 6, 7
70,10,1, 4, 6, 7
71,10,1, 5, 6, 7
72,10,1, 6, 6, 7
73,17,1, 7, 6, 7
74,17,1, 8, 6, 7
75,17,1, 9, 6, 7
76,15,1, 1, 5, 6
77,15,1, 2, 5, 6
78,13,1, 3, 5, 6
79,15,1, 4, 5, 6
80,15,1, 5, 5, 6
81,15,1, 6, 5, 6
82,15,1, 7, 5, 6
83,15,1, 8, 5, 6
84,15,1, 9, 5, 6
85,15,1, 1, 4, 5
86,15,1, 2, 4, 5
87,13,1, 3, 4, 5
88,15,1, 4, 4, 5
89,15,1, 5, 4, 5
90,15,1, 6, 4, 5
91,15,1, 7, 4, 5
92,15,1, 8, 4, 5
93,15,1, 9, 4, 5
94,15,1, 1, 3, 4
95,15,1, 2, 3, 4
96,13,1, 3, 3, 4
97,15,1, 4, 3, 4
98,15,1, 5, 3, 4
99,15,1, 6, 3, 4
100,15,1,7,3,4
101,15,1,8,3,4
102,15,1,9,3,4
103,19,1,1,2,3
104,19,1,2,2,3

105,14,1,3,2,3
106,19,1,4,2,3
107,19,1,5,2,3
108,19,1,6,2,3
109,19,1,7,2,3
110,19,1,8,2,3
111,19,1,9,2,3
112,16,1,1,1,2
113,16,1,2,1,2
114,16,1,3,1,2
115,16,1,4,1,2
116,16,1,5,1,2
117,16,1,6,1,2
118,16,1,7,1,2
119,16,1,8,1,2
120,16,1,9,1,2
121,20,1,1,0,1
122,20,1,2,0,1
123,20,1,3,0,1
124,20,1,4,0,1
125,20,1,5,0,1
126,20,1,6,0,1
127,20,1,7,0,1
128,20,1,8,0,1
129,20,1,9,0,1
130, 2, 2, 3, 16, 17
131, 24, 2, 4, 16, 17
132, 2, 2, 5, 16, 17
133, 21, 2, 6, 16, 17
134, 4, 2, 2, 15, 16
135, 3, 2, 3, 15, 16
136, 4, 2, 4, 15, 16
137, 3, 2, 5, 15, 16
138, 1, 2, 6, 15, 16
139, 4, 2, 2, 14, 15
140, 3, 2, 3, 14, 15
141, 4, 2, 4, 14, 15
142, 3, 2, 5, 14, 15
143, 1, 2, 6, 14, 15
144, 9, 2, 2, 13, 14
145, 6, 2, 3, 13, 14
146, 9, 2, 4, 13, 14
147, 6, 2, 5, 13, 14
148, 6, 2, 6, 13, 14
149, 9, 2, 2, 12, 13
150, 6, 2, 3, 12, 13
151, 9, 2, 4, 12, 13
152, 6, 2, 5, 12, 13
153, 6, 2, 6, 12, 13
154, 9, 2, 2, 11, 12
155, 6, 2, 3, 11, 12

156,9,2, 4, 11, 12
157,6, 2, 5, 11, 12
158,6, 2, 6, 11, 12
159,22, 2, 1, 10, 11
160,26,2, 2, 10, 11
161,7,2, 3, 10, 11
162,26,2, 4, 10, 11
163,7,2, 5, 10, 11
164,7,2, 6, 10, 11
165,26,2, 7, 10, 11
166,7,2, 8, 10, 11
167,7,2, 9, 10, 11
168,26,2,10, 10, 11
169,22, 2,11, 10, 11
170,23,2, 1, 9, 10
171,28,2, 2, 9, 10
172,10,2, 3, 9, 10
173,28,2, 4, 9, 10
174,10,2, 5, 9, 10
175,10,2, 6, 9, 10
176,27,2, 7, 9, 10
177,25,2, 8, 9, 10
178,25,2, 9, 9, 10
179,28,2, 10, 9, 10
180,25,2, 11, 9, 10
181,23,2, 1, 8, 9
182,28,2, 2, 8, 9
183,10,2, 3, 8, 9
184,28,2, 4, 8, 9
185,10,2, 5, 8, 9
186,10,2, 6, 8, 9
187,27,2, 7, 8, 9
188,25,2, 8, 8, 9
189,25,2, 9, 8, 9
190,28,2, 10, 8, 9
191,25,2, 11, 8, 9
192,23,2, 1, 7, 8
193,28,2, 2, 7, 8
194,10,2, 3, 7, 8
195,28,2, 4, 7, 8
196,10,2, 5, 7, 8
197,10,2, 6, 7, 8
198,27,2, 7, 7, 8
199,25,2, 8, 7, 8
200,25,2, 9, 7, 8
201,28,2, 10, 7, 8
202,25,2, 11, 7, 8
203,23,2, 1, 6, 7
204,28,2, 2, 6, 7
205,10,2, 3, 6, 7
206,28,2, 4, 6, 7

207,10,2, 5, 6, 7
208,10,2, 6, 6, 7
209,27,2, 7, 6, 7
210,25,2, 8, 6, 7
211,25,2, 9, 6, 7
212,28,2, 10, 6, 7
213,25,2, 11, 6, 7
214,25,2, 1, 5, 6
215,30,2, 2, 5, 6
216,15,2, 3, 5, 6
217,30,2, 4, 5, 6
218,15,2, 5, 5, 6
219,15,2, 6, 5, 6
220,28,2, 7, 5, 6
221,10,2, 8, 5, 6
222,10,2, 9, 5, 6
223,30,2, 10, 5, 6
224,10,2, 11, 5, 6
225,25,2, 1, 4, 5
226,30,2, 2, 4, 5
227,15,2, 3, 4, 5
228,30,2, 4, 4, 5
229,15,2,5,4,5
230,15,2,6,4,5
231,28,2,7,4,5
232,10,2,8,4,5
233,10,2,9,4,5
234,30,2,10,4,5
235,10,2,11,4,5
236,25,2,1,3,4
237,30,2,2,3,4
238,15,2,3,3,4
239,30,2,4,3,4
240,15,2,5,3,4
241,15,2,6,3,4
242,28,2,7,3,4
243,10,2,8,3,4
244,10,2,9,3,4
245,30,2,10,3,4
246,10,2,11,3,4
247,25,2,1,2,3
248,14,2,2,2,3
249,19,2,3,2,3
250,14,2,4,2,3
251,19,2,5,2,3
252,19,2,6,2,3
253,29,2,7,2,3
254,29,2,8,2,3
255,29,2,9,2,3
256,14,2,10,2,3
257,29,2,11,2,3

258,16,2,1,1,2
259,16,2,2,1,2
260,16,2,3,1,2
261,16,2,4,1,2
262,16,2,5,1,2
263,16,2,6,1,2
264,16,2,7,1,2
265,16,2,8,1,2
266,16,2,9,1,2
267,16,2,10,1,2
268,16,2,11,1,2
269,20,2,1,0,1
270,20,2,2,0,1
271,20,2,3,0,1
272,20,2,4,0,1
273,20,2,5,0,1
274,20,2,6,0,1
275,20,2,7,0,1
276,20,2,8,0,1
277,20,2,9,0,1
278,20,2,10,0,1
279,20,2,11,0,1
280,24,3,4,16,17
281,2,3,5,16,17
282,2,3,6,16,17
283,24,3,7,16,17
284,2,3,8,16,17
285,2,3,9,16,17
286,24,3,10,16,17
287,4,3,4,15,16
288,3,3,5,15,16
289,3,3,6,15,16
290,4,3,7,15,16
291,3,3,8,15,16
292,3,3,9,15,16
293,4,3,10,15,16
294,4,3,4,14,15
295,3,3,5,14,15
296,3,3,6,14,15
297,9,3,7,14,15
298,3,3,8,14,15
299,3,3,9,14,15
300,4,3,10,14,15
301,9,3,4,13,14
302,6,3,5,13,14
303,6,3,6,13,14
304,9,3,7,13,14
305,6,3,8,13,14
306,6,3,9,13,14
307,6,3,10,13,14
308,9,3,4,12,13

309,6,3,5,12,13
310,6,3,6,12,13
311,9,3,7,12,13
312,6,3,8,12,13
313,6,3,9,12,13
314,6,3,10,12,13
315,1,3,2,11,12
316,1,3,3,11,12
317,9,3,4,11,12
318,6,3,5,11,12
319,6,3,6,11,12
320,9,3,7,11,12
321,6,3,8,11,12
322,6,3,9,11,12
323,6,3,10,11,12
324,22,3,1,10,11
325,22,3,2,10,11
326,22,3,3,10,11
327,26,3,4,10,11
328,7,3,5,10,11
329,7,3,6,10,11
330,26,3,7,10,11
331,7,3,8,10,11
332,7,3,9,10,11
333,7,3,10,10,11
334,22,3,11,10,11
335,23,3,1,9,10
336,23,3,2,9,10
337,23,3,3,9,10
338,25,3,4,9,10
339,25,3,5,9,10
340,25,3,6,9,10
341,27,3,7,9,10
342,25,3,8,9,10
343,25,3,9,9,10
344,25,3,10,9,10
345,8,3,11,9,10
346,8,3,1,8,9
347,25,3,2,8,9
348,10,3,3,8,9
349,28,3,4,8,9
350,10,3,5,8,9
351,10,3,6,8,9
352,28,3,7,8,9
353,10,3,8,8,9
354,10,3,9,8,9
355,28,3,10,8,9
356,23,3,11,8,9
357,23,3,1,7,8
358,25,3,2,7,8
359,10,3,3,7,8

360,28,3,4,7,8
361,10,3,5,7,8
362,10,3,6,7,8
363,28,3,7,7,8
364,10,3,8,7,8
365,10,3,9,7,8
366,28,3,10,7,8
367,23,3,11,7,8
368,23,3,1,6,7
369,25,3,2,6,7
370,10,3,3,6,7
371,28,3,4,6,7
372,10,3,5,6,7
373,10,3,6,6,7
374,28,3,7,6,7
375,10,3,8,6,7
376,10,3,9,6,7
377,28,3,10,6,7
378,23,3,11,6,7
379,23,3,1,5,6
380,25,3,2,5,6
381,10,3,3,5,6
382,28,3,4,5,6
383,10,3,5,5,6
384,10,3,6,5,6
385,28,3,7,5,6
386,10,3,8,5,6
387,10,3,9,5,6
388,28,3,10,5,6
389,23,3,11,5,6
390,25,3,1,4,5
391,25,3,2,4,5
392,25,3,3,4,5
393,30,3,4,4,5
394,15,3,5,4,5
395,15,3,6,4,5
396,30,3,7,4,5
397,15,3,8,4,5
398,15,3,9,4,5
399,30,3,10,4,5
400,27,3,11,4,5
401,25,3,1,3,4
402,25,3,2,3,4
403,15,3,3,3,4
404,30,3,4,3,4
405,15,3,5,3,4
406,15,3,6,3,4
407,30,3,7,3,4
408,15,3,8,3,4
409,15,3,9,3,4
410,30,3,10,3,4

411,27,3,11,3,4
412,25,3,1,2,3
413,27,3,2,2,3
414,19,3,3,2,3
415,14,3,4,2,3
416,19,3,5,2,3
417,19,3,6,2,3
418,14,3,7,2,3
419,19,3,8,2,3
420,19,3,9,2,3
421,14,3,10,2,3
422,27,3,11,2,3
423,25,3,1,1,2
424,27,3,2,1,2
425,15,3,3,1,2
426,30,3,4,1,2
427,15,3,5,1,2
428,15,3,6,1,2
429,30,3,7,1,2
430,19,3,8,1,2
431,15,3,9,1,2
432,30,3,10,1,2
433,27,3,11,1,2
434,31,3,1,0,1
435,31,3,2,0,1
436,31,3,3,0,1
437,31,3,4,0,1
438,31,3,5,0,1
439,31,3,6,0,1
440,31,3,7,0,1
441,31,3,8,0,1
442,31,3,9,0,1
443,31,3,10,0,1
444,31,3,11,0,1
445,5,4,2,10,11
446,5,4,3,10,11
447,5,4,4,10,11
448,5,4,5,10,11
449,5,4,6,10,11
450,5,4,7,10,11
451,5,4,8,10,11
452,5,4,9,10,11
453,5,4,10,10,11
454,32,4,2,9,10
455,32,4,3,9,10
456,32,4,4,9,10
457,32,4,5,9,10
458,32,4,6,9,10
459,32,4,7,9,10
460,32,4,8,9,10
461,32,4,9,9,10

462,32,4,10,9,10
463,32,4,2,8,9
464,32,4,3,8,9
465,32,4,4,8,9
466,32,4,5,8,9
467,32,4,6,8,9
468,32,4,7,8,9
469,32,4,8,8,9
470,32,4,9,8,9
471,32,4,10,8,9
472,32,4,2,7,8
473,32,4,3,7,8
474,32,4,4,7,8
475,32,4,5,7,8
476,32,4,6,7,8
477,32,4,7,7,8
478,32,4,8,7,8
479,32,4,9,7,8
480,32,4,10,7,8
481,32,4,2,6,7
482,32,4,3,6,7
483,32,4,4,6,7
484,32,4,5,6,7
485,32,4,6,6,7
486,32,4,7,6,7
487,32,4,8,6,7
488,32,4,9,6,7
489,32,4,10,6,7
490,32,4,2,5,6
491,32,4,3,5,6
492,32,4,4,5,6
493,32,4,5,5,6
494,32,4,6,5,6
495,32,4,7,5,6
496,32,4,8,5,6
497,32,4,9,5,6
498,32,4,10,5,6
499,17,4,2,4,5
500,17,4,3,4,5
501,17,4,4,4,5
502,17,4,5,4,5
503,17,4,6,4,5
504,17,4,7,4,5
505,17,4,8,4,5
506,17,4,9,4,5
507,17,4,10,4,5
508,17,4,2,3,4
509,17,4,3,3,4
510,17,4,4,3,4
511,17,4,5,3,4
512,17,4,6,3,4

513,17,4,7,3,4
514,17,4,8,3,4
515,17,4,9,3,4
516,17,4,10,3,4
517,17,4,2,2,3
518,17,4,3,2,3
519,17,4,4,2,3
520,17,4,5,2,3
521,17,4,6,2,3
522,17,4,7,2,3
523,17,4,8,2,3
524,17,4,9,2,3
525,17,4,10,2,3
526,17,4,2,1,2
527,17,4,3,1,2
528,17,4,4,1,2
529,17,4,5,1,2
530,17,4,6,1,2
531,17,4,7,1,2
532,17,4,8,1,2
533,17,4,9,1,2
534,17,4,10,1,2
535,31,4,2,0,1
536,31,4,3,0,1
537,31,4,4,0,1
538,31,4,5,0,1
539,31,4,6,0,1
540,31,4,7,0,1
541,31,4,8,0,1
542,31,4,9,0,1
543,31,4,10,0,1
beam connectivities
1, 1, 17, 1, 2, 3
2, 1, 17, 1, 3, 4
3, 1, 17, 1, 4, 5
4, 1, 16, 1, 2, 3
5, 1, 16, 1, 3, 4
6, 1, 16, 1, 4, 5
7, 3, 15, 1, 2, 3
8, 3, 15, 1, 3, 4
9, 3, 15, 1, 4, 5
10, 3, 15, 1, 5, 6
11, 3, 14, 1, 1, 2
12, 3, 14, 1, 2, 3
13, 3, 14, 1, 3, 4
14, 3, 14, 1, 4, 5
15, 3, 14, 1, 5, 6
16, 4, 13, 1, 1, 2
17, 4, 13, 1, 2, 3
18, 4, 13, 1, 3, 4
19, 4, 13, 1, 4, 5

20,4, 13, 1, 5, 6
21,4, 12, 1, 1, 2
22,4, 12, 1, 2, 3
23,4, 12, 1, 3, 4
24,4, 12, 1, 4, 5
25,4, 12, 1, 5, 6
26,2, 11, 1, 1, 2
27,2, 11, 1, 2, 3
28,2, 11, 1, 3, 4
29,2, 11, 1, 4, 5
30,2, 11, 1, 5, 6
31,2, 11, 1, 6, 7
32,2, 11, 1, 7, 8
33,2, 10, 1, 1, 2
34,2, 10, 1, 2, 3
35,2, 10, 1, 3, 4
36,2, 10, 1, 4, 5
37,2, 10, 1, 5, 6
38,2, 10, 1, 6, 7
39,2, 10, 1, 7, 8
40,2, 10, 1, 8, 9
41,3, 8, 1, 1, 2
42,3, 8, 1, 2, 3
43,3, 8, 1, 3, 4
44,3, 8, 1, 4, 5
45,3, 8, 1, 5, 6
46,3, 8, 1, 6, 7
47,3, 8, 1, 7, 8
48,3, 8, 1, 8, 9
49,3, 6, 1, 1, 2
50,3, 6, 1, 5, 6
51,3, 6, 1, 6, 7
52,3, 6, 1, 7, 8
53,3, 6, 1, 8, 9
54,5, 2, 1, 1, 2
55,5, 2, 1, 2, 3
56,5, 2, 1, 3, 4
57,5, 2, 1, 4, 5
58,5, 2, 1, 5, 6
59,5, 2, 1, 6, 7
60,5, 2, 1, 7, 8
61,5, 2, 1, 8, 9
62, 1, 17, 2, 3, 4
63, 1, 17, 2, 4, 5
64, 1, 17, 2, 5, 6
65, 1, 16, 2, 2, 3
66, 1, 16, 2, 3, 4
67, 1, 16, 2, 4, 5
68, 1, 16, 2, 5, 6
69, 2, 15, 2, 2, 3
70, 2, 15, 2, 3, 4

71,2, 15, 2, 4, 5
72,2, 15, 2, 5, 6
73,2, 14, 2, 2, 3
74,2, 14, 2, 3, 4
75,2, 14, 2, 4, 5
76,2, 14, 2, 5, 6
77,3, 13, 2, 2, 3
78,3, 13, 2, 3, 4
79,3, 13, 2, 4, 5
80,3, 13, 2, 5, 6
81,3, 12, 2, 2, 3
82,3, 12, 2, 3, 4
83,3, 12, 2, 4, 5
84,3, 12, 2, 5, 6
85,2, 11, 2, 1, 2
86,2, 11, 2, 2, 3
87,2, 11, 2, 3, 4
88,2, 11, 2, 4, 5
89,2, 11, 2, 5, 6
90,2, 11, 2, 6, 7
91,2, 11, 2, 7, 8
92,2, 11, 2, 8, 9
93,2, 11, 2, 9, 10
94,2, 11, 2, 10, 11
95,2, 10, 2, 1, 2
96,2, 10, 2, 2, 3
97,2, 10, 2, 3, 4
98,2, 10, 2, 4, 5
99,2, 10, 2, 5, 6
100,2, 10, 2, 6, 7
101,2, 10, 2, 7, 8
102,2, 10, 2, 8, 9
103,2, 10, 2, 9, 10
104,2, 10, 2, 10, 11
105,2, 8, 2, 1, 2
106,2, 8, 2, 2, 3
107,2, 8, 2, 3, 4
108,2, 8, 2, 4, 5
109,2, 8, 2, 5, 6
110,2, 8, 2, 6, 7
111,2, 8, 2, 7, 8
112,2, 8, 2, 8, 9
113,2, 8, 2, 9, 10
114,2, 8, 2, 10, 11
115,2, 6, 2, 1, 2
116,2, 6, 2, 2, 3
117,2, 6, 2, 3, 4
118,2, 6, 2, 4, 5
119,2, 6, 2, 5, 6
120,2, 6, 2, 6, 7
121,2, 6, 2, 7, 8

122,2, 6, 2, 8, 9
123,2, 6, 2, 9, 10
124,2, 6, 2, 10, 11
125,2, 4, 2, 2, 3
126,6, 4, 2, 3, 4
127,6, 4, 2, 4, 5
128,6, 4, 2, 5, 6
129,6, 4, 2, 6, 7
130,6, 4, 2, 7, 8
131,6, 4, 2, 8, 9
132,6, 4, 2, 9, 10
133,2, 4, 2, 10, 11
134,5, 2, 2, 1, 2
135,5, 2, 2, 2, 3
136,5, 2, 2, 3, 4
137,5, 2, 2, 4, 5
138,5, 2, 2, 5, 6
139,5, 2, 2, 6, 7
140,5, 2, 2, 7, 8
141,5, 2, 2, 8, 9
142,5, 2, 2, 9, 10
143,5, 2, 2, 10, 11
144,1,17,3,4,5
145,1,17,3,5,6
146,1,17,3,6,7
147,1,17,3,7,8
148,1,17,3,8,9
149,1,17,3,9,10
150,1,16,3,4,5
151,1,16,3,5,6
152,1,16,3,6,7
153,1,16,3,7,8
154,1,16,3,8,9
155,1,16,3,9,10
156,2,15,3,4,5
157,2,15,3,5,6
158,2,15,3,6,7
159,2,15,3,7,8
160,2,15,3,8,9
161,2,15,3,9,10
162,2,14,3,4,5
163,2,14,3,5,6
164,2,14,3,6,7
165,2,14,3,7,8
167,2,14,3,8,9
168,2,14,3,9,10
169,2,13,3,4,5
170,2,13,3,5,6
171,2,13,3,6,7
172,2,13,3,7,8
173,2,13,3,8,9

174,2,13,3,9,10
175,2,12,3,2,3
176,2,12,3,3,4
177,2,12,3,4,5
178,2,12,3,5,6
179,2,12,3,6,7
180,2,12,3,7,8
181,2,12,3,8,9
182,2,12,3,9,10
183,2,11,3,1,2
184,2,11,3,2,3
185,2,11,3,3,4
186,2,11,3,4,5
187,2,11,3,5,6
188,2,11,3,6,7
189,2,11,3,7,8
190,2,11,3,8,9
191,2,11,3,9,10
192,2,11,3,10,11
193,2,9,3,1,2
194,2,9,3,2,3
195,2,9,3,3,4
196,2,9,3,4,5
197,2,9,3,5,6
198,2,9,3,6,7
199,2,9,3,7,8
200,2,9,3,8,9
201,2,9,3,9,10
202,2,9,3,10,11
203,2,7,3,1,2
204,2,7,3,2,3
205,2,7,3,3,4
206,2,7,3,4,5
207,2,7,3,5,6
208,2,7,3,6,7
209,2,7,3,7,8
210,2,7,3,8,9
211,2,7,3,9,10
212,2,7,3,10,11
213,2,5,3,1,2
214,2,5,3,2,3
215,2,5,3,3,4
216,2,5,3,4,5
217,2,5,3,5,6
218,2,5,3,6,7
219,2,5,3,7,8
220,2,5,3,8,9
221,2,5,3,9,10
222,2,5,3,10,11
223,2,4,3,1,2
224,2,4,3,2,3

225,2,4,3,3,4
226,2,4,3,4,5
227,2,4,3,5,6
228,2,4,3,6,7
229,2,4,3,7,8
230,2,4,3,8,9
231,2,4,3,9,10
232,2,4,3,10,11
233,5,3,3,1,2
234,5,3,3,2,3
235,5,3,3,3,4
236,5,3,3,4,5
237,5,3,3,5,6
238,5,3,3,6,7
239,5,3,3,7,8
240,5,3,3,8,9
241,5,3,3,9,10
242,5,3,3,10,11
243,6,11,4,2,3
244,6,11,4,3,4
245,6,11,4,4,5
246,6,11,4,5,6
247,6,11,4,6,7
248,6,11,4,7,8
249,6,11,4,8,9
250,6,11,4,9,10
251,6,9,4,2,3
252,6,9,4,3,4
253,6,9,4,4,5
254,6,9,4,5,6
255,6,9,4,6,7
256,6,9,4,7,8
257,6,9,4,8,9
258,6,9,4,9,10
259,6,7,4,2,3
260,6,7,4,3,4
261,6,7,4,4,5
262,6,7,4,5,6
263,6,7,4,6,7
264,6,7,4,7,8
265,6,7,4,8,9
266,6,7,4,9,10
267,6,5,4,2,3
268,6,5,4,3,4
269,6,5,4,4,5
270,6,5,4,5,6
271,6,5,4,6,7
272,6,5,4,7,8
273,6,5,4,8,9
274,6,5,4,9,10
275,6,3,4,2,3

276,6,3,4,3,4
277,6,3,4,4,5
278,6,3,4,5,6
279,6,3,4,6,7
280,6,3,4,7,8
281,6,3,4,8,9
282,6,3,4,9,10
283,5,1,4,2,3
284,5,1,4,3,4
285,5,1,4,4,5
286,5,1,4,5,6
287,5,1,4,6,7
288,5,1,4,7,8
289,5,1,4,8,9
290,5,1,4,9,10
type of analysis
2
static loads
0,0,0,0
Monotonic Pushover Analysis (1=force control; 2=displacement control)
1
FORCE CONTROLLED ANALYSIS
1
0.5,150,5
Snapshot Control Data
0
0,0,0,0,0
OUTPUT CONTROL
10,1,1,3,5,7,9,11,12,13,15,17
story1
story3
story5
story7
story9
story11
story12
story13
story15
story17
ELEMENT HYSTERESIS OUTPUT
0,0,0,0,0,0

CASE STUDY #9

Note: This example file is for one of the cases discussed in Section IV for case #9.

*input filename: idarc.dat
data filename: case9_3.dat
output filename: idarc.out
results filename: case9_3.out*

file: idarc.dat

case9_3.dat
case9_3.out

file: case9_3.dat

CASE 9: 70% reduction 1st fl. 35% 2nd & 10% 3rd. consider col. compre

Control Data

3,1,0,0,0,0,1, 1

Element types

6,9,0,0,0,0,0,1,0

Element data

12,9,0,0,0,0,0,1,0

Unit system

1

Floor elevations

45.0, 93.0, 141.0

Number of duplicate frames

2

No of column lines

4

Nodal weights

1, 1, 3.375, 3.375, 3.375, 3.375

2, 1, 3.375, 3.375, 3.375, 3.375

3, 1, 3.375, 3.375, 3.375, 3.375

Env generation option

1

Hysteretic Control

3

1, 1, 15.0, 0.1, 0.01, 1.0, 2

2, 1, 15.0, 0.1, 0.01, 1.0, 2

3, 1, 15.0, 0.1, 0.01, 0.1, 0

Column input option

1

Column data

1

1, 10, 50, 20, 48.0,0,3.0

 1, 72264.6, 1140.0, 7.0, 16.0, 0.0008, 0.03, 0.55

 7.0, 16.0, 0.0008, 0.03, 0.55

 1, 72264.6, 1140.0, 7.0, 16.0, 0.0008, 0.03, 0.55

 7.0, 16.0, 0.0008, 0.03, 0.55

1

2, 10, 50, 20, 48.0,0,3.0

1, 369360.0, 2322.0, 24.0, 72.0, 0.0006, 0.01, 0.16
 24.0, 72.0, 0.0006, 0.01, 0.16
 1, 369360.0, 2322.0, 24.0, 72.0, 0.0006, 0.01, 0.16
 24.0, 72.0, 0.0006, 0.01, 0.16
 1
 3, 10, 50, 20, 48.0, 0, 3.0
 1, 47559, 887, 11.0, 21.0, 0.0008, 0.03, 0.84
 11.0, 21.0, 0.0008, 0.03, 0.84
 1, 47559, 887, 11.0, 21.0, 0.0008, 0.03, 0.84
 11.0, 21.0, 0.0008, 0.03, 0.84
 1
 4, 10, 50, 20, 48.0, 0, 3.0
 1, 250800.0, 1995.0, 32.0, 84.0, 0.001, 0.03, 0.24
 32.0, 84.0, 0.001, 0.03, 0.24
 1, 250800.0, 1995.0, 32.0, 84.0, 0.001, 0.03, 0.24
 32.0, 84.0, 0.001, 0.03, 0.24
 1
 5, 10, 50, 20, 45.0, 0, 0, 3.0
 3, 14453.2, 380.0, 8, 10.0, 0.0025, 0.06, 0.28
 8, 10.0, 0.0025, 0.06, 0.28
 3, 14453.2, 380.0, 1, 2.0, 0.0025, 0.06, 0.28
 1, 2.0, 0.0025, 0.06, 0.28
 1
 6, 10, 50, 20, 45.0, 0, 0, 3.0
 1, 62496.0, 885.0, 115, 120, 0.003, 0.08, 0.96
 115, 120, 0.003, 0.08, 0.96
 1, 82496.0, 885.0, 115, 120, 0.003, 0.08, 0.96
 115, 120, 0.003, 0.08, 0.96

Beam input type

1

Beam data

1

1, 72.0, 2.0, 7.0

 2, 181980.0, 7.38, 37.0, 0.0004, 0.03, 1.32
 7.38, 37.0, 0.0004, 0.03, 1.32
 2, 181980.0, 7.38, 37.0, 0.0004, 0.03, 1.32
 7.38, 37.0, 0.0004, 0.03, 1.32

1

2, 72.0, 7.0, 7.0

 2, 181980.0, 7.38, 37.0, 0.0004, 0.03, 1.32
 7.38, 37.0, 0.0004, 0.03, 1.32
 2, 181980.0, 7.38, 37.0, 0.0004, 0.03, 1.32
 7.38, 37.0, 0.0004, 0.03, 1.32

1

3, 72.0, 7.0, 2.0

 2, 181980.0, 7.38, 37.0, 0.0004, 0.03, 1.32
 7.38, 37.0, 0.0004, 0.03, 1.32
 2, 181980.0, 7.38, 37.0, 0.0004, 0.03, 1.32
 7.38, 37.0, 0.0004, 0.03, 1.32

1

4, 72.0, 2.0, 7.0

2, 123186.0,	7.38, 37.0, 0.0004, 0.03,	1.95
	7.38, 37.0, 0.0004, 0.03,	1.95
2, 123186.0,	7.38, 37.0, 0.0004, 0.03,	1.95
	7.38, 37.0, 0.0004, 0.03,	1.95
1		
5, 72.0, 7.0, 7.0		
2, 123186.0,	7.38, 37.0, 0.0004, 0.03,	1.95
	7.38, 37.0, 0.0004, 0.03,	1.95
2, 123186.0,	7.38, 37.0, 0.0004, 0.03,	1.95
	7.38, 37.0, 0.0004, 0.03,	1.95
1		
6, 72.0, 7.0, 2.0		
2, 123186.0,	7.38, 37.0, 0.0004, 0.03,	1.95
	7.38, 37.0, 0.0004, 0.03,	1.95
2, 123186.0,	7.38, 37.0, 0.0004, 0.03,	1.95
	7.38, 37.0, 0.0004, 0.03,	1.95
1		
7, 72.0, 2.0, 7.0		
2, 43675.0,	7.38, 37.0, 0.001, 0.03,	5.50
	7.38, 37.0, 0.001, 0.03,	5.50
2, 43675.0,	7.38, 37.0, 0.001, 0.03,	5.50
	7.38, 37.0, 0.001, 0.03,	5.50
1		
8, 72.0, 7.0, 7.0		
2, 43675.0,	7.38, 37.0, 0.001, 0.03,	5.50
	7.38, 37.0, 0.001, 0.03,	5.50
2, 43675.0,	7.38, 37.0, 0.001, 0.03,	5.50
	7.38, 37.0, 0.001, 0.03,	5.50
1		
9, 72.0, 7.0, 2.0		
2, 43675.0,	7.38, 37.0, 0.001, 0.03,	5.50
	7.38, 37.0, 0.001, 0.03,	5.50
2, 43675.0,	7.38, 37.0, 0.001, 0.03,	5.50
	7.38, 37.0, 0.001, 0.03,	5.50

HYSERETIC DAMPER BRACES PROPERTIES

0

1, 1, 1.0, 80, 3.0

Column connectivity

1,1,1,1,2,3

2,2,1,2,2,3

3,2,1,3,2,3

4,1,1,4,2,3

5,3,1,1,1,2

6,4,1,2,1,2

7,4,1,3,1,2

8,3,1,4,1,2

9,5,1,1,0,1

10,6,1,2,0,1

11,6,1,3,0,1

12,5,1,4,0,1

Beam connectivity

```
1,1,3,1,1,2  
2,2,3,1,2,3  
3,3,3,1,3,4  
4,4,2,1,1,2  
5,5,2,1,2,3  
6,6,2,1,3,4  
7,7,1,1,1,2  
8,8,1,1,2,3  
9,9,1,1,3,4  
BRACE CONNECTIVITY  
1,1,3,1,2,1,2,3,76  
Type of Analysis  
3  
Static loads  
0,0,0,0  
Dynamic Analysis Control Data  
0.30, 0.0, 0.0005, 32.0, 6, 3  
Wave data  
0, 0, 6400, 0.005  
El-Centro - EARTHQUAKE  
flea30.a  
Output options  
0  
0 0 0 0 0  
STORY OUTPUT CONTROL  
3, 0.005,1,2,3  
floor1h.out  
floor2h.out  
floor3h.out  
Hys output  
0,0,0,0,0,0  
1
```

NOTES : The earthquake ground acceleration record is read separately from a file named 'flea30.a' as specified in the input data

CASE STUDY #10

input filename: idarc.dat
data filename: case10.dat
output filename: idarc.out
results filename: case10.out

file: idarc.dat

case10.dat
case10.out

file: case10.dat

CASE 10: MASONRY INFILLED FRAME TESTED IN SEISMIC LAB

Control Data

3,1,0,0,1,0, 0, 1, 1

Element types

2,1,0,0,0,0,0,0,1

Element data

6,3,0,0,0,0,0,0,1

Unit system

1

Floor elevations

12,82.512,94.512

Number of duplicate frames

1

No of column lines

2

Nodal weights

1, 1, 3.375, 3.375

2, 1, 3.375, 3.375

3, 1, 3.375, 3.375

Env generation option

0

Masonry properties

1,3.408,0.123,0.003,0.115,0.120,0.3

Hysteretic Control

1

1, 1, 10.0, 0.01, 0.01, 1.0, 2

Column input option

1

Column data

1

1, 10, 50, 20, 70.512,4.0,4.0

1, 456228, 553.2, 142.96, 146.19, 0.000735, 0.003, 0.6247

142.96, 146.19, 0.000735, 0.003, 0.6247

1, 456228, 553.2, 142.96, 146.19, 0.000735, 0.003, 0.6247

142.96, 146.19, 0.000735, 0.003, 0.6247

1

2, 10, 50, 20, 16.0,4.0,4.0

1, 456228, 3250., 142.96, 146.19, 0.000735, 0.003, 0.6247

142.96, 146.19, 0.000735, 0.003, 0.6247

1, 456228, 3250., 142.96, 146.19, 0.000735, 0.003, 0.6247
 142.96, 146.19, 0.000735, 0.003, 0.6247
 Beam input type
 1
 Beam data
 1
 1,100.5,4.0,4.0
 1, 414903, 124.45, 127.3, 0.000725, 0.003, 0.5724
 124.45, 127.3, 0.000725, 0.003, 0.5724
 1, 414903, 124.45, 127.3, 0.000725, 0.003, 0.5724
 124.45, 127.3, 0.000725, 0.003, 0.5724
 Infill Wall input
 Infill panel geometry
 1,0
 1,3.504,92.008,62.480
 175.23,165.504,112.726
 1.0,0.1,0.9,2.0,0.02
 1,0.22,0.05,0.1
 0.2,0.8,1.0,10.0
 Column connectivity
 1,2,1,1,0,1
 2,1,1,1,1,2
 3,2,1,1,2,3
 4,2,1,2,0,1
 5,1,1,2,1,2
 6,2,1,2,2,3
 Beam connectivity
 1,1,1,1,1,2
 2,1,2,1,1,2
 3,1,3,1,1,2
 Infill wall connectivity
 1,1,1,2,1,1,2,1
 Type of Analysis
 4
 Static loads
 0,0,0,0
 Quasi Static Analysis Control Data
 1
 1
 3
 37
 0.0,0.175,0.,-0.175,0.,0.35,0.,-0.35,0.,0.525,0.,-0.525,0.,0.7,0.,-0.7,0.,0.875,0.,-0.875,0.,1.05,0.,-1.05,0.,1.225,0.,-1.225,0.,1.4,0.,-1.4,0.,1.4,0.,-1.4,0.
 0.001
 Snapshot Output
 0
 0,0,0,0,0
 Output options
 3,1,1,2,3
 FR11.out
 FR22.out

FR33.out
Hys output
0,0,0,0,0,1
Infill Wall # TO BE PRINTED
1
END OF INPUT FILE

=====

Type of Analysis
3
Static loads
0,0,0,0
Dynamic Analysis Control Data
0.68, 0.0, 0.001,32.0, 2, 3
Wave data
0, 0,6400,0.005
El-Centro - EARTHQUAKE
vwta20.a0
Snapshot Output
0
0,0,0,0,0
Output options
3,0.001,1,2,3
FR11.out
FR22.out
FR33.out
Hys output
0,0,0,0,0,1
Infill Wall # TO BE PRINTED
1

CASE STUDY #11

*input filename: idarc.dat
data filename: case11.dat
output filename: idarc.out
results filename: case11.out*

file: idarc.dat

case11.dat
case11.out

file: case11.dat

CASE 11: FOR DEEP BEAM TEST: Deep Column (DC4)

CONTROL DATA

1,1,1,1,0,0,0,1,1

ELEMENT TYPES

1,1,0,0,0,0,0,0,0

ELEMENT DATA

2,1,0,0,0,0,0,0

UNITS SYSTEM : KN - MM

2

FLOOR ELEVATIONS

1500.0

DESCRIPTION OF IDENTICAL FRAMES

1

PLAN CONFIGURATION: NO OF COLUMN LINES

2

NODAL WEIGHTS

1,1, 22.24, 22.24

CODE FOR SPECIFICATION OF USER PROPERTIES

0

CONCRETE PROPERTIES

1, 0.0402, 0.0, 0.0, 0.0, 0.0, 0.0

REINFORCEMENT PROPERTIES

1, 0.4, 0.0, 0.0, 0.0, 0.0

HYSTERETIC MODELING RULES

3

1, 1, 4.0, 0.01, 0.01, 1.0, 2

2, 1, 4.0, 0.01, 0.01 1.0, 2

3, 1, 200.0, 0.01, 0.01, 1.0, 2

MOMENT CURVATURE ENVELOPE GENERATION

1

COLUMN PROPERTIES

2

1 30 60 150 1500.0, 0.0, 50.0

-2, 2.62E+8, 2.62E+5, 15000.0, 17000.0, 0.00011, 0.001, 1.0
15000.0, 17000.0, 0.00011, 0.001, 1.0

1, 500.0, 6.0, 7.0, 0.03, 0.5, 1.0

6.0, 7.0, 0.03, 0.5, 1.0

BEAM MOMENT CURVATURE ENVELOPE GENERATION

1

BEAM DIMENSIONS

1

1, 2000.0, 50.0, 50.0
 -2, 2.62E+8, 15000.0, 17000.0, 0.00011, 0.001, 1.0
 15000.0, 17000.0, 0.00011, 0.001, 1.0

COLUMN CONNECTIVITY

1,1,1,0,1

2,1,1,2,0,1

BEAM CONNECTIVITY

1,1,1,1,1,2

ANALYSIS TYPE

4

STATIC ANALYSIS OPTION

0,0,0,0

QUASI-STATIC CYCLIC ANALYSIS

1

1

1

260

0.0000	6.8580	0.0000	-6.8580	0.0000	10.1600
0.0000	-10.1600	0.0000	12.7000	25.4000	32.4104
25.4000	12.7000	0.0000	-12.7000	-25.4000	-32.4104
-25.4000	-12.7000	0.0000	12.7000	25.4000	32.4104
25.4000	12.7000	0.0000	-12.7000	-25.4000	-32.4104
-25.4000	-12.7000	12.7000	25.4000	32.4104	25.4000
12.7000	0.0000	-12.7000	-25.4000	-32.4104	-25.4000
-12.7000	0.0000	12.7000	25.4000	32.4104	50.8000
55.8800	50.8000	32.4104	25.4000	12.7000	0.0000
-12.7000	-25.4000	-32.4104	-50.8000	-55.8800	-50.8000
-32.4104	-25.4000	-12.7000	0.0000	12.7000	25.4000
32.4104	50.8000	55.8800	50.8000	32.4104	25.4000
12.7000	0.0000	-12.7000	-25.4000	-32.4104	-50.8000
-55.8800	-50.8000	-32.4104	-25.4000	-12.7000	0.0000
12.7000	25.4000	32.4104	50.8000	55.8800	50.8000
32.4104	25.4000	12.7000	0.0000	-12.7000	-25.4000
-32.4104	-50.8000	-55.8800	-50.8000	-32.4104	-25.4000
-12.7000	0.0000	25.4000	50.8000	76.2000	86.8680
76.2000	50.8000	25.4000	0.0000	-25.4000	-50.8000
-76.2000	-86.8680	-76.2000	-50.8000	-25.4000	0.0000
25.4000	50.8000	76.2000	86.8680	76.2000	50.8000
25.4000	0.0000	-25.4000	-50.8000	-76.2000	-86.8680
-76.2000	-50.8000	-25.4000	0.0000	25.4000	50.8000
76.2000	86.8680	76.2000	50.8000	25.4000	0.0000
-25.4000	-50.8000	-76.2000	-86.8680	-76.2000	-50.8000
-25.4000	0.0000	38.1000	76.2000	106.6800	114.3000
106.6800	76.2000	38.1000	0.0000	-38.1000	-76.2000
-106.6800	-114.3000	-106.6800	-76.2000	-38.1000	0.0000
38.1000	76.2000	106.6800	114.3000	106.6800	76.2000
38.1000	0.0000	-38.1000	-76.2000	-106.6800	-114.3000
-106.6800	-76.2000	-38.1000	0.0000	38.1000	76.2000
106.6800	114.3000	106.6800	76.2000	38.1000	0.0000

-38.1000	-76.2000	-106.6800	-114.3000	-106.6800	-76.2000
-38.1000	0.0000	38.1000	76.2000	114.3000	139.7000
147.8280	139.7000	114.3000	76.2000	38.1000	0.0000
-38.1000	-76.2000	-114.3000	-139.7000	-147.8280	-139.7000
-114.3000	-76.2000	-38.10000	0.0000	38.1000	76.2000
114.3000	139.7000	147.8280	139.7000	114.3000	76.2000
38.1000	0.0000	-38.1000	-76.2000	-114.3000	-139.7000
-147.8280	-139.7000	-114.3000	-76.2000	-38.1000	0.0000
38.1000	76.2000	114.3000	139.7000	147.8280	139.7000
114.3000	76.2000	38.1000	0.0000	-38.1000	-76.2000
-114.3000	-139.7000	-147.8280	-139.7000	-114.3000	-76.2000
-38.10000	0.0000				

0.02

SNAPSHOT OUTPUT CONTROL

0

0,0,0,0

STORY OUTPUT CONTROL

1,1,1

LEVEL1.OUT

ELEMENT HYSTERESIS OUTPUT INFORMATION

2,1,0,0,0,0

COLUMN OUTPUT

1 2

BEAM OUTPUT

1

CASE STUDY #12

input filename: idarc.dat
data filename: case12.dat
output filename: idarc.out
results filename: case12.out

file: idarc.dat

case12.dat
case12.out

file: case12.dat

CASE12: Dynamic analysis for a weakened structure: Alterantive C(SA) for upper bound
(Original structure: Case Study 4)

Control Data

3,2,0,0,0,0,0,1

Element types

8,1,0,0,0,0,0,0,0

Element data

24,18,0,0,0,0,0,0,0

Unit system

1

Floor elevations

45.0, 93.0, 141.0

Number of duplicate frames

1, 1

No of column lines

4, 4

Nodal weights

1, 1, 2.25, 4.5, 4.5, 2.25

2, 2.25, 4.5, 4.5, 2.25

2, 1, 2.25, 4.5, 4.5, 2.25

2, 2.25, 4.5, 4.5, 2.25

3, 1, 2.25, 4.5, 4.5, 2.25

2, 2.25, 4.5, 4.5, 2.25

Env generation option

1

Hysteretic Control

3

1, 1, 8.0, 0.30, 0.15, 1.0, 0

2, 1, 10.0, 0.30, 0.15, 1.0, 0

3, 1, 200.0, 0.01, 0.01, 1.0, 3

Column input option

1

Column data

1

1, 2.25, 50, 20, 48.0, 3.0, 3.0

1, 45400.0, 843.0, 10.0, 18.0, 0.002, 0.080, 0.88

10.0, 18.0, 0.002, 0.080, 0.88

1, 45400.0, 843.0, 10.0, 18.0, 0.002, 0.080, 0.88

10.0, 18.0, 0.002, 0.080, 0.88

1
 2, 4.5, 50, 20, 48.0, 3.0, 3.0
 1, 45400.0, 843.0, 10.0, 22.0, 0.002, 0.080, 0.88
 10.0, 22.0, 0.002, 0.080, 0.88
 1, 45400.0, 843.0, 10.0, 22.0, 0.002, 0.080, 0.88
 10.0, 22.0, 0.002, 0.080, 0.88
 1
 3, 4.5, 50, 20, 48.0, 3.0, 3.0
 1, 45900.0, 900.0, 10.0, 22.0, 0.003, 0.120, 0.87
 10.0, 22.0, 0.003, 0.120, 0.87
 1, 45900.0, 900.0, 10.0, 22.0, 0.003, 0.120, 0.87
 10.0, 22.0, 0.003, 0.120, 0.87
 1
 4, 9.0, 50, 20, 48.0, 3.0, 3.0
 1, 45900.0, 900.0, 14.0, 29.0, 0.003, 0.120, 0.87
 14.0, 29.0, 0.003, 0.120, 0.87
 1, 45900.0, 900.0, 14.0, 29.0, 0.003, 0.120, 0.87
 14.0, 29.0, 0.003, 0.120, 0.87
 1
 5, 6.75, 50, 20, 45.0, 0.0, 3.0
 1, 45200.0, 960.0, 12.0, 28.0, 0.003, 0.120, 0.88
 12.0, 28.0, 0.003, 0.120, 0.88
 1, 45200.0, 960.0, 12.0, 28.0, 0.003, 0.120, 0.88
 12.0, 28.0, 0.003, 0.120, 0.88
 1
 6, 13.5, 50, 20, 45.0, 0.0, 3.0
 1, 45200.0, 960.0, 16.0, 38.0, 0.003, 0.120, 0.88
 16.0, 38.0, 0.003, 0.120, 0.88
 1, 45200.0, 960.0, 16.0, 38.0, 0.003, 0.120, 0.88
 16.0, 38.0, 0.003, 0.120, 0.88
 3
 7, 2.25, 50, 20, 48.0, 3.0, 3.0, 1
 -3, 22901.33, 60800.0, 1.5002, 4.2594, 0.0011162, 0.0020825, 0.0198120, 0.2724
 1.5002, 4.2594, 0.0011162, 0.0020825, 0.0198120, 0.2724
 3
 8, 4.5, 50, 20, 48.0, 3.0, 3.0, 1
 -3, 22901.33, 60800.0, 3.0003, 8.0365, 0.0012523, 0.0021693, 0.0180340, 1.1428
 3.0003, 8.0365, 0.0012523, 0.0021693, 0.0180340, 1.1428

Beam input type

1

Beam data

1

1, 72.0, 2.0, 2.0

2, 140000.0, 30.0, 70.0, 0.001, 0.04,	1.71
30.0, 70.0, 0.001, 0.04,	1.71
2, 140000.0, 30.0, 70.0, 0.001, 0.04,	1.71
30.0, 70.0, 0.001, 0.04,	1.71

Column connectivity

1,1,1,1,2,3

2,2,1,2,2,3

3,2,1,3,2,3

4,1,1,4,2,3
5,3,1,1,1,2
6,4,1,2,1,2
7,4,1,3,1,2
8,3,1,4,1,2
9,5,1,1,0,1
10,6,1,2,0,1
11,6,1,3,0,1
12,5,1,4,0,1
13,7,2,1,2,3
14,8,2,2,2,3
15,8,2,3,2,3
16,7,2,4,2,3
17,7,2,1,1,2
18,8,2,2,1,2
19,8,2,3,1,2
20,7,2,4,1,2
21,7,2,1,0,1
22,8,2,2,0,1
23,8,2,3,0,1
24,7,2,4,0,1
Beam connectivity
1,1,3,1,1,2
2,1,3,1,2,3
3,1,3,1,3,4
4,1,2,1,1,2
5,1,2,1,2,3
6,1,2,1,3,4
7,1,1,1,1,2
8,1,1,1,2,3
9,1,1,1,3,4
10,1,3,2,1,2
11,1,3,2,2,3
12,1,3,2,3,4
13,1,2,2,1,2
14,1,2,2,2,3
15,1,2,2,3,4
16,1,1,2,1,2
17,1,1,2,2,3
18,1,1,2,3,4
Type of Analysis
3
Static loads
0,0,0,0
Dynamic Analysis Control Data
0.3, 0.0, 0.001, 30.0, 1.3362, 1
Wave data
0, 0, 3000, 0.01
WHITENOISE-EARTHQUAKE
whitenoise.txt
SNAPSHOT CONTROL DATA

0
0,0,0,0,0
Output options
3, 0.001, 1,2,3
story_1.out
story_2.out
story_3.out
Hys output
6,0,0,0,0,0
COLUMN
13, 14, 17, 18, 21, 22

APPENDIX C

DEFAULT SETTINGS IN FILE IDDEFN.FOR

The following table contains the list of the control variables used in IDARC to dimension the variables used during analysis. The executable PC version of the program is compiled using the default values listed below. The default value for each variable may be changed in the file IDDEFN.FOR, and the program recompiled to take into account the new variable sizes.

Table C.1 Default Maximum Settings in File IDDEFN.FOR

Variable Name	Default Setting	Variable Description
NN1	20	Maximum Number of Stories
NN2	10	Maximum Number of Frames
NN4	30	Maximum Number of Vertical Lines
NN5	1000	Maximum Number of Degrees of Freedom
NN6	300	Maximum Half Band Width
NNC	100	Maximum Number of Column Elements
NNB	100	Maximum Number of Beam Elements
NNW	50	Maximum Number of Shear Wall Elements
NNE	50	Maximum Number of Edge Beams
NNT	50	Maximum Number of Transverse Beams
NNR	50	Maximum Number of Rotational Spring Elements
NND1	40	Maximum Number of Viscoelastic Damper Elements
NND2	40	Maximum Number of Friction Damper Elements
NND3	40	Maximum Number of Hysteretic Damper Elements
NND4	50	Maximum Number of Infill Panels
NP1	10	Maximum Number of Concrete Types
NP2	5	Maximum Number of Steel Reinforcement Types
NZ1	10	Maximum Number of Output Histories for Dynamic Analysis
NZ2	8000	Maximum Number of Points in Earthquake Wave
NZ3	10	Maximum Number of Hysteretic Properties Specified
NZ4	500	Maximum Number of Points in Monotonic Analysis and Quasi-Static Input

APPENDIX D

IMPLEMENTATION OF POLYGONAL HYSTERETIC MODEL

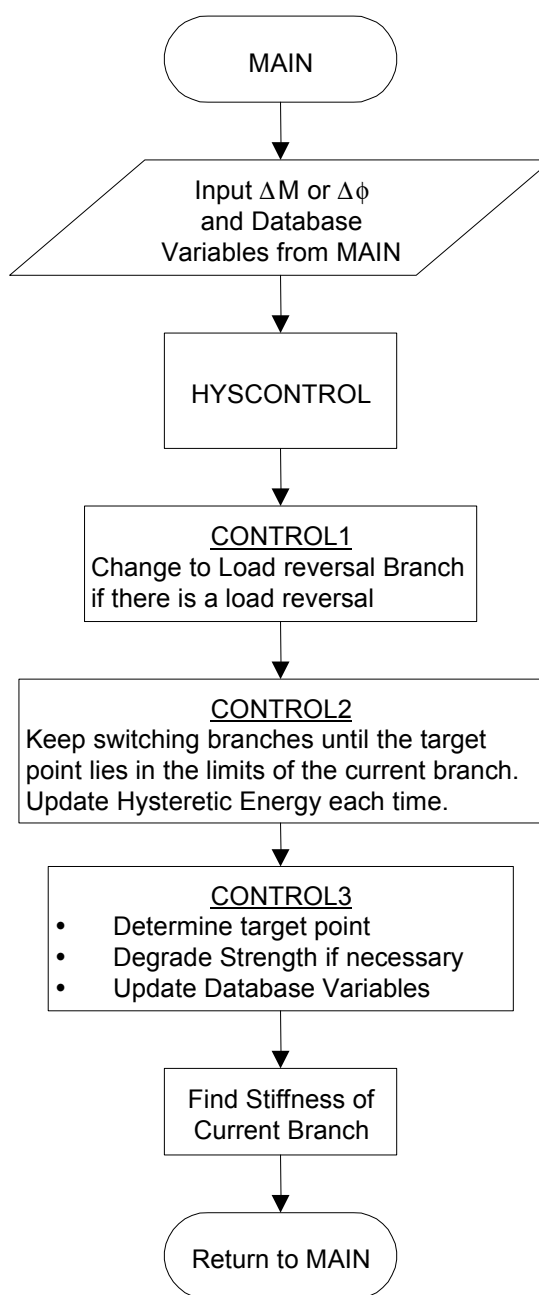


Fig. D.1 Overall flow of PHM module

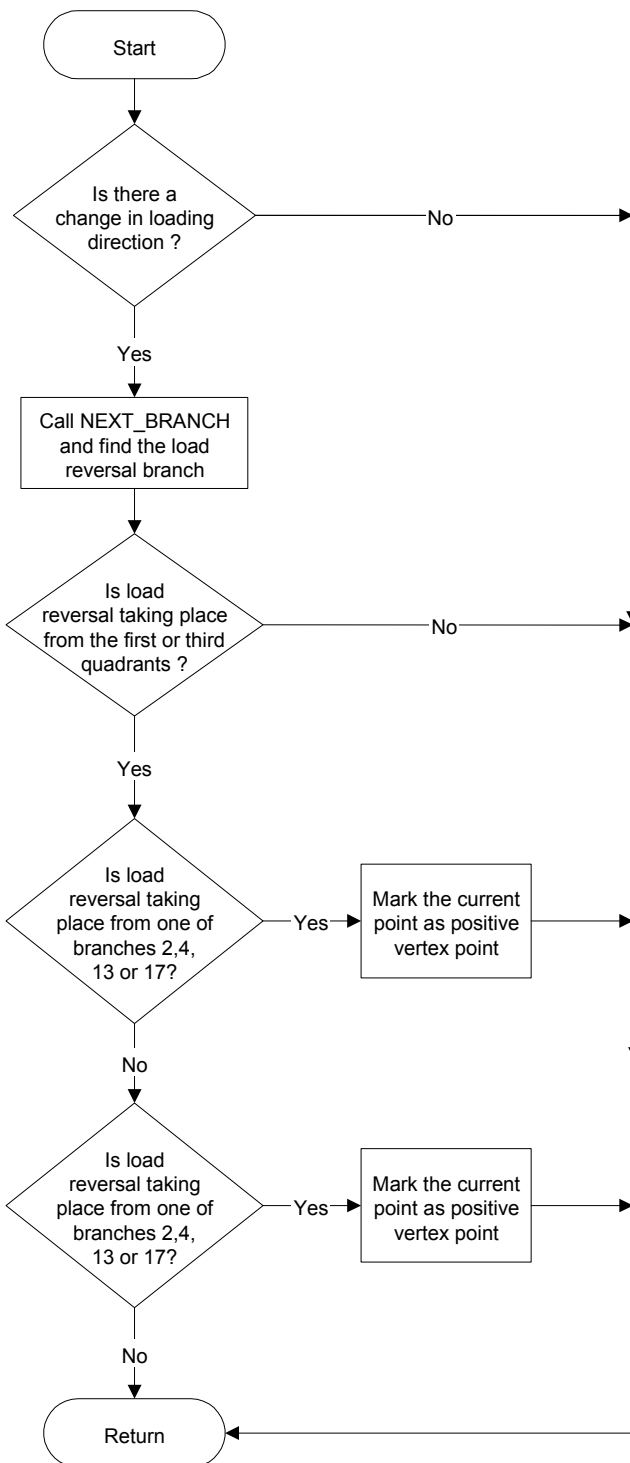


Fig. D.2 Flowchart for Subroutine CONTROL1

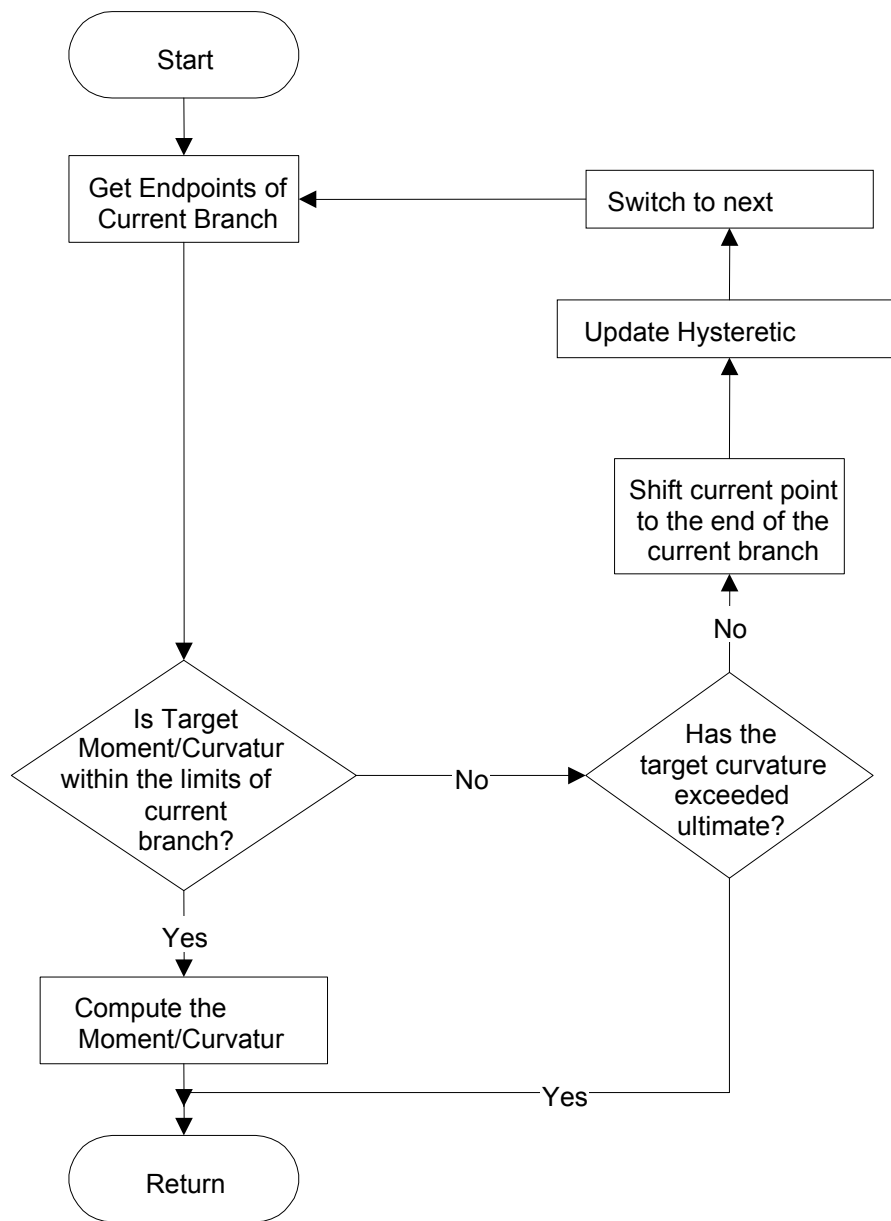


Fig. D.3 Flowchart for Subroutine CONTROL2

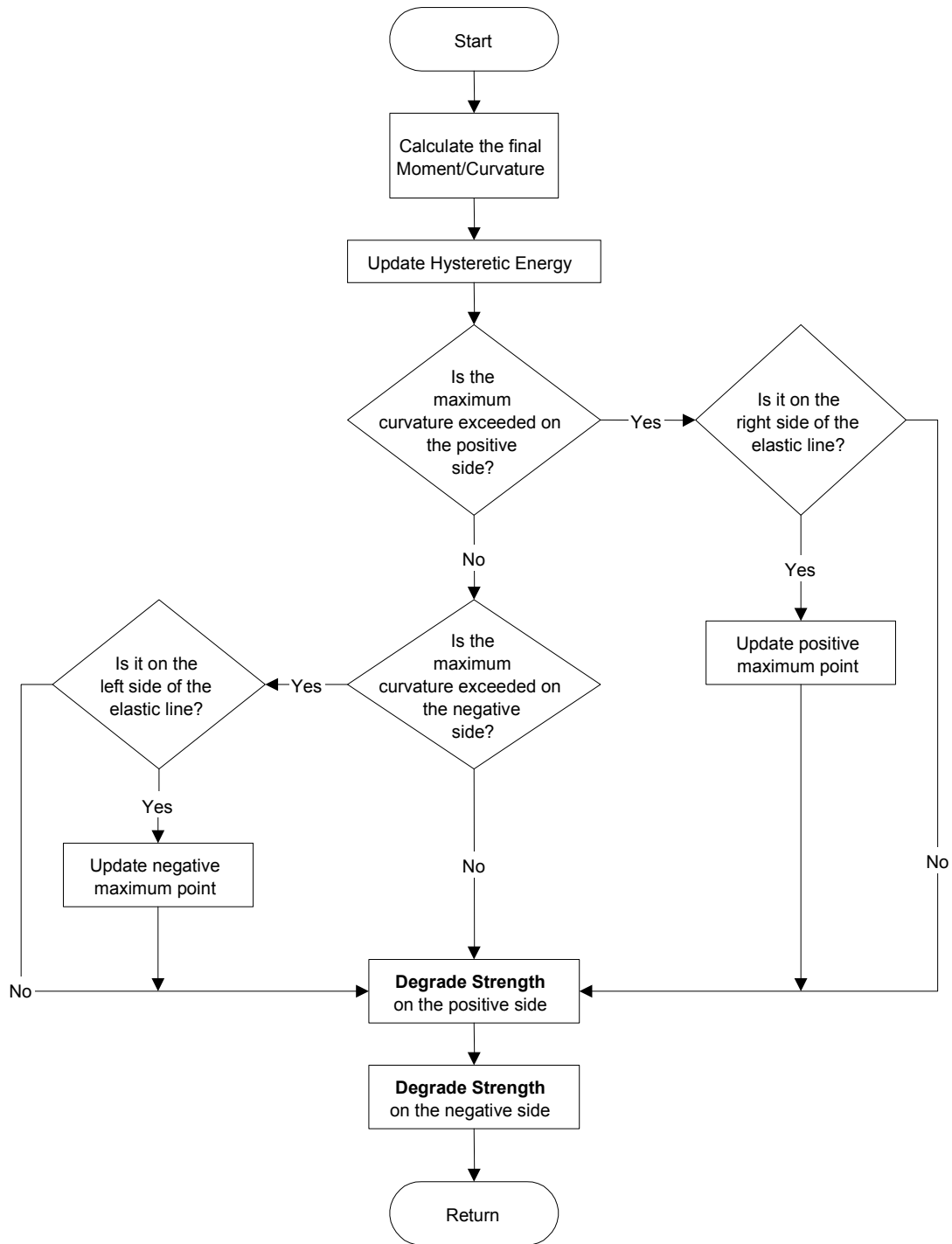


Fig. D.4 Flowchart for Subroutine CONTROL3

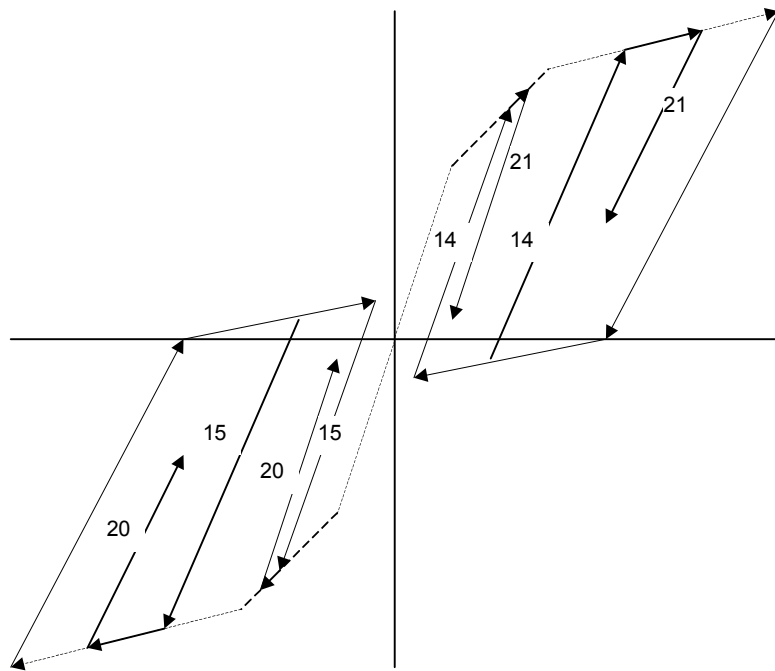


Fig. D.5: Explanation for Rules which change Branches from 2 to 21 and 3 to 20

Table D.1 Subroutines and their functions

SUBROUTINE	FUNCTION
HYSCONTROL	Main Hysteretic Model Control Subroutine. (Figure A.1)
CONTROL1	This subroutine changes to a Load-reversal branch when there is a change in the direction of loading. (Figure A.2)
CONTROL2	If the target point does not lie on the current branch, this subroutine keeps switching branches till target-point lies on current branch, each time setting the current point to the end point of the current branch and updating the hysteretic energy each time. (Figure A.3)
CONTROL3	When this subroutine is called, the target point always lies on the current branch. The target point is found by interpolating between the end points of the current branch. It also degrades the strength, causing a drop in the backbone curve. (Figure A.4)
POINTS	Computes the coordinates of any of the control points, given the database variables.
NEXT_BRANCH	Uses the branch-transition rules to determine the number of the next branch, given the load increment and the database variables.

Table D.2 Variables Governing PHM

SYMBOL	MEANING
M_{cur}	Current Moment level in the section
ϕ_{cur}	Current Curvature of the section
ΔM	Moment Increment
EI	Slope of the current branch
M_{\max}^+	Maximum positive moment reach by the section at any time
ϕ_{\max}^+	Maximum positive curvature reached by the section at any time
M_{\max}^-	Maximum negative moment reach by the section at any time
ϕ_{\max}^-	Maximum negative curvature reached by the section at any time
M_y^+	Current (degraded) value of positive yield moment
M_y^-	Current (degraded) value of negative yield moment
M_{vertex}^+	Moment at the current vertex point on the positive side.
ϕ_{vertex}^+	Curvature at the current vertex point on the positive side.
M_{vertex}^-	Moment at the current vertex point on the negative side.
ϕ_{vertex}^-	Curvature at the current vertex point on the negative side.
M_{cr}^+	Positive Cracking Moment
M_{cr}^-	Negative Cracking Moment
K_O	Initial Elastic slope

(Boxed variables are Backbone Parameters. Others are *database* or *internal* variables)

Table D.2 Variables Governing PHM (contd.)

SYMBOL	MEANING
M_{y0}^+	Initial Positive Yielding Moment
ϕ_{y0}^+	Initial Positive Yield curvature
M_{y0}^-	Initial Negative Yielding Moment
ϕ_{y0}^-	Initial Negative Yield curvature
ϕ_u^+	Ultimate Positive Curvature
ϕ_u^-	Ultimate Negative Curvature
a^+	Positive Post-yield slope as a fraction of the initial elastic slope
a^-	Negative Post-yield slope as a fraction of the initial elastic slope
α	Stiffness Degradation Parameter
β	Strength Degradation Parameter
γ	Slip (or pinching) Parameter.

(Boxed variables are Backbone Parameters. Others are *database* or *internal* variables)

Table D.3 Point Formulas

POINT	FORMULA		
	ϕ	M	Other Terms Used
1	M_{cr}^+ / K_0	M_{cr}^+	-
2	M_{cr}^- / K_0	M_{cr}^-	-
3	ϕ_{y0}^+	M_y^+	-
4	ϕ_{y0}^-	M_y^-	-
5	ϕ_{\max}^+	M_{\max}^+	-
6	ϕ_{\max}^-	M_{\max}^-	-
7	ϕ_u^+	$M_y^+ + K_{sh}^+ (\phi_u^+ - \phi_{y0}^+)$	$K_{sh}^+ = a^+ K_0$
8	ϕ_u^-	$M_y^- + K_{sh}^- (\phi_u^- - \phi_{y0}^-)$	$K_{sh}^- = a^- K_0$
9	9'	Point of intersection of: Line joining point 4 and point 8 Line passing through point $(M_{vertex}^+, \phi_{vertex}^+)$ and having slope $R_K^+ K_0$	$R_K^+ = \frac{M_{vertex}^+ + \alpha M_y^+}{K_0 \phi_{vertex}^+ + \alpha M_y^+}$
	9	$\phi_{vertex}^+ - \frac{M_{vertex}^+}{R_K^+ K_0}$	
10	10'	Point of intersection of: Line joining point 3 and point 7 Line passing through point $(M_{vertex}^-, \phi_{vertex}^-)$ and having slope $R_K^- K_0$	$R_K^- = \frac{M_{vertex}^- + \alpha M_y^-}{K_0 \phi_{vertex}^- + \alpha M_y^-}$
	10	$\phi_{vertex}^- - \frac{M_{vertex}^-}{R_K^- K_0}$	

Table D.3 Point Formulas (contd.)

POINT	FORMULA		
	ϕ	M	Other Terms Used
11	Point of intersection of: Line joining point 9 and point 13 Branch 1		-
12	Point of intersection of: Line joining point 10 and point 14 Branch 1		-
13	$WF\phi_y^- + (1 - WF)\phi_{yu}^-$	γM_y^-	$R_{K,\max}^+ = \frac{M_{\max}^+ + \alpha M_y^+}{K_0\phi_{\max}^+ + \alpha M_y^+}$
	If $M_{\max}^- > M_y^-$ and $M < M_{cr}^-$ then		$\phi_{yu}^- = \phi_{\max}^- - \frac{M_{\max}^- - \gamma M_y^-}{R_{K,\max}^- K_0}$
	$M_{cr}^- \cancel{/} K_0$	M_{cr}^-	$\phi_y^- = M_y^- \cancel{/} K_0$ $\phi_y^- = \gamma \phi_y^-$ Weighting Factor, $WF = \gamma$
13'	Point of intersection of: Line joining point 8 and point 4 Branch 1		-
13''	If $\phi_{vertex}^- > M_y^- \cancel{/} K_0$ then same as Point 2		-
	Else Point of intersection of: Line joining point 9 and $(\phi_{vertex}^-, M_{vertex}^-)$ Branch 1		-

Table D.3 Point Formulas (contd.)

POINT		FORMULA			
		ϕ	M	Other Terms Used	
14	14	$WF\phi_{yy}^+ + (1-WF)\phi_{yu}^+$	γM_y^+	$R_{K,\max}^- = \frac{M_{\max}^- + \alpha M_y^-}{K_0 \phi_{\max}^- + \alpha M_y^-}$ $\phi_{yu}^+ = \phi_{\max}^+ - \frac{M_{\max}^+ - \gamma M_y^+}{R_{K,\max}^+ K_0}$ $\phi_y^- = M_y^- / K_0$ $\phi_{yy}^- = \gamma \phi_y^-$ <p>Weighting Factor, $WF = \gamma$</p>	
		If $M_{\max}^+ < M_y^+$ and $M > M_{cr}^+$ then			
		M_{cr}^- / K_0	M_{cr}^-		
	14'	Point of intersection of: Line joining point 7 and point 3 Branch 1		-	
14''		If $\phi_{vertex}^+ < M_y^+ / K_0$ then same as Point 1		-	
		Else Point of intersection of: Line joining point 10 and $(\phi_{vertex}^P, M_{vertex}^+)$ Branch 1		-	
15		ϕ_{\max}^+	M_{\max}^+	-	
16		ϕ_{\max}^-	M_{\max}^-	-	

Table D.3 Point Formulas (contd.)

POINT	FORMULA		
	ϕ	M	Other Terms Used
17	A	Point of intersection of: Line joining point 1 and point 3 Line passing through current point and having slope $R_K^+ K_0$	$R_K^+ = \frac{M_{cur} + \alpha M_y^+}{K_0 \phi_{cur} + \alpha M_y^+}$
	B	Point of intersection of: Line joining point 3 and point 5 Line passing through current point and having slope $R_K^+ K_0$	
	C	Point of intersection of: Line joining point 10 and point 14 Line passing through current point and having slope $R_K^+ K_0$	
	D	Point of intersection of: Line joining point 14 and point 15 Line passing through current point and having slope $R_K^+ K_0$	

Table D.3 Point Formulas (contd.)

POINT	FORMULA		
	ϕ	M	Other Terms Used
18	A	Point of intersection of: Line joining point 2 and point 4 Line passing through current point and having slope $R_K^- K_0$	$R_K^- = \frac{M_{cur} + \alpha M_y^-}{K_0 \phi_{cur} + \alpha M_y^-}$
	B	Point of intersection of: Line joining point 4 and point 6 Line passing through current point and having slope $R_K^- K_0$	
	C	Point of intersection of: Line joining point 9 and point 13 Line passing through current point and having slope $R_K^- K_0$	
	D	Point of intersection of: Line joining point 9 and point 13 Line passing through current point and having slope $R_K^- K_0$	

Table D.3 Point Formulas (contd.)

POINT	FORMULA		
	ϕ	M	Other Terms Used
19	Point of intersection of: Line joining point 14 and point 15 Line passing through current point and having slope $R_K^+ K_0$		$R_K^+ = \frac{M_{cur} + \alpha M_y^+}{K_0 \phi_{cur} + \alpha M_y^+}$
20	Point of intersection of: Line joining point 10 and point 14 Line passing through current point and having slope $R_K^- K_0$		$R_K^- = \frac{M_{cur} + \alpha M_y^-}{K_0 \phi_{cur} + \alpha M_y^-}$
21	$\phi_{current}$	$M_{current}$	-

Table D.4 Map of Branch Connectivity

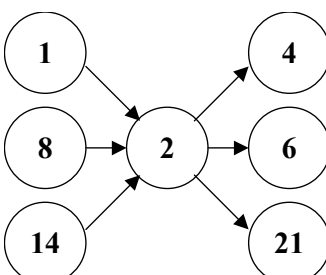
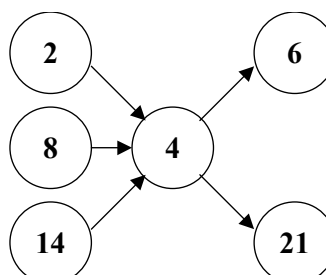
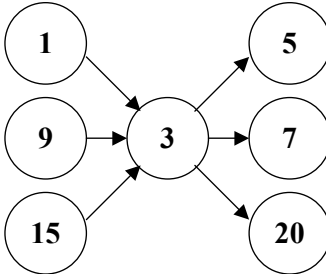
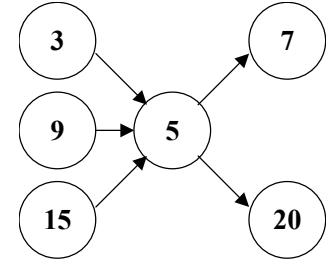
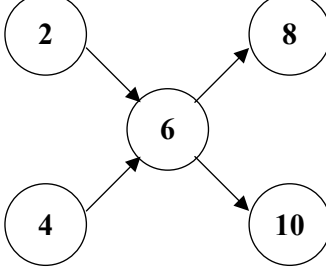
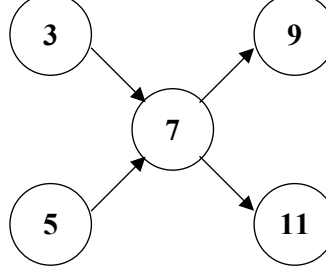
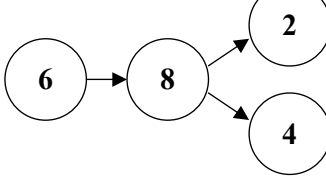
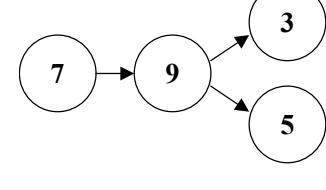
Branch 2	Branch 4
	
Branch 3	Branch 5
	
Branch 6	Branch 7
	
Branch 8	Branch 9
	

Table D.4 Map of Branch Connectivity (contd.)

Branch 10	Branch 11
Branch 12	Branch 13
Branch 14	Branch 15
Branch 16	Branch 17

Table D.4 Map of Branch Connectivity (contd.)

Branch 20	Branch 21
Branch 22	Branch 23
Branch 24	Branch 25

Table D.5 Starting and ending points of branches

Branch	1	2	3	4	5	6	7	8	9	10	11	12	13	14	15	16	17	20	21	22	23	24	25
Start Pt	1	1	2	3	4	5	6	9	10	9	10	11	12	21	21	13	14	21	21	21	21	21	21
End Pt	2	3	4	7	8	9	10	5	6	11	12	13	14	17	18	16	15	10	9	18	17	19	20

Table D.6 Rules for Change of Branch

Current Branch	Next Branch	Condition	
		Force Control	Displacement Control
1	1	In this case, $(\phi_{start}^1, M_{start}^1)$ is always on the negative end of Branch 1 and $(\phi_{end}^1, M_{end}^1)$ is always on the positive side. $M_{start}^1 < M_{cur} + \Delta M < M_{end}^1$	$\Delta\phi \square (\phi_{end}^1 - \phi_{start}^1) < 0$, i.e., there is a load reversal. Also swap Start and Endpoints of Branch 1 in this case
	2	Not on Branch 1 and $\Delta M > 0$	$\Delta\phi \square (\phi_{end}^1 - \phi_{start}^1) > 0$ $\Delta\phi > 0$
	3	Not on Branch 1 and $\Delta M < 0$	$\Delta\phi \square (\phi_{end}^1 - \phi_{start}^1) > 0$ $\Delta\phi < 0$
2	4	$\Delta M > 0$	$\Delta\phi > 0$
	6	$\Delta M < 0, M_{cur} > M_{max}^+$	$\Delta\phi < 0, M_{cur} > M_{max}^+$
	21	$\Delta M < 0, M_{cur} < M_{max}^+$ (See Fig. D.5)	$\Delta\phi < 0, M_{cur} < M_{max}^+$ (See Fig. D.5)
3	5	$\Delta M < 0$	$\Delta\phi < 0$
	7	$\Delta M > 0, M_{cur} < M_{max}^-$	$\Delta\phi > 0, M_{cur} < M_{max}^-$
	20	$\Delta M > 0, M_{cur} > M_{max}^-$ (See Fig. D.5)	$\Delta\phi > 0, M_{cur} > M_{max}^-$ (See Fig. D.5)
4	6	$M_{cur} > M_{max}^+$	$M_{cur} > M_{max}^+$
	21	$M_{cur} < M_{max}^+$	$M_{cur} < M_{max}^+$
5	7	$M_{cur} < M_{max}^-$	$M_{cur} < M_{max}^-$
	20	$M_{cur} > M_{max}^-$	$M_{cur} > M_{max}^-$
6	8	$\Delta M > 0$	$\Delta\phi > 0$
	10	$\Delta M < 0$	$\Delta\phi < 0$

Note: $(\phi_{start}^i, M_{start}^i)$ and $(\phi_{end}^i, M_{end}^i)$ denote the start and end points of Branch "i"

Table D.6 Rules for Change of Branch (contd.)

7	9	$\Delta M < 0$	$\Delta\phi < 0$
	11	$\Delta M > 0$	$\Delta\phi > 0$
8	2	$M_{start}^2 < M_{end}^8 < M_{end}^2$, i.e., end point of Branch 8 lies on Branch 2	$\phi_{start}^2 < \phi_{end}^8 < \phi_{end}^2$, i.e., end point of Branch 8 lies on Branch 2
	4	Otherwise	Otherwise
9	3	$M_{start}^3 > M_{end}^9 > M_{end}^3$, i.e., end point of Branch 9 lies on Branch 3	$\phi_{start}^3 > \phi_{end}^9 > \phi_{end}^3$, i.e., end point of Branch 9 lies on Branch 3
	5	Otherwise	Otherwise
10	1	$\Delta M < 0$ and $M_{max}^- > M_y^-$, i.e., section has not yielded on the negative side	$\Delta\phi < 0$ and $M_{max}^- > M_y^-$, i.e., section has not yielded on the negative side
	12	$\Delta M < 0$ and $M_{max}^- < M_y^-$	$\Delta\phi < 0$ and $M_{max}^- < M_y^-$
	14	$\Delta M > 0$	$\Delta\phi > 0$
11	1	$\Delta M > 0$ and $M_{max}^+ < M_y^+$, i.e., section has not yielded on the positive side	$\Delta\phi > 0$ and $M_{max}^+ < M_y^+$, i.e., section has not yielded on the positive side
	13	$\Delta M > 0$ and $M_{max}^+ > M_y^+$	$\Delta\phi > 0$ and $M_{max}^+ > M_y^+$
	15	$\Delta M < 0$	$\Delta\phi < 0$
12	16	$\Delta M < 0$	$\Delta\phi < 0$
	20	$\Delta M > 0$	$\Delta\phi > 0$
13	17	$\Delta M > 0$	$\Delta\phi > 0$
	21	$\Delta M < 0$	$\Delta\phi < 0$

Note: $(\phi_{start}^i, M_{start}^i)$ and $(\phi_{end}^i, M_{end}^i)$ denote the start and end points of Branch "i"

Table D.6 Rules for Change of Branch (contd.)

14	2	$\Delta M > 0, M_{\max}^- < M_y^-$ (i.e., yielded on negative side), $M_{\max}^+ < M_y^+$ (i.e., not yielded on positive side) OR $\Delta M > 0, M_{\max}^- > M_y^-$ (i.e., not yielded on negative side), $M_{start}^2 < M_{end}^{14} < M_{end}^2$ (i.e., end point of Branch 14 lies on Branch 2)	$\Delta\phi > 0, M_{\max}^- < M_y^-$ (i.e., yielded on negative side), $M_{\max}^+ < M_y^+$ (i.e., not yielded on positive side) OR $\Delta\phi > 0, M_{\max}^- > M_y^-$ (i.e., not yielded on negative side), $\phi_{start}^2 < \phi_{end}^{14} < \phi_{end}^2$ (i.e., end point of Branch 14 lies on Branch 2)
		$\Delta M > 0, M_{\max}^- > M_y^-$ (i.e., not yielded on negative side), $M_{end}^{14} > M_{end}^2$ (i.e., end point of Branch 14 lies on Branch 4)	$\Delta\phi > 0, M_{\max}^- > M_y^-$ (i.e., not yielded on negative side), $\phi_{end}^{14} > \phi_{end}^2$ (i.e., end point of Branch 14 lies on Branch 4)
	13	$\Delta M > 0, M_{\max}^- < M_y^-$ (i.e., yielded on negative side), $M_{\max}^+ > M_y^+$ (i.e., yielded on positive side), $M_{start}^{13} < M_{end}^{14} < M_{end}^{13}$ (i.e., end point of Branch 14 lies on Branch 13)	$\Delta\phi > 0, M_{\max}^- < M_y^-$ (i.e., yielded on negative side), $M_{\max}^+ > M_y^+$ (i.e., yielded on positive side), $\phi_{start}^{13} < \phi_{end}^{14} < \phi_{end}^{13}$ (i.e., end point of Branch 14 lies on Branch 13)
	17	$\Delta M > 0, M_{\max}^- < M_y^-$ (i.e., yielded on negative side), $M_{\max}^+ > M_y^+$ (i.e., yielded on positive side), $M_{end}^{14} > M_{end}^{13}$ (i.e., end point of Branch 14 lies on Branch 17)	$\Delta\phi > 0, M_{\max}^- < M_y^-$ (i.e., yielded on negative side), $M_{\max}^+ > M_y^+$ (i.e., yielded on positive side), $\phi_{end}^{14} > \phi_{end}^{13}$ (i.e., end point of Branch 14 lies on Branch 17)
	24	$\Delta M < 0$	$\Delta\phi < 0$

Note: $(\phi_{start}^i, M_{start}^i)$ and $(\phi_{end}^i, M_{end}^i)$ denote the start and end points of Branch "i"

Table D.6 Rules for Change of Branch (contd.)

15	3	$\Delta M < 0, M_{\max}^+ > M_y^+$ (i.e., yielded on positive side), $M_{\max}^- > M_y^-$ (i.e., not yielded on negative side) OR $\Delta M < 0, M_{\max}^+ < M_y^+$ (i.e., not yielded on positive side), $M_{start}^3 > M_{end}^{15} > M_{end}^3$ (i.e., end point of Branch 15 lies on Branch 3)	$\Delta\phi < 0, M_{\max}^+ > M_y^+$ (i.e., yielded on positive side), $M_{\max}^- > M_y^-$ (i.e., not yielded on negative side) OR $\Delta\phi < 0, M_{\max}^+ < M_y^+$ (i.e., not yielded on positive side), $\phi_{start}^3 > \phi_{end}^{15} > \phi_{end}^3$ (i.e., end point of Branch 15 lies on Branch 3)
	5	$\Delta M < 0, M_{\max}^+ < M_y^+$ (i.e., not yielded on positive side), $M_{end}^{15} < M_{end}^3$ (i.e., end point of Branch 15 lies on Branch 5)	$\Delta\phi < 0, M_{\max}^+ < M_y^+$ (i.e., not yielded on positive side), $\phi_{end}^{15} < \phi_{end}^3$ (i.e., end point of Branch 15 lies on Branch 5)
	12	$\Delta M < 0, M_{\max}^+ > M_y^+$ (i.e., yielded on positive side), $M_{\max}^- < M_y^-$ (i.e., yielded on negative side), $M_{start}^{12} > M_{end}^{15} > M_{end}^{12}$ (i.e., end point of Branch 15 lies on Branch 12)	$\Delta\phi < 0, M_{\max}^+ > M_y^+$ (i.e., yielded on positive side), $M_{\max}^- < M_y^-$ (i.e., yielded on negative side), $\phi_{start}^{12} > \phi_{end}^{15} > \phi_{end}^{12}$ (i.e., end point of Branch 15 lies on Branch 12)
	16	$\Delta M < 0, M_{\max}^+ > M_y^+$ (i.e., yielded on positive side), $M_{\max}^- < M_y^-$ (i.e., yielded on negative side), $M_{end}^{15} < M_{end}^{12}$ (i.e., end point of Branch 15 lies on Branch 16)	$\Delta\phi < 0, M_{\max}^+ > M_y^+$ (i.e., yielded on positive side), $M_{\max}^- < M_y^-$ (i.e., yielded on negative side), $\phi_{end}^{15} < \phi_{end}^{12}$ (i.e., end point of Branch 15 lies on Branch 16)
	25	$\Delta M > 0$	$\Delta\phi > 0$

Note: $(\phi_{start}^i, M_{start}^i)$ and $(\phi_{end}^i, M_{end}^i)$ denote the start and end points of Branch "i"

Table D.6 Rules for Change of Branch (contd.)

22	3	$\Delta M < 0, M_{\max}^+ > M_y^+$ (i.e., yielded on positive side), $M_{\max}^- > M_y^-$ (i.e., not yielded on negative side) OR $\Delta M < 0, M_{\max}^+ < M_y^+$ (i.e., not yielded on positive side), $M_{start}^3 > M_{end}^{22} > M_{end}^3$ (i.e., end point of Branch 22 lies on Branch 3)	$\Delta\phi < 0, M_{\max}^+ > M_y^+$ (i.e., yielded on positive side), $M_{\max}^- > M_y^-$ (i.e., not yielded on negative side) OR $\Delta\phi < 0, M_{\max}^+ < M_y^+$ (i.e., not yielded on positive side), $\phi_{start}^3 > \phi_{end}^{22} > \phi_{end}^3$ (i.e., end point of Branch 22 lies on Branch 3)
		$\Delta M < 0, M_{\max}^+ < M_y^+$ (i.e., not yielded on positive side), $M_{end}^{22} < M_{end}^3$ (i.e., end point of Branch 22 lies on Branch 5)	$\Delta\phi < 0, M_{\max}^+ < M_y^+$ (i.e., not yielded on positive side), $\phi_{end}^{22} < \phi_{end}^3$ (i.e., end point of Branch 22 lies on Branch 5)
	12	$\Delta M < 0, M_{\max}^+ > M_y^+$ (i.e., yielded on positive side), $M_{\max}^- < M_y^-$ (i.e., yielded on negative side), $M_{start}^{12} > M_{end}^{22} > M_{end}^{12}$ (i.e., end point of Branch 22 lies on Branch 12)	$\Delta\phi < 0, M_{\max}^+ > M_y^+$ (i.e., yielded on positive side), $M_{\max}^- < M_y^-$ (i.e., yielded on negative side), $\phi_{start}^{12} > \phi_{end}^{22} > \phi_{end}^{12}$ (i.e., end point of Branch 22 lies on Branch 12)
	16	$\Delta M < 0, M_{\max}^+ > M_y^+$ (i.e., yielded on positive side), $M_{\max}^- < M_y^-$ (i.e., yielded on negative side), $M_{end}^{22} < M_{end}^{12}$ (i.e., end point of Branch 22 lies on Branch 16)	$\Delta\phi < 0, M_{\max}^+ > M_y^+$ (i.e., yielded on positive side), $M_{\max}^- < M_y^-$ (i.e., yielded on negative side), $\phi_{end}^{22} < \phi_{end}^{12}$ (i.e., end point of Branch 22 lies on Branch 16)
	20	$\Delta M > 0$	$\Delta\phi > 0$

Note: $(\phi_{start}^i, M_{start}^i)$ and $(\phi_{end}^i, M_{end}^i)$ denote the start and end points of Branch "i"

Table D.6 Rules for Change of Branch (contd.)

23	2	$\Delta M > 0, M_{\max}^- < M_y^-$ (i.e., yielded on negative side), $M_{\max}^+ < M_y^+$ (i.e., not yielded on positive side) OR $\Delta M > 0, M_{\max}^- > M_y^-$ (i.e., not yielded on negative side), $M_{start}^2 < M_{end}^{23} < M_{end}^2$ (i.e., end point of Branch 23 lies on Branch 2)	$\Delta \phi > 0, M_{\max}^- < M_y^-$ (i.e., yielded on negative side), $M_{\max}^+ < M_y^+$ (i.e., not yielded on positive side) OR $\Delta \phi > 0, M_{\max}^- > M_y^-$ (i.e., not yielded on negative side), $\phi_{start}^2 < \phi_{end}^{23} < \phi_{end}^2$ (i.e., end point of Branch 23 lies on Branch 2)
	4	$\Delta M > 0, M_{\max}^- > M_y^-$ (i.e., not yielded on negative side), $M_{end}^{23} > M_{end}^2$ (i.e., end point of Branch 23 lies on Branch 4)	$\Delta \phi > 0, M_{\max}^- > M_y^-$ (i.e., not yielded on negative side), $\phi_{end}^{23} > \phi_{end}^2$ (i.e., end point of Branch 23 lies on Branch 4)
	13	$\Delta M > 0, M_{\max}^- < M_y^-$ (i.e., yielded on negative side), $M_{\max}^+ > M_y^+$ (i.e., yielded on positive side), $M_{start}^{13} < M_{end}^{23} < M_{end}^{13}$ (i.e., end point of Branch 23 lies on Branch 13)	$\Delta \phi > 0, M_{\max}^- < M_y^-$ (i.e., yielded on negative side), $M_{\max}^+ > M_y^+$ (i.e., yielded on positive side), $\phi_{start}^{13} < \phi_{end}^{23} < \phi_{end}^{13}$ (i.e., end point of Branch 23 lies on Branch 13)
	17	$\Delta M > 0, M_{\max}^- < M_y^-$ (i.e., yielded on negative side), $M_{\max}^+ > M_y^+$ (i.e., yielded on positive side), $M_{end}^{23} > M_{end}^{13}$ (i.e., end point of Branch 23 lies on Branch 17)	$\Delta \phi > 0, M_{\max}^- < M_y^-$ (i.e., yielded on negative side), $M_{\max}^+ > M_y^+$ (i.e., yielded on positive side), $\phi_{end}^{23} > \phi_{end}^{13}$ (i.e., end point of Branch 23 lies on Branch 17)
	21	$\Delta M < 0$	$\Delta \phi < 0$

Note: $(\phi_{start}^i, M_{start}^i)$ and $(\phi_{end}^i, M_{end}^i)$ denote the start and end points of Branch "i"

Table D.6 Rules for Change of Branch (contd.)

16	4	$\Delta M < 0$	$\Delta\phi < 0$
	20	$\Delta M > 0$	$\Delta\phi > 0$
17	5	$\Delta M > 0$	$\Delta\phi > 0$
	21	$\Delta M < 0$	$\Delta\phi < 0$
20	11	$\Delta M > 0$	$\Delta\phi > 0$
	22	$\Delta M < 0$	$\Delta\phi < 0$
21	10	$\Delta M < 0$	$\Delta\phi < 0$
	23	$\Delta M > 0$	$\Delta\phi > 0$
24	10	$\Delta M < 0$	$\Delta\phi < 0$
	14	$\Delta M > 0$	$\Delta\phi > 0$
25	11	$\Delta M > 0$	$\Delta\phi > 0$
	15	$\Delta M < 0$	$\Delta\phi < 0$

Note: $(\phi_{start}^i, M_{start}^i)$ and $(\phi_{end}^i, M_{end}^i)$ denote the start and end points of Branch "i"

Table D.7 Variables governing nonlinear elastic-cyclic model (NECM)

Symbol	Definition
M_{cur}	Current moment level in the section
ϕ_{cur}	Current curvature level in the section
M_y^+	Current (degraded) value of positive yield moment
M_y^-	Current (degraded) value of negative yield moment
M_r^+	Current (degraded) value of positive rocking moment
M_r^-	Current (degraded) value of negative rocking moment
M_{ot}^+	Current (degraded) value of positive overturning moment
M_{ot}^-	Current (degraded) value of negative overturning moment
M_{cr}^+	Positive cracking moment
M_{cr}^-	Negative cracking moment
EI_0	Initial elastic slope
EI_3	Slope of the yielding to overturning state
M_{yo}^+	Initial positive yielding moment
ϕ_y^+	Initial positive yield curvature
M_{yo}^-	Initial negative yielding moment
ϕ_y^-	Initial negative yield curvature
ϕ_r^+	Positive rocking curvature
ϕ_r^-	Negative rocking curvature
ϕ_{ot}^+	Overshoot positive curvature
ϕ_{ot}^-	Overshoot negative curvature
a^+	Positive post-yield slope as a fraction of the initial elastic slope
a^-	Negative post-yield slope as a fraction of the initial elastic slope

Table D.8 Definition of benchmark points in NECM (Fig. 5.10)

Point	Definition		
	ϕ	M	Other terms used
1	M_{cr}^+ / K_0	M_{cr}^+	-
2	M_{cr}^- / K_0	M_{cr}^-	-
3	ϕ_{y0}^+	M_y^+	Follow Eqs. 5.5~5.7 after rocking
4	ϕ_{y0}^-	M_y^-	Follow Eqs. 5.5~5.7 after rocking
5	ϕ_r^+	M_r^+	
6	ϕ_r^-	M_r^-	
7	ϕ_{ot}^+	$M_{ot}^+ = M_y^+ + EI_3^+ (\phi_{ot}^+ - \phi_y^+)$	$EI_3^+ = a^+ EI_0$
8	ϕ_{ot}^-	$M_{ot}^- = M_y^- + EI_3^- (\phi_{ot}^- - \phi_y^-)$	$EI_3^- = a^- EI_0$

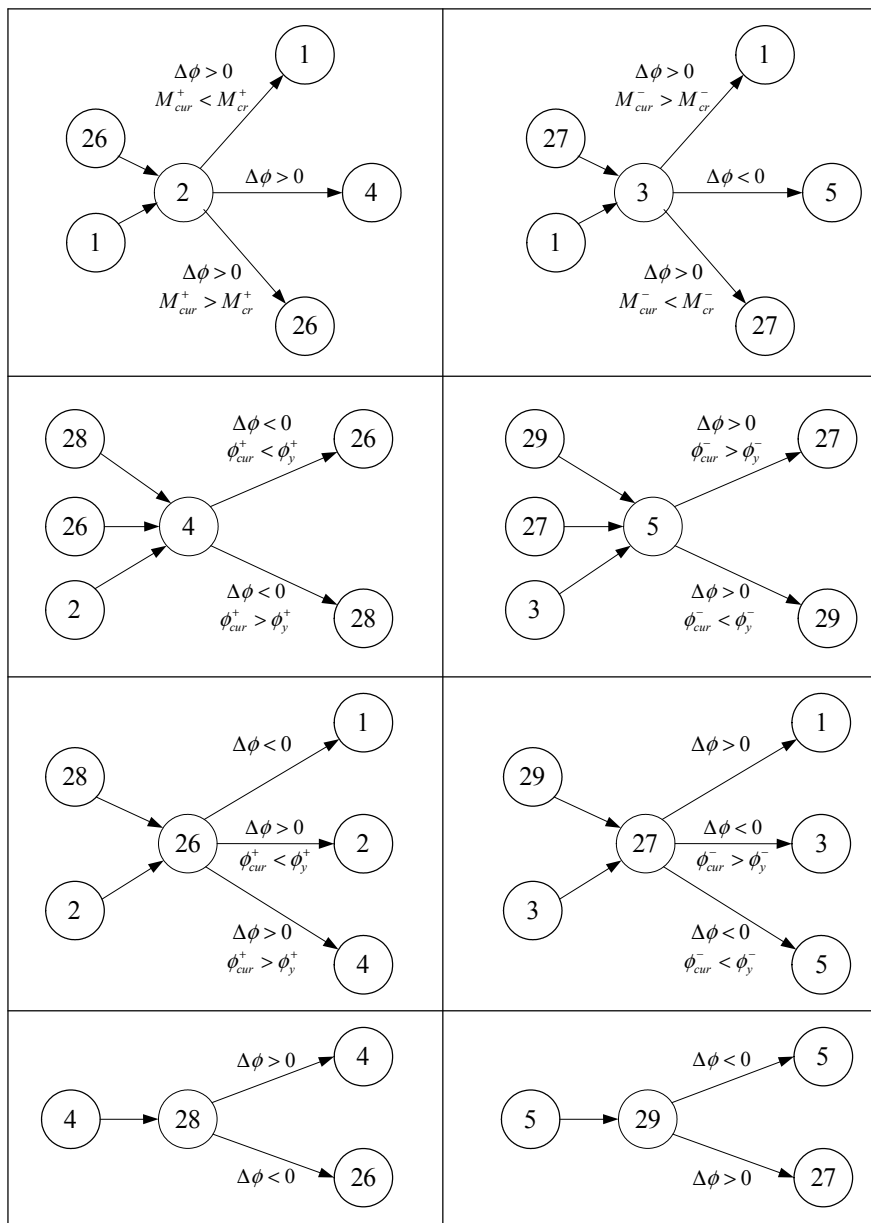
Table D.9 Map of Branch Connectivity

Branch 2	Branch 3
Branch 4	Branch 5
Branch 26	Branch 27
Branch 28	Branch 29
# : Nonlinear elastic hysteretic model for rocking column	
# : Existing hysteretic model in current IDARC2D	

Table D.10 Starting and ending points of branches

Branch	26	27	28	29
Start Pt	3	4	7	8
End Pt	1	2	3	4

Table D.11 Rules of Branch Transition



APPENDIX E

FORMULATION FOR MASONRY INFILL FRAMES

The following formulation is used in the program to calculate the hysteretic parameters for masonry infill frames. The formulation is adapted from Saneinejad and Hobbs (1995).

The permissible stress f_a or the masonry strut in compression is calculated as:

$$f_a = f_c \left[1 - \left(\frac{l_{eff}}{40t} \right)^2 \right] \quad \text{where } f_c = 0.6\phi f_m' \quad \text{and} \quad \phi=0.65 \quad (\text{E.1})$$

The upper bound or failure normal uniform contact stresses at the column-infill interface σ_{c0} and beam-infill interface σ_{b0} are calculated from the Tresca hexagonal yield criterion as:

$$\sigma_{c0} = \frac{f_c}{\sqrt{1+3\mu_f^2 r^4}}; \quad \sigma_{b0} = \frac{f_c}{\sqrt{1+3\mu_f^2}} \quad (\text{E.2})$$

where r is the aspect ratio of the infill, i.e. $r = h/l$; and μ_f is the coefficient of friction of the frame-infill surface. The contact lengths at the column-infill interface $\alpha_c h$ and beam-infill interface $\alpha_b l$ are calculated from equilibrium as:

$$\alpha_c h = \sqrt{\frac{2M_{pj} + 2\beta_c M_{pc}}{\sigma_{co} t}} \leq 0.4h' \quad (\text{E.3})$$

$$\alpha_b h = \sqrt{\frac{2M_{pj} + 2\beta_c M_{pc}}{\sigma_{bo} t}} \leq 0.4l' \quad (\text{E.4})$$

in which $\beta_0 = 0.2$.

The actual normal contact stresses σ_c and σ_b are calculated form the rotational

equilibrium of the infill panel using the following methodology:

If $A_c \geq A_b$ then

$$\sigma_b = \sigma_{b0} \quad \text{and} \quad \sigma_c = \sigma_{c0} \left(\frac{A_b}{A_c} \right) \quad (\text{E.5})$$

If $A_b \geq A_c$ then:

$$\sigma_c = \sigma_{c0} \quad \text{and} \quad \sigma_b = \sigma_{b0} \left(\frac{A_c}{A_b} \right) \quad (\text{E.6})$$

where:

$$A_c = r^2 \sigma_{c0} \alpha_c (1 - \alpha_c - \mu_f r) \quad (\text{E.7})$$

$$A_b = \sigma_{b0} \alpha_b (1 - \alpha_b - \mu_f r) \quad (\text{E.8})$$

The contact shear stresses at the column-infill interface τ_c and beam-infill interface τ_b are given as:

$$\tau_c = \mu_f r^2 \sigma_c \quad (\text{E.9})$$

$$\tau_b = \mu_f \sigma_b \quad (\text{E.10})$$

The sloping angle θ' of the masonry diagonal strut at shear failure is given as:

$$\theta' = \tan^{-1} \left[(1 - \alpha_c) h' / l' \right] \quad (\text{E.11})$$

The controlling parameters of the smooth hysteretic model exhibit well defined physical characteristics if the following constraint is imposed:

$$A = \beta + \gamma \quad (\text{E.12})$$

When using masonry infill panel elements, the following are suggested values of the smooth hysteretic parameters (Reinhorn et al., 1995d):

$$A=1.0, \beta=0.1, \gamma=0.9, \eta=2.0$$

$$\mu_c=5.0$$

$$A_s=0.3$$

$$Z_s=0.1$$

$$\bar{Z}=0.0$$

$$s_k=0.1$$

$$s_{p1}=0.8$$

$$s_{p2}=1.0$$

Other values can be used to achieve different hysteretic response characteristics.

MCEER Technical Reports

MCEER publishes technical reports on a variety of subjects written by authors funded through MCEER. These reports are available from both MCEER Publications and the National Technical Information Service (NTIS). Requests for reports should be directed to MCEER Publications, MCEER, University at Buffalo, State University of New York, Red Jacket Quadrangle, Buffalo, New York 14261. Reports can also be requested through NTIS, 5285 Port Royal Road, Springfield, Virginia 22161. NTIS accession numbers are shown in parenthesis, if available.

- NCEER-87-0001 "First-Year Program in Research, Education and Technology Transfer," 3/5/87, (PB88-134275, A04, MF-A01).
- NCEER-87-0002 "Experimental Evaluation of Instantaneous Optimal Algorithms for Structural Control," by R.C. Lin, T.T. Soong and A.M. Reinhorn, 4/20/87, (PB88-134341, A04, MF-A01).
- NCEER-87-0003 "Experimentation Using the Earthquake Simulation Facilities at University at Buffalo," by A.M. Reinhorn and R.L. Ketter, to be published.
- NCEER-87-0004 "The System Characteristics and Performance of a Shaking Table," by J.S. Hwang, K.C. Chang and G.C. Lee, 6/1/87, (PB88-134259, A03, MF-A01). This report is available only through NTIS (see address given above).
- NCEER-87-0005 "A Finite Element Formulation for Nonlinear Viscoplastic Material Using a Q Model," by O. Gyebi and G. Dasgupta, 11/2/87, (PB88-213764, A08, MF-A01).
- NCEER-87-0006 "Symbolic Manipulation Program (SMP) - Algebraic Codes for Two and Three Dimensional Finite Element Formulations," by X. Lee and G. Dasgupta, 11/9/87, (PB88-218522, A05, MF-A01).
- NCEER-87-0007 "Instantaneous Optimal Control Laws for Tall Buildings Under Seismic Excitations," by J.N. Yang, A. Akbarpour and P. Ghaemmaghami, 6/10/87, (PB88-134333, A06, MF-A01). This report is only available through NTIS (see address given above).
- NCEER-87-0008 "IDARC: Inelastic Damage Analysis of Reinforced Concrete Frame - Shear-Wall Structures," by Y.J. Park, A.M. Reinhorn and S.K. Kunath, 7/20/87, (PB88-134325, A09, MF-A01). This report is only available through NTIS (see address given above).
- NCEER-87-0009 "Liquefaction Potential for New York State: A Preliminary Report on Sites in Manhattan and Buffalo," by M. Budhu, V. Vijayakumar, R.F. Giese and L. Baumgras, 8/31/87, (PB88-163704, A03, MF-A01). This report is available only through NTIS (see address given above).
- NCEER-87-0010 "Vertical and Torsional Vibration of Foundations in Inhomogeneous Media," by A.S. Veletsos and K.W. Dotson, 6/1/87, (PB88-134291, A03, MF-A01). This report is only available through NTIS (see address given above).
- NCEER-87-0011 "Seismic Probabilistic Risk Assessment and Seismic Margins Studies for Nuclear Power Plants," by Howard H.M. Hwang, 6/15/87, (PB88-134267, A03, MF-A01). This report is only available through NTIS (see address given above).
- NCEER-87-0012 "Parametric Studies of Frequency Response of Secondary Systems Under Ground-Acceleration Excitations," by Y. Yong and Y.K. Lin, 6/10/87, (PB88-134309, A03, MF-A01). This report is only available through NTIS (see address given above).
- NCEER-87-0013 "Frequency Response of Secondary Systems Under Seismic Excitation," by J.A. HoLung, J. Cai and Y.K. Lin, 7/31/87, (PB88-134317, A05, MF-A01). This report is only available through NTIS (see address given above).
- NCEER-87-0014 "Modelling Earthquake Ground Motions in Seismically Active Regions Using Parametric Time Series Methods," by G.W. Ellis and A.S. Cakmak, 8/25/87, (PB88-134283, A08, MF-A01). This report is only available through NTIS (see address given above).
- NCEER-87-0015 "Detection and Assessment of Seismic Structural Damage," by E. DiPasquale and A.S. Cakmak, 8/25/87, (PB88-163712, A05, MF-A01). This report is only available through NTIS (see address given above).

- NCEER-87-0016 "Pipeline Experiment at Parkfield, California," by J. Isenberg and E. Richardson, 9/15/87, (PB88-163720, A03, MF-A01). This report is available only through NTIS (see address given above).
- NCEER-87-0017 "Digital Simulation of Seismic Ground Motion," by M. Shinozuka, G. Deodatis and T. Harada, 8/31/87, (PB88-155197, A04, MF-A01). This report is available only through NTIS (see address given above).
- NCEER-87-0018 "Practical Considerations for Structural Control: System Uncertainty, System Time Delay and Truncation of Small Control Forces," J.N. Yang and A. Akbarpour, 8/10/87, (PB88-163738, A08, MF-A01). This report is only available through NTIS (see address given above).
- NCEER-87-0019 "Modal Analysis of Nonclassically Damped Structural Systems Using Canonical Transformation," by J.N. Yang, S. Sarkani and F.X. Long, 9/27/87, (PB88-187851, A04, MF-A01).
- NCEER-87-0020 "A Nonstationary Solution in Random Vibration Theory," by J.R. Red-Horse and P.D. Spanos, 11/3/87, (PB88-163746, A03, MF-A01).
- NCEER-87-0021 "Horizontal Impedances for Radially Inhomogeneous Viscoelastic Soil Layers," by A.S. Veletsos and K.W. Dotson, 10/15/87, (PB88-150859, A04, MF-A01).
- NCEER-87-0022 "Seismic Damage Assessment of Reinforced Concrete Members," by Y.S. Chung, C. Meyer and M. Shinozuka, 10/9/87, (PB88-150867, A05, MF-A01). This report is available only through NTIS (see address given above).
- NCEER-87-0023 "Active Structural Control in Civil Engineering," by T.T. Soong, 11/11/87, (PB88-187778, A03, MF-A01).
- NCEER-87-0024 "Vertical and Torsional Impedances for Radially Inhomogeneous Viscoelastic Soil Layers," by K.W. Dotson and A.S. Veletsos, 12/87, (PB88-187786, A03, MF-A01).
- NCEER-87-0025 "Proceedings from the Symposium on Seismic Hazards, Ground Motions, Soil-Liquefaction and Engineering Practice in Eastern North America," October 20-22, 1987, edited by K.H. Jacob, 12/87, (PB88-188115, A23, MF-A01). This report is available only through NTIS (see address given above).
- NCEER-87-0026 "Report on the Whittier-Narrows, California, Earthquake of October 1, 1987," by J. Pantelic and A. Reinhorn, 11/87, (PB88-187752, A03, MF-A01). This report is available only through NTIS (see address given above).
- NCEER-87-0027 "Design of a Modular Program for Transient Nonlinear Analysis of Large 3-D Building Structures," by S. Srivastav and J.F. Abel, 12/30/87, (PB88-187950, A05, MF-A01). This report is only available through NTIS (see address given above).
- NCEER-87-0028 "Second-Year Program in Research, Education and Technology Transfer," 3/8/88, (PB88-219480, A04, MF-A01).
- NCEER-88-0001 "Workshop on Seismic Computer Analysis and Design of Buildings With Interactive Graphics," by W. McGuire, J.F. Abel and C.H. Conley, 1/18/88, (PB88-187760, A03, MF-A01). This report is only available through NTIS (see address given above).
- NCEER-88-0002 "Optimal Control of Nonlinear Flexible Structures," by J.N. Yang, F.X. Long and D. Wong, 1/22/88, (PB88-213772, A06, MF-A01).
- NCEER-88-0003 "Substructuring Techniques in the Time Domain for Primary-Secondary Structural Systems," by G.D. Manolis and G. Juhn, 2/10/88, (PB88-213780, A04, MF-A01).
- NCEER-88-0004 "Iterative Seismic Analysis of Primary-Secondary Systems," by A. Singhal, L.D. Lutes and P.D. Spanos, 2/23/88, (PB88-213798, A04, MF-A01).
- NCEER-88-0005 "Stochastic Finite Element Expansion for Random Media," by P.D. Spanos and R. Ghanem, 3/14/88, (PB88-213806, A03, MF-A01).

- NCEER-88-0006 "Combining Structural Optimization and Structural Control," by F.Y. Cheng and C.P. Pantelides, 1/10/88, (PB88-213814, A05, MF-A01).
- NCEER-88-0007 "Seismic Performance Assessment of Code-Designed Structures," by H.H-M. Hwang, J-W. Jaw and H-J. Shau, 3/20/88, (PB88-219423, A04, MF-A01). This report is only available through NTIS (see address given above).
- NCEER-88-0008 "Reliability Analysis of Code-Designed Structures Under Natural Hazards," by H.H-M. Hwang, H. Ushiba and M. Shinohara, 2/29/88, (PB88-229471, A07, MF-A01). This report is only available through NTIS (see address given above).
- NCEER-88-0009 "Seismic Fragility Analysis of Shear Wall Structures," by J-W Jaw and H.H-M. Hwang, 4/30/88, (PB89-102867, A04, MF-A01).
- NCEER-88-0010 "Base Isolation of a Multi-Story Building Under a Harmonic Ground Motion - A Comparison of Performances of Various Systems," by F-G Fan, G. Ahmadi and I.G. Tadjbakhsh, 5/18/88, (PB89-122238, A06, MF-A01). This report is only available through NTIS (see address given above).
- NCEER-88-0011 "Seismic Floor Response Spectra for a Combined System by Green's Functions," by F.M. Lavelle, L.A. Bergman and P.D. Spanos, 5/1/88, (PB89-102875, A03, MF-A01).
- NCEER-88-0012 "A New Solution Technique for Randomly Excited Hysteretic Structures," by G.Q. Cai and Y.K. Lin, 5/16/88, (PB89-102883, A03, MF-A01).
- NCEER-88-0013 "A Study of Radiation Damping and Soil-Structure Interaction Effects in the Centrifuge," by K. Weissman, supervised by J.H. Prevost, 5/24/88, (PB89-144703, A06, MF-A01).
- NCEER-88-0014 "Parameter Identification and Implementation of a Kinematic Plasticity Model for Frictional Soils," by J.H. Prevost and D.V. Griffiths, to be published.
- NCEER-88-0015 "Two- and Three- Dimensional Dynamic Finite Element Analyses of the Long Valley Dam," by D.V. Griffiths and J.H. Prevost, 6/17/88, (PB89-144711, A04, MF-A01).
- NCEER-88-0016 "Damage Assessment of Reinforced Concrete Structures in Eastern United States," by A.M. Reinhorn, M.J. Seidel, S.K. Kunnath and Y.J. Park, 6/15/88, (PB89-122220, A04, MF-A01). This report is only available through NTIS (see address given above).
- NCEER-88-0017 "Dynamic Compliance of Vertically Loaded Strip Foundations in Multilayered Viscoelastic Soils," by S. Ahmad and A.S.M. Israil, 6/17/88, (PB89-102891, A04, MF-A01).
- NCEER-88-0018 "An Experimental Study of Seismic Structural Response With Added Viscoelastic Dampers," by R.C. Lin, Z. Liang, T.T. Soong and R.H. Zhang, 6/30/88, (PB89-122212, A05, MF-A01). This report is available only through NTIS (see address given above).
- NCEER-88-0019 "Experimental Investigation of Primary - Secondary System Interaction," by G.D. Manolis, G. Juhn and A.M. Reinhorn, 5/27/88, (PB89-122204, A04, MF-A01).
- NCEER-88-0020 "A Response Spectrum Approach For Analysis of Nonclassically Damped Structures," by J.N. Yang, S. Sarkani and F.X. Long, 4/22/88, (PB89-102909, A04, MF-A01).
- NCEER-88-0021 "Seismic Interaction of Structures and Soils: Stochastic Approach," by A.S. Veletsos and A.M. Prasad, 7/21/88, (PB89-122196, A04, MF-A01). This report is only available through NTIS (see address given above).
- NCEER-88-0022 "Identification of the Serviceability Limit State and Detection of Seismic Structural Damage," by E. DiPasquale and A.S. Cakmak, 6/15/88, (PB89-122188, A05, MF-A01). This report is available only through NTIS (see address given above).
- NCEER-88-0023 "Multi-Hazard Risk Analysis: Case of a Simple Offshore Structure," by B.K. Bhartia and E.H. Vanmarcke, 7/21/88, (PB89-145213, A05, MF-A01).

- NCEER-88-0024 "Automated Seismic Design of Reinforced Concrete Buildings," by Y.S. Chung, C. Meyer and M. Shinozuka, 7/5/88, (PB89-122170, A06, MF-A01). This report is available only through NTIS (see address given above).
- NCEER-88-0025 "Experimental Study of Active Control of MDOF Structures Under Seismic Excitations," by L.L. Chung, R.C. Lin, T.T. Soong and A.M. Reinhorn, 7/10/88, (PB89-122600, A04, MF-A01).
- NCEER-88-0026 "Earthquake Simulation Tests of a Low-Rise Metal Structure," by J.S. Hwang, K.C. Chang, G.C. Lee and R.L. Ketter, 8/1/88, (PB89-102917, A04, MF-A01).
- NCEER-88-0027 "Systems Study of Urban Response and Reconstruction Due to Catastrophic Earthquakes," by F. Kozin and H.K. Zhou, 9/22/88, (PB90-162348, A04, MF-A01).
- NCEER-88-0028 "Seismic Fragility Analysis of Plane Frame Structures," by H.H-M. Hwang and Y.K. Low, 7/31/88, (PB89-131445, A06, MF-A01).
- NCEER-88-0029 "Response Analysis of Stochastic Structures," by A. Kardara, C. Bucher and M. Shinozuka, 9/22/88, (PB89-174429, A04, MF-A01).
- NCEER-88-0030 "Nonnormal Accelerations Due to Yielding in a Primary Structure," by D.C.K. Chen and L.D. Lutes, 9/19/88, (PB89-131437, A04, MF-A01).
- NCEER-88-0031 "Design Approaches for Soil-Structure Interaction," by A.S. Veletsos, A.M. Prasad and Y. Tang, 12/30/88, (PB89-174437, A03, MF-A01). This report is available only through NTIS (see address given above).
- NCEER-88-0032 "A Re-evaluation of Design Spectra for Seismic Damage Control," by C.J. Turkstra and A.G. Tallin, 11/7/88, (PB89-145221, A05, MF-A01).
- NCEER-88-0033 "The Behavior and Design of Noncontact Lap Splices Subjected to Repeated Inelastic Tensile Loading," by V.E. Sagan, P. Gergely and R.N. White, 12/8/88, (PB89-163737, A08, MF-A01).
- NCEER-88-0034 "Seismic Response of Pile Foundations," by S.M. Mamoon, P.K. Banerjee and S. Ahmad, 11/1/88, (PB89-145239, A04, MF-A01).
- NCEER-88-0035 "Modeling of R/C Building Structures With Flexible Floor Diaphragms (IDARC2)," by A.M. Reinhorn, S.K. Kunath and N. Panahshahi, 9/7/88, (PB89-207153, A07, MF-A01).
- NCEER-88-0036 "Solution of the Dam-Reservoir Interaction Problem Using a Combination of FEM, BEM with Particular Integrals, Modal Analysis, and Substructuring," by C-S. Tsai, G.C. Lee and R.L. Ketter, 12/31/88, (PB89-207146, A04, MF-A01).
- NCEER-88-0037 "Optimal Placement of Actuators for Structural Control," by F.Y. Cheng and C.P. Pantelides, 8/15/88, (PB89-162846, A05, MF-A01).
- NCEER-88-0038 "Teflon Bearings in Aseismic Base Isolation: Experimental Studies and Mathematical Modeling," by A. Mokha, M.C. Constantinou and A.M. Reinhorn, 12/5/88, (PB89-218457, A10, MF-A01). This report is available only through NTIS (see address given above).
- NCEER-88-0039 "Seismic Behavior of Flat Slab High-Rise Buildings in the New York City Area," by P. Weidlinger and M. Ettouney, 10/15/88, (PB90-145681, A04, MF-A01).
- NCEER-88-0040 "Evaluation of the Earthquake Resistance of Existing Buildings in New York City," by P. Weidlinger and M. Ettouney, 10/15/88, to be published.
- NCEER-88-0041 "Small-Scale Modeling Techniques for Reinforced Concrete Structures Subjected to Seismic Loads," by W. Kim, A. El-Attar and R.N. White, 11/22/88, (PB89-189625, A05, MF-A01).
- NCEER-88-0042 "Modeling Strong Ground Motion from Multiple Event Earthquakes," by G.W. Ellis and A.S. Cakmak, 10/15/88, (PB89-174445, A03, MF-A01).

- NCEER-88-0043 "Nonstationary Models of Seismic Ground Acceleration," by M. Grigoriu, S.E. Ruiz and E. Rosenblueth, 7/15/88, (PB89-189617, A04, MF-A01).
- NCEER-88-0044 "SARCF User's Guide: Seismic Analysis of Reinforced Concrete Frames," by Y.S. Chung, C. Meyer and M. Shinouzuka, 11/9/88, (PB89-174452, A08, MF-A01).
- NCEER-88-0045 "First Expert Panel Meeting on Disaster Research and Planning," edited by J. Pantelic and J. Stoyle, 9/15/88, (PB89-174460, A05, MF-A01).
- NCEER-88-0046 "Preliminary Studies of the Effect of Degrading Infill Walls on the Nonlinear Seismic Response of Steel Frames," by C.Z. Chrysostomou, P. Gergely and J.F. Abel, 12/19/88, (PB89-208383, A05, MF-A01).
- NCEER-88-0047 "Reinforced Concrete Frame Component Testing Facility - Design, Construction, Instrumentation and Operation," by S.P. Pessiki, C. Conley, T. Bond, P. Gergely and R.N. White, 12/16/88, (PB89-174478, A04, MF-A01).
- NCEER-89-0001 "Effects of Protective Cushion and Soil Compliancy on the Response of Equipment Within a Seismically Excited Building," by J.A. HoLung, 2/16/89, (PB89-207179, A04, MF-A01).
- NCEER-89-0002 "Statistical Evaluation of Response Modification Factors for Reinforced Concrete Structures," by H.H-M. Hwang and J-W. Jaw, 2/17/89, (PB89-207187, A05, MF-A01).
- NCEER-89-0003 "Hysteretic Columns Under Random Excitation," by G-Q. Cai and Y.K. Lin, 1/9/89, (PB89-196513, A03, MF-A01).
- NCEER-89-0004 "Experimental Study of 'Elephant Foot Bulge' Instability of Thin-Walled Metal Tanks," by Z-H. Jia and R.L. Ketter, 2/22/89, (PB89-207195, A03, MF-A01).
- NCEER-89-0005 "Experiment on Performance of Buried Pipelines Across San Andreas Fault," by J. Isenberg, E. Richardson and T.D. O'Rourke, 3/10/89, (PB89-218440, A04, MF-A01). This report is available only through NTIS (see address given above).
- NCEER-89-0006 "A Knowledge-Based Approach to Structural Design of Earthquake-Resistant Buildings," by M. Subramani, P. Gergely, C.H. Conley, J.F. Abel and A.H. Zaghw, 1/15/89, (PB89-218465, A06, MF-A01).
- NCEER-89-0007 "Liquefaction Hazards and Their Effects on Buried Pipelines," by T.D. O'Rourke and P.A. Lane, 2/1/89, (PB89-218481, A09, MF-A01).
- NCEER-89-0008 "Fundamentals of System Identification in Structural Dynamics," by H. Imai, C-B. Yun, O. Maruyama and M. Shinouzuka, 1/26/89, (PB89-207211, A04, MF-A01).
- NCEER-89-0009 "Effects of the 1985 Michoacan Earthquake on Water Systems and Other Buried Lifelines in Mexico," by A.G. Ayala and M.J. O'Rourke, 3/8/89, (PB89-207229, A06, MF-A01).
- NCEER-89-R010 "NCEER Bibliography of Earthquake Education Materials," by K.E.K. Ross, Second Revision, 9/1/89, (PB90-125352, A05, MF-A01). This report is replaced by NCEER-92-0018.
- NCEER-89-0011 "Inelastic Three-Dimensional Response Analysis of Reinforced Concrete Building Structures (IDARC-3D), Part I - Modeling," by S.K. Kunnath and A.M. Reinhorn, 4/17/89, (PB90-114612, A07, MF-A01). This report is available only through NTIS (see address given above).
- NCEER-89-0012 "Recommended Modifications to ATC-14," by C.D. Poland and J.O. Malley, 4/12/89, (PB90-108648, A15, MF-A01).
- NCEER-89-0013 "Repair and Strengthening of Beam-to-Column Connections Subjected to Earthquake Loading," by M. Corazao and A.J. Durrani, 2/28/89, (PB90-109885, A06, MF-A01).
- NCEER-89-0014 "Program EXKAL2 for Identification of Structural Dynamic Systems," by O. Maruyama, C-B. Yun, M. Hoshiya and M. Shinouzuka, 5/19/89, (PB90-109877, A09, MF-A01).

- NCEER-89-0015 "Response of Frames With Bolted Semi-Rigid Connections, Part I - Experimental Study and Analytical Predictions," by P.J. DiCorso, A.M. Reinhorn, J.R. Dickerson, J.B. Radziminski and W.L. Harper, 6/1/89, to be published.
- NCEER-89-0016 "ARMA Monte Carlo Simulation in Probabilistic Structural Analysis," by P.D. Spanos and M.P. Mignolet, 7/10/89, (PB90-109893, A03, MF-A01).
- NCEER-89-P017 "Preliminary Proceedings from the Conference on Disaster Preparedness - The Place of Earthquake Education in Our Schools," Edited by K.E.K. Ross, 6/23/89, (PB90-108606, A03, MF-A01).
- NCEER-89-0017 "Proceedings from the Conference on Disaster Preparedness - The Place of Earthquake Education in Our Schools," Edited by K.E.K. Ross, 12/31/89, (PB90-207895, A012, MF-A02). This report is available only through NTIS (see address given above).
- NCEER-89-0018 "Multidimensional Models of Hysteretic Material Behavior for Vibration Analysis of Shape Memory Energy Absorbing Devices, by E.J. Graesser and F.A. Cozzarelli, 6/7/89, (PB90-164146, A04, MF-A01).
- NCEER-89-0019 "Nonlinear Dynamic Analysis of Three-Dimensional Base Isolated Structures (3D-BASIS)," by S. Nagarajaiah, A.M. Reinhorn and M.C. Constantinou, 8/3/89, (PB90-161936, A06, MF-A01). This report has been replaced by NCEER-93-0011.
- NCEER-89-0020 "Structural Control Considering Time-Rate of Control Forces and Control Rate Constraints," by F.Y. Cheng and C.P. Pantelides, 8/3/89, (PB90-120445, A04, MF-A01).
- NCEER-89-0021 "Subsurface Conditions of Memphis and Shelby County," by K.W. Ng, T-S. Chang and H-H.M. Hwang, 7/26/89, (PB90-120437, A03, MF-A01).
- NCEER-89-0022 "Seismic Wave Propagation Effects on Straight Jointed Buried Pipelines," by K. Elhmadi and M.J. O'Rourke, 8/24/89, (PB90-162322, A10, MF-A02).
- NCEER-89-0023 "Workshop on Serviceability Analysis of Water Delivery Systems," edited by M. Grigoriu, 3/6/89, (PB90-127424, A03, MF-A01).
- NCEER-89-0024 "Shaking Table Study of a 1/5 Scale Steel Frame Composed of Tapered Members," by K.C. Chang, J.S. Hwang and G.C. Lee, 9/18/89, (PB90-160169, A04, MF-A01).
- NCEER-89-0025 "DYNA1D: A Computer Program for Nonlinear Seismic Site Response Analysis - Technical Documentation," by Jean H. Prevost, 9/14/89, (PB90-161944, A07, MF-A01). This report is available only through NTIS (see address given above).
- NCEER-89-0026 "1:4 Scale Model Studies of Active Tendon Systems and Active Mass Dampers for Aseismic Protection," by A.M. Reinhorn, T.T. Soong, R.C. Lin, Y.P. Yang, Y. Fukao, H. Abe and M. Nakai, 9/15/89, (PB90-173246, A10, MF-A02). This report is available only through NTIS (see address given above).
- NCEER-89-0027 "Scattering of Waves by Inclusions in a Nonhomogeneous Elastic Half Space Solved by Boundary Element Methods," by P.K. Hadley, A. Askar and A.S. Cakmak, 6/15/89, (PB90-145699, A07, MF-A01).
- NCEER-89-0028 "Statistical Evaluation of Deflection Amplification Factors for Reinforced Concrete Structures," by H.H.M. Hwang, J-W. Jaw and A.L. Ch'ng, 8/31/89, (PB90-164633, A05, MF-A01).
- NCEER-89-0029 "Bedrock Accelerations in Memphis Area Due to Large New Madrid Earthquakes," by H.H.M. Hwang, C.H.S. Chen and G. Yu, 11/7/89, (PB90-162330, A04, MF-A01).
- NCEER-89-0030 "Seismic Behavior and Response Sensitivity of Secondary Structural Systems," by Y.Q. Chen and T.T. Soong, 10/23/89, (PB90-164658, A08, MF-A01).
- NCEER-89-0031 "Random Vibration and Reliability Analysis of Primary-Secondary Structural Systems," by Y. Ibrahim, M. Grigoriu and T.T. Soong, 11/10/89, (PB90-161951, A04, MF-A01).

- NCEER-89-0032 "Proceedings from the Second U.S. - Japan Workshop on Liquefaction, Large Ground Deformation and Their Effects on Lifelines, September 26-29, 1989," Edited by T.D. O'Rourke and M. Hamada, 12/1/89, (PB90-209388, A22, MF-A03).
- NCEER-89-0033 "Deterministic Model for Seismic Damage Evaluation of Reinforced Concrete Structures," by J.M. Bracci, A.M. Reinhorn, J.B. Mander and S.K. Kunnath, 9/27/89, (PB91-108803, A06, MF-A01).
- NCEER-89-0034 "On the Relation Between Local and Global Damage Indices," by E. DiPasquale and A.S. Cakmak, 8/15/89, (PB90-173865, A05, MF-A01).
- NCEER-89-0035 "Cyclic Undrained Behavior of Nonplastic and Low Plasticity Silts," by A.J. Walker and H.E. Stewart, 7/26/89, (PB90-183518, A10, MF-A01).
- NCEER-89-0036 "Liquefaction Potential of Surficial Deposits in the City of Buffalo, New York," by M. Budhu, R. Giese and L. Baumgrass, 1/17/89, (PB90-208455, A04, MF-A01).
- NCEER-89-0037 "A Deterministic Assessment of Effects of Ground Motion Incoherence," by A.S. Veletsos and Y. Tang, 7/15/89, (PB90-164294, A03, MF-A01).
- NCEER-89-0038 "Workshop on Ground Motion Parameters for Seismic Hazard Mapping," July 17-18, 1989, edited by R.V. Whitman, 12/1/89, (PB90-173923, A04, MF-A01).
- NCEER-89-0039 "Seismic Effects on Elevated Transit Lines of the New York City Transit Authority," by C.J. Costantino, C.A. Miller and E. Heymsfield, 12/26/89, (PB90-207887, A06, MF-A01).
- NCEER-89-0040 "Centrifugal Modeling of Dynamic Soil-Structure Interaction," by K. Weissman, Supervised by J.H. Prevost, 5/10/89, (PB90-207879, A07, MF-A01).
- NCEER-89-0041 "Linearized Identification of Buildings With Cores for Seismic Vulnerability Assessment," by I-K. Ho and A.E. Aktan, 11/1/89, (PB90-251943, A07, MF-A01).
- NCEER-90-0001 "Geotechnical and Lifeline Aspects of the October 17, 1989 Loma Prieta Earthquake in San Francisco," by T.D. O'Rourke, H.E. Stewart, F.T. Blackburn and T.S. Dickerman, 1/90, (PB90-208596, A05, MF-A01).
- NCEER-90-0002 "Nonnormal Secondary Response Due to Yielding in a Primary Structure," by D.C.K. Chen and L.D. Lutes, 2/28/90, (PB90-251976, A07, MF-A01).
- NCEER-90-0003 "Earthquake Education Materials for Grades K-12," by K.E.K. Ross, 4/16/90, (PB91-251984, A05, MF-A05). This report has been replaced by NCEER-92-0018.
- NCEER-90-0004 "Catalog of Strong Motion Stations in Eastern North America," by R.W. Busby, 4/3/90, (PB90-251984, A05, MF-A01).
- NCEER-90-0005 "NCEER Strong-Motion Data Base: A User Manual for the GeoBase Release (Version 1.0 for the Sun3)," by P. Friberg and K. Jacob, 3/31/90 (PB90-258062, A04, MF-A01).
- NCEER-90-0006 "Seismic Hazard Along a Crude Oil Pipeline in the Event of an 1811-1812 Type New Madrid Earthquake," by H.H.M. Hwang and C-H.S. Chen, 4/16/90, (PB90-258054, A04, MF-A01).
- NCEER-90-0007 "Site-Specific Response Spectra for Memphis Sheahan Pumping Station," by H.H.M. Hwang and C.S. Lee, 5/15/90, (PB91-108811, A05, MF-A01).
- NCEER-90-0008 "Pilot Study on Seismic Vulnerability of Crude Oil Transmission Systems," by T. Ariman, R. Dobry, M. Grigoriu, F. Kozin, M. O'Rourke, T. O'Rourke and M. Shinozuka, 5/25/90, (PB91-108837, A06, MF-A01).
- NCEER-90-0009 "A Program to Generate Site Dependent Time Histories: EQGEN," by G.W. Ellis, M. Srinivasan and A.S. Cakmak, 1/30/90, (PB91-108829, A04, MF-A01).
- NCEER-90-0010 "Active Isolation for Seismic Protection of Operating Rooms," by M.E. Talbott, Supervised by M. Shinozuka, 6/8/9, (PB91-110205, A05, MF-A01).

- NCEER-90-0011 "Program LINEARID for Identification of Linear Structural Dynamic Systems," by C-B. Yun and M. Shinozuka, 6/25/90, (PB91-110312, A08, MF-A01).
- NCEER-90-0012 "Two-Dimensional Two-Phase Elasto-Plastic Seismic Response of Earth Dams," by A.N. Yiagos, Supervised by J.H. Prevost, 6/20/90, (PB91-110197, A13, MF-A02).
- NCEER-90-0013 "Secondary Systems in Base-Isolated Structures: Experimental Investigation, Stochastic Response and Stochastic Sensitivity," by G.D. Manolis, G. Juhn, M.C. Constantinou and A.M. Reinhorn, 7/1/90, (PB91-110320, A08, MF-A01).
- NCEER-90-0014 "Seismic Behavior of Lightly-Reinforced Concrete Column and Beam-Column Joint Details," by S.P. Pessiki, C.H. Conley, P. Gergely and R.N. White, 8/22/90, (PB91-108795, A11, MF-A02).
- NCEER-90-0015 "Two Hybrid Control Systems for Building Structures Under Strong Earthquakes," by J.N. Yang and A. Danielians, 6/29/90, (PB91-125393, A04, MF-A01).
- NCEER-90-0016 "Instantaneous Optimal Control with Acceleration and Velocity Feedback," by J.N. Yang and Z. Li, 6/29/90, (PB91-125401, A03, MF-A01).
- NCEER-90-0017 "Reconnaissance Report on the Northern Iran Earthquake of June 21, 1990," by M. Mehrain, 10/4/90, (PB91-125377, A03, MF-A01).
- NCEER-90-0018 "Evaluation of Liquefaction Potential in Memphis and Shelby County," by T.S. Chang, P.S. Tang, C.S. Lee and H. Hwang, 8/10/90, (PB91-125427, A09, MF-A01).
- NCEER-90-0019 "Experimental and Analytical Study of a Combined Sliding Disc Bearing and Helical Steel Spring Isolation System," by M.C. Constantinou, A.S. Mokha and A.M. Reinhorn, 10/4/90, (PB91-125385, A06, MF-A01). This report is available only through NTIS (see address given above).
- NCEER-90-0020 "Experimental Study and Analytical Prediction of Earthquake Response of a Sliding Isolation System with a Spherical Surface," by A.S. Mokha, M.C. Constantinou and A.M. Reinhorn, 10/11/90, (PB91-125419, A05, MF-A01).
- NCEER-90-0021 "Dynamic Interaction Factors for Floating Pile Groups," by G. Gazetas, K. Fan, A. Kaynia and E. Kausel, 9/10/90, (PB91-170381, A05, MF-A01).
- NCEER-90-0022 "Evaluation of Seismic Damage Indices for Reinforced Concrete Structures," by S. Rodriguez-Gomez and A.S. Cakmak, 9/30/90, PB91-171322, A06, MF-A01).
- NCEER-90-0023 "Study of Site Response at a Selected Memphis Site," by H. Desai, S. Ahmad, E.S. Gazetas and M.R. Oh, 10/11/90, (PB91-196857, A03, MF-A01).
- NCEER-90-0024 "A User's Guide to Strongmo: Version 1.0 of NCEER's Strong-Motion Data Access Tool for PCs and Terminals," by P.A. Friberg and C.A.T. Susch, 11/15/90, (PB91-171272, A03, MF-A01).
- NCEER-90-0025 "A Three-Dimensional Analytical Study of Spatial Variability of Seismic Ground Motions," by L-L. Hong and A.H.-S. Ang, 10/30/90, (PB91-170399, A09, MF-A01).
- NCEER-90-0026 "MUMOID User's Guide - A Program for the Identification of Modal Parameters," by S. Rodriguez-Gomez and E. DiPasquale, 9/30/90, (PB91-171298, A04, MF-A01).
- NCEER-90-0027 "SARCF-II User's Guide - Seismic Analysis of Reinforced Concrete Frames," by S. Rodriguez-Gomez, Y.S. Chung and C. Meyer, 9/30/90, (PB91-171280, A05, MF-A01).
- NCEER-90-0028 "Viscous Dampers: Testing, Modeling and Application in Vibration and Seismic Isolation," by N. Makris and M.C. Constantinou, 12/20/90 (PB91-190561, A06, MF-A01).
- NCEER-90-0029 "Soil Effects on Earthquake Ground Motions in the Memphis Area," by H. Hwang, C.S. Lee, K.W. Ng and T.S. Chang, 8/2/90, (PB91-190751, A05, MF-A01).

- NCEER-91-0001 "Proceedings from the Third Japan-U.S. Workshop on Earthquake Resistant Design of Lifeline Facilities and Countermeasures for Soil Liquefaction, December 17-19, 1990," edited by T.D. O'Rourke and M. Hamada, 2/1/91, (PB91-179259, A99, MF-A04).
- NCEER-91-0002 "Physical Space Solutions of Non-Proportionally Damped Systems," by M. Tong, Z. Liang and G.C. Lee, 1/15/91, (PB91-179242, A04, MF-A01).
- NCEER-91-0003 "Seismic Response of Single Piles and Pile Groups," by K. Fan and G. Gazetas, 1/10/91, (PB92-174994, A04, MF-A01).
- NCEER-91-0004 "Damping of Structures: Part 1 - Theory of Complex Damping," by Z. Liang and G. Lee, 10/10/91, (PB92-197235, A12, MF-A03).
- NCEER-91-0005 "3D-BASIS - Nonlinear Dynamic Analysis of Three Dimensional Base Isolated Structures: Part II," by S. Nagarajaiah, A.M. Reinhorn and M.C. Constantinou, 2/28/91, (PB91-190553, A07, MF-A01). This report has been replaced by NCEER-93-0011.
- NCEER-91-0006 "A Multidimensional Hysteretic Model for Plasticity Deforming Metals in Energy Absorbing Devices," by E.J. Graesser and F.A. Cozzarelli, 4/9/91, (PB92-108364, A04, MF-A01).
- NCEER-91-0007 "A Framework for Customizable Knowledge-Based Expert Systems with an Application to a KBES for Evaluating the Seismic Resistance of Existing Buildings," by E.G. Ibarra-Anaya and S.J. Fenves, 4/9/91, (PB91-210930, A08, MF-A01).
- NCEER-91-0008 "Nonlinear Analysis of Steel Frames with Semi-Rigid Connections Using the Capacity Spectrum Method," by G.G. Deierlein, S-H. Hsieh, Y-J. Shen and J.F. Abel, 7/2/91, (PB92-113828, A05, MF-A01).
- NCEER-91-0009 "Earthquake Education Materials for Grades K-12," by K.E.K. Ross, 4/30/91, (PB91-212142, A06, MF-A01). This report has been replaced by NCEER-92-0018.
- NCEER-91-0010 "Phase Wave Velocities and Displacement Phase Differences in a Harmonically Oscillating Pile," by N. Makris and G. Gazetas, 7/8/91, (PB92-108356, A04, MF-A01).
- NCEER-91-0011 "Dynamic Characteristics of a Full-Size Five-Story Steel Structure and a 2/5 Scale Model," by K.C. Chang, G.C. Yao, G.C. Lee, D.S. Hao and Y.C. Yeh, 7/2/91, (PB93-116648, A06, MF-A02).
- NCEER-91-0012 "Seismic Response of a 2/5 Scale Steel Structure with Added Viscoelastic Dampers," by K.C. Chang, T.T. Soong, S-T. Oh and M.L. Lai, 5/17/91, (PB92-110816, A05, MF-A01).
- NCEER-91-0013 "Earthquake Response of Retaining Walls; Full-Scale Testing and Computational Modeling," by S. Alampalli and A-W.M. Elgamal, 6/20/91, to be published.
- NCEER-91-0014 "3D-BASIS-M: Nonlinear Dynamic Analysis of Multiple Building Base Isolated Structures," by P.C. Tsopelas, S. Nagarajaiah, M.C. Constantinou and A.M. Reinhorn, 5/28/91, (PB92-113885, A09, MF-A02).
- NCEER-91-0015 "Evaluation of SEAOC Design Requirements for Sliding Isolated Structures," by D. Theodossiou and M.C. Constantinou, 6/10/91, (PB92-114602, A11, MF-A03).
- NCEER-91-0016 "Closed-Loop Modal Testing of a 27-Story Reinforced Concrete Flat Plate-Core Building," by H.R. Somaprasad, T. Toksoy, H. Yoshiyuki and A.E. Aktan, 7/15/91, (PB92-129980, A07, MF-A02).
- NCEER-91-0017 "Shake Table Test of a 1/6 Scale Two-Story Lightly Reinforced Concrete Building," by A.G. El-Attar, R.N. White and P. Gergely, 2/28/91, (PB92-222447, A06, MF-A02).
- NCEER-91-0018 "Shake Table Test of a 1/8 Scale Three-Story Lightly Reinforced Concrete Building," by A.G. El-Attar, R.N. White and P. Gergely, 2/28/91, (PB93-116630, A08, MF-A02).
- NCEER-91-0019 "Transfer Functions for Rigid Rectangular Foundations," by A.S. Veletsos, A.M. Prasad and W.H. Wu, 7/31/91, to be published.

- NCEER-91-0020 "Hybrid Control of Seismic-Excited Nonlinear and Inelastic Structural Systems," by J.N. Yang, Z. Li and A. Danielians, 8/1/91, (PB92-143171, A06, MF-A02).
- NCEER-91-0021 "The NCEER-91 Earthquake Catalog: Improved Intensity-Based Magnitudes and Recurrence Relations for U.S. Earthquakes East of New Madrid," by L. Seeber and J.G. Armbruster, 8/28/91, (PB92-176742, A06, MF-A02).
- NCEER-91-0022 "Proceedings from the Implementation of Earthquake Planning and Education in Schools: The Need for Change - The Roles of the Changemakers," by K.E.K. Ross and F. Winslow, 7/23/91, (PB92-129998, A12, MF-A03).
- NCEER-91-0023 "A Study of Reliability-Based Criteria for Seismic Design of Reinforced Concrete Frame Buildings," by H.H.M. Hwang and H-M. Hsu, 8/10/91, (PB92-140235, A09, MF-A02).
- NCEER-91-0024 "Experimental Verification of a Number of Structural System Identification Algorithms," by R.G. Ghanem, H. Gavin and M. Shinozuka, 9/18/91, (PB92-176577, A18, MF-A04).
- NCEER-91-0025 "Probabilistic Evaluation of Liquefaction Potential," by H.H.M. Hwang and C.S. Lee," 11/25/91, (PB92-143429, A05, MF-A01).
- NCEER-91-0026 "Instantaneous Optimal Control for Linear, Nonlinear and Hysteretic Structures - Stable Controllers," by J.N. Yang and Z. Li, 11/15/91, (PB92-163807, A04, MF-A01).
- NCEER-91-0027 "Experimental and Theoretical Study of a Sliding Isolation System for Bridges," by M.C. Constantinou, A. Kartoum, A.M. Reinhorn and P. Bradford, 11/15/91, (PB92-176973, A10, MF-A03).
- NCEER-92-0001 "Case Studies of Liquefaction and Lifeline Performance During Past Earthquakes, Volume 1: Japanese Case Studies," Edited by M. Hamada and T. O'Rourke, 2/17/92, (PB92-197243, A18, MF-A04).
- NCEER-92-0002 "Case Studies of Liquefaction and Lifeline Performance During Past Earthquakes, Volume 2: United States Case Studies," Edited by T. O'Rourke and M. Hamada, 2/17/92, (PB92-197250, A20, MF-A04).
- NCEER-92-0003 "Issues in Earthquake Education," Edited by K. Ross, 2/3/92, (PB92-222389, A07, MF-A02).
- NCEER-92-0004 "Proceedings from the First U.S. - Japan Workshop on Earthquake Protective Systems for Bridges," Edited by I.G. Buckle, 2/4/92, (PB94-142239, A99, MF-A06).
- NCEER-92-0005 "Seismic Ground Motion from a Haskell-Type Source in a Multiple-Layered Half-Space," A.P. Theoharis, G. Deodatis and M. Shinozuka, 1/2/92, to be published.
- NCEER-92-0006 "Proceedings from the Site Effects Workshop," Edited by R. Whitman, 2/29/92, (PB92-197201, A04, MF-A01).
- NCEER-92-0007 "Engineering Evaluation of Permanent Ground Deformations Due to Seismically-Induced Liquefaction," by M.H. Baziar, R. Dobry and A-W.M. Elgamal, 3/24/92, (PB92-222421, A13, MF-A03).
- NCEER-92-0008 "A Procedure for the Seismic Evaluation of Buildings in the Central and Eastern United States," by C.D. Poland and J.O. Malley, 4/2/92, (PB92-222439, A20, MF-A04).
- NCEER-92-0009 "Experimental and Analytical Study of a Hybrid Isolation System Using Friction Controllable Sliding Bearings," by M.Q. Feng, S. Fujii and M. Shinozuka, 5/15/92, (PB93-150282, A06, MF-A02).
- NCEER-92-0010 "Seismic Resistance of Slab-Column Connections in Existing Non-Ductile Flat-Plate Buildings," by A.J. Durrani and Y. Du, 5/18/92, (PB93-116812, A06, MF-A02).
- NCEER-92-0011 "The Hysteretic and Dynamic Behavior of Brick Masonry Walls Upgraded by Ferrocement Coatings Under Cyclic Loading and Strong Simulated Ground Motion," by H. Lee and S.P. Prawel, 5/11/92, to be published.
- NCEER-92-0012 "Study of Wire Rope Systems for Seismic Protection of Equipment in Buildings," by G.F. Demetriades, M.C. Constantinou and A.M. Reinhorn, 5/20/92, (PB93-116655, A08, MF-A02).

- NCEER-92-0013 "Shape Memory Structural Dampers: Material Properties, Design and Seismic Testing," by P.R. Witting and F.A. Cozzarelli, 5/26/92, (PB93-116663, A05, MF-A01).
- NCEER-92-0014 "Longitudinal Permanent Ground Deformation Effects on Buried Continuous Pipelines," by M.J. O'Rourke, and C. Nordberg, 6/15/92, (PB93-116671, A08, MF-A02).
- NCEER-92-0015 "A Simulation Method for Stationary Gaussian Random Functions Based on the Sampling Theorem," by M. Grigoriu and S. Balopoulou, 6/11/92, (PB93-127496, A05, MF-A01).
- NCEER-92-0016 "Gravity-Load-Designed Reinforced Concrete Buildings: Seismic Evaluation of Existing Construction and Detailing Strategies for Improved Seismic Resistance," by G.W. Hoffmann, S.K. Kunnath, A.M. Reinhorn and J.B. Mander, 7/15/92, (PB94-142007, A08, MF-A02).
- NCEER-92-0017 "Observations on Water System and Pipeline Performance in the Limón Area of Costa Rica Due to the April 22, 1991 Earthquake," by M. O'Rourke and D. Ballantyne, 6/30/92, (PB93-126811, A06, MF-A02).
- NCEER-92-0018 "Fourth Edition of Earthquake Education Materials for Grades K-12," Edited by K.E.K. Ross, 8/10/92, (PB93-114023, A07, MF-A02).
- NCEER-92-0019 "Proceedings from the Fourth Japan-U.S. Workshop on Earthquake Resistant Design of Lifeline Facilities and Countermeasures for Soil Liquefaction," Edited by M. Hamada and T.D. O'Rourke, 8/12/92, (PB93-163939, A99, MF-E11).
- NCEER-92-0020 "Active Bracing System: A Full Scale Implementation of Active Control," by A.M. Reinhorn, T.T. Soong, R.C. Lin, M.A. Riley, Y.P. Wang, S. Aizawa and M. Higashino, 8/14/92, (PB93-127512, A06, MF-A02).
- NCEER-92-0021 "Empirical Analysis of Horizontal Ground Displacement Generated by Liquefaction-Induced Lateral Spreads," by S.F. Bartlett and T.L. Youd, 8/17/92, (PB93-188241, A06, MF-A02).
- NCEER-92-0022 "IDARC Version 3.0: Inelastic Damage Analysis of Reinforced Concrete Structures," by S.K. Kunnath, A.M. Reinhorn and R.F. Lobo, 8/31/92, (PB93-227502, A07, MF-A02).
- NCEER-92-0023 "A Semi-Empirical Analysis of Strong-Motion Peaks in Terms of Seismic Source, Propagation Path and Local Site Conditions, by M. Kamiyama, M.J. O'Rourke and R. Flores-Berrones, 9/9/92, (PB93-150266, A08, MF-A02).
- NCEER-92-0024 "Seismic Behavior of Reinforced Concrete Frame Structures with Nonductile Details, Part I: Summary of Experimental Findings of Full Scale Beam-Column Joint Tests," by A. Beres, R.N. White and P. Gergely, 9/30/92, (PB93-227783, A05, MF-A01).
- NCEER-92-0025 "Experimental Results of Repaired and Retrofitted Beam-Column Joint Tests in Lightly Reinforced Concrete Frame Buildings," by A. Beres, S. El-Borgi, R.N. White and P. Gergely, 10/29/92, (PB93-227791, A05, MF-A01).
- NCEER-92-0026 "A Generalization of Optimal Control Theory: Linear and Nonlinear Structures," by J.N. Yang, Z. Li and S. Vongchavalitkul, 11/2/92, (PB93-188621, A05, MF-A01).
- NCEER-92-0027 "Seismic Resistance of Reinforced Concrete Frame Structures Designed Only for Gravity Loads: Part I - Design and Properties of a One-Third Scale Model Structure," by J.M. Bracci, A.M. Reinhorn and J.B. Mander, 12/1/92, (PB94-104502, A08, MF-A02).
- NCEER-92-0028 "Seismic Resistance of Reinforced Concrete Frame Structures Designed Only for Gravity Loads: Part II - Experimental Performance of Subassemblages," by L.E. Aycardi, J.B. Mander and A.M. Reinhorn, 12/1/92, (PB94-104510, A08, MF-A02).
- NCEER-92-0029 "Seismic Resistance of Reinforced Concrete Frame Structures Designed Only for Gravity Loads: Part III - Experimental Performance and Analytical Study of a Structural Model," by J.M. Bracci, A.M. Reinhorn and J.B. Mander, 12/1/92, (PB93-227528, A09, MF-A01).

- NCEER-92-0030 "Evaluation of Seismic Retrofit of Reinforced Concrete Frame Structures: Part I - Experimental Performance of Retrofitted Subassemblages," by D. Choudhuri, J.B. Mander and A.M. Reinhorn, 12/8/92, (PB93-198307, A07, MF-A02).
- NCEER-92-0031 "Evaluation of Seismic Retrofit of Reinforced Concrete Frame Structures: Part II - Experimental Performance and Analytical Study of a Retrofitted Structural Model," by J.M. Bracci, A.M. Reinhorn and J.B. Mander, 12/8/92, (PB93-198315, A09, MF-A03).
- NCEER-92-0032 "Experimental and Analytical Investigation of Seismic Response of Structures with Supplemental Fluid Viscous Dampers," by M.C. Constantinou and M.D. Symans, 12/21/92, (PB93-191435, A10, MF-A03). This report is available only through NTIS (see address given above).
- NCEER-92-0033 "Reconnaissance Report on the Cairo, Egypt Earthquake of October 12, 1992," by M. Khater, 12/23/92, (PB93-188621, A03, MF-A01).
- NCEER-92-0034 "Low-Level Dynamic Characteristics of Four Tall Flat-Plate Buildings in New York City," by H. Gavin, S. Yuan, J. Grossman, E. Pekelis and K. Jacob, 12/28/92, (PB93-188217, A07, MF-A02).
- NCEER-93-0001 "An Experimental Study on the Seismic Performance of Brick-Infilled Steel Frames With and Without Retrofit," by J.B. Mander, B. Nair, K. Wojtkowski and J. Ma, 1/29/93, (PB93-227510, A07, MF-A02).
- NCEER-93-0002 "Social Accounting for Disaster Preparedness and Recovery Planning," by S. Cole, E. Pantoja and V. Razak, 2/22/93, (PB94-142114, A12, MF-A03).
- NCEER-93-0003 "Assessment of 1991 NEHRP Provisions for Nonstructural Components and Recommended Revisions," by T.T. Soong, G. Chen, Z. Wu, R-H. Zhang and M. Grigoriu, 3/1/93, (PB93-188639, A06, MF-A02).
- NCEER-93-0004 "Evaluation of Static and Response Spectrum Analysis Procedures of SEAOC/UBC for Seismic Isolated Structures," by C.W. Winters and M.C. Constantinou, 3/23/93, (PB93-198299, A10, MF-A03).
- NCEER-93-0005 "Earthquakes in the Northeast - Are We Ignoring the Hazard? A Workshop on Earthquake Science and Safety for Educators," edited by K.E.K. Ross, 4/2/93, (PB94-103066, A09, MF-A02).
- NCEER-93-0006 "Inelastic Response of Reinforced Concrete Structures with Viscoelastic Braces," by R.F. Lobo, J.M. Bracci, K.L. Shen, A.M. Reinhorn and T.T. Soong, 4/5/93, (PB93-227486, A05, MF-A02).
- NCEER-93-0007 "Seismic Testing of Installation Methods for Computers and Data Processing Equipment," by K. Kosar, T.T. Soong, K.L. Shen, J.A. HoLung and Y.K. Lin, 4/12/93, (PB93-198299, A07, MF-A02).
- NCEER-93-0008 "Retrofit of Reinforced Concrete Frames Using Added Dampers," by A. Reinhorn, M. Constantinou and C. Li, to be published.
- NCEER-93-0009 "Seismic Behavior and Design Guidelines for Steel Frame Structures with Added Viscoelastic Dampers," by K.C. Chang, M.L. Lai, T.T. Soong, D.S. Hao and Y.C. Yeh, 5/1/93, (PB94-141959, A07, MF-A02).
- NCEER-93-0010 "Seismic Performance of Shear-Critical Reinforced Concrete Bridge Piers," by J.B. Mander, S.M. Waheed, M.T.A. Chaudhary and S.S. Chen, 5/12/93, (PB93-227494, A08, MF-A02).
- NCEER-93-0011 "3D-BASIS-TABS: Computer Program for Nonlinear Dynamic Analysis of Three Dimensional Base Isolated Structures," by S. Nagarajaiah, C. Li, A.M. Reinhorn and M.C. Constantinou, 8/2/93, (PB94-141819, A09, MF-A02).
- NCEER-93-0012 "Effects of Hydrocarbon Spills from an Oil Pipeline Break on Ground Water," by O.J. Helweg and H.H.M. Hwang, 8/3/93, (PB94-141942, A06, MF-A02).
- NCEER-93-0013 "Simplified Procedures for Seismic Design of Nonstructural Components and Assessment of Current Code Provisions," by M.P. Singh, L.E. Suarez, E.E. Matheu and G.O. Maldonado, 8/4/93, (PB94-141827, A09, MF-A02).
- NCEER-93-0014 "An Energy Approach to Seismic Analysis and Design of Secondary Systems," by G. Chen and T.T. Soong, 8/6/93, (PB94-142767, A11, MF-A03).

- NCEER-93-0015 "Proceedings from School Sites: Becoming Prepared for Earthquakes - Commemorating the Third Anniversary of the Loma Prieta Earthquake," Edited by F.E. Winslow and K.E.K. Ross, 8/16/93, (PB94-154275, A16, MF-A02).
- NCEER-93-0016 "Reconnaissance Report of Damage to Historic Monuments in Cairo, Egypt Following the October 12, 1992 Dahshur Earthquake," by D. Sykora, D. Look, G. Croci, E. Karaesmen and E. Karaesmen, 8/19/93, (PB94-142221, A08, MF-A02).
- NCEER-93-0017 "The Island of Guam Earthquake of August 8, 1993," by S.W. Swan and S.K. Harris, 9/30/93, (PB94-141843, A04, MF-A01).
- NCEER-93-0018 "Engineering Aspects of the October 12, 1992 Egyptian Earthquake," by A.W. Elgamal, M. Amer, K. Adalier and A. Abul-Fadl, 10/7/93, (PB94-141983, A05, MF-A01).
- NCEER-93-0019 "Development of an Earthquake Motion Simulator and its Application in Dynamic Centrifuge Testing," by I. Krstelj, Supervised by J.H. Prevost, 10/23/93, (PB94-181773, A-10, MF-A03).
- NCEER-93-0020 "NCEER-Taisei Corporation Research Program on Sliding Seismic Isolation Systems for Bridges: Experimental and Analytical Study of a Friction Pendulum System (FPS)," by M.C. Constantinou, P. Tsopelas, Y-S. Kim and S. Okamoto, 11/1/93, (PB94-142775, A08, MF-A02).
- NCEER-93-0021 "Finite Element Modeling of Elastomeric Seismic Isolation Bearings," by L.J. Billings, Supervised by R. Shepherd, 11/8/93, to be published.
- NCEER-93-0022 "Seismic Vulnerability of Equipment in Critical Facilities: Life-Safety and Operational Consequences," by K. Porter, G.S. Johnson, M.M. Zadeh, C. Scawthorn and S. Eder, 11/24/93, (PB94-181765, A16, MF-A03).
- NCEER-93-0023 "Hokkaido Nansei-oki, Japan Earthquake of July 12, 1993, by P.I. Yanev and C.R. Scawthorn, 12/23/93, (PB94-181500, A07, MF-A01).
- NCEER-94-0001 "An Evaluation of Seismic Serviceability of Water Supply Networks with Application to the San Francisco Auxiliary Water Supply System," by I. Markov, Supervised by M. Grigoriu and T. O'Rourke, 1/21/94, (PB94-204013, A07, MF-A02).
- NCEER-94-0002 "NCEER-Taisei Corporation Research Program on Sliding Seismic Isolation Systems for Bridges: Experimental and Analytical Study of Systems Consisting of Sliding Bearings, Rubber Restoring Force Devices and Fluid Dampers," Volumes I and II, by P. Tsopelas, S. Okamoto, M.C. Constantinou, D. Ozaki and S. Fujii, 2/4/94, (PB94-181740, A09, MF-A02 and PB94-181757, A12, MF-A03).
- NCEER-94-0003 "A Markov Model for Local and Global Damage Indices in Seismic Analysis," by S. Rahman and M. Grigoriu, 2/18/94, (PB94-206000, A12, MF-A03).
- NCEER-94-0004 "Proceedings from the NCEER Workshop on Seismic Response of Masonry Infills," edited by D.P. Abrams, 3/1/94, (PB94-180783, A07, MF-A02).
- NCEER-94-0005 "The Northridge, California Earthquake of January 17, 1994: General Reconnaissance Report," edited by J.D. Goltz, 3/11/94, (PB94-193943, A10, MF-A03).
- NCEER-94-0006 "Seismic Energy Based Fatigue Damage Analysis of Bridge Columns: Part I - Evaluation of Seismic Capacity," by G.A. Chang and J.B. Mander, 3/14/94, (PB94-219185, A11, MF-A03).
- NCEER-94-0007 "Seismic Isolation of Multi-Story Frame Structures Using Spherical Sliding Isolation Systems," by T.M. Al-Hussaini, V.A. Zayas and M.C. Constantinou, 3/17/94, (PB94-193745, A09, MF-A02).
- NCEER-94-0008 "The Northridge, California Earthquake of January 17, 1994: Performance of Highway Bridges," edited by I.G. Buckle, 3/24/94, (PB94-193851, A06, MF-A02).
- NCEER-94-0009 "Proceedings of the Third U.S.-Japan Workshop on Earthquake Protective Systems for Bridges," edited by I.G. Buckle and I. Friedland, 3/31/94, (PB94-195815, A99, MF-A06).

- NCEER-94-0010 "3D-BASIS-ME: Computer Program for Nonlinear Dynamic Analysis of Seismically Isolated Single and Multiple Structures and Liquid Storage Tanks," by P.C. Tsopelas, M.C. Constantinou and A.M. Reinhorn, 4/12/94, (PB94-204922, A09, MF-A02).
- NCEER-94-0011 "The Northridge, California Earthquake of January 17, 1994: Performance of Gas Transmission Pipelines," by T.D. O'Rourke and M.C. Palmer, 5/16/94, (PB94-204989, A05, MF-A01).
- NCEER-94-0012 "Feasibility Study of Replacement Procedures and Earthquake Performance Related to Gas Transmission Pipelines," by T.D. O'Rourke and M.C. Palmer, 5/25/94, (PB94-206638, A09, MF-A02).
- NCEER-94-0013 "Seismic Energy Based Fatigue Damage Analysis of Bridge Columns: Part II - Evaluation of Seismic Demand," by G.A. Chang and J.B. Mander, 6/1/94, (PB95-18106, A08, MF-A02).
- NCEER-94-0014 "NCEER-Taisei Corporation Research Program on Sliding Seismic Isolation Systems for Bridges: Experimental and Analytical Study of a System Consisting of Sliding Bearings and Fluid Restoring Force/Damping Devices," by P. Tsopelas and M.C. Constantinou, 6/13/94, (PB94-219144, A10, MF-A03).
- NCEER-94-0015 "Generation of Hazard-Consistent Fragility Curves for Seismic Loss Estimation Studies," by H. Hwang and J-R. Huo, 6/14/94, (PB95-181996, A09, MF-A02).
- NCEER-94-0016 "Seismic Study of Building Frames with Added Energy-Absorbing Devices," by W.S. Pong, C.S. Tsai and G.C. Lee, 6/20/94, (PB94-219136, A10, A03).
- NCEER-94-0017 "Sliding Mode Control for Seismic-Excited Linear and Nonlinear Civil Engineering Structures," by J. Yang, J. Wu, A. Agrawal and Z. Li, 6/21/94, (PB95-138483, A06, MF-A02).
- NCEER-94-0018 "3D-BASIS-TABS Version 2.0: Computer Program for Nonlinear Dynamic Analysis of Three Dimensional Base Isolated Structures," by A.M. Reinhorn, S. Nagarajaiah, M.C. Constantinou, P. Tsopelas and R. Li, 6/22/94, (PB95-182176, A08, MF-A02).
- NCEER-94-0019 "Proceedings of the International Workshop on Civil Infrastructure Systems: Application of Intelligent Systems and Advanced Materials on Bridge Systems," Edited by G.C. Lee and K.C. Chang, 7/18/94, (PB95-252474, A20, MF-A04).
- NCEER-94-0020 "Study of Seismic Isolation Systems for Computer Floors," by V. Lambrou and M.C. Constantinou, 7/19/94, (PB95-138533, A10, MF-A03).
- NCEER-94-0021 "Proceedings of the U.S.-Italian Workshop on Guidelines for Seismic Evaluation and Rehabilitation of Unreinforced Masonry Buildings," Edited by D.P. Abrams and G.M. Calvi, 7/20/94, (PB95-138749, A13, MF-A03).
- NCEER-94-0022 "NCEER-Taisei Corporation Research Program on Sliding Seismic Isolation Systems for Bridges: Experimental and Analytical Study of a System Consisting of Lubricated PTFE Sliding Bearings and Mild Steel Dampers," by P. Tsopelas and M.C. Constantinou, 7/22/94, (PB95-182184, A08, MF-A02).
- NCEER-94-0023 "Development of Reliability-Based Design Criteria for Buildings Under Seismic Load," by Y.K. Wen, H. Hwang and M. Shinozuka, 8/1/94, (PB95-211934, A08, MF-A02).
- NCEER-94-0024 "Experimental Verification of Acceleration Feedback Control Strategies for an Active Tendon System," by S.J. Dyke, B.F. Spencer, Jr., P. Quast, M.K. Sain, D.C. Kaspari, Jr. and T.T. Soong, 8/29/94, (PB95-212320, A05, MF-A01).
- NCEER-94-0025 "Seismic Retrofitting Manual for Highway Bridges," Edited by I.G. Buckle and I.F. Friedland, published by the Federal Highway Administration (PB95-212676, A15, MF-A03).
- NCEER-94-0026 "Proceedings from the Fifth U.S.-Japan Workshop on Earthquake Resistant Design of Lifeline Facilities and Countermeasures Against Soil Liquefaction," Edited by T.D. O'Rourke and M. Hamada, 11/7/94, (PB95-220802, A99, MF-E08).

- NCEER-95-0001 "Experimental and Analytical Investigation of Seismic Retrofit of Structures with Supplemental Damping: Part 1 - Fluid Viscous Damping Devices," by A.M. Reinhorn, C. Li and M.C. Constantinou, 1/3/95, (PB95-266599, A09, MF-A02).
- NCEER-95-0002 "Experimental and Analytical Study of Low-Cycle Fatigue Behavior of Semi-Rigid Top-And-Sear Angle Connections," by G. Pekcan, J.B. Mander and S.S. Chen, 1/5/95, (PB95-220042, A07, MF-A02).
- NCEER-95-0003 "NCEER-ATC Joint Study on Fragility of Buildings," by T. Anagnos, C. Rojahn and A.S. Kiremidjian, 1/20/95, (PB95-220026, A06, MF-A02).
- NCEER-95-0004 "Nonlinear Control Algorithms for Peak Response Reduction," by Z. Wu, T.T. Soong, V. Gattulli and R.C. Lin, 2/16/95, (PB95-220349, A05, MF-A01).
- NCEER-95-0005 "Pipeline Replacement Feasibility Study: A Methodology for Minimizing Seismic and Corrosion Risks to Underground Natural Gas Pipelines," by R.T. Eguchi, H.A. Seligson and D.G. Honegger, 3/2/95, (PB95-252326, A06, MF-A02).
- NCEER-95-0006 "Evaluation of Seismic Performance of an 11-Story Frame Building During the 1994 Northridge Earthquake," by F. Naeim, R. DiSilio, K. Benuska, A. Reinhorn and C. Li, to be published.
- NCEER-95-0007 "Prioritization of Bridges for Seismic Retrofitting," by N. Basöz and A.S. Kiremidjian, 4/24/95, (PB95-252300, A08, MF-A02).
- NCEER-95-0008 "Method for Developing Motion Damage Relationships for Reinforced Concrete Frames," by A. Singhal and A.S. Kiremidjian, 5/11/95, (PB95-266607, A06, MF-A02).
- NCEER-95-0009 "Experimental and Analytical Investigation of Seismic Retrofit of Structures with Supplemental Damping: Part II - Friction Devices," by C. Li and A.M. Reinhorn, 7/6/95, (PB96-128087, A11, MF-A03).
- NCEER-95-0010 "Experimental Performance and Analytical Study of a Non-Ductile Reinforced Concrete Frame Structure Retrofitted with Elastomeric Spring Dampers," by G. Pekcan, J.B. Mander and S.S. Chen, 7/14/95, (PB96-137161, A08, MF-A02).
- NCEER-95-0011 "Development and Experimental Study of Semi-Active Fluid Damping Devices for Seismic Protection of Structures," by M.D. Symans and M.C. Constantinou, 8/3/95, (PB96-136940, A23, MF-A04).
- NCEER-95-0012 "Real-Time Structural Parameter Modification (RSPM): Development of Innervated Structures," by Z. Liang, M. Tong and G.C. Lee, 4/11/95, (PB96-137153, A06, MF-A01).
- NCEER-95-0013 "Experimental and Analytical Investigation of Seismic Retrofit of Structures with Supplemental Damping: Part III - Viscous Damping Walls," by A.M. Reinhorn and C. Li, 10/1/95, (PB96-176409, A11, MF-A03).
- NCEER-95-0014 "Seismic Fragility Analysis of Equipment and Structures in a Memphis Electric Substation," by J-R. Huo and H.H.M. Hwang, 8/10/95, (PB96-128087, A09, MF-A02).
- NCEER-95-0015 "The Hanshin-Awaji Earthquake of January 17, 1995: Performance of Lifelines," Edited by M. Shinozuka, 11/3/95, (PB96-176383, A15, MF-A03).
- NCEER-95-0016 "Highway Culvert Performance During Earthquakes," by T.L. Youd and C.J. Beckman, available as NCEER-96-0015.
- NCEER-95-0017 "The Hanshin-Awaji Earthquake of January 17, 1995: Performance of Highway Bridges," Edited by I.G. Buckle, 12/1/95, to be published.
- NCEER-95-0018 "Modeling of Masonry Infill Panels for Structural Analysis," by A.M. Reinhorn, A. Madan, R.E. Valles, Y. Reichmann and J.B. Mander, 12/8/95, (PB97-110886, MF-A01, A06).
- NCEER-95-0019 "Optimal Polynomial Control for Linear and Nonlinear Structures," by A.K. Agrawal and J.N. Yang, 12/11/95, (PB96-168737, A07, MF-A02).

- NCEER-95-0020 "Retrofit of Non-Ductile Reinforced Concrete Frames Using Friction Dampers," by R.S. Rao, P. Gergely and R.N. White, 12/22/95, (PB97-133508, A10, MF-A02).
- NCEER-95-0021 "Parametric Results for Seismic Response of Pile-Supported Bridge Bents," by G. Mylonakis, A. Nikolaou and G. Gazetas, 12/22/95, (PB97-100242, A12, MF-A03).
- NCEER-95-0022 "Kinematic Bending Moments in Seismically Stressed Piles," by A. Nikolaou, G. Mylonakis and G. Gazetas, 12/23/95, (PB97-113914, MF-A03, A13).
- NCEER-96-0001 "Dynamic Response of Unreinforced Masonry Buildings with Flexible Diaphragms," by A.C. Costley and D.P. Abrams," 10/10/96, (PB97-133573, MF-A03, A15).
- NCEER-96-0002 "State of the Art Review: Foundations and Retaining Structures," by I. Po Lam, to be published.
- NCEER-96-0003 "Ductility of Rectangular Reinforced Concrete Bridge Columns with Moderate Confinement," by N. Wehbe, M. Saidi, D. Sanders and B. Douglas, 11/7/96, (PB97-133557, A06, MF-A02).
- NCEER-96-0004 "Proceedings of the Long-Span Bridge Seismic Research Workshop," edited by I.G. Buckle and I.M. Friedland, to be published.
- NCEER-96-0005 "Establish Representative Pier Types for Comprehensive Study: Eastern United States," by J. Kulicki and Z. Prucz, 5/28/96, (PB98-119217, A07, MF-A02).
- NCEER-96-0006 "Establish Representative Pier Types for Comprehensive Study: Western United States," by R. Imbsen, R.A. Schamber and T.A. Osterkamp, 5/28/96, (PB98-118607, A07, MF-A02).
- NCEER-96-0007 "Nonlinear Control Techniques for Dynamical Systems with Uncertain Parameters," by R.G. Ghanem and M.I. Bujakow, 5/27/96, (PB97-100259, A17, MF-A03).
- NCEER-96-0008 "Seismic Evaluation of a 30-Year Old Non-Ductile Highway Bridge Pier and Its Retrofit," by J.B. Mander, B. Mahmoodzadegan, S. Bhadra and S.S. Chen, 5/31/96, (PB97-110902, MF-A03, A10).
- NCEER-96-0009 "Seismic Performance of a Model Reinforced Concrete Bridge Pier Before and After Retrofit," by J.B. Mander, J.H. Kim and C.A. Ligozio, 5/31/96, (PB97-110910, MF-A02, A10).
- NCEER-96-0010 "IDARC2D Version 4.0: A Computer Program for the Inelastic Damage Analysis of Buildings," by R.E. Valles, A.M. Reinhorn, S.K. Kunnath, C. Li and A. Madan, 6/3/96, (PB97-100234, A17, MF-A03).
- NCEER-96-0011 "Estimation of the Economic Impact of Multiple Lifeline Disruption: Memphis Light, Gas and Water Division Case Study," by S.E. Chang, H.A. Seligson and R.T. Eguchi, 8/16/96, (PB97-133490, A11, MF-A03).
- NCEER-96-0012 "Proceedings from the Sixth Japan-U.S. Workshop on Earthquake Resistant Design of Lifeline Facilities and Countermeasures Against Soil Liquefaction, Edited by M. Hamada and T. O'Rourke, 9/11/96, (PB97-133581, A99, MF-A06).
- NCEER-96-0013 "Chemical Hazards, Mitigation and Preparedness in Areas of High Seismic Risk: A Methodology for Estimating the Risk of Post-Earthquake Hazardous Materials Release," by H.A. Seligson, R.T. Eguchi, K.J. Tierney and K. Richmond, 11/7/96, (PB97-133565, MF-A02, A08).
- NCEER-96-0014 "Response of Steel Bridge Bearings to Reversed Cyclic Loading," by J.B. Mander, D-K. Kim, S.S. Chen and G.J. Premus, 11/13/96, (PB97-140735, A12, MF-A03).
- NCEER-96-0015 "Highway Culvert Performance During Past Earthquakes," by T.L. Youd and C.J. Beckman, 11/25/96, (PB97-133532, A06, MF-A01).
- NCEER-97-0001 "Evaluation, Prevention and Mitigation of Pounding Effects in Building Structures," by R.E. Valles and A.M. Reinhorn, 2/20/97, (PB97-159552, A14, MF-A03).
- NCEER-97-0002 "Seismic Design Criteria for Bridges and Other Highway Structures," by C. Rojahn, R. Mayes, D.G. Anderson, J. Clark, J.H. Hom, R.V. Nutt and M.J. O'Rourke, 4/30/97, (PB97-194658, A06, MF-A03).

- NCEER-97-0003 "Proceedings of the U.S.-Italian Workshop on Seismic Evaluation and Retrofit," Edited by D.P. Abrams and G.M. Calvi, 3/19/97, (PB97-194666, A13, MF-A03).
- NCEER-97-0004 "Investigation of Seismic Response of Buildings with Linear and Nonlinear Fluid Viscous Dampers," by A.A. Seleemah and M.C. Constantinou, 5/21/97, (PB98-109002, A15, MF-A03).
- NCEER-97-0005 "Proceedings of the Workshop on Earthquake Engineering Frontiers in Transportation Facilities," edited by G.C. Lee and I.M. Friedland, 8/29/97, (PB98-128911, A25, MR-A04).
- NCEER-97-0006 "Cumulative Seismic Damage of Reinforced Concrete Bridge Piers," by S.K. Kunnath, A. El-Bahy, A. Taylor and W. Stone, 9/2/97, (PB98-108814, A11, MF-A03).
- NCEER-97-0007 "Structural Details to Accommodate Seismic Movements of Highway Bridges and Retaining Walls," by R.A. Imbsen, R.A. Schamber, E. Thorkildsen, A. Kartoum, B.T. Martin, T.N. Rosser and J.M. Kulicki, 9/3/97, (PB98-108996, A09, MF-A02).
- NCEER-97-0008 "A Method for Earthquake Motion-Damage Relationships with Application to Reinforced Concrete Frames," by A. Singhal and A.S. Kiremidjian, 9/10/97, (PB98-108988, A13, MF-A03).
- NCEER-97-0009 "Seismic Analysis and Design of Bridge Abutments Considering Sliding and Rotation," by K. Fishman and R. Richards, Jr., 9/15/97, (PB98-108897, A06, MF-A02).
- NCEER-97-0010 "Proceedings of the FHWA/NCEER Workshop on the National Representation of Seismic Ground Motion for New and Existing Highway Facilities," edited by I.M. Friedland, M.S. Power and R.L. Mayes, 9/22/97, (PB98-128903, A21, MF-A04).
- NCEER-97-0011 "Seismic Analysis for Design or Retrofit of Gravity Bridge Abutments," by K.L. Fishman, R. Richards, Jr. and R.C. Divito, 10/2/97, (PB98-128937, A08, MF-A02).
- NCEER-97-0012 "Evaluation of Simplified Methods of Analysis for Yielding Structures," by P. Tsopelas, M.C. Constantinou, C.A. Kircher and A.S. Whittaker, 10/31/97, (PB98-128929, A10, MF-A03).
- NCEER-97-0013 "Seismic Design of Bridge Columns Based on Control and Repairability of Damage," by C-T. Cheng and J.B. Mander, 12/8/97, (PB98-144249, A11, MF-A03).
- NCEER-97-0014 "Seismic Resistance of Bridge Piers Based on Damage Avoidance Design," by J.B. Mander and C-T. Cheng, 12/10/97, (PB98-144223, A09, MF-A02).
- NCEER-97-0015 "Seismic Response of Nominally Symmetric Systems with Strength Uncertainty," by S. Balopoulos and M. Grigoriu, 12/23/97, (PB98-153422, A11, MF-A03).
- NCEER-97-0016 "Evaluation of Seismic Retrofit Methods for Reinforced Concrete Bridge Columns," by T.J. Wipf, F.W. Klaiber and F.M. Russo, 12/28/97, (PB98-144215, A12, MF-A03).
- NCEER-97-0017 "Seismic Fragility of Existing Conventional Reinforced Concrete Highway Bridges," by C.L. Mullen and A.S. Cakmak, 12/30/97, (PB98-153406, A08, MF-A02).
- NCEER-97-0018 "Loss Assessment of Memphis Buildings," edited by D.P. Abrams and M. Shinozuka, 12/31/97, (PB98-144231, A13, MF-A03).
- NCEER-97-0019 "Seismic Evaluation of Frames with Infill Walls Using Quasi-static Experiments," by K.M. Mosalam, R.N. White and P. Gergely, 12/31/97, (PB98-153455, A07, MF-A02).
- NCEER-97-0020 "Seismic Evaluation of Frames with Infill Walls Using Pseudo-dynamic Experiments," by K.M. Mosalam, R.N. White and P. Gergely, 12/31/97, (PB98-153430, A07, MF-A02).
- NCEER-97-0021 "Computational Strategies for Frames with Infill Walls: Discrete and Smeared Crack Analyses and Seismic Fragility," by K.M. Mosalam, R.N. White and P. Gergely, 12/31/97, (PB98-153414, A10, MF-A02).

- NCEER-97-0022 "Proceedings of the NCEER Workshop on Evaluation of Liquefaction Resistance of Soils," edited by T.L. Youd and I.M. Idriss, 12/31/97, (PB98-155617, A15, MF-A03).
- MCEER-98-0001 "Extraction of Nonlinear Hysteretic Properties of Seismically Isolated Bridges from Quick-Release Field Tests," by Q. Chen, B.M. Douglas, E.M. Maragakis and I.G. Buckle, 5/26/98, (PB99-118838, A06, MF-A01).
- MCEER-98-0002 "Methodologies for Evaluating the Importance of Highway Bridges," by A. Thomas, S. Eshenaur and J. Kulicki, 5/29/98, (PB99-118846, A10, MF-A02).
- MCEER-98-0003 "Capacity Design of Bridge Piers and the Analysis of Overstrength," by J.B. Mander, A. Dutta and P. Goel, 6/1/98, (PB99-118853, A09, MF-A02).
- MCEER-98-0004 "Evaluation of Bridge Damage Data from the Loma Prieta and Northridge, California Earthquakes," by N. Basoz and A. Kiremidjian, 6/2/98, (PB99-118861, A15, MF-A03).
- MCEER-98-0005 "Screening Guide for Rapid Assessment of Liquefaction Hazard at Highway Bridge Sites," by T. L. Youd, 6/16/98, (PB99-118879, A06, not available on microfiche).
- MCEER-98-0006 "Structural Steel and Steel/Concrete Interface Details for Bridges," by P. Ritchie, N. Kauhl and J. Kulicki, 7/13/98, (PB99-118945, A06, MF-A01).
- MCEER-98-0007 "Capacity Design and Fatigue Analysis of Confined Concrete Columns," by A. Dutta and J.B. Mander, 7/14/98, (PB99-118960, A14, MF-A03).
- MCEER-98-0008 "Proceedings of the Workshop on Performance Criteria for Telecommunication Services Under Earthquake Conditions," edited by A.J. Schiff, 7/15/98, (PB99-118952, A08, MF-A02).
- MCEER-98-0009 "Fatigue Analysis of Unconfined Concrete Columns," by J.B. Mander, A. Dutta and J.H. Kim, 9/12/98, (PB99-123655, A10, MF-A02).
- MCEER-98-0010 "Centrifuge Modeling of Cyclic Lateral Response of Pile-Cap Systems and Seat-Type Abutments in Dry Sands," by A.D. Gadre and R. Dobry, 10/2/98, (PB99-123606, A13, MF-A03).
- MCEER-98-0011 "IDARC-BRIDGE: A Computational Platform for Seismic Damage Assessment of Bridge Structures," by A.M. Reinhorn, V. Simeonov, G. Mylonakis and Y. Reichman, 10/2/98, (PB99-162919, A15, MF-A03).
- MCEER-98-0012 "Experimental Investigation of the Dynamic Response of Two Bridges Before and After Retrofitting with Elastomeric Bearings," by D.A. Wendichansky, S.S. Chen and J.B. Mander, 10/2/98, (PB99-162927, A15, MF-A03).
- MCEER-98-0013 "Design Procedures for Hinge Restrainers and Hinge Sear Width for Multiple-Frame Bridges," by R. Des Roches and G.L. Fenves, 11/3/98, (PB99-140477, A13, MF-A03).
- MCEER-98-0014 "Response Modification Factors for Seismically Isolated Bridges," by M.C. Constantinou and J.K. Quarshie, 11/3/98, (PB99-140485, A14, MF-A03).
- MCEER-98-0015 "Proceedings of the U.S.-Italy Workshop on Seismic Protective Systems for Bridges," edited by I.M. Friedland and M.C. Constantinou, 11/3/98, (PB2000-101711, A22, MF-A04).
- MCEER-98-0016 "Appropriate Seismic Reliability for Critical Equipment Systems: Recommendations Based on Regional Analysis of Financial and Life Loss," by K. Porter, C. Scawthorn, C. Taylor and N. Blais, 11/10/98, (PB99-157265, A08, MF-A02).
- MCEER-98-0017 "Proceedings of the U.S. Japan Joint Seminar on Civil Infrastructure Systems Research," edited by M. Shinozuka and A. Rose, 11/12/98, (PB99-156713, A16, MF-A03).
- MCEER-98-0018 "Modeling of Pile Footings and Drilled Shafts for Seismic Design," by I. PoLam, M. Kapuskar and D. Chaudhuri, 12/21/98, (PB99-157257, A09, MF-A02).

- MCEER-99-0001 "Seismic Evaluation of a Masonry Infilled Reinforced Concrete Frame by Pseudodynamic Testing," by S.G. Buonopane and R.N. White, 2/16/99, (PB99-162851, A09, MF-A02).
- MCEER-99-0002 "Response History Analysis of Structures with Seismic Isolation and Energy Dissipation Systems: Verification Examples for Program SAP2000," by J. Scheller and M.C. Constantinou, 2/22/99, (PB99-162869, A08, MF-A02).
- MCEER-99-0003 "Experimental Study on the Seismic Design and Retrofit of Bridge Columns Including Axial Load Effects," by A. Dutta, T. Kokorina and J.B. Mander, 2/22/99, (PB99-162877, A09, MF-A02).
- MCEER-99-0004 "Experimental Study of Bridge Elastomeric and Other Isolation and Energy Dissipation Systems with Emphasis on Uplift Prevention and High Velocity Near-source Seismic Excitation," by A. Kasalanati and M. C. Constantinou, 2/26/99, (PB99-162885, A12, MF-A03).
- MCEER-99-0005 "Truss Modeling of Reinforced Concrete Shear-flexure Behavior," by J.H. Kim and J.B. Mander, 3/8/99, (PB99-163693, A12, MF-A03).
- MCEER-99-0006 "Experimental Investigation and Computational Modeling of Seismic Response of a 1:4 Scale Model Steel Structure with a Load Balancing Supplemental Damping System," by G. Pekcan, J.B. Mander and S.S. Chen, 4/2/99, (PB99-162893, A11, MF-A03).
- MCEER-99-0007 "Effect of Vertical Ground Motions on the Structural Response of Highway Bridges," by M.R. Button, C.J. Cronin and R.L. Mayes, 4/10/99, (PB2000-101411, A10, MF-A03).
- MCEER-99-0008 "Seismic Reliability Assessment of Critical Facilities: A Handbook, Supporting Documentation, and Model Code Provisions," by G.S. Johnson, R.E. Sheppard, M.D. Quilici, S.J. Eder and C.R. Scawthorn, 4/12/99, (PB2000-101701, A18, MF-A04).
- MCEER-99-0009 "Impact Assessment of Selected MCEER Highway Project Research on the Seismic Design of Highway Structures," by C. Rojahn, R. Mayes, D.G. Anderson, J.H. Clark, D'Appolonia Engineering, S. Gloyd and R.V. Nutt, 4/14/99, (PB99-162901, A10, MF-A02).
- MCEER-99-0010 "Site Factors and Site Categories in Seismic Codes," by R. Dobry, R. Ramos and M.S. Power, 7/19/99, (PB2000-101705, A08, MF-A02).
- MCEER-99-0011 "Restrainer Design Procedures for Multi-Span Simply-Supported Bridges," by M.J. Randall, M. Saiidi, E. Maragakis and T. Isakovic, 7/20/99, (PB2000-101702, A10, MF-A02).
- MCEER-99-0012 "Property Modification Factors for Seismic Isolation Bearings," by M.C. Constantinou, P. Tsopelas, A. Kasalanati and E. Wolff, 7/20/99, (PB2000-103387, A11, MF-A03).
- MCEER-99-0013 "Critical Seismic Issues for Existing Steel Bridges," by P. Ritchie, N. Kauhl and J. Kulicki, 7/20/99, (PB2000-101697, A09, MF-A02).
- MCEER-99-0014 "Nonstructural Damage Database," by A. Kao, T.T. Soong and A. Vender, 7/24/99, (PB2000-101407, A06, MF-A01).
- MCEER-99-0015 "Guide to Remedial Measures for Liquefaction Mitigation at Existing Highway Bridge Sites," by H.G. Cooke and J. K. Mitchell, 7/26/99, (PB2000-101703, A11, MF-A03).
- MCEER-99-0016 "Proceedings of the MCEER Workshop on Ground Motion Methodologies for the Eastern United States," edited by N. Abrahamson and A. Becker, 8/11/99, (PB2000-103385, A07, MF-A02).
- MCEER-99-0017 "Quindío, Colombia Earthquake of January 25, 1999: Reconnaissance Report," by A.P. Asfura and P.J. Flores, 10/4/99, (PB2000-106893, A06, MF-A01).
- MCEER-99-0018 "Hysteretic Models for Cyclic Behavior of Deteriorating Inelastic Structures," by M.V. Sivaselvan and A.M. Reinhorn, 11/5/99, (PB2000-103386, A08, MF-A02).

- MCEER-99-0019 "Proceedings of the 7th U.S.- Japan Workshop on Earthquake Resistant Design of Lifeline Facilities and Countermeasures Against Soil Liquefaction," edited by T.D. O'Rourke, J.P. Bardet and M. Hamada, 11/19/99, (PB2000-103354, A99, MF-A06).
- MCEER-99-0020 "Development of Measurement Capability for Micro-Vibration Evaluations with Application to Chip Fabrication Facilities," by G.C. Lee, Z. Liang, J.W. Song, J.D. Shen and W.C. Liu, 12/1/99, (PB2000-105993, A08, MF-A02).
- MCEER-99-0021 "Design and Retrofit Methodology for Building Structures with Supplemental Energy Dissipating Systems," by G. Pekcan, J.B. Mander and S.S. Chen, 12/31/99, (PB2000-105994, A11, MF-A03).
- MCEER-00-0001 "The Marmara, Turkey Earthquake of August 17, 1999: Reconnaissance Report," edited by C. Scawthorn; with major contributions by M. Bruneau, R. Eguchi, T. Holzer, G. Johnson, J. Mander, J. Mitchell, W. Mitchell, A. Papageorgiou, C. Scaethorn, and G. Webb, 3/23/00, (PB2000-106200, A11, MF-A03).
- MCEER-00-0002 "Proceedings of the MCEER Workshop for Seismic Hazard Mitigation of Health Care Facilities," edited by G.C. Lee, M. Ettouney, M. Grigoriu, J. Hauer and J. Nigg, 3/29/00, (PB2000-106892, A08, MF-A02).
- MCEER-00-0003 "The Chi-Chi, Taiwan Earthquake of September 21, 1999: Reconnaissance Report," edited by G.C. Lee and C.H. Loh, with major contributions by G.C. Lee, M. Bruneau, I.G. Buckle, S.E. Chang, P.J. Flores, T.D. O'Rourke, M. Shinozuka, T.T. Soong, C-H. Loh, K-C. Chang, Z-J. Chen, J-S. Hwang, M-L. Lin, G-Y. Liu, K-C. Tsai, G.C. Yao and C-L. Yen, 4/30/00, (PB2001-100980, A10, MF-A02).
- MCEER-00-0004 "Seismic Retrofit of End-Sway Frames of Steel Deck-Truss Bridges with a Supplemental Tendon System: Experimental and Analytical Investigation," by G. Pekcan, J.B. Mander and S.S. Chen, 7/1/00, (PB2001-100982, A10, MF-A02).
- MCEER-00-0005 "Sliding Fragility of Unrestrained Equipment in Critical Facilities," by W.H. Chong and T.T. Soong, 7/5/00, (PB2001-100983, A08, MF-A02).
- MCEER-00-0006 "Seismic Response of Reinforced Concrete Bridge Pier Walls in the Weak Direction," by N. Abo-Shadi, M. Saiidi and D. Sanders, 7/17/00, (PB2001-100981, A17, MF-A03).
- MCEER-00-0007 "Low-Cycle Fatigue Behavior of Longitudinal Reinforcement in Reinforced Concrete Bridge Columns," by J. Brown and S.K. Kunath, 7/23/00, (PB2001-104392, A08, MF-A02).
- MCEER-00-0008 "Soil Structure Interaction of Bridges for Seismic Analysis," I. PoLam and H. Law, 9/25/00, (PB2001-105397, A08, MF-A02).
- MCEER-00-0009 "Proceedings of the First MCEER Workshop on Mitigation of Earthquake Disaster by Advanced Technologies (MEDAT-1), edited by M. Shinozuka, D.J. Inman and T.D. O'Rourke, 11/10/00, (PB2001-105399, A14, MF-A03).
- MCEER-00-0010 "Development and Evaluation of Simplified Procedures for Analysis and Design of Buildings with Passive Energy Dissipation Systems, Revision 01," by O.M. Ramirez, M.C. Constantinou, C.A. Kircher, A.S. Whittaker, M.W. Johnson, J.D. Gomez and C. Chrysostomou, 11/16/01, (PB2001-105523, A23, MF-A04).
- MCEER-00-0011 "Dynamic Soil-Foundation-Structure Interaction Analyses of Large Caissons," by C-Y. Chang, C-M. Mok, Z-L. Wang, R. Settgast, F. Waggoner, M.A. Ketchum, H.M. Gonnermann and C-C. Chin, 12/30/00, (PB2001-104373, A07, MF-A02).
- MCEER-00-0012 "Experimental Evaluation of Seismic Performance of Bridge Restrainers," by A.G. Vlassis, E.M. Maragakis and M. Saiid Saiidi, 12/30/00, (PB2001-104354, A09, MF-A02).
- MCEER-00-0013 "Effect of Spatial Variation of Ground Motion on Highway Structures," by M. Shinozuka, V. Saxena and G. Deodatis, 12/31/00, (PB2001-108755, A13, MF-A03).
- MCEER-00-0014 "A Risk-Based Methodology for Assessing the Seismic Performance of Highway Systems," by S.D. Werner, C.E. Taylor, J.E. Moore, II, J.S. Walton and S. Cho, 12/31/00, (PB2001-108756, A14, MF-A03).

- MCEER-01-0001 "Experimental Investigation of P-Delta Effects to Collapse During Earthquakes," by D. Vian and M. Bruneau, 6/25/01, (PB2002-100534, A17, MF-A03).
- MCEER-01-0002 "Proceedings of the Second MCEER Workshop on Mitigation of Earthquake Disaster by Advanced Technologies (MEDAT-2)," edited by M. Bruneau and D.J. Inman, 7/23/01, (PB2002-100434, A16, MF-A03).
- MCEER-01-0003 "Sensitivity Analysis of Dynamic Systems Subjected to Seismic Loads," by C. Roth and M. Grigoriu, 9/18/01, (PB2003-100884, A12, MF-A03).
- MCEER-01-0004 "Overcoming Obstacles to Implementing Earthquake Hazard Mitigation Policies: Stage 1 Report," by D.J. Alesch and W.J. Petak, 12/17/01, (PB2002-107949, A07, MF-A02).
- MCEER-01-0005 "Updating Real-Time Earthquake Loss Estimates: Methods, Problems and Insights," by C.E. Taylor, S.E. Chang and R.T. Eguchi, 12/17/01, (PB2002-107948, A05, MF-A01).
- MCEER-01-0006 "Experimental Investigation and Retrofit of Steel Pile Foundations and Pile Bents Under Cyclic Lateral Loadings," by A. Shama, J. Mander, B. Blabac and S. Chen, 12/31/01, (PB2002-107950, A13, MF-A03).
- MCEER-02-0001 "Assessment of Performance of Bolu Viaduct in the 1999 Duzce Earthquake in Turkey" by P.C. Roussis, M.C. Constantinou, M. Erdik, E. Durukal and M. Dicleli, 5/8/02, (PB2003-100883, A08, MF-A02).
- MCEER-02-0002 "Seismic Behavior of Rail Counterweight Systems of Elevators in Buildings," by M.P. Singh, Rildova and L.E. Suarez, 5/27/02. (PB2003-100882, A11, MF-A03).
- MCEER-02-0003 "Development of Analysis and Design Procedures for Spread Footings," by G. Mylonakis, G. Gazetas, S. Nikolaou and A. Chauncey, 10/02/02, (PB2004-101636, A13, MF-A03, CD-A13).
- MCEER-02-0004 "Bare-Earth Algorithms for Use with SAR and LIDAR Digital Elevation Models," by C.K. Huyck, R.T. Eguchi and B. Houshmand, 10/16/02, (PB2004-101637, A07, CD-A07).
- MCEER-02-0005 "Review of Energy Dissipation of Compression Members in Concentrically Braced Frames," by K.Lee and M. Bruneau, 10/18/02, (PB2004-101638, A10, CD-A10).
- MCEER-03-0001 "Experimental Investigation of Light-Gauge Steel Plate Shear Walls for the Seismic Retrofit of Buildings" by J. Berman and M. Bruneau, 5/2/03, (PB2004-101622, A10, MF-A03, CD-A10).
- MCEER-03-0002 "Statistical Analysis of Fragility Curves," by M. Shinotuka, M.Q. Feng, H. Kim, T. Uzawa and T. Ueda, 6/16/03, (PB2004-101849, A09, CD-A09).
- MCEER-03-0003 "Proceedings of the Eighth U.S.-Japan Workshop on Earthquake Resistant Design f Lifeline Facilities and Countermeasures Against Liquefaction," edited by M. Hamada, J.P. Bardet and T.D. O'Rourke, 6/30/03, (PB2004-104386, A99, CD-A99).
- MCEER-03-0004 "Proceedings of the PRC-US Workshop on Seismic Analysis and Design of Special Bridges," edited by L.C. Fan and G.C. Lee, 7/15/03, (PB2004-104387, A14, CD-A14).
- MCEER-03-0005 "Urban Disaster Recovery: A Framework and Simulation Model," by S.B. Miles and S.E. Chang, 7/25/03, (PB2004-104388, A07, CD-A07).
- MCEER-03-0006 "Behavior of Underground Piping Joints Due to Static and Dynamic Loading," by R.D. Meis, M. Maragakis and R. Siddharthan, 11/17/03, (PB2005-102194, A13, MF-A03, CD-A00).
- MCEER-04-0001 "Experimental Study of Seismic Isolation Systems with Emphasis on Secondary System Response and Verification of Accuracy of Dynamic Response History Analysis Methods," by E. Wolff and M. Constantinou, 1/16/04 (PB2005-102195, A99, MF-E08, CD-A00).
- MCEER-04-0002 "Tension, Compression and Cyclic Testing of Engineered Cementitious Composite Materials," by K. Kesner and S.L. Billington, 3/1/04, (PB2005-102196, A08, CD-A08).

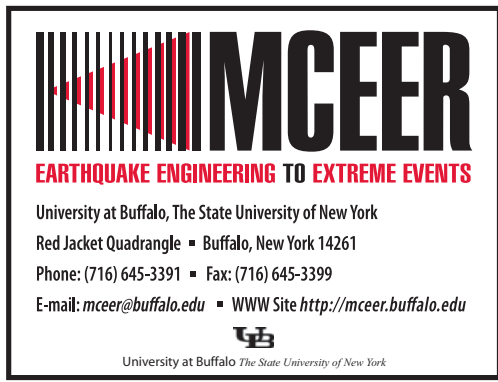
- MCEER-04-0003 "Cyclic Testing of Braces Laterally Restrained by Steel Studs to Enhance Performance During Earthquakes," by O.C. Celik, J.W. Berman and M. Bruneau, 3/16/04, (PB2005-102197, A13, MF-A03, CD-A00).
- MCEER-04-0004 "Methodologies for Post Earthquake Building Damage Detection Using SAR and Optical Remote Sensing: Application to the August 17, 1999 Marmara, Turkey Earthquake," by C.K. Huyck, B.J. Adams, S. Cho, R.T. Eguchi, B. Mansouri and B. Houshmand, 6/15/04, (PB2005-104888, A10, CD-A00).
- MCEER-04-0005 "Nonlinear Structural Analysis Towards Collapse Simulation: A Dynamical Systems Approach," by M.V. Sivaselvan and A.M. Reinhorn, 6/16/04, (PB2005-104889, A11, MF-A03, CD-A00).
- MCEER-04-0006 "Proceedings of the Second PRC-US Workshop on Seismic Analysis and Design of Special Bridges," edited by G.C. Lee and L.C. Fan, 6/25/04, (PB2005-104890, A16, CD-A00).
- MCEER-04-0007 "Seismic Vulnerability Evaluation of Axially Loaded Steel Built-up Laced Members," by K. Lee and M. Bruneau, 6/30/04, (PB2005-104891, A16, CD-A00).
- MCEER-04-0008 "Evaluation of Accuracy of Simplified Methods of Analysis and Design of Buildings with Damping Systems for Near-Fault and for Soft-Soil Seismic Motions," by E.A. Pavlou and M.C. Constantinou, 8/16/04, (PB2005-104892, A08, MF-A02, CD-A00).
- MCEER-04-0009 "Assessment of Geotechnical Issues in Acute Care Facilities in California," by M. Lew, T.D. O'Rourke, R. Dobry and M. Koch, 9/15/04, (PB2005-104893, A08, CD-A00).
- MCEER-04-0010 "Scissor-Jack-Damper Energy Dissipation System," by A.N. Sigaher-Boyle and M.C. Constantinou, 12/1/04 (PB2005-108221).
- MCEER-04-0011 "Seismic Retrofit of Bridge Steel Truss Piers Using a Controlled Rocking Approach," by M. Pollino and M. Bruneau, 12/20/04 (PB2006-105795).
- MCEER-05-0001 "Experimental and Analytical Studies of Structures Seismically Isolated with an Uplift-Restraint Isolation System," by P.C. Roussis and M.C. Constantinou, 1/10/05 (PB2005-108222).
- MCEER-05-0002 "A Versatile Experimentation Model for Study of Structures Near Collapse Applied to Seismic Evaluation of Irregular Structures," by D. Kusumastuti, A.M. Reinhorn and A. Rutenberg, 3/31/05 (PB2006-101523).
- MCEER-05-0003 "Proceedings of the Third PRC-US Workshop on Seismic Analysis and Design of Special Bridges," edited by L.C. Fan and G.C. Lee, 4/20/05, (PB2006-105796).
- MCEER-05-0004 "Approaches for the Seismic Retrofit of Braced Steel Bridge Piers and Proof-of-Concept Testing of an Eccentrically Braced Frame with Tubular Link," by J.W. Berman and M. Bruneau, 4/21/05 (PB2006-101524).
- MCEER-05-0005 "Simulation of Strong Ground Motions for Seismic Fragility Evaluation of Nonstructural Components in Hospitals," by A. Wanitkorkul and A. Filiatrault, 5/26/05 (PB2006-500027).
- MCEER-05-0006 "Seismic Safety in California Hospitals: Assessing an Attempt to Accelerate the Replacement or Seismic Retrofit of Older Hospital Facilities," by D.J. Alesch, L.A. Arendt and W.J. Petak, 6/6/05 (PB2006-105794).
- MCEER-05-0007 "Development of Seismic Strengthening and Retrofit Strategies for Critical Facilities Using Engineered Cementitious Composite Materials," by K. Kesner and S.L. Billington, 8/29/05 (PB2006-111701).
- MCEER-05-0008 "Experimental and Analytical Studies of Base Isolation Systems for Seismic Protection of Power Transformers," by N. Murota, M.Q. Feng and G-Y. Liu, 9/30/05 (PB2006-111702).
- MCEER-05-0009 "3D-BASIS-ME-MB: Computer Program for Nonlinear Dynamic Analysis of Seismically Isolated Structures," by P.C. Tsopelas, P.C. Roussis, M.C. Constantinou, R. Buchanan and A.M. Reinhorn, 10/3/05 (PB2006-111703).
- MCEER-05-0010 "Steel Plate Shear Walls for Seismic Design and Retrofit of Building Structures," by D. Vian and M. Bruneau, 12/15/05 (PB2006-111704).

- MCEER-05-0011 "The Performance-Based Design Paradigm," by M.J. Astrella and A. Whittaker, 12/15/05 (PB2006-111705).
- MCEER-06-0001 "Seismic Fragility of Suspended Ceiling Systems," H. Badillo-Almaraz, A.S. Whittaker, A.M. Reinhorn and G.P. Cimellaro, 2/4/06 (PB2006-111706).
- MCEER-06-0002 "Multi-Dimensional Fragility of Structures," by G.P. Cimellaro, A.M. Reinhorn and M. Bruneau, 3/1/06 (PB2007-106974, A09, MF-A02, CD A00).
- MCEER-06-0003 "Built-Up Shear Links as Energy Dissipators for Seismic Protection of Bridges," by P. Dusicka, A.M. Itani and I.G. Buckle, 3/15/06 (PB2006-111708).
- MCEER-06-0004 "Analytical Investigation of the Structural Fuse Concept," by R.E. Vargas and M. Bruneau, 3/16/06 (PB2006-111709).
- MCEER-06-0005 "Experimental Investigation of the Structural Fuse Concept," by R.E. Vargas and M. Bruneau, 3/17/06 (PB2006-111710).
- MCEER-06-0006 "Further Development of Tubular Eccentrically Braced Frame Links for the Seismic Retrofit of Braced Steel Truss Bridge Piers," by J.W. Berman and M. Bruneau, 3/27/06 (PB2007-105147).
- MCEER-06-0007 "REDARS Validation Report," by S. Cho, C.K. Huyck, S. Ghosh and R.T. Eguchi, 8/8/06 (PB2007-106983).
- MCEER-06-0008 "Review of Current NDE Technologies for Post-Earthquake Assessment of Retrofitted Bridge Columns," by J.W. Song, Z. Liang and G.C. Lee, 8/21/06 (PB2007-106984).
- MCEER-06-0009 "Liquefaction Remediation in Silty Soils Using Dynamic Compaction and Stone Columns," by S. Thevanayagam, G.R. Martin, R. Nashed, T. Shenthal, T. Kanagalingam and N. Ecemis, 8/28/06 (PB2007-106985).
- MCEER-06-0010 "Conceptual Design and Experimental Investigation of Polymer Matrix Composite Infill Panels for Seismic Retrofitting," by W. Jung, M. Chiewanichakorn and A.J. Aref, 9/21/06 (PB2007-106986).
- MCEER-06-0011 "A Study of the Coupled Horizontal-Vertical Behavior of Elastomeric and Lead-Rubber Seismic Isolation Bearings," by G.P. Warn and A.S. Whittaker, 9/22/06 (PB2007-108679).
- MCEER-06-0012 "Proceedings of the Fourth PRC-US Workshop on Seismic Analysis and Design of Special Bridges: Advancing Bridge Technologies in Research, Design, Construction and Preservation," Edited by L.C. Fan, G.C. Lee and L. Ziang, 10/12/06 (PB2007-109042).
- MCEER-06-0013 "Cyclic Response and Low Cycle Fatigue Characteristics of Plate Steels," by P. Dusicka, A.M. Itani and I.G. Buckle, 11/1/06 06 (PB2007-106987).
- MCEER-06-0014 "Proceedings of the Second US-Taiwan Bridge Engineering Workshop," edited by W.P. Yen, J. Shen, J-Y. Chen and M. Wang, 11/15/06 (PB2008-500041).
- MCEER-06-0015 "User Manual and Technical Documentation for the REDARS™ Import Wizard," by S. Cho, S. Ghosh, C.K. Huyck and S.D. Werner, 11/30/06 (PB2007-114766).
- MCEER-06-0016 "Hazard Mitigation Strategy and Monitoring Technologies for Urban and Infrastructure Public Buildings: Proceedings of the China-US Workshops," edited by X.Y. Zhou, A.L. Zhang, G.C. Lee and M. Tong, 12/12/06 (PB2008-500018).
- MCEER-07-0001 "Static and Kinetic Coefficients of Friction for Rigid Blocks," by C. Kafali, S. Fathali, M. Grigoriu and A.S. Whittaker, 3/20/07 (PB2007-114767).
- MCEER-07-0002 "Hazard Mitigation Investment Decision Making: Organizational Response to Legislative Mandate," by L.A. Arendt, D.J. Alesch and W.J. Petak, 4/9/07 (PB2007-114768).
- MCEER-07-0003 "Seismic Behavior of Bidirectional-Resistant Ductile End Diaphragms with Unbonded Braces in Straight or Skewed Steel Bridges," by O. Celik and M. Bruneau, 4/11/07 (PB2008-105141).

- MCEER-07-0004 "Modeling Pile Behavior in Large Pile Groups Under Lateral Loading," by A.M. Dodds and G.R. Martin, 4/16/07 (PB2008-105142).
- MCEER-07-0005 "Experimental Investigation of Blast Performance of Seismically Resistant Concrete-Filled Steel Tube Bridge Piers," by S. Fujikura, M. Bruneau and D. Lopez-Garcia, 4/20/07 (PB2008-105143).
- MCEER-07-0006 "Seismic Analysis of Conventional and Isolated Liquefied Natural Gas Tanks Using Mechanical Analogs," by I.P. Christovasilis and A.S. Whittaker, 5/1/07.
- MCEER-07-0007 "Experimental Seismic Performance Evaluation of Isolation/Restrain Systems for Mechanical Equipment – Part 1: Heavy Equipment Study," by S. Fathali and A. Filiatral, 6/6/07 (PB2008-105144).
- MCEER-07-0008 "Seismic Vulnerability of Timber Bridges and Timber Substructures," by A.A. Sharma, J.B. Mander, I.M. Friedland and D.R. Allicock, 6/7/07 (PB2008-105145).
- MCEER-07-0009 "Experimental and Analytical Study of the XY-Friction Pendulum (XY-FP) Bearing for Bridge Applications," by C.C. Marin-Artieda, A.S. Whittaker and M.C. Constantinou, 6/7/07 (PB2008-105191).
- MCEER-07-0010 "Proceedings of the PRC-US Earthquake Engineering Forum for Young Researchers," Edited by G.C. Lee and X.Z. Qi, 6/8/07 (PB2008-500058).
- MCEER-07-0011 "Design Recommendations for Perforated Steel Plate Shear Walls," by R. Purba and M. Bruneau, 6/18/07, (PB2008-105192).
- MCEER-07-0012 "Performance of Seismic Isolation Hardware Under Service and Seismic Loading," by M.C. Constantinou, A.S. Whittaker, Y. Kalpakidis, D.M. Fenz and G.P. Warn, 8/27/07, (PB2008-105193).
- MCEER-07-0013 "Experimental Evaluation of the Seismic Performance of Hospital Piping Subassemblies," by E.R. Goodwin, E. Maragakis and A.M. Itani, 9/4/07, (PB2008-105194).
- MCEER-07-0014 "A Simulation Model of Urban Disaster Recovery and Resilience: Implementation for the 1994 Northridge Earthquake," by S. Miles and S.E. Chang, 9/7/07, (PB2008-106426).
- MCEER-07-0015 "Statistical and Mechanistic Fragility Analysis of Concrete Bridges," by M. Shinozuka, S. Banerjee and S-H. Kim, 9/10/07, (PB2008-106427).
- MCEER-07-0016 "Three-Dimensional Modeling of Inelastic Buckling in Frame Structures," by M. Schachter and AM. Reinhorn, 9/13/07, (PB2008-108125).
- MCEER-07-0017 "Modeling of Seismic Wave Scattering on Pile Groups and Caissons," by I. Po Lam, H. Law and C.T. Yang, 9/17/07 (PB2008-108150).
- MCEER-07-0018 "Bridge Foundations: Modeling Large Pile Groups and Caissons for Seismic Design," by I. Po Lam, H. Law and G.R. Martin (Coordinating Author), 12/1/07 (PB2008-111190).
- MCEER-07-0019 "Principles and Performance of Roller Seismic Isolation Bearings for Highway Bridges," by G.C. Lee, Y.C. Ou, Z. Liang, T.C. Niu and J. Song, 12/10/07 (PB2009-110466).
- MCEER-07-0020 "Centrifuge Modeling of Permeability and Pinning Reinforcement Effects on Pile Response to Lateral Spreading," by L.L Gonzalez-Lagos, T. Abdoun and R. Dobry, 12/10/07 (PB2008-111191).
- MCEER-07-0021 "Damage to the Highway System from the Pisco, Perú Earthquake of August 15, 2007," by J.S. O'Connor, L. Mesa and M. Nykamp, 12/10/07, (PB2008-108126).
- MCEER-07-0022 "Experimental Seismic Performance Evaluation of Isolation/Restrain Systems for Mechanical Equipment – Part 2: Light Equipment Study," by S. Fathali and A. Filiatral, 12/13/07 (PB2008-111192).
- MCEER-07-0023 "Fragility Considerations in Highway Bridge Design," by M. Shinozuka, S. Banerjee and S.H. Kim, 12/14/07 (PB2008-111193).

- MCEER-07-0024 "Performance Estimates for Seismically Isolated Bridges," by G.P. Warn and A.S. Whittaker, 12/30/07 (PB2008-112230).
- MCEER-08-0001 "Seismic Performance of Steel Girder Bridge Superstructures with Conventional Cross Frames," by L.P. Carden, A.M. Itani and I.G. Buckle, 1/7/08, (PB2008-112231).
- MCEER-08-0002 "Seismic Performance of Steel Girder Bridge Superstructures with Ductile End Cross Frames with Seismic Isolators," by L.P. Carden, A.M. Itani and I.G. Buckle, 1/7/08 (PB2008-112232).
- MCEER-08-0003 "Analytical and Experimental Investigation of a Controlled Rocking Approach for Seismic Protection of Bridge Steel Truss Piers," by M. Pollino and M. Bruneau, 1/21/08 (PB2008-112233).
- MCEER-08-0004 "Linking Lifeline Infrastructure Performance and Community Disaster Resilience: Models and Multi-Stakeholder Processes," by S.E. Chang, C. Pasion, K. Tatebe and R. Ahmad, 3/3/08 (PB2008-112234).
- MCEER-08-0005 "Modal Analysis of Generally Damped Linear Structures Subjected to Seismic Excitations," by J. Song, Y-L. Chu, Z. Liang and G.C. Lee, 3/4/08 (PB2009-102311).
- MCEER-08-0006 "System Performance Under Multi-Hazard Environments," by C. Kafali and M. Grigoriu, 3/4/08 (PB2008-112235).
- MCEER-08-0007 "Mechanical Behavior of Multi-Spherical Sliding Bearings," by D.M. Fenz and M.C. Constantinou, 3/6/08 (PB2008-112236).
- MCEER-08-0008 "Post-Earthquake Restoration of the Los Angeles Water Supply System," by T.H.P. Tabucchi and R.A. Davidson, 3/7/08 (PB2008-112237).
- MCEER-08-0009 "Fragility Analysis of Water Supply Systems," by A. Jacobson and M. Grigoriu, 3/10/08 (PB2009-105545).
- MCEER-08-0010 "Experimental Investigation of Full-Scale Two-Story Steel Plate Shear Walls with Reduced Beam Section Connections," by B. Qu, M. Bruneau, C-H. Lin and K-C. Tsai, 3/17/08 (PB2009-106368).
- MCEER-08-0011 "Seismic Evaluation and Rehabilitation of Critical Components of Electrical Power Systems," S. Ersoy, B. Feizi, A. Ashrafi and M. Ala Saadeghvaziri, 3/17/08 (PB2009-105546).
- MCEER-08-0012 "Seismic Behavior and Design of Boundary Frame Members of Steel Plate Shear Walls," by B. Qu and M. Bruneau, 4/26/08 . (PB2009-106744).
- MCEER-08-0013 "Development and Appraisal of a Numerical Cyclic Loading Protocol for Quantifying Building System Performance," by A. Filiatralt, A. Wanitkorkul and M. Constantinou, 4/27/08 (PB2009-107906).
- MCEER-08-0014 "Structural and Nonstructural Earthquake Design: The Challenge of Integrating Specialty Areas in Designing Complex, Critical Facilities," by W.J. Petak and D.J. Alesch, 4/30/08 (PB2009-107907).
- MCEER-08-0015 "Seismic Performance Evaluation of Water Systems," by Y. Wang and T.D. O'Rourke, 5/5/08 (PB2009-107908).
- MCEER-08-0016 "Seismic Response Modeling of Water Supply Systems," by P. Shi and T.D. O'Rourke, 5/5/08 (PB2009-107910).
- MCEER-08-0017 "Numerical and Experimental Studies of Self-Centering Post-Tensioned Steel Frames," by D. Wang and A. Filiatralt, 5/12/08 (PB2009-110479).
- MCEER-08-0018 "Development, Implementation and Verification of Dynamic Analysis Models for Multi-Spherical Sliding Bearings," by D.M. Fenz and M.C. Constantinou, 8/15/08 (PB2009-107911).
- MCEER-08-0019 "Performance Assessment of Conventional and Base Isolated Nuclear Power Plants for Earthquake Blast Loadings," by Y.N. Huang, A.S. Whittaker and N. Luco, 10/28/08 (PB2009-107912).

- MCEER-08-0020 "Remote Sensing for Resilient Multi-Hazard Disaster Response – Volume I: Introduction to Damage Assessment Methodologies," by B.J. Adams and R.T. Eguchi, 11/17/08.
- MCEER-08-0021 "Remote Sensing for Resilient Multi-Hazard Disaster Response – Volume II: Counting the Number of Collapsed Buildings Using an Object-Oriented Analysis: Case Study of the 2003 Bam Earthquake," by L. Gusella, C.K. Huyck and B.J. Adams, 11/17/08.
- MCEER-08-0022 "Remote Sensing for Resilient Multi-Hazard Disaster Response – Volume III: Multi-Sensor Image Fusion Techniques for Robust Neighborhood-Scale Urban Damage Assessment," by B.J. Adams and A. McMillan, 11/17/08.
- MCEER-08-0023 "Remote Sensing for Resilient Multi-Hazard Disaster Response – Volume IV: A Study of Multi-Temporal and Multi-Resolution SAR Imagery for Post-Katrina Flood Monitoring in New Orleans," by A. McMillan, J.G. Morley, B.J. Adams and S. Chesworth, 11/17/08.
- MCEER-08-0024 "Remote Sensing for Resilient Multi-Hazard Disaster Response – Volume V: Integration of Remote Sensing Imagery and VIEWSTM Field Data for Post-Hurricane Charley Building Damage Assessment," by J.A. Womble, K. Mehta and B.J. Adams, 11/17/08 (PB2009-115532).
- MCEER-08-0025 "Building Inventory Compilation for Disaster Management: Application of Remote Sensing and Statistical Modeling," by P. Sarabandi, A.S. Kiremidjian, R.T. Eguchi and B. J. Adams, 11/20/08 (PB2009-110484).
- MCEER-08-0026 "New Experimental Capabilities and Loading Protocols for Seismic Qualification and Fragility Assessment of Nonstructural Systems," by R. Retamales, G. Mosqueda, A. Filiatrault and A. Reinhorn, 11/24/08 (PB2009-110485).
- MCEER-08-0027 "Effects of Heating and Load History on the Behavior of Lead-Rubber Bearings," by I.V. Kalpakidis and M.C. Constantinou, 12/1/08 (PB2009-115533).
- MCEER-08-0028 "Experimental and Analytical Investigation of Blast Performance of Seismically Resistant Bridge Piers," by S.Fujikura and M. Bruneau, 12/8/08 (PB2009-115534).
- MCEER-08-0029 "Evolutionary Methodology for Aseismic Decision Support," by Y. Hu and G. Dargush, 12/15/08.
- MCEER-08-0030 "Development of a Steel Plate Shear Wall Bridge Pier System Conceived from a Multi-Hazard Perspective," by D. Keller and M. Bruneau, 12/19/08.
- MCEER-09-0001 "Modal Analysis of Arbitrarily Damped Three-Dimensional Linear Structures Subjected to Seismic Excitations," by Y.L. Chu, J. Song and G.C. Lee, 1/31/09.
- MCEER-09-0002 "Air-Blast Effects on Structural Shapes," by G. Ballantyne, A.S. Whittaker, A.J. Aref and G.F. Dargush, 2/2/09.
- MCEER-09-0003 "Water Supply Performance During Earthquakes and Extreme Events," by A.L. Bonneau and T.D. O'Rourke, 2/16/09.
- MCEER-09-0004 "Generalized Linear (Mixed) Models of Post-Earthquake Ignitions," by R.A. Davidson, 7/20/09.
- MCEER-09-0005 "Seismic Testing of a Full-Scale Two-Story Light-Frame Wood Building: NEESWood Benchmark Test," by I.P. Christovasilis, A. Filiatrault and A. Wanitkorkul, 7/22/09.
- MCEER-09-0006 "IDARC2D Version 7.0: A Program for the Inelastic Damage Analysis of Structures," by A.M. Reinhorn, H. Roh, M. Sivaselvan, S.K. Kunnath, R.E. Valles, A. Madan, C. Li, R. Lobo and Y.J. Park, 7/28/09.



ISSN 1520-295X